

**Faculty of Science and Engineering  
Department of Applied Geology**

**Ordovician Carbonate-Shale System of the part of the Canning Basin,  
W.A.**

**Ying Jia Teoh**

**This thesis is presented for the Degree of**

**Doctor of Philosophy**

**of**

**Curtin University**

**September 2013**

## DECLARATION

“This thesis contains no material which has been accepted for the award of any other degree or diploma in any university To the best of my knowledge and belief, this thesis contains no material previously published by any other person except where due acknowledgement has been made.”.

Ying Jia Teoh

Signature: 

Date: 27<sup>th</sup> September 2013

## COPYRIGHT DECLARATION

“I warrant that I have obtained, where necessary, permission from the copyright owners to use any third-party copyright material reproduced in the thesis, or to use any of my own work in which copyright is held by another party”.

Ying Jia Teoh

Signature: 

Date: 27<sup>th</sup> September 2013

## ACKNOWLEDGEMENTS

Special appreciation goes to my supervisor, Prof. Lindsay Collins, for his supervision and constant support. His invaluable help of constructive comments and suggestions throughout the works have contributed to the success of this research. Not forgotten, my appreciation to my associate supervisor, Dr. Mehrooz Aspandiar for all his support and his permission to use his TSG-Core software.

A special thank you is given to the Universiti Sains Malaysia and Ministry of Higher Education (KPT) for awarding me with a Ph.D. scholarship.

I would like to thank the Geological Survey of Western Australia (GSWA) for permission to use the CycloLog® software, TSG-Core software and collect samples from Perth core library at Carlisle. I appreciate Dr. Peter Haines, Dr. Lena Hancock and other staffs from GSWA for sharing their knowledge.

I would like to express my appreciation to all the office staffs in the Department of Applied Geology, Curtin University for their co-operation. I also appreciate the stimulating discussions I have had with Ricardo Jahnert and Saad Alawwad. Sincere thanks to all my friends especially Ming Yi, Eva, Siyu, Ni, Huiqing, Lingling, Yue, Weihua, Qian, Fiona, Giada, Alex, Tubagus, Omar, Khalid, Moataz, Leo and others for their kindness and moral support during my study. Thanks for the friendship and memories.

Last but not least, my deepest gratitude goes to my family members for their encouragement and understanding. To those who indirectly contributed in this research, your kindness means a lot to me. Thank you very much.

## ABSTRACT

The Canning Basin is located between the Kimberley and Pilbara Precambrian cratonic blocks. It is a large but relatively poorly explored Paleozoic basin in remote Western Australia. During the early Ordovician period, the Australian continent was located near the equator. Middle Ordovician age Nita and Goldwyer Formations in Canning Basin are therefore warm water carbonates. The Nita Formation carbonates are a regressive sequence which conformably overlies the Goldwyer Formation. It contains numerous progradational cycles of limestone, vuggy dolomitized carbonate beds and shale deposited in subtidal to supratidal environments. The Goldwyer Formation contains transgressive shale sequences and regressive carbonates deposited in shallow subtidal conditions. The shales contain oil-prone *Gloeocapsormorpha prisca*-bearing source rocks.

For cores studied, the Nita Formation (major part of Leo Member and part of Cudalgarra Member) from well Looma 1 (Broome Platform) has been classified into 6 microfacies, which are, from deepest to shallowest: 1) burrowed, fossiliferous mudstone/ wackestone; 2) oolitic/ peloidal/ intraclastic and bioclastic packstone/ grainstone; 3) interlaminated shale and wackestone/packstone; 4) microbial laminites; 5) evaporitic wackestone; and 6) terrestrial shale. These lithofacies are interpreted to have been deposited in low energy tidal flat shallowing upward sequence, which from shallow subtidal (microfacies 1); shoal (microfacies 2); intertidal (microfacies 3); intertidal/supratidal (microfacies 4); and supratidal (microfacies 5 and 6).

The Goldwyer middle carbonate (Unit 3) shallows upward from microfacies of gastropod bioclastic burrowed wackestone (subtidal below wave-base) to oncoidal-peloidal packstone/floatstone (shallow subtidal above wave-base) in well Acacia 2 (Barbwire Terrace). Wave energy was probably low in this shallow epeiric sea which is reflected in the overall muddy character of the facies present.

The Nita Leo Member carbonate sediments in well Canopus 1 (Mowla Terrace) is shale-rich and is interbedded with dolomitised, stylolitic carbonates. Microfacies are weakly cemented burrowed mudstone with peloids and bioclasts with a depositional environment of subtidal below wave-base, coarsening upwards and capped by

peloidal/intraclastic packstone/floatstone which was deposited during storms or periods of lowered wave-base.

The Nita and Goldwyer Formations section log for well Kunzea 1 (Crossland Platform) was studied and investigated. Goldwyer Unit 3 consists of upward coarsening thin cycles from below wave-base wackestone/packstone to oncoidal/peloidal packstone/floatstone. The interval at depth 404.6m contains thin stromatolite layers which likely represent shallow subtidal to lowermost intertidal zone near the top of this unit. Goldwyer Unit 4 is strongly shaly at its base and this unit consists of upward coarsening cycles from shale to packstone. Near the top of this unit is oncoidal/peloidal packstone which may represent shoaling before onset of deposition of the Nita Leo Member regressive carbonate package. Nita Leo Member in this well consists of thin cyclicity from shallow subtidal zone (microfacies stylonodular burrowed wackestone) to storm lags (bioclastic floatstone horizons) intervals, a few centimetres to decimetre scale. Bioclastic rudstone is found at the boundary of Nita Leo Member and Nita Cudalgarra Member. This matches with the positive bounding surface (the turning point between Leo Member and Cudalgarra Member) from integrated prediction error filter analysis (INPEFA) which indicates a maximum regressive surface. Nita Cudalgarra Member is heavily dolomitised mudstone and diagenesis has prevented identification of microfacies and environmental analysis.

In summary, the Nita Formation carbonates consist of thin upward shallowing sequences of Milankovitch origin and grade from muddy below wave-base facies to intertidal-supratidal zone microbial laminites, sometimes capped by evaporitic and supratidal deposits. The Goldwyer Formation carbonates are similarly in thin (Milankovitch) packages of bioclastic to oolitic, shallow water below-to-above wave-base carbonates. The carbonate packages are interbedded with transgressive shales in both Formations.

The lack of available cores necessitated use of correlation techniques such as INPEFA analysis by using 'CycloLog software'. The technique of generating INPEFA curve data, integrated with facies analysis of available cores, has been successfully applied to basin mapping. The INPEFA curves show that the Goldwyer Formation forms by transgressive systems tract (interval Or1000P), regressive

systems tract (interval Or2000) and a further transgressive systems tract (interval Or2000P) for the top Goldwyer. Interval Or1000P matches the Goldwyer lower shale (Goldwyer Unit 1 and Unit 2) with transgressive systems tract. Interval Or2000 matches the Goldwyer middle carbonate (Goldwyer Unit 3) with regressive systems tract. Interval Or2000P matches the Goldwyer upper shale (Goldwyer Unit 4) with transgressive systems tract and increasing relative sea-level. The Goldwyer Formation can be concluded as largely transgressive due to the fact that it forms by mostly transgressive systems tracts for the shale packages but is regressive for the shallow subtidal cyclic carbonate packages. INPEFA curves show that the Nita Formation forms by regressive systems tract, transgressive systems tract and regressive systems tract. Long-term (third order scale) evolution of the cyclicity packages through the Nita and Goldwyer Formations are three cycles of shallowing upwards from transgression to regression from larger scale cycles in the Goldwyer Formation and similar but thinner cycles in the Nita Formation. Willara Sub-basin (106.8Tcf), Mowla Terrace (83.9Tcf), Broome Platform (261.1Tcf) and Kidson Sub-basin (276.1Tcf) contain high values of the estimated maximum total gas in place while the Barbwire Terrace contains estimated maximum total gas in place of 32.5Tcf. Therefore, these tectonic sub-divisions could be an important potential area for shale gas exploration. The total gas in place that is estimated in these study areas ranges from 253.5-760.4Tcf (minimum 253.5Tcf, median 506.9Tcf, and maximum 760.4Tcf). The minimum value is comparable to the EIA (2011) estimate, the median value is almost twice the previous estimate, and the maximum value of 760.4Tcf is three times the EIA estimate. Shale gas in place (adsorbed gas) estimation was derived from INPEFA data (139-418 Tcf) and estimated total gas in place (253.5-760.4 Tcf) for the Goldwyer shales with significant 5% TOC value and 10% shale porosity reinforce the resource potential of the Ordovician strata for future shale gas exploration and production.

Llanvirnian relative sea-level fluctuations were reconstructed by using Fischer plots methodology for three key wells (wells McLarty 1, Looma 1 and Robert 1) in Broome Platform and compared with INPEFA data. The Goldwyer lower shale (interval Or1000P) shows increasing relative sea-level and this matches with a transgressive systems tract. Goldwyer middle carbonate (interval Or2000) shows relative sea-level drop and this matches with a regressive systems tract. Goldwyer

upper shale (interval Or2000P) shows relative sea-level drop and this matches with a transgressive systems tract. Nita Formation Leo Member (interval Or3000) shows a relative sea level drop and this matches with a regressive systems tract. The Nita Formation Cudalgarra Member (intervals Or3000P and Or4000) with transgressive systems tract then this is followed by a regressive systems tract. This pattern matches with the relative sea-level curves in wells McLarty 1 and Robert 1. The correlation is weak for parts of well Looma 1. This is probably influenced by the fact that the thickness of this section is quite small. As a conclusion, Fischer plots for the Llanvirnian Goldwyer and Nita Formations show good agreement with the third order global sea level cycles of Haq and others. Fischer plots are generally correlated well with trend and cyclicity determined by INPEFA curves and as a method of cross-checking INPEFA data and sea-level change.

# TABLE OF CONTENTS

<b>DECLARATION</b> .....	i
<b>COPYRIGHT DECLARATION</b> .....	ii
<b>ACKNOWLEDGEMENTS</b> .....	iii
<b>ABSTRACT</b> .....	iv
<b>TABLE OF CONTENTS</b> .....	viii
<b>LIST OF FIGURES</b> .....	xvi
<b>LIST OF TABLES</b> .....	xxxiii
<b>CHAPTER 1: INTRODUCTION</b> .....	<b>1</b>
<b>1.1 Overview of Canning Basin</b> .....	<b>1</b>
<b>1.2 Study areas</b> .....	<b>3</b>
<b>1.3 Ordovician Nita and Goldwyer Formations</b> .....	<b>4</b>
<b>1.4 Aims and objectives (present study)</b> .....	<b>10</b>
<b>1.5 Significance</b> .....	<b>11</b>
<b>1.6 Methods and techniques</b> .....	<b>11</b>
1.6.1 Sedimentary logging techniques.....	11
1.6.2 Thin section analysis.....	11
1.6.3 Cycle analysis.....	12
1.6.3.1 CycloLog® software-INPEFA curves.....	12
1.6.3.2 Gamma ray logs.....	14
1.6.3.3 Sonic logs.....	15
1.6.3.4 Spontaneous potential logs.....	15
1.6.3.5 Caliper logs.....	15
1.6.4 Fischer plots analysis.....	16
<b>1.7 Structure of the thesis</b> .....	<b>16</b>

<b>CHAPTER 2: REGIONAL GEOLOGICAL SETTING OF CANNING BASIN</b> .....	<b>18</b>
<b>2.1 Introduction</b> .....	<b>18</b>
<b>2.2 Geology of the Canning Basin</b> .....	<b>18</b>
<b>2.3 Petroleum exploration history</b> .....	<b>18</b>
<b>2.4 Basin evolution</b> .....	<b>20</b>
<b>2.5 Basin subdivision</b> .....	<b>22</b>
<b>2.6 Hydrocarbon potential</b> .....	<b>25</b>
2.6.1 Petroleum systems.....	25
2.6.2 Shale gas.....	26
2.6.2.1 Shale gas prospectivity in Western Australia.....	27
<b>CHAPTER 3: SEDIMENTARY LOGGING AND FACIES ANALYSIS FOR NITA AND GOLDWYER FORMATIONS, MIDDLE ORDOVICIAN</b> .....	<b>28</b>
<b>3.1 Introduction</b> .....	<b>28</b>
<b>3.2 Carbonate depositional environment</b> .....	<b>31</b>
<b>3.3 Results</b> .....	<b>32</b>
3.3.1 Well Looma 1 of the Broome Platform.....	32
3.3.1.1 Sediment log (well Looma 1).....	33
3.3.1.2 Microfacies associations for Looma 1.....	39
3.3.1.2.1 Microfacies 1 (S <sub>1</sub> ): Burrowed, fossiliferous mudstone/wackestone.....	39
3.3.1.2.2 Microfacies 2 (S <sub>2</sub> ): Oolitic/peloidal/intraclastic and bioclastic packstone/grainstone.....	42
3.3.1.2.3 Microfacies 3 (S <sub>3</sub> ): Interlaminated shale and wackestone/packstone.....	45
3.3.1.2.4 Microfacies 4 (S <sub>4</sub> ): Microbial laminites.....	46
3.3.1.2.5 Microfacies 5 (S <sub>5</sub> ): Evaporitic wackestone.....	47
3.3.1.2.6 Microfacies 6 (S <sub>6</sub> ): Terrestrial shale.....	52
3.3.1.3 Discussion (Well Looma 1).....	53
3.3.1.3.1 Depositional environment.....	53
3.3.2 Well Acacia 2 of the Barbwire Terrace.....	54
3.3.2.1 Sediment log (well Acacia 2).....	55
3.3.2.2 Microfacies associations for Acacia 2.....	56
3.3.2.2.1 Microfacies 1: Gastropod bioclastic burrowed wackestone.....	56

3.3.2.2.2 Microfacies 2: Oncoidal-peloidal packstone/floatstone with ooids and bioclasts.....	57
3.3.2.3 Discussion (Well Acacia 2) .....	62
3.3.3 Well Canopus 1 of the Mowla Terrace.....	63
3.3.3.1 Sediment log (well Canopus 1 with part of Leo Member).....	63
3.3.3.2 Microfacies associations for Canopus 1.....	64
3.3.3.2.1 Microfacies A: Weakly cemented burrowed mudstone with peloids and bioclasts .....	64
3.3.3.2.2 Microfacies B: Peloidal/intraclastic packstone/floatstone .....	68
3.3.3.3 Discussion (Well Canopus 1).....	73
3.3.4 Well Kunzea 1 of the Crossland Platform .....	74
3.3.4.1 Sediment log (Well Kunzea 1).....	74
3.3.4.2 Microfacies associations for Kunzea 1 .....	76
3.3.4.2.1 Microfacies I: Dolomitised mudstone (Depth 307.16m, Cudalgarra Member).....	76
3.3.4.2.2 Microfacies II: Bioclastic rudstone (Depth 317.6m, boundary at Leo Member and Cudalgarra Member).....	76
3.3.4.2.3 Microfacies III: Stylonodular burrowed wackestone (Depths 328.5m, 329.67m, 333.34m, 337.40m, 337.85m, 341.40m, 344.80m and 349.20m, Leo Member).....	77
3.3.4.2.3 Microfacies IV: Oncoidal-peloidal packstone/floatstone with ooids and bioclasts (Depth 356.26m, Goldwyer upper shale or Unit 4).....	81
3.3.4.3 Discussion (Well Kunzea 1).....	83
3.3.4.3.1 Goldwyer Formation Middle Carbonate (Unit 3).....	83
3.3.4.3.2 Goldwyer Formation Upper Shale (Unit 4).....	83
3.3.4.3.3 Nita Formation (Leo Member).....	83
3.3.4.3.4 Nita Formation (Cudalgarra Member).....	84
<b>3.4 Summary of core lithofacies and their stratigraphic occurrence.....</b>	<b>84</b>

<b>CHAPTER 4: SUBSURFACE CORRELATION OF NITA AND GOLDWYER FORMATIONS (MIDDLE ORDOVICIAN) IN PART OF THE CANNING BASIN, WA</b> .....	<b>86</b>
<b>4.1 Introduction</b> .....	<b>86</b>
<b>4.2 Climate stratigraphy</b> .....	<b>88</b>
<b>4.3 Global Cyclostratigraphy</b> .....	<b>88</b>
<b>4.4 Systems tracts</b> .....	<b>88</b>
4.4.1 Regressive systems tract (RST).....	89
4.4.2 Transgressive systems tract (TST).....	90
4.4.3 Maximum regressive surface/ Transgressive surface/Flooding surface (MRS).....	90
4.4.4 Maximum flooding surface/Maximum transgressive surface (MFS).....	91
4.4.5 Application of systems tract model in this study.....	91
<b>4.5 Results</b> .....	<b>95</b>
4.5.1 Broome Platform.....	95
4.5.1.1 Well McLarty 1.....	96
4.5.1.1.1 Interpretation for McLarty 1 (Figure 4.8).....	97
4.5.1.2 Well Looma 1.....	98
4.5.1.2.1 Interpretation for Looma 1 (Figure 4.9).....	99
4.5.1.2.2 Core to log correlation for Looma 1.....	99
4.5.1.3 Well Robert 1.....	100
4.5.1.3.1 Interpretation for Robert 1, Nita Formation and part of Goldwyer Formation (Figure 4.10).....	101
4.5.1.4 Well correlation of wells McLarty 1, Looma 1 and Robert 1 (Figure 4.11)..	101
4.5.1.5 Well Sharon Ann 1.....	103
4.5.1.5.1 Interpretation for Sharon Ann 1 (Figure 4.12).....	104
4.5.1.6 Well Goldwyer 1.....	105
4.5.1.6.1 Interpretation for Goldwyer 1 (Figure 4.13).....	106
4.5.1.7 Well Hedonia 1.....	107
4.5.1.7.1 Interpretation for Hedonia 1 (Figure 4.14).....	108
4.5.1.8 Well correlation of wells Sharon Ann 1, Goldwyer 1 and Hedonia 1 (Figure 4.15).....	108

4.5.2 Barbwire Terrace.....	110
4.5.2.1 Well Barbwire 1.....	111
4.5.2.1.1 Interpretation for Barbwire 1 (Figure 4.17).....	112
4.5.2.2 Well Dodonea 1.....	113
4.5.2.2.1 Interpretation for Dodonea 1 (Figure 4.18).....	114
4.5.2.3 Well Percival 1.....	115
4.5.2.3.1 Interpretation for Percival 1 (Figure 4.19).....	116
4.5.2.4 Well correlation of wells Barbwire 1, Dodonea 1 and Percival 1 (Figure 4.20).....	116
4.5.2.5 Well Setaria 1.....	118
4.5.2.5.1 Interpretation for Setaria 1 (Figure 4.21).....	119
4.5.2.6 Well Solanum 1.....	120
4.5.2.6.1 Interpretation for Solanum 1 (Figure 4.22).....	121
4.5.2.7 Well Acacia 2.....	122
4.5.2.7.1 Interpretation for Acacia 2 (Figure 4.23).....	123
4.5.2.7.2 Core to log correlation for Acacia 2.....	123
4.5.2.8 Well correlation of wells Setaria 1, Solanum 1, Acacia 2 and Barbwire 1 (Figure 4.24).....	124
4.5.3 Crossland Platform.....	126
4.5.3.1 Well Missing 1.....	127
4.5.3.1.1 Interpretation for Missing 1 (Figure 4.26).....	128
4.5.3.2 Well Santalum 1A.....	129
4.5.1.3.1 Interpretation for Santalum 1A, Nita Formation and part of Goldwyer Formation (Figure 4.27).....	130
4.5.3.3 Well Kunzea 1.....	131
4.5.3.3.1 Interpretation for Kunzea 1, Nita Formation and part of Goldwyer Formation (Figure 4.28).....	132
4.5.3.3.2 Core to log correlation for Kunzea 1.....	132
4.5.3.4 Well correlation of wells Missing 1, Santalum 1A and Kunzea 1 (Figure 4.29).....	132

4.5.4 Mowla Terrace.....	134
4.5.4.1 Well Crystal Creek 1.....	135
4.5.4.1.1 Interpretation for Crystal Creek 1 (Figure 4.31).....	136
4.5.4.2 Well Pictor 1.....	137
4.5.4.2.1 Interpretation for Pictor 1 (Figure 4.32).....	138
4.5.4.3 Well Canopus 1.....	139
4.5.4.3.1 Interpretation for Canopus 1 (Figure 4.33).....	140
4.5.4.3.2 Core to log correlation for Canopus 1.....	140
4.5.4.4 Well correlation for Crystal Creek 1, Pictor 1 and Canopus 1 (Figure 4.34).....	141
4.5.4.5 Well Matches Springs 1.....	143
4.5.4.5.1 Interpretation for Matches Springs 1, Nita Formation and part of Goldwyer Formation (Figure 4.35).....	144
4.5.4.6 Well correlation for Matches Springs 1 and Pictor 1 (Figure 4.36).....	145
4.5.5 Willara Sub-Basin.....	147
4.5.5.1 Well Willara 1.....	148
4.5.5.1.1 Interpretation for Willara 1 (Figure 4.38).....	149
4.5.5.2 Well Woods Hills 1.....	150
4.5.5.2.1 Interpretation for Woods Hills 1 (Figure 4.39).....	151
4.5.5.3 Well Munro 1.....	152
4.5.5.3.1 Interpretation for Munro 1 (Figure 4.40).....	153
4.5.5.4 Well correlation for Willara 1, Woods Hills 1 and Munro 1 (Figure 4.41).....	153
<b>4.6 Discussions.....</b>	<b>156</b>
4.6.1 Comparison between the previous lithofacies and INPEFA curve in the Goldwyer Formation.....	156
4.6.2 Comparison between the previous lithofacies and INPEFA curve in the Nita Formation.....	157
4.6.3 Application of Embry's transgressive-regressive model (2002) to components of INPEFA stratigraphy.....	157
<b>4.7 Summary.....</b>	<b>159</b>

<b>CHAPTER 5: SHALE GAS PROSPECTIVITY OF GOLDWYER FORMATION IN CANNING BASIN</b> .....	<b>161</b>
<b>5.1 Introduction</b> .....	161
<b>5.2 Middle Ordovician Goldwyer Formation as shale gas resource</b> .....	162
<b>5.3 Results</b> .....	164
5.3.1 Section A-A' (yellow line) (Figures 5.3, 5.4 and Table 5.2).....	166
5.3.2 Section B-B' (Green line) (Figures 5.5, 5.6 and Table 5.3).....	167
5.3.3 Section C-C' (Red line) (Figures 5.7, 5.8 and Table 5.4).....	168
5.3.4 Section D-D' (Orange line) (Figures 5.9, 5.10 and Table 5.5).....	169
5.3.5 Section E-E' (Dark blue line) (Figures 5.11, 5.12 and Table 5.6).....	169
5.3.6 Section F-F' (Purple line) (Figures 5.13, 5.14 and Table 5.7).....	170
5.3.7 Section G-G' (Brown line) (Figures 5.15, 5.16 and Table 5.8).....	171
5.3.8 Section H-H' (Grey line) (Figures 5.17, 5.18 and Table 5.9).....	171
<b>5.4 Discussion</b> .....	197
<b>5.5 Isopach maps</b> .....	197
5.5.1 Isopach map of the top Goldwyer Formation.....	198
5.5.2 Isopach map of the total Goldwyer shale thicknesses.....	200
<b>5.6 Estimation resource</b> .....	202
<b>5.7 Summary</b> .....	204
<b>CHAPTER 6: MIDDLE ORDOVICIAN (LLANVIRNIAN) RELATIVE SEA-LEVEL FLUCTUATIONS</b> .....	<b>206</b>
<b>6.1 Introduction</b> .....	206
<b>6.2 Middle Ordovician sea-level</b> .....	208
<b>6.3 Parasequences stacking patterns and Fischer plots</b> .....	208
<b>6.4 Sea-level fluctuations</b> .....	210
6.4.1 Fischer plots for well Looma 1.....	213
6.4.1.1 Interpretation for Looma 1.....	213
6.4.2 Fischer plots for well McLarty 1.....	214
6.4.2.1 Interpretation for McLarty 1.....	214
6.4.3 Fischer plots for well Robert 1.....	215

6.4.3.1 Interpretation for Robert 1.....	215
<b>6.5 Relationship of systems tracts with relative sea-level curves.....</b>	<b>216</b>
<b>6.6 Comparison of Middle to Late Llanvirnian age relative sea-level curves.....</b>	<b>221</b>
<b>6.7 Summary.....</b>	<b>222</b>
<b>CHAPTER 7: CONCLUSIONS.....</b>	<b>223</b>
<b>7.1 Conclusions of this study.....</b>	<b>223</b>
<b>7.2 Recommendations for future research.....</b>	<b>227</b>
<b>REFERENCES.....</b>	<b>228</b>
<b>APPENDIX 1: Core photos generated by TSG software.....</b>	<b>241</b>
<b>APPENDIX 2: List of well completion reports.....</b>	<b>268</b>
<b>APPENDIX 3: Fischer plots calculation.....</b>	<b>271</b>

## LIST OF FIGURES

### CHAPTER 1

- Figure 1.1: Location map of Canning Basin. ....2
- Figure 1.2: The location map of the study areas in Canning Basin, WA. ....3
- Figure 1.3: The generalised stratigraphy of the Canning Basin (After Brown et al., 1984). Note stratigraphic position of Nita and Goldwyer Formation. ....5
- Figure 1.4: The stratigraphic subdivision from Ordovician to Silurian period of Canning Basin (after Jones et al. (1998) and Haines (2004)). ....6
- Figure 1.5: Tectonic setting of Western Australia’s sedimentary basins in early Ordovician period (after Baillie et al., 1994). ....9
- Figure 1.6: The oil and gas shows for Ordovician- Silurian successions in Canning Basin, WA (after Haines and Ghori, 2006). ....9

### CHAPTER 2

- Figure 2.1: Basin evolution of Canning Basin (After Middleton, 1990). Note the increasing tectonic disturbance of parts of the initial Ordovician sag basin through time and also tectono-stratigraphic domains and sub-basins developed. ....21
- Figure 2.2: Principal structural elements of the Canning Basin (After Tyler and Hocking, 2001; Haines, 2004). ....23
- Figure 2.3: Cross–sections of Canning Basin’s sub-basins, terraces and deep depocentre (after Yeates et al., 1984; Ghori, 2013). ....24

### CHAPTER 3

- Figure 3.1: The location map of the study wells in Canning Basin, WA. ....28
- Figure 3.2: The settings of carbonate depositional environments (Flüger, 2010). ....31
- Figure 3.3: Legend for the graphic logs of selected drillcore for the Nita and Goldwyer Formations. ....32
- Figure 3.4: Sketch shows the logged interval from part 1 to part 5 for the following pages here for well Looma 1. The Nita Leo Member was logged from 1275.5-1350.0m while the Cudalgarra Member was logged from 1259.0-1275.5m.

Note that the available core of well Looma 1 does not cover the complete Nita Formation. ....	33
Figure 3.5: Sediment log of well Looma 1, part 1 from depth 1333.8m to 1350.0 m. Depositional environments and microfacies of the Leo Member, Nita Formation. Mineralogical composition was checked and determined by using TSG-core software. For legend see Figure 3.3. ....	34
Figure 3.6: Sediment log of well Looma 1, part 2 from depth 1313.9m to 1333.8m. Depositional environments and microfacies of the Leo Member, Nita Formation. Mineralogical composition was checked and determined by using TSG-core software. For legend see Figure 3.3. ....	35
Figure 3.7: Sediment log of well Looma 1, part 3 from depth 1295.0m to 1313.9m. Depositional environments and microfacies of the Leo Member, Nita Formation. Mineralogical composition was checked and determined by using TSG-core software. For legend see Figure 3.3. ....	36
Figure 3.8: Sediment log of well Looma 1, part 4 from depth 1276.4m to 1295.0m. Depositional environments and microfacies of the Leo Member, Nita Formation. Mineralogical composition was checked and determined by using TSG-core software. For legend see Figure 3.3. ....	37
Figure 3.9: Sediment log of well Looma 1, part 5 from depth 1259.0m to 1276.4m. Depositional environments and microfacies of the Leo Member, Nita Formation. Mineralogical composition was checked and determined by using TSG-core software. For legend see Figure 3.3. ....	38
Figure 3.10: <b>A.</b> Core photo of depth 1348.8m for microfacies S <sub>1</sub> : burrowed, fossiliferous lime mudstone/ wackestone, well Looma 1. <b>B.</b> Photomicrograph of microfacies S <sub>1</sub> : burrowed, fossiliferous lime mudstone/ wackestone for well Looma 1. ( <b>B:</b> scale bar (bottom right) = 1mm) <b>C.</b> Detail of part of dolomitised burrow-fill shown in <b>B.</b> Note rhombic dolomite crystals. ( <b>C:</b> scale bar (bottom right) = 1mm). ....	40
Figure 3.11: <b>A.</b> Core photo of depth 1310.6m, for microfacies S <sub>1</sub> : burrowed, fossiliferous lime mudstone/ wackestone, well Looma 1, showing wispy lamination and wackestone fabric. <b>B.</b> Shale seam (S), 1310.6m, PPL, scale bar = 1mm. <b>C.</b> Recrystallized bivalve (I), stylolites (Sty) and s (S), 1310.6m, PPL, scale bar = 1mm. For location of section see Fig 3.7. ....	41
Figure 3.12: Core photos of microfacies S <sub>2</sub> : Oolitic/peloidal/intraclastic and bioclastic packstone/grainstone for well Looma 1. <b>A.</b> Packstone/grainstone fabric at 1317.81m. <b>B.</b> Packstone/grainstone fabric at 1291.51m. ....	43
Figure 3.13: Photomicrograph of microfacies S <sub>2</sub> : Oolitic/peloidal/intraclastic and bioclastic packstone/grainstone from A to F for well Looma 1, showing	

constituents and fabrics. **A.** A brachiopod wall (A), recrystallised bivalve (I) and peloid (P). 1317.81m, PPL, scale bar = 0.1mm. **B.** Bryozoans (B), crinoids (C), peloid (P), brachiopod (B) and ooid (O). 1317.81m, PPL, scale bar = 1mm. **C.** Bryozoan (B) and trilobite (T). 1317.81m, PPL, scale bar = 0.1mm. **D.** Bivalve (I), brachiopod (A), crinoid (C), ooid (O), peloid (P) and pellet (Pe). 1291.51m, PPL, scale bar = 1mm. **E.** Nautiloid (N) and intraclast (Int). 1291.51m, PPL, scale bar = 1mm. **F.** Brachiopod (A) and crinoids (C). 1291.51m, PPL, scale bar (at bottom right) = 1mm. ....44

Figure 3.14: Core photos of microfacies S<sub>3</sub>: Shows mixing between microfacies. **A.** Depth 1334.754-1334.801m. **B.** Depth 1316.926-1316.973m. **C.** 1299.643-1299.69m. Note the interlaminated character of this muddy low energy microfacies, shale/wackestone packstone. Shale laminae are dark, carbonate are light coloured. ....45

Figure 3.15: Core photos of microfacies S<sub>4</sub>: microbial laminites. **A.** Depth 1261-1261.137m. **B.** 1261.184-1261.231m. Note well developed laminar fabric with only small disturbance by burrowers. ....46

Figure 3.16: **A.** Core photo of depth 1289.8m, well Looma 1. **B and C.** Photomicrographs of microfacies S<sub>5</sub>: Evaporitic wackestone. Note the anhydrite crystals with different colours in **C**. 1289.8m, **B** is PPL and **C** is XPL, scale bar (at bottom right) = 1mm. ....48

Figure 3.17: **A.** Core photo of depth 1275.9m, well Looma 1. **B-E:** Photomicrographic of microfacies S<sub>5</sub>: Evaporitic wackestone. **B:** Crinoid/Pelmatozoan arm plate (**C**). **C and D:** Note the anhydrite crystal (**A**) with different colour in **D** and bivalve (**B**). **E:** Burrows (Bu). 1275.9m, **B, C and E** is PPL; **D** is XPL; scale bar (at bottom right) = 1mm. ....49

Figure 3.18: **A.** Core photo of depth 1277.9m, well Looma 1, for microfacies S<sub>5</sub>: Evaporitic wackestone. Note that the white colour dots are anhydrite nodules. **B-E:** Photomicrographic of microfacies S<sub>5</sub>: Evaporitic wackestone. **B and C:** Note the anhydrite crystal with different colour in **C**. **D and E:** Note the bivalve fragment has dissolved and created a secondary porosity. 1277.9m, **B and D** are PPL and **C and E** are XPL, scale bar (at bottom right) = 1mm. ...50

Figure 3.19: **A.** Core photo of depth 1262.5m, well Looma 1 for microfacies S<sub>5</sub>: Evaporitic wackestone. **B and C:** Photomicrographic of microfacies S<sub>5</sub>: Evaporitic wackestone. **B and C:** Note the anhydrite crystal with different colour in **C**. 1262.5m, **B** is PPL and **C** is XPL, scale bar (at bottom right) = 1mm. ....51

Figure 3.20: **A.** Core photo of 1259.5m, well Looma 1. Note that probable root material (black colour) is present. **B and C:** Oil stained recrystallised mudstone. 1259.5m, PPL, scale bar (at bottom right) = 1mm. ....52

- Figure 3.21: Sediment log of well Acacia 2, part of Goldwyer Formation Unit 3. Burrowed wackestones alternate with peloidal packstone/floatstone in metre to decimetre scale units representing upward coarsening cycles. Legend of this sediment log is in Figure 3.3. ....55
- Figure 3.22: An example of microfacies gastropod bioclastic burrowed wackestone at depth 840.54m. Note the burrows and wispy lamination in this microfacies. ....56
- Figure 3.23: An example of microfacies oncoidal-peloidal packstone/floatstone at depth 847.324m. Note the oncoidals and peloids in this microfacies at depth 847.324m show the packstone/floatstone fabric. ....57
- Figure 3.24: An example of microfacies oncoidal-peloidal packstone/floatstone at depth 847.324m. Note the buff to dark colour of this section is due to the presence of iron. ....58
- Figure 3.25: Photomicrograph of microfacies peloidal packstone/floatstone with ooids and bioclasts. Peloids dominate this microfacies in this section. Peloids and oolites shows packstone fabric while intraclast with >2mm shows floatstone fabric. 840.52m, PPL, scale bar (at bottom right) = 1mm. ....58
- Figure 3.26: Photomicrograph of microfacies peloidal packstone/floatstone with ooids and bioclasts. Note that ooid was filled with dolomitised grains in the centre part. 840.52m, PPL, scale bar (at bottom right) = 0.1mm. ....59
- Figure 3.27: Photomicrograph of microfacies peloidal packstone/floatstone with ooids and bioclasts. Brachiopod in floatstone facies. This is an example of an impunctate shell wall in the brachiopod *Platystropha cypha*. This shell has an extremely thin primary layer and a thick secondary layer. Note the typical low-angle fibrous structure and the substantial lateral variations in shell thickness. 847.39m, PPL, scale bar (at bottom right) = 0.1mm. ....59
- Figure 3.28: Photomicrograph of microfacies peloidal packstone/floatstone with ooids and bioclasts. Note the oncoids in the centre part, ooid at top right and crinoids/pelmatozoan at bottom right. 847.39m, PPL, scale bar (at bottom right) = 0.1mm. ....60
- Figure 3.29: Photomicrograph of microfacies peloidal packstone/floatstone with ooids and bioclasts. Green algae and peloids are in top part. *Codiacean* (green algae) are common in warm shallow seas with good light penetration. 852.16m, PPL, scale bar (at bottom right) = 1mm. ....60
- Figure 3.30: Photomicrograph of microfacies peloidal packstone/floatstone with ooids and bioclasts. Gastropod at middle right is surrounded by peloids and pellets. This gastropod shell still is recognizable by shape; most of this original gastropod shell was dissolved and was later filled with peloids and pellets.

This is the norm for most gastropod remains and in the absence of diagnostic shell shapes it would be impossible to differentiate from leached neomorphosed remains of other organisms (bivalves or algae etc.). Facies is gastropod – peloidal mud – dominated, of shallow subtidal origin. 852.16m, PPL, scale bar (at bottom right) = 0.1mm. ....61

Figure 3.31: Photomicrograph of microfacies peloidal packstone/floatstone with ooids and bioclasts. Trilobite in floatstone facies (bedding is top left to bottom right). This trilobite fragment shows characteristic complex curvature of the shell and homogenous prismatic shell structure. Same view but under cross-polarized light is shown on the right. Note the characteristic dark extinction bands at the centre and left of the grain. As the grain is rotated under cross-polarized light, the extinction bands sweep through the entire grain. Note presence of ooids and peloids shows packstone fabric. 852.16m, PPL on left and XPL on right, scale bar (at bottom right) = 1mm. ....61

Figure 3.32: Sediment log of well Canopus 1, part of Nita Formation Leo Member. The burrowed wackestones are capped by thin packstone/floatstone intervals in the cycles. For legend see Figure 3.3. ....63

Figure 3.33: An example of microfacies weakly cemented burrowed mudstone with peloids and bioclast at depth 1148.56-1148.61m. Note the presence of peloids at depth 1148.595m. Dark colour of this microfacies confirmed the mudstone fabric. ....64

Figure 3.34: An example of microfacies weakly cemented burrowed mudstone with peloids and bioclasts at depth 1154.66-1154.72m. Note the abundance of dolomitised filled burrows. ....65

Figure 3.35: Photomicrograph of microfacies weakly cemented burrowed mudstone with peloids and bioclasts. Note the weakly cemented dolomitised mudstone. 1148.56-1148.61m, PPL, scale bar (at bottom right) = 1mm. ....65

Figure 3.36: Photomicrograph of microfacies weakly cemented burrowed mudstone with peloids and bioclasts. Note the red colour lime mudstone. The red colour is limestone while the grey colour is dolostone. 1148.79-1148.85m, PPL, scale bar (at bottom right) = 1mm. ....66

Figure 3.37: Photomicrograph of microfacies weakly cemented burrowed mudstone with peloids and bioclast. Note the brown colour mudstone. A burrow is shown at top right. White colour bivalves also present. The red colour is limestone while the grey colour is dolostone. 1154.66-1154.72m, PPL, scale bar (at bottom right) = 1mm. ....66

Figure 3.38: Photomicrograph of microfacies weakly cemented burrowed mudstone with peloids and bioclasts. Note the red colour lime mudstone. The red colour

- is limestone. Occasional shell fragments (white) are present. 1154.80m, PPL, scale bar (at bottom right) = 1mm. ....67
- Figure 3.39: Photomicrograph of microfacies weakly cemented burrowed mudstone with peloids and bioclast. Note the brown colour mudstone in the top part. Pellets filled in fossils are found at bottom right. Pelmatozoan/crinoids are at the top left. 1155.66-1155.69m, PPL, scale bar (at bottom right) = 1mm. ...67
- Figure 3.40: Photomicrograph of microfacies weakly cemented burrowed mudstone with peloids and bioclasts. Note the brown colour mudstone. Grey colour dolomite grains filled in the burrows. The red colour is limestone while the grey colour is dolostone. 1156.32-1156.37m, PPL, scale bar (at bottom right) = 1mm. ....68
- Figure 3.41: An example of microfacies peloidal/intraclastic packstone/floatstone at depth 1148.4-1148.45m. Note the presence of intraclasts at depth 1148.407m shows the packstone/floatstone fabric. ....69
- Figure 3.42: An example of microfacies peloidal/intraclastic packstone/floatstone at depth 1150.79-1150.84m. Note the fabric of packstone/floatstone at depth 1150.802m. ....69
- Figure 3.43: Photomicrograph of microfacies peloidal/intraclastic packstone/floatstone. Note the bivalves >2mm show floatstone matrix while the peloids and ooids which are dolomitised and filled in the middle are found at bottom left and show packstone matrix. The red colour is limestone while the grey colour is dolostone. 1148.35m, PPL, scale bar (at bottom right) = 1mm. ....70
- Figure 3.44: Photomicrograph of microfacies peloidal/intraclastic packstone/floatstone. Note the peloids and intraclasts show the packstone/floatstone fabric. The peloids form around a shell fragment (possibly brachiopod wall). They can be found quite typically in shallow-to-outer-shelf settings (Scholle and Ulmer-Scholle, 2003). 1148.4-1148.45m, PPL, scale bar (at bottom right) = 1mm. ....70
- Figure 3.45: Photomicrograph of microfacies peloidal/intraclastic packstone/floatstone. Note the bivalves >2mm show floatstone matrix and crinoids/pelmatozoan arm plate is at top right. The red colour is limestone while the grey colour is dolostone. 1149.60-1149.66m, PPL, scale bar (at bottom right) = 1mm. ....71
- Figure 3.46: Photomicrograph of microfacies peloidal/intraclastic packstone/floatstone. Note the brachiopod and peloids encrustations around pelmatozoan/crinoid in the middle part. The red colour is limestone while the grey colour is dolostone. 1150.79-1150.84m, PPL, scale bar (at bottom right) = 1mm. ....71

- Figure 3.47: Photomicrograph of microfacies peloidal/intraclastic packstone/floatstone. Note the bivalves >2mm show floatstone matrix. 1151.95-1152.0m, PPL, scale bar (at bottom right) = 1mm. ....72
- Figure 3.48: Photomicrograph of microfacies peloidal/intraclastic packstone/floatstone. Note the trilobite >2mm at top left show floatstone matrix. 1152.60-1152.66m, PPL, scale bar (at bottom right) = 1mm. ....72
- Figure 3.49: Photomicrograph of microfacies peloidal/intraclastic packstone/floatstone. Note the recrystallised fossil fragments >2mm showing floatstone fabric. 1153.92-1153.97m, PPL, scale bar (at bottom right) = 1mm. ....73
- Figure 3.50: Sediment log of well Kunzea 1 covers complete Nita Formation, Goldwyer Unit 3 and Goldwyer Unit 4. The burrowed wackestones are capped by thin packstone/floatstone intervals in the cycles of part of the Nita Leo Member based on the thin section analysis in this study (Grain size and sedimentary structures after Haines (2004)). For legend see Figure 3.3. ....75
- Figure 3.51: Photomicrograph of microfacies dolomitised mudstone. Note the horizontal lamination shows the low energy condition of the mudstone. 307.16m, PPL, scale bar (at bottom right) = 1mm. ....76
- Figure 3.52: Photomicrograph of microfacies bioclastic rudstone. Note the contact of grains (pelmatozoan/crinoids, ooid and dolomite grains) show the rudstone fabric. The red colour is limestone while the grey colour is dolostone. 317.6m, PPL, scale bar (at bottom right) = 1mm. ....76
- Figure 3.53: Photomicrograph of microfacies stylonodular burrowed wackestone. Note the dolomitised-filled burrows are at the bottom right. The fossil fragments up to 25% show a wackestone fabric. The red colour is limestone while the grey colour is dolostone. 328.5m, PPL, scale bar (at bottom right) = 1mm. ....77
- Figure 3.54: Photomicrograph of microfacies stylonodular burrowed wackestone. The prominent boundary is between wackestone (red) and dolomitised dilled burrow (grey). The fossil fragments in red colour limestone of 25% show a wackestone fabric. The red colour is limestone while the grey colour is dolostone. 329.67m, PPL, scale bar (at bottom right) = 1mm. ....77
- Figure 3.55: Photomicrograph of microfacies stylonodular burrowed wackestone. Note brachiopods are at the central part in a thin bioclastic horizon (storm lag). Bedding is lower left to top right. The red colour is limestone while the grey colour is dolostone. 333.34m, PPL, scale bar (at bottom right) = 1mm. ....78
- Figure 3.56: Photomicrograph of microfacies stylonodular burrowed wackestone. Note the crinoids/pelmatozoan arm plate is at the central part with red colour.

- The bioclastic horizon in burrowed wackestone probably represents storm lags deposited during period of lowered wave-base. The red colour is limestone while the grey colour is dolostone. 337.40m, PPL, scale bar (at bottom right) = 1mm. ....78
- Figure 3.57: Photomicrograph of microfacies stylonodular burrowed wackestone. Note the brachiopods followed by trilobites from lower right to top left margin, present as a thin bioclastic storm lag (millimetre to decimetre scale). The red colour is limestone while the grey colour is dolostone. 337.85m, PPL, scale bar (at bottom right) = 1mm. ....79
- Figure 3.58: Photomicrograph of microfacies stylonodular burrowed wackestone. Note the red colour limestone is probably a middle part of two dolomitised-filled burrows. The red colour is limestone while the grey colour is dolostone. 341.40m, PPL, scale bar (at bottom right) = 1mm. ....79
- Figure 3.59: Photomicrograph of microfacies stylonodular burrowed wackestone. Note the gastropods and trilobites at the middle part, present as a thin bioclastic storm lag. Bedding is lower right to top left. The red colour is limestone while the grey colour is dolostone. 344.80m, PPL, scale bar (at bottom right) = 1mm. ....80
- Figure 3.60: Photomicrograph of microfacies stylonodular burrowed wackestone. Note the bryozoans and pelmatozoan/crinoids are in an oriented layer most likely represents a storm lag. The red colour is limestone while the grey colour is dolostone. 349.20m, PPL, scale bar (at bottom right) = 1mm. ....80
- Figure 3.61: Photomicrograph of microfacies oncoidal-peloidal packstone/ floatstone with ooids and bioclasts. Note the brachiopod shell at the middle part and peloids at the bottom part. The red colour is limestone while the grey colour is dolostone. 356.26m, PPL, scale bar (at bottom right) = 1mm. ....81
- Figure 3.62: Photomicrograph of microfacies oncoidal-peloidal packstone/ floatstone with ooids and bioclasts. Note the presence of pelmatozoan/crinoids, oncoids and ooids in this microfacies. The red colour is limestone while the grey colour is dolostone. 356.26m, PPL, scale bar (at bottom right) = 1mm. ....81
- Figure 3.63: Photomicrograph of microfacies oncoidal-peloidal packstone/ floatstone with ooids and bioclasts. Note the bivalves >2mm along the left side show floatstone fabric while peloids, ooids and pellets show packstone fabric. The red colour is limestone while the grey colour is dolostone. 356.26m, PPL, scale bar (at bottom right) = 1mm. ....82
- Figure 3.64: Photomicrographic for microfacies stromatolite boundstone. Note the overgrowth stromatolite along the centre part with the white colour crystals like dog tooth spar. 404.6m, PPL, scale bar (at bottom right) = 1mm. ....82

## CHAPTER 4

- Figure 4.1: Schematic overview the principal tools within the stratigraphic toolkit (Doyle and Bennet, 1998; ENRES International, 2011). .....87
- Figure: 4.2: The material-based two systems tracts defined by Embry (1993). The occurrence of the low diachroneity maximum flooding surface (MFS) allows the sequence to be subdivided into two systems tracts – TST and RST, (Embry, 2009). .....89
- Figure 4.3: The maximum regressive surfaces (MRS) have been delineated in this subsurface succession of Jurassic strata from the Loughheed Island area (Embry, 2009). .....91
- Figure 4.4: Summary of various systems tract classification schemes that have been proposed. The sequence boundaries are in red and internal systems tract boundaries are in blue (Embry, 2009). .....93
- Figure 4.5: Application of Embry’s models (1993) to components of INPEFA stratigraphy including the stratigraphic packages. ....93
- Figure 4.6: Terminology and definitions associated with the interpretation of INPEFA curves (after ENRES International, 2011). A negative bounding surface (NBS) is a point at which the trends changes from positive (P-Trend) to negative (N-Trend). A positive bounding surface (PBS) is the point at which trend changes from negative to positive. There are 15 classes of colour in colour gamma ray log, where red, orange and yellow represent low gamma ray value while blue and green represent higher gamma ray value. ....94
- Figure 4.7: Location maps of wells Sharon Ann 1, Goldwyer 1, Hedonia 1, McLarty 1, Looma 1 and Robert 1 in Broome Platform, Canning Basin, WA. ....95
- Figure 4.8: Well composite chart of well McLarty 1 with interpreted stratigraphic packages using the INPEFA curves. Note the Goldwyer Formation is complete here but only the lower part of the Nita Formation is covered. There are 15 classes of colour in colour gamma ray log, where red, orange and yellow represent low gamma ray value while blue and green represent higher gamma ray value. For the lithology log, green colour represents shale and purple colour represents limestone. ....96
- Figure 4.9: Well composite chart of well Looma 1 with interpreted stratigraphic packages using the INPEFA curves. Well Looma 1 covered the complete Nita and Goldwyer Formations. Note that logged cored section is from 1259-1350m (see Figures 3.4-3.8). Colours are described in Figure 4.8. ....98
- Figure 4.10: Well composite chart of well Robert 1 with interpreted stratigraphic packages using the INPEFA curves. Note the Nita Formation is complete here

but only part of the Goldwyer Formation (Goldwyer upper shale and part of the Goldwyer middle carbonate) only is covered due to the well total depth being reached. Colours are described in Figure 4.8. ....100

Figure 4.11: Well-to-well correlation of the INPEFA curves of wells McLarty 1, Looma 1 and Robert 1 on the Broome Platform, showing the subdivision of the Nita and Goldwyer formations (Or1000P: Goldwyer lower shale (Transgression); Or2000: Goldwyer middle limestone (Regression); Or2000P: Goldwyer upper shale (Transgression); Or3000: Leo Member (Regression); Or3000P: Cudalgarra Member part 1 (Transgression); and, Or4000: Cudalgarra part 2 (Regression)). ....102

Figure 4.12: Well composite chart of well Sharon Ann 1 with interpreted stratigraphic packages using the INPEFA curves. Note the Goldwyer Formation is complete here but only part of the Nita Formation (part of Nita Leo Member) is covered due to the erosion by the Permian Grant Group. Colours are described in Figure 4.8. ....103

Figure 4.13: Well composite chart of well Goldwyer 1 with interpreted stratigraphic packages using the INPEFA curves. Note the upper part of the Goldwyer Formation (Goldwyer upper shale) is partly eroded by Permian Grant Group; this erosion process is a reason of the absence of Nita Formation. Colours are described in Figure 4.8. ....105

Figure 4.14: Well composite chart of well Hedonia 1 with interpreted stratigraphic packages using the INPEFA curves. Note the Permian Grant Group eroded the Nita and Goldwyer Formations and left only part of the Goldwyer lower shale. The Goldwyer Formation overlies conformably on top of the Willara Formation. Colours are described in Figure 4.8. ....107

Figure 4.15: Well-to-well correlation of the INPEFA curves of wells Sharon Ann 1, Goldwyer 1 and Hedonia 1 on the Broome Platform, well Sharon Ann 1 shows the subdivision of the Nita and Goldwyer Formations (Or1000P: Goldwyer lower shale (Transgression); Or2000: Goldwyer middle limestone (Regression); Or2000P: Goldwyer upper shale (Transgression); Or3000: Leo Member (Regression)). Note that Nita Cudalgarra Member (intervals Or3000P and Or 4000) is absence due to the erosion by Permian Grant Group. Due to this erosion process, well Goldwyer 1 consists of intervals Or1000P, Or2000 and Or2000P while well Hedonia 1 only consists of interval Or1000P. ....109

Figure 4.16: Location maps of wells Acacia 2, Barbwire 1, Dodonea 1, Percival 1, Setaria 1 and Solanum 1 in Barbwire Terrace, Canning Basin, WA. ....110

- Figure 4.17: Well composite chart of well Barbwire 1 with interpreted stratigraphic packages using the INPEFA curves. Note the Goldwyer Formation is complete here but only part of the Nita Formation (part of Nita Leo Member) is covered due to either the erosion by Pegasus Dolomite Member or the formation pinched out. Colours are described in Figure 4.8. ....111
- Figure 4.18: Well composite chart of well Dodonea 1 with interpreted stratigraphic packages using the INPEFA curves. Note the upper part of the Goldwyer Formation (Goldwyer upper shale) is partly eroded by Pegasus Dolomite Member in Carribuddy Group; this erosion process might be a reason for the absence of Nita Formation. Colours are described in Figure 4.8. ....113
- Figure 4.19: Well composite chart of well Percival 1 with interpreted stratigraphic packages using the INPEFA curves. Note the Goldwyer Formation is complete here and major part of the Nita Formation is covered. Colours are described in Figure 4.8. ....115
- Figure 4.20: Well-to-well correlation of the INPEFA curves of wells Barbwire 1, Dodonea 1 and Percival 1 on the Barbwire Terrace. Well Barbwire 1 shows the subdivision of the Nita and Goldwyer Formations (Or1000P: Goldwyer lower shale (Transgression); Or2000: Goldwyer middle limestone (Regression); Or2000P: Goldwyer upper shale (Transgression); Or3000: Leo Member (Regression) and well Dodonea 1 consists of intervals Or1000P, Or2000 and Or2000P. Note that Nita Formation is thinning from well Barbwire 1 to well Dodonea 1. The Nita Formation is either eroded by Pegasus Dolomite Member or died out from well Barbwire 1 towards well Dodonea 1. However, Nita Formation (Leo Member and Cudalgarra Member part 1) can be found in well Percival 1. This is probably due to the Barbwire Terrace which is essentially divided into the northern Barbwire High and southern Percival High (France, 1986). ....117
- Figure 4.21: Well composite chart of well Setaria 1 with interpreted stratigraphic packages using the INPEFA curves. Note the the top of Goldwyer Formation Unit 3 (Goldwyer middle carbonate) is eroded by the Permian glaciations events; this erosion process might be a reason for the absence of Nita Formation. Colours are described in Figure 4.8. ....118
- Figure 4.22: Well composite chart of well Solanum 1 with interpreted stratigraphic packages using the INPEFA curves. Well Solanum 1 covered the complete Nita and Goldwyer Formations. Colours are described in Figure 4.8. ....120
- Figure 4.23: Well composite chart for well Acacia 2 with interpreted stratigraphic packages using the INPEFA curves. Well Acacia 2 covered the complete Nita and Goldwyer Formations. Note that logged cored section is from 837-

855.12m which shows stacked and thin subtidal carbonate cycles (see Figures 3.21). Colours are described in Figure 4.8. ....122

Figure 4.24: Well-to-well correlation of the INPEFA curves of wells Setaria 1, Solanum 1, Acacia 2 and Barbwire 1 on the Barbwire Terrace, wells Solanum 1 and Acacia 2 show the complete subdivision of the Nita and Goldwyer Formations (Or1000P1: Goldwyer Unit 1 (Transgression); Or1000P2: Goldwyer Unit 2 (Transgression); Or2000: Goldwyer middle limestone (Regression); Or2000P: Goldwyer upper shale (Transgression); Or3000: Leo Member (Regression); Or3000P: Cudalgarra Member part 1 (Transgression); Or4000: Cudalgarra Member part 2 (Regression)). Note that Nita Formation and Goldwyer Unit 4 are eroded by the Permian Grant Group in well Setaria 1. In well Barbwire 1, Nita Formation Cudalgarra Member is absent; this is probably due to the erosion by Pegasus Dolomite Member or pinches out. ....125

Figure 4.25: Location maps of wells Missing 1, Santalum 1A and Kunzea 1 in Crossland Platform, Canning Basin, WA. ....126

Figure 4.26: Well composite chart of well Missing 1 with interpreted stratigraphic packages using the INPEFA curves. Well Missing 1 covered the complete Nita and Goldwyer Formations. Colours are described in Figure 4.8. ....127

Figure 4.27: Well composite chart of well Santalum 1A with interpreted stratigraphic packages using the INPEFA curves. Note the Nita Formation is complete here but the lower part of the Goldwyer lower shale is not covered due to the well total depth being reached. Colours are described in Figure 4.8. ....129

Figure 4.28: Well composite chart of well Kunzea 1 with interpreted stratigraphic packages using the INPEFA curves. Note the Nita Formation is complete here but only part of the Goldwyer Formation (Goldwyer upper shale and part of the Goldwyer middle carbonate) is covered due to the well total depth being reached. Note that logged cored section is investigated from approximately 292-450m (see Figures 3.50). Colours are described in Figure 4.8. ....131

Figure 4.29: Well-to-well correlation of the INPEFA curves of wells Missing 1, Santalum 1A and Kunzea 1 on the Crossland Platform, well Missing 1 shows the complete subdivision of the Nita and Goldwyer Formations (Or1000P: Goldwyer lower shale (Transgression); Or2000: Goldwyer middle carbonate (Regression); Or2000P: Goldwyer upper shale (Transgression); Or3000: Leo Member (Regression); Or3000P: Cudalgarra Member part 1 (Transgression); Or4000: Cudalgarra Member part 2 (Regression)). Note that Goldwyer Formation lower shale reaches the well total depth in well Santalum 1A. In

well Kunzea 1, Goldwyer middle carbonate reaches the well total depth. The wells are correlated from west to east on the Crossland Platform. ....	131
Figure 4.30: Location maps of wells Crystal Creek 1, Pictor 1, Canopus 1 and Matches Springs 1 in Mowla Terrace, Canning Basin, WA. ....	134
Figure 4.31: Well composite chart of well Crystal Creek 1 with interpreted stratigraphic packages using the INPEFA curves. Well Crystal Creek 1 covered the complete Nita and Goldwyer Formations. Colours are described in Figure 4.8. ....	135
Figure 4.32: Well composite chart of well Pictor 1 with interpreted stratigraphic packages using the INPEFA curves. Well Pictor 1 covered the complete Nita and Goldwyer Formations. Colours are described in Figure 4.8. ....	137
Figure 4.33: Well composite chart of well Canopus 1 with interpreted stratigraphic packages using the INPEFA curves. Well Canopus 1 covered the complete Nita and Goldwyer Formations. Note that logged cored section is from 1148.2-1156.6m (see Figure 3.32). ....	139
Figure 4.34: Well-to-well correlation of the INPEFA curves of wells Crystal Creek 1, Pictor 1 and Canopus 1 on the Mowla terrace, all these three wells show the complete subdivision of the Nita and Goldwyer Formations (Or1000P: Goldwyer lower shale (Transgression); Or2000: Goldwyer middle carbonate (Regression); Or2000P: Goldwyer upper shale (Transgression); Or3000: Leo Member (Regression); Or3000P: Cudalgarra Member part 1 (Transgression); Or4000: Cudalgarra Member part 2 (Regression)). Note that the distance between wells Crystal Creek 1- Pictor 1 and Pictor 1 – Canopus 1 is the same, which is 27.6km. ....	142
Figure 4.35: Well composite chart of well Matches Springs 1 with interpreted stratigraphic packages using the INPEFA curves. Note the Nita Formation is complete here but only the lower part of the Goldwyer lower shale is not covered due to the well total depth. Colours are described in Figure 4.8. ....	143
Figure 4.36: Well-to-well correlation of the INPEFA curves of wells Matches Springs 1 and Pictor 1 on the Mowla terrace, well Pictor 1 shows the complete subdivision of the Nita and Goldwyer Formations (Or1000P: Goldwyer lower shale (Transgression); Or2000: Goldwyer middle carbonate (Regression); Or2000P: Goldwyer upper shale (Transgression); Or3000: Leo Member (Regression); Or3000P: Cudalgarra Member part 1 (Transgression); Or4000: Cudalgarra Member part 2 (Regression)). Note the Nita Formation is	

complete for well Matches Springs 1 but the lower part of the Goldwyer lower shale is not covered due to the well total depth. ....	146
Figure 4.37: Location maps of wells Willara 1, Woods Hills 1 and Munro 1 in Willara Sub-basin, Canning Basin, WA. ....	147
Figure 4.38: Well composite chart of well Willara 1 with interpreted stratigraphic packages using the INPEFA curves. Well Willara 1 covered the complete Nita and Goldwyer Formations. Colours are described in Figure 4.8. ....	148
Figure 4.39: Well composite chart of well Woods Hills 1 with interpreted stratigraphic packages using the INPEFA curves. Well Woods Hills 1 covered the complete Nita and Goldwyer Formations. Colours are described in Figure 4.8. ....	150
Figure 4.40: Well composite chart of well Munro 1 with interpreted stratigraphic packages using the INPEFA curves. Well Munro 1 covered the complete Nita and Goldwyer Formations. Colours are described in Figure 4.8. ....	152
Figure 4.41: Well-to-well correlation of the INPEFA curves of wells Willara 1, Woods Hills 1 and Munro 1 on the Willara Sub-basin, all these three wells show the complete subdivision of the Nita and Goldwyer Formations (Or1000P: Goldwyer lower shale (Transgression); Or2000: Goldwyer middle carbonate (Regression); Or2000P: Goldwyer upper shale (Transgression); Or3000: Leo Member (Regression); Or3000P: Cudalgarra Member part 1 (Transgression); Or4000: Cudalgarra Member part 2 (Regression)). ....	155
Figure 4.42: A schematic cross section illustrating the boundaries of the various types of systems tracts that have been defined by various authors (Van Wagoner et al. 1988; Embry, 1993; Helland-Hansen and Gjelberg, 1994; Posamentier and Allen, 1999). Embry (2002) argued that only the transgressive systems tracts (TST) and the regressive systems tract (RST) have boundaries that can be determined by objective scientific analysis. The other types have one or more unrecognizable boundaries (hypothetical time lines) which have no practical use. This study applies the results of INPEFA curves analysis to match with the transgressive-regressive model of Embry (2002). Note that this diagram is not to scale. ....	159
Figure 4.43.: Application of Embry's models (1993) to components of INPEFA stratigraphy including the stratigraphic packages and compare with the results of this study. ....	160

## CHAPTER 5

- Figure 5.1: Prospective areas for shale gas resources in the Canning Basin (Energy Information Administration, 2011). .....163
- Figure 5.2: Well correlation lines, Canning Basin for Goldwyer Formation shale assessment. Each of the sections studied has three figures, first location map, then correlation diagrams and tables of shale distribution thickness. All of these figures are found after section 5.38 and following page 171. ....165
- Figure 5.3: Map location of section A-A' (yellow line) for the Goldwyer Formation correlation from southwest to northeast in the Canning Basin. ....173
- Figure 5.4: Well-to-well correlation for the section A-A' (yellow line) from southwest to northeast across Willara Sub-basin to Broome Platform in the Canning Basin for the Goldwyer Formation. ....174
- Figure 5.5: Map location of section B-B' (green line) for the Goldwyer Formation correlation from southwest to northeast in the Canning Basin. ....176
- Figure 5.6: Well-to-well correlation for the section B-B' (green line) from southwest to northeast across Willara Sub-basin, Broome Platform, Mowla Terrace, Jurgurra Terrace, Fitzroy Trough to Lennard Shelf in the Canning Basin. ....177
- Figure 5.7: Map location of section C-C' (red line) for the Goldwyer Formation correlation from southwest to northeast in the Canning Basin. ....179
- Figure 5.8: Well-to-well correlation for the section C-C' (red line) from southwest to northeast across Munro Arch, Kidson Sub-basin, Broome Platform, Crossland Platform and Barbwire Terrace in the Canning Basin. ....180
- Figure 5.9: Map location of section D-D' (orange line) for the Goldwyer Formation correlation from southwest to northeast in the Canning Basin. ....182
- Figure 5.10: Well-to-well correlation for the section D-D' (orange line) from southwest to northeast across Kidson Sub-basin, Crossland Platform and Barbwire Terrace in the Canning Basin. ....183
- Figure 5.11: Map location of section E-E' (dark blue line) for the Goldwyer Formation correlation from northwest to southeast in the Canning Basin. ....185
- Figure 5.12: Well-to-well correlation for the section E-E' (dark blue line) from northwest to southeast across Broome Platform, Willara Sub-basin, Munro Arch, Kidson Sub-basin and Ryan Shelf in the Canning Basin. ....186

Figure 5.13: Map location of section F-F' (purple line) for the Goldwyer Formation correlation from northwest to southeast in the Canning Basin. ....	188
Figure 5.14: Well-to-well correlation for section F-F' (purple line) from northwest to southeast across Broome Platform in the Canning Basin. ....	189
Figure 5.15: Map location of section G-G' (brown line) for the Goldwyer Formation correlation from northwest to southeast in the Canning Basin. ....	191
Figure 5.16: Well-to-well correlation for the section G-G' (brown line) from northwest to southeast across Broome Platform in the Canning Basin. ....	192
Figure 5.17: Map location of section H-H' (grey line) for the Goldwyer Formation correlation from northwest to southeast in the Canning Basin. ....	194
Figure 5.18: Well-to-well correlation for the section H-H' (grey line) from northwest to southeast across Broome Platform, Mowla Terrace and Barbwire Terrace in the Canning Basin. ....	195
Figure 5.19: Contour map represents topography for the top Goldwyer Formation to show the depth and distribution of this formation in the subsurface of the Canning Basin. Note that negative symbol of the depth means the depth is at the subsurface. The deepest depth of this formation is found in the Kidson Sub-basin while the shallowest of the top of this formation is in the Broome Platform. ....	199
Figure 5.20: An isopach map of Canning Basin showing the thickness of the Goldwyer shale which is the total thickness of Goldwyer Unit 1, Unit 2 and Unit 4. This figure shows the thickness distribution of the Goldwyer shale in part of the Canning Basin where data is available. Note that the thickest Goldwyer shale is found in the Willara Sub-basin. ....	201

## CHAPTER 6

Figure 6.1: Comparison of North American and Baltoscandian third-order sea level curves. Ross and Ross (1992, 1995) defined the North American sea level curve while Nielsen (2012) illustrated the Baltoscandian sea level curve (after Nielsen, 2012). The middle to late Llanvirnian is approximately from 460.5 Ma to 465 million years, during where the Nita and Goldwyer Formations were deposited. ....	207
Figure 6.2: Ordovician sea level changes (Haq and Schutter, 2008). ....	209
Figure 6.3: An example of Fischer plot showing changes in accommodation space as a function of cycle number. Thin green vertical line is individual cycle thickness. Increase in accommodation is shown by red line sloping up to the	

right while decrease in accommodation is shown by blue line (after Husinec et al., 2008). .....	210
Figure 6.4: Excel spreadsheet for data entry. Required input is number of covered intervals, thickness of each cycle in stratigraphic section between each covered interval and thickness of each covered interval (Husinec et al., 2008). .....	211
Figure 6.5: Well location maps of the studied wells in Broome Platform, Canning Basin, WA. ....	212
Figure 6.6 Fischer plots illustrated relative sea-level curve of well Looma 1 by showing changes in accommodation space as a function of cycle number. Increase in accommodation is shown by red arrow line sloping up to the right while decrease in accommodation is shown by blue arrow line. ....	213
Figure 6.7: Fischer plots illustrated sea level curve of well McLarty 1 by showing changes in accommodation space as a function of cycle number. Increase in accommodation is shown by red arrow line sloping up to the right while decrease in accommodation is shown by blue arrow line. ....	214
Figure 6.8: Fischer plots illustrated sea level curve of well Robert 1 by showing changes in accommodation space as a function of cycle number. Increase in accommodation is shown by red arrow line sloping up to the right while decrease in accommodation is shown by blue arrow line. ....	215
Figure 6.9: Comparison of Fischer plot and well composite chart for well Looma 1. There is a good match between the transgressive-regressive cycles for Goldwyer Formation as determined by the INPEFA curve and the sea-level curve (right hand column) as interpreted from the Fischer plots. But for the Nita Formation the correlation is weak. ....	218
Figure 6.10: Comparison of Fischer plot and well composite chart for well McLarty 1. There is a good match between the transgressive-regressive cycles for Goldwyer lower shale and Goldwyer middle carbonate as determined by the INPEFA curve and the sea-level curve (right hand column) as interpreted from the Fischer plots. But for the Goldwyer upper shale the correlation is weak. Nita Leo Member with regressive trend matches with the decreasing sea-level curve. ....	219
Figure 6.11: Comparison of Fischer plot and well composite chart for well Robert 1. In this well, there is a good match between the transgressive-regressive cycles for Nita and Goldwyer Formations as determined by the INPEFA curve and the sea-level curve (right hand column) as interpreted from the Fischer plots. ....	220

Figure 6.12: Comparison of third-order sea-level curves for Middle to Late Llanvirnian with various studies and this study. The middle to late Llanvirnian is approximately from 460.5 Ma to 465 million years, during where the Nita and Goldwyer Formations were deposited. The third-order sea-level illustrated with Fischer plots in this study correlates well with others shown. ....221

## LIST OF TABLES

### CHAPTER 1

Table 1.1: Sub-units of the Goldwyer Formation show the description of each sub-unit according to Foster et al. (1986) and Haines (2004). The Goldwyer Formation can be subdivided into Goldwyer lower shale (Goldwyer Unit 1 and Unit 2), Goldwyer middle carbonate (Goldwyer Unit 3) and Goldwyer upper shale (Goldwyer Unit 4). ....7

Table 1.2: Sub-units of the Nita Formation show shallowing upwards cycles and description of each sub-unit is according to McCracken (1994) and Haines (2004). The Nita Formation was subdivided into Leo Member and Cudalgarra Member by McCracken (1994). Before that, the well completion reports (Appendix2) mentioned and subdivided Nita Formation into Lower Nita, Middle Nita and Upper Nita. ....8

Table 1.3: Interpretation of INPEFA trends and turning-points (Nio et al., 2005; Nio et al., 2006; De Jong et al., 2006). ....14

### CHAPTER 2

Table 2.1: Western Australia shale play parameters in the Canning Basin and Perth Basin. Goldwyer Formation from the Canning Basin shows the biggest potential for shale gas exploration based on the thickness and original gas-in-place (DMP, 2012). ....27

### CHAPTER 3

Table 3.1: Previous work published on the Middle Ordovician Nita and Goldwyer Formations in the Canning Basin with respect to facies descriptions. ....29

Table 3.2: Four studied wells from the Canning Basin, Western Australia in this study by using the methods of sedimentary logging, microfacies and thin section analysis. ....29

Table 3.3: Depicts the relationship between the cored intervals, their facies associations, and positions within the stratigraphy. ....85

## CHAPTER 4

Table 4.1: The studied wells located at different areas in the Canning Basin, WA. N and G indicate logged core for Nita and Goldwyer Formations described in Chapter 3. ....	86
--	----

## CHAPTER 5

Table 5.1: Historical and projected US gas Production, year 1990-2030 (EIA, 2011). ....	162
Table 5.2: Thickness correlation for the Goldwyer Formation based on the sub-units along the section A-A' (yellow line). ....	175
Table 5.3: Thickness correlation for the Goldwyer Formation based on the sub-units along the section B-B' (green line). ....	178
Table 5.4: Thickness correlation for the Goldwyer Formation based on the sub-units along the section C-C' (red line). ....	181
Table 5.5: Thickness correlation for the Goldwyer Formation based on the sub-units along the section D-D' (orange line). ....	184
Table 5.6: Thickness correlation for the Goldwyer Formation based on the sub-units along the E-E' (dark blue line). ....	187
Table 5.7: Thickness correlation for the Goldwyer Formation based on the sub-units along the section F-F' (purple line). ....	190
Table 5.8: Thickness correlation for the Goldwyer Formation based on the sub-units along the section G-G' (brown line). ....	193
Table 5.9: Thickness correlation for the Goldwyer Formation based on the sub-units along the section H-H' (grey line). ....	196
Table 5.10: Gas in place (adsorbed gas) was estimated for Goldwyer shale on Willara Sub-basin, Barbwire Terrace, Mowla Terrace, Broome Platform and Kidson Sub-basin in the Canning Basin. ....	205

# CHAPTER 1

## INTRODUCTION

### 1.1 Overview of Canning Basin

The Canning Basin (Figure 1.1) is the largest Paleozoic sedimentary basin in north-western Australia. The basin covers approximately 506,000 km<sup>2</sup> of which approximately 430,000 km<sup>2</sup> is on land (Brown et. al., 1984).

The Paleozoic of the Canning Basin is subdivided into three megasequences (Warris, 1993):-

Megasequence I: Nambheet to Worrall Formations;

Megasequence II: Tandalgoon to Anderson Formations;

Megasequence III: Grant Group and younger.

The lower to middle Ordovician rocks of Canning Basin resting unconformably on Precambrian basement and succeeded disconformably by Upper Silurian (?) – Lower Devonian strata (Yeates et. al., 1984), have been investigated from many different perspectives, including sedimentology and stratigraphy, particularly as a consequence of their hydrocarbon resources (Haines, 2004; Haines, 2009). Paleogeographic constraints are important to develop basin-scale hydrocarbon system models and accessing exploration risks. A ubiquitous feature in Ordovician paleogeographic reconstructions for Canning and Amadeus basins is the Larapinta seaway, an early illustration of the shallow east-west transcontinental seaway across Australia during the Ordovician (Haines and Wingate, 2005; Baillie et al., 1994).

From Early Ordovician to the Cretaceous, the basin preserves a multi-phase depositional history (Forman and Wales, 1981; Brown et. al., 1984; Kennard et. al., 1994). Karajas and Taylor (1983) focuses on the depositional environment of Nita Formation (Middle Ordovician age) of well Aquila 1, Broome Platform, Canning Basin. Aquila 1 lies within the Broome Platform, a mid-basement ridge which was emergent during considerable periods of Canning Basin sedimentation. The Aquila section provides a useful model for predicting the distribution of porous carbonate facies in the Nita Formation (Karajas & Kernick, 1984). About one third of world's

petroleum is preserved in carbonates and they are very important reservoir rocks throughout the oil and gas industries; approximately 80% of North America's hydrocarbons in carbonates occur in dolomite (Zenger et.al., 1980).

Despite containing several demonstrated petroleum systems, such as the Larapintine petroleum system which is the early illustration of the shallow east-west transcontinental seaway across Australia during the Ordovician (Browne, 1947; David, 1950; Baillie et al., 1994), most of the basin remains underexplored or unexplored for petroleum resources. These pioneering studies laid an important foundation for later research in this region. However, the early studies focused mainly on the Devonian Reef (Begg, 1987; Playford et al., 1989; Wallace et al., 1991; Wood, 1998; Gregory, 2001; Playford, 2009; Frost III, 2010; etc.), and little research was carried out on the Ordovician carbonates of Canning Basin. The Canning Basin may still be the least explored of the known Paleozoic basins with proven petroleum systems (Carlsen and Ghori, 2005).

This research is intended to obtain a detailed understanding of facies associations and depositional environments of the Ordovician carbonates from Nita and Goldwyer Formations to determine the petroleum potential for these formations.

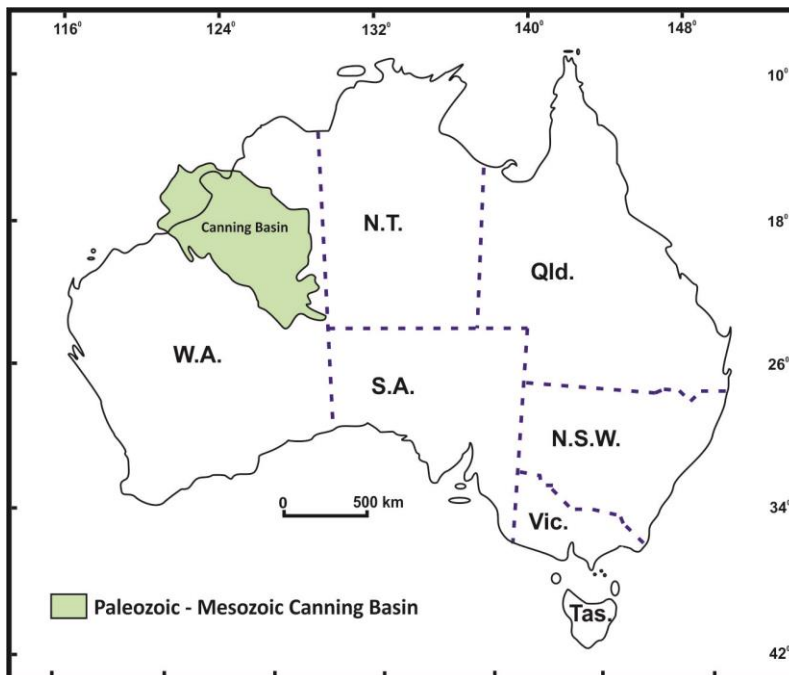


Figure 1.1: Location map of Canning Basin

## 1.2 Study areas

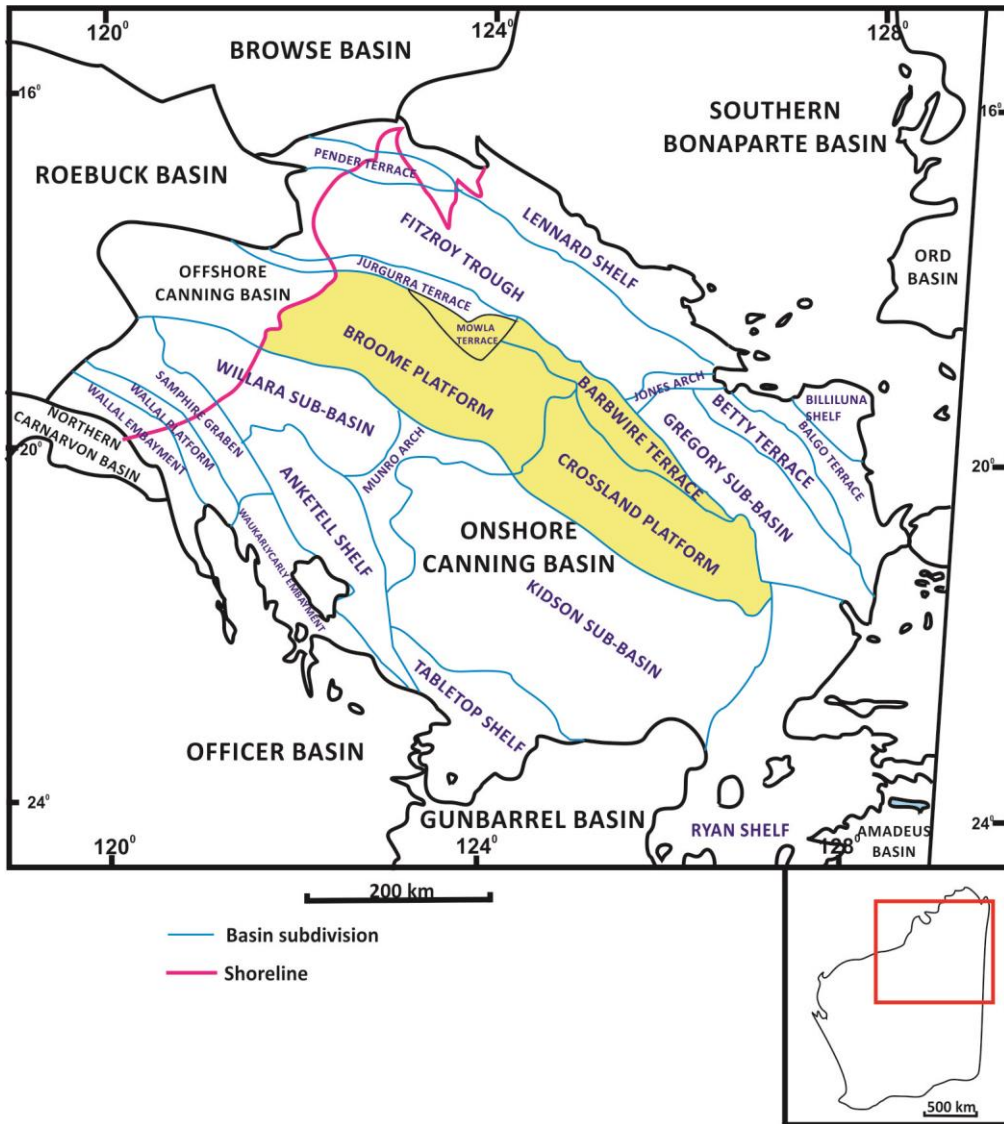


Figure 1.2: Location map of the study areas in Canning Basin, WA

The carbonates sequences of Nita and Goldwyer Formations are well developed across Broome Platform, Mowla Terrace and Barbwire Terrace and seem to thin towards Kidson Sub-basin (Haines, pers comms). This is the reason that the study areas are focused on the Broome Platform, Mowla Terrace, Barbwire Terrace and Crossland Platform (Figure 1.2), in what is a large basin (greater in area than the State of Texas, USA).

### 1.3 Ordovician Nita and Goldwyer Formations

The generalised stratigraphy of the Canning Basin is shown in Figure 1.3 and Figure 1.4. Deposition in the Canning Basin commenced in the Early Ordovician and the Ordovician age formations are rarely exposed exploration targets. The Ordovician period of the Paleozoic era is an interval exhibiting increased animal diversity and an abundance of marine life. Figure 1.5 shows that during the early Ordovician period, the Australian continent was located near the equator (Baillie et al., 1994); this indicates carbonates of Middle Ordovician age Nita and Goldwyer Formations in Canning Basin are warm water carbonates. Although the surface environment today is desert, evidence suggests that the basin was a deep water marine environment of relatively high faunal diversity during the Ordovician period.

Paralic sandstones (Lower Nambheet Formation) and intertidal and subtidal shale, siltstone and carbonate (Upper Nambheet Formation) were deposited at this time, (see Figs 1.3, 1.4). The Willara Formation was carbonate platforms developed on basement highs during the Arenigian (Brown et al., 1984; Cadman et al., 1993). Romine et al. (1994) identified a general upward shallowing megasequence from middle Goldwyer Formation to Carribuddy Group. The Goldwyer Formation is a transgressive sequence (see Table 1.1) and deposited in shallow subtidal conditions during the early Llanvirnian and contains oil-prone *Gloeocapsormorpha prisca*-bearing source rocks (Foster et al., 1986; Haines, 2004). The Nita Formation is a regressive sequence with Llanvirnian age (see Table 1.2) and conformably overlies the Goldwyer Formation. The Nita Formation was subdivided into Leo Member and Cudalgarra Member by McCracken (1994). Before that, the well completion reports (Appendix 2) mentioned and subdivided Nita Formation into Lower Nita, Middle Nita and Upper Nita. It contains numerous progradational cycles of limestone, vuggy dolomitized carbonate beds and shale deposited in subtidal to supratidal environments with limited reservoir potential as shown in Figure 1.6 (Karajas and Kernick, 1984; McCracken, 1997; Haines, 2004). Regression eventually ended Ordovician sedimentation during the late Llanvirnian.

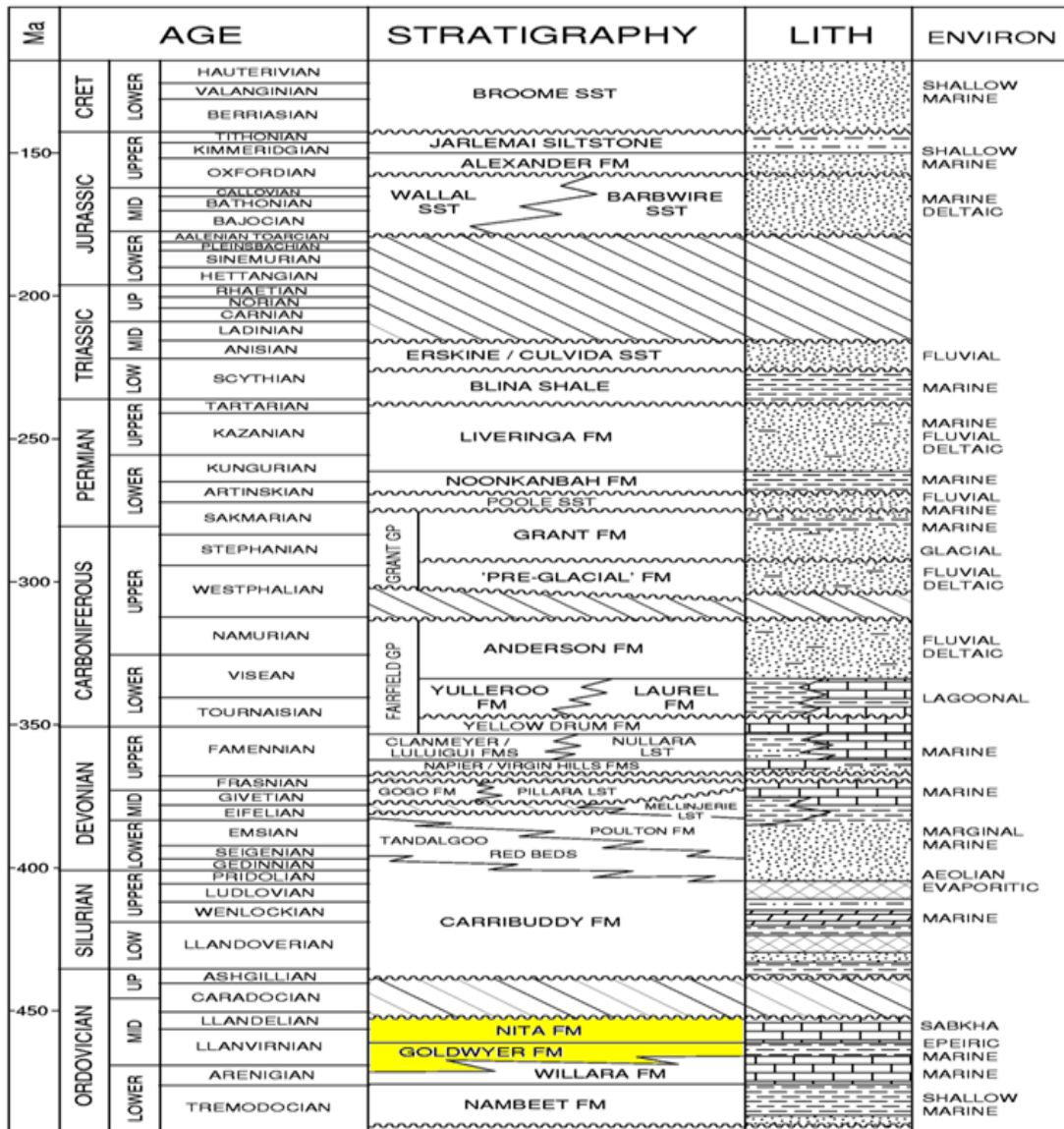
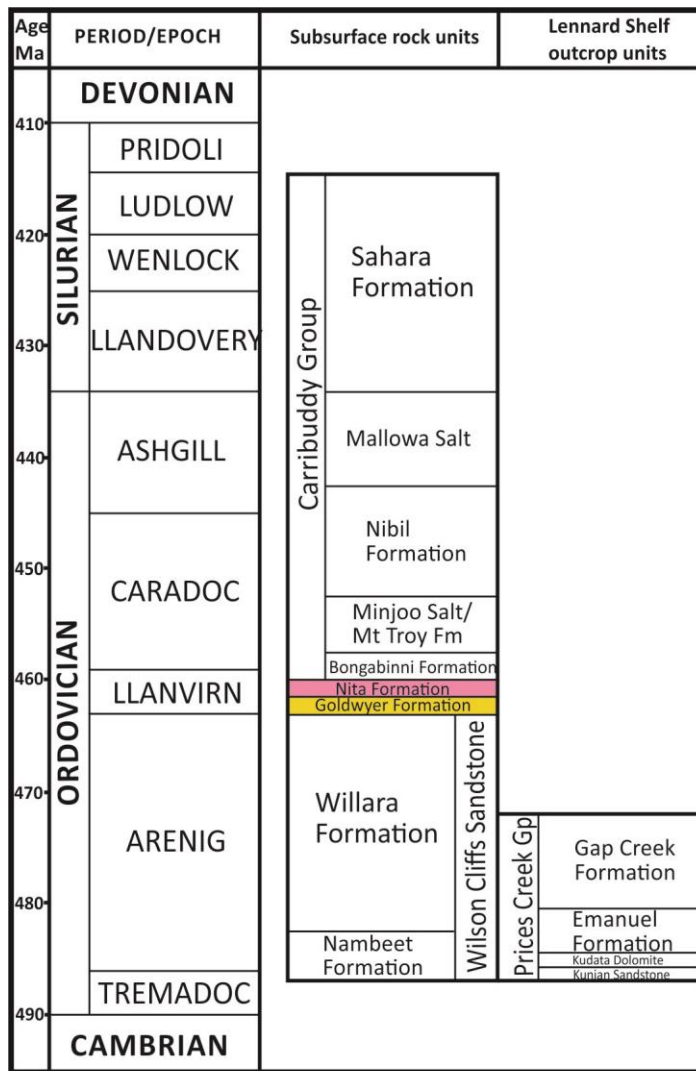


Figure 1.3: The generalised stratigraphy of the Canning Basin (After Brown et al., 1984). Note stratigraphic position of Nita and Goldwyer Formation.



Fm: Formation  
Gp: Group

Figure 1.4: The stratigraphic subdivision from Ordovician to Silurian period of Canning Basin (after Jones et al. (1998) and Haines (2004)).

Goldwyer upper shale	Goldwyer Unit 4	Transgressive shale: Dominated by abundant <i>G.Prisca</i>
Goldwyer middle carbonate	Goldwyer Unit 3	Regressive carbonates: Major carbonate build-ups present locally; Pale to medium grey slightly pyritic wackestone with lesser amounts of packstone & grainstone; Macrofossils are abundant.
Goldwyer lower shale (Transgressive shale and can be sub-divided into Goldwyer Units 1 and 2)	Goldwyer Unit 2	Thickly bedded transgressive shale
	Goldwyer Unit 1	Thinly bedded transgressive shale

Table 1.1: Sub-units of the Goldwyer Formation show the description of each sub-unit according to Foster et al. (1986) and Haines (2004). The Goldwyer Formation can be subdivided into Goldwyer lower shale (Goldwyer Unit 1 and Unit 2), Goldwyer middle carbonate (Goldwyer Unit 3) and Goldwyer upper shale (Goldwyer Unit 4).

<p>Upper Nita Formation (Cudalgarra Member part 2)</p>	<p>Consists of up to 7 shallowing upward cycles of tidal flats (Admiral Bay Fault Zone); Mostly supratidal origin; Top part: Interbedded grey-green and reddish mudstone, microbial lamination and evaporites; Dolostone: fine grained ; primary features preserved; Very early diagenetic origin; Fragmentary bioclasts and bioturbation decrease in abundance from Leo Member to Cudalgarra Member.</p>
<p>Middle Nita Formation (Cudalgarra Member part 1)</p>	<p>Dolostone: Grey to brown, coarsely crystalline &amp; destructive of primary facies, late diagenetic replacement, vuggy secondary porosity and replacement of burrow infillings.</p>
<p>Lower Nita Formation (Leo Member)</p>	<p>Bioturbated crinoidal wackestone, packstone &amp; mudstone (grey); Cyclicality is shallowing upwards units.</p>

Table 1.2: Sub-units of the Nita Formation show shallowing upwards. (After McCracken (1994); Haines (2004)).

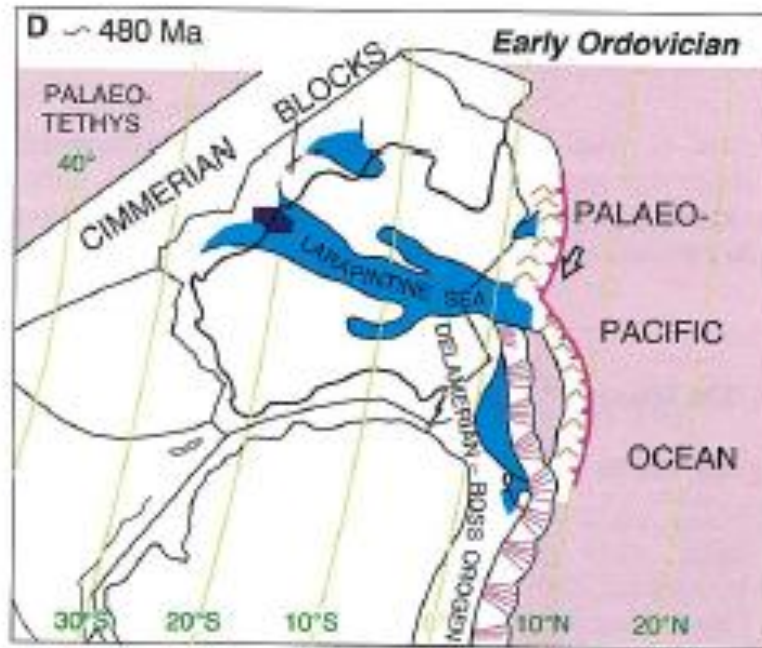


Figure 1.5: Tectonic setting of Western Australia's sedimentary basins in early Ordovician period (after Baillie et al., 1994).

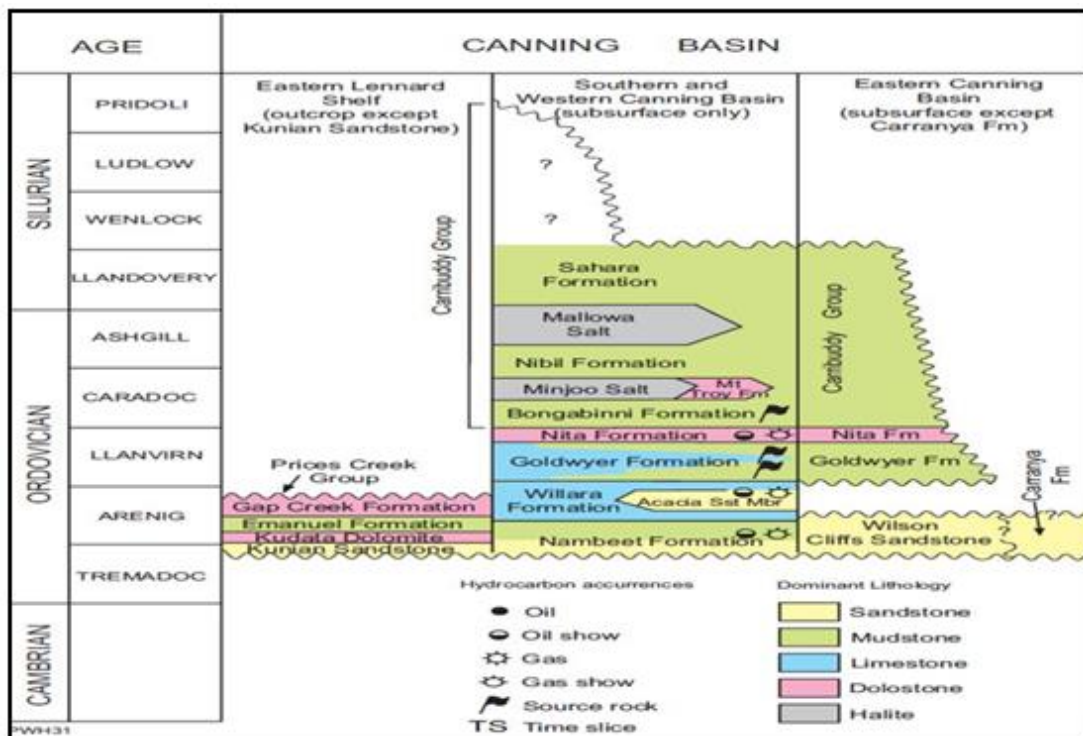


Figure 1.6: The oil and gas shows for Ordovician- Silurian successions in Canning Basin, WA (after Haines and Ghori, 2006).

#### **1.4 Aims and objectives (present study)**

The main aim of the project is to have detailed understanding of the basin, facies development, depositional environment of the Ordovician carbonates and determining hydrocarbon/ shale gas potentiality of the Nita and Goldwyer Formations. The objectives of this research project are as follows:

- (i) To obtain a detailed understanding of the relationship between the carbonate sequence and build-ups and the regional geology of the Goldwyer and Nita Formations in the study areas and recognise the Nita-Goldwyer cyclicity package.
- (ii) To characterise and correlate cycles within wireline log data by using “CycloLog” software as a regional correlation tool.
- (iii) To determine the depositional environment of the sediments of Goldwyer and Nita Formations by core study and facies analysis.
- (iv) To estimate total gas in place for the Goldwyer Formation (a potential shale gas).
- (v) To construct Llanvirnian sea-level curve based on Nita and Goldwyer deposits.

This study relies heavily on open file data provided in well completion reports submitted to the Geological Survey of Western Australia as a statutory requirement of petroleum exploration licenses. The lack of available cores necessitated use of correlation techniques such as ‘CycloLog software’. The study also describes the use of the fundamentals of sedimentology, which includes the study of four cores with 275.52m total thickness of core inspected and logged and thirty eight thin sections for lithology and facies variation. Twenty two well composite charts are analysed for the stratigraphic sequences by using the CycloLog software. Thirty eight wells are studied for the Goldwyer Formation and understand the thickness of the Goldwyer shale units. Three Fischer plots are plotted from three wells to understand the relative sea-level fluctuations during Llanvirn for Nita and Goldwyer Formations. As a conclusion, this research project is subdivided into three categories:

- (i) The study methods, the regional geology, the sedimentary and sequence analysis models which form the Middle Ordovician Nita and Goldwyer Formations.
- (ii) The interpretations based on the results of the core logging, facies analysis, well correlation, sequence analysis, resource estimation and Llanvirnian sea-level curve.
- (iii) The relationship between the sequence stratigraphic models proposed as a result of analysis of the Nita and Goldwyer Formations and published cyclicity packages.

## **1.5 Significance**

The Canning Basin is a large but relatively poorly explored Paleozoic basin in remote Western Australia. According to GSWA (2013), the main issues and uncertainties in this basin include: (1) unreliable and poorly distributed geochemical data; (2) inconsistent stratigraphic nomenclature across the basin, especially for the Paleozoic section; (3) lack of biostratigraphic data in many wells; (4) uncertain validity of the structural and tectonic framework; (5) lack of good quality well and seismic data and issues regarding the quality and distribution of the data. Core data are also limited to scarce. The Nita and Goldwyer Formations' carbonate sequences are of particular interest as subtidal to supratidal depositional environments (Hillock, 1988; King, 1998; Haines, 2004). The Nita Formation is a primary exploration target with hydrocarbon shows occurring above the Goldwyer Formation which is source rock and below the Carribuddy Group which contains evaporitic seals (Figure 1.6). The Goldwyer shale is not only the source and seal rocks for hydrocarbons, but also has become a target of shale gas exploration recently.

## **1.6 Methods and techniques**

### **1.6.1 Sedimentary logging techniques**

The sedimentary logs of four available cores for Nita and Goldwyer Formations in Canning Basin, WA were constructed through descriptions of bed thickness, colour, sedimentary structures, grain size and mineralogy (using the Dunham (1962) scheme) in Chapter 3. Total thickness of core interpreted and logged is 275.52m. The cores are stored in the GSWA, Perth Core Library in Carisle, WA. Photographs of the cores were taken in association with the Hylogging methodology. The goals of Hylogging methodology are to improve the objectivity of drillcore logging, increase the quality of information obtained from exploration activity, determine the signatures of mineralized environments and characterize primary rock types (Huntington et al., 2007; Hancock and Huntington, 2010). The Hylogger hardware and TSG-Core software which is developed by CSIRO is used for the mineralogical interpretation.

### **1.6.2 Thin section analysis**

Thirty eight thin sections were studied for this thesis in Chapter 3. Most of the thin sections are on loan from the Geological Survey Western Australia (GSWA). The

rest of them were sampled from the core and sent to Minerex Pty. Ltd. for the thin section preparation. The microscopic study of thin sections of Nita and Goldwyer Formations provides the basic microfacies data, where it is available. The combination of thin section studies and sedimentary logging interpretation provide key information on the depositional environment of these two formations, to support the CycloLog regional analysis.

Petrographic descriptions were made on a textural level using the Dunham (1962) scheme; grain identifications were made using Scholle and Ulmer-Scholle (2003) and were further classified using the microfacies scheme provided with the sedimentary logs in Chapter 3. Polarizing microscopes and binocular microscopes in the lab of Department of Applied Geology, Curtin University were essential tools for thin section studies in this project.

### **1.6.3 Cycle analysis**

After twenty two well logs and integrated prediction error filter analysis (INPEFA) curve observations had been collated, the results could be used to characterise the metre-scale cyclicity for the Nita and Goldwyer Formations in Chapter 4. Metre-scale cyclicity has been a subject of study in sedimentary sequences for many years and it is a fundamental aspect of carbonate platforms (Goldhammer et al., 1987). Cyclicity was determined by assessing the vertical stacking in the successions. The Nita-Goldwyer cyclicity packages in this study start from the boundary of Willara and Goldwyer Formations towards the top of the Nita Formation. Cycles could be either transgressive-regressive or wholly regressive. Fischer plots were then constructed to identify the trends by keying the cycle thickness which could be a result of longer term relative sea level fluctuations. These cycle stacking patterns can be used as a tool for correlation.

#### **1.6.3.1 CycloLog® software – INPEFA curves**

Thirty eight wells are studied for the Goldwyer Formation and understand the thickness of the Goldwyer shale units based on the integrated prediction error filter analysis (INPEFA) curves by using the CycloLog software in Chapter 5. Twenty two wells are studied for the Nita and Goldwyer Formations in Chapter 4 to understand the systems tracts and stratigraphic packages of these formations by using the

INPEFA curves that generated by CycloLog software as well. To generate the INPEFA curves, a LAS file of each well was imported to the CycloLog software. Well completion reports of each well were read and interpreted to mark the top Nita Formation, top Goldwyer Formation and top Willara Formation. With the information from well completion reports, the lithology logs were constructed by using the Winlog software. CycloLog software developed by ENRES International was used to predict stratigraphic packaging in the subsurface by transforming a standard wireline log data (ENRES, 2011). Besides, the contour map was constructed based on INPEFA analysis to estimate the gas in place for the Goldwyer shale for sub-basin study in this research.

The Gamma Ray log which is a facies sensitive log is transformed to an integrated prediction error filter analysis curve (INPEFA curve), which shows uphole changes in the waveform properties concealed in the numerical log data and displays discontinuity surfaces and trends. This INPEFA curve with its emphasis on changes in the frequency content is an analytical tool that looks at the pattern of vertical lithofacies change and this can help to reveal the pattern imposed on the depositional system by the succession of climate change (Nio et al, 2005). Besides, this method of ‘climate stratigraphy’ allows the development of a framework of well-to-well correlations by identification of trends in wireline log data and vertical lithofacies changes.

The waveform properties can only be analysed for sections that have been preserved. Therefore, the interpretation of INPEFA curves focuses on identifying equivalent breaks and trends rather than on finding identical patterns (Nio et al, 2008). A positive trend in the INPEFA curve is from left-to-right while a negative trend is from right-to-left and these both positive and negative trends are separated by turning-points (Table 1.3). A positive turning point is a point at which the trend changes from negative to positive; a negative turning point is a point at which the trend changes from positive to negative. After identification the trends and turning points then are calibrated in lithological terms and interpreted in stratigraphic terms (Nio et al, 2008). Turning points that signify changes in depositional trends (Embry, 2002) are called bounding or stratigraphic surfaces and these are correlatable between wells. Negative turning-points are called negative bounding surfaces (NBS) while positive turning-points are called positive bounding surface (PBS). These turning-points are time-

equivalent, primarily ‘climate-controlled’ and record vertical lithofacies changes. Usually, an NBS marks the base of a trend with a progradational (regression) or related component, whereas PBS represents the beginning of a period of retrogradation (transgression) or related process (Nio et al., 2005).

A hierarchy of change is commonly observable in the INPEFA\_GR curve, this indicating a hierarchy of vertical lithofacies trends and changes. ‘StratPacs’ (stratigraphic packages) are bounded by adjacent negative bounding surfaces (NBS) of the same hierarchical rank and StratPacs represent systematic changes in lithofacies controlled by climatic variations. They are stratigraphically time-synchronous.

INPEFA Feature		Mathematical Interpretation	Geological Interpretation
Positive Trend		Persistent under estimation of log properties	Shale prone character of “transgressive” trend or transgressive surface
Positive Turning-Point (PBS)			Base level rise- “flooding” surface
Negative Trend		Persistent over estimation of log properties	Sand prone or “regressive” trend
Negative Turning-Point (NBS)			Low base level- possible erosion surface- new influx of coarser grained sediment

Table 1.3: Interpretation of INPEFA trends and turning-points (Nio et al., 2005; Nio et al., 2006; De Jong et al., 2006).

The lack of core data and relative abundance of well log data provided an opportunity to apply CycloLog analysis on a regional basin to the large depositional system. CycloLog has been successfully used in a variety of settings (Nio et al., 2005; De Jong et al., 2006; De Jong et al., 2007). Haines (2009) used CycloLog software to define the units of Upper Ordovician to Silurian Carribuddy Group and Worrall Formation from the Canning Basin, Western Australia; furthermore, the stratigraphic correlations have been carried out successfully.

### 1.6.3.2 Gamma ray logs

Gamma ray logs which scale in API (American Petroleum Institute) units are electric logs that measure the natural radioactivity in formations. Three radioactive isotopes usually measured in gamma ray logs are Uranium, Potassium and Thorium. Gamma ray logs are useful for shale logs which show high gamma ray reading when shale content increases because of the relatively large concentration of radioactive

material in shale. Shale-free sandstones and carbonates usually have low gamma ray readings, however, clean sands or carbonates might also produce a high gamma ray response when they contain potassium feldspars, micas, shale, heavy minerals (zircon, monazite), glauconite or uranium-rich waters (Asquith and Krygowski, 2004). Besides identifying shale and shale-free sandstones and carbonates, gamma log can also be used to correlate between formations.

#### **1.6.3.3 Sonic logs**

The sonic log is a porosity log and is used to measure interval transit time ( $\Delta t$ ) of a compressional sound wave travelling through one foot of formation. The interval transit time is related to formation porosity (Asquith and Krygowski, 2004). The sonic log is used to measure porosity and lithology by responding to both grains and fluids. The clean sandstones, carbonates and anhydrite have low transit time; coals and shales have higher transit time, and salt has intermediate transit time.

#### **1.6.3.4 Spontaneous potential logs**

The spontaneous potential (SP) log is used to identify impermeable zones (shale) and permeable zones (sandstone or carbonates). It is a record of direct current (DC) voltage differences between the naturally occurring potential of a moveable electrode in the well bore and the potential of a fixed electrode located at the surface which is measured in millivolts (Doll, 1948; Asquith and Krygowski, 2004).

The SP log is used to detect permeable beds and the boundaries of these beds. The SP log can also be used to determine formation water resistivity ( $R_w$ ) and the volume of shale in permeable beds (Asquith and Gibson, 1982). The variations in the SP log are the results of differences in salinities between mud filtrate and formation water. This salinity difference produces a resistivity difference between resistivity of mud filtrate ( $R_{mf}$ ) and resistivity of formation water ( $R_w$ ).

#### **1.6.3.5 Caliper logs**

The caliper log is used to indicate borehole diameter and volume, input for environmental corrections for other measurements, log quality control, qualitative indication of permeability and correlation (Krygowski, 2003). In this study, the caliper log provides a control for log quality by allowing identification of ‘caving’

intervals in the well bore; these intervals are likely to produce poor quality log data which needs to be identified and allowed for in well log analysis. The caliper value is checked in casing against the casing diameter and the shale values should be similar to those in nearby wells. The curves should have the same values and character as those from previous runs or repeat sections (Krygowski, 2003).

#### **1.6.4 Fischer plots analysis**

Three Fischer plots are plotted from three wells to understand the relative sea-level fluctuations during the Llanvirnian for Nita and Goldwyer Formations in Chapter 6. Fischer plots are a tool for graphically illustrating deviations from average cycle thickness plotted against cycle number to determine the cycle stratigraphy for “cyclic” carbonate platforms (Fischer, 1964; Sadler et al., 1993). The thicker-than-average cycles or periods of increased accommodation are with positive slope (which generally matches times of open marine, subtidal parasequence development) while thinner-than-average cycles or periods of decreased accommodation are with a negative slope (which generally matches with thin, shallow, peritidal parasequences) and this provides an objective plot of cycle thickness variation. The plots are used to recognize changes in accommodation space from cyclic carbonate successions and pick depositional sequences (Husinec et al., 2008). One method to generate Fischer plots is by using an Excel spreadsheet program developed by Husinec et al. (2008) and the data input is the number and thickness of covered intervals in core and cycle thickness data.

#### **1.7 Structure of Thesis**

In outline, the Thesis consists of:-

Chapter 1: Brief introduction to the Canning Basin and Nita and Goldwyer Formations, including aims and objectives, methodology and software used in this study.

Chapter 2: The geological background of the Canning Basin and the study area are discussed, with a brief overview of the basin evolution and subdivision, petroleum systems and exploration history of the basin.

Chapter 3: Description and interpretation of the tidal flat carbonate lithofacies identified for the Nita and Goldwyer Formations in the study area by using the best

available cored sections for the study area. Four wells and 38 thin sections are studied from Broome Platform (well Looma 1), Crossland Platform (well Kunzea 1), Mowla Terrace (well Canopus 1) and Barbwire Terrace (well Acacia 2).

Chapter 4: CycloLog software is used to construct INPEFA\_GR curves and well logs to aid correlation between successions by analysing 22 subsurface wells in part of the Canning Basin.

Chapter 5: Preliminary analysis of the shale gas potential prospectivity of Goldwyer Formation in Canning Basin with the short term INPEFA\_curves are used to correlate the Goldwyer Formation distribution for the Goldwyer lower shale and the Goldwyer upper shale across the Canning Basin.

Chapter 6: Discussion of the relative sea-level fluctuations in the Middle Ordovician. The metre-scale cyclicity in the study area is discussed. Fischer plots are constructed to aid understanding of the Middle Ordovician sea-level fluctuations.

Chapter 7: Conclusions.

# **CHAPTER 2**

## **REGIONAL GEOLOGICAL SETTING OF CANNING BASIN**

### **2.1 Introduction**

This chapter reviews studies of the regional geology of Canning Basin in Western Australia. The key research topic areas of this study are basin evolution, basin subdivision and the Ordovician palaeogeography of Canning Basin. The aim of this chapter is to understand the geological settings of the study areas.

### **2.2 Geology of the Canning Basin**

Canning Basin is a large basin covering an onshore area approximately 430,000 km<sup>2</sup> and ranging in age from Ordovician to Cretaceous. The maximum sediment thickness is 15 km. The northern border of Canning Basin is the Proterozoic Kimberley Block while the southern border is Archean Pilbara craton. Both the Kimberley and Pilbara are cratonic crystalline rocks with metasediments and volcanics. The Canning Basin is separated from the Amadeus Basin to the east and the Officer Basin to the southeast by high basement ridges. The east to south east border of Canning Basin is formed by the Precambrian Musgrave Block (Brown et al., 1984; Yeates et al., 1984; Kennard et al., 1994).

### **2.3 Petroleum exploration history**

The potential of hydrocarbon resources of Canning Basin has drawn geologists of the Australian Government and the exploration industry to the area. In the Canning Basin, the petroleum exploration activity began in the early 1920s when the Freney Oil Company encountered oil shows in drill holes on the Lennard Shelf (Purcell, 1984). The company struggled along for decades and it was restructured several times, lastly drilling the Sisters 1 well in 1956 (Purcell, 1984). By then, the Freney period was over and West Australian Petroleum Pty Ltd (WAPET) had entered the basin.

Exploration was intensified during the WAPET period (1953-1974). Bureau of Mineral Resources (BMR) and WAPET conducted gravity, magnetic and seismic reflection surveys in the northern and western part of Canning Basin. Many Australian and international oil companies served an apprenticeship with WAPET. Important geological results obtained by WAPET during this period where the identification of reef anomalies from seismic data, the discoveries of oil in Ordovician carbonates on the Broome Platform and the discovery of oil shows in the Fairfield Group (Cadman et al., 1993).

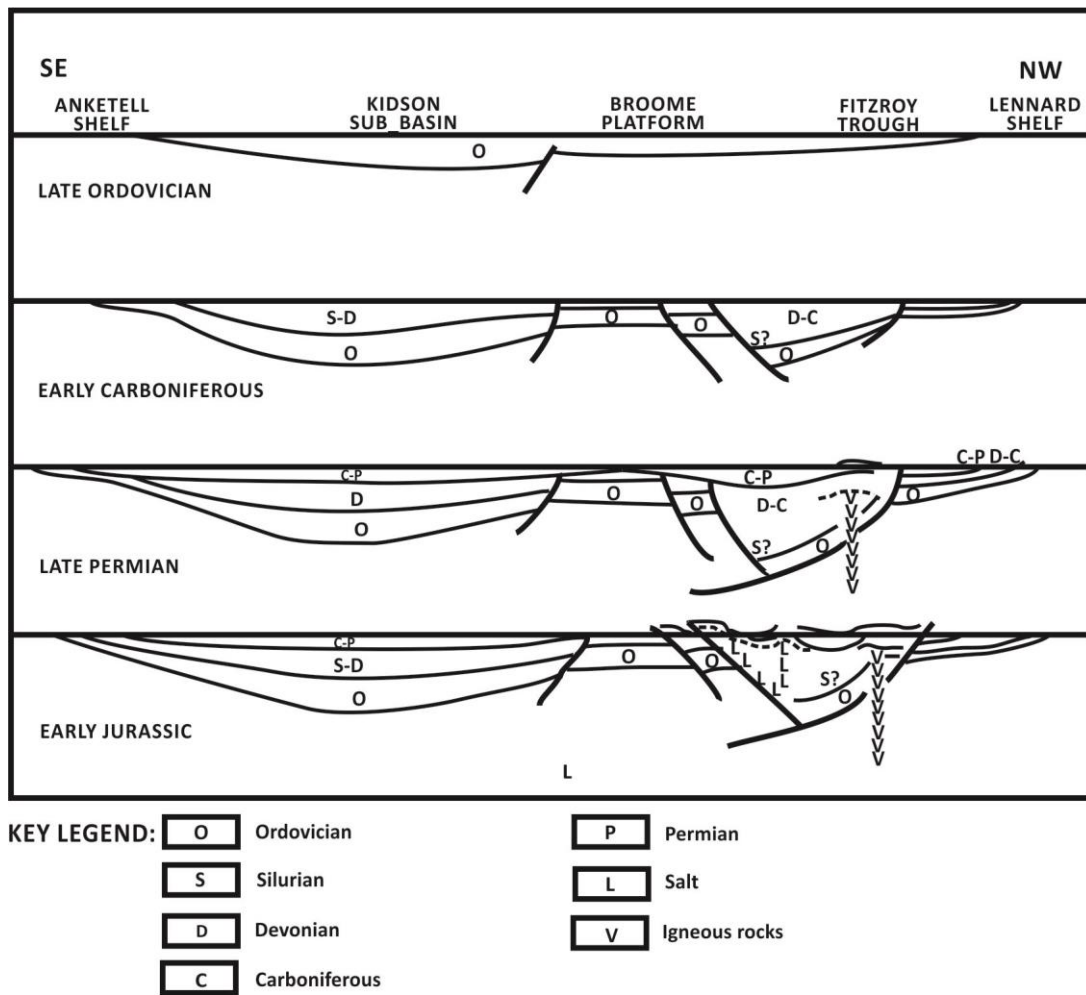
The multi-company period began late in 1976 when Whitestone Petroleum Australia, Ltd. was granted permit EP 97 in the central Fitzroy Valley. This company had recognized the possibility of an intra-rift horst-block in the Fitzroy Trough on the northern flank of the St. George Ranges structure from seismic evidence (Purcell, 1984). A new phase of exploration began in 1977 when the Amax/Whitestone group had acquired three other permits and Esso (Australia) Limited also held a permit. Up until the mid-1980s, exploration largely focused on the northern and central parts of the Canning Basin. The primary targets of exploration were the Devonian reef complexes, Permo-carboniferous clastics and the Ordovician strata (Cadman et al., 1993). Many exploration wells had oil shows, but few yielded commercial hydrocarbons. The basin is substantially under explored but the oil shows encourage continued optimism about the basin's potential (Purcell, 1984).

More recently, the subsalt Ordovician section has been the target of companies such as Shell, who recovered hydrocarbons at its Looma 1 discovery in the southern Canning Basin. Buru Energy and its joint venture partner Mitsubishi Corporation purchased two new parcels of acreage, boosting its holdings in the region to 69,000km<sup>2</sup> in the Canning Basin in year 2013, and Buru has started test production of oil at Ungani and it is continuing its production at the Blina and Sundown oilfields (Prospect, 2013).

## **2.4 Basin evolution**

The Ordovician of the Canning Basin forms as an extensional intracratonic sag basin and there are mainly carbonates within the Ordovician (Middleton, 1990) (Figure 2.1). A rift system started to develop and concentrated sedimentation found in the Fitzroy Graben from Silurian to Early Carboniferous. In the Late Permian, intrusive igneous activity was pervasive in the north-western part of basin and this short period of regional upwelling of the mantle caused localized uplift. This was associated with the initiation of Gondwana break-up and a hot spot under the North-Western of the basin (Brown et. al., 1984).

A main rifting stage happened at Early Jurassic time, when wrench movement occurred along Fitzroy Trough (Fitzroy movement) attributed to stress and continental break-up of North-West Shelf associated with uplift, with the uplift due to thermal domes and mantle material upwelling (Brown et. al., 1984). The same tectonism may have initiated the salt structures on the north and west part of the Kidson evaporite basin. No significant tectonic activity occurred in the Onshore Canning Basin after the Late Triassic- Early Jurassic event. Continental break-up in offshore Canning Basin (Middle-Late Jurassic) led to a thin (<500m) cover of Jurassic and younger sediment accumulated over the whole basin (Brown et. al., 1984; Haines, 2004).



GSWA 24258

Figure 2.1: Basin evolution of Canning Basin (After Middleton, 1990). Note the increasing tectonic disturbance of parts of the initial Ordovician sag basin through time and also tectono-stratigraphic domains and sub-basins developed.

## 2.5 Basin subdivision

The main structural elements in the Canning Basin are shown in Figure 2.2. The basin has been divided into a series of platforms, terraces, sub-basins and shelves and is cut by major fault systems which trend southeast, parallel to the long margin of basin (Shaw et al., 1994; Hocking et al., 1994). The major fault systems control the major thickness changes and these can be used to subdivide the basin into a series of tectono-stratigraphic domains.

The onshore Canning Basin has elongate northern and southern depocentres separated by Broome and Crossland Platforms. These platforms have a thinner succession. Figure 2.3 shows Broome Platform has thinner succession compared with other subdivisions. In the north, approximately 15km of strata is preserved in the Fitzroy Trough and Gregory Sub-basin. To the south, thinner sequences are preserved in the Willara and Kidson Sub-basins. Fitzroy Trough and Gregory Sub-basin are flanked to the south by Jurgurra, Mowla and Barbwire Terraces; transitional domains to the Broome and Crossland platforms respectively. The present northern margin is defined by the Lennard Shelf, the Billiluna Shelf and transitional Balgo and Betty Terraces while the south-eastern margin of the basin is defined by thin successions on the Ryan Shelf, flanking the Crossland Platform and Kidson Sub-basin. The areas of shallow basement along the southern flank of the Kidson and Willara Sub-Basin are referred to as Tabletop and Anketell Shelves (Smith, 1984; Brown et. al., 1984; Yeates et. al., 1984).

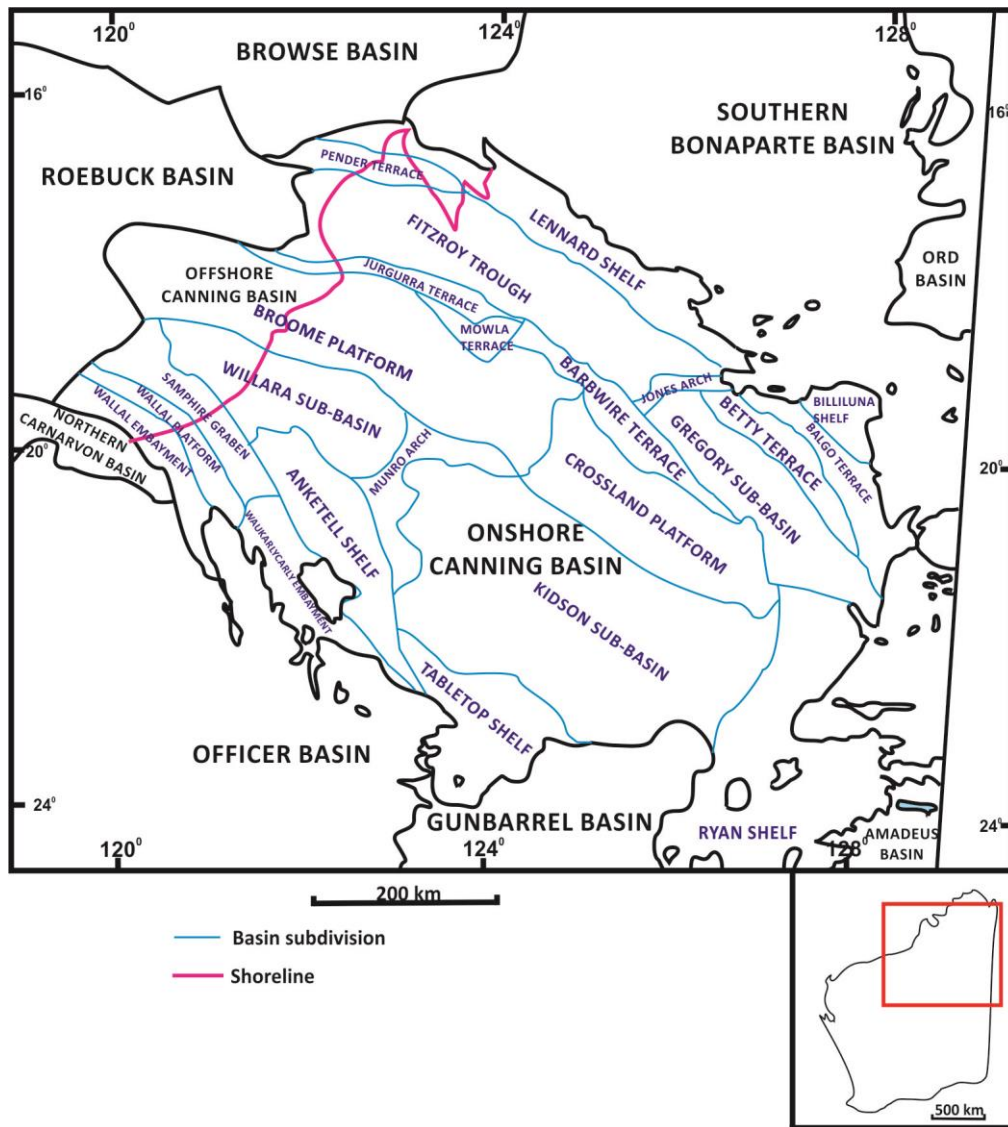


Figure 2.2: Principal structural elements of the Canning Basin (After Tyler and Hocking, 2001; Haines, 2004).

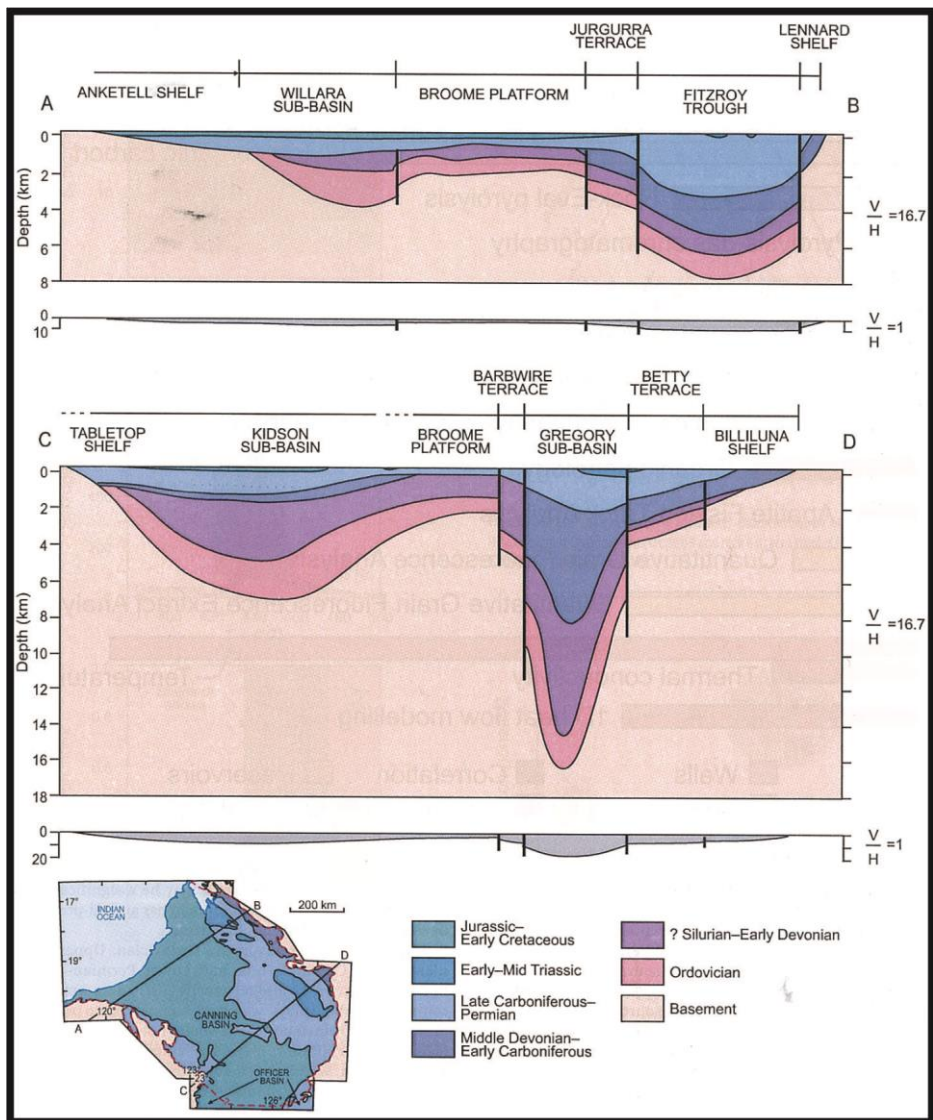


Figure 2.3: Cross-sections of Canning Basin's sub-basins, terraces and deep depocentre (after Yeates et al., 1984; Ghori, 2013).

## **2.6 Hydrocarbon potential**

### **2.6.1 Petroleum systems**

Early illustration of the shallow east-west transcontinental seaway across Australia during the Ordovician can be found in Browne (1947) and David (1950). Three active petroleum systems are recognized in the Canning Basin (Larapintine Supersystem, Systems L2, L3 and L4) with source rocks of Ordovician to Permian age, where L2 is Goldwyer and Bongabinni Formations, L3 is Devonian Gogo Formation and L4 is Early Carboniferous Laurel and Anderson Formations (Bradshaw et al., 1994; Kennard et al., 1994; Romine et al., 1994; Edwards et al., 1997). Edwards et al. (1997) identified hydrocarbons from these petroleum systems from isotopic and biomarker data.

The 'Larapintine 2' petroleum system is characterized by organic-rich Ordovician marine shales with the oil-prone microfossil *Gloeocapsomorpha prisca*. The best source rocks in the Larapintine 2 petroleum system occur in the Goldwyer Formation (Romine et al., 1994). Edwards et al. (1997) further supported the G.*prisca* link to the Goldwyer Formation. The oil generated from G.*prisca* contains low concentrations of pristane, phytane and steranes. Zalessky (1917) proposed two possible scenarios for G.*prisca*. First, it was thought to be planktonic organism that bloomed on the surface of saline lakes, subsequently sank and became incorporated into the bottom sediments (in-situ) and secondly, it was considered to be a benthonic mat. Hoffman et al. (1987) agree with the first scenario while Reed et al. (1986) support the second scenario.

In the Canning Basin, the geographic distribution of Goldwyer source rock quality is poorly known, although richness appears to increase towards the east from the Broome Platform and adjacent terraces to the central Barrow Terrace (Foster et al., 1986; Haines, 2004; Haines and Wingate, 2005). Due to limited well data, trends further east are poorly known and the Willara Sub-basin appears to have low source potential (McCracken, 1997; Edwards et al., 1997).

The Canning Basin may be the least explored of the known Paleozoic basins with proven petroleum systems (Carlsen and Ghori, 2005). Ghori and Haines (2007) concluded that oil and gas is geographically and stratigraphically widespread, the timing of petroleum charge varies greatly across the Canning Basin. More studies on this basin are required for further exploration as a low level of exploration and wide

geographic and stratigraphic distribution of hydrocarbons demonstrate the high potential for significant new discoveries.

### **2.6.2 Shale gas**

Shales are formed through depositional sedimentary processes, usually from the consolidation of clay-sized particle (muds) in low-energy, aqueous depositional environments such as tidal flats or deep-water basins (O'Brien and Slatt, 1990). Any algae, plant or animal matter that may be present in these environments may settle amongst the clay particles during deposition, resulting in the formation of a mudstone with high organic content. Shales are the source rocks for hydrocarbon migrating into porous and permeable reservoir rocks and act as seal rocks for trapping oil and gas in the reservoir rocks. Until recently, geologists and engineers have begun to view a specific type of shale, organic-rich shale, with a newfound appreciation. Organic-rich shales have the potential to serve not only as sources and seals of hydrocarbons but also as reservoirs to be produced.

Even though the Earth has vast amounts of shale deposits, not all of it can be developed into hydrocarbon reservoirs. In order for the shales to become hydrocarbon reservoirs, they should have been buried in such a way that at least a substantial fraction of the original organic matter was preserved so that it could serve as a source for hydrocarbon. After hydrocarbon is produced, they become trapped in the ultra-low permeable matrix.

High levels of organic matter combined with low levels of oxygen are the critical conditions required for formation of hydrocarbons. Such conditions were widespread during the Devonian Period. The climate was warm and the Earth was covered by tropical seas. Thick organic-rich shale deposits had also formed during other periods like the Precambrian (Alexander et al., 2011).

Finding and producing gas from shale formations, initially a North American phenomenon has become a global pursuit for many exploration companies (Boyer et al., 2011). The catalyst for the recent boom in shale exploration is the Barnett Shale in Texas. It took 20 years of experimenting before the play was considered economically viable. Fracture stimulation and horizontal drilling were the two techniques applied to enable this success (Boyer et al., 2011). The success of Barnett Shale in the US

energy industry has created a lot of excitement in Australia. The possibility of bringing new sources of natural gas to market for Western Australia would help to mitigate the foreseen shortfall in domestic gas supply and to increase the diversity of available gas resources.

### 2.6.2.1 Shale gas prospectivity in Western Australia

The Goldwyer shale contained 764 Trillion cubic feet (Tcf) of risked gas in place and 229 Tcf of risked recoverable gas, the largest estimate for any basin in Australia, according an April 2011 report by the U.S. Energy Information Administration on world shale gas resources. Table 2.1 shows the shale play parameters in Western Australia (DMP, 2012). The Goldwyer Formation (Ordovician age) has been favourable compare with other plays and this formation remains highly underexplored but it is predicted to contain approximately 21.6Tm<sup>3</sup> (764 Tcf) of gas-in-place (EIA, 2011). However, shale gas exploration has only recently commenced in the Canning Basin and the material has not yet been fully assessed.

<b>SHALE PLAY</b>	<b>WESTERN AUSTRALIA</b>				
<b>Basin</b>	Canning	Canning	Canning	Perth	Perth
<b>Formation</b>	Goldwyer	Laurel	Gogo	Carynginia	Kockatea
<b>Area Extent of Basin (km<sup>2</sup>)</b>	48,100	48,100	48,100	2180	2180
<b>Geologic Age</b>	Ordovician	Carboniferous	Devonian	Permian	Triassic
<b>Depth (m)</b>	800-2300	800-2880	330-2800	1220-5030	1000-5300
<b>Thickness</b>	400-750	550	420	90-450	90-900
<b>Richness (TOC%) / Maturity (R<sub>0</sub>%)</b>	6.4/1.6	4.8/2	4/0.8	4/1.4	5.6/1.3
<b>Original Gas-in-Place (Gm<sup>3</sup>/Tcf)</b>	21,634/764	Not available	Not available	2775/98	2831/100
<b>Recoverable Resource (Gm<sup>3</sup>/Tcf)</b>	6484/229	Not available	Not available	821/29	849/30

Table 2.1: Western Australia shale play parameters in the Canning Basin and Perth Basin. Goldwyer Formation from the Canning Basin shows the biggest potential for shale gas exploration based on the thickness and original gas-in-place (DMP, 2012).

# CHAPTER 3

## SEDIMENTARY LOGGING AND MICROFACIES ANALYSIS OF CARBONATE SUCCESSIONS FOR NITA AND GOLDWYER FORMATIONS, MIDDLE ORDOVICIAN

### 3.1 Introduction

This chapter describes and discusses the sedimentary logs and microfacies for Middle Ordovician carbonate successions of Nita and Goldwyer Formations of the Canning Basin, Western Australia, using the best available cored sections for the study area. Four wells and 38 thin sections are studied from Broome Platform (well Looma 1), Crossland Platform (well Kunzea 1), Mowla Terrace (well Canopus 1) and Barbwire Terrace (well Acacia 2) (Figure 3.1; Table 3.1, 3.2). The sedimentological analysis is based primarily on drilled cores from the Geological Survey Western Australia (GSWA) Perth Core Library, Carisle, Western Australia.

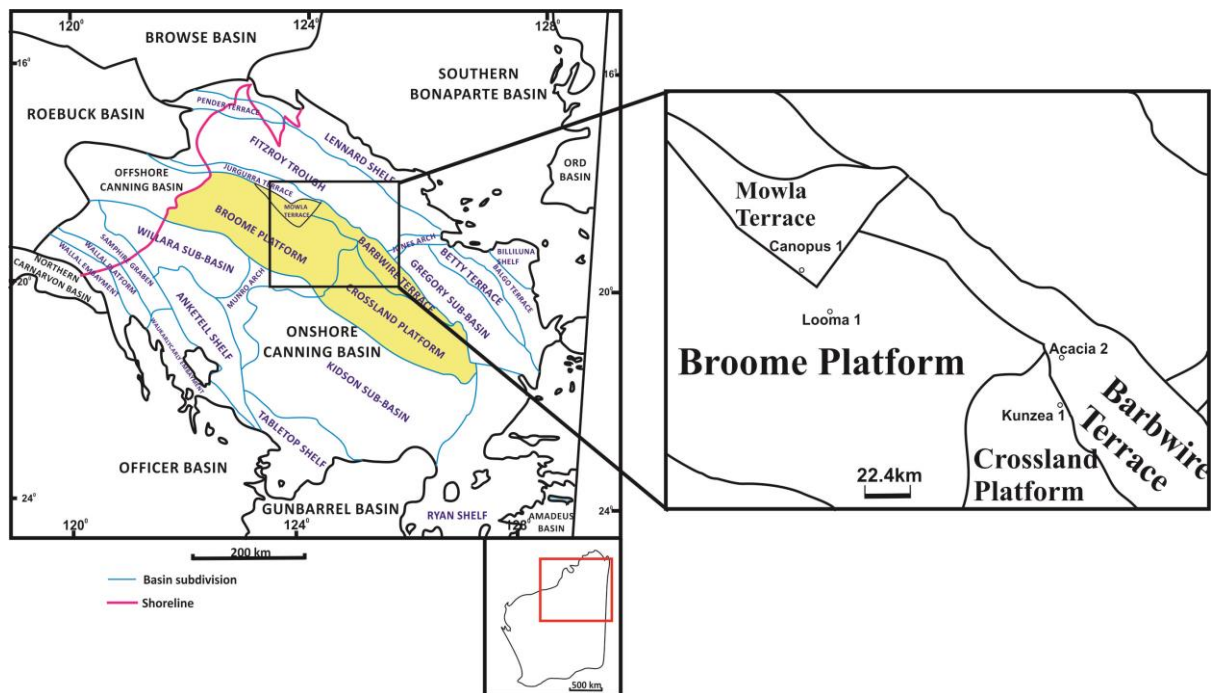


Figure 3.1: The location map of the study wells in Canning Basin, WA.

<b>Study Formation</b>	<b>References</b>
Nita Formation	Karajas and Kernick, 1984 McCracken, 1997 Hillock, 1988 King, 1998 Haines, 2004
Goldwyer Formation	Foster et al., 1986 McCracken, 1997 Haines, 2004

Table 3.1: Previous work published on the Middle Ordovician Nita and Goldwyer Formations in the Canning Basin with respect to facies descriptions.

<b>Wells</b>	<b>Formations</b>	<b>Depth (m)</b>
Acacia 2 (Barbwire Terrace)	Goldwyer Formation: Part of Unit 3	837-855.12
Looma 1 (Broome Platform)	Nita Formation: Part of Cudalgarra Member	1259-1272.5
	Nita Formation: Major part of Leo Member	1272.5-1350
Canopus 1 (Mowla Terrace)	Nita Formation: Part of Leo Member	1148.2-1156.6
Kunzea 1 (After Haines, 2004) (Crossland Platform)	Nita Formation: Full Cudalgarra Member	292-315
	Nita Formation: Full Leo Member	315-350
	Goldwyer Formation: Full Unit 4	350-400
	Goldwyer Formation: Major part of Unit 3	400-450
	Total thickness of core inspected and logged	275.52m

Table 3.2: Four studied wells from the Canning Basin, Western Australia in this study by using the methods of sedimentary logging, microfacies and thin section analysis.

The Nita and Goldwyer Formations are Middle Ordovician units which are not exposed but frequently intersected in the petroleum wells in the Canning Basin. Table 3.1 shows these two formations have been studied with respect to facies characteristics by several authors. The Nita Formation is dominated by dolostone and limestone with some amounts of mudstone. Previous lithofacies analysis of the Nita Formation suggested an intertidal to supratidal environment (Karajas and Kernick, 1984; McCracken, 1994; McCracken, 1997; King, 1998; Haines, 2004). McCracken (1994) named the upper Nita Formation as Cudalgarra Member whilst the lower Nita Formation is called the Leo Member in the subdivision of Admiral Bay Fault Zone.

Limestone in the Leo Member is characterised by cyclic subtidal carbonate rocks (McCracken, 1997) and is generally grey stylonodular wackestone, packstone, and lesser grainstone (Haines, 2004). A complete cycle of Cudalgarra Member in Admiral Bay Fault Zone consists of bioclastic and intraclastic grainstones and packstones (surf-zone sands), burrowed lime mudstones and wackestones (subtidal lagoonal mud) capped by a bored hardground, intertidal bioturbated, dolomitic algal mats and evaporitic terrigenous mudstones (McCracken, 1994). According to Karajas and Kernick (1984), the Cudalgarra Member in Broome Platform is dolomitised and was deposited in a supratidal environment. Dolostone of the Cudalgarra Member is commonly fine-grained and delicate primary features are often preserved; bioclasts and bioturbation become rare at this level. Towards the top of the Cudalgarra Member, interbedded grey, green and reddish mudstones increases in abundance and are finely laminated or flaser-bedded. Microbial laminations and evaporites are common near to the top of Cudalgarra Member (Haines, 2004).

The Goldwyer Formation is widely known from the subsurface Canning Basin, Western Australia. Microfossils of acritarchs, chitinozoans, macrofossils and conodonts indicate this formation deposited in a normal marine environment in Middle Ordovician time (Combaz and Peniguel, 1972; Legg, 1978; Nicoll, 1984; Playford and Martin, 1984; Watson, 1988; Winchester-Seeto et al., 2000; Quintavalle and Playford, 2008). Foster et al. (1986) subdivided the Goldwyer Formation into four lithologic members: Goldwyer Unit 1, Goldwyer Unit 2, Goldwyer Unit 3 and Goldwyer Unit 4 in ascending stratigraphic order in the Barbwire Terrace based on the gamma ray logs.

However, a significant limitation must be taken into account, because core is not available for most intervals of interest. Four wells were studied by using sedimentary

logging, microfacies analysis and thin section analysis (see Table 3.2), utilising what were considered to be the best available stratigraphic intervals.

### 3.2 Carbonate depositional environment

Major depositional environments of carbonates are shown in Figure 3.2. The carbonate platform is a shallow illuminated seafloor where carbonate is accumulated and precipitated easily (James and Kendall, 1992; Walker and James, 1992). The production, distribution and deposition of these shallow carbonates depend on the complex interaction of several external and internal controls. Many researchers have tried to identify the parameters controlling carbonate production and carbonate contents during the last two decades. The fourth-fifth order meter-scale and shallowing-upward carbonate cycles are the basic building blocks of most carbonate platform deposits in Proterozoic through Holocene periods (James, 1984; Wright, 1986; Elrick, 1995). A detailed model of cyclic carbonate sedimentation with the revival of the Milankovitch theory of orbital forcing has been refined greatly in the last decade (Goldhammer et al., 1990).

Folk (1973) described a variety settings on carbonate ramps or shelves and platforms associated with low-energy peritidal environments, especially tidal flats. Tidal flats may accrete from the shorelines of land areas and from around islands; they also occur on the leeward, protected sides of barriers on ramps and behind shoals and reefs on rimmed shelves. Three main zones are recognized for the peritidal environments which are subtidal, intertidal and supratidal.

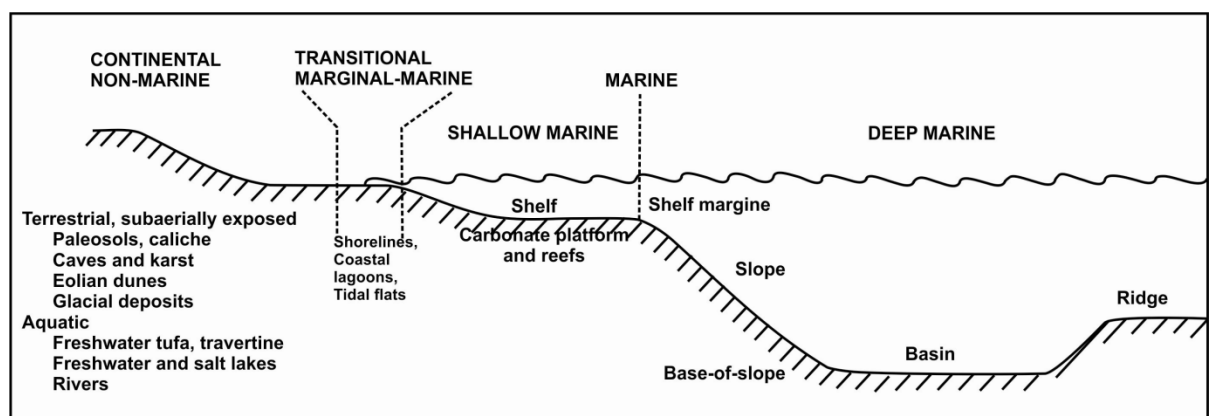


Figure 3.2: The settings of carbonate depositional environments (Flügel, 2010).

### 3.3 Results

Four cores were logged for the Nita and Goldwyer Formations in the Canning Basin. The legend of the sediment logs is shown in Figure 3.3. The core photos are attached as Appendix 1. Microfacies analysis of Nita Formation is based on core study and photomicrographs which were taken of thirty eight thin sections of representative microfacies. The microfacies are named according to the Dunham (1962) and Dunham extended classification for the interpretation of depositional environment.

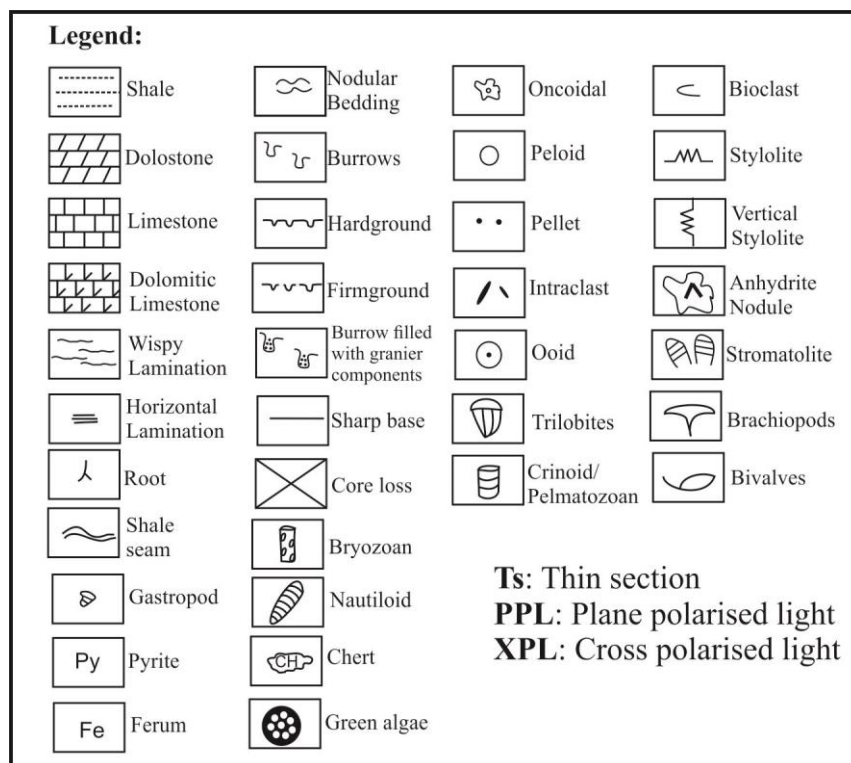


Figure 3.3: Legend for the graphic logs of selected drillcore for the Nita and Goldwyer Formations.

#### 3.3.1 Well Looma 1 of the Broome Platform

Well Looma 1 from Broome Platform (Latitude: 19° 07' 29.892"S; Longitude: 123° 59' 34.733"E) was drilled in Permit EP 353 in the Canning Basin of Western Australia by Shell Development Australia Pty. Ltd. The well spudded on July 4, 1996 with total depth of 2535m, which was reached on August 31, 1996 (Phipps et al., 1998). Well Looma 1 contains the transition zone of Cudalgarra and Leo Members

and a major part of Leo Member from depth 1259-1350m. The Goldwyer Formation is not available to study in this well.

### 3.3.1.1 Sediment log (well Looma 1)

The Nita Formation of well Looma 1 is logged from depth 1259m to 1350m (Figure 3.5-3.9) based on the legend in Figure 3.3. Depth from 1259m to 1272.5m is part of the Cudalgarra Member while 1272.5m to 1350m covers a major part of Leo Member. A sketch shows the logged intervals for well Looma 1 (Figure 3.4).

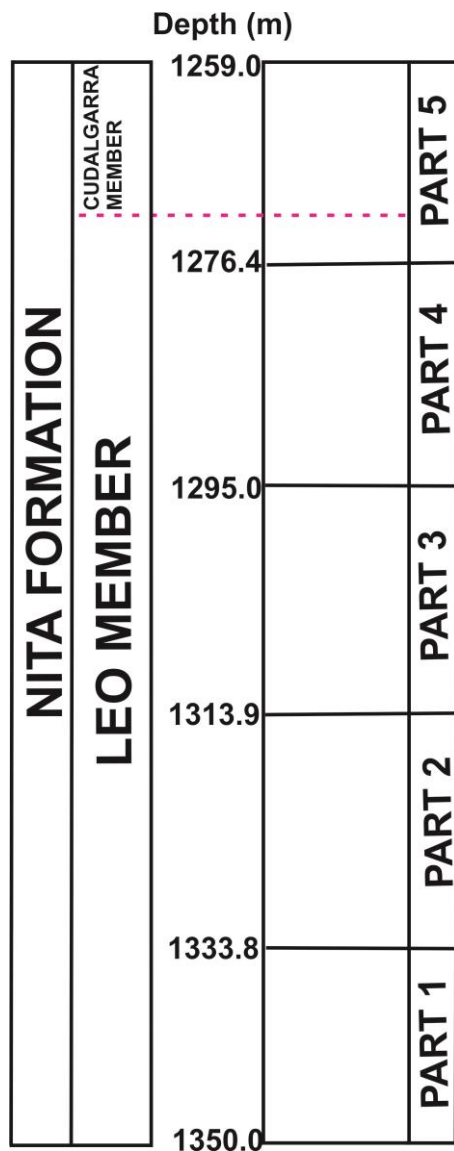


Figure 3.4: Sketch shows the logged interval from part 1 to part 5 for the following pages here for well Looma 1.

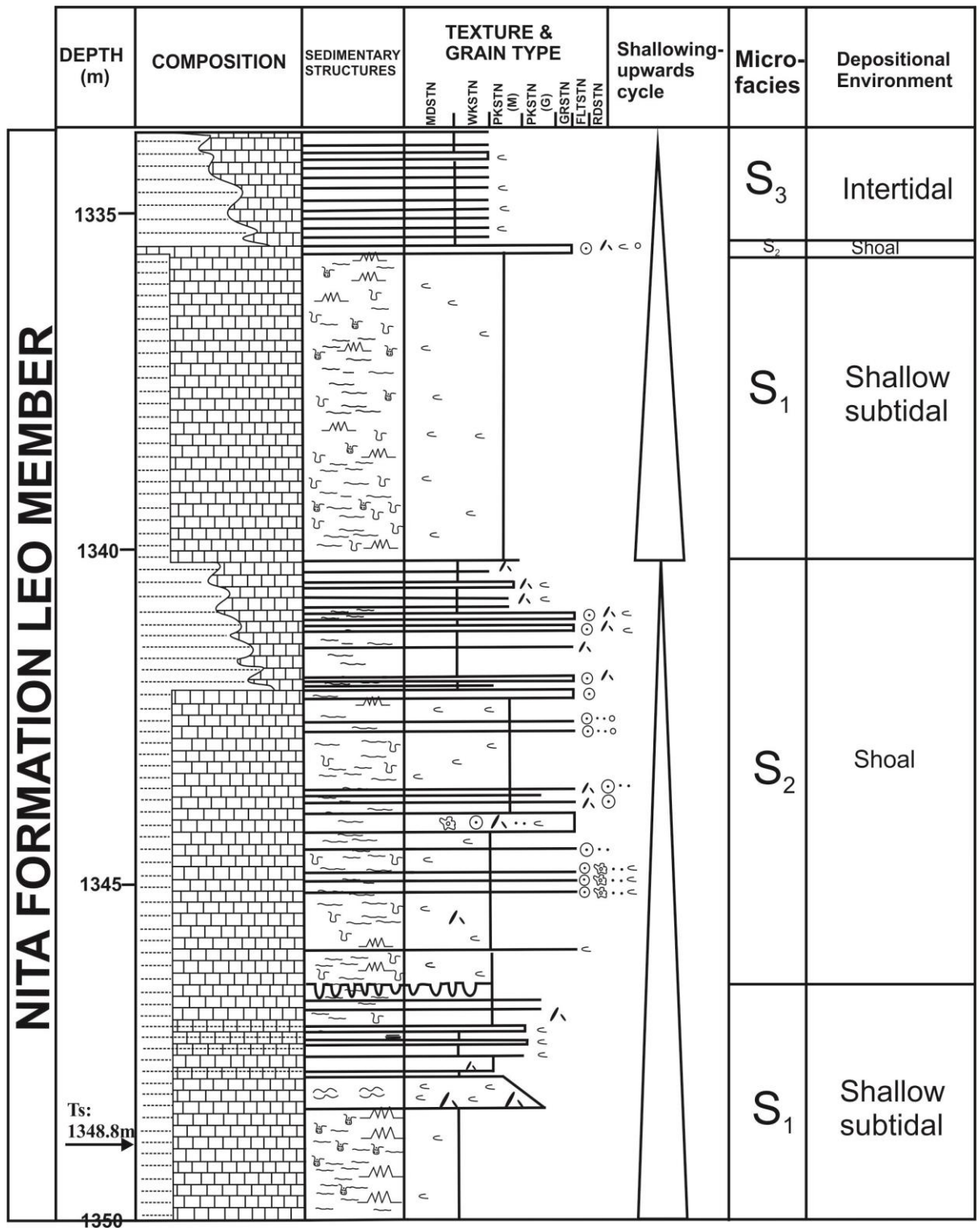


Figure 3.5: Sediment log of well Looma 1, part 1 from depth 1333.8m to 1350.0 m. Depositional environments and microfacies of the Leo Member, Nita Formation. Mineralogical composition was checked and determined by using TSG-core software. Refer legend Figure 3.3, page 32.

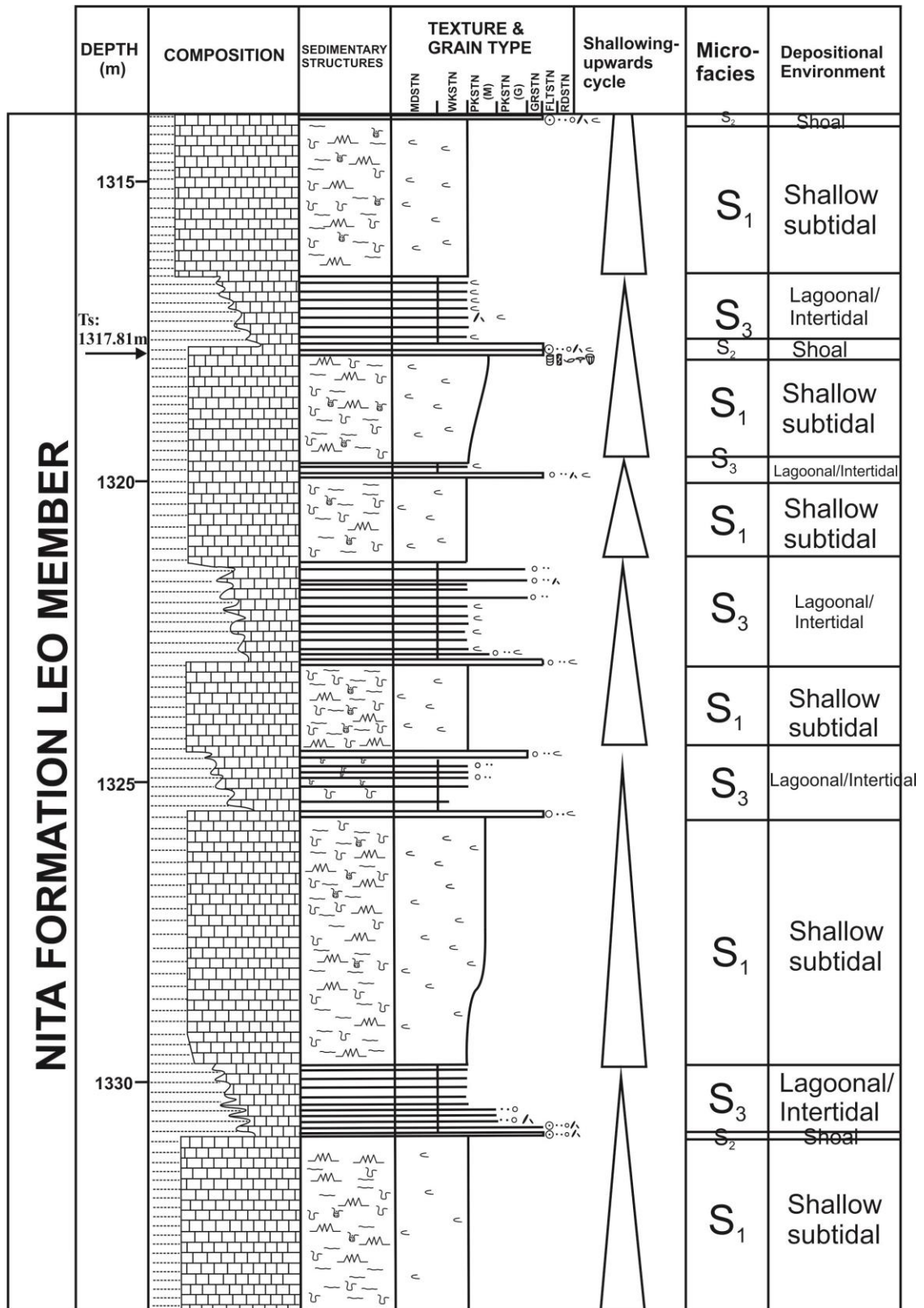


Figure 3.6: Sediment log of well Looma 1, part 2 from depth 1313.9m to 1333.8m. Depositional environments and microfacies of the Leo Member, Nita Formation. Mineralogical composition was checked and determined by using TSG-core software. For legend see Figure 3.3.

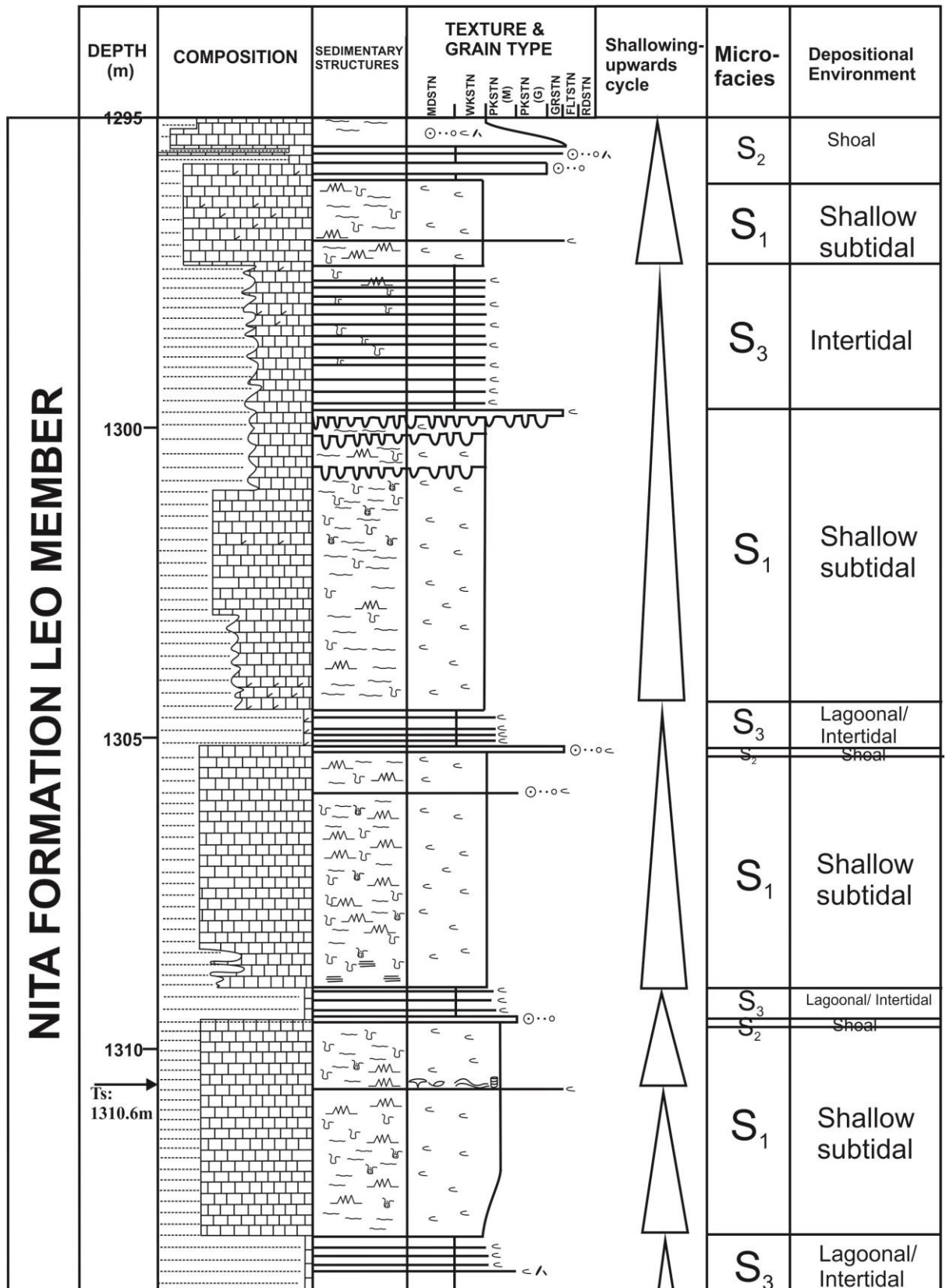


Figure 3.7: Sediment log of well Looma 1, part 3 from depth 1295.0m to 1313.9m. Depositional environments and microfacies of the Leo Member, Nita Formation. Mineralogical composition was checked and determined by using TSG-core software. For legend see Figure 3.3.

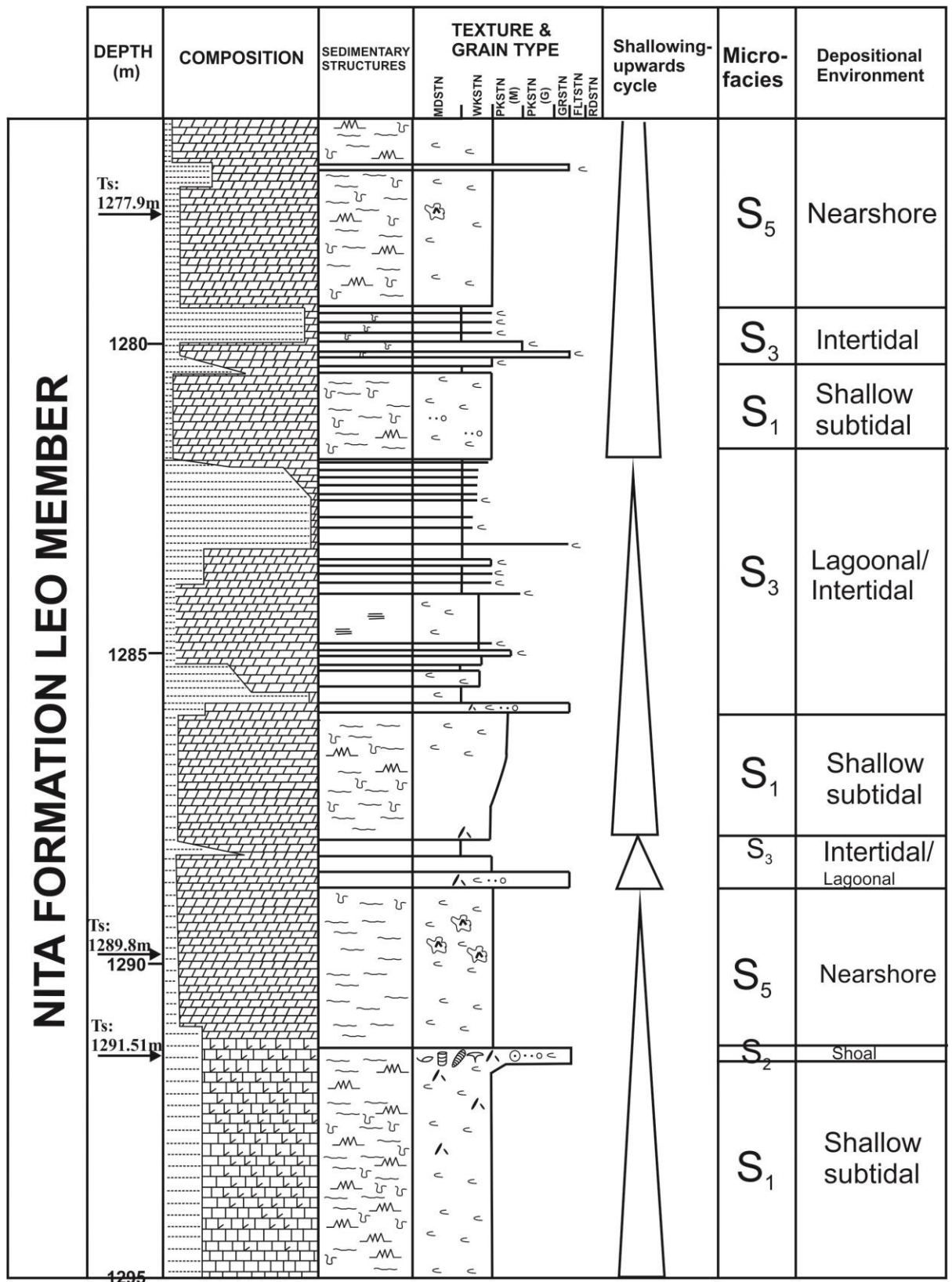


Figure 3.8: Sediment log of well Looma 1, part 4 from depth 1276.4m to 1295.0m. Depositional environments and microfacies of the Leo Member, Nita Formation. Mineralogical composition was checked and determined by using TSG-core software. For legend see Figure 3.3.

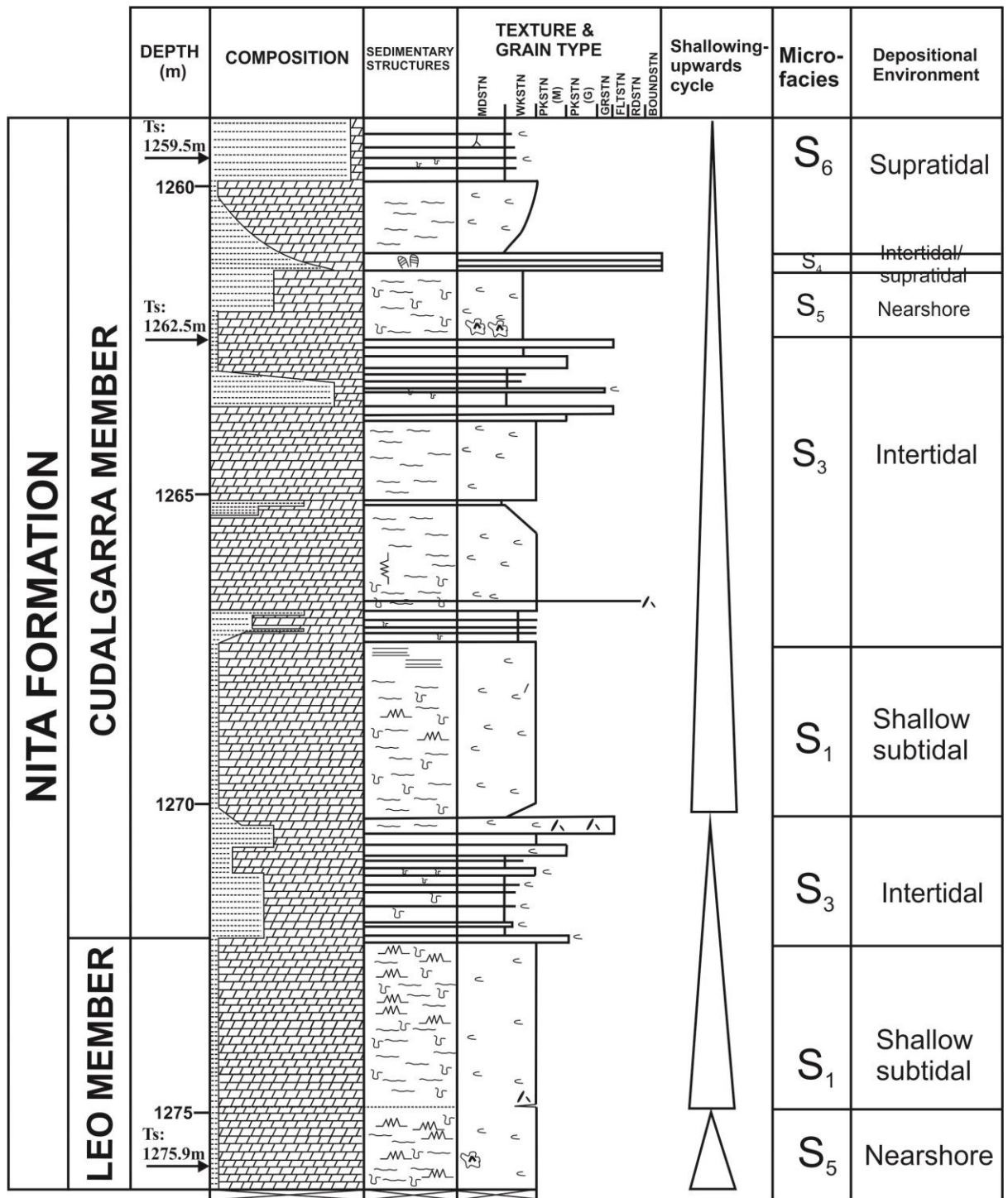


Figure 3.9: Sediment log of well Looma 1, part 5 from depth 1259.0m to 1276.4m. Depositional environments and microfacies of the Leo Member, Nita Formation. Mineralogical composition was checked and determined by using TSG-core software. For legend see Figure 3.3.

### **3.3.1.2 Microfacies associations for Looma 1**

The carbonate and mudstone of Middle Ordovician rocks for the well Looma 1 (depth 1259m-1350m) from Broome Platform, Canning Basin consists of six different microfacies. The microfacies associations are described as below.

#### **3.3.1.2.1 Microfacies 1 (S<sub>1</sub>): Burrowed, fossiliferous mudstone/wackestone**

The burrowed, fossiliferous mudstone/wackestone is present throughout the Nita Formation in well Looma 1. Figure 3.10A and Figure 3.11A show the core photo of this microfacies at depths 1348.8m and 1310.6m respectively. This microfacies has wispy lamination and is light grey in colour. Partially dolomitized strata commonly show burrow-associated patterns of selective replacement. The photomicrograph of the thin sections of depth 1348.8m shows the dolomitised burrow-fill wackestone (Figure 3.11B). Selectively dolomitized, burrow mottled carbonate rocks are common in this microfacies (Figure 3.10B and Figure 3.10C). Bioturbation or burrows also resulted in the reworking of terrigenous material which was deposited from suspension. The fossil fragments were not dolomitized and have been subsequently dissolved, leaving moldic porosity (Figure 3.11C). Such reservoir rocks with moldic porosity have high porosity but low to moderate permeability because the large moldic pores are connected to each other only through small intercrystalline conduits (Scholle and Ulmer-Scholle, 2003).

The main elements at depth 1310.6m are shale seam, bioclasts and stylolites. The bioclasts include bivalves (Figure 3.11C), pelmatozoans and brachiopods. The bivalves were dissolved and the molds were later filled with sparry calcite. The shale seam is compressed between two different minerals, which are dolomite and calcite (Figure 3.11B). Stylolite is found near to the shale seam (Figure 3.11C).

The dominant microfacies of this association, burrowed, fossiliferous mudstone/wackestone are consistent with deposition in shallow subtidal settings. Burrows are the most common features that can be observed in shelf carbonates both in intertidal and especially subtidal settings (Flügel, 2010). Hillock (1988) suggested the environment of deposition where a large population of burrowing fauna populated cohesive sediment (which destroyed most layering that formed) is the shallow subtidal zone.

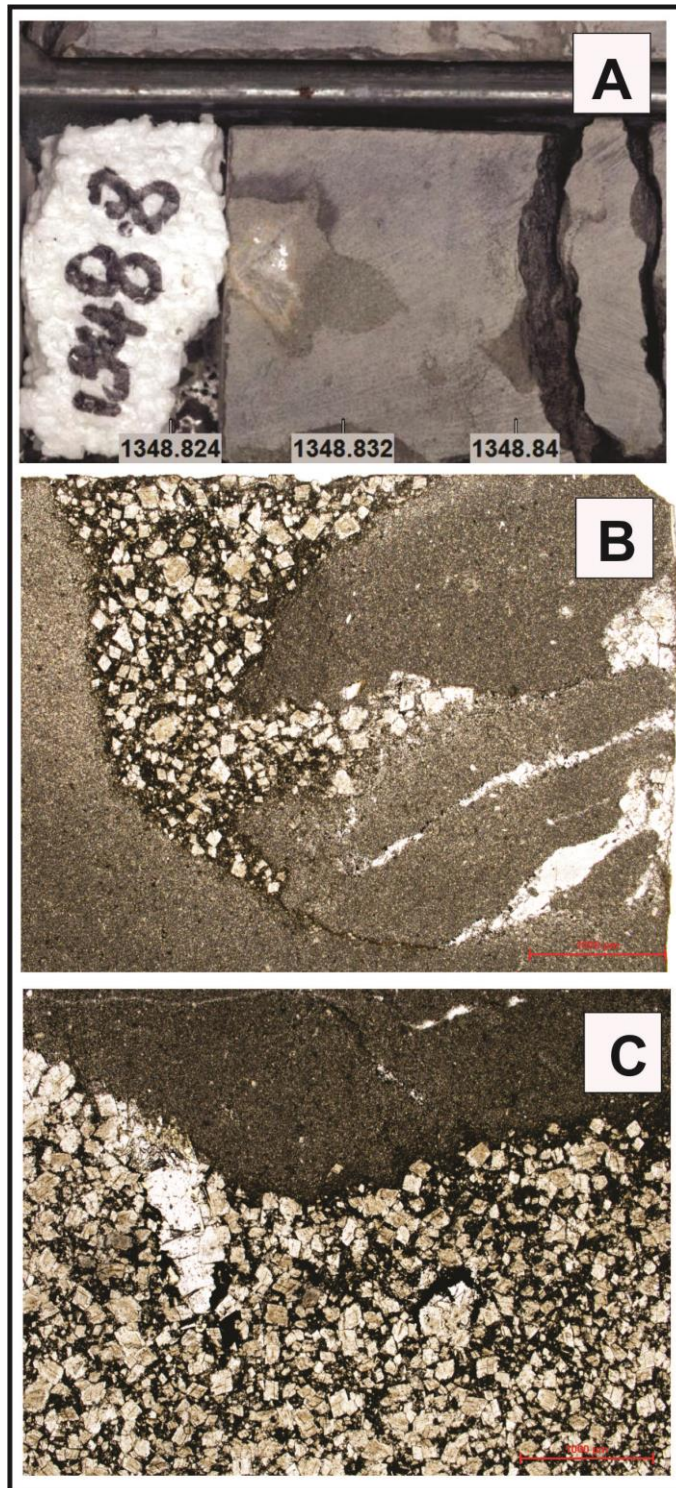


Figure 3.10: **A.** Core photo of depth 1348.8m for microfacies  $S_1$ : burrowed, fossiliferous lime mudstone/ wackestone, well Looma 1. **B.** Photomicrograph of microfacies  $S_1$ : burrowed, fossiliferous lime mudstone/ wackestone for well Looma 1. (**B:** scale bar (bottom right) = 1mm) **C.** Detail of part of dolomitised burrow-fill shown in **B.** Note rhombic dolomite crystals. (**C:** scale bar (bottom right) = 1mm).

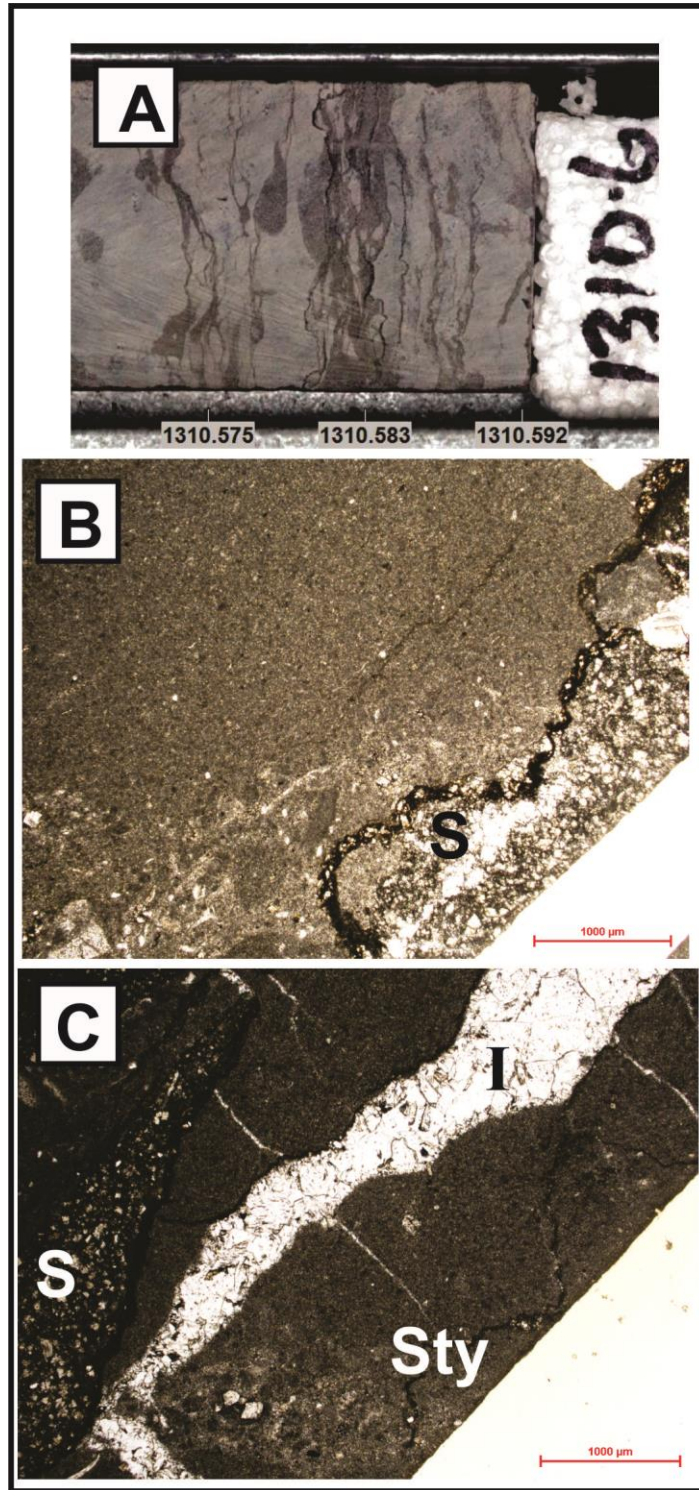


Figure 3.11: **A.** Core photo of depth 1310.6m, for microfacies  $S_1$ : burrowed, fossiliferous lime mudstone/ wackestone, well Looma 1, showing wispy lamination and wackestone fabric. **B.** Shale seam (S), 1310.6m, PPL, scale bar = 1mm. **C.** Recrystallized bivalve (I), stylolites (Sty) and s (S), 1310.6m, PPL, scale bar = 1mm. For location of section see Fig 3.7.

### **3.3.1.2.2 Microfacies 2 (S<sub>2</sub>): Oolitic/peloidal/intraclastic and bioclastic packstone/grainstone**

The oolitic/peloidal/intraclastic and bioclastic packstone/grainstone is present throughout the Nita Formation Leo Member in well Looma 1. Figure 3.12 shows the core photo of this microfacies. Figure 3.13 shows the photomicrograph of the thin sections of this microfacies at depths 1317.81m and 1291.51m. Ooids, peloids and intraclasts can be identified in this microfacies (Figure 3.13). They have been micritized and dolomitized in the centre part. The ooids that have been micritized and dolomitized (Figure 3.13B and 3.13D) with no remnant structure visible in this section and the grain would have to be classed as peloids because other than size and shape, no textural characteristics remain that would allow identification of these grains as ooids. In this section, bivalve shells, brachiopod walls, nautiloids, bryozoans, trilobites and crinoids can also be identified.

The impunctate brachiopod shell wall in this microfacies has an extremely thin (or diagenetically altered) primary layer and a thick secondary layer. This type of brachiopod resembles *Platystropha cypha* (Scholle and Ulmer-Scholle, 2003). Bivalve/Pelecypod shells found in this microfacies were dissolved and the molds were later filled with sparry calcite (Figure 3.13A and 3.13D). Crinoids/pelmatozoans in Figure 3.13F have bioclasts with characteristic single-crystal or unit extinction and uniform “honeycomb” microtexture, with the small pores filled with micrite with central canal. Crinoid arm plates with U-shape and Trilobites (Figure 3.13C), nautiloid (Figure 3.13E) and bryozoans (Figure 3.13B) are found in this microfacies, The bryozoans are in cryptostomid forms (Figure 3.13B) and are regarded as autochthonous components of the assemblage; this type of bryozoans are well preserved indicating only limited reworking (Flügel, 2010).

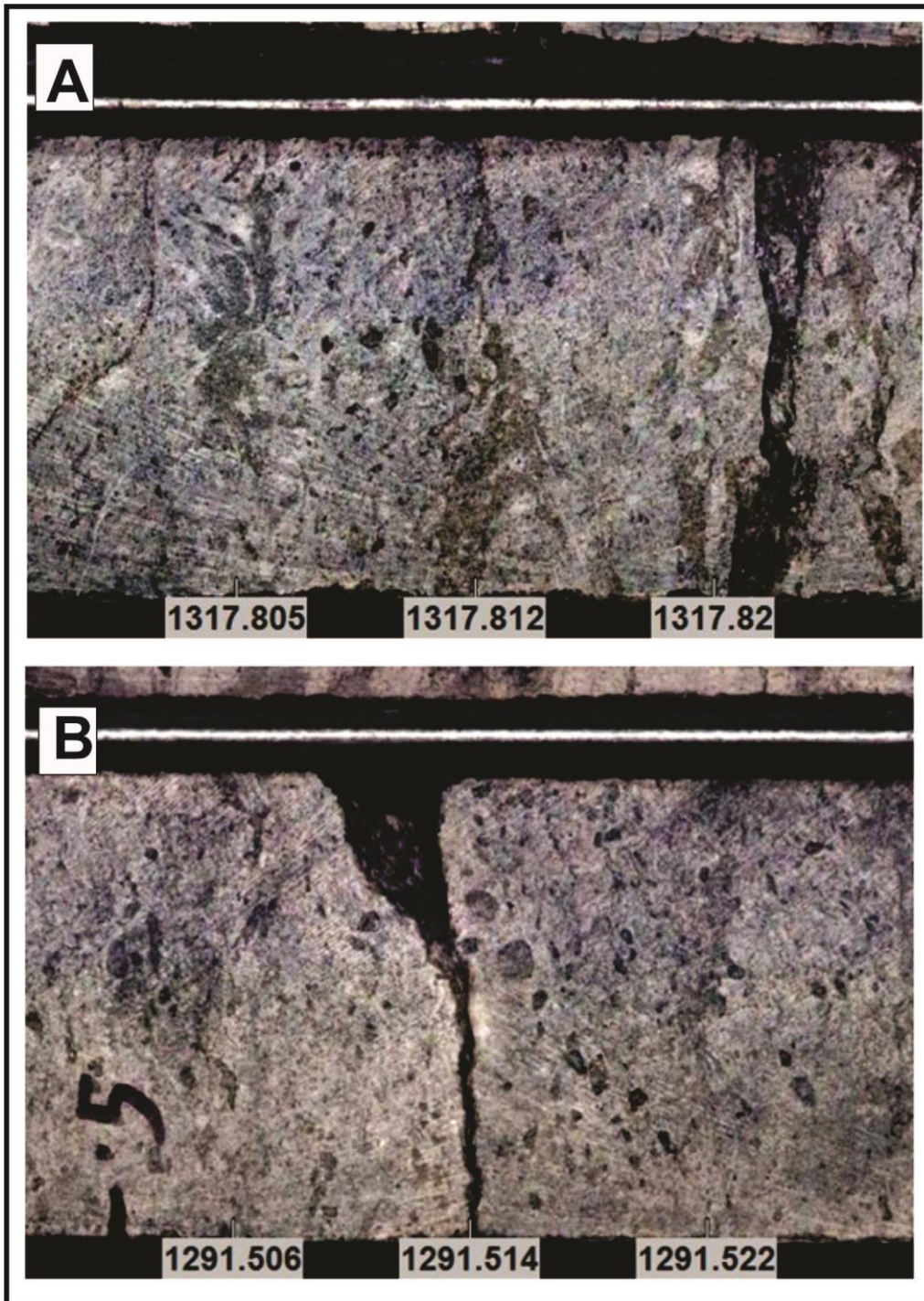


Figure 3.12: Core photos of microfacies S<sub>2</sub>: Oolitic/peloidal/intraclastic and bioclastic packstone/grainstone for well Looma 1. **A.** Packstone/grainstone fabric at 1317.81m. **B.** Packstone/grainstone fabric at 1291.51m.

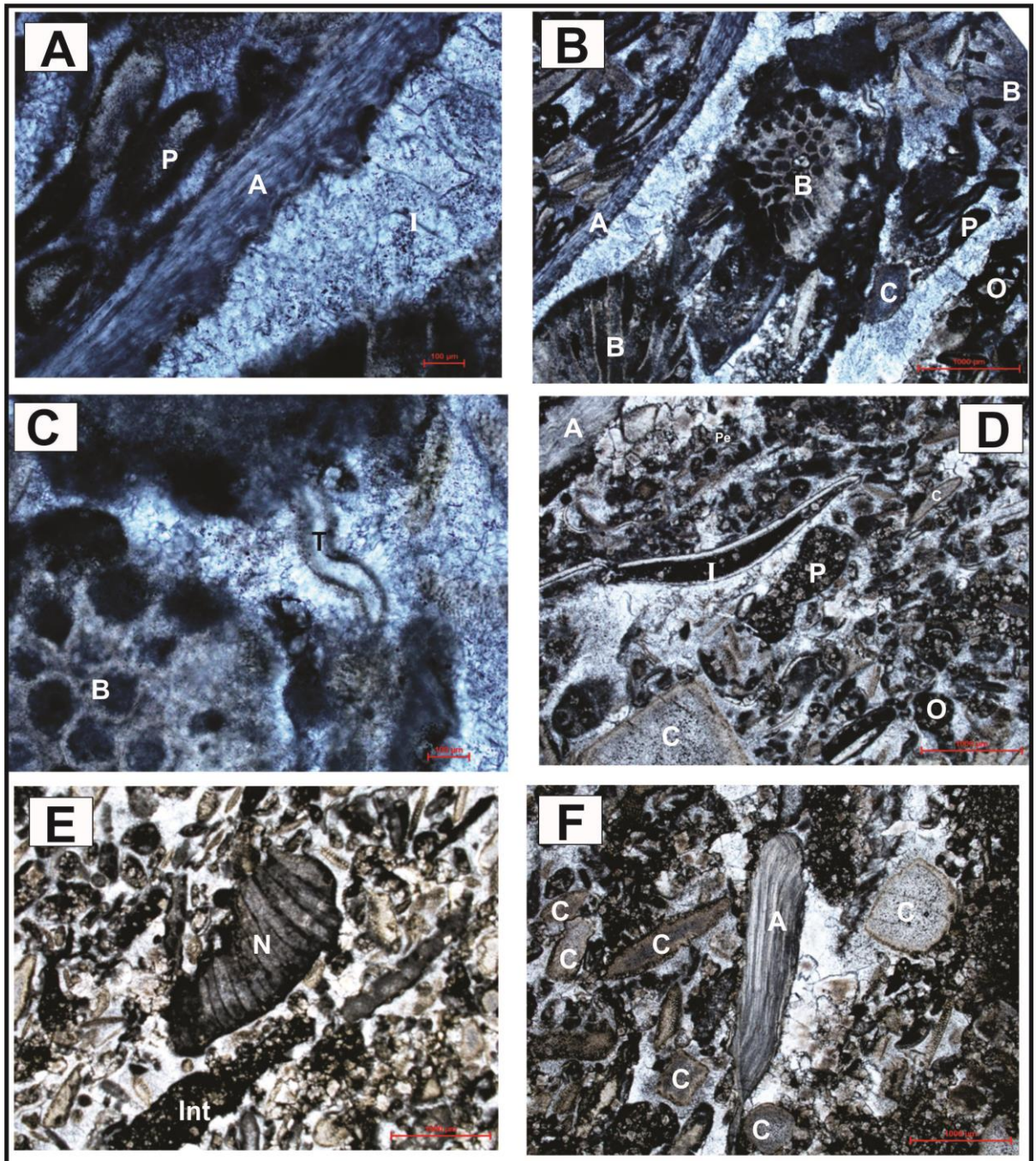


Figure 3.13: Photomicrograph of microfacies  $S_2$ : Oolitic/peloidal/intraclastic and bioclastic packstone/grainstone from A to F for well Looma 1, showing constituents and fabrics. **A.** A brachiopod wall (A), recrystallised bivalve (I) and peloid (P). 1317.81m, PPL, scale bar = 0.1mm. **B.** Bryozoans (B), crinoids (C), peloid (P), brachiopod (B) and ooid (O). 1317.81m, PPL, scale bar = 1mm. **C.** Bryozoan (B) and trilobite (T). 1317.81m, PPL, scale bar = 0.1mm. **D.** Bivalve (I), brachiopod (A), crinoid (C), ooid (O), peloid (P) and pellet (Pe). 1291.51m, PPL, scale bar = 1mm. **E.** Nautiloid (N) and intraclast (Int). 1291.51m, PPL, scale bar = 1mm. **F.** Brachiopod (A) and crinoids (C). 1291.51m, PPL, scale bar (at bottom right) = 1mm.

### 3.3.1.2.3 Microfacies 3 (S<sub>3</sub>): Interlaminated shale and wackestone/packstone

Interlamination between shale and wackestone-packstone are common in the Nita Formation, well Looma 1 (Figure 3.14). This muddy laminated microfacies was likely deposited in an intertidal environment. Where this type of microfacies overlies the shoal environment sediments and peloids are present, the depositional environment might be lagoonal/intertidal, as upward shallowing took place.

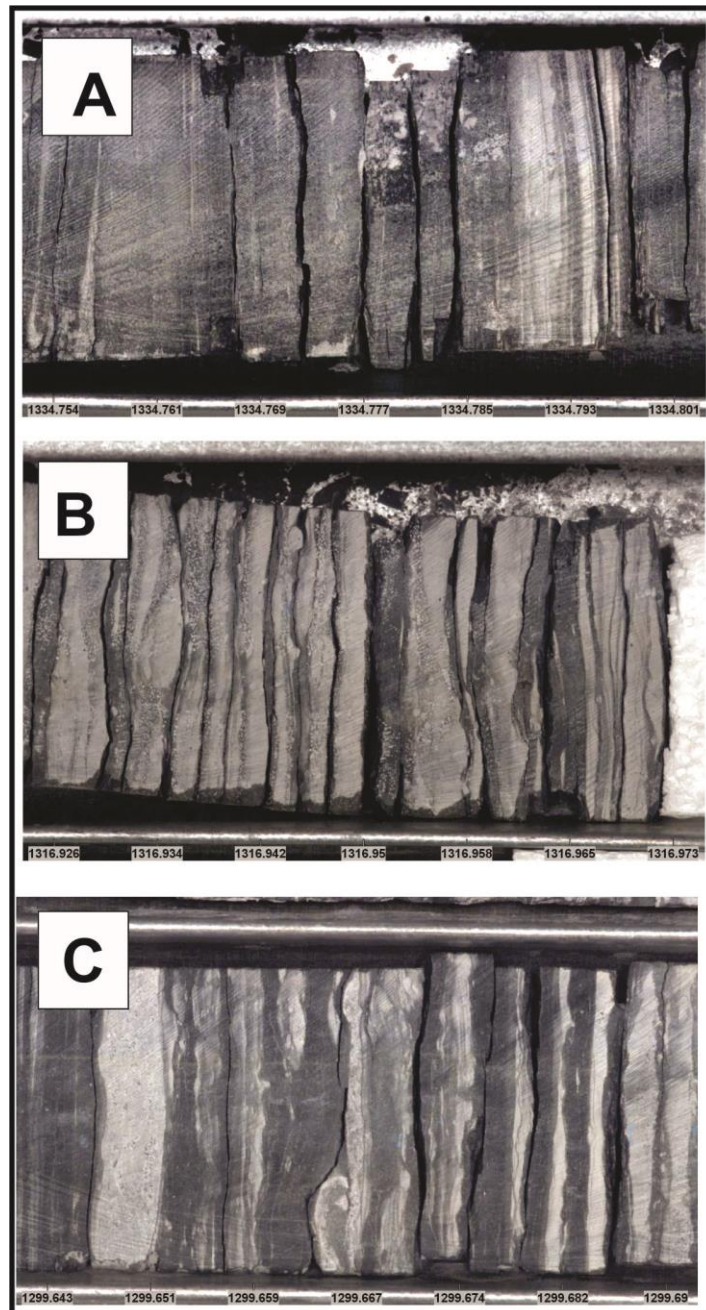


Figure 3.14: Core photos of microfacies S<sub>3</sub>. Shows mixing between microfacies. A. Depth 1334.754-1334.801m. B. Depth 1316.926-1316.973m. C. 1299.643-1299.69m. Note the interlaminated character of this muddy low energy microfacies, shale/wackestone packstone. Shale laminae are dark, carbonate are light coloured.

#### 3.3.1.2.4 Microfacies 4 (S<sub>4</sub>): Microbial laminites

Sediments with microbial lamination are very common within the rock-record, however, their origins are not easy to determine since there are many mechanisms which can produce the microbial laminations and these processes can occur in several different environments (Demico and Hardie, 1994). This microfacies is probably produced by cyanobacteria because it has continuous and wavy laminae (Figure 3.15), so it resembles microbially influenced sedimentation. The microbial mat is preserved as laminites at the top part of the sediment log, from depth 1261m to 1262m.

In this study area the microbial laminites are identified as high intertidal-supratidal deposits because a terrigenous shale with the supratidal environment is above the microbial mats. Karajas and Kernick (1984) identified the facies as intertidal, and, where rhombic dolomite crystals or molds were present, they diagnosed an intertidal to supratidal environment. Also, solution of dolomite crystals has generated secondary porosity of potential reservoir significance in some wells.

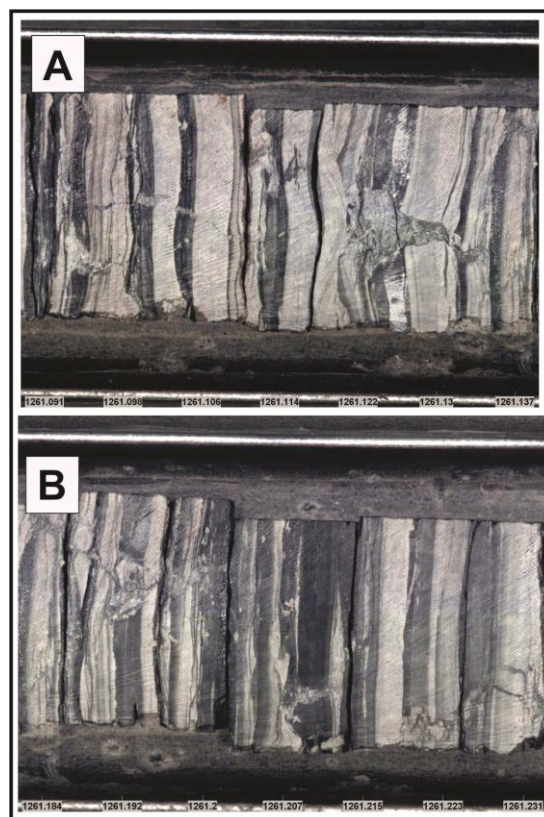


Figure 3.15: Core photos of microfacies S<sub>4</sub>: microbial laminites. **A.** Depth 1261-1261.137m. **B.** 1261.184-1261.231m. Note well developed laminar fabric with only small disturbance by burrowers.

### **3.3.1.2.5 Microfacies 5 (S<sub>5</sub>): Evaporitic wackestone**

The microfacies evaporitic wackestone contains the element of white nodular anhydrite. Figure 3.16A, Figure 3.17A, Figure 3.18A and Figure 3.19A are the core photos as the examples of this microfacies. Note that the white colour dots are anhydrite nodules (Figure 3.16A). The photomicrograph of anhydrite under the cross polarised light has different colours (Figure 3.16C). Burrows or bioturbation are rare in this microfacies. The original tidal-flat dolomicrite has been overprinted and filled with anhydrite (Figure 3.16B). Anhydrite cements are commonly found as early porosity filling agents in arid-region, coastal, evaporitic carbonates (Scholle and Ulmer-Scholle, 2003).

The evaporite deposits are products of arid environments. According to Haines (2004), evaporites or their pseudomorphs may be present near the top of the formation, particularly within the Cudalgarra Member when differentiated. Phipps et al. (1998) suggested that lack of fossils, presence of distorted anhydrite nodules and bands with microcrystalline texture characterise sediments that are deposited in nearshore environments.

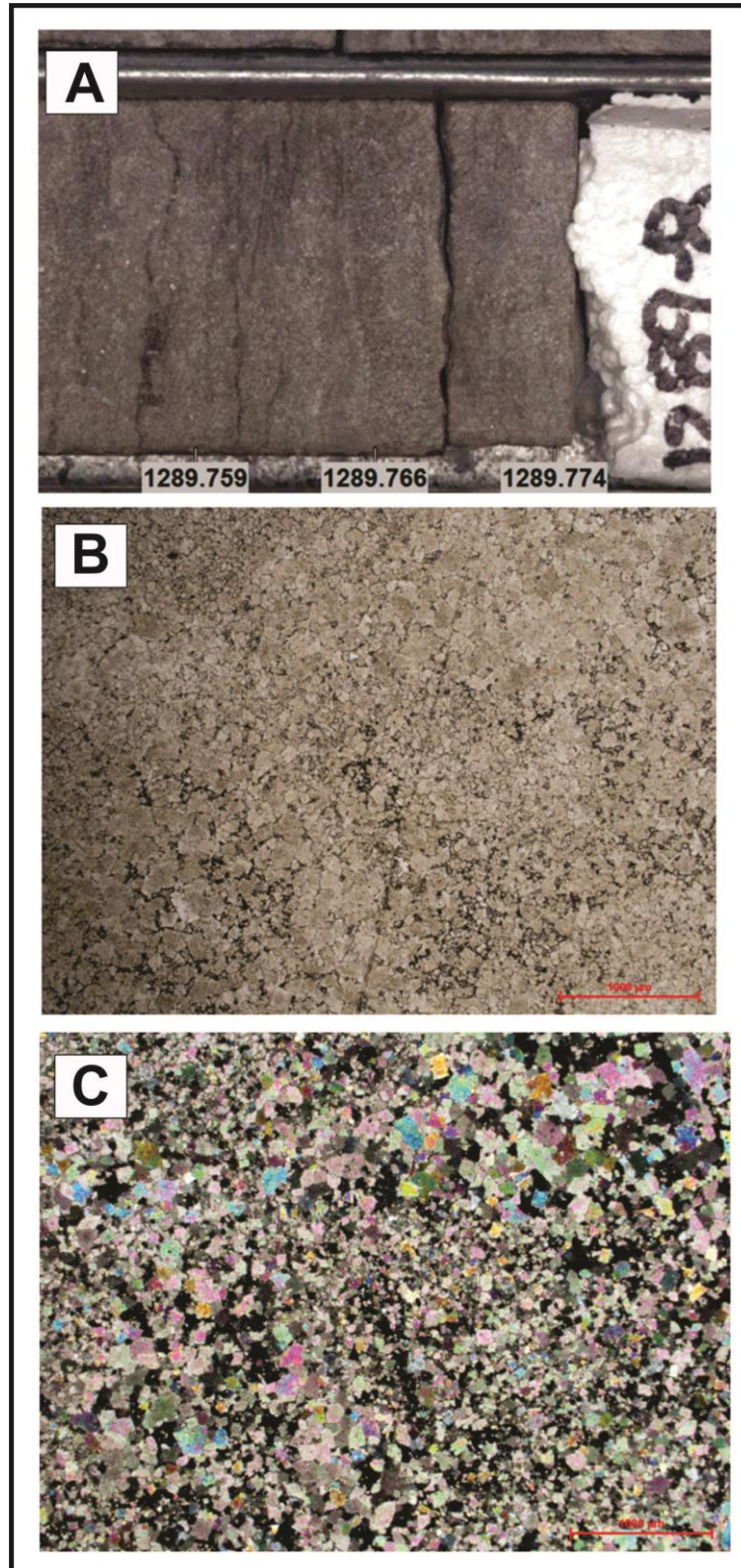


Figure 3.16: **A.** Core photo of depth 1289.8m, well Looma 1. **B and C.** Photomicrographs of microfacies  $S_5$ : Evaporitic wackestone. Note the anhydrite crystals with different colours in **C**. 1289.8m, **B** is PPL and **C** is XPL, scale bar (at bottom right) = 1mm.

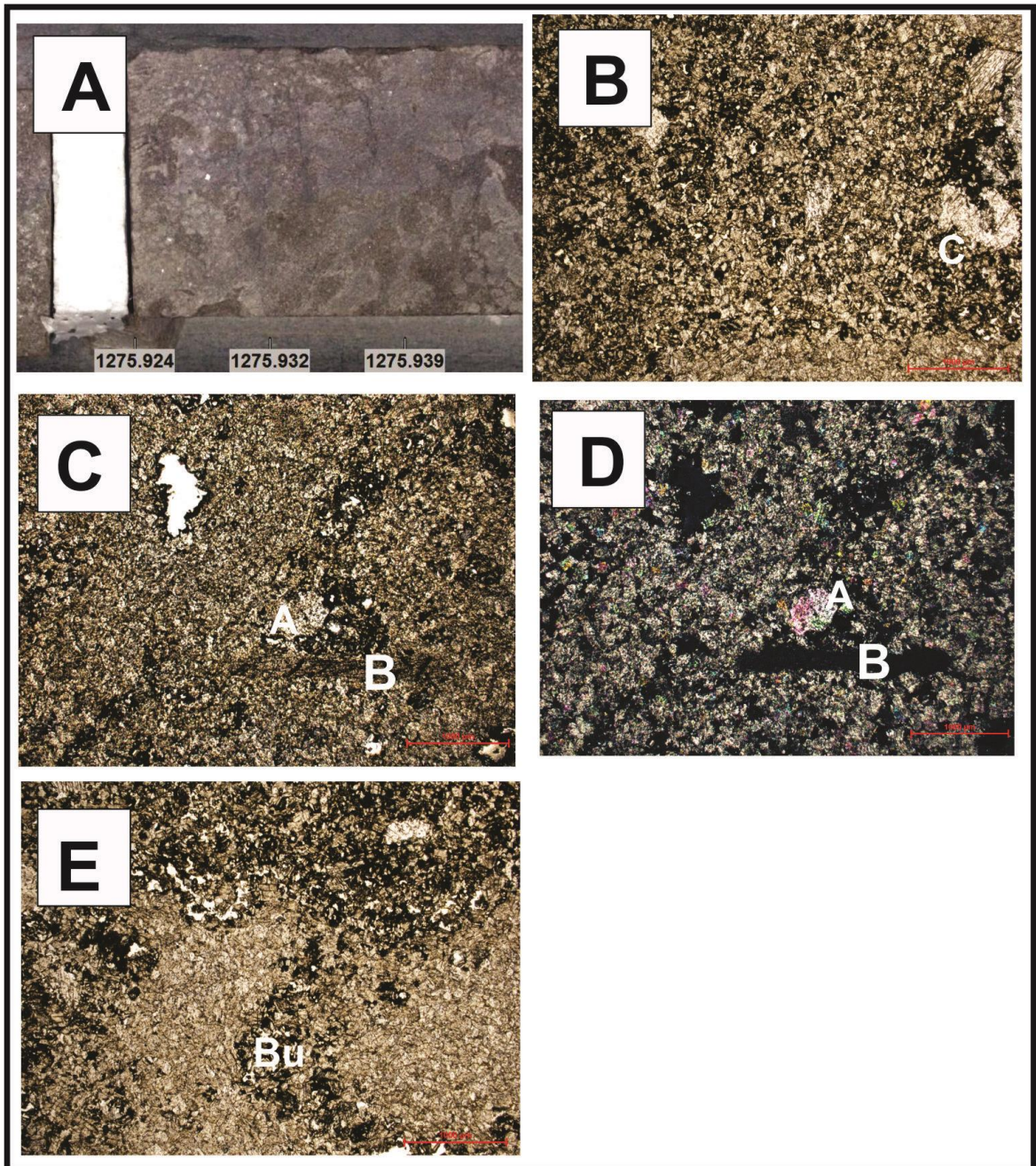


Figure 3.17: A. Core photo of depth 1275.9m, well Looma 1.

**B-E:** Photomicrographic of microfacies S<sub>5</sub>: Evaporitic wackestone.

**B:** Crinoid/Pelmatozoan arm plate (C).

**C and D:** Note the anhydrite crystal (A) with different colour in **D** and bivalve (B).

**E:** Burrows (Bu).

1275.9m, **B, C and E** is PPL; **D** is XPL; scale bar (at bottom right) = 1mm.

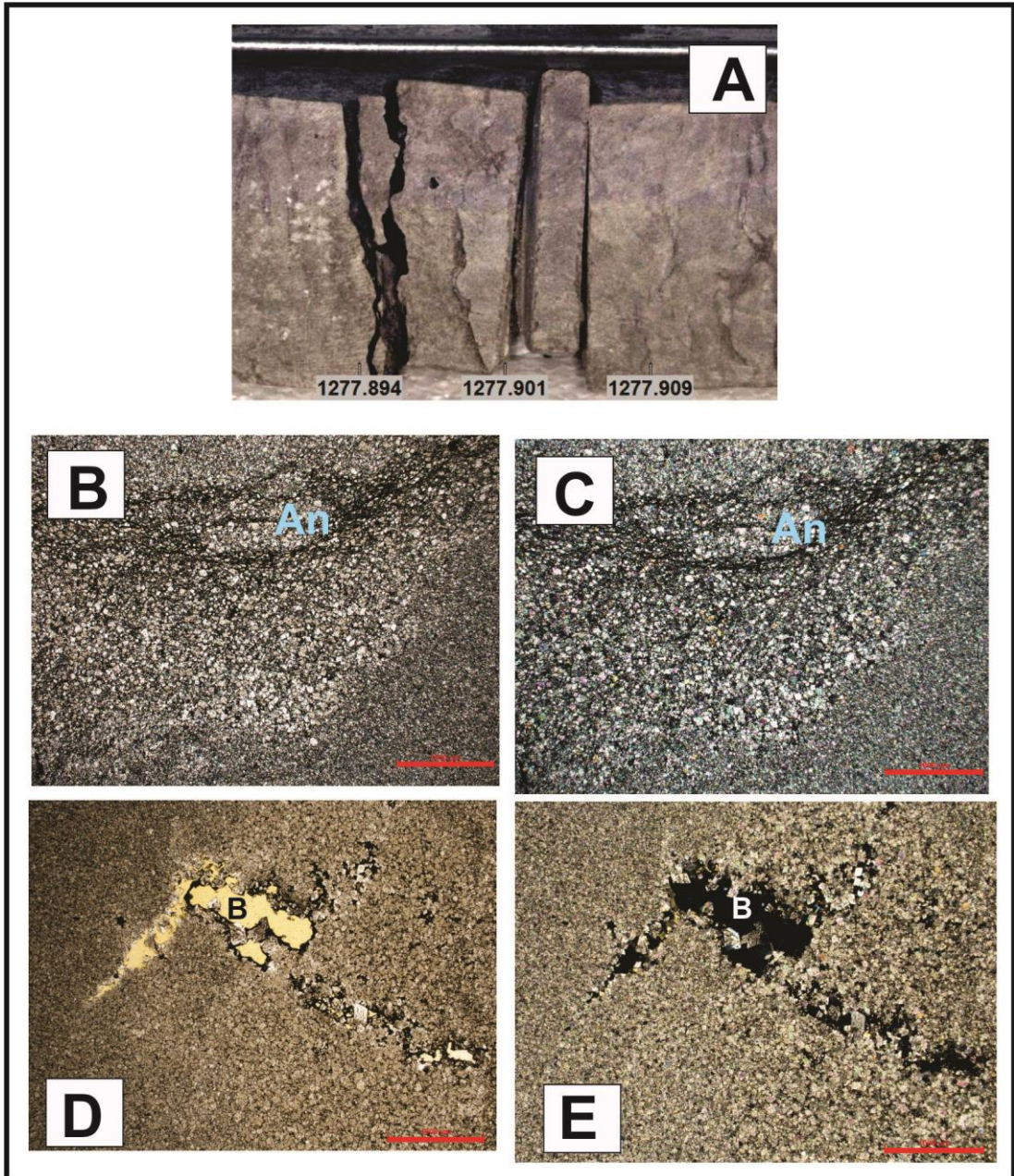


Figure 3.18: **A.** Core photo of depth 1277.9m, well Looma 1, for microfacies  $S_5$ : Evaporitic wackestone. Note that the white colour dots are anhydrite nodules

**B-E:** Photomicrographic of microfacies  $S_5$ : Evaporitic wackestone.

**B and C:** Note the anhydrite crystal (An) with different colour in **C**.

**D and E:** Note the bivalve fragment (**B**) has dissolved and created a secondary porosity.

1277.9m, **B and D** are PPL and **C and E** are XPL, scale bar (at bottom right) = 1mm.

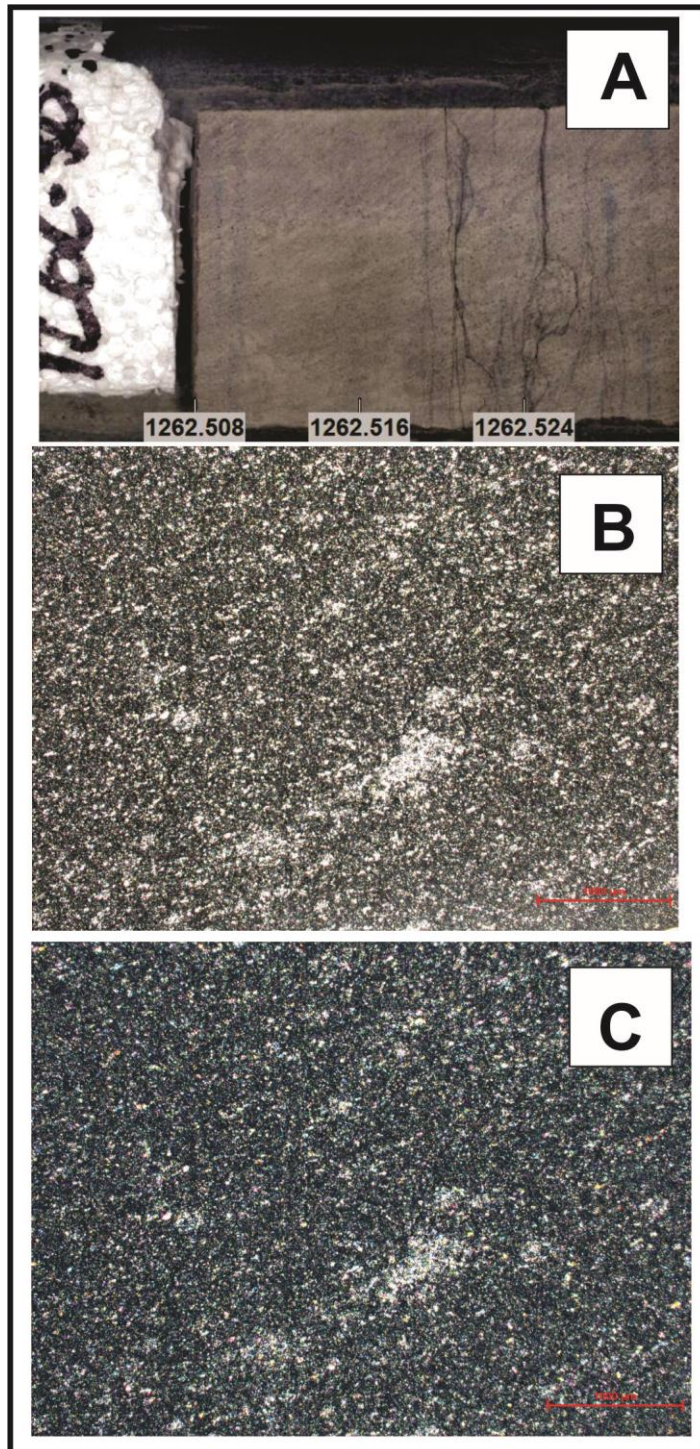


Figure 3.19: **A**. Core photo of depth 1262.5m, well Looma 1 for microfacies S<sub>5</sub>: Evaporitic wackestone.

**B and C**: Photomicrographic of microfacies S<sub>5</sub>: Evaporitic wackestone.

**B and C**: Note the anhydrite crystal with different colour in **C**.

1262.5m, **B** is PPL and **C** is XPL, scale bar (at bottom right) = 1mm.

### 3.3.1.2.6 Microfacies 6 (S<sub>6</sub>): Terrestrial shale

The terrestrial shale is a red dolomitic mudstone. It is distinguished by its colour due to iron oxidation or exposure. Roots are found at this microfacies (Figure 3.20A). Mudstone is interbedded with this terrestrial shale and the core photo is shown in Figure 3.20A. Generated fabrics produced by root structuring are present. The photomicrograph of depth 1259.5m shows that the mudstone contains oil staining (Figure 3.20B; Figure 3.20C).

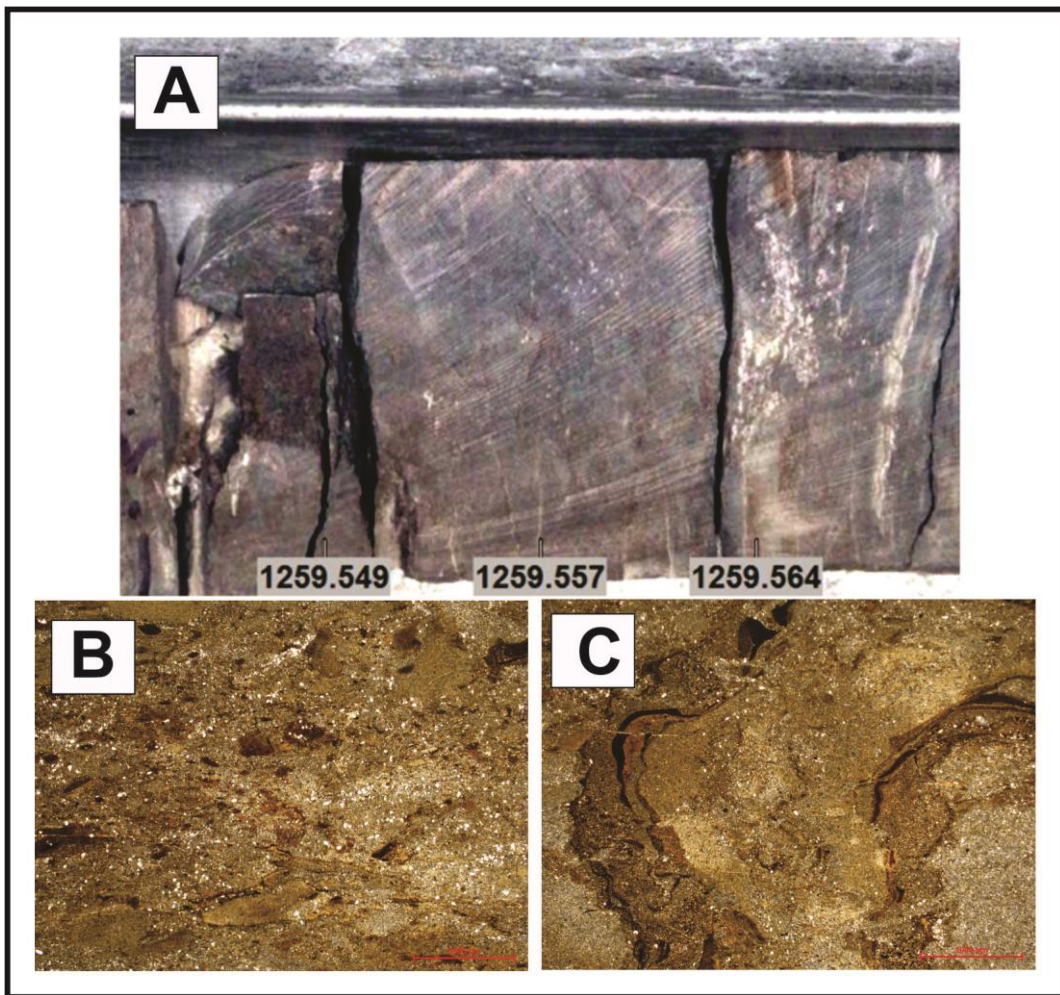


Figure 3.20: **A**. Core photo of 1259.5m, well Looma 1. Note that probable root material (black colour) is present. **B and C**: Oil stained recrystallised mudstone. 1259.5m, PPL, scale bar (at bottom right) = 1mm.

### 3.3.1.3 Discussion (Well Looma 1)

The Nita Formation available to study in well Looma 1 covers an interval from 1350-1260m. There are approximately 20 cycles identified throughout Nita Formation in well Looma 1. From these approximately 20 cycles, the sequence can be divided into 5 types of cycles based on the sedimentology.

Cycle I: Shallow subtidal - shoal facies

Cycle II: Shallow subtidal – shoal – lagoonal/intertidal facies

Cycle III: Shallow subtidal – intertidal facies

Cycle IV: Shallow subtidal – shoal – nearshore facies

Cycle V: Shallow subtidal – intertidal – intertidal/supratidal – supratidal facies

#### 3.3.1.3.1 Depositional environment

Depositional environment for Nita Formation sediments in well Looma 1, Broome Platform is a low energy tidal flat shallowing upward sequence. Based on the sediment log and photomicrographic observations, the Nita sediments were deposited in shallowing upward sequence (Figures 3.5-3.9), which is from shallow subtidal, shoal, lagoonal/intertidal to supratidal environments, as follows:

<b>Microfacies</b>	<b>Depositional environment</b>
Burrowed, fossiliferous mudstone/wackestone	Shallow subtidal
Oolitic/peloidal/intraclastic and bioclastic packstone/grainstone	Shoal
Interlaminated shale and wackestone/packstone	Intertidal
Microbial laminites	Intertidal/ supratidal
Evaporitic wackestone	Supratidal
Terrestrial shale	Supratidal

Garland (1997) suggested that bivalves inhabited restricted conditions within a lagoon. Crinoids are tolerant of normal or near normal-marine conditions and therefore they can be used as environmental indicators. Palaeozoic forms of crinoids occurred mainly as attached organisms (pelmatozoans) in shelf or shelf-marine settings (Scholle and Ulmer-Scholle, 2003). Crinoids are common in both warm- and cold- water settings, even extending into Arctic and Antarctic waters (Scholle and Ulmer-Scholle, 2003). Trilobites are common in shallow shelf settings (Scholle and Ulmer-Scholle, 2003). As a conclusion, the presence of these bioclasts suggested that Nita Formation was deposited in a shallow marine environment. The presence of ooids, microbial mats and evaporites suggest that conditions during deposition were warm water, tropical with shallow seas with relatively thin upward-shallowing cycles capped by arid microbial to evaporitic tidal flats.

Although there is shale towards the top of the sediment log from depth 1275m to 1259m, the microbial mat (microfacies S<sub>4</sub>) and terrigenous shale (microfacies S<sub>6</sub>) show that there is a shallowing upwards sequence. The shaly sediment may indicate transgression during sea level rise. These strongly expressed upward shallowing thin cycles represent stacked microbial tidal flats and Milankovitch scale sea-level fluctuations.

### **3.3.2 Well Acacia 2 of the Barbwire Terrace**

Well Acacia 2 from Barbwire Terrace (Latitude: 19° 07' 29.892"S; Longitude: 123° 59' 34.733"E) was drilled in Permit EP 143 in the Canning Basin of Western Australia by a National 610 UE rig operated by ATCO APM Drilling Pty. Ltd. The well spudded in on July 2, 1982 with total depth of 1573m, which was reached on July 6, 1982 (Watson and Derrington, 1982). Well Acacia 2 contains part of the Goldwyer Formation Unit 3 (Goldwyer middle carbonate) from depth 837-855.12m.

### 3.3.2.1 Sediment log (well Acacia 2)

The Goldwyer middle carbonate (Goldwyer Unit 3) of well Acacia 2 is logged from depth 837m to 855.12m (Figure 3.21). Note that the legend is in Figure 3.3.

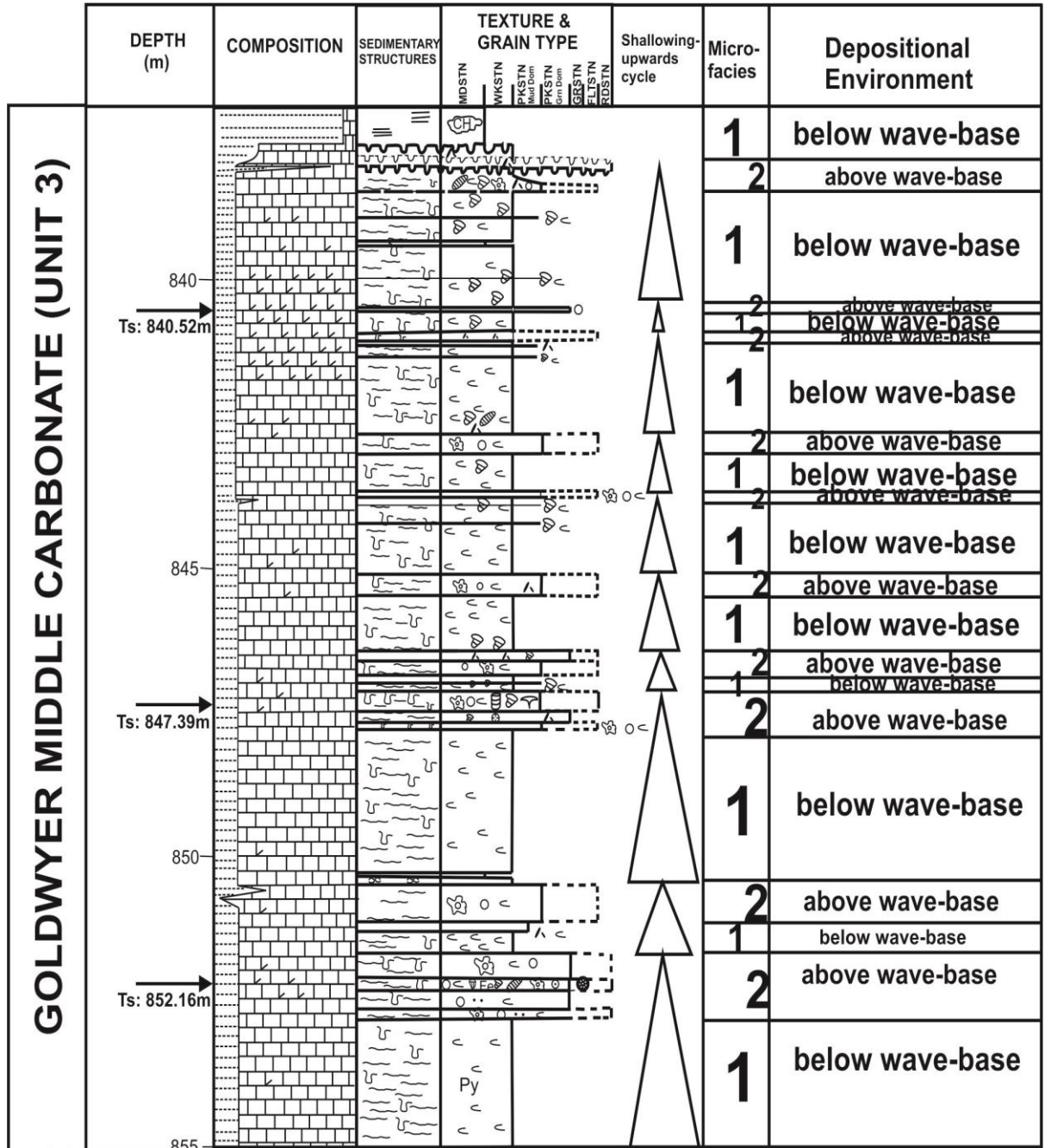


Figure 3.21: Sediment log of well Acacia 2, part of Goldwyer Formation Unit 3. Burrowed wackestones alternate with peloidal packstone/floatstone in metre to decimetre scale units representing upward coarsening cycles. Legend of this sediment log is in Figure 3.3.

### 3.3.2.2 Microfacies associations for Acacia 2

From the sediment log shown in Figure 3.21, part of the Goldwyer middle carbonate for the well Acacia 2 (depth 837m-855.12) from Barbwire Terrace, Canning Basin consists of two different microfacies. The microfacies associations are described as below.

#### 3.3.2.2.1 Microfacies 1: Gastropod bioclastic burrowed wackestone

The microfacies gastropod bioclastic burrowed wackestone with meter scale has the sedimentary structures of burrows and wispy lamination. Figure 3.22 is the core photo as the example of this microfacies. Note the burrows and wispy lamination in this microfacies at depth 840.54m (Figure3.22). Burrows are the most common features that can be observed in shelf carbonates both in intertidal and especially subtidal settings (Flügel, 2010). However, the decimetre-scale peloidal packstone/floatstone units that cap this microfacies show an upward coarsening cycle. Thus, it is suggested that the microfacies gastropod bioclastic burrowed wackestone is deposited in a subtidal setting, below wave-base.

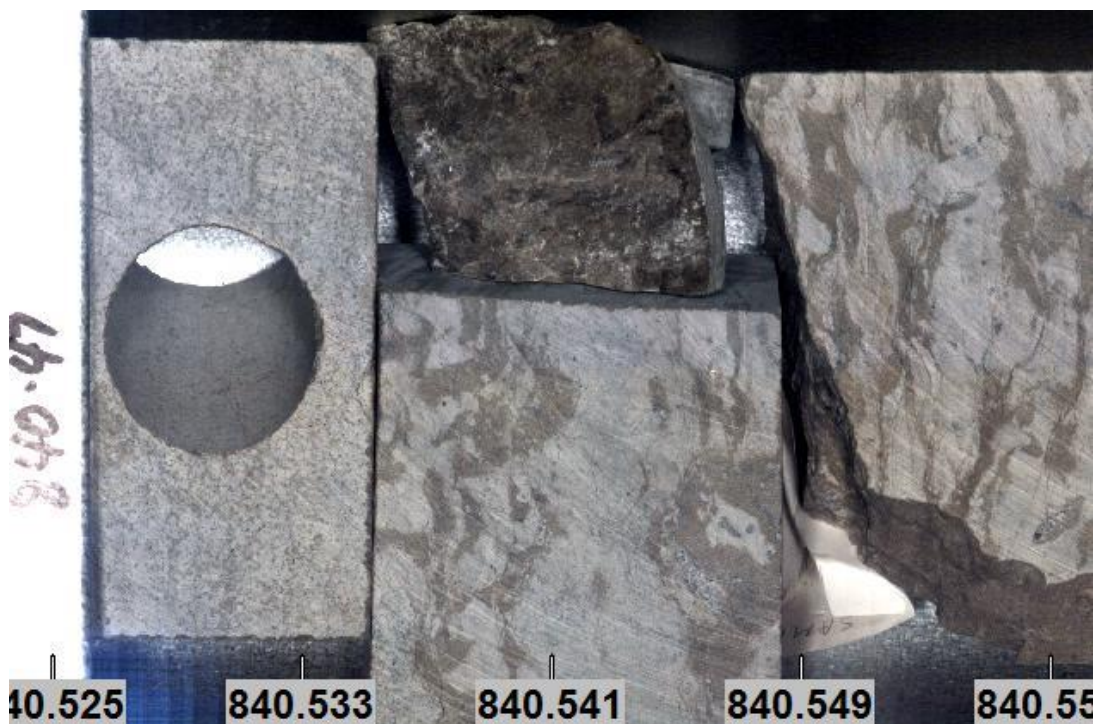


Figure 3.22: An example of microfacies gastropod bioclastic burrowed wackestone at depth 840.54m. Note the burrows and wispy lamination in this microfacies.

### 3.3.2.2.2 Microfacies 2: Oncoidal-peloidal packstone/floatstone with ooids and bioclasts

The microfacies oncoidal-peloidal packstone/floatstone with ooids and bioclasts (decimetre scale) has the wispy lamination sedimentary structures and occasionally with burrows. Figure 3.23 is the core photo as the examples of this microfacies. Note the oncoids and peloids in this microfacies at depth 847.324m (Figure 3.23). Figure 3.24 shows another example of this microfacies at depth 847.32m. The buff colour of the rocks is due to the presence of iron (see Figure 3.21).

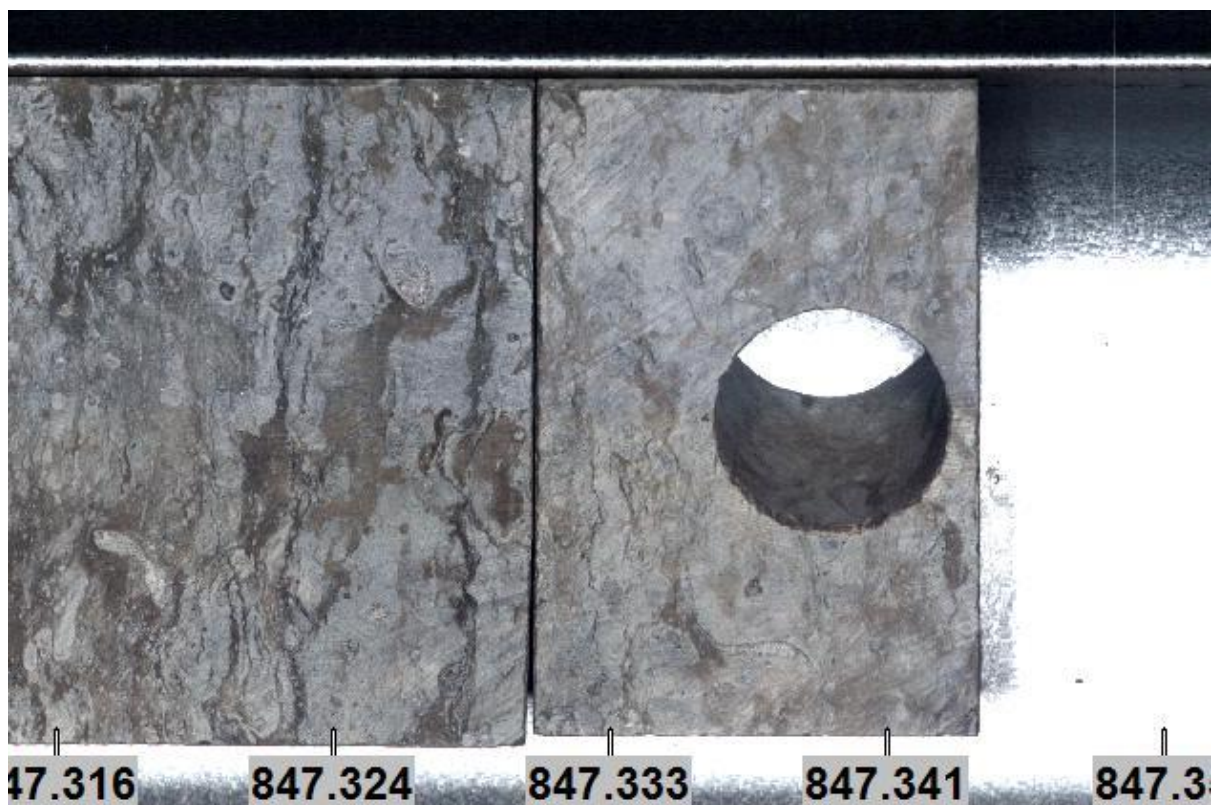


Figure 3.23: An example of microfacies oncoidal-peloidal packstone/floatstone at depth 847.324m. Note the oncoids and peloids in this microfacies at depth 847.324m show the packstone/floatstone fabric.

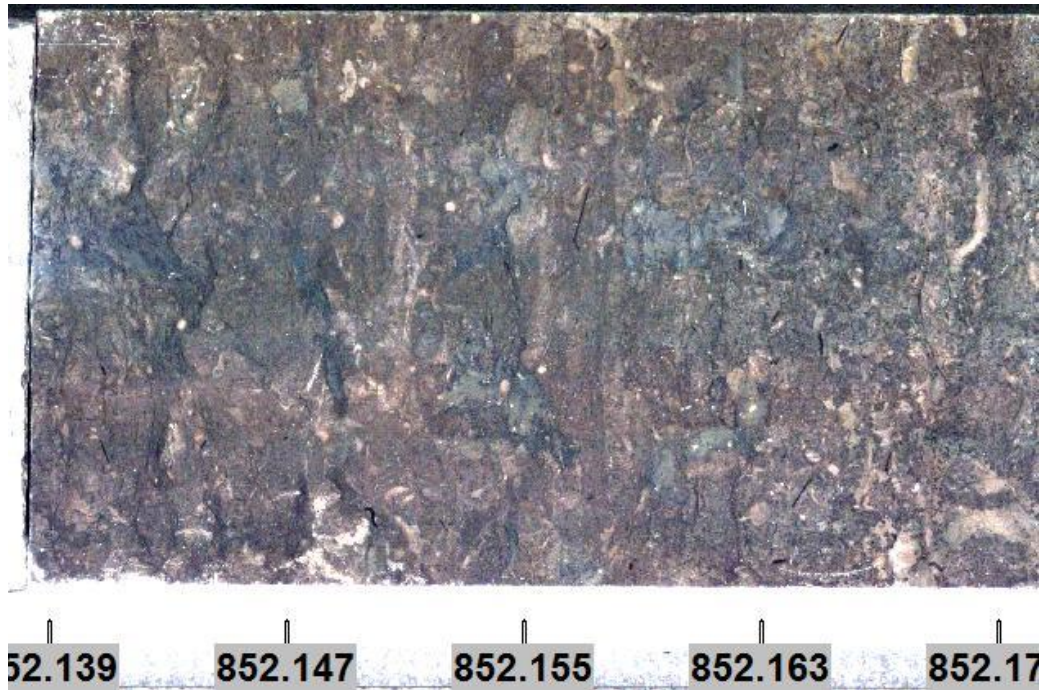


Figure 3.24: An example of microfacies oncolidal-peloidal packstone/floatstone at depth 847.324m. Note the buff to dark colour of this section is due to the presence of iron.

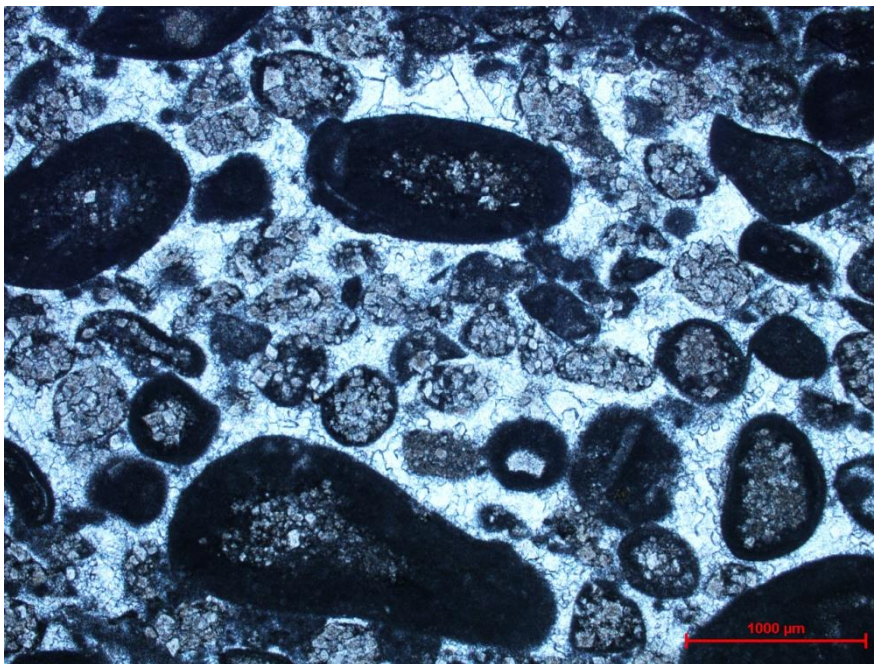


Figure 3.25: Photomicrograph of microfacies peloidal packstone/floatstone with ooids and bioclasts. Peloids dominate this microfacies in this section. Peloids and oolites shows packstone fabric while intraclast with  $>2\text{mm}$  shows floatstone fabric. 840.52m, PPL, scale bar (at bottom right) = 1mm.

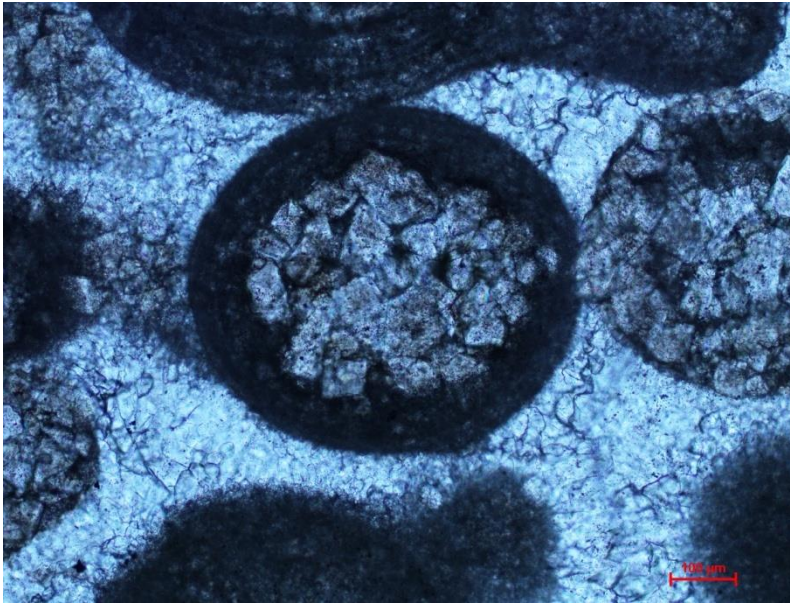


Figure 3.26: Photomicrograph of microfacies peloidal packstone/floatstone with ooids and bioclasts. Note that ooid was filled with dolomitised grains in the centre part. 840.52m, PPL, scale bar (at bottom right) = 0.1mm.

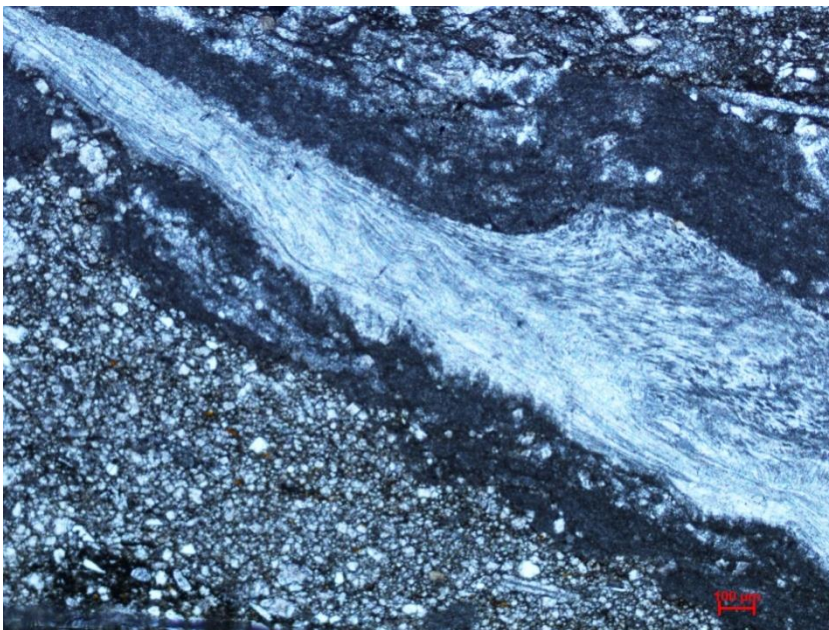


Figure 3.27: Photomicrograph of microfacies peloidal packstone/floatstone with ooids and bioclasts. Brachiopod in floatstone facies. This is an example of an impunctate shell wall in the brachiopod *Platystropha cypha*. This shell has an extremely thin primary layer and a thick secondary layer. Note the typical low-angle fibrous structure and the substantial lateral variations in shell thickness. 847.39m, PPL, scale bar (at bottom right) = 0.1mm.

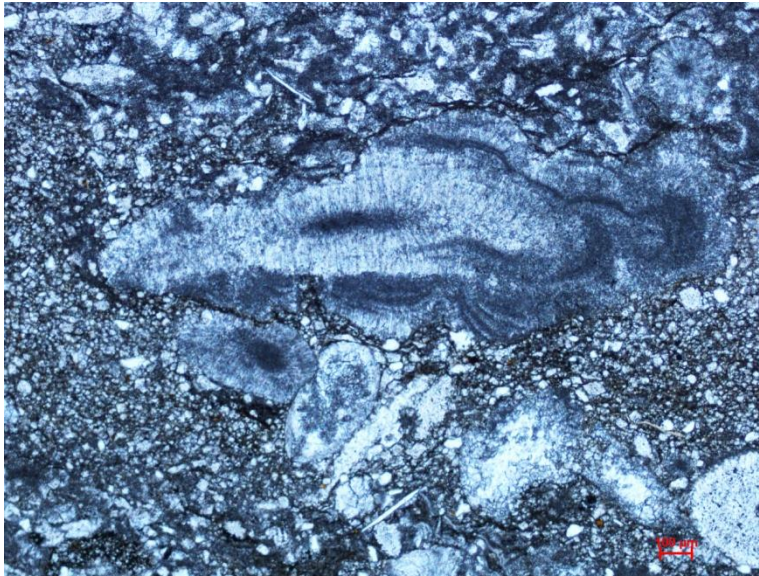


Figure 3.28: Photomicrograph of microfacies peloidal packstone/floatstone with ooids and bioclasts. Note the oncoids in the centre part, ooid at top right and crinoids/pelmatozoan at bottom right. 847.39m, PPL, scale bar (at bottom right) = 0.1mm.

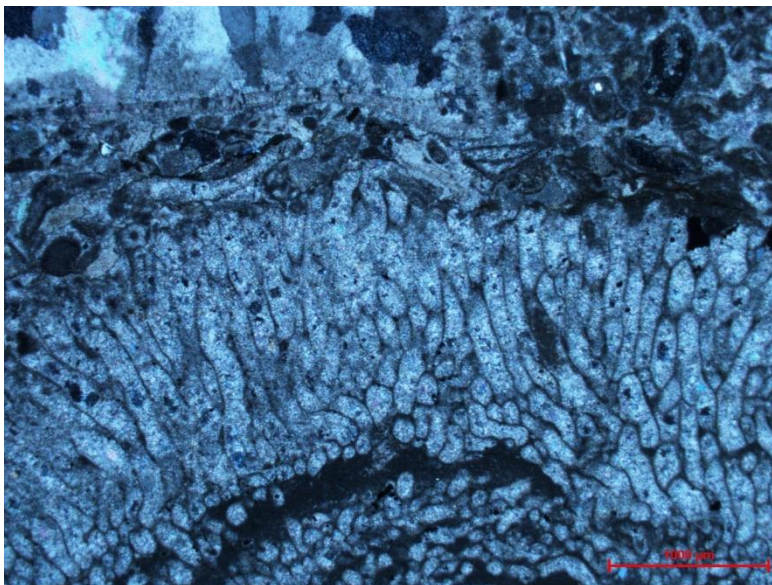


Figure 3.29: Photomicrograph of microfacies peloidal packstone/floatstone with ooids and bioclasts. Green algae and peloids are in top part. *Codiacean* (green algae) are common in warm shallow seas with good light penetration. 852.16m, PPL, scale bar (at bottom right) = 1mm.

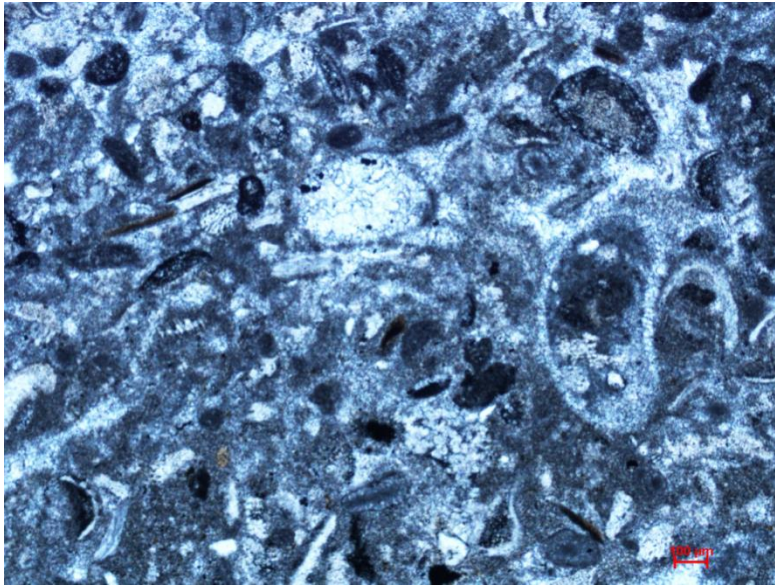


Figure 3.30: Photomicrograph of microfacies peloidal packstone/floatstone with ooids and bioclasts. Gastropod at middle right is surrounded by peloids and pellets. This gastropod shell still is recognizable by shape; most of this original gastropod shell was dissolved and was later filled with peloids and pellets. This is the norm for most gastropod remains and in the absence of diagnostic shell shapes it would be impossible to differentiate from leached neomorphosed remains of other organisms (bivalves or algae etc.). Facies is gastropod – peloidal mud – dominated, of shallow subtidal origin. 852.16m, PPL, scale bar (at bottom right) = 0.1mm.

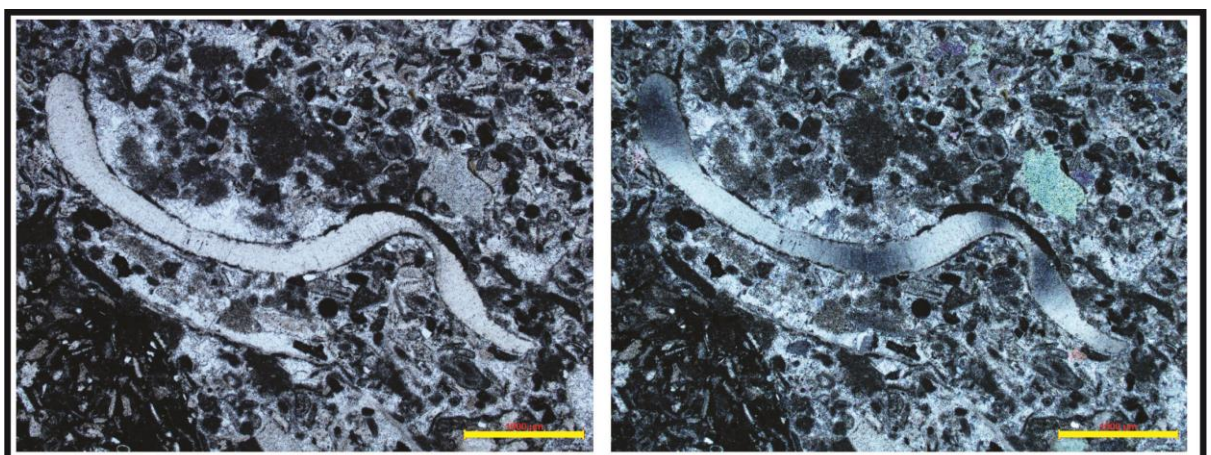


Figure 3.31: Photomicrograph of microfacies peloidal packstone/floatstone with ooids and bioclasts. Trilobite in floatstone facies (bedding is top left to bottom right). This trilobite fragment shows characteristic complex curvature of the shell and homogenous prismatic shell structure. Same view but under cross-polarized light is shown on the right. Note the characteristic dark extinction bands at the centre and left

of the grain. As the grain is rotated under cross-polarized light, the extinction bands sweep through the entire grain. Note presence of ooids and peloids shows packstone fabric. 852.16m, PPL on left and XPL on right, scale bar (at bottom right) = 1mm.

### 3.3.2.3 Discussion (Well Acacia 2)

The Goldwyer middle carbonate sediments were deposited in shallowing upward sequence (Figures 3.22), which is from subtidal to shallow subtidal environments, as follows:

<b>Microfacies</b>	<b>Depositional environment</b>
Oncoidal-peloidal packstone/floatstone	Shallow subtidal (above wave base)
Gastropod bioclastic burrowed wackestone	Subtidal (below wave-base)

Essentially two alternating facies are present in the formation: 1) Gastropod bioclastic burrowed wackestone (meter scale at cycle bases), and 2) Oncoid-peloidal floatstone with packstone matrix (decimetre scale with thin cycle tops). Rapid alternation of the two facies in decimetre to metre scale units constitute the cycles present. These upward shallowing, upward coarsening cycles grade from subtidal, muddy bioclastic intervals (deposited below wave – base) to more grainy, oncoid-peloidal thin – intervals of shallower (above wave – base) character. Note the absence of microbial laminites and lack of intertidal/supratidal facies here, in contrast to the Nita Formation. Wave energy was probably low in this shallow epeiric sea, and this is reflected in the overall muddy character of the facies present. This facies also contains nautiloids of pelagic origin.

### 3.3.3 Well Canopus 1 of the Mowla Terrace

#### 3.3.3.1 Sediment log (well Canopus 1 with part of Leo Member)

The Goldwyer middle carbonate (Goldwyer Unit 3) of well Acacia 2 is logged from depth 837m to 855.12m (Figure 3.21). Note that the legend is in Figure 3.3.

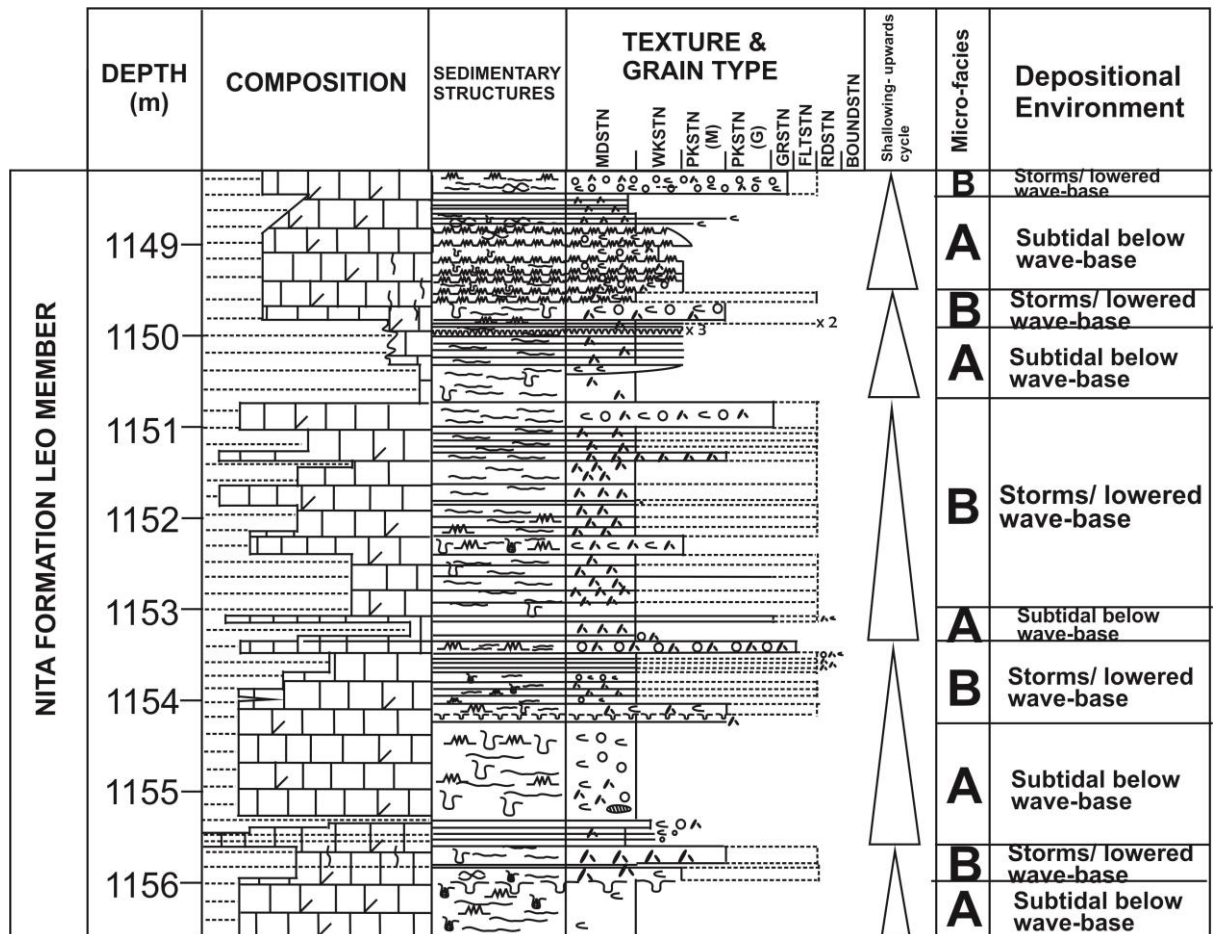


Figure 3.32: Sediment log of well Canopus 1, part of Nita Formation Leo Member. The burrowed wackestones are capped by thin packstone/floatstone intervals in the cycles. For legend see Figure 3.3.

### 3.3.3.2 Microfacies associations for Canopus 1

#### 3.3.3.2.1 Microfacies A: Weakly cemented burrowed mudstone with peloids and bioclasts

The microfacies weakly cemented burrowed mudstone with peloids and bioclasts has the sedimentary structures of burrows and wispy lamination. Figure 3.33 is the core photo as the example of this microfacies and shows the mudstone fabric. Note the burrows and wispy lamination in this microfacies at depth 1154.66-1154.72m (Figure3.34). Burrows are the most common features that can be observed in shelf carbonates both in intertidal and especially subtidal settings (Flügel, 2010). However, the thinly peloidal/intraclastic packstone/floatstone units that cap this microfacies show an upward shallowing cycle. Thus, it is suggested that the microfacies weakly cemented burrowed mudstone with peloids and bioclasts is deposited in a subtidal setting.



Figure 3.33: An example of microfacies weakly cemented burrowed mudstone with peloids and bioclast at depth 1148.56-1148.61m. Note the presence of peloids at depth 1148.595m. Dark colour of this microfacies confirmed the mudstone fabric.

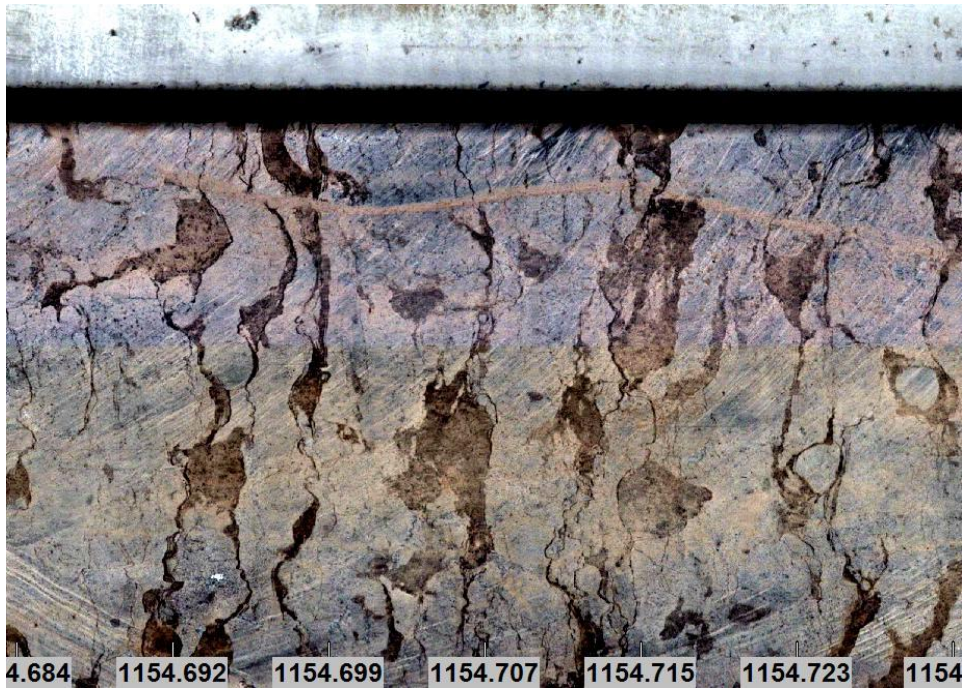


Figure 3.34: An example of microfacies weakly cemented burrowed mudstone with peloids and bioclasts at depth 1154.66-1154.72m. Note the abundance of dolomitised filled burrows.



Figure 3.35: Photomicrograph of microfacies weakly cemented burrowed mudstone with peloids and bioclasts. Note the weakly cemented dolomitised mudstone. 1148.56-1148.61m, PPL, scale bar (at bottom right) = 1mm.

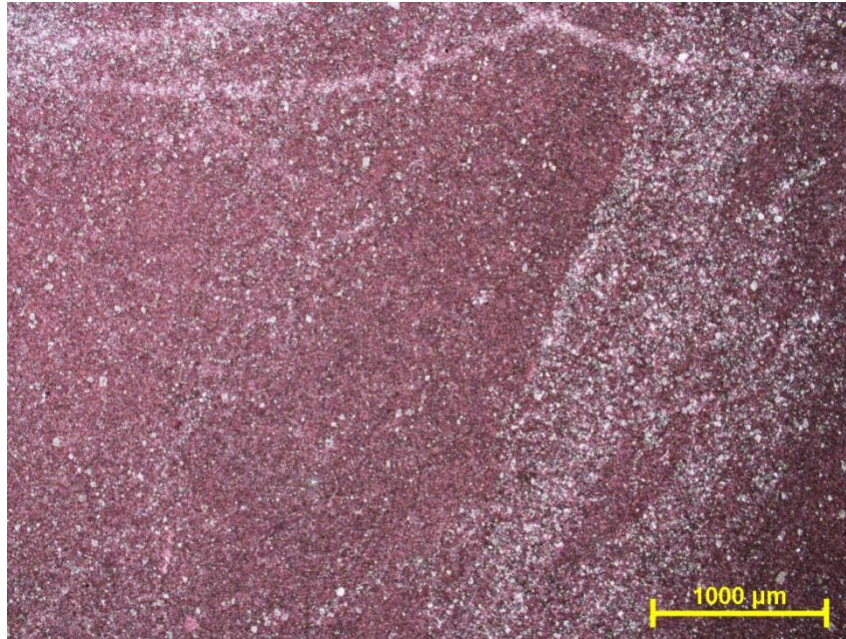


Figure 3.36: Photomicrograph of microfacies weakly cemented burrowed mudstone with peloids and bioclasts. Note the red colour lime mudstone. The red colour is limestone while the grey colour is dolostone. 1148.79-1148.85m, PPL, scale bar (at bottom right) = 1mm.



Figure 3.37: Photomicrograph of microfacies weakly cemented burrowed mudstone with peloids and bioclast. Note the brown colour mudstone. A burrow is shown at top right. White colour bivalves also present. The red colour is limestone while the grey colour is dolostone. 1154.66-1154.72m, PPL, scale bar (at bottom right) = 1mm.

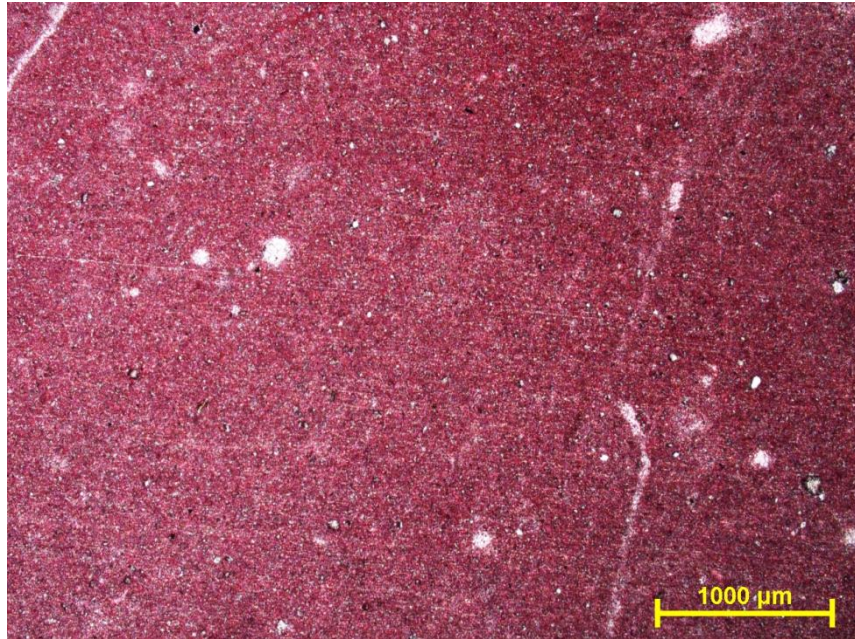


Figure 3.38: Photomicrograph of microfacies weakly cemented burrowed mudstone with peloids and bioclasts. Note the red colour lime mudstone. The red colour is limestone. Occasional shell fragments (white) are present. 1154.80m, PPL, scale bar (at bottom right) = 1mm.

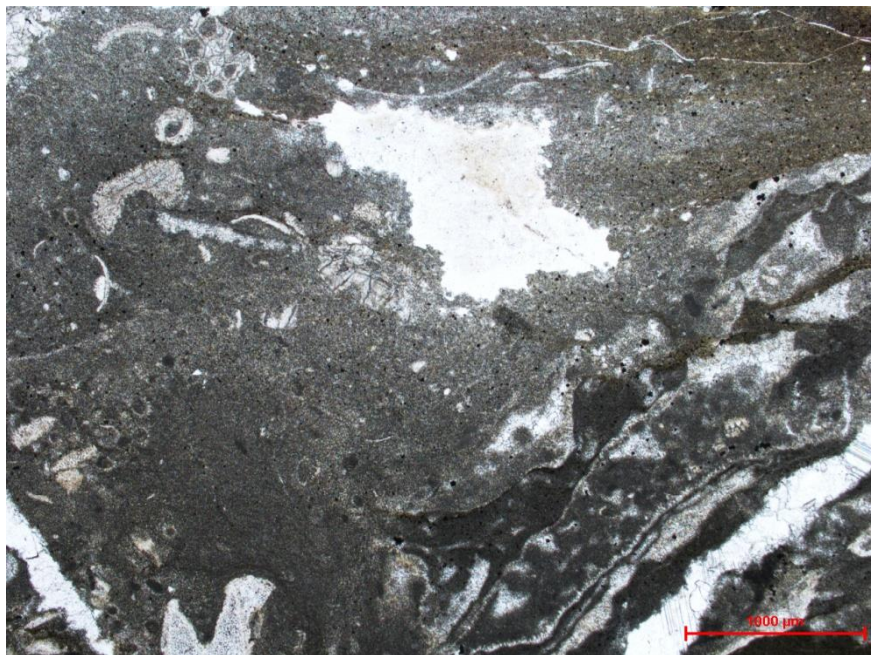


Figure 3.39: Photomicrograph of microfacies weakly cemented burrowed mudstone with peloids and bioclast. Note the brown colour mudstone in the top part. Pellets filled in fossils are found at bottom right. Pelmatozoan/crinoids are at the top left. 1155.66-1155.69m, PPL, scale bar (at bottom right) = 1mm.

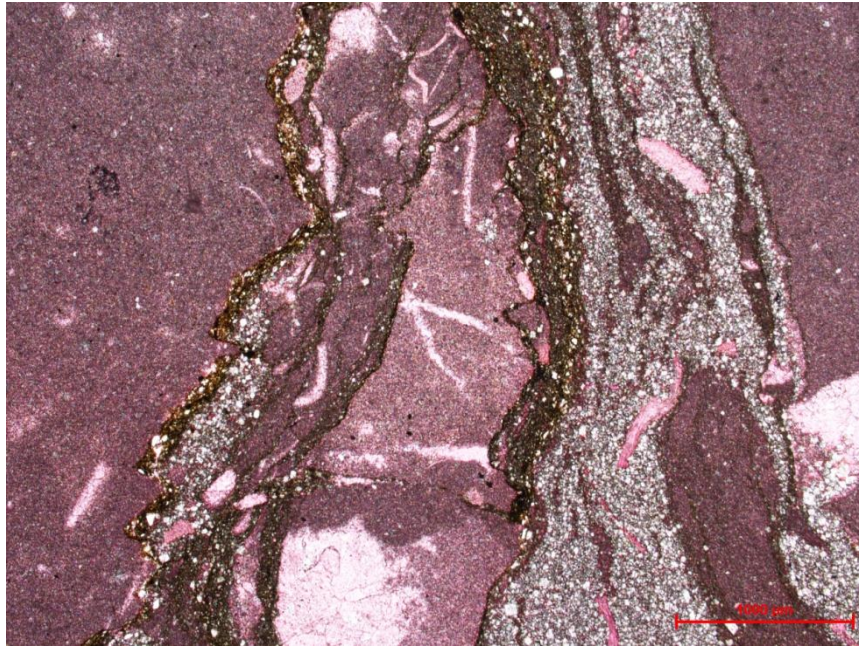


Figure 3.40: Photomicrograph of microfacies weakly cemented burrowed mudstone with peloids and bioclasts. Note the brown colour mudstone. Grey colour dolomite grains filled in the burrows. The red colour is limestone while the grey colour is dolostone. 1156.32-1156.37m, PPL, scale bar (at bottom right) = 1mm.

#### **3.3.3.2.2 Microfacies B: Peloidal/intraclastic packstone/floatstone**

The microfacies peloidal/intraclastic packstone/floatstone has the wispy lamination sedimentary structures and occasionally with burrows. Figure 3.41 is the core photo as the example of this microfacies. Note that the peloidal/intraclastic particles in this microfacies at depth 1148.407m (Figure 3.41). Another example of the core photo is at depth 1150.79-1150.84m (Figure 3.42) The fabric of packstone/floatstone can be found at depth 1150.802m.



Figure 3.41: An example of microfacies peloidal/intraclastic packstone/floatstone at depth 1148.4-1148.45m. Note the presence of intraclasts at depth 1148.407m shows the packstone/floatstone fabric.

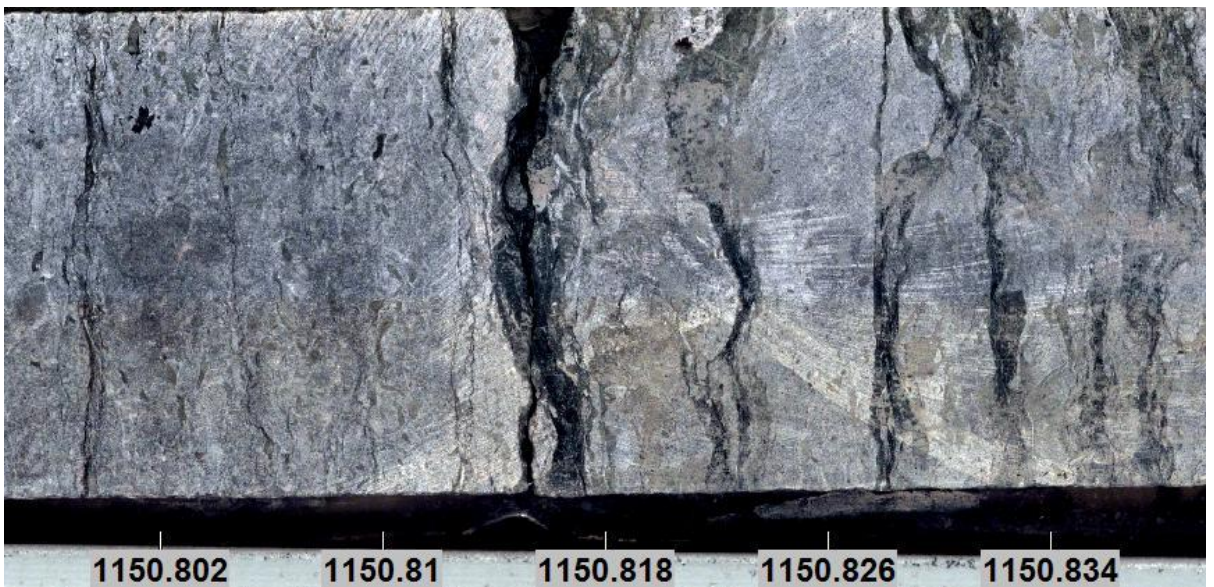


Figure 3.42: An example of microfacies peloidal/intraclastic packstone/floatstone at depth 1150.79-1150.84m. Note the fabric of packstone/floatstone at depth 1150.802m.

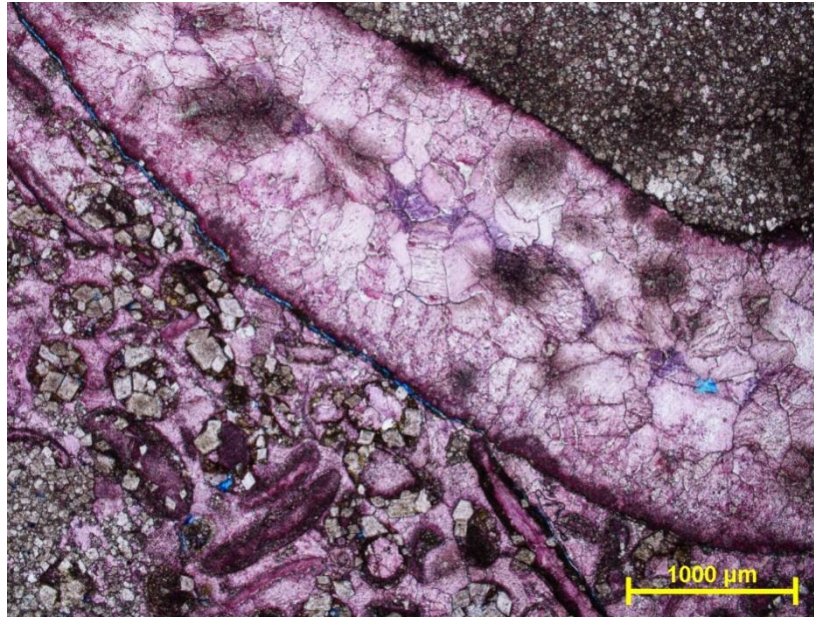


Figure 3.43: Photomicrograph of microfacies peloidal/intraclastic packstone/floatstone. Note the bivalves >2mm show floatstone matrix while the peloids and ooids which are dolomitised and filled in the middle are found at bottom left and show packstone matrix. The red colour is limestone while the grey colour is dolostone. 1148.35m, PPL, scale bar (at bottom right) = 1mm.



Figure 3.44: Photomicrograph of microfacies peloidal/intraclastic packstone/floatstone. Note the peloids and intraclasts show the packstone/floatstone fabric. The peloids form around a shell fragment (possibly brachiopod wall). They can be found quite typically in shallow-to-outer-shelf settings (Scholle and Ulmer-Scholle, 2003). 1148.4-1148.45m, PPL, scale bar (at bottom right) = 1mm.

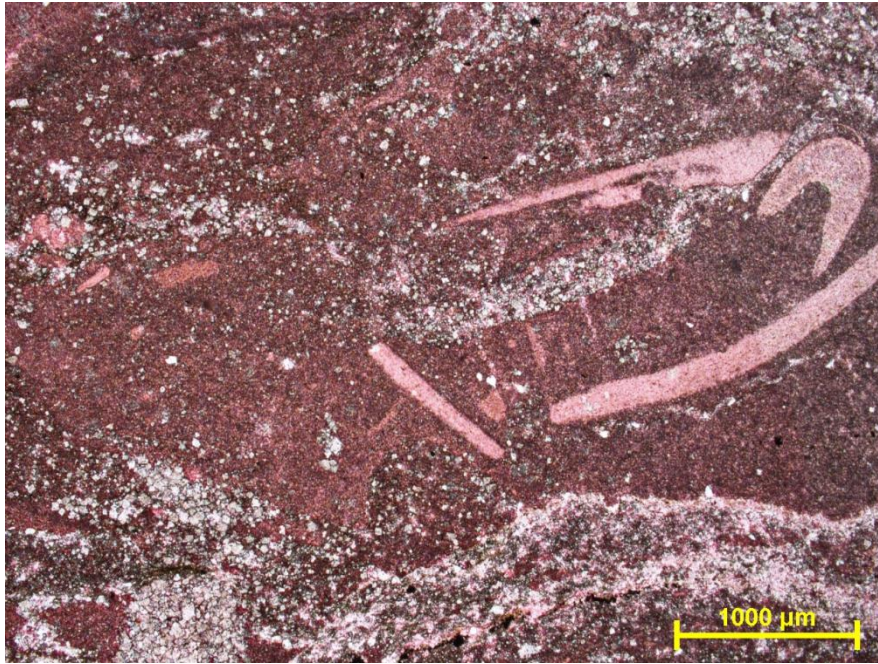


Figure 3.45: Photomicrograph of microfacies peloidal/intraclastic packstone/floatstone. Note the bivalves >2mm show floatstone matrix and crinoids/pelmatozoan arm plate is at top right. The red colour is limestone while the grey colour is dolostone. 1149.60-1149.66m, PPL, scale bar (at bottom right) = 1mm.



Figure 3.46: Photomicrograph of microfacies peloidal/intraclastic packstone/floatstone. Note the brachiopod and peloids encrustations around pelmatozoan/crinoid in the middle part. The red colour is limestone while the grey colour is dolostone. 1150.79-1150.84m, PPL, scale bar (at bottom right) = 1mm.



Figure 3.47: Photomicrograph of microfacies peloidal/intraclastic packstone/floatstone. Note the bivalves >2mm show floatstone matrix. 1151.95-1152.0m, PPL, scale bar (at bottom right) = 1mm.

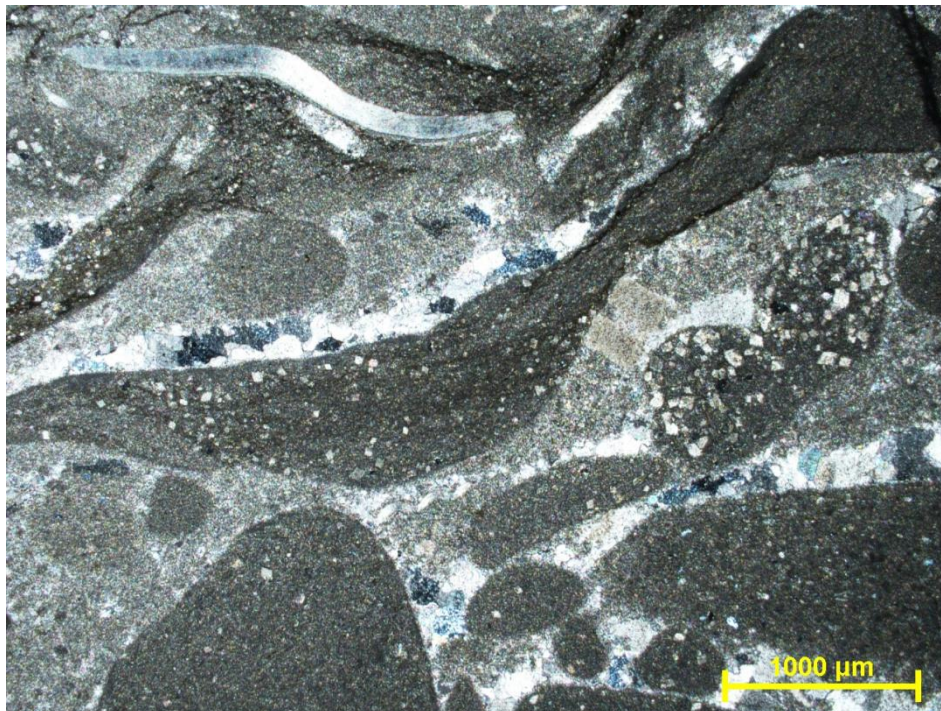


Figure 3.48: Photomicrograph of microfacies peloidal/intraclastic packstone/floatstone. Note the trilobite >2mm at top left show floatstone matrix. 1152.60-1152.66m, PPL, scale bar (at bottom right) = 1mm.

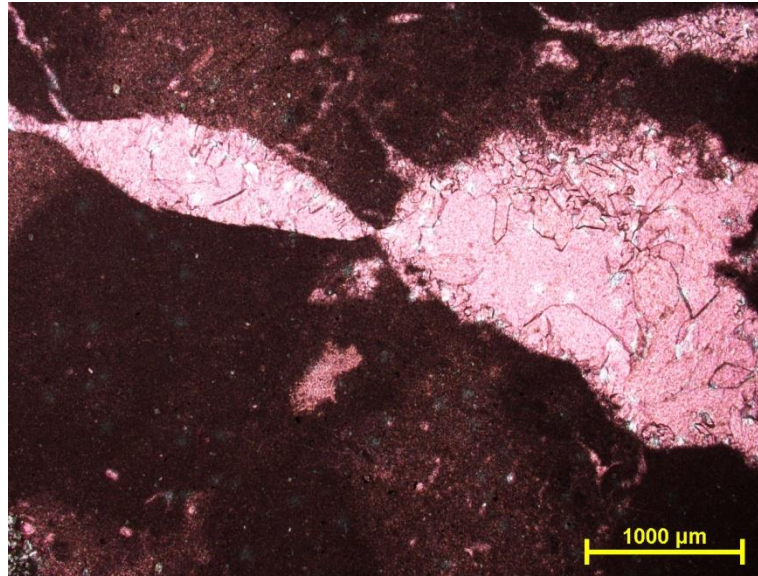


Figure 3.49: Photomicrograph of microfacies peloidal/intraclastic packstone/floatstone. Note the recrystallised fossil fragments >2mm showing floatstone fabric. 1153.92-1153.97m, PPL, scale bar (at bottom right) = 1mm.

### 3.3.3.3 Discussion (Well Canopus 1)

The Nita Formation Leo Member carbonate sediments were deposited in shallowing upward sequence or upward coarsening cycles (Figures 3.32), which is from below wave-base to periods of lowered wave-base (or storms), as follows:

Microfacies	Depositional environment
Peloidal/intraclastic packstone/floatstone Thickness range: 0.04m-0.26m	Storms or periods of lowered wave-base
Weakly cemented burrowed mudstone with peloids and bioclasts Thickness range: 0.39-1.13m	Subtidal (below wave-base)

The Nita Formation (Leo Member) in Canopus 1 of the Mowla Terrace is shale-rich and is interbedded with dolomitized, stylolitic carbonates. Mudstones which are weakly cemented, burrowed with peloids and bioclasts dominate the carbonates; and these are subtidal below wave base deposits. These intervals are capped by thin (10-20cm) intervals of packstone/floatstones with peloids and intraclasts as dominant

particles. Such intervals may represent storms or periods of lowered wave - base in this low energy subtidal to shallow/ shelf setting.

---

### **3.3.4 Well Kunzea 1 of the Crossland Platform**

#### **3.3.4.1 Sediment log (Well Kunzea 1)**

The Nita and Goldwyer Formations of well Kunzea 1 was inspected and logged from depth 292m to 450m (Figure 3.50). Haines (2004) logged the well Kunzea 1 and this sediment log was used to inspect in this study and 12 thin sections were analysed to add more data to Haines (2004) sediment log. Sediment log of well Kunzea 1 covers the complete Nita Formation (Leo Member and Cudalgarra Member), Goldwyer upper shale and Goldwyer middle carbonate. Well Kunzea 1 reaches the well total depth at the base of Goldwyer middle carbonate and this is the reason for the absence of Goldwyer lower shale which was not cored. Note that the legend is in Figure 3.3.

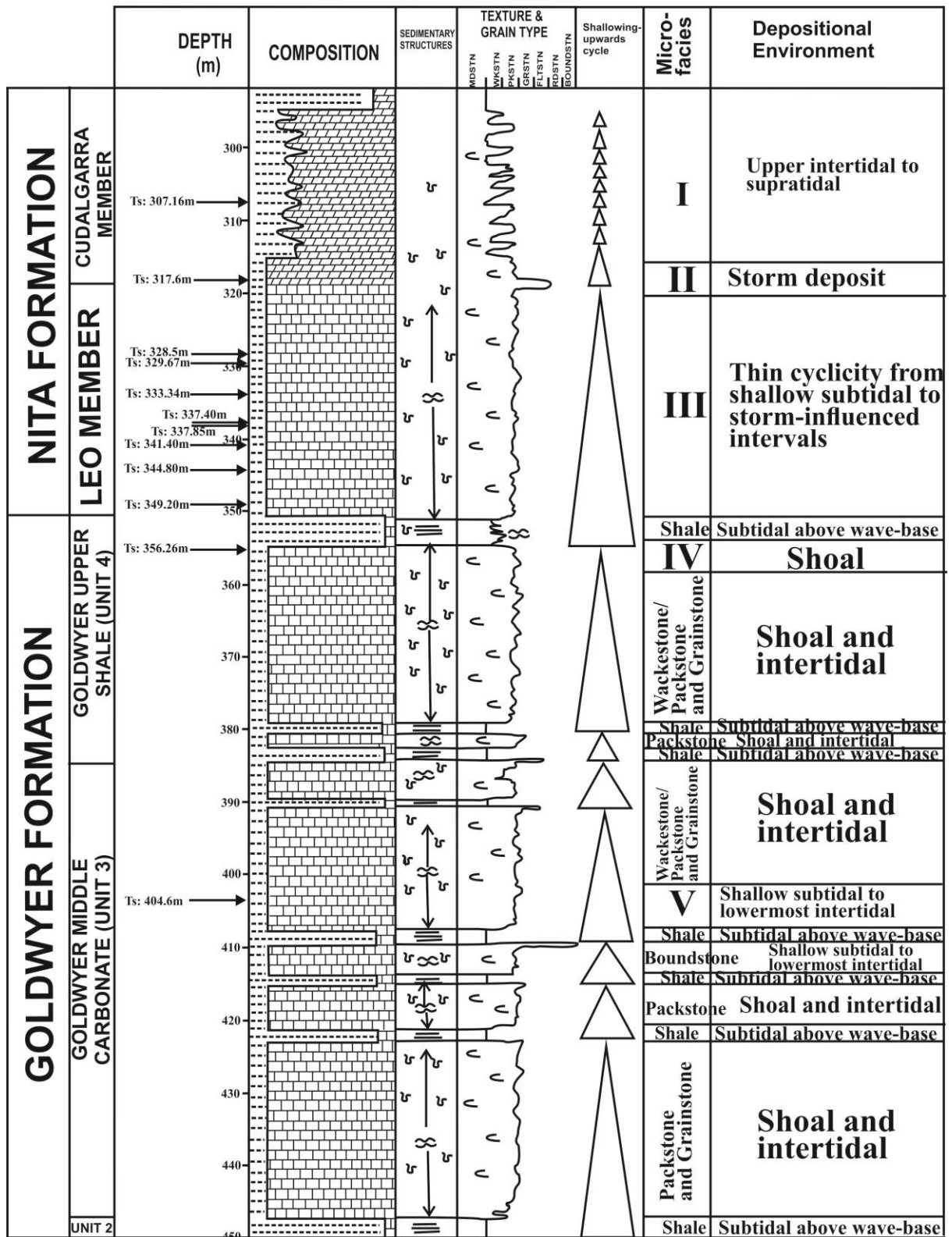


Figure 3.50: Sediment log of well Kunzea 1 covers complete Nita Formation, Goldwyer Unit 3 and Goldwyer Unit 4. The burrowed wackestones are capped by thin packstone/floatstone intervals in the cycles of part of the Nita Leo Member based on the thin section analysis in this study (Grain size and sedimentary structures after Haines (2004)). For legend see Figure 3.3.

### 3.3.4.2 Microfacies associations for Kunzea 1

#### 3.3.4.2.1 Microfacies I: Dolomitised mudstone (Depth 307.16m, Cudalgarra Member)

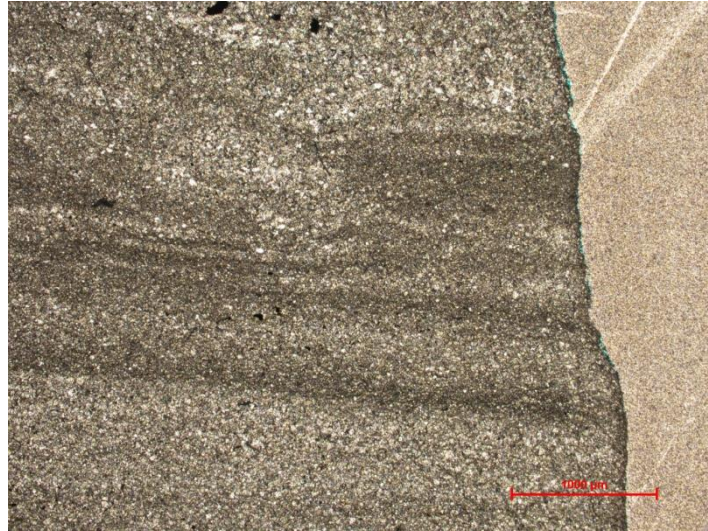


Figure 3.51: Photomicrograph of microfacies dolomitised mudstone. Note the horizontal lamination shows the low energy condition of the mudstone. 307.16m, PPL, scale bar (at bottom right) = 1mm.

#### 3.3.4.2.2 Microfacies II: Bioclastic rudstone (Depth 317.6m, boundary at Leo Member and Cudalgarra Member)



Figure 3.52: Photomicrograph of microfacies bioclastic rudstone. Note the contact of grains (pelmatozoan/crinoids, ooid and dolomite grains) show the rudstone fabric. The red colour is limestone while the grey colour is dolomite. 317.6m, PPL, scale bar (at bottom right) = 1mm.

**3.3.4.2.3 Microfacies III: Stylonodular burrowed wackestone (Depths 328.5m, 329.67m, 333.34m, 337.40m, 337.85m, 341.40m, 344.80m and 349.20m, Leo Member)**

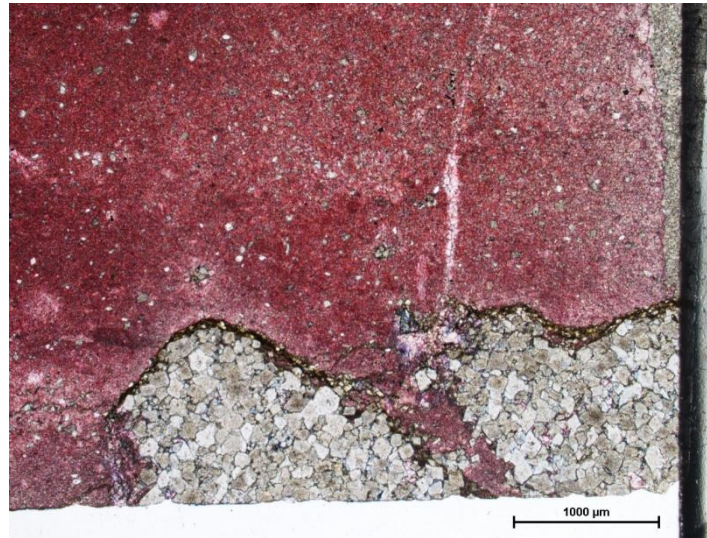


Figure 3.53: Photomicrograph of microfacies stylonodular burrowed wackestone. Note the dolomitised-filled burrows are at the bottom right. The fossil fragments up to 25% show a wackestone fabric. The red colour is limestone while the grey colour is dolostone. 328.5m, PPL, scale bar (at bottom right) = 1mm.

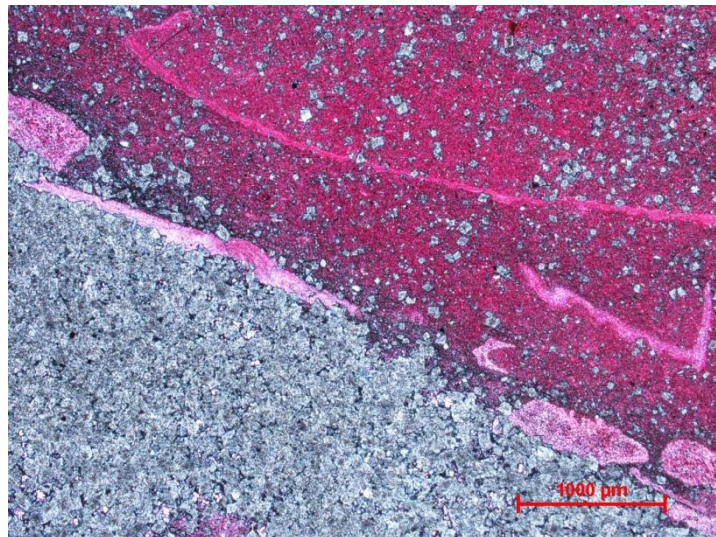


Figure 3.54: Photomicrograph of microfacies stylonodular burrowed wackestone. The prominent boundary is between wackestone (red) and dolomitised dilled burrow (grey). The fossil fragments in red colour limestone of 25% show a wackestone fabric. The red colour is limestone while the grey colour is dolostone. 329.67m, PPL, scale bar (at bottom right) = 1mm.



Figure 3.55: Photomicrograph of microfacies stylonodular burrowed wackestone. Note brachiopods are at the central part in a thin bioclastic horizon (storm lag). Bedding is lower left to top right. The red colour is limestone while the grey colour is dolostone. 333.34m, PPL, scale bar (at bottom right) = 1mm.



Figure 3.56: Photomicrograph of microfacies stylonodular burrowed wackestone. Note the crinoids/pelmatozoan arm plate is at the central part with red colour. The bioclastic horizon in burrowed wackestone probably represents storm lags deposited during period of lowered wave-base. The red colour is limestone while the grey colour is dolostone. 337.40m, PPL, scale bar (at bottom right) = 1mm.



Figure 3.57: Photomicrograph of microfacies stylonodular burrowed wackestone. Note the brachiopods followed by trilobites from lower right to top left margin, present as a thin bioclastic storm lag (millimetre to decimetre scale). The red colour is limestone while the grey colour is dolostone. 337.85m, PPL, scale bar (at bottom right) = 1mm.

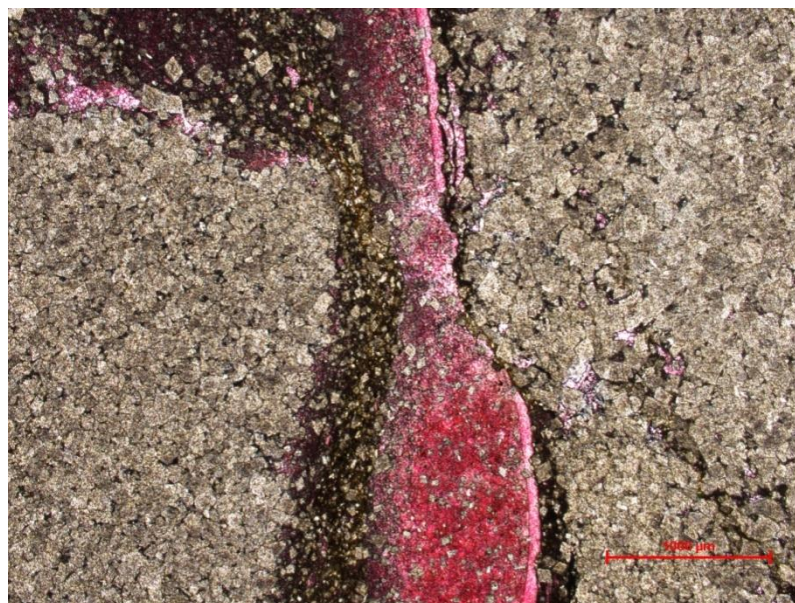


Figure 3.58: Photomicrograph of microfacies stylonodular burrowed wackestone. Note the red colour limestone is probably a middle part of two dolomitised-filled burrows. The red colour is limestone while the grey colour is dolostone. 341.40m, PPL, scale bar (at bottom right) = 1mm.

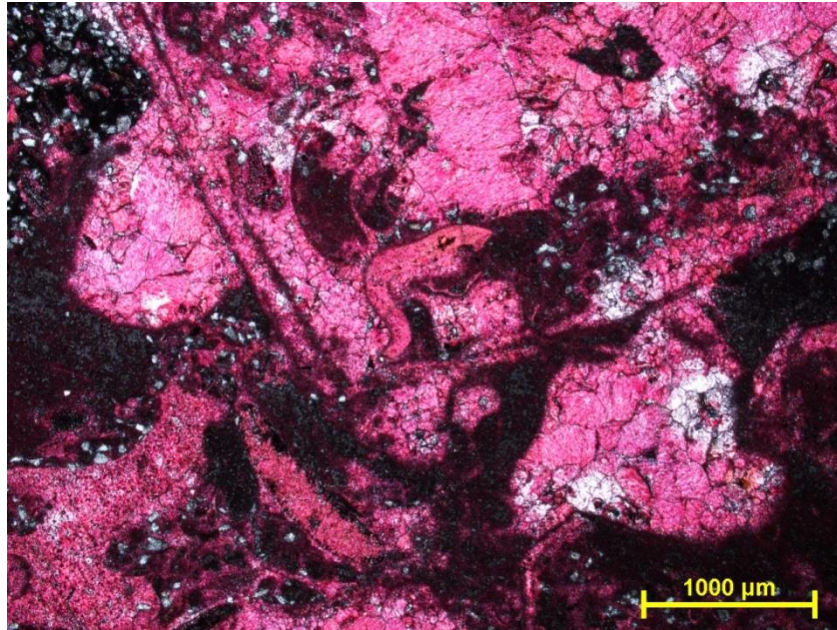


Figure 3.59: Photomicrograph of microfacies stylonodular burrowed wackestone. Note the gastropods and trilobites at the middle part, present as a thin bioclastic storm lag. Bedding is lower right to top left. The red colour is limestone while the grey colour is dolostone. 344.80m, PPL, scale bar (at bottom right) = 1mm.

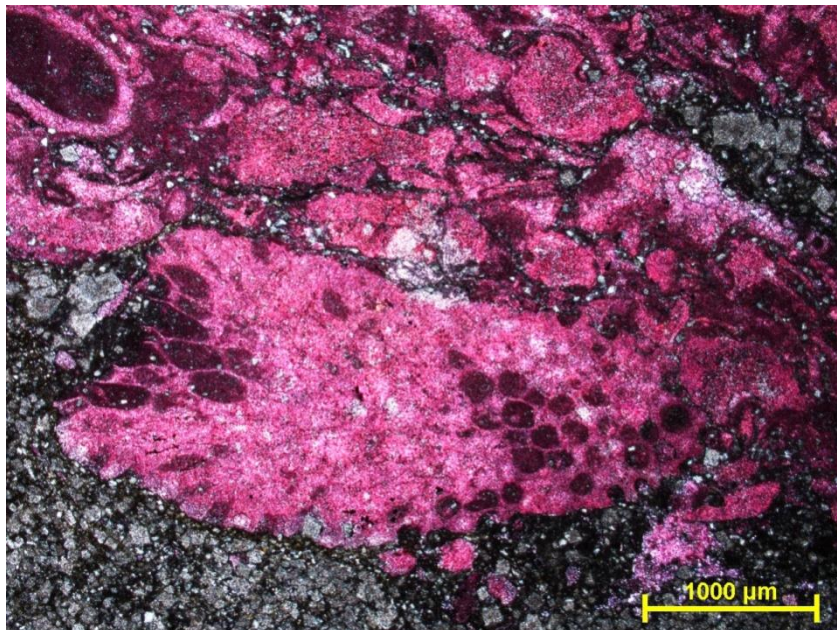


Figure 3.60: Photomicrograph of microfacies stylonodular burrowed wackestone. Note the bryozoans and pelmatozoan/crinoids are in an oriented layer most likely represents a storm lag. The red colour is limestone while the grey colour is dolostone. 349.20m, PPL, scale bar (at bottom right) = 1mm.

**3.3.4.2.3 Microfacies IV: Oncoidal-peloidal packstone/floatstone with ooids and bioclasts (Depth 356.26m, Goldwyer upper shale or Unit 4)**

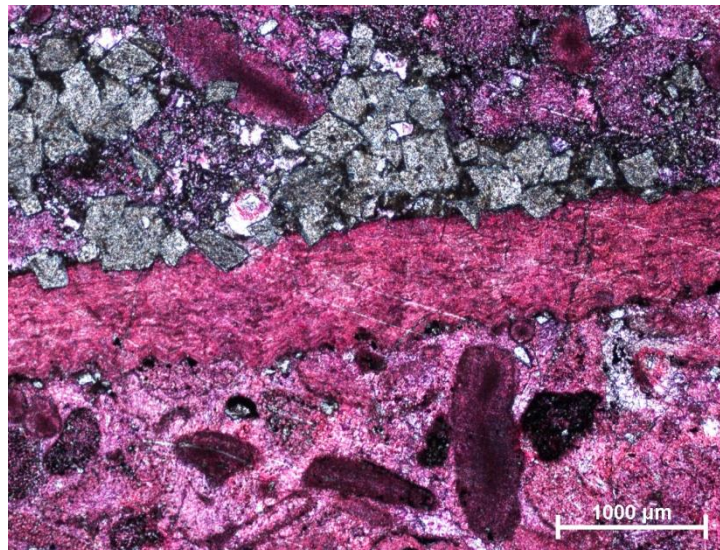


Figure 3.61: Photomicrograph of microfacies oncoidal-peloidal packstone/ floatstone with ooids and bioclasts. Note the brachiopod shell at the middle part and peloids at the bottom part. The red colour is limestone while the grey colour is dolostone. 356.26m, PPL, scale bar (at bottom right) = 1mm.

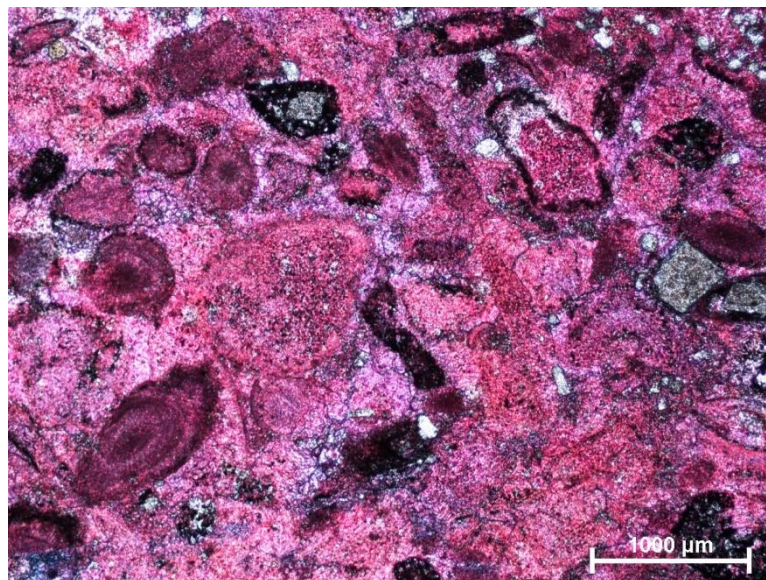


Figure 3.62: Photomicrograph of microfacies oncoidal-peloidal packstone/ floatstone with ooids and bioclasts. Note the presence of pelmatozoan/crinoids, oncoids and ooids in this microfacies. The red colour is limestone while the grey colour is dolostone. 356.26m, PPL, scale bar (at bottom right) = 1mm.

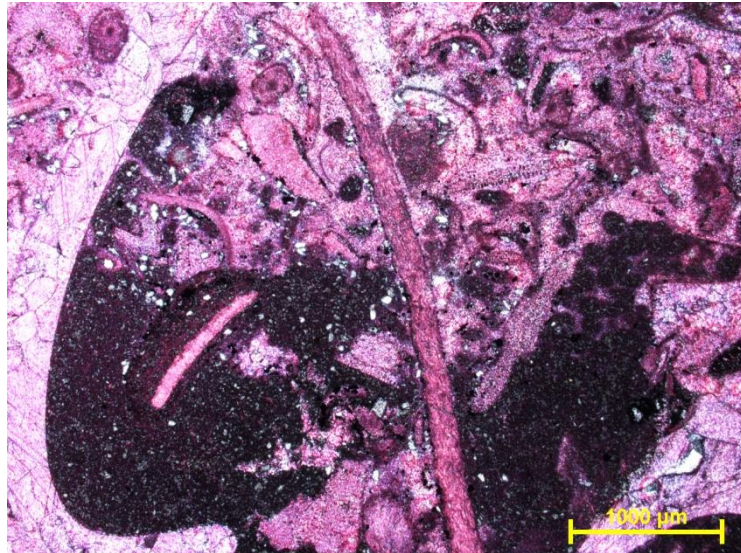


Figure 3.63: Photomicrograph of microfacies oncolidal-peloidal packstone/ floatstone with ooids and bioclasts. Note the bivalves >2mm along the left side show floatstone fabric while peloids, ooids and pellets show packstone fabric. The red colour is limestone while the grey colour is dolostone. 356.26m, PPL, scale bar (at bottom right) = 1mm.

#### 3.3.4.2.3 Microfacies V: Stromatolite boundstone (Depth 404.6m, Goldwyer middle carbonate or Unit 3)

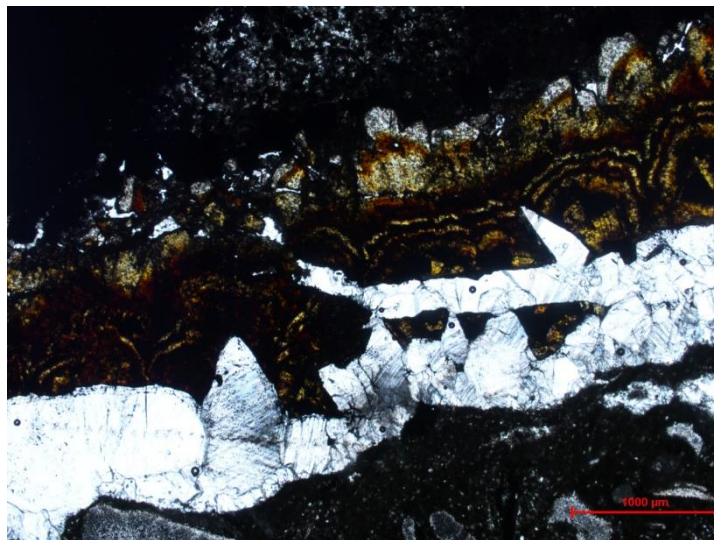


Figure 3.64: Photomicrographic for microfacies stromatolite boundstone. Note the overgrowth stromatolite along the centre part with the white colour crystals like dog tooth spar. 404.6m, PPL, scale bar (at bottom right) = 1mm.

### **3.3.4.3 Discussion (Well Kunzea 1)**

The 128m section log of Haines (2004; see Fig 3.50) is a condensed summary log for the Goldwyer Formation (Units 3 and Unit 4, carbonate middle unit and Goldwyer upper shale unit, respectively) and the Nita Formation (Leo and Cudalgarra Members). Petrographic study for this project focused on the Leo Member (Nita Formation) with the addition of a thin interval in Goldwyer Unit 3.

#### **3.3.4.3.1 Goldwyer Formation Middle Carbonate (Unit 3)**

This unit consists of burrowed bioclastic packstones with laminated shale intervals. This is broadly consistent with the more detailed logs provided by this study (see Figures 3.21-3.31, upward coarsening thin cycles of below wave-base wackestone/packstone and oncoid-peloidal packstone/floatstone). The interval at 404.6m was confirmed to contain thin stromatolite layers (microfacies V, page 82 and Figure 3.64) which likely represent shallow sub-tidal to lowermost intertidal conditions near the top of this overall regressive package.

#### **3.3.4.3.2 Goldwyer Formation Upper Shale (Unit 4)**

This unit is strongly shaly at its base but otherwise is logged as bioturbated wackestone/packstone (upward coarsening cycles from shale to packstone). Near the top of the unit the microfacies studied was oncoid-peloidal packstone (microfacies IV, page 81 and Figures 3.61 to 3.63) which may represent shoaling before onset of deposition of the Nita Formation (Leo Member) regressive carbonate package.

#### **3.3.4.3.3 Nita Formation (Leo Member)**

Where examined in eight thin sections for Nita Leo Member, the microfacies identified was stylonodular burrowed wackestone (microfacies III, pages 77 to 80 and Figures 3.53-3.60). Within the generally muddy, bioturbated wackestone (microfacies III) the bioclastic floatstone horizons (Figures 3.55, 3.56, 3.57, 3.59 and 3.60) occur as thin (a few millimetre to decimetre scale) intervals and likely represent periods of lowered wave base which produced storm lags in the otherwise quiescent sub-wave base and shallow subtidal setting. These microfacies are similar to those encountered in the Canopus 1 well (Mowla Terrace) which exhibits thin cyclicity from shallow subtidal to storm – influenced intervals (see Fig 3.32). However, they differ from the

Nita Formation in the Looma 1 well (Figs 3.5 to 3.9) in that no microbial laminites are present. The bioclastic rudstone was found at the boundary of Leo Member and Cudalgarra Member (microfacies II, page 76 and Figure 3.52). This matches with the positive bounding surface (the turning point between Leo Member and Cudalgarra Member) from INPEFA analysis in Chapter 4 which indicates maximum regressive surface.

#### **3.3.4.3.4 Nita Formation (Cudalgarra Member)**

Aside from the thin bioclastic mudstone storm lag present at its basal contact, this unit is heavily dolomitised mudstone (microfacies I, page 76 and Figure 3.51), and diagenesis has prevented identification of microfacies and environments and detailed environmental analysis (see Haines, 2004). According to Haines (2004), dolostone of Cudalgarra Member deposited in upper intertidal to supratidal environment is fine grained, bioclasts and bioturbation become rare, and evaporites are common. In addition, terrestrial shale with root material was found in Cudalgarra Member from well Looma 1 in this study (Figure 3.20 and page 52).

### **3.4 Summary of core lithofacies and their stratigraphic occurrence**

The summary of core lithofacies and their stratigraphic occurrence for four different wells in this Chapter (wells Looma 1, Acacia 2, Canopus 1 and Kunzea 1) is shown in Table 3.3. Well Looma 1 (part of Nita Formation) consists of six different lithofacies and deposited from shallow subtidal, shoal, intertidal/lagoonal, nearshore to supratidal. Well Acacia 2 covers part of Unit 3 of Goldwyer Formation with two different lithofacies deposited from below wave-base to above wave-base. Part of Leo Member, Nita Formation from well Canopus 1 is deposited from subtidal below wave-base to storms. The Nita and Goldwyer Formations for well Kunzea 1 (Crossland Platform) were further investigated in cores in this study.

<b>WELL</b>	<b>FORMATION</b>	<b>MICRO-FACIES</b>	<b>LITHOFACIES</b>	<b>DEPOSITIONAL ENVIRONMENT</b>
Looma 1	Nita Formation (major part of Leo Member and part of Cudalgarra Member)	S <sub>6</sub>	Terrestrial shale	Supratidal
		S <sub>5</sub>	Evaporitic wackestone	Nearshore
		S <sub>4</sub>	Microbial laminites	Intertidal to supratidal
		S <sub>3</sub>	Interlaminated shale and wackestone/packstone	Intertidal/lagoonal
		S <sub>2</sub>	Oolitic/peloidal/intraclastic and bioclastic packstone/grainstone	Shoal
		S <sub>1</sub>	Burrowed, fossiliferous mudstone/wackestone	Shallow subtidal
Acacia 2	Goldwyer Formation (part of Unit 3)	2	Oncoidal-peloidal packstone/floatstone with ooids and bioclasts	Above wave-base
		1	Gastropod bioclastic burrowed wackestone	Below wave-base
Canopus 1	Nita Formation (part of Leo Member)	B	Peloidal/intraclastic packstone/floatstone	Storms/ lowered wave-base
		A	Weakly cemented burrowed mudstone with peloids and bioclasts	Subtidal below wave-base
Kunzea 1	Nita Formation (Cudalgarra member)	I	Dolomitised mudstone	Upper intertidal to supratidal
	Nita Formation (Leo member)	II	Bioclastic rudstone	Storm deposit
		III	Thin bioclastic horizon	Storm lag
			Stylonodular burrowed wackestone	Shallow subtidal
	Goldwyer Formation (Unit 4)	IV	Oncoidal/peloidal packstone/floatstone with ooids and bioclasts	Shoal
		Haines, 2004	Wackestone, packstone and grainstone	Shoal and intertidal
		Haines, 2004	Shale	Subtidal above wave-base
	Goldwyer Formation (Unit 3)	Haines, 2004	Wackestone, packstone and grainstone	Shoal and intertidal
		V	Stromatolite boundstone	Shallow subtidal to lowermost intertidal
		Haines, 2004	Shale	Subtidal above wave-base

Table 3.3: Depicts the relationship between the cored intervals, their facies associations, and positions within the stratigraphy.

# CHAPTER 4

## SUBSURFACE CORRELATION OF NITA AND GOLDWYER FORMATIONS (MIDDLE ORDOVICIAN) IN PART OF CANNING BASIN, WA

### 4.1 Introduction

This chapter uses the CycloLog software developed by ENRES International to analyse 22 subsurface wells in part of the Canning Basin as shown in table 4.1. A facies sensitive log, usually the gamma ray (GR) log is transformed to the integrated prediction error filter analysis (INPEFA) curve. The INPEFA curve shows uphole changes in the waveform properties concealed in the numerical log data and displays discontinuity surfaces and trends. The stratigraphic packages interpreted from the INPEFA curve should be calibrated with sequencing and time tools (Figure 4.1). The objectives are to demonstrate a scheme of stratigraphic packages based on interpretation of INPEFA curves. This INPEFA stratigraphy is data-driven and obtained from wireline log data. The components of INPEFA stratigraphy are discussed in Chapter 1. The comparison between litho-stratigraphy and the depositional environment using this technique provides a methodology for regionally mapping the subsurface cycles at basin scale for the Nita and Goldwyer Formations.

AREA	SUBSURFACE WELL
Broome Platform	Looma 1 <sup>N</sup> , McLarty 1, Robert 1, Goldwyer 1, Hedonea 1. Sharon Ann 1
Barbwire Terrace	Acacia 2 <sup>G</sup> , Barbwire 1, Dodonea 1, Percival 1, Setaria 1, Solanum 1
Crossland Platform	Missing 1, Kunzea 1 <sup>N&amp;G</sup> , Santalum 1A
Mowla Terrace	Canopus 1 <sup>N</sup> , Crystal Creek 1, Matches Springs 1, Pictor 1
Willara Sub-basin	Munro 1, Willara 1, Woods Hills 1

Table 4.1: The studied wells located at different areas in the Canning Basin, WA. N and G indicate logged core for Nita and Goldwyer Formations described in Chapter 3.

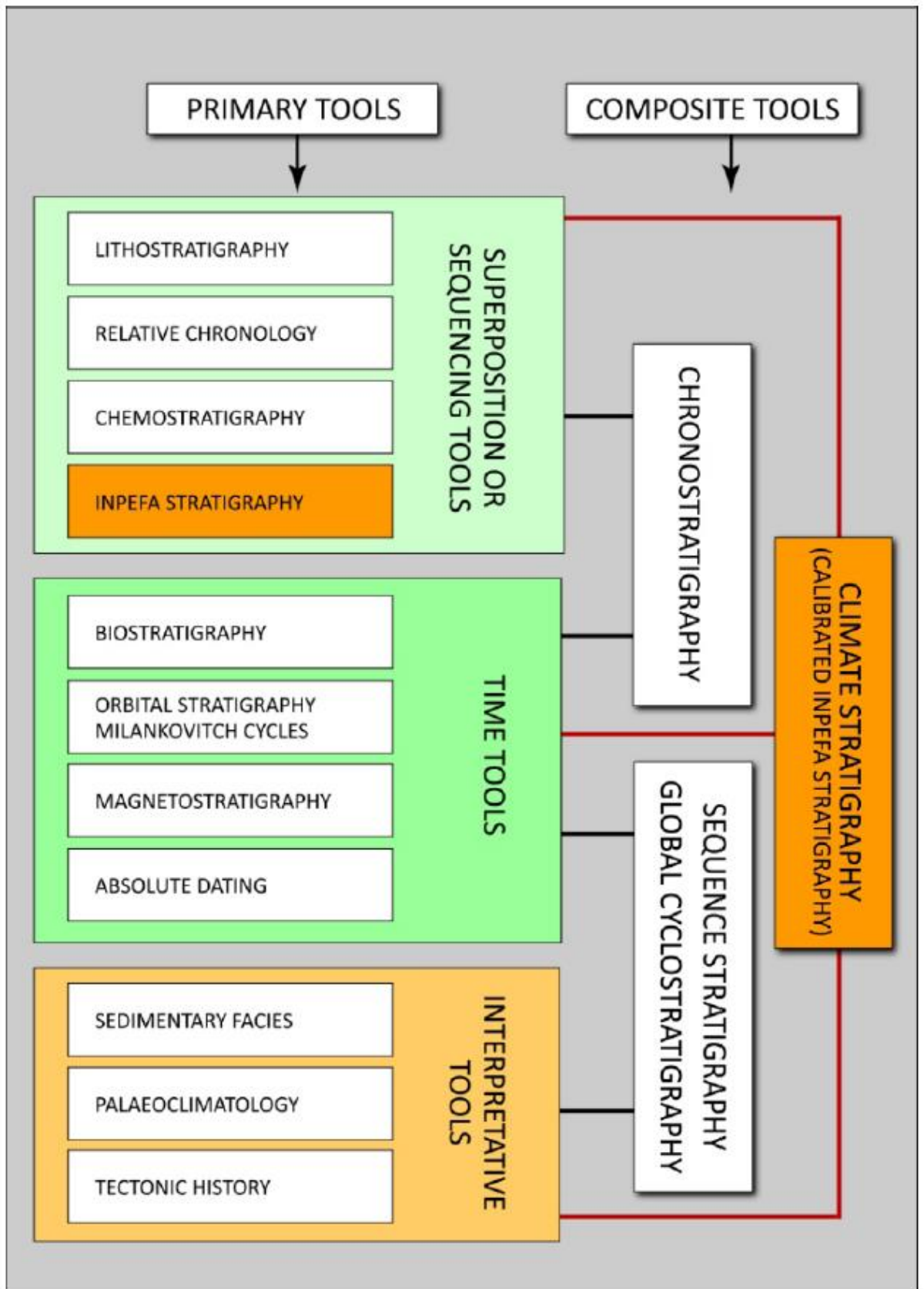


Figure 4.1: Schematic overview the principal tools within the stratigraphic toolkit (Doyle and Bennet, 1998; ENRES, 2011).

## **4.2 Climate stratigraphy**

The term climate stratigraphy which was developed by ENRES International is an application of aspects of global cyclostratigraphy. According to Nio et al. (2005, 2006), De Jong et al. (2007) and ENRES (2011), the principles of the method of climate stratigraphy are based on: 1) Climate is a primary control on vertical lithofacies patterns which retain a record of nested orbital periodicities and is accessible through the spectral (wavelength, amplitude, phase) properties of facies-sensitive logs; 2) Climate stratigraphy uses an important part of the insights of sequence stratigraphy which emphasizes facies relationships and stratal architecture marking climatic changes that are near-synchronous, the recognition of genetic units that result from the interplay of accommodation and sedimentation; 3) Climate stratigraphy uses the fundamental findings of Global Cyclostratigraphy as the basis of a method of reservoir-scale stratigraphic analysis and correlation which includes the principle that climate change is quasi-cyclic as a result of primary (Milankovitch) orbital control.

Given the above principles, climate stratigraphy operates by extracting a curve representing the downhole changes in the spectral prosperities of a facies-sensitive wireline logs and correlating key features of those spectral change curves between wells (Kongkanoi, 2008).

## **4.3 Global Cyclostratigraphy**

Perlmutter and Matthews (1992) introduced Global Cyclostratigraphy as the study of cyclic depositional patterns produced by climate and tectonic processes. They assumed that the theory of orbitally-forced (Milankovitch) climate change was sufficiently well-established that it could drive predictive models of the stratigraphic succession of lithofacies. ENRES International has developed the CycloLog software to recognise the predicted stratigraphic packaging in the subsurface by using a spectral analytic method to transform standard wireline log data, especially gamma ray logs.

## **4.4 Systems tracts**

The sequence is best defined by bounding unconformity surfaces in sequence stratigraphy and this sequence can be subdivided into distinctive units that are called systems tracts (Embry, 2002). Two systems tracts model which are material-based that are defined by Embry (1993) and Embry and Johannessen (1993) consist of a

lower transgressive systems tract (TST) that follows the definition of Van Wagoner et al. (1998) and an upper regressive systems tract (RST) (Figure 4.2). A systems tract must be bound by a specific sequence stratigraphical surface like a sequence, such as maximum regressive surface (MRS) and maximum flooding surface (MFS). A TST is bound by a maximum regressive surface (MRS) and its correlative surface below and a maximum flooding surface (MFS) above while RST is just the opposite being defined as a sequence stratigraphy bound by a maximum flooding surface (MFS) below and by a maximum regressive surface (MRS) above (Embry, 2009).

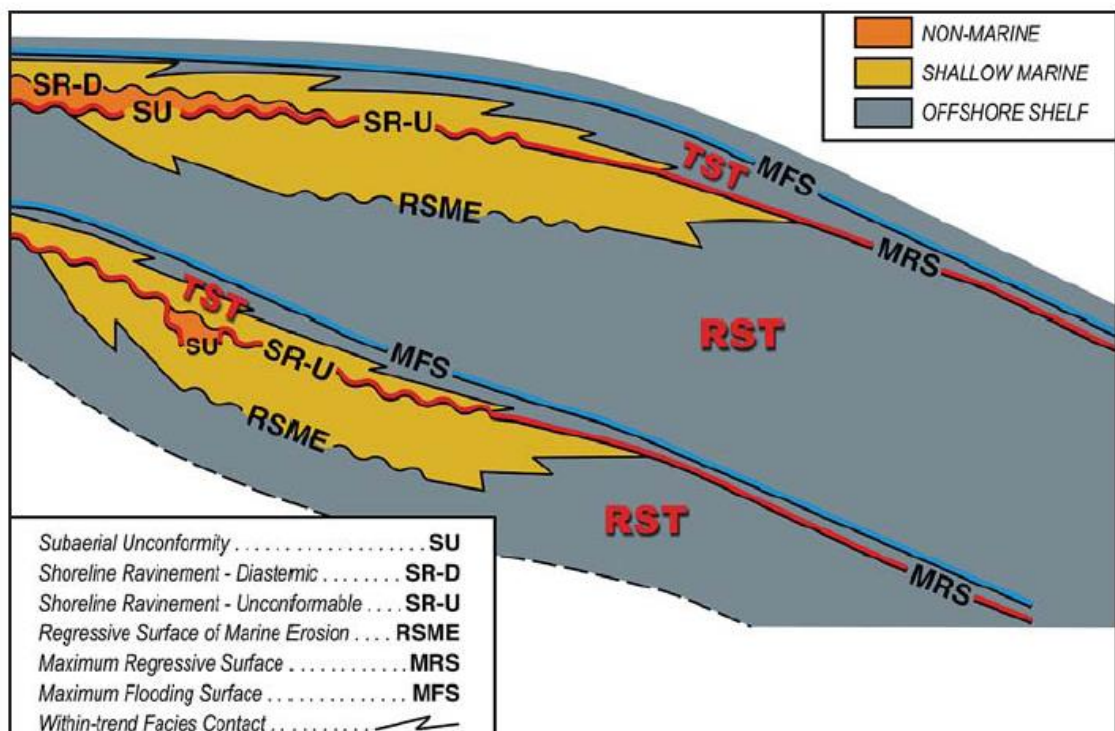


Figure: 4.2: The material-based two systems tracts defined by Embry (1993). The occurrence of the low diachroneity maximum flooding surface (MFS) allows the sequence to be subdivided into two systems tracts – TST and RST, (Embry, 2009).

#### 4.4.1 Regressive systems tract (RST)

The regressive systems tract was defined by Embry and Johannessen in 1992, and in their definition the regressive systems tract is “overlying a transgressive systems tract with the base of a maximum flooding surface and top with maximum regressive surface”. This complete sequence is known as a transgressive-regressive sequence (T-R sequence) (Embry, 2002). The sediments of this systems tract include the highstand system tract and early lowstand systems tract (Posamentier and Allen, 1999).

#### **4.4.2 Transgressive systems tract (TST)**

The transgressive systems tract (TST) is defined by the maximum regressive surface (MRS) or transgressive surface at the base and the maximum flooding surface (MFS) at the top. This was originally defined by Van Wagoner et al. (1988).

#### **4.4.3 Maximum regressive surface/Transgressive surface/Flooding surface (MRS)**

Maximum regressive surface (MRS) marks the start of transgression and at this time sediment supply to the adjacent marine shelf decreases and water depth at nearshore localities begins to increase (Embry, 2002).

MRS can be delineated with gamma ray log and sonic log. The MRS is placed at the change in gamma log trend from decreasing gamma ray to increasing gamma ray and the change in this trend is interpreted to reflect a change from shallowing-upward (decreasing clay content) to deepening-upward (increasing clay content (Figure 4.3). The sonic log is a mirror image of gamma ray log to assist the determination of the MRS. In pure carbonate systems, gamma ray are no help for MRS identification and facies data from core or cuttings are required (Embry, 2009). However, Nita and Goldwyer Formations from Canning Basin, Western Australia contain both carbonate and shale, and this helps to identify the MRS, MFS, transgression trend and regression trend with gamma ray and sonic logs (Figure 4.3) and CycloLog software.

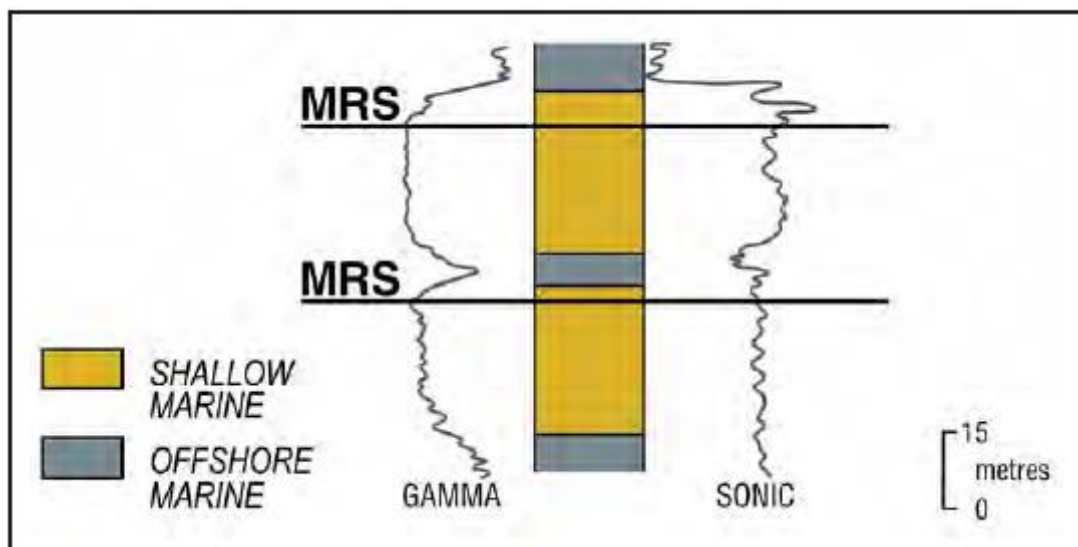


Figure 4.3: The maximum regressive surfaces (MRS) have been delineated in this subsurface succession of Jurassic strata from the Loughheed Island area (Embry, 2009).

#### 4.4.4 Maximum flooding surface/ Maximum transgressive surface (MFS):

Maximum flooding surface (MFS) is the shaliest point that represents the major condensed sections that mark the top of the transgressive systems units, and often include the base of the highstand systems units. MFS is used to correlate well log sections and is called “markers” (Oliver and Cowper, 1963). Frazier (1974) called MFS a “hiatal surface” while Vail et al. (1977) called the seismic reflector which encompassed this surface a downlap surface.

In carbonate strata, the MFS marks a change in trend from fining to coarsening. MFS will mark the horizon of change between deepening upward to shallowing upward in shallow water carbonate settings (Embry, 2009).

#### 4.4.5 Application of systems tract model in this study

Figure 4.4 shows the summary of various systems tract classification schemes that have been proposed (Van Wagoner et al. 1988; Embry, 1993; Helland-Hansen and Gielberg, 1994; Posamentier and Allen, 1999). In this study, the transgressive-regressive model proposed by Embry (1993; 2002) is used to interpret the integrated prediction error filter analysis (INPEFA) curve that generated by CycloLog software developed by ENRES international (Figure 4.5).

Figure 4.6 shows an example of the terminology and definitions associated with the interpretation of INPEFA curves. A negative INPEFA trend results from a cumulatively negative set of prediction error values which imply over-estimation of the gamma ray (GR) value by filter (Nio et al., 2005). Therefore, the actual values in the case of a GR log of negative trend are more ‘sandy’ than predicted, implying a regressive systems tract in Embry’s model. A sanding-up trend could imply (a) increased supply of coarse sediment, (b) shallowing-up, or (c) decreasing distance from shoreline (Nio et al., 2005). Conversely, a positive trend results from a cumulatively positive set of prediction error values which the actual values are more ‘shaley’ than predicted, implying a transgressive systems tract in Embry’s model. This might represent (a) decreased sediment supply, (b) increased in water depth or accommodation space, or (c) increasing distance from shoreline (Nio et al., 2005). In Figure 4.4, maximum flooding surface (MFS) is interpreted as start of regression; it is a negative turning point shown in the INPEFA curve which is called a negative bounding surface (NBS). Maximum regressive surface (MRS) is interpreted as the start of transgression in Embry’s model; it is a positive turning point or positive bounding surface (PBS) which is separated by a negative trend below and positive trend on top in INPEFA curves.

The systematic changes in litho-facies by climatic variation can be represented by stratigraphic packages (StratPacs). From a negative bounding surface to a next negative bounding surface forms a complete set of StratPac (Figure 4.5 and Figure 4.6). This Chapter attempts to analyse the subsurface stratigraphy by using the system described here.

Approach	Material-Based		Time-Based		Interpreted Events
Sequence Model	Exxon 1988 All Models Van Wagoner et al., 1988	All Models Embry, 1993	All Models Helland-Hansen and Gjelberg, 1994	All Models Posamentier and Allen, 1999	
<b>Systems Tracts</b>	MFS HST	MFS RST	MFS HST	MFS HST	Start Regression
	MRS TST	MRS TST	MRS TST	MRS TST	Start Transgression
	LST	RST	CC LST	LST	Start Base Level Rise
	FACIES CHANGE		FRST (FSST)	LST	Start Base Level Rise
	MFS HST	MFS	BSFR HST	BSFR HST	Start Base Level Fall
	MRS TST	MRS TST	MRS TST	MRS TST	Start Regression
	LST	RST	CC LST	LST	Start Base Level Rise
	FACIES CHANGE		FRST (FSST)	LST	Start Base Level Rise
	MFS HST	MFS	BSFR HST	BSFR HST	Start Base Level Fall
	MRS TST	MRS TST	MRS TST	MRS TST	Start Transgression
LST	RST	CC LST	LST	Start Base Level Rise	
FACIES CHANGE		FRST (FSST)	LST	Start Base Level Rise	
MFS HST	MFS	BSFR HST	BSFR HST	Start Base Level Fall	

Figure 4.4: Summary of various systems tract classification schemes that have been proposed. The sequence boundaries are in red and internal systems tract boundaries are in blue (Embry, 2009).

Interpreted Events	All models Embry, 1993	Components of INPEFA stratigraphy	Stratigraphic packages (StratPac)
Start Regression	MFS RST	NEGATIVE TREND	One complete set of StratPac
Start Transgression	MRS TST	POSITIVE TREND	
Start Regression	MFS RST	NEGATIVE TREND	
Start Transgression	MRS TST	POSITIVE TREND	
	MFS RST	NEGATIVE TREND	
	MRS TST	POSITIVE TREND	
	MFS RST	NEGATIVE TREND	
	MRS TST	POSITIVE TREND	

Figure 4.5: Application of Embry's models (1993) to components of INPEFA stratigraphy including the stratigraphic packages.

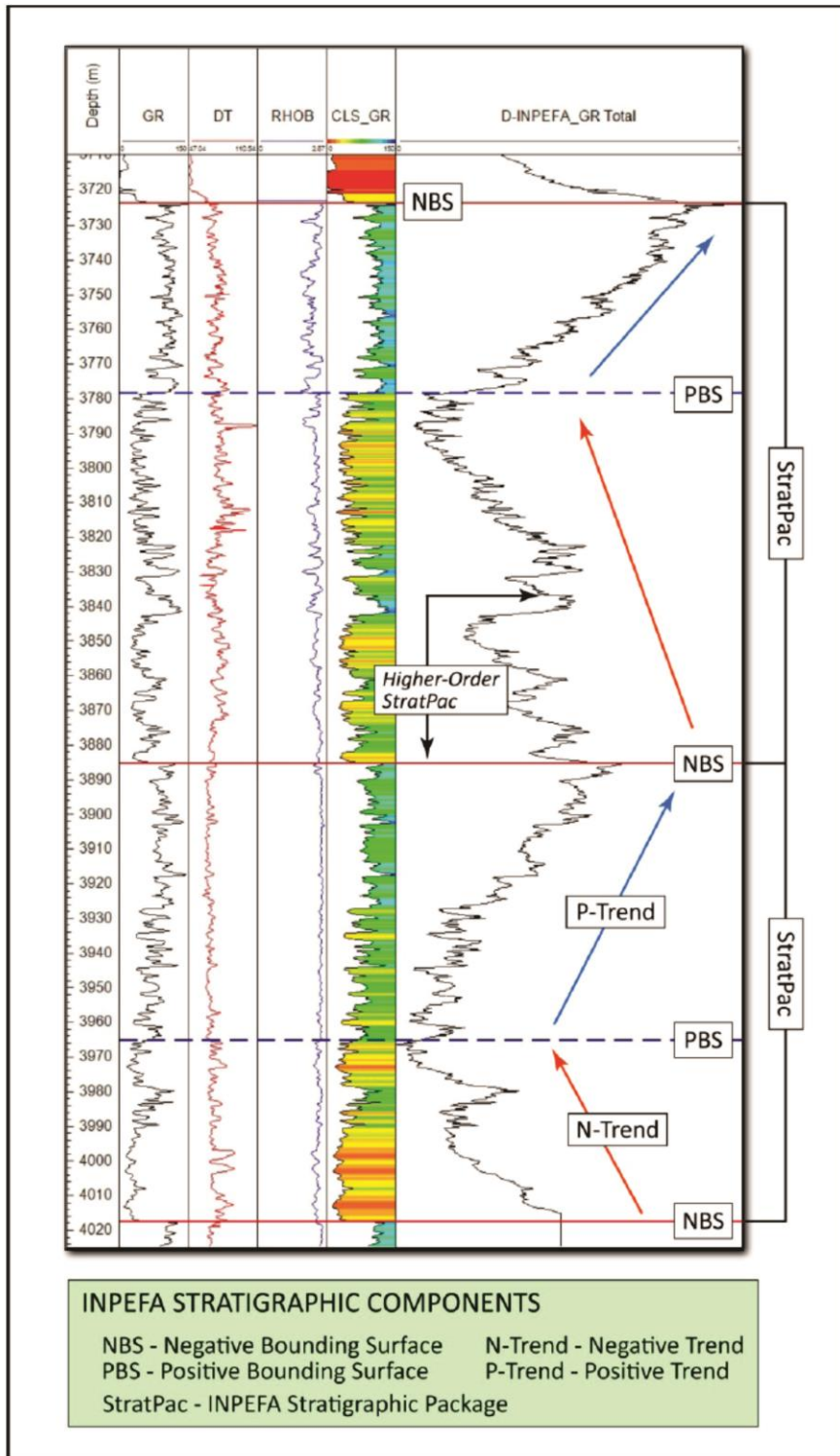


Figure 4.6: Terminology and definitions associated with the interpretation of INPEFA curves (after ENRES, 2011). A negative bounding surface (NBS) is a point at which the trends changes from positive (P-Trend) to negative (N-Trend). A positive bounding surface (PBS) is the point at which trend changes from negative to positive. There are 15 classes of colour in colour gamma ray log, where red, orange and yellow represent low gamma ray value while blue and green represent higher gamma ray value.

## 4.6 Results

### 4.6.5 Broome Platform

This study presents results from the 6 wells: Sharon Ann 1, Goldwyer 1, Hedonia 1, McLarty 1, Looma 1 and Robert 1 in Broome Platform (Figure 4.7) and data analysis in relation to the objectives of the research. Wells Sharon Ann 1, Goldwyer 1 and Hedonia 1 are located at the north-western part of the Broome Platform near to offshore Canning Basin while wells MacLarty 1, Looma 1 and Robert 1 are located at the south-eastern part of Broome Platform near to Mowla Terrace. The Broome Platform has had a complex history because the Ordovician isopachs indicate thickening to the north which suggests a phase of post-Ordovician structural rotation (tilting) but now this platform dips to the south (Broad, 1973).

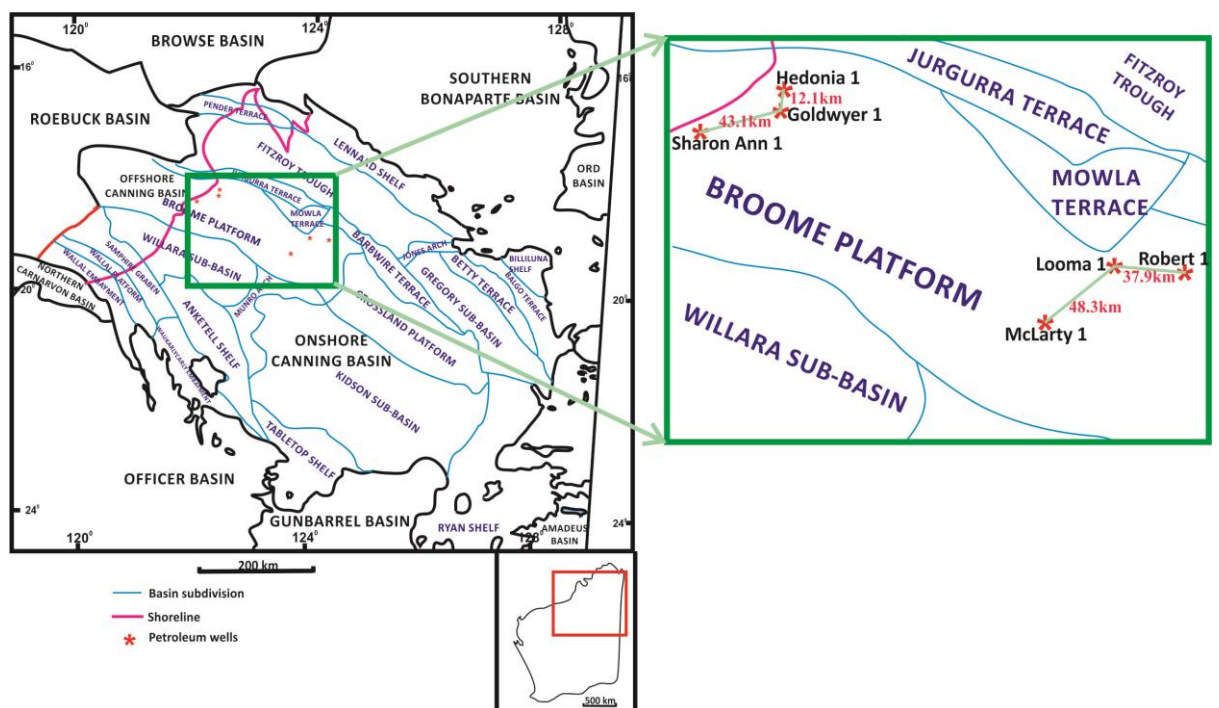


Figure 4.7: Location maps of wells Sharon Ann 1, Goldwyer 1, Hedonia 1, McLarty 1, Looma 1 and Robert 1 in Broome Platform, Canning Basin, WA.

### 4.5.1.1 Well McLarty 1

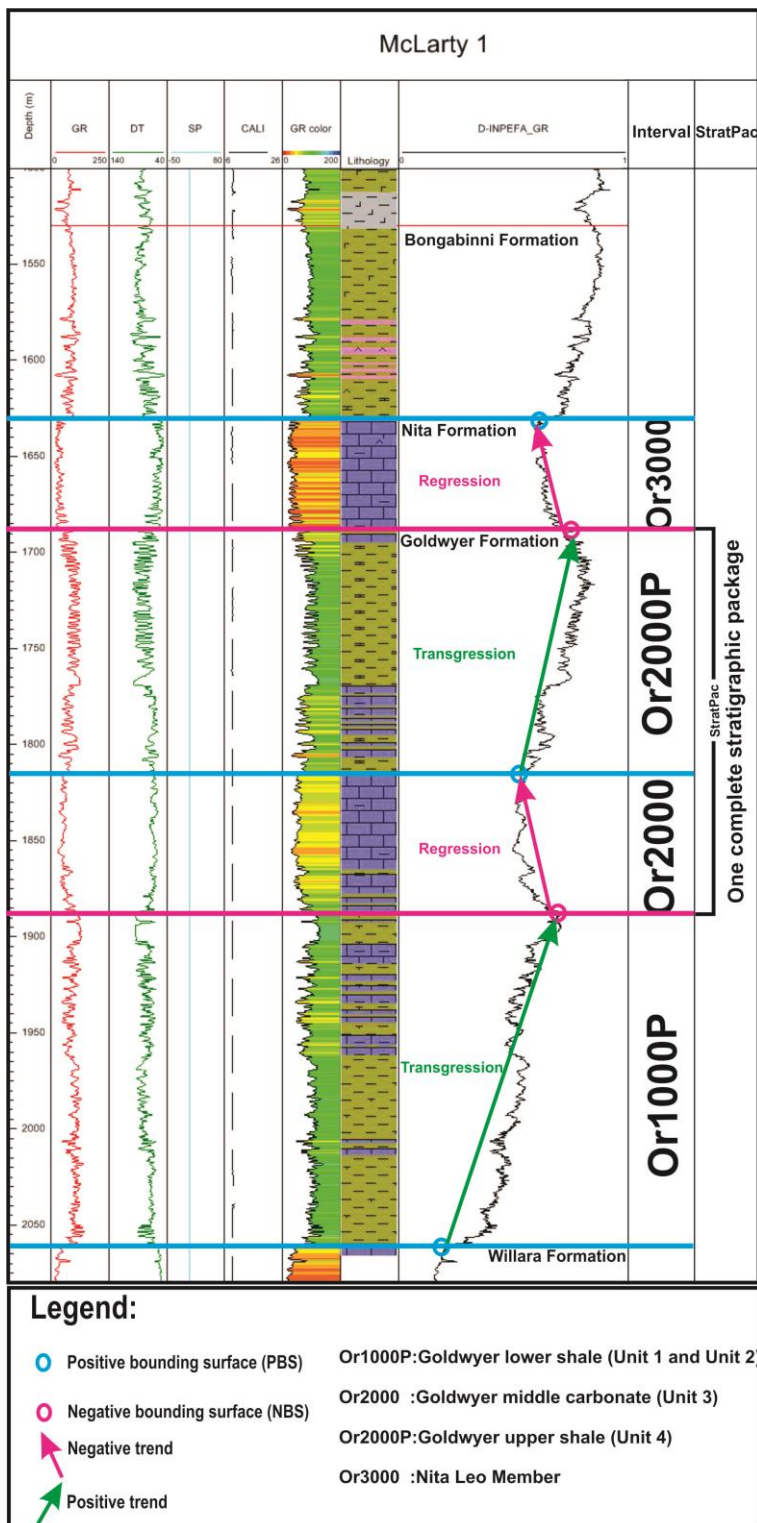


Figure 4.8: Well composite chart of well McLarty 1 with interpreted stratigraphic packages using the INPEFA curves. Note the Goldwyer Formation is complete here but only the lower part of the Nita Formation is covered. There are 15 classes of colour in colour gamma ray log, where red, orange and yellow represent low gamma ray value while blue and green represent higher gamma ray value. For the lithology log, green colour represents shale and purple colour represents limestone.

#### **4.5.1.1.1 Interpretation for McLarty 1 (Figure 4.8)**

The base of the interval studied is Or1000P, a positive trend which is clockwise in an upward direction. Or1000P is a transgressive succession and following this is a regressive trend which is Or2000. The positive bounding surface (PBS) between intervals Or2000 and Or2000P represents a transgressive surface and these two intervals are a complete stratigraphic package. The Goldwyer Formation covers from interval Or1000P to interval Or2000P and it can be suggested that the Goldwyer Formation consists of a transgression (TST), regression (RST) and another transgression (TST), three systems tracts in all. The Goldwyer Formation overlies the Willara Formation (Figure 4.8). Interval Or3000 indicates a regressive succession (Nita Formation) with a negative trend. This is overlain by the shaly Bongabinni Formation at the top of the section (Figure 4.8). The stratigraphic sequences for well McLarty 1 (Figure 4.8) cover the complete Goldwyer Formation and lower part of the Nita Formation. The upper Nita is possibly either eroded by the Bongabinni Formation or Nita Formation was not deposited as the transgressive trend Or3000P and the regressive trend Or4000 are missing compared with well Looma 1 (Figure 4.9). There are 15 classes of colour in colour gamma ray log, where red, orange and yellow represent low gamma ray value while blue and green represent higher gamma ray value. The red, orange and yellow colour gamma ray log matches with the regressive trends in intervals Or3000 and Or2000 because low gamma ray value represents sand prone units or regression (Figure 4.8). Intervals Or1000P and Or2000P in Figure 4.8 matches with the colour gamma ray log which dominated by green colour (high gamma ray value) which represents shale prone units or transgression.

The interval between two main negative bounding surfaces (NBS) is defined as an INPEFA stratigraphic package or Stratpac (ENRES, 2011). There is one Stratpac identified in well McLarty 1 which is a progradational trend (regression) overlain by a retrogradational trend (transgression). This Stratpac is made up of Goldwyer Formation Unit 3 and Unit 4.

### 4.5.1.2 Well Looma 1

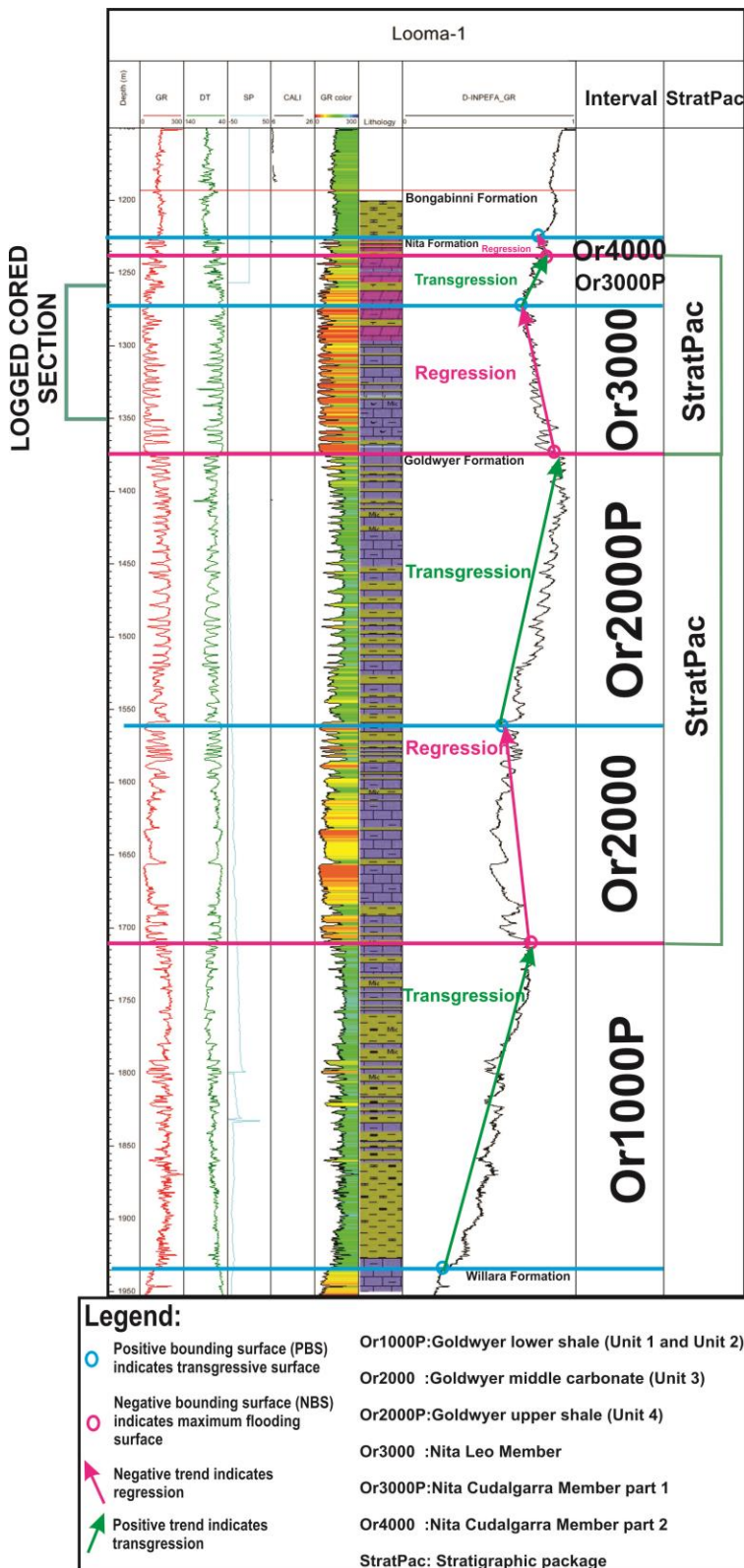


Figure 4.9: Well composite chart of well Looma 1 with interpreted stratigraphic packages using the INPEFA curves. Well Looma 1 covered the complete Nita and Goldwyer Formations. Note that logged cored section is from 1259-1350m (see Figures 3.4-3.8). Colours are described in Figure 4.8.

#### **4.5.1.2.1 Interpretation for Looma 1 (Figure 4.9)**

The stratigraphic packages for well Looma 1 cover most of the stratigraphic interval analyzed and it shows the major breaks and trends clearly. The base of this interval study is Or1000P; this is a positive trend and represents shaly upwards or transgression. The top of interval Or1000P marked by the first prominent negative turning point (NBS) which coincides with the base of Or2000. The NBS at this point is a maximum flooding surface and marks the base of regression trend, which represents Or2000 consists of a stacking of predominant sand prone units. In addition, the colour gamma ray log of interval Or2000 (Figure 4.9) shows low value of gamma ray with majority of yellow to orange colour which represents sand prone units. The positive bounding surface (PBS) of interval Or2000P is a transgressive surface because the transgressive trend is followed by this point. Or2000P has a positive trend that represents a transgressive succession and stops at the negative turning point (NBS). This is followed by interval Or3000 which indicates regression with a negative trend and interval Or3000P with a positive trend (transgression). On top of interval Or3000P is Or4000 which is a regression trend becoming sandy upwards.

The intervals of Or2000 (regression; Goldwyer Unit 3) and Or2000P (transgression; Goldwyer Unit 4) in Goldwyer Formation are a complete stratigraphic package (regression trend then followed by transgression trend) and the intervals of Or3000 and Or3000P are another set of stratigraphic packages. There are two Stratpacs identified in well Looma 1.

#### **4.5.1.2.2 Core to log correlation for Looma 1**

The studied core (Figure 3.8) comes from near the top of the Nita regressive package (interval Or3000), and consists of shallow subtidal to intertidal (and occasionally supratidal) upward shallowing thin carbonate cycles, including microbial laminites, deposited in a low energy tidal flat setting. Based on similarity of log character, it is likely that the whole 91m thick regressive package consists of this cycle type with small sea level fluctuations creating limited accommodation space, followed by repeated infilling by warm water shallow carbonates with known hydrocarbon reservoir potential. Slow subsidence covered with Milankovitch scale sea level change are likely controls.

### 4.5.1.3 Well Robert 1

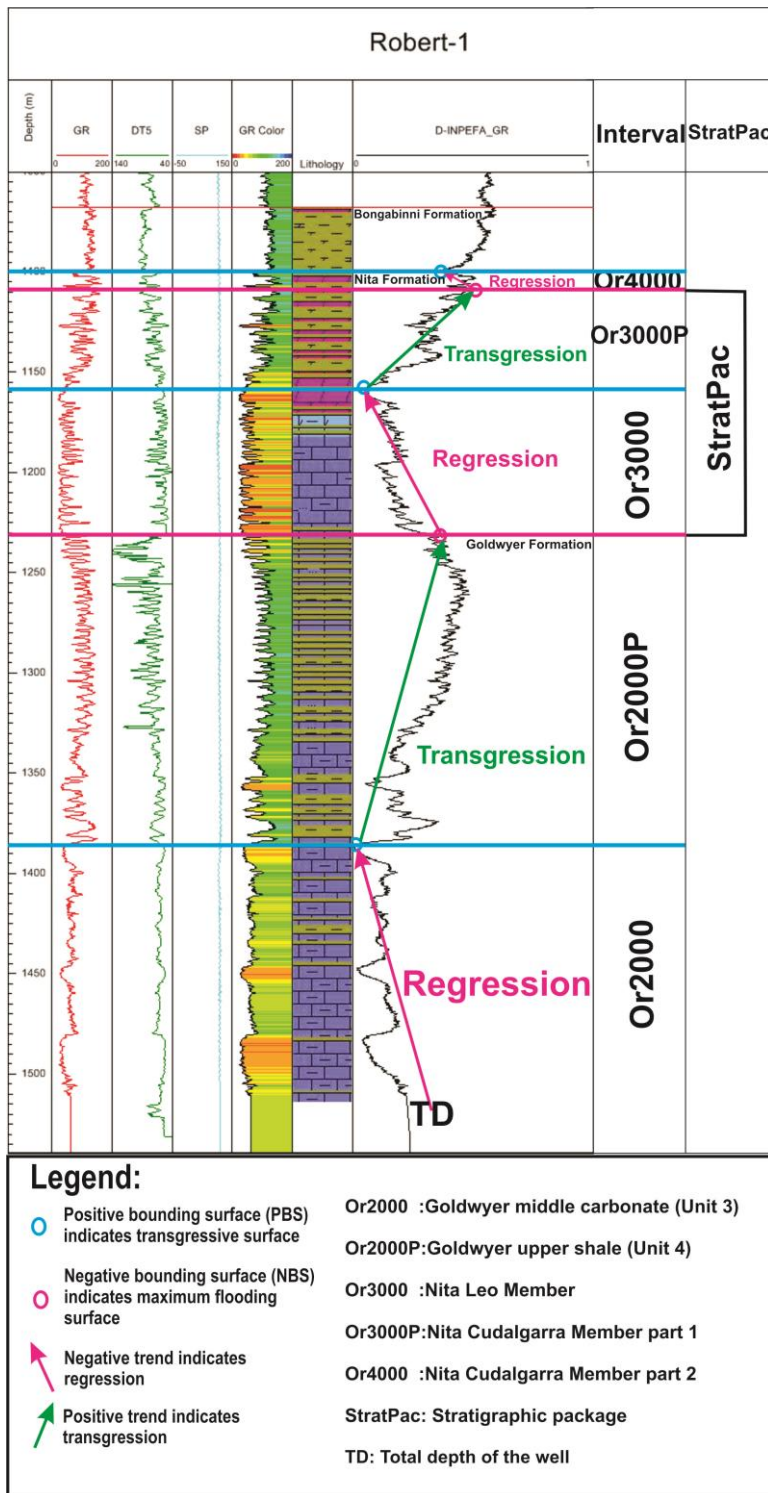


Figure 4.10: Well composite chart of well Robert 1 with interpreted stratigraphic packages using the INPEFA curves. Note the Nita Formation is complete here but only part of the Goldwyer Formation (Goldwyer upper shale and part of the Goldwyer middle carbonate) only is covered due to the well total depth being reached. Colours are described in Figure 4.8.

#### **4.5.1.3.1 Interpretation for Robert 1, Nita Formation and part of Goldwyer Formation (Figure 4.10)**

The stratigraphic packages for well Robert 1 cover the complete Nita Formation and part of the Goldwyer Formation as indicated by borehole data (Figure 4.10). For the Goldwyer Formation, the base starts from Or2000 where the interval Or1000P does not exist in this well. Or2000 is a regression trend and is followed by the Or2000P which is a transgressive succession. The intervals that cover the Nita Formation are Or3000, Or3000P and Or4000 where the Nita Formation is dominated by a regressive succession. However, the Nita is represented by a complete StratPac (Regression then Transgression). The caliper log (and therefore the self potential log) is not available for well Robert 1.

There is one Stratpac identified in well Robert 1 which is a progradational trend (regression) overlain by a retrogradational trend (transgression). This Stratpac is made up by Nita Formation Leo Member and Cudalgarra Member part 1.

#### **4.5.1.4 Well correlation of wells McLarty 1, Looma 1 and Robert 1 (Figure 4.11)**

The regional correlations of the INPEFA curves of well McLarty 1, well Looma 1 and well Robert 1 are shown in Figure 4.11. Compared to well Looma 1, well McLarty 1 consists of intervals Or1000P, Or2000, Or2000P and Or3000 while intervals Or3000P and Or4000 do not exist due to erosion processes. This indicates top Nita Formation of well McLarty 1 is an unconformity due to erosion. The Nita Formation in well McLarty1 was probably eroded by the Carribuddy Group which overlies it. A different stratigraphy occurs with well McLarty 1. Well Robert 1 consists of intervals from Or2000, Or2000P, Or3000, Or3000P and Or4000. Well Robert 1 does not contain the full Goldwyer Formation due to the wireline data stopping at the middle part of the Goldwyer Formation. The regression successions which are the reservoir rocks (Or2000, Or3000 and Or4000) are thickening towards the basin centre and thinner towards the basin margin.

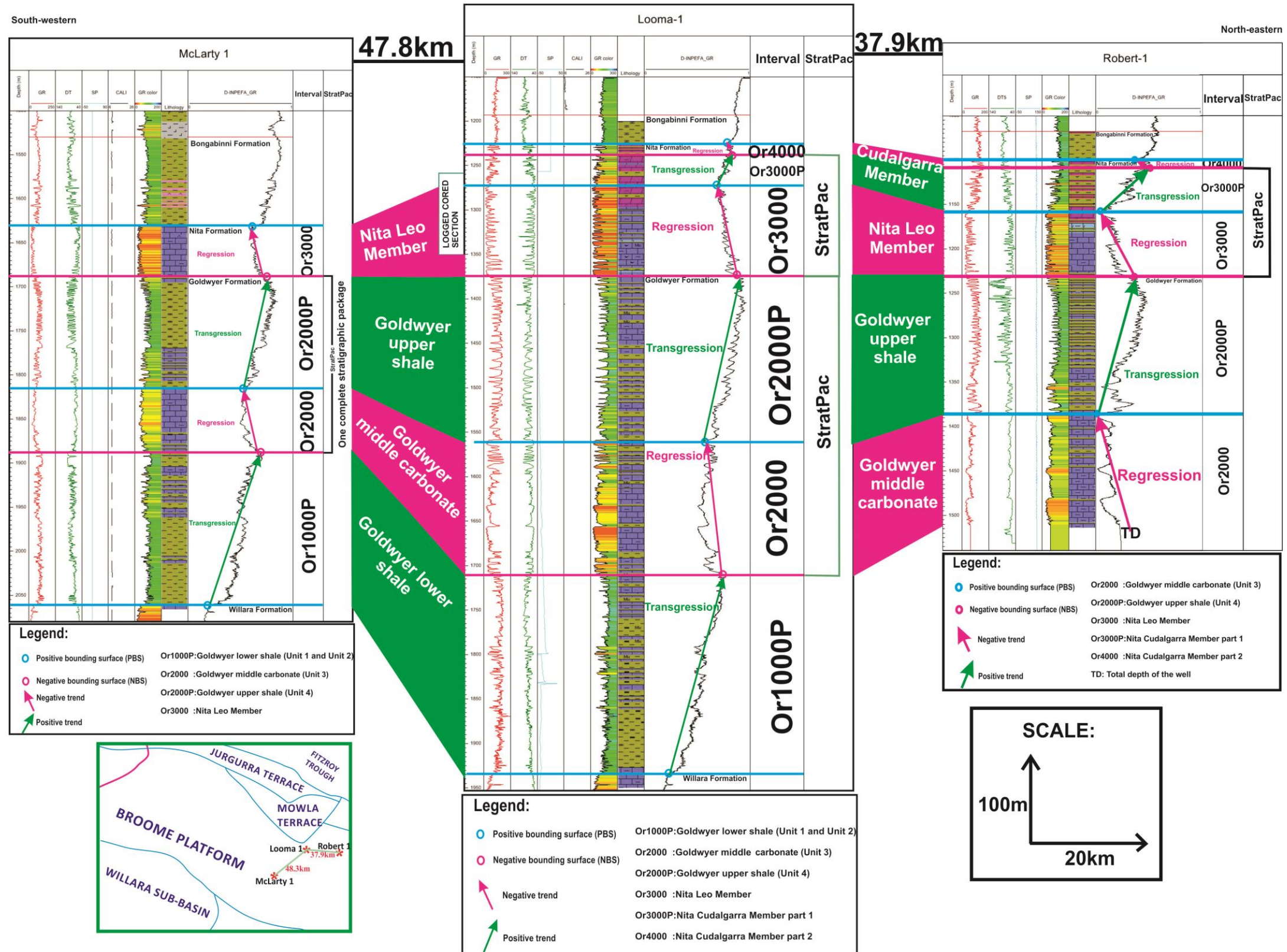


Figure 4.11: Well-to-well correlation of the INPEFA curves of wells McLarty 1, Looma 1 and Robert 1 on the Broome Platform, showing the subdivision of the Nita and Goldwyer formations (Or1000P: Goldwyer lower shale (Transgression); Or2000: Goldwyer middle limestone (Regression); Or2000P: Goldwyer upper shale (Transgression); Or3000: Leo Member (Regression); Or3000P: Cudalgarra Member part 1 (Transgression); and, Or4000: Cudalgarra part 2 (Regression)).

### 4.5.1.5 Well Sharon Ann 1

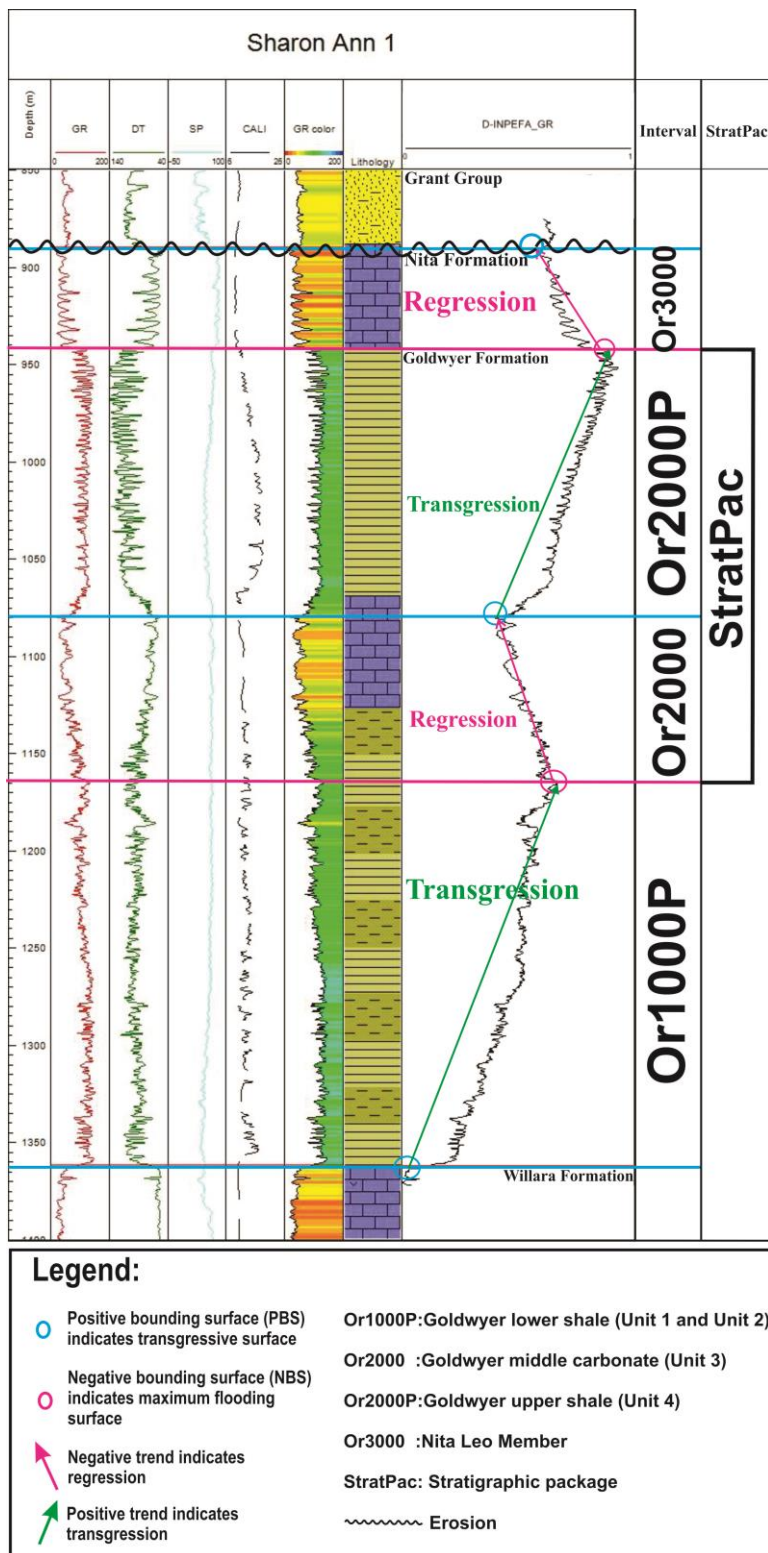


Figure 4.12: Well composite chart of well Sharon Ann 1 with interpreted stratigraphic packages using the INPEFA curves. Note the Goldwyer Formation is complete here but only part of the Nita Formation (part of Nita Leo Member) is covered due to the erosion by the Permian Grant Group. Colours are described in Figure 4.8.

#### **4.5.1.5.1 Interpretation for Sharon Ann 1 (Figure 4.12)**

The base of the interval studied of well Sharon Ann 1 is Or1000P, a positive trend which is clockwise in an upward direction. As a positive trend indicates transgression, interval Or1000P is a transgressive succession and following this is a regressive trend which is interval Or2000 with a negative trend. The positive bounding surface (PBS) between intervals Or2000 and Or2000P represents a transgressive surface and these two intervals are a complete stratigraphic package (StratPac). The Goldwyer Formation covers from interval Or1000P to interval Or2000P and it can be suggested that the Goldwyer Formation started from a transgressive trend followed by a regressive trend and finally a transgressive trend. The Goldwyer Formation is overlain conformably on top of the Willara Formation (Figure 4.12). Interval Or3000 indicates a regressive succession (Nita Formation Leo Member). The upper Nita (Nita Formation Cudalgarra Member) is eroded by the Permian Grant Group as the transgressive trend Or3000P and the regressive trend Or4000 are missing compared with well Looma 1 (Figure 4.9).

There is one stratigraphic package identified in well Sharon Ann 1 (intervals Or2000 and Or2000P). This stratigraphic package for well Sharon Ann 1 (Figure 4.12) covers Goldwyer Formation Unit 3 and Unit 4.

#### 4.5.1.6 Well Goldwyer 1

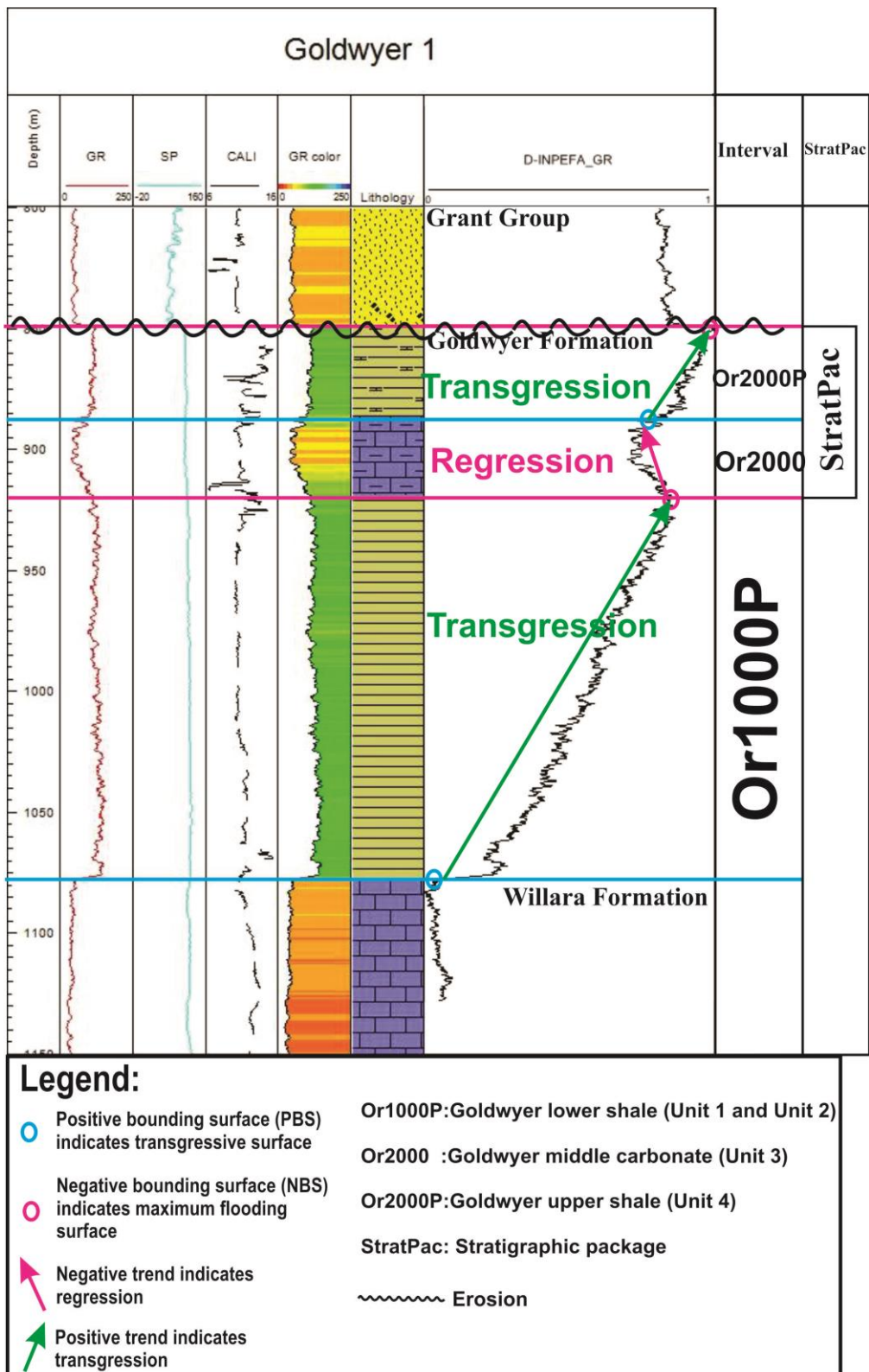


Figure 4.13: Well composite chart of well Goldwyer 1 with interpreted stratigraphic packages using the INPEFA curves. Note the upper part of the Goldwyer Formation (Goldwyer upper shale) is partly eroded by Permian Grant Group; this erosion process is a reason of the absence of Nita Formation. Colours are described in Figure 4.8.

#### **4.5.1.6.1 Interpretation for Goldwyer 1 (Figure 4.13)**

The stratigraphic sequences for well Goldwyer 1 (Figure 4.13) cover the complete Goldwyer Formation with part of the Goldwyer upper shale eroded by Permian Grant Group and the Nita Formation is absent in this well.

The base of the interval studied of well Goldwyer 1 is Or1000P, a positive trend which is clockwise in an upward direction (Figure 4.13). As a positive trend indicates transgression, interval Or1000P is a transgressive succession and following this is a regressive trend which is interval Or2000 with a negative trend. The positive bounding surface (PBS) between intervals Or2000 and Or2000P represents a transgressive surface and these two intervals are a complete stratigraphic package (StratPac). The Goldwyer Formation covers from interval Or1000P to interval Or2000P and it can be suggested that the Goldwyer Formation started from a transgressive trend followed by a regressive trend and finally a transgressive trend. This matches previous ideas that the Goldwyer lower shale indicates transgression, Goldwyer middle carbonate indicates regression and Goldwyer upper shale indicates transgression. The upper part of the Goldwyer Formation (Goldwyer upper shale) is partly eroded by the Permian Grant Group; this erosion process is a reason for the absence of the Nita Formation. The Goldwyer Formation lies conformably on top of the Willara Formation in well Goldwyer 1.

There is one stratigraphic package identified in well Goldwyer 1 (intervals Or2000 and Or2000P). This stratigraphic package for well Sharon Ann 1 (Figure 4.12) covers Goldwyer Formation Unit 3 and Unit 4.

#### 4.5.1.7 Well Hedonia 1

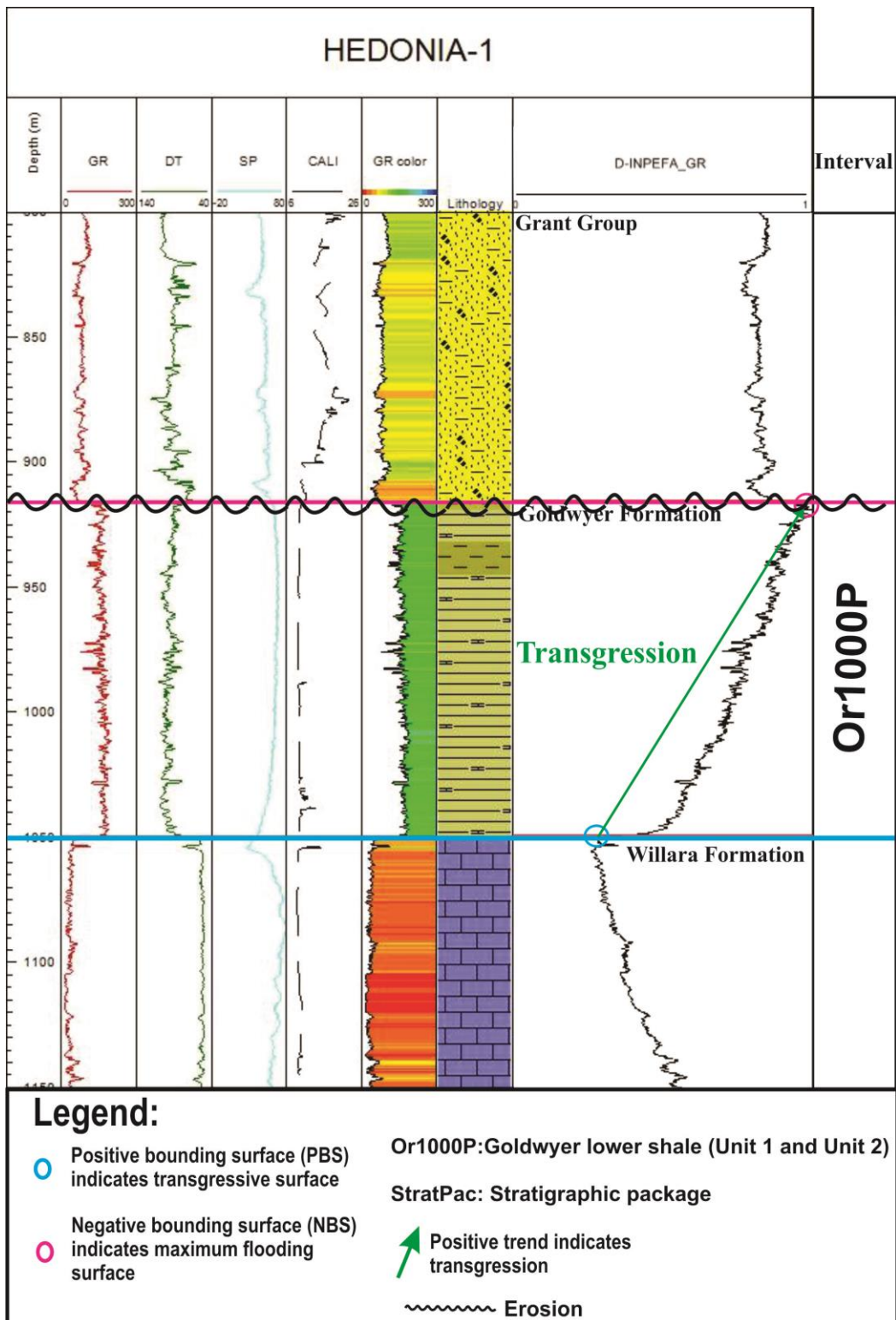


Figure 4.14: Well composite chart of well Hedonia 1 with interpreted stratigraphic packages using the INPEFA curves. Note the Permian Grant Group eroded the Nita and Goldwyer Formations and left only part of the Goldwyer lower shale. The Goldwyer Formation overlies conformably on top of the Willara Formation. Colours are described in Figure 4.8.

#### **4.5.1.7.1 Interpretation for Hedonia 1 (Figure 4.14)**

The interval studied of well Hedonia 1 is Or1000P, a positive trend which is clockwise in an upward direction (Figure 4.14). As a positive trend indicates transgression, interval Or1000P is a transgressive succession. This matches the Goldwyer lower shale which indicates transgression. The intervals Or2000, Or2000P, Or3000, Or3000P and Or4000 (Goldwyer middle carbonate, Goldwyer upper shale and Nita Formation) are absent in this well. This is due to the erosion process which happened in Permian time. The Goldwyer Formation is lies conformably on top of the Willara Formation in well Goldwyer 1.

The stratigraphic sequences for well Hedonia 1 (Figure 4.14) only consists of Goldwyer lower shale (Or1000P) as other parts of the intervals (Or2000, Or2000P, Or3000, Or3000P and Or4000) were eroded by the Permian Grant Group. Therefore, there is no stratpac identified in well Hedonia 1.

#### **4.5.1.8 Well correlation of wells Sharon Ann 1, Goldwyer 1 and Hedonia 1 (Figure 4.15)**

The regional correlations of the INPEFA curves of well Sharon Ann 1, well Goldwyer 1 and well Hedonia 1 are shown in Figure 4.15. Well Sharon Ann 1 consists of intervals Or1000P, Or2000, Or2000P and Or3000. Intervals Or3000P and Or4000 (Nita Formation Cudalgarra Member) do not exist in Sharon Ann 1 compared with Looma 1 (see Figure 4.9), the Nita Cudalgarra Member was probably eroded by Permian successions because the Permian Grant Group lies unconformably on top of the Nita Leo Member. Well Goldwyer 1 consists of intervals Or1000P, Or2000 and Or2000P (Goldwyer Formation) while intervals Or3000, Or3000P and Or4000 (Nita Formation) do not exist. This indicates Nita Formation in well Goldwyer 1 was eroded by the Permian Grant Group. Well Hedonia 1 only consists of interval Or1000P, which indicates that the Goldwyer lower shale was truncated due to erosion processes in the Permian. The Nita and Goldwyer Formations packages are thickening towards well Sharon Ann 1 from well Hedonia 1. Erosion in the Permian influenced the successions in well Hedonia 1 the most, followed by well Goldwyer 1 and well Sharon Ann 1.

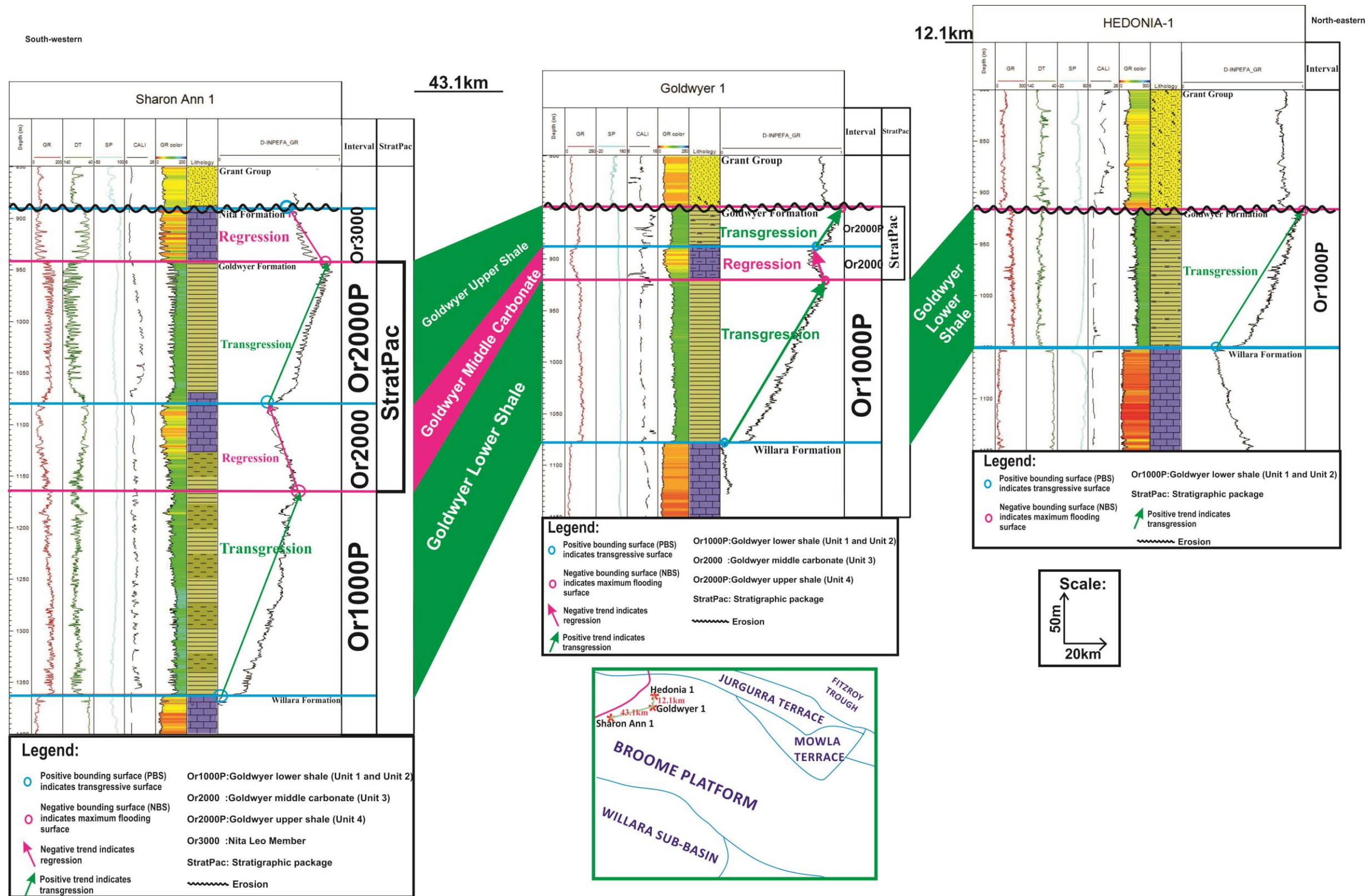


Figure 4.15: Well-to-well correlation of the INPEFA curves of wells Sharon Ann 1, Goldwyer 1 and Hedonia 1 on the Broome Platform, well Sharon Ann 1 shows the subdivision of the Nita and Goldwyer Formations (Or1000P: Goldwyer lower shale (Transgression); Or2000: Goldwyer middle limestone (Regression); Or2000P: Goldwyer upper shale (Transgression); Or3000: Leo Member (Regression)). Note that Nita Cudalgarra Member (intervals Or3000P and Or 4000) is absent due to the erosion by Permian Grant Group. Due to this erosion process, well Goldwyer 1 consists of intervals Or1000P, Or2000 and Or2000P while well Hedonia 1 only consists of interval Or1000P.

#### 4.6.5 Barbwire Terrace

This study presents results from the 6 wells: Acacia 2, Barbwire 1, Dodonea 1, Percival 1, Setaria 1, Solanum 1 in Barbwire terrace (Figure 4.16) and data analysis in relation to the objectives of the research. Wells Acacia 2, Barbwire 1, Dodonea 1, Setaria 1, Solanum 1 are located at the north-western part of the Barbwire Terrace while well Percival 1 is located at the south-eastern part of Broome Platform. The Barbwire Terrace is essentially divided into the northern Barbwire High and southern Percival High (France, 1986). The Ordovician sequence on the Barbwire Terrace is significantly block-faulted with minor folding; these faults pass down into basement rocks and tend to die out into the overlying Carribuddy Group (France, 1986).

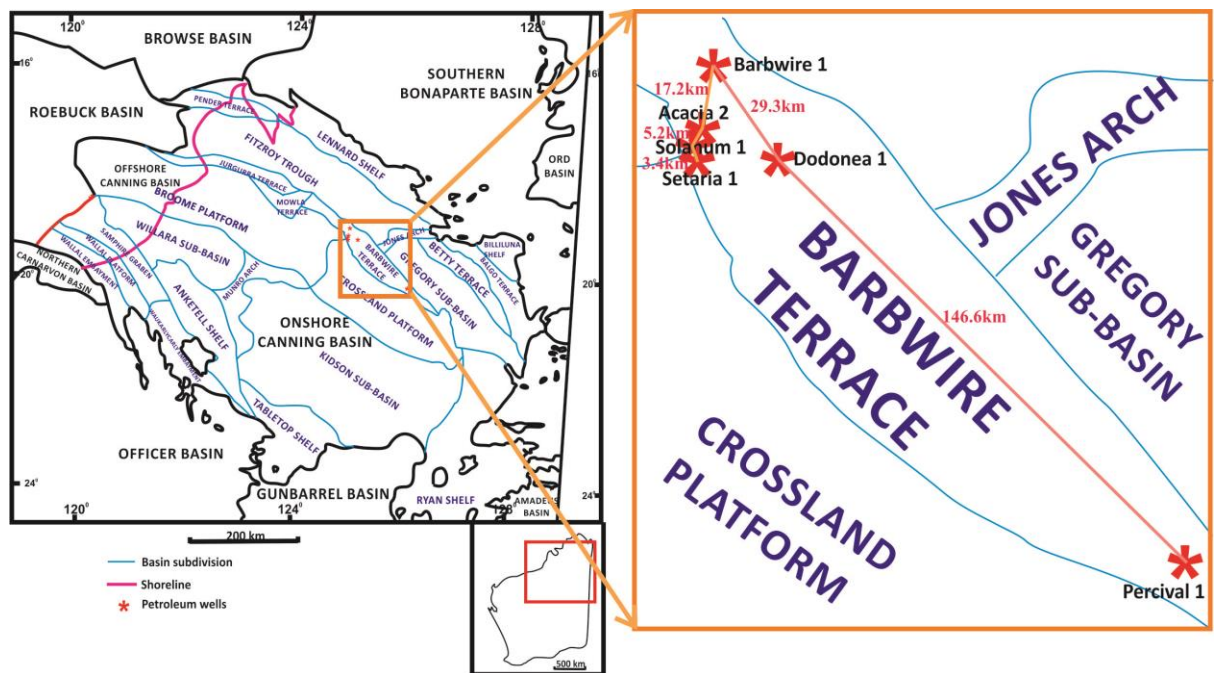


Figure 4.16: Location maps of wells Acacia 2, Barbwire 1, Dodonea 1, Percival 1, Setaria 1 and Solanum 1 in Barbwire Terrace, Canning Basin, WA.

### 4.5.2.1 Well Barbwire 1

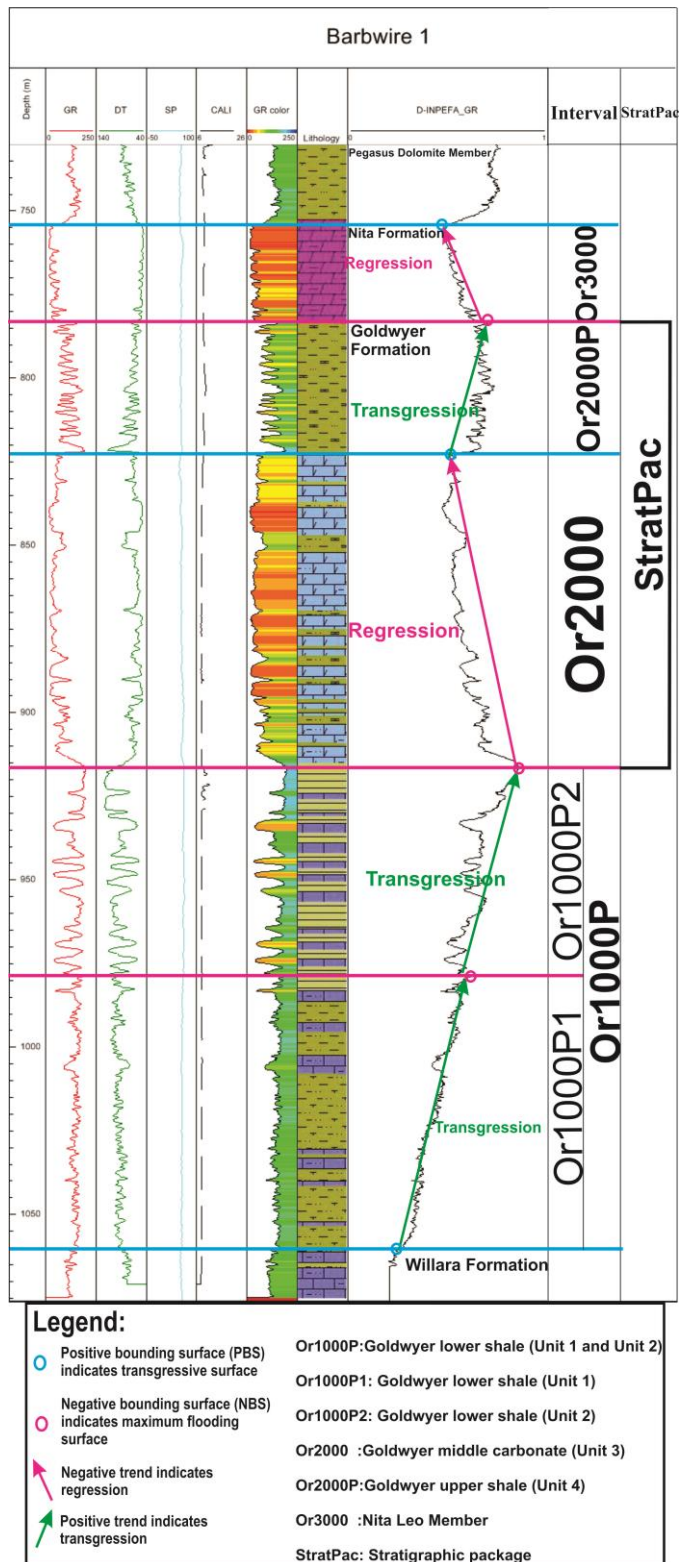


Figure 4.17: Well composite chart of well Barbwire 1 with interpreted stratigraphic packages using the INPEFA curves. Note the Goldwyer Formation is complete here but only part of the Nita Formation (part of Nita Leo Member) is covered due to either the erosion by Pegasus Dolomite Member or the formation pinched out. Colours are described in Figure 4.8.

#### **4.5.2.1.1 Interpretation for Barbwire 1 (Figure 4.17)**

The stratigraphic sequences for well Barbwire cover the complete Goldwyer Formation and lower part of the Nita Formation (Nita Leo Member). The base of the interval studied of well Barbwire 1 is Or1000P, a positive trend which is clockwise in an upward direction (Figure 4.17). As a positive trend indicates transgression, interval Or1000P (Goldwyer lower shale) is a transgressive succession. This interval Or1000P can be sub-divided into two parts by the different log characters, which are Or1000P1 and Or1000P2. Goldwyer lower shale has been sub-divided into Goldwyer Unit 1 and Goldwyer Unit 2 in Barbwire Terrace by Foster et al. (1986); this matches the Or1000P1 as Goldwyer Unit 1 and Or1000P2 as Goldwyer Unit 2. Following this is a regressive trend which is interval Or2000 with a negative trend. The positive bounding surface (PBS) between intervals Or2000 and Or2000P represents a transgressive surface and these two intervals are a complete stratigraphic package (StratPac). The Goldwyer Formation covers from interval Or1000P to interval Or2000P and it can be suggested that the Goldwyer Formation started from a transgressive trend followed by a regressive trend and finally a transgressive trend. The Goldwyer Formation is overlain conformably on top of the Willara Formation (Figure 4.17). Interval Or3000 indicates a regressive succession (Nita Formation Leo Member). Nita Formation Cudalgarra Member (transgressive trend Or3000P and the regressive trend Or4000 in Figure 4.9) are not found in this well. The Nita Cudalgarra Member probably pinched out in this section or was eroded by the Pegasus Dolomite Member from the Carribuddy Group (Upper Ordovician – Silurian).

There is one stratigraphic package identified in well Barbwire 1 (intervals Or2000 and Or2000P). This stratigraphic package for well Barbwire 1 (Figure 4.17) covers Goldwyer Formation Unit 3 and Unit 4.

### 4.5.2.2 Well Dodonea 1

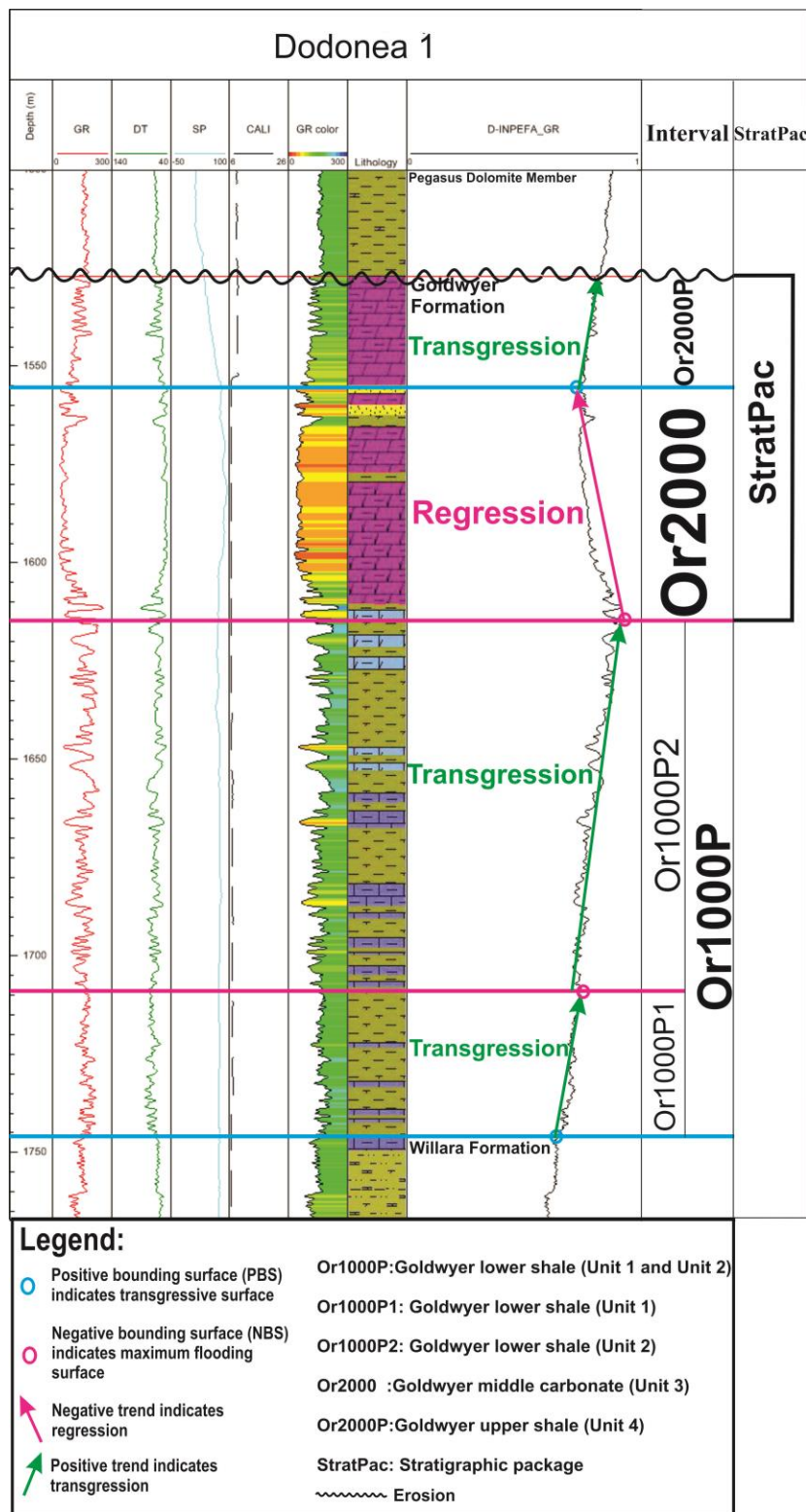


Figure 4.18: Well composite chart of well Dodonea 1 with interpreted stratigraphic packages using the INPEFA curves. Note the upper part of the Goldwyer Formation (Goldwyer upper shale) is partly eroded by Pegasus Dolomite Member in Carribuddy Group; this erosion process might be a reason for the absence of Nita Formation. Colours are described in Figure 4.8.

#### **4.5.2.2.1 Interpretation for Dodonea 1 (Figure 4.18)**

The stratigraphic sequences for well Dodonea 1 (Figure 4.18) cover the complete Goldwyer Formation with the possibility that part of the Goldwyer upper shale was eroded by Pegasus Dolomite Member since the Nita Formation is absent in this well.

The base of the interval studied of well Dodonea 1 is Or1000P, a positive trend which is clockwise in an upward direction (Figure 4.18). As a positive trend indicates transgression, interval Or1000P (Goldwyer lower shale) is a transgressive succession. This interval Or1000P can be sub-divided into two parts by the different log characters, which are Or1000P1 and Or1000P2. Goldwyer lower shale has been sub-divided into Goldwyer Unit 1 and Goldwyer Unit 2 in Barbwire Terrace by Foster et al. (1986); this matches the Or1000P1 as Goldwyer Unit 1 and Or1000P2 as Goldwyer Unit 2. Following this is a regressive trend which is interval Or2000 with a negative trend. The positive bounding surface (PBS) between intervals Or2000 and Or2000P represents a transgressive surface. The Goldwyer Formation covers from interval Or1000P to interval Or2000P and it can be suggested that the Goldwyer Formation started from a transgressive trend followed by a regressive trend and finally a transgressive trend. These matches the Goldwyer lower shale indicates transgression, Goldwyer middle carbonate indicates regression and Goldwyer upper shale indicates transgression. The upper part of the Goldwyer Formation (Goldwyer upper shale) is possibly eroded by Pegasus Dolomite Member from the Carribuddy Group (Upper Ordovician-Silurian) because the Nita Formation which should overlie conformably on top of the Goldwyer Formation is absent. The Goldwyer Formation is overlain conformably on top of the Willara Formation in well Dodonea 1.

There is one stratigraphic package identified in well Dodonea 1 (intervals Or2000 and Or2000P). This stratigraphic package for well Dodonea 1 (Figure 4.18) covers Goldwyer Formation Unit 3 and Unit 4. The top part of the Goldwyer Formation Unit 4 is eroded by the Pegasus Dolomite Member.

### 4.5.2.3 Well Percival 1

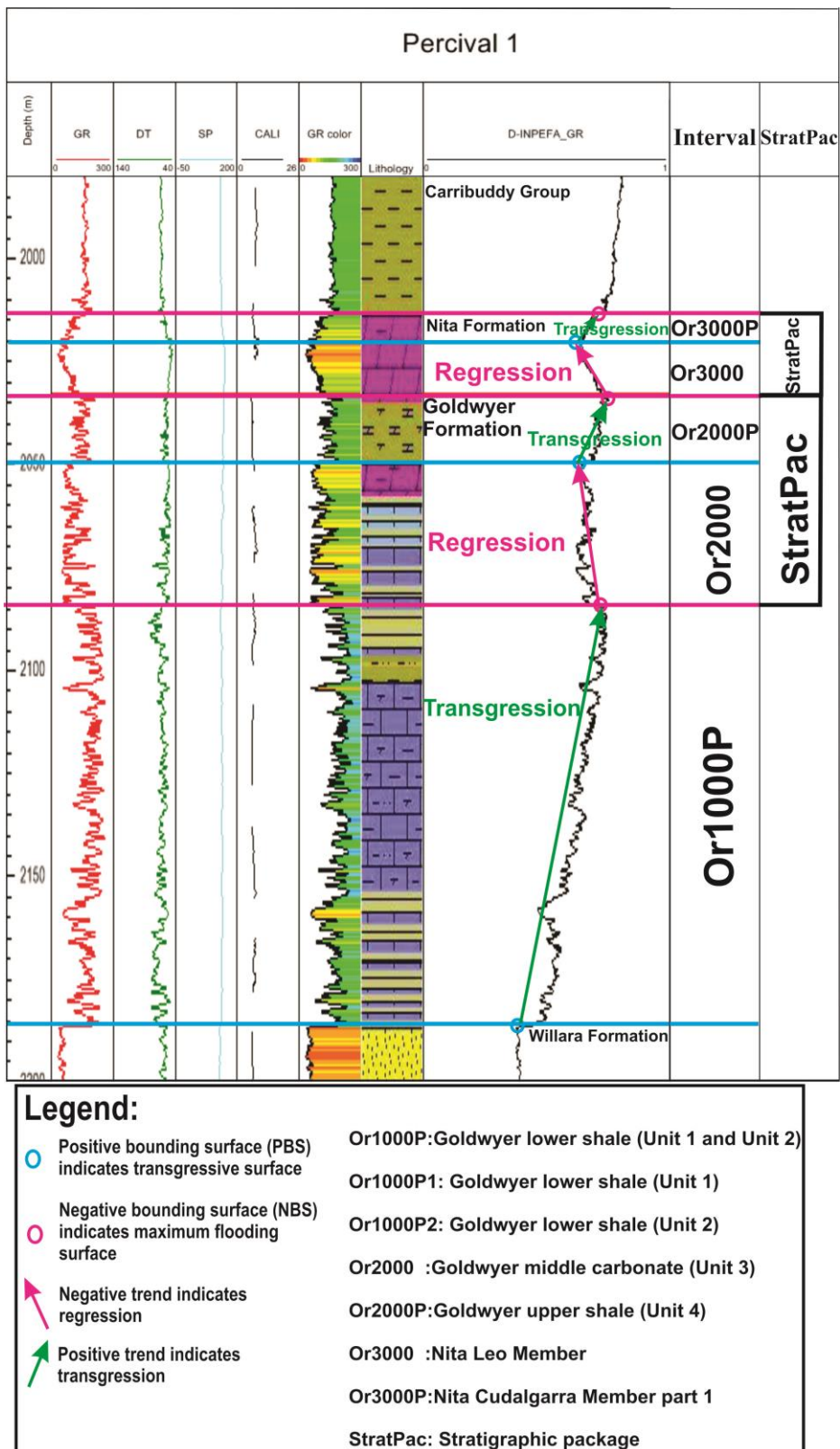


Figure 4.19: Well composite chart of well Percival 1 with interpreted stratigraphic packages using the INPEFA curves. Note the Goldwyer Formation is complete here and major part of the Nita Formation is covered. Colours are described in Figure 4.8.

#### **4.5.2.3.1 Interpretation for Percival 1 (Figure 4.19)**

The base of the interval studied is Or1000P, a positive trend which is clockwise in an upward direction (Figure 4.19). Or1000P is a transgressive succession and following this is a regressive trend which is Or2000. The positive bounding surface (PBS) between intervals Or2000 and Or2000P represents a transgressive surface and these two intervals are a complete stratigraphic package. The Goldwyer Formation covers from interval Or1000P to interval Or2000P and it can be suggested that the Goldwyer Formation started from a transgressive trend followed by a regressive trend and finally a transgressive trend. The Goldwyer Formation is overlain on top of the Willara Formation. The intervals of Or3000 and Or3000P are another set of stratigraphic packages. Interval Or3000 indicates a regressive succession (Nita Formation Leo Member) while interval Or3000P indicates a transgressive succession (Nita Formation Cudalgarra Member part 1). The interval Or4000 (Nita Formation Cudalgarra Member part 2) is not found in this well. The Nita Formation is overlain by the shaly Carribuddy Group at the top of the section (Figure 4.19).

The intervals of Or2000 (regression; Goldwyer Unit 3) and Or2000P (transgression; Goldwyer Unit 4) in Goldwyer Formation are a complete stratigraphic package (regression trend then followed by transgression trend) and the intervals of Or3000 and Or3000P are another set of stratigraphic packages. Therefore, there are two Stratpacs identified in well Percival 1.

#### **4.5.2.4 Well correlation of wells Barbwire 1, Dodonea 1 and Percival 1 (Figure 4.20)**

The regional correlations of the INPEFA curves of wells Barbwire 1, Dodonea 1 and Percival 1 are shown in Figure 4.20. Well Barbwire 1 shows the subdivision of the Nita and Goldwyer Formations (Or1000P: Goldwyer lower shale (Transgression); Or2000: Goldwyer middle limestone (Regression); Or2000P: Goldwyer upper shale (Transgression); Or3000: Leo Member (Regression)) and well Dodonea 1 consists of intervals Or1000P, Or2000 and Or2000P. Note that Nita Formation is thinning from well Barbwire 1 to well Dodonea 1. The Nita Formation is either eroded by Pegasus Dolomite Member or died out from well Barbwire 1 towards well Dodonea 1. However, Nita Formation (Leo Member and Cudalgarra Member part 1) can be found in well Percival 1. This is probably due to the Barbwire Terrace which is essentially divided into the northern Barbwire High and southern Percival High (France, 1986).

North-western

South-eastern

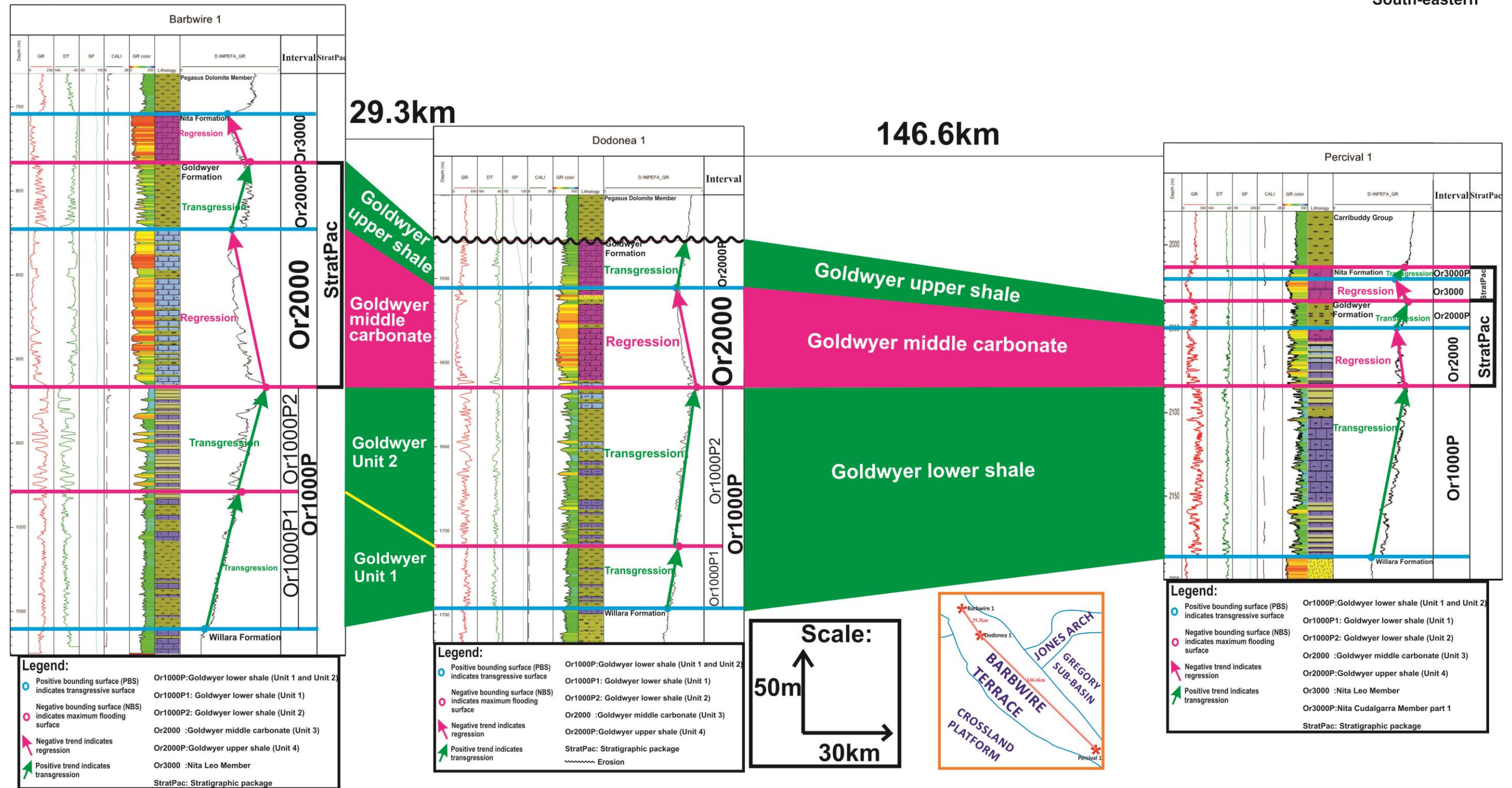


Figure 4.20: Well-to-well correlation of the INPEFA curves of wells Barbwire 1, Dodonea 1 and Percival 1 on the Barbwire Terrace. Well Barbwire 1 shows the subdivision of the Nita and Goldwyer Formations (Or1000P: Goldwyer lower shale (Transgression); Or2000: Goldwyer middle limestone (Regression); Or2000P: Goldwyer upper shale (Transgression); Or3000: Leo Member (Regression) and well Dodonea 1 consists of intervals Or1000P, Or2000 and Or2000P. Note that Nita Formation is thinning from well Barbwire 1 to well Dodonea 1. The Nita Formation is either eroded by Pegasus Dolomite Member or died out from well Barbwire 1 towards well Dodonea 1. However, Nita Formation (Leo Member and Cudalgarra Member part 1) can be found in well Percival 1. This is probably due to the Barbwire Terrace which is essentially divided into the northern Barbwire High and southern Percival High (France, 1986).

#### 4.5.2.5 Well Setaria 1

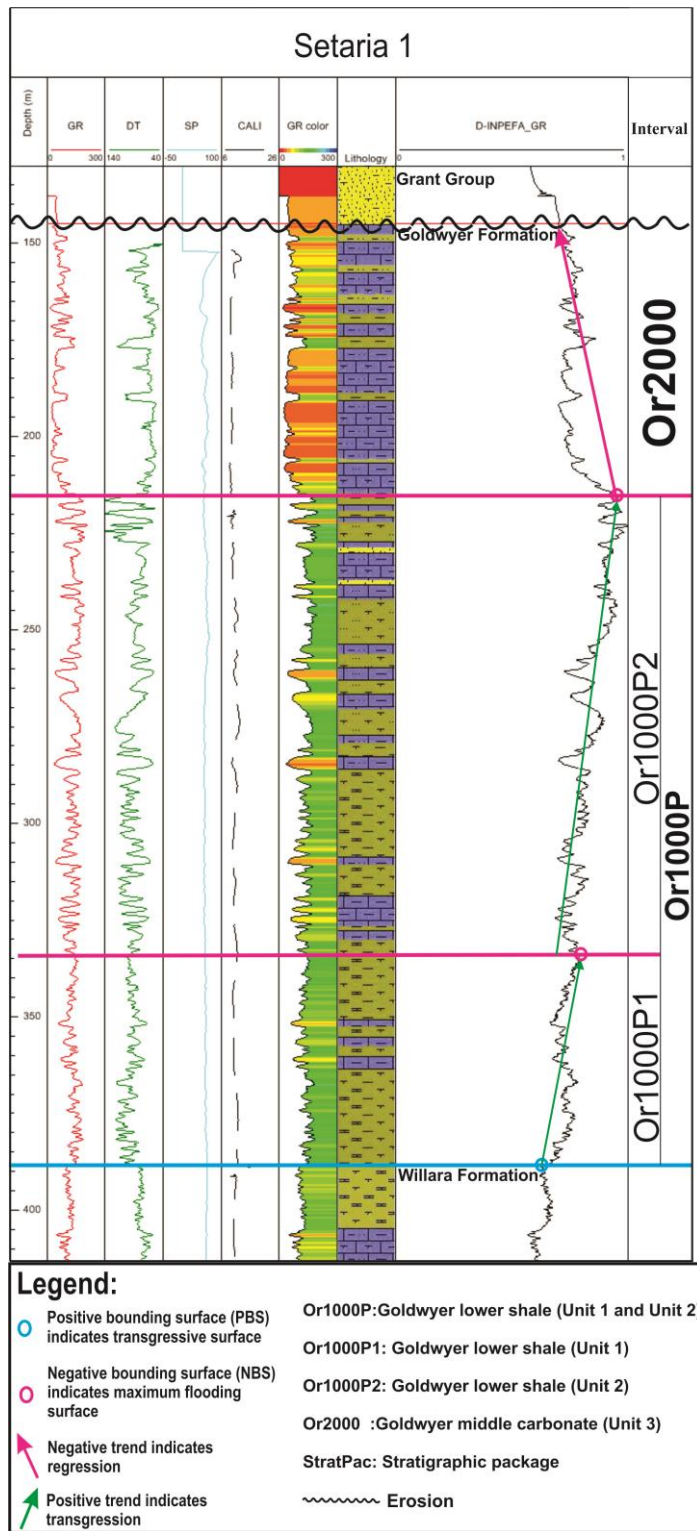


Figure 4.21: Well composite chart of well Setaria 1 with interpreted stratigraphic packages using the INPEFA curves. Note the the top of Goldwyer Formation Unit 3 (Goldwyer middle carbonate) is eroded by the Permian glaciations events; this erosion process might be a reason for the absence of Nita Formation. Colours are described in Figure 4.8.

#### **4.5.2.5.1 Interpretation for Setaria 1 (Figure 4.21)**

The base of the interval studied of well Setaria 1 is Or1000P, a positive trend which is clockwise in an upward direction (Figure 4.21). As a positive trend indicates transgression, interval Or1000P is a transgressive succession. This interval Or1000P can be sub-divided into two parts by the different log characters, which are Or1000P1 and Or1000P2. Goldwyer lower shale has been sub-divided into Goldwyer Unit 1 and Goldwyer Unit 2 in Barbwire Terrace by Foster et al. (1986); this matches the Or1000P1 as Goldwyer Unit 1 and Or1000P2 as Goldwyer Unit 2. Following this is a regressive trend which is interval Or2000 with a negative trend.

The Goldwyer Formation covers from interval Or1000P (transgression) to interval Or2000 (regression) in this well. This match the Goldwyer lower shale indicates transgression and the Goldwyer middle carbonate indicates regression. The upper part of the Goldwyer Formation (Goldwyer upper shale) and the Nita Formation which should lie on top of the Goldwyer upper shale are eroded by the Permian Grant Group; this erosion process is a reason for the absence of Goldwyer upper shale and Nita Formation. The Goldwyer Formation is overlain conformably on top of the Willara Formation in well Setaria 1.

The stratigraphic sequences for well Setaria 1 (Figure 4.21) cover the Goldwyer lower shale (Or1000P) and Goldwyer middle carbonate (Or2000). The Goldwyer upper shale and Nita Formation are eroded by Permian Grant Group. With only two intervals in well Setaria 1, there is no Stratpac identified in this well.

### 4.5.2.6 Well Solanum 1

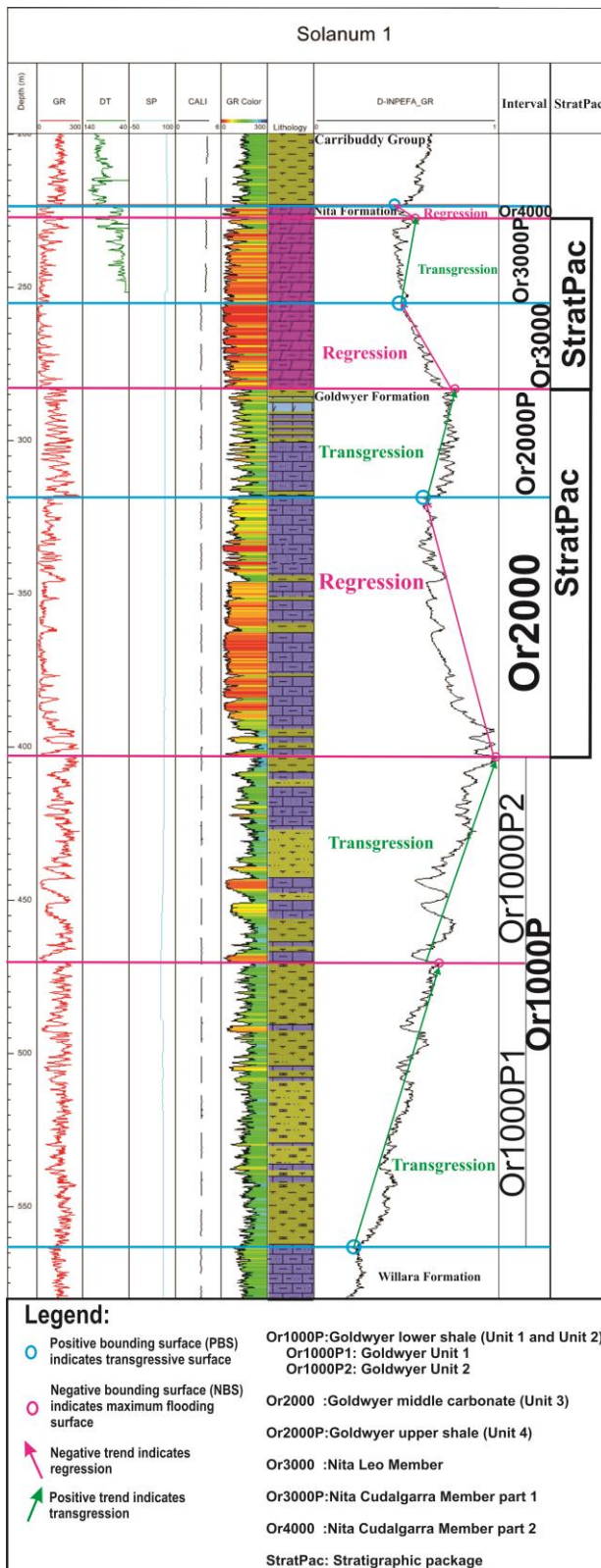


Figure 4.22: Well composite chart of well Solanum 1 with interpreted stratigraphic packages using the INPEFA curves. Well Solanum 1 covered the complete Nita and Goldwyer Formations. Colours are described in Figure 4.8.

#### **4.5.2.6.1 Interpretation for Solanum 1 (Figure 4.22)**

The stratigraphic packages for well Solanum 1 cover the complete Nita Formation and Goldwyer Formations as indicated by borehole data (Figure 4.22). The stratigraphic packages for well Solanum 1 cover most of the stratigraphic interval analysed and it shows the major breaks and trends clearly. The base of this interval study is Or1000P; this is a positive trend and represents shaly upwards or transgression. This interval Or1000P can be sub-divided into two parts by the different log characters, which are Or1000P1 and Or1000P2. Goldwyer lower shale has been sub-divided into Goldwyer Unit 1 and Goldwyer Unit 2 in Barbwire Terrace by Foster et al. (1986); this matches the Or1000P1 as Goldwyer Unit 1 and Or1000P2 as Goldwyer Unit 2.

The top of interval Or1000P marked by the first prominent negative turning point (NBS) which coincides with the base of Or2000. The NBS at this point is a maximum flooding surface and marks the base of regression trend, which represents Or2000 consists of a stacking of predominant sand prone units. In addition, the colour gamma ray log of interval Or2000 (Figure 4.22) shows low value of gamma ray with majority of yellow to orange colour which indicates sand prone units. The positive bounding surface (PBS) of interval Or2000P is a transgressive surface because the transgressive trend is followed by this point. Or2000P has a positive trend that represents a transgressive succession and stops at the negative turning point (NBS). The intervals of Or2000 and Or2000P are a complete stratigraphic package (regression trend then followed by transgression trend) and the intervals of Or3000 and Or3000P are another set of stratigraphic packages (Figure 4.22). On top of interval Or3000P is Or4000 which is a regression trend becoming sandy upwards.

The Goldwyer Formation is overlain conformably on top of the Willara Formation in well Solanum 1. The stratigraphic sequences for well Solanum 1 (Figure 4.22) cover the complete Nita Formation (intervals Or3000, Or3000P and Or4000) and Goldwyer Formation (intervals Or1000P, Or2000 and Or2000P). The intervals of Or2000 (regression; Goldwyer Unit 3) and Or2000P (transgression; Goldwyer Unit 4) in Goldwyer Formation are a complete stratigraphic package (regression trend then followed by transgression trend) and the intervals of Or3000 and Or3000P are another set of stratigraphic packages. There are two Stratpacs identified in well Solanum 1.

### 4.5.2.7 Well Acacia 2

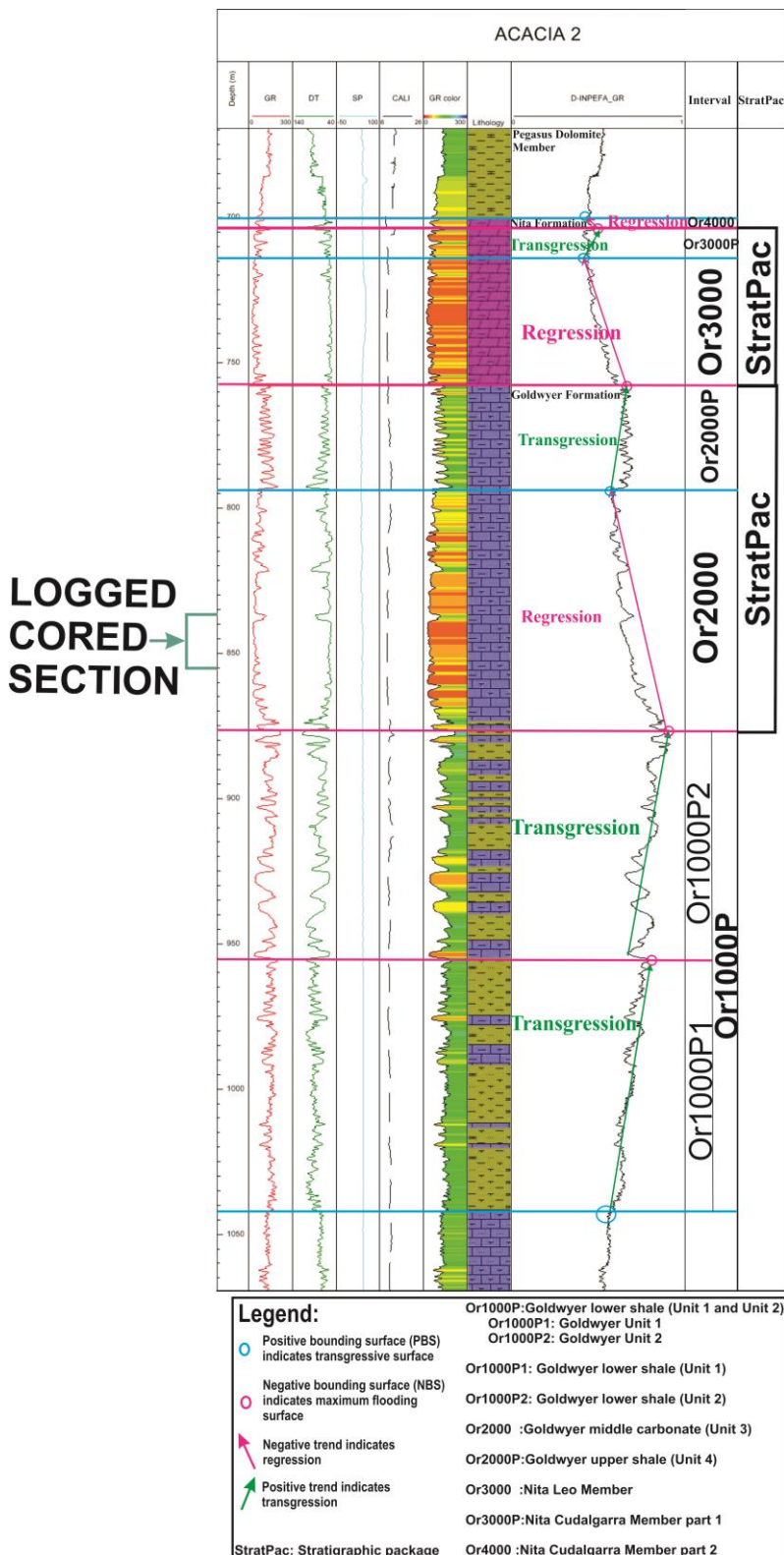


Figure 4.23: Well composite chart for well Acacia 2 with interpreted stratigraphic packages using the INPEFA curves. Well Acacia 2 covered the complete Nita and Goldwyer Formations. Note that logged cored section is from 837-855.12m which shows stacked and thin subtidal carbonate cycles (see Figures 3.21). Colours are described in Figure 4.8.

#### **4.5.2.7.1 Interpretation for Acacia 2 (Figure 4.23)**

The stratigraphic sequences for well Acacia 2 cover the complete Nita Formation and Goldwyer Formation as indicated by borehole data (Figure 4.23) and it shows the major breaks and trends clearly. The base of this interval study is Or1000P; this is a positive trend and represents shaly upwards or transgression. This interval Or1000P can be sub-divided into two parts by the different log characters, which are Or1000P1 and Or1000P2. Goldwyer lower shale has been sub-divided into Goldwyer Unit 1 and Goldwyer Unit 2 in Barbwire Terrace by Foster et al. (1986); this matches the Or1000P1 as Goldwyer Unit 1 and Or1000P2 as Goldwyer Unit 2.

The top of interval Or1000P marked by the first prominent negative turning point (NBS) which coincides with the base of Or2000. The NBS at this point is a maximum flooding surface and marks the base of regression trend, which represents Or2000 consists of a stacking of predominant sand prone units. In addition, the colour gamma ray log of interval Or2000 (Figure 4.23) shows low value of gamma ray (15 classes by log value, red representing the lowest GR value and blue representing the highest GR value) with majority of yellow to orange colour. The positive bounding surface (PBS) of interval Or2000P is a transgressive surface because the transgressive trend is followed by this point. Or2000P has a positive trend that represents a transgressive succession and stops at the negative turning point (NBS). The intervals of Or2000 and Or2000P are a complete stratigraphic package (regression trend then followed by transgression trend) and the intervals of Or3000 and Or3000P are another set of stratigraphic packages (Figure 4.23). On top of interval Or3000P is Or4000 which is a regression trend becoming sandy upwards. The Goldwyer Formation lies conformably on top of the Willara Formation in well Acacia 2.

There are two Stratpacs identified in well Acacia 2. The intervals of Or2000 (regression; Goldwyer Unit 3) and Or2000P (transgression; Goldwyer Unit 4) in Goldwyer Formation are a complete Stratpac (regression trend then followed by transgression trend) and the intervals of Or3000 and Or3000P are another set of Stratpac.

#### **4.5.2.7.2 Core to log correlation for Acacia 2**

Unit 3 of Goldwyer Formation (see Figure 3.21) consists of shallow warm water subtidal carbonates which are cyclic and shallow upwards (where core is available for study within this regression package), (see Figure 3.21). They represent a muddy carbonate shoreface association.

#### **4.5.2.8 Well correlation of wells Setaria 1, Solanum 1, Acacia 2 and Barbwire 1 (Figure 4.24)**

The regional correlations of the INPEFA curves of well Setaria 1, well Solanum 1, well Acacia 2 and well Barbwire 1 are shown in Figure 4.24. Well Solanum 1 and well Acacia 2 show the complete subdivision of the Nita and Goldwyer Formations (Or1000P1: Goldwyer Unit 1 (Transgression); Or1000P2: Goldwyer Unit 2 (Transgression); Or2000: Goldwyer middle limestone (Regression); Or2000P: Goldwyer upper shale (Transgression); Or3000: Leo Member (Regression); Or3000P: Cudalgarra Member part 1 (Transgression); Or4000: Cudalgarra Member part 2 (Regression)). These two wells match very well with the intervals interpreted in well Looma 1 (see Figure 4.9) except the Goldwyer lower shale can be sub-divided into Goldwyer Unit 1 and Goldwyer Unit 2 clearly in well Acacia 2 and well Solanum 1.

Foster et al. (1986) has defined that the Goldwyer Formation consists of four units, which are Unit 1, Unit 2, Unit 3 and Unit 4. According to Foster et al. (1986), Unit 1 and Unit 4 are thinly bedded shale and carbonate, Unit 2 is thickly bedded shale and carbonate while Unit 3 is dominated by carbonates. Menezes (2012) also confirmed that the Goldwyer Formation on the Barbwire Terrace can be subdivided into four units by using the electrofacies analysis. Nita Formation and Goldwyer Unit 4 are eroded by the Permian Grant Group in well Setaria 1. In well Barbwire 1, Nita Formation Cudalgarra Member is absent; this is probably due to the erosion by Pegasus Dolomite Member or stratigraphic pinchout.

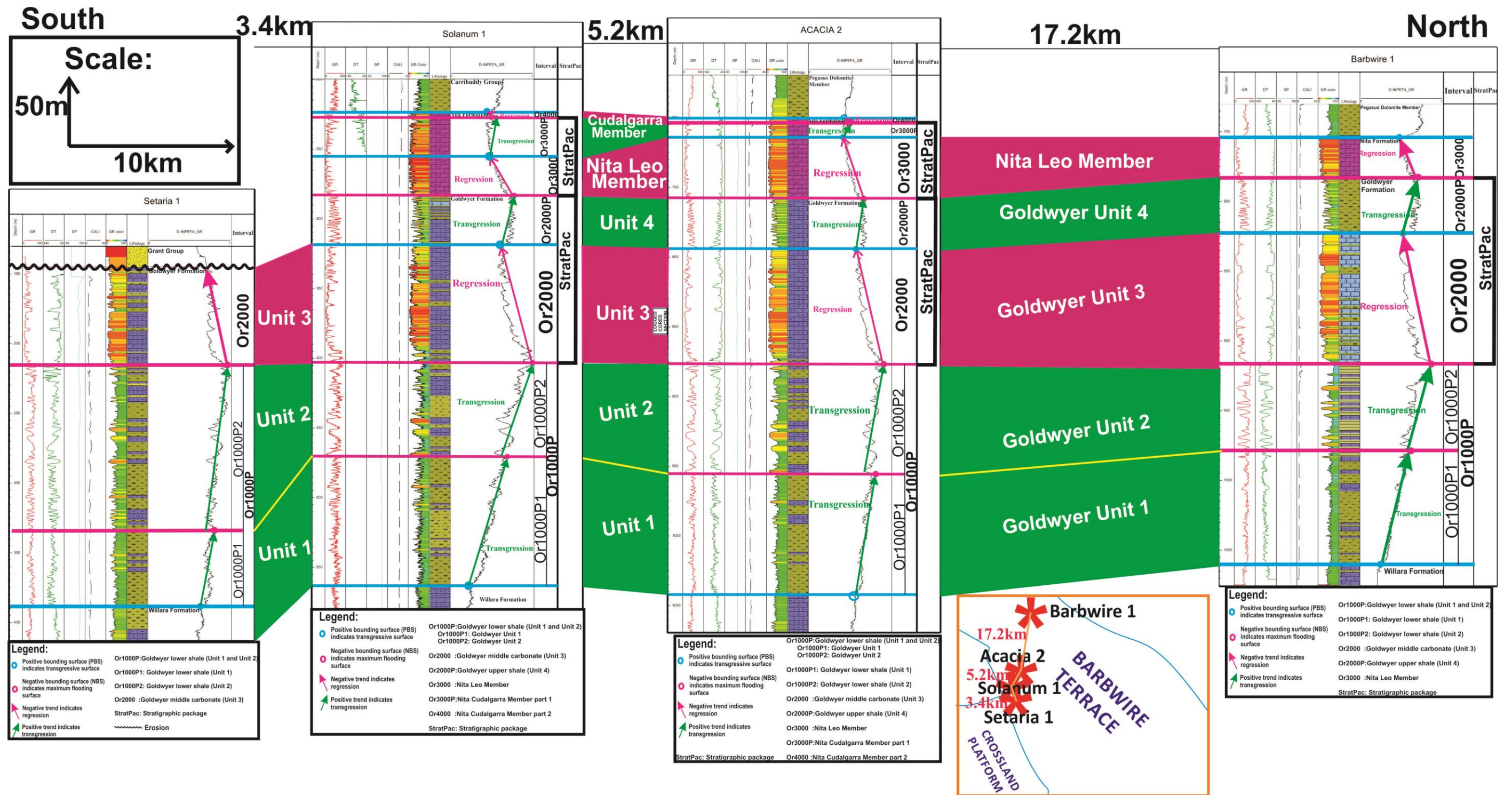


Figure 4.24: Well-to-well correlation of the INPEFA curves of wells Setaria 1, Solanum 1, Acacia 2 and Barbwire 1 on the Barbwire Terrace, wells Solanum 1 and Acacia 2 show the complete subdivision of the Nita and Goldwyer Formations (Or1000P1: Goldwyer Unit 1 (Transgression); Or1000P2: Goldwyer Unit 2 (Transgression); Or2000: Goldwyer middle limestone (Regression); Or2000P: Goldwyer upper shale (Transgression); Or3000: Leo Member (Regression); Or3000P: Cudalgarra Member part 1 (Transgression); Or4000: Cudalgarra Member part 2 (Regression)). Note that Nita Formation and Goldwyer Unit 4 are eroded by the Permian Grant Group in well Setaria 1. In well Barbwire 1, Nita Formation Cudalgarra Member is absent; this is probably due to the erosion by Pegasus Dolomite Member or pinches out.

#### 4.6.5 Crossland Platform

This study presents results from the three wells: Missing 1, Santalum 1A and Kunzea 1 in Crossland Platform (Figure 4.25) and data analysis in relation to the objectives of the research. Wells Missing 1, Santalum 1A and Kunzea 1 are located at the north-western part of the Crossland Platform. The Crossland Platform is located in the central part of the Canning Basin (Figure 4.25). Wells that penetrate to Ordovician succession are rare in the Crossland Platform and the three wells studied in this area are near to the Broome Platform and Barbwire Terrace.

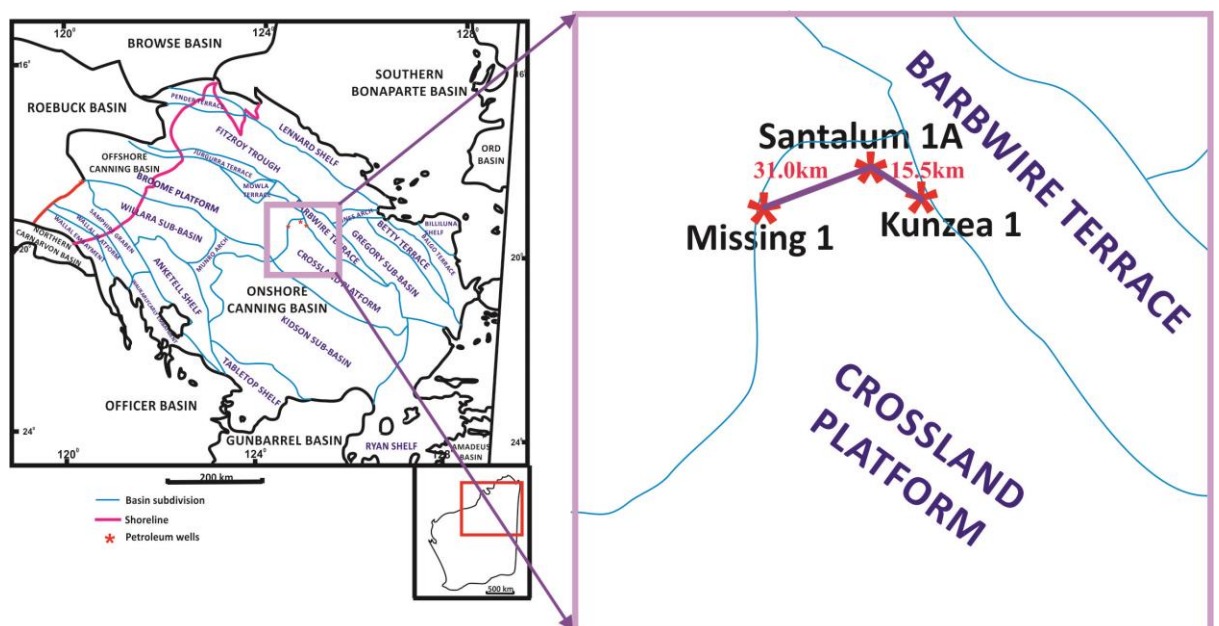


Figure 4.25: Location maps of wells Missing 1, Santalum 1A and Kunzea 1 in Crossland Platform, Canning Basin, WA.

### 4.5.3.1 Well Missing 1

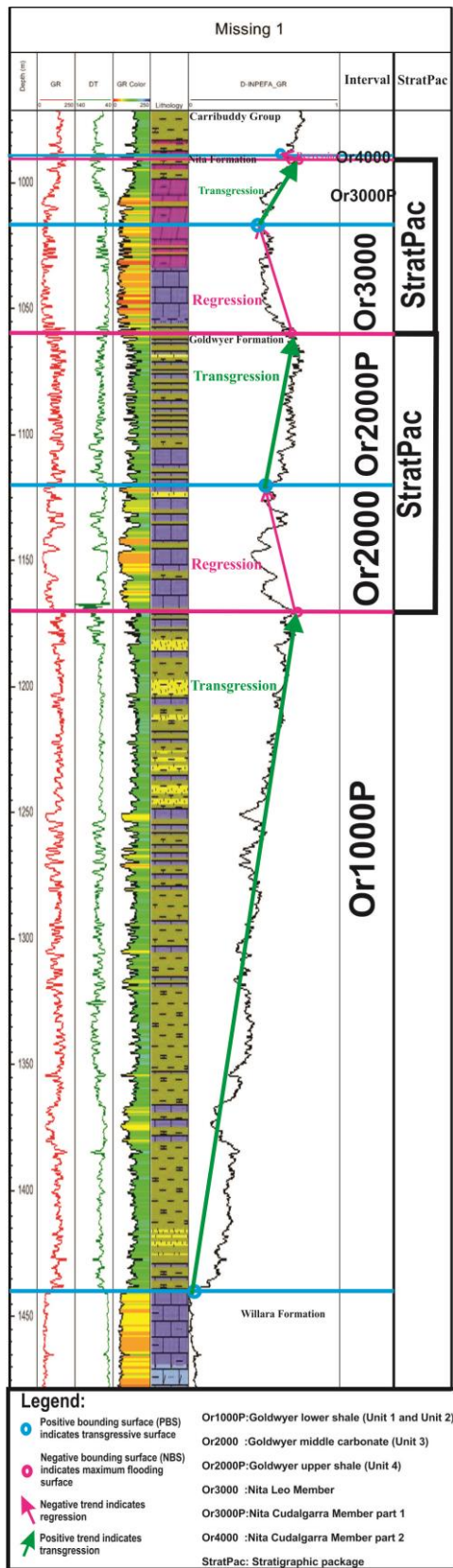


Figure 4.26: Well composite chart of well Missing 1 with interpreted stratigraphic packages using the INPEFA curves. Well Missing 1 covered the complete Nita and Goldwyer Formations. Colours are described in Figure 4.8.

#### **4.5.3.1.1 Interpretation for Missing 1 (Figure 4.26)**

The stratigraphic packages for well Missing 1 cover most of the stratigraphic interval analyzed and it shows the major breaks and trends clearly. The base of this interval study is Or1000P; this is a positive trend and represents shaly upwards or transgression. The top of interval Or1000P marked by the first prominent negative turning point (NBS) which coincides with the base of Or2000. The NBS at this point is a maximum flooding surface and marks the base of a regression trend, which represents Or2000 consists of a stacking of predominant sand prone units. In addition, the colour gamma ray log of interval Or2000 (Figure 4.26) shows low value of gamma ray with majority of yellow to orange colour which represents sand prone units. The positive bounding surface (PBS) of interval Or2000P is a transgressive surface because the transgressive trend is followed by this point. Or2000P has a positive trend that represents a transgressive succession and stops at the negative turning point (NBS). The intervals of Or2000 and Or2000P are a complete stratigraphic package (regression trend then followed by transgression trend) and the intervals of Or3000 and Or3000P are another set of stratigraphic packages. On top of interval Or3000P is Or4000 which is a regression trend becoming sandy upwards.

The Goldwyer Formation is overlain conformably on top of the Willara Formation in well Missing 1. The stratigraphic sequences for well Missing 1 (Figure 4.26) cover the complete Nita Formation (intervals Or3000, Or3000P and Or4000) and Goldwyer Formation (intervals Or1000P, Or2000 and Or2000P).

There are two Stratpacs identified in well Missing 1. The intervals of Or2000 (regression; Goldwyer Unit 3) and Or2000P (transgression; Goldwyer Unit 4) in Goldwyer Formation are a complete Stratpac (regression trend then followed by transgression trend) and the intervals of Or3000 and Or3000P in Nita Formation are another set of Stratpac.

### 4.5.3.2 Well Santalum 1A

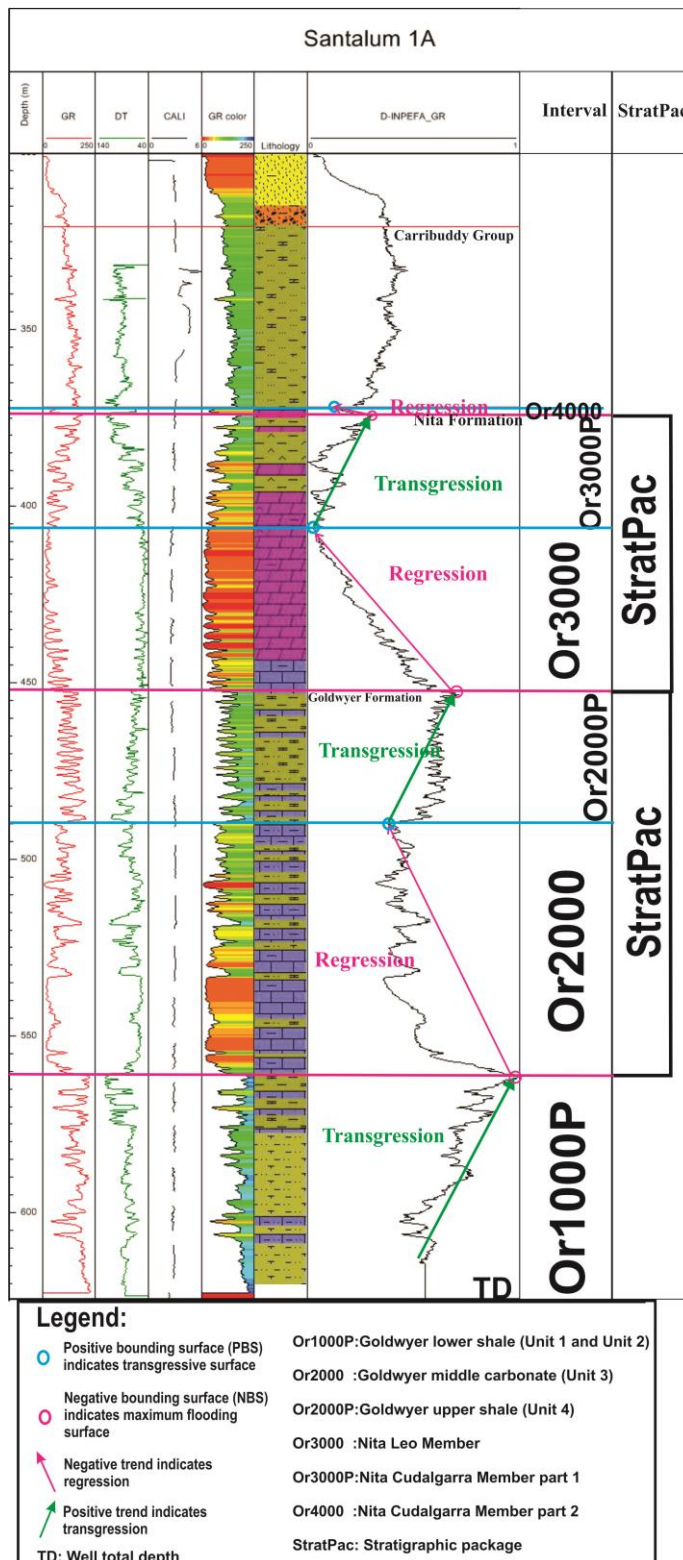


Figure 4.27: Well composite chart of well Santalum 1A with interpreted stratigraphic packages using the INPEFA curves. Note the Nita Formation is complete here but the lower part of the Goldwyer lower shale is not covered due to the well total depth being reached. Colours are described in Figure 4.8.

#### **4.5.1.3.1 Interpretation for Santalum 1A, Nita Formation and part of Goldwyer Formation (Figure 4.27)**

The stratigraphic packages for well Santalum 1A cover the complete Nita Formation and part of the Goldwyer lower shale as indicated by borehole data (Figure 4.27). For the Goldwyer Formation, the base starts from incomplete interval Or1000P because it reaches well total depth. Or2000 is a regression trend and is followed by the Or2000P which is a transgressive succession. The intervals that cover the Nita Formation are Or3000, Or3000P and Or4000 where the Nita Formation is overall dominated by a regressive succession. The top of interval Or1000P marked by the first prominent negative turning point (NBS) which coincides with the base of Or2000. The NBS at this point is a maximum flooding surface and marks the base of regression trend, which represents Or2000 consists of a stacking of predominant sand prone units. In addition, the colour gamma ray log of interval Or2000 (Figure 4.27) shows low value of gamma ray with red, orange and colour which indicates sand prone units. The positive bounding surface (PBS) of interval Or2000P is a transgressive surface because the transgressive trend is followed by this point. Or2000P has a positive trend that represents a transgressive succession and stops at the negative turning point (NBS). The intervals of Or2000 and Or2000P are a complete stratigraphic package (regression trend then followed by transgression trend) and the intervals of Or3000 and Or3000P are another set of stratigraphic packages.

The stratigraphic sequences for well Santalum 1A (Figure 4.27) cover the complete Nita Formation (intervals Or3000, Or3000P and Or4000) and Goldwyer Formation (intervals Or1000P, Or2000 and Or2000P), where the interval Or1000P consists only part of the Goldwyer lower shale due to the well total depth.

There are two Stratpacs identified in well Santalum 1A (Figure 4.27). The intervals of Or2000 (regression; Goldwyer Unit 3) and Or2000P (transgression; Goldwyer Unit 4) in Goldwyer Formation are a complete Stratpac (regression trend then followed by transgression trend) and the intervals of Or3000 (Nita Leo Member) and Or3000P (Nita Cudalgarra Member part 1) are another set of Stratpac.

### 4.5.3.3 Well Kunzea 1

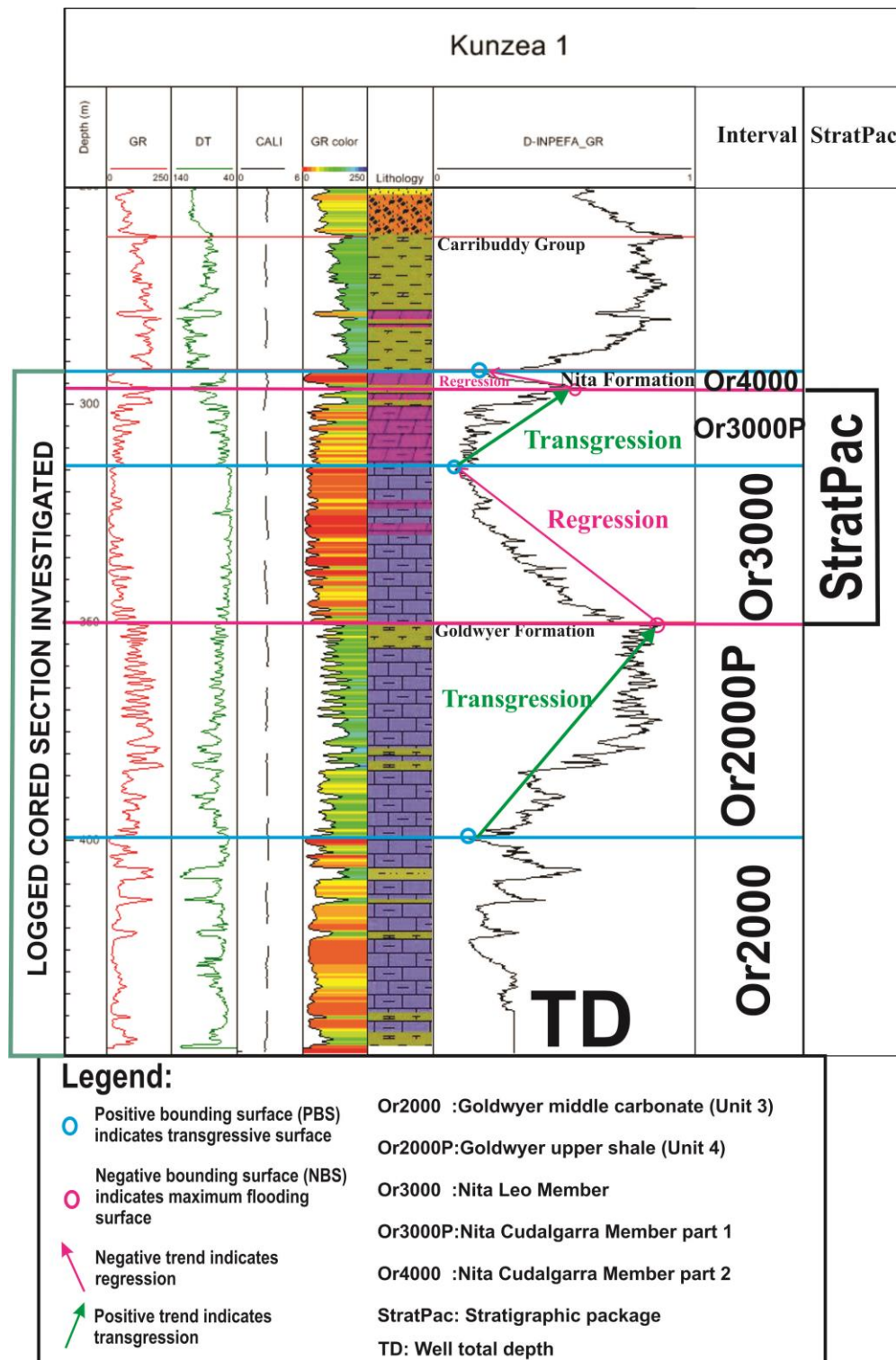


Figure 4.28: Well composite chart of well Kunzea 1 with interpreted stratigraphic packages using the INPEFA curves. Note the Nita Formation is complete here but only part of the Goldwyer Formation (Goldwyer upper shale and part of the Goldwyer middle carbonate) is covered due to the well total depth being reached. Note that logged cored section is investigated from approximately 292-450m (see Figures 3.50). Colours are described in Figure 4.8.

#### **4.5.3.3.1 Interpretation for Kunzea 1, Nita Formation and part of Goldwyer Formation (Figure 4.28)**

The stratigraphic packages for well Kunzea 1 cover the complete Nita Formation and part of the Goldwyer Formation as indicated by borehole data (Figure 4.28). For the Goldwyer Formation, the base starts from part of the interval Or2000P where the interval Or1000P does not exist in this well while interval Or2000 does not have a clear trend due to the absence of interval Or1000P. Or2000P is a transgressive trend which is then followed by the intervals Or3000 (regressive trend), Or3000P (transgressive trend) and Or4000 (regressive trend) which cover the Nita Formation. However, the Nita is represented by a complete StratPac (regression then transgression).

Well Kunzea 1 (Figure 4.28) covers the complete Nita Formation (intervals Or3000, Or3000P and Or4000) and part of the Goldwyer Formation (intervals Or2000P). The Goldwyer middle carbonate which is usually with a negative trend (interval Or 2000) remains unclear for this trend although the colour gamma ray log of this section shows low value of gamma ray with majority of yellow to orange colour which indicates sand prone units. This may be due to the absence of Goldwyer lower shale as the well total depth being reached.

#### **4.5.3.3.2 Core to log correlation for Kunzea 1**

The studied core (Figure 3.50) comes from the top of the Nita Formation until the well total depth (intervals Or4000, Or3000P, Or3000, Or2000P and part of Or2000). It consists of shallow subtidal to intertidal (and occasionally supratidal) upward shallowing thin carbonate cycles.

#### **4.5.3.4 Well correlation of wells Missing 1, Santalum 1A and Kunzea 1 (Figure 4.29)**

The regional correlations of the INPEFA curves of wells Missing 1, Santalum 1A and Kunzea 1 are shown in Figure 4.29. Goldwyer lower shale reaches the well total depth in well Santalum 1A. In well Kunzea 1, Goldwyer middle carbonate reaches the well total depth. The wells are correlated from west to east on the Crossland Platform.

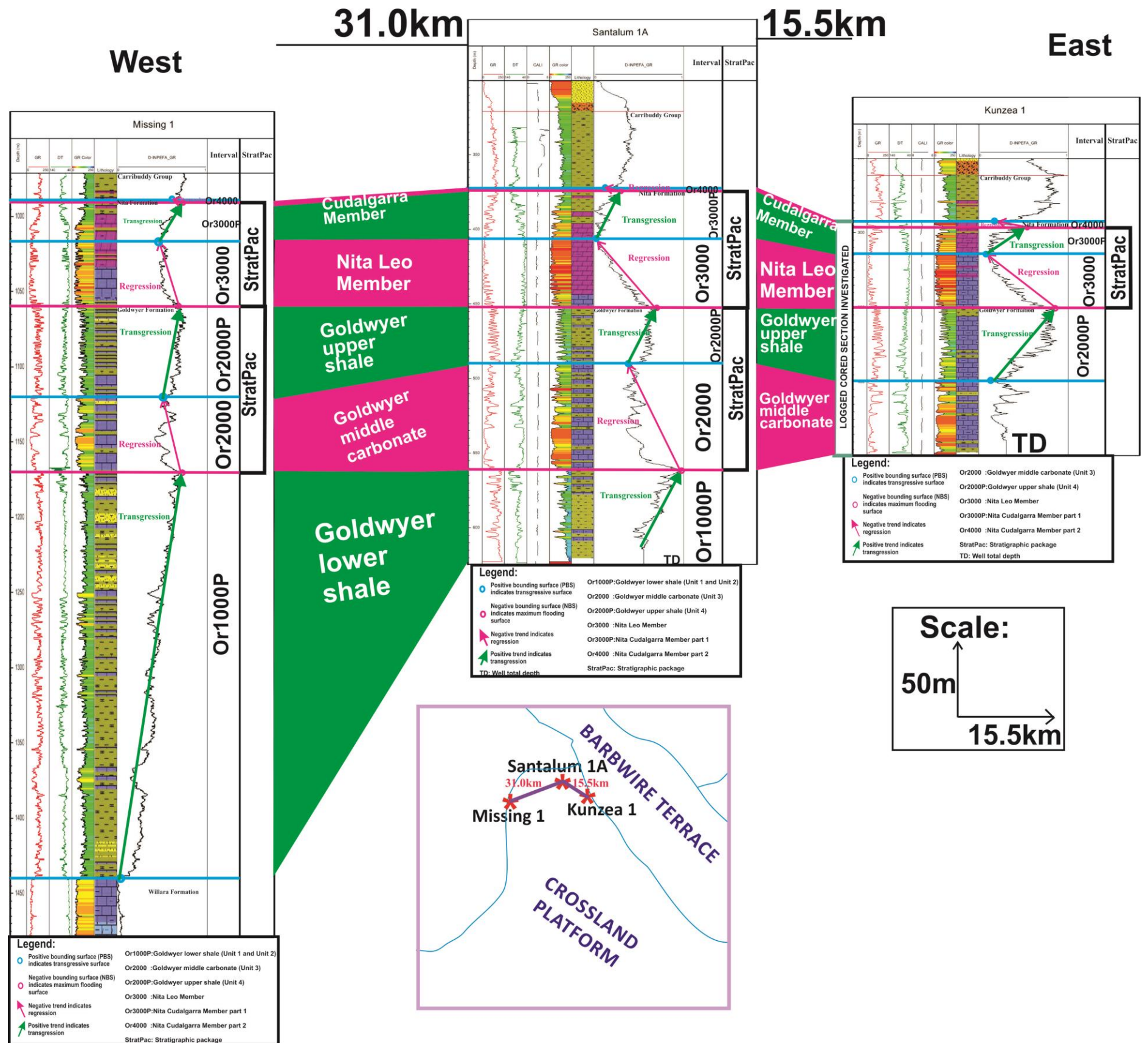


Figure 4.29: Well-to-well correlation of the INPEFA curves of wells Missing 1, Santalum 1A and Kunzea 1 on the Crossland Platform, well Missing 1 shows the complete subdivision of the Nita and Goldwyer Formations (Or1000P: Goldwyer lower shale (Transgression); Or2000: Goldwyer middle carbonate (Regression); Or2000P: Goldwyer upper shale (Transgression); Or3000: Leo Member (Regression); Or3000P: Cudalgarra Member part 1 (Transgression); Or4000: Cudalgarra Member part 2 (Regression)). Note that Goldwyer Formation lower shale reaches the well total depth in well Santalum 1A. In well Kunzea 1, Goldwyer middle carbonate reaches the well total depth. The wells are correlated from west to east on the Crossland Platform.

#### 4.6.5 Mowla Terrace

This study presents results and data analysis in relation to the objectives of the research from the four wells: Crystal Creek 1, Pictor 1, Canopus 1 and Matches Springs 1 in Mowla Terrace. The wells location is shown in Figure 4.30. Wells Crystal Creek 1, Pictor 1 and Canopus 1 are located at the western part of the Mowla Terrace while well Matches Springs 1 is located in the eastern part of the Mowla Terrace. Mowla Terrace has a complex structural and located at northern Barbwire Terrace region (Copp, 2008).

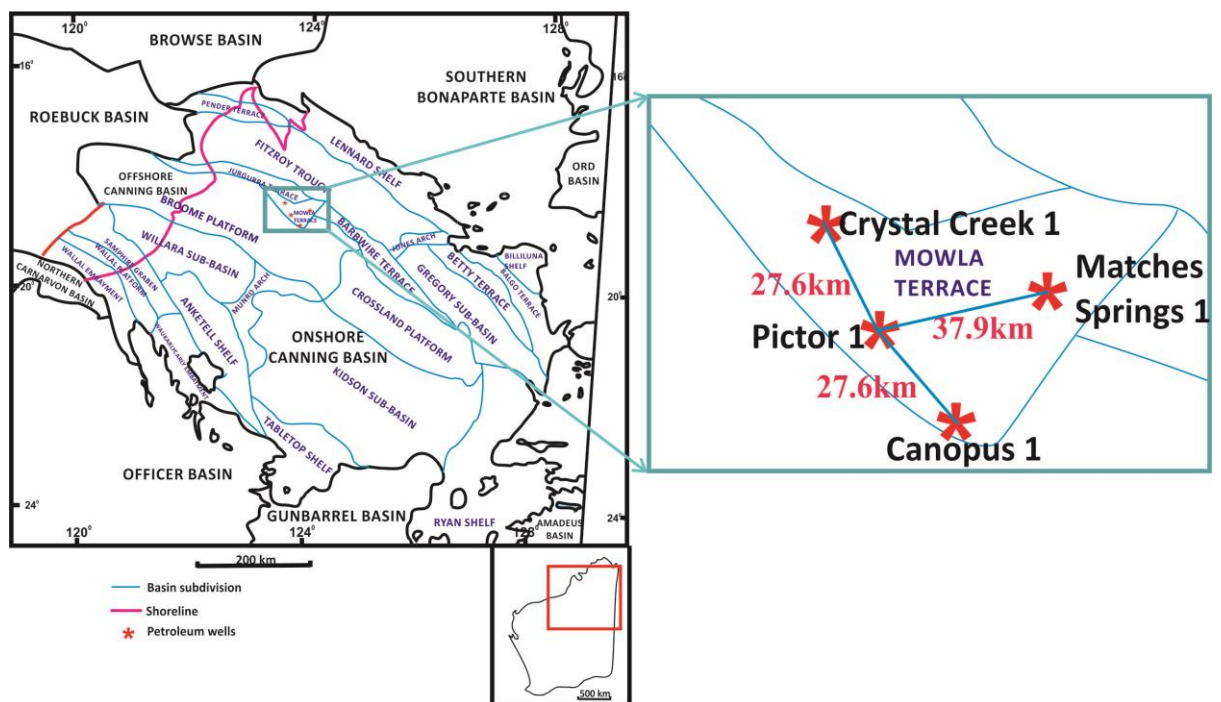


Figure 4.30: Location maps of wells Crystal Creek 1, Pictor 1, Canopus 1 and Matches Springs 1 in Mowla Terrace, Canning Basin, WA.

### 4.5.4.1 Well Crystal Creek 1

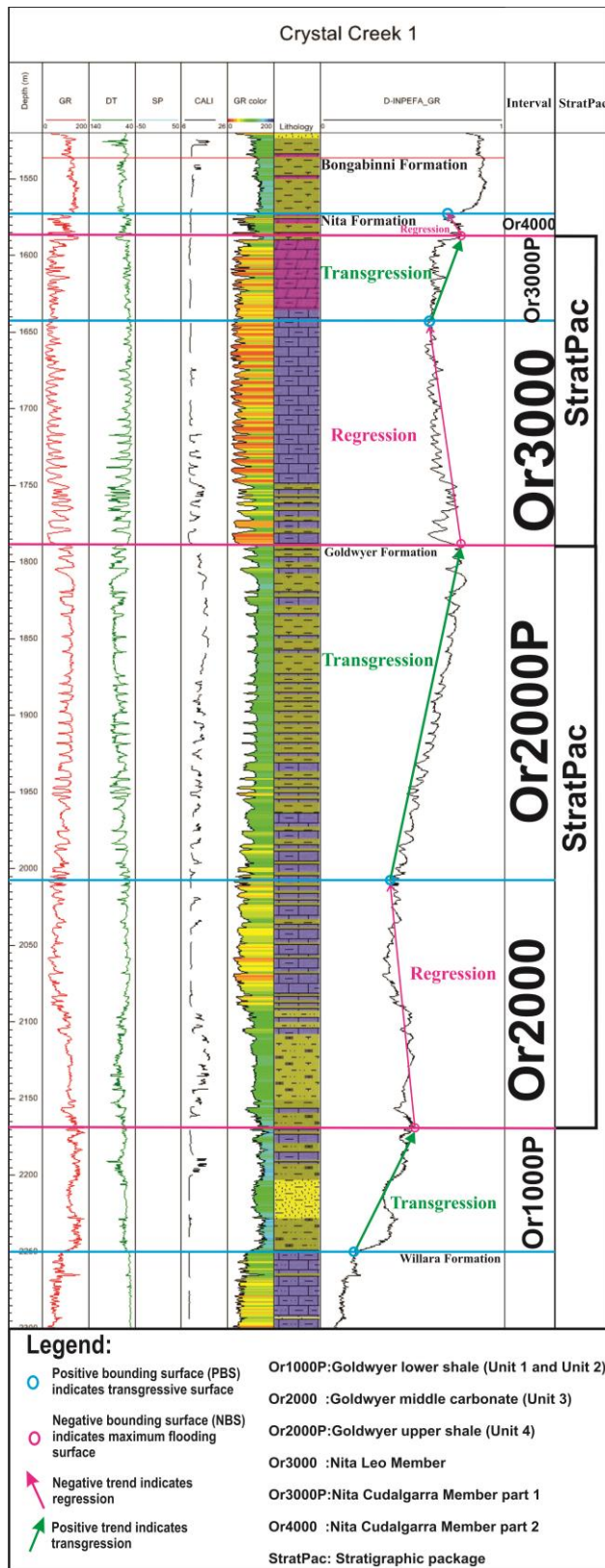


Figure 4.31: Well composite chart of well Crystal Creek 1 with interpreted stratigraphic packages using the INPEFA curves. Well Crystal Creek 1 covered the complete Nita and Goldwyer Formations. Colours are described in Figure 4.8.

#### **4.5.4.1.1 Interpretation for Crystal Creek 1 (Figure 4.31)**

The stratigraphic sequences for well Crystal Creek 1 cover the complete stratigraphic interval analysed and it shows the major breaks and trends clearly. The base of this interval study is Or1000P; this is a positive trend and represents shaly upwards or transgression. The top of interval Or1000P is marked by the first prominent negative turning point (NBS) which coincides with the base of Or2000. The NBS at this point is a maximum flooding surface and marks the base of regression trend, which represents Or2000 consists of a stacking of predominant sand prone units. In addition, the colour gamma ray log of interval Or2000 (Figure 4.31) shows low value of gamma ray with majority of yellow colour (indicates sand prone units which matches the regression systems tract). The positive bounding surface (PBS) of interval Or2000P is a transgressive surface because the transgressive trend is followed by this point. Or2000P has a positive trend that represents a transgressive succession and stops at the negative turning point (NBS). The intervals of Or2000 and Or2000P are a complete stratigraphic package (regression trend then followed by transgression trend) and the intervals of Or3000 and Or3000P are another set of stratigraphic packages. On top of interval Or3000P is Or4000 which is a regression trend becoming sandy upwards. Bongabinni Formation from the Carribuddy Group (Upper Ordovician to Silurian) overlies conformably on top of the interval Or4000.

The Goldwyer Formation lies conformably on top of the Willara Formation in well Crystal Creek 1. The stratigraphic sequences for well Crystal Creek 1 (Figure 4.31) cover the complete Nita Formation (intervals Or3000, Or3000P and Or4000) and Goldwyer Formation (intervals Or1000P, Or2000 and Or2000P).

There are two Stratpacs identified in well Crystal Creek 1. The intervals of Or2000 (regression; Goldwyer Unit 3) and Or2000P (transgression; Goldwyer Unit 4) in Goldwyer Formation are a complete Stratpac (regression trend then followed by transgression trend) and the intervals of Or3000 and Or3000P in Nita Formation are another set of Stratpac (see Figure 4.31).

#### 4.5.4.2 Well Pictor 1

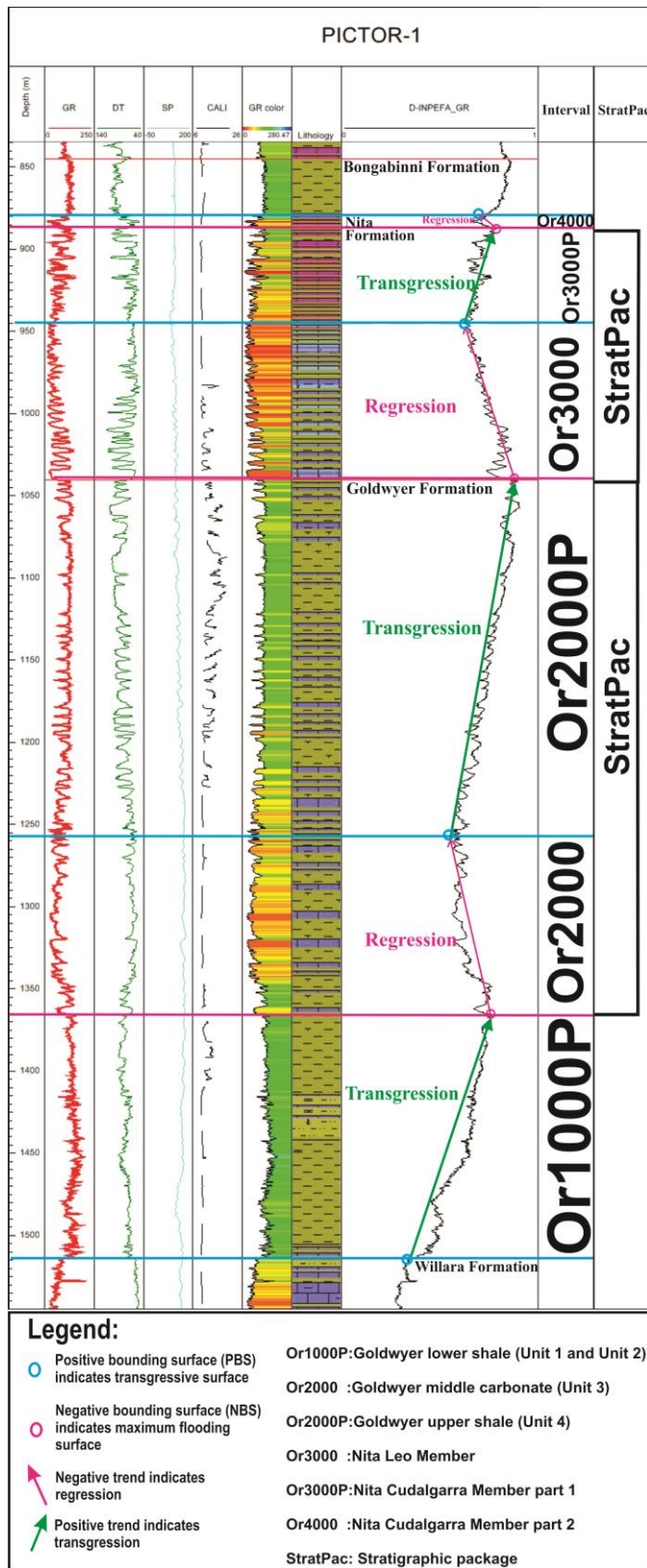


Figure 4.32: Well composite chart of well Pictor 1 with interpreted stratigraphic packages using the INPEFA curves. Well Pictor 1 covered the complete Nita and Goldwyer Formations. Colours are described in Figure 4.8.

#### **4.5.4.2.1 Interpretation for Pictor 1 (Figure 4.32)**

The stratigraphic sequences for well Pictor 1 cover the complete stratigraphic interval analysed and it shows the major breaks and trends clearly. The base of this interval study is Or1000P; this is a positive trend and represents shaly upwards or transgression. The top of interval Or1000P marked by the first prominent negative turning point (NBS) which coincides with the base of Or2000. The NBS at this point is a maximum flooding surface and marks the base of regression trend, which represents Or2000 consists of a stacking of predominant sand prone units. In addition, the colour gamma ray log of interval Or2000 (Figure 4.32) shows low value of gamma ray with majority of yellow colour which indicates sand prone units. The positive bounding surface (PBS) of interval Or2000P is a transgressive surface because the transgressive trend is followed by this point. Or2000P has a positive trend that represents a transgressive succession and stops at the negative turning point (NBS). The intervals of Or2000 and Or2000P are a complete stratigraphic package (regression trend then followed by transgression trend) and the intervals of Or3000 and Or3000P are another set of stratigraphic packages. On top of interval Or3000P is Or4000 which is a regression trend becoming sandy upwards. Bongabinni Formation from the Carribuddy Group (Upper Ordovician to Silurian) overlies conformably on top of the interval Or4000. The Goldwyer Formation is overlain conformably on top of the Willara Formation in well Pictor 1.

Well Pictor 1 consists of two Stratpacs. The intervals of Or2000 (progradational trend) and Or2000P (retrogradational trend) in Goldwyer Formation are a complete Stratpac (regression trend then followed by transgression trend) and the intervals of Or3000 (progradational trend) and Or3000P (retrogradational trend) in Nita Formation are another set of Stratpac (see Figure 4.32).

### 4.5.4.3 Well Canopus 1

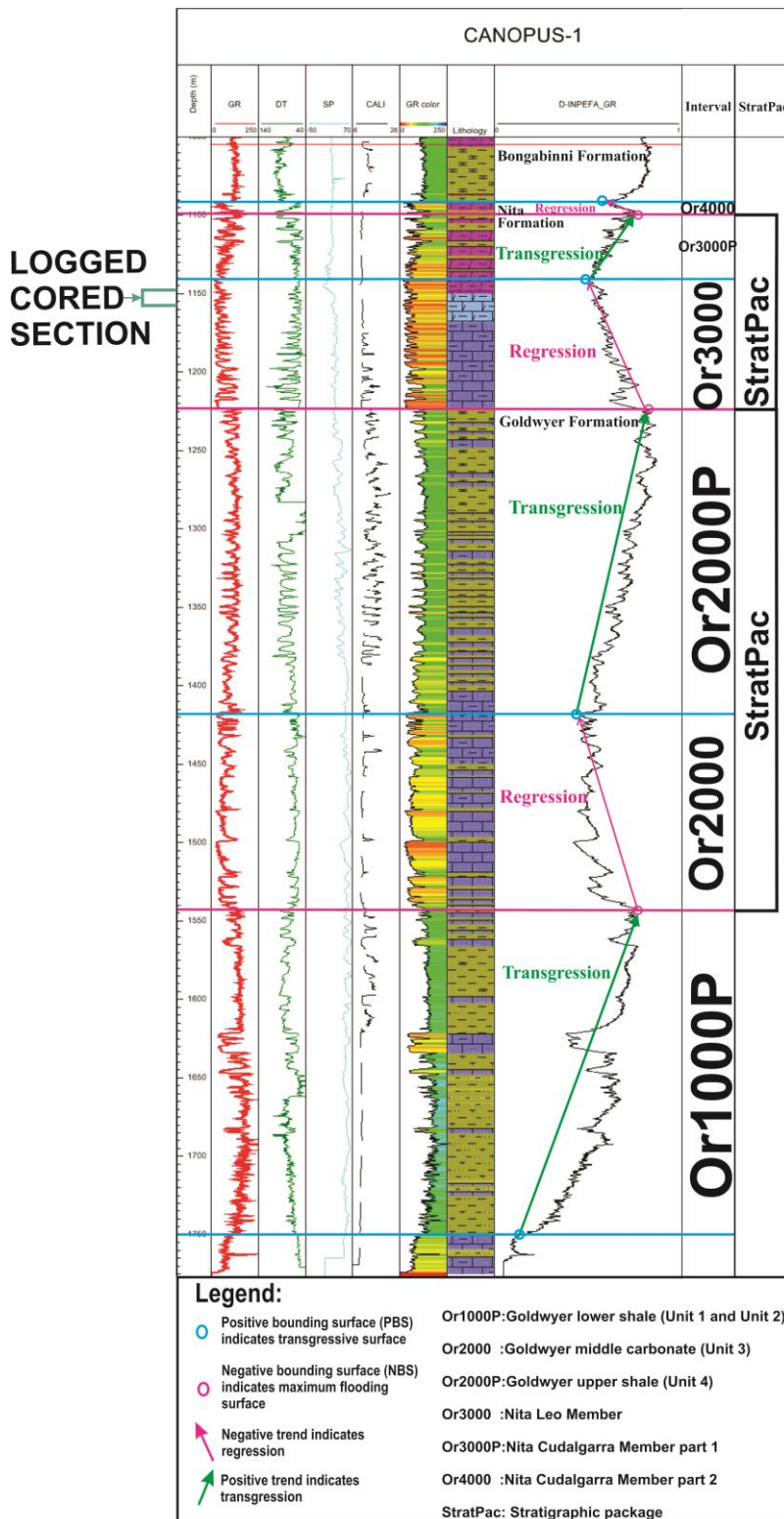


Figure 4.33: Well composite chart of well Canopus 1 with interpreted stratigraphic packages using the INPEFA curves. Well Canopus 1 covered the complete Nita and Goldwyer Formations. Note that logged cored section is from 1148.2-1156.6m (see Figure 3.32).

#### **4.5.4.3.1 Interpretation for Canopus 1 (Figure 4.33)**

The stratigraphic sequences for well Canopus 1 cover the complete stratigraphic interval analysed (Nita and Goldwyer Formations) and it shows the major breaks and trends clearly. The base of this interval study is Or1000P; this is a positive trend and represents shaly upwards or transgression. The top of interval Or1000P marked by the first prominent negative turning point (NBS) which coincides with the base of Or2000. The NBS at this point is a maximum flooding surface and marks the base of regression trend, which represents Or2000 consists of a stacking of predominant sand prone units. In addition, the colour gamma ray log of intervals Or2000 and Or3000 which indicate regressive trend (Figure 4.33) shows low value of gamma ray with majority of yellow and orange colour which indicates sand prone units. The positive bounding surface (PBS) of interval Or2000P is a transgressive surface because the transgressive trend is followed by this point. Or2000P has a positive trend that represents a transgressive succession and stops at the negative turning point (NBS). The intervals of Or2000 and Or2000P are a complete stratigraphic package (regression trend then followed by transgression trend) and the intervals of Or3000 and Or3000P are another set of stratigraphic packages. On top of interval Or3000P is Or4000 which is a regression trend becoming sandy upwards. Bongabinni Formation from the Carribuddy Group (Upper Ordovician to Silurian) lies conformably on top of the interval Or4000.

The Goldwyer Formation lies conformably on top of the Willara Formation in well Canopus 1. Well Canopus 1 consists of two Stratpacs. The intervals of Or2000 (progradational trend) and Or2000P (retrogradational trend) in Goldwyer Formation Unit 3 and Unit 4 are a complete Stratpac (regression trend then followed by transgression trend) and the intervals of Or3000 (progradational trend) and Or3000P (retrogradational trend) in Nita Formation are another set of Stratpac (Figure 4.33).

#### **4.5.4.3.2 Core to log correlation for Canopus 1**

The available core for Nita Formation Leo Member in well Canopus 1 is from 1148.2-1156.6m (see Figure 3.32). From the core logging, this part of Nita Leo Member consists of shallow warm water subtidal carbonates which are cyclic and shallow upwards (where core is available for study within this regression package (see Figure 3.32)). Figure 4.33 shows that Nita Leo Member fall into the interval Or3000

which is a negative trend and indicates regression. This matches with the core study in Chapter 3 for well Canopus 1.

#### **4.5.4.4 Well correlation for Crystal Creek 1, Pictor 1 and Canopus 1 (Figure 4.34)**

The regional correlations of the INPEFA curves of well Crystal Creek 1, well Pictor 1 and well Canopus 1 are shown in Figure 4.34 which is from north-western to south-east in the Mowla Terrace. These three wells consist of the complete subdivision of the Nita and Goldwyer Formations (Or1000P: Goldwyer lower shale (Transgression); Or2000: Goldwyer middle carbonate (Regression); Or2000P: Goldwyer upper shale (Transgression); Or3000: Leo Member (Regression); Or3000P: Cudalgarra Member part 1 (Transgression); Or4000: Cudalgarra Member part 2 (Regression)). Figure 4.34 shows that these three wells correlate very well.

These three wells match with the intervals interpreted in well Looma 1 which also consists of the complete Nita and Goldwyer Formations on the Broome Platform (see Figure 4.9). Besides, they also match with wells Solanum 1 (Figure 4.22) and Acacia 2 (Figure 4.23) on Barbwire Terrace except the Goldwyer lower shale (Or1000P) from wells Acacia 2 and Solanum 1 can be sub-divided into Goldwyer Unit 1 (Or1000P1) and Goldwyer Unit 2 (Or1000P2).

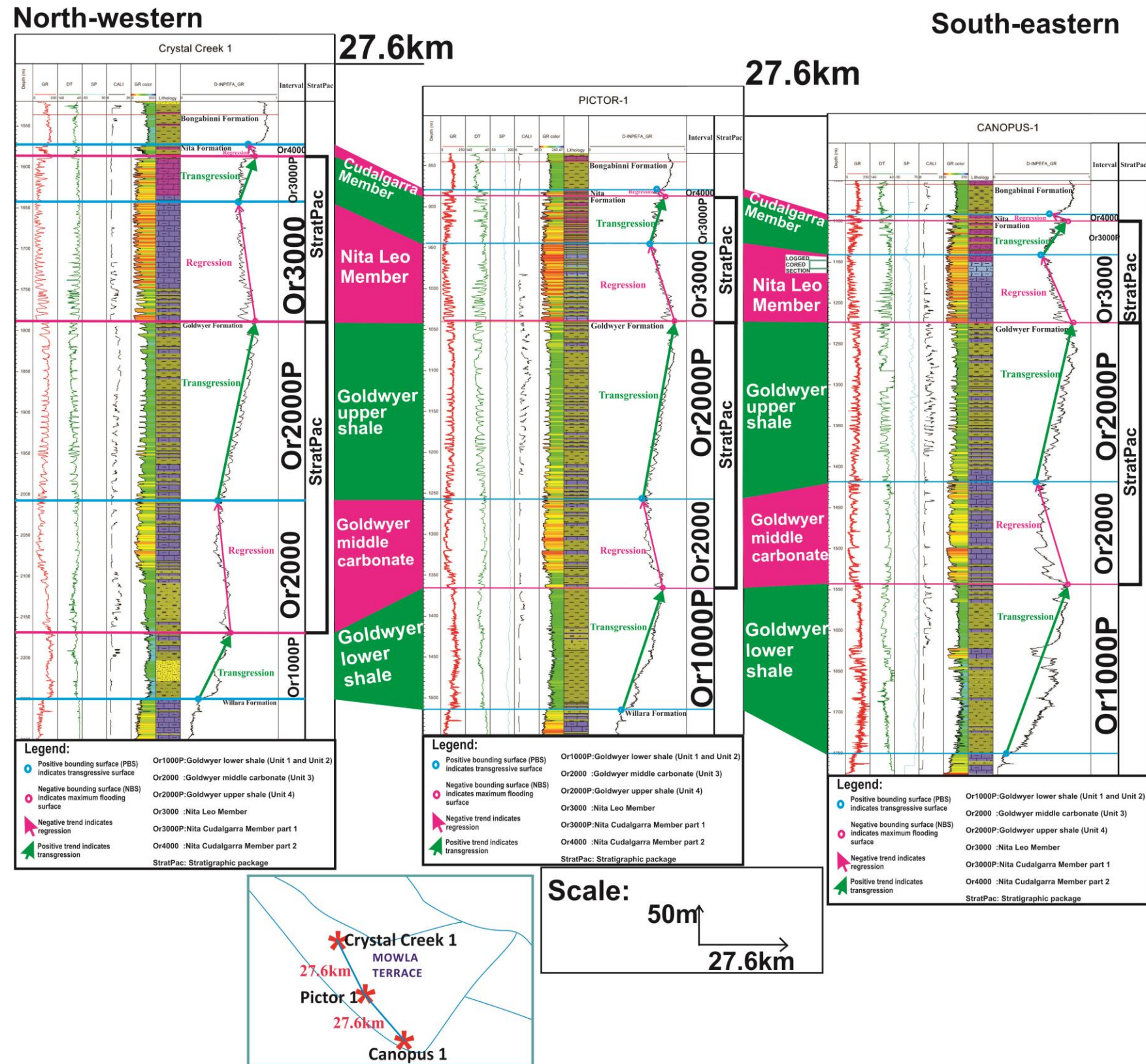


Figure 4.34: Well-to-well correlation of the INPEFA curves of wells Crystal Creek 1, Pictor 1 and Canopus 1 on the Mowla terrace, all these three wells show the complete subdivision of the Nita and Goldwyer Formations (Or1000P: Goldwyer lower shale (Transgression); Or2000: Goldwyer middle carbonate (Regression); Or2000P: Goldwyer upper shale (Transgression); Or3000: Leo Member (Regression); Or3000P: Cudalgarra Member part 1 (Transgression); Or4000: Cudalgarra Member part 2 (Regression)). Note that the distance between wells Crystal Creek 1- Pictor 1 and Pictor 1 – Canopus 1 is the same, which is 27.6km.

### 4.5.4.5 Well Matches Springs 1

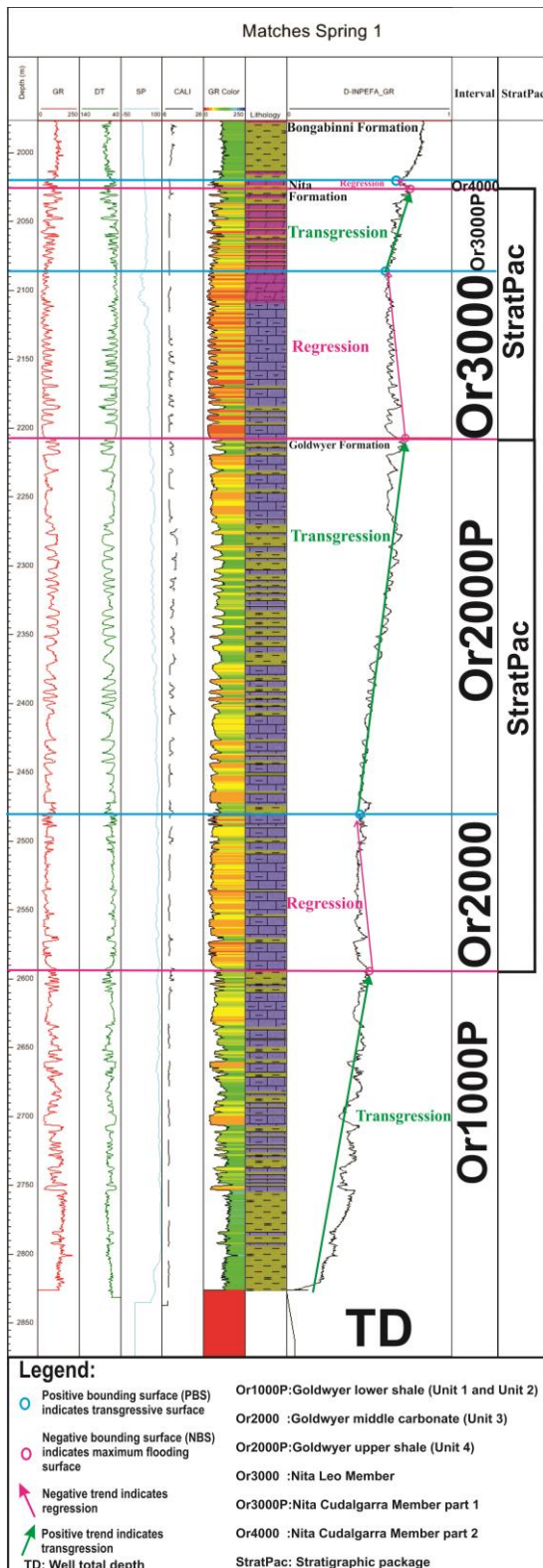


Figure 4.35: Well composite chart of well Matches Springs 1 with interpreted stratigraphic packages using the INPEFA curves. Note the Nita Formation is complete here but only the lower part of the Goldwyer lower shale is not covered due to the well total depth. Colours are described in Figure 4.8.

#### **4.5.4.5.1 Interpretation for Matches Springs 1, Nita Formation and part of Goldwyer Formation (Figure 4.35)**

The stratigraphic sequences for well Matches Springs 1 cover the complete Nita Formation and part of the Goldwyer lower shale as indicated by borehole data (Figure 4.35). For the Goldwyer Formation, the base starts from incomplete interval Or1000P because it reaches well total depth. Or2000 is a regression trend and is followed by the Or2000P which is a transgressive succession. The intervals that cover the Nita Formation are Or3000, Or3000P and Or4000 where the Nita Formation is overall dominated by a regressive succession. The top of interval Or1000P marked by the first prominent negative turning point (NBS) which coincides with the base of Or2000. The NBS at this point is a maximum flooding surface and marks the base of regression trend, which represents Or2000 consists of a stacking of predominant sand prone units. In addition, the colour gamma ray log of intervals Or2000 and Or3000 which indicate regression (Figure 4.35) shows low value of gamma ray with majority of yellow to orange colour which indicates sand prone units. The positive bounding surface (PBS) of interval Or2000P is a transgressive surface because the transgressive trend is followed by this point. Or2000P has a positive trend that represents a transgressive succession and stops at the negative turning point (NBS). The intervals of Or2000 and Or2000P are a complete stratigraphic package (regression trend then followed by transgression trend) and the intervals of Or3000 and Or3000P are another set of stratigraphic packages.

The stratigraphic sequences for well Matches Springs 1 (Figure 4.35) cover the complete Nita Formation (intervals Or3000, Or3000P and Or4000) and Goldwyer Formation (intervals Or1000P, Or2000 and Or2000P), where the interval Or1000P consists of only part of the Goldwyer lower shale due to the well total depth.

Well Matches Springs 1 consists of two Stratpacs. The intervals of Or2000 (progradational trend) and Or2000P (retrogradational trend) in Goldwyer Formation Unit 3 and Unit 4 are a complete Stratpac (regression trend then followed by transgression trend) and the intervals of Or3000 (progradational trend) and Or3000P (retrogradational trend) in Nita Formation are another set of Stratpac

#### **4.5.4.6 Well correlation for Matches Springs 1 and Pictor 1 (Figure 4.36)**

The regional correlations of the INPEFA curves of well Matches Springs 1 and well Pictor 1 are shown in Figure 4.36 from west to east in the Mowla Terrace. Well Pictor 1 consists of the complete subdivision of the Nita and Goldwyer Formations (Or1000P: Goldwyer lower shale (Transgression); Or2000: Goldwyer middle carbonate (Regression); Or2000P: Goldwyer upper shale (Transgression); Or3000: Leo Member (Regression); Or3000P: Cudalgarra Member part 1 (Transgression); Or4000: Cudalgarra Member part 2 (Regression)). Well Matches Springs 1 consists major part of the Nita and Goldwyer Formation and cover only part of the Goldwyer lower shale (interval Or1000P), because this interval reaches the well total depth. Figure 4.36 shows that these three wells correlate very well for each sub-unit for Nita and Goldwyer Formations.

Well Pictor 1 matches with the intervals interpreted in well Looma 1 which also consists of the complete Nita and Goldwyer Formations on the Broome Platform (see Figure 4.9). Besides, they also match with wells Solanum 1 (Figure 4.22) and Acacia 2 (Figure 4.23) on the Barbwire Terrace except the Goldwyer lower shale (Or1000P) from wells Acacia 2 and Solanum 1 which can be sub-divided into Goldwyer Unit 1 (Or1000P1) and Goldwyer Unit 2 (Or1000P2).

West

East

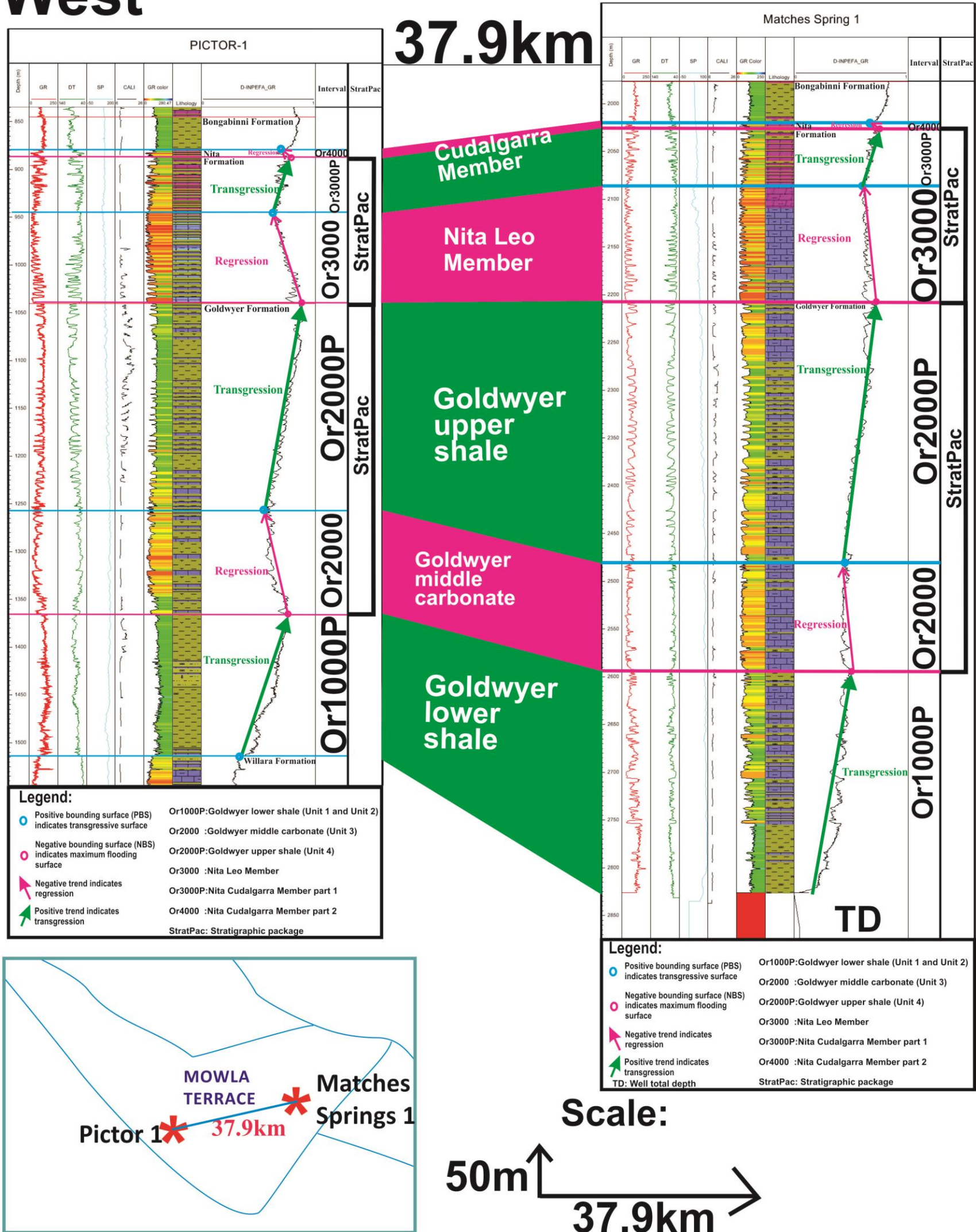


Figure 4.36: Well-to-well correlation of the INPEFA curves of wells Matches Springs 1 and Pictor 1 on the Mowla terrace, well Pictor 1 shows the complete subdivision of the Nita and Goldwyer Formations (Or1000P: Goldwyer lower shale (Transgression); Or2000: Goldwyer middle carbonate (Regression); Or2000P: Goldwyer upper shale (Transgression); Or3000: Leo Member (Regression); Or3000P: Cudalgarra Member part 1 (Transgression); Or4000: Cudalgarra Member part 2 (Regression)). Note the Nita Formation is complete for well Matches Springs 1 but the lower part of the Goldwyer lower shale is not covered due to the well total depth.

#### 4.6.5 Willara Sub-Basin

This study presents results from the three wells: Willara 1, Woods Hills 1 and Munro 1 in Willara Sub-basin (Figure 4.37) and data analysis in relation to the objectives of the research. Wells Willara 1, Woods Hills 1 and Munro are located at the central part of the onshore Willara Sub-basin.

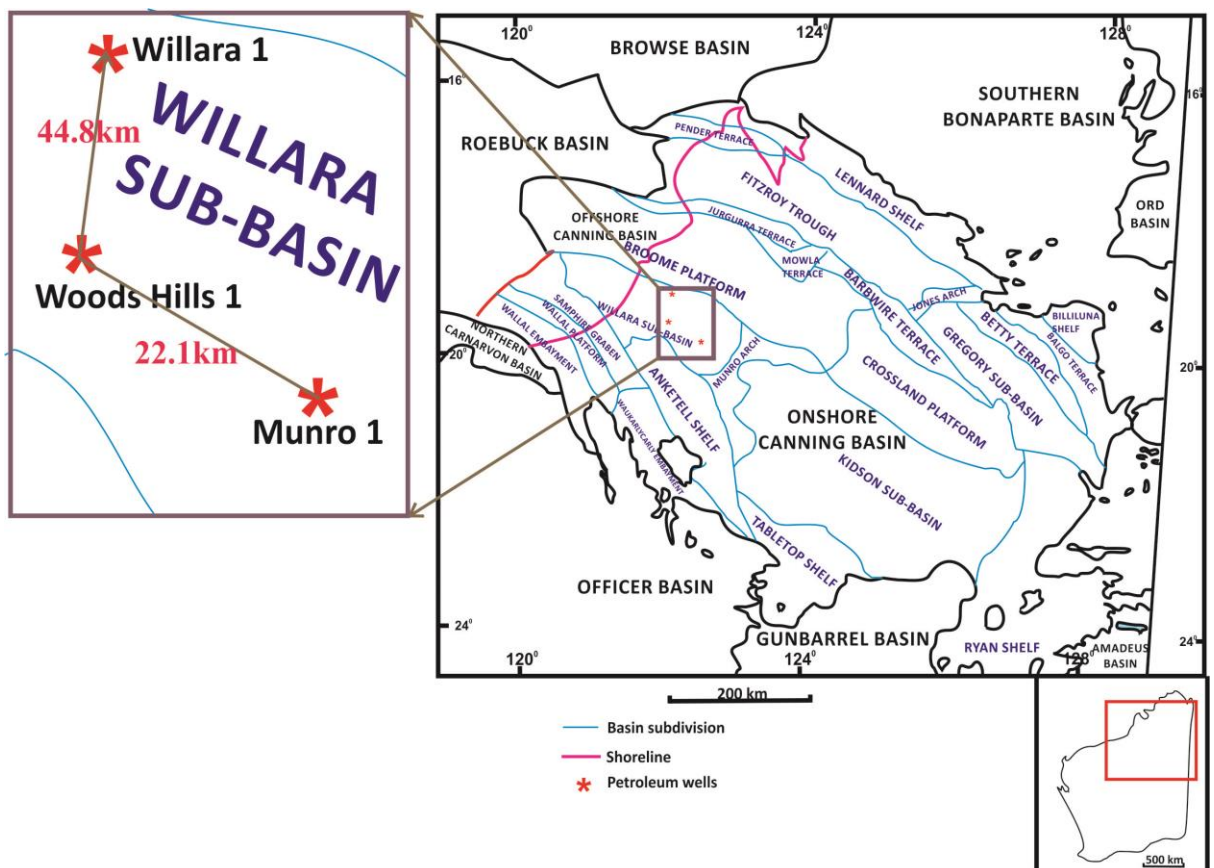


Figure 4.37: Location maps of wells Willara 1, Woods Hills 1 and Munro 1 in Willara Sub-basin, Canning Basin, WA.

### 4.5.5.1 Well Willara 1

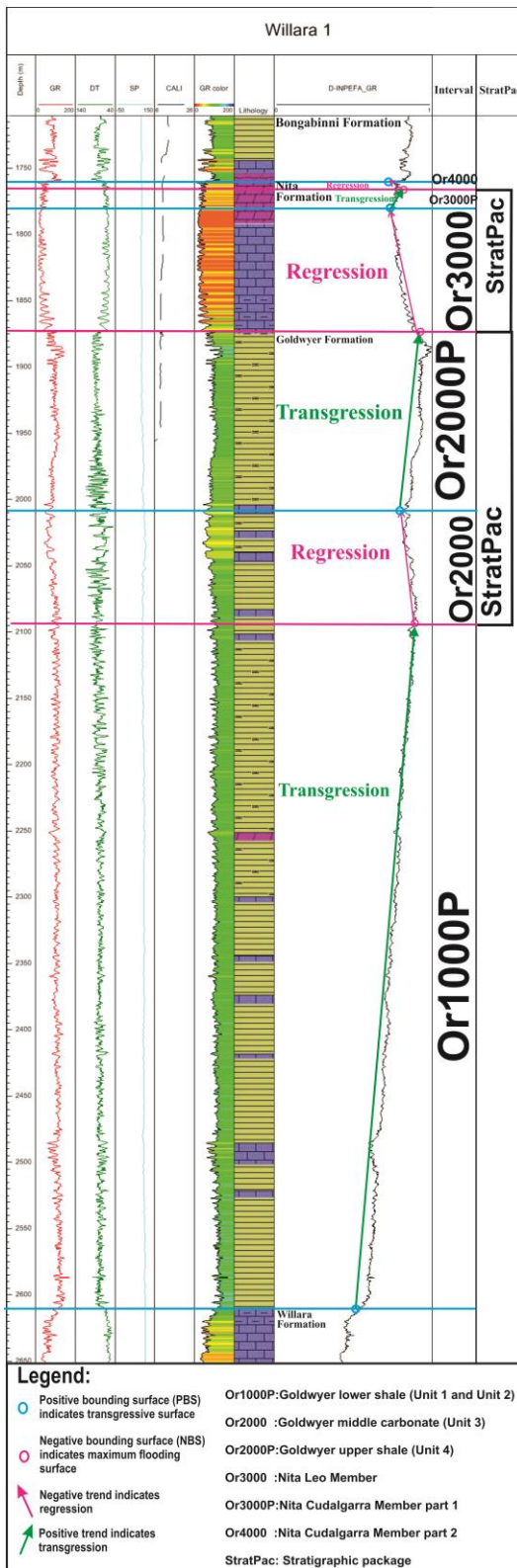


Figure 4.38: Well composite chart of well Willara 1 with interpreted stratigraphic packages using the INPEFA curves. Well Willara 1 covered the complete Nita and Goldwyer Formations. Colours are described in Figure 4.8.

#### **4.5.5.1.1 Interpretation for Willara 1 (Figure 4.38)**

The stratigraphic sequences for well Willara 1 cover the complete stratigraphic interval analysed and it shows the major breaks and trends clearly in Figure 4.38. The base of this interval study is Or1000P; this is a positive trend and represents shaly upwards or transgression. The top of interval Or1000P marked by the first prominent negative turning point (NBS) which coincides with the base of Or2000. The NBS at this point is a maximum flooding surface and marks the base of regression trend, which represents Or2000 consists of a stacking of predominant sand prone units. In addition, the colour gamma ray log of intervals Or2000 and Or3000 which indicates regressive trend (Figure 4.38) shows low value of gamma ray with majority of yellow or orange colour which indicates sand prone units. The positive bounding surface (PBS) of interval Or2000P is a transgressive surface because the transgressive trend is followed by this point. Or2000P has a positive trend that represents a transgressive succession and stops at the negative turning point (NBS). The intervals of Or2000 and Or2000P are a complete stratigraphic package (regression trend then followed by transgression trend) and the intervals of Or3000 and Or3000P are another set of stratigraphic packages. On top of interval Or3000P is Or4000 which is a regression trend becoming sandy upwards. Bongabinni Formation from the Carribuddy Group (Upper Ordovician to Silurian) overlies conformably on top of the interval Or4000.

The Goldwyer Formation is overlain conformably on top of the Willara Formation in well Willara 1. In this well, the complete Nita Formation can be sub-divided into intervals Or3000 (regression), Or3000P (transgression) and Or4000 (regression) while the Goldwyer Formation can be sub-divided into intervals Or1000P (transgression), Or2000 (regression) and Or2000P (transgression).

Well Willara 1 consists of two Stratpacs. The intervals of Or2000 (progradational trend) and Or2000P (retrogradational trend) in Goldwyer Formation Unit 3 and Unit 4 are a complete Stratpac (regression trend then followed by transgression trend) and the intervals of Or3000 (progradational trend) and Or3000P (retrogradational trend) in Nita Formation are another set of Stratpac

### 4.5.5.2 Well Woods Hills 1

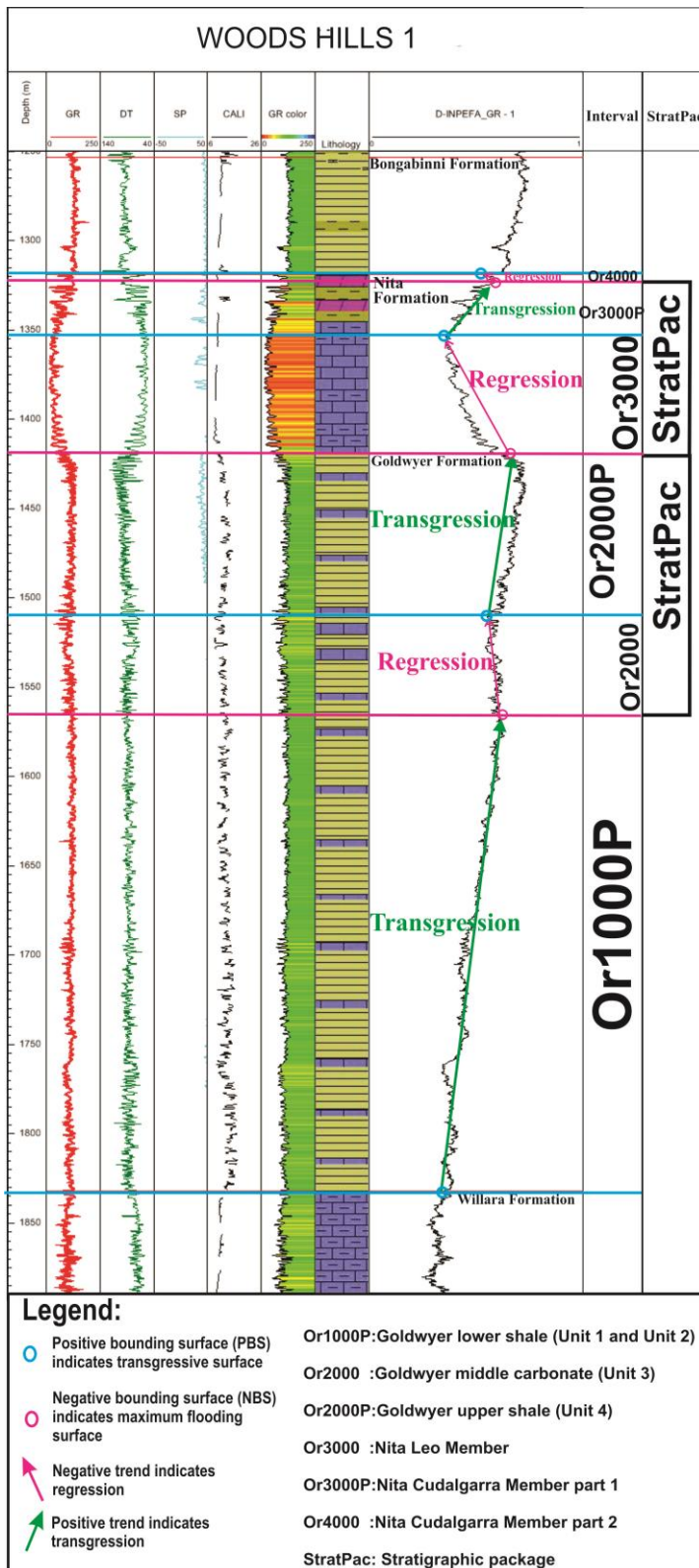


Figure 4.39: Well composite chart of well Woods Hills 1 with interpreted stratigraphic packages using the INPEFA curves. Well Woods Hills 1 covered the complete Nita and Goldwyer Formations. Colours are described in Figure 4.8.

#### **4.5.5.2.1 Interpretation for Woods Hills 1 (Figure 4.39)**

The stratigraphic sequences for well Woods Hills 1 cover the complete stratigraphic interval analysed and it shows the major breaks and trends clearly in Figure 4.39. The base of this interval study is Or1000P; this is a positive trend and represents shaly upwards or transgression. The top of interval Or1000P marked by the first prominent negative turning point (NBS) which coincides with the base of Or2000. The NBS at this point is a maximum flooding surface and marks the base of regression trend, which represents Or2000 consists of a stacking of predominant sand prone units. The positive bounding surface (PBS) of interval Or2000P is a transgressive surface because the transgressive trend is followed by this point. Or2000P has a positive trend that represents a transgressive succession and stops at the negative turning point (NBS). The intervals of Or2000 and Or2000P are a complete stratigraphic package (regression trend then followed by transgression trend) and the intervals of Or3000 and Or3000P are another set of stratigraphic packages. Furthermore, the colour gamma ray log of interval Or3000 which indicate regressive trend (Figure 4.39) shows a low value of gamma ray with majority of yellow and orange colour which indicates sand prone units. On top of interval Or3000P is Or4000 which is a regression trend becoming sandy upwards. Bongabinni Formation from the Carribuddy Group (Upper Ordovician to Silurian) overlies conformably on top of the interval Or4000.

The Goldwyer Formation is overlain conformably on top of the Willara Formation in well Woods Hills 1. In this well, the Nita Formation can be sub-divided into intervals Or3000 (regression), Or3000P (transgression) and Or4000 (regression) while the Goldwyer Formation can be sub-divided into intervals Or1000P (transgression), Or2000 (regression) and Or2000P (transgression).

Well Woods Hills 1 consists of two Stratpacs. The intervals of Or2000 (progradational trend) and Or2000P (retrogradational trend) in Goldwyer Formation Unit 3 and Unit 4 are a complete Stratpac (regression trend then followed by transgression trend) and the intervals of Or3000 (progradational trend) and Or3000P (retrogradational trend) in Nita Formation are another set of Stratpac

### 4.5.5.3 Well Munro 1

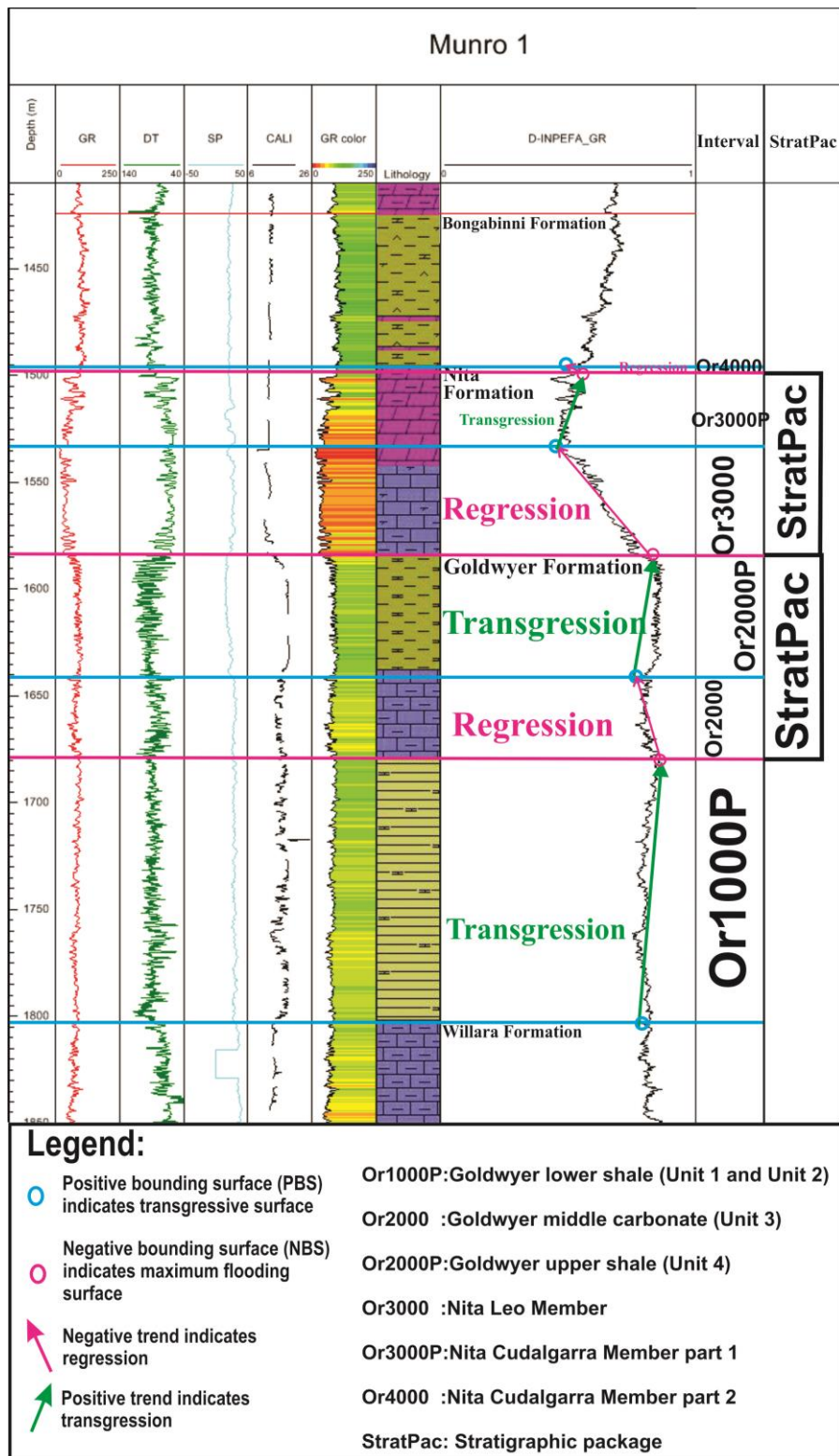


Figure 4.40: Well composite chart of well Munro 1 with interpreted stratigraphic packages using the INPEFA curves. Well Munro 1 covered the complete Nita and Goldwyer Formations. Colours are described in Figure 4.8.

#### **4.5.5.3.1 Interpretation for Munro 1 (Figure 4.40)**

The stratigraphic packages for well Munro 1 cover the complete stratigraphic interval analysed and it shows the major breaks and trends clearly in Figure 4.40. The base of this interval study is Or1000P; this is a positive trend and represents shaly upwards or transgression. The top of interval Or1000P marked by the first prominent negative turning point (NBS) which coincides with the base of Or2000. The NBS at this point is a maximum flooding surface and marks the base of regression trend, which represents Or2000 consists of a stacking of predominant sand prone units. The positive bounding surface (PBS) of interval Or2000P is a transgressive surface because the transgressive trend is followed by this point. Or2000P has a positive trend that represents a transgressive succession and stops at the negative turning point (NBS). The intervals of Or2000 and Or2000P are a complete stratigraphic package (regression trend then followed by transgression trend) and the intervals of Or3000 and Or3000P are another set of stratigraphic packages. In addition, the colour gamma ray log of interval Or3000 which indicate regressive trend (Figure 4.40) shows low value of gamma ray shows the sand prone units with the yellow and orange colours. On top of interval Or3000P is Or4000 which is a regression trend becoming sandy upwards. Bongabinni Formation from the Carribuddy Group (Upper Ordovician to Silurian) overlies conformably on top of the interval Or4000.

The Goldwyer Formation is overlain conformably on top of the Willara Formation in well Munro 1. The stratigraphic sequences for well Munro 1 (Figure 4.40) cover the complete Nita Formation (intervals Or3000, Or3000P and Or4000) and Goldwyer Formation (intervals Or1000P, Or2000 and Or2000P).

Well Munro 1 consists of two Stratpacs. The intervals of Or2000 (progradational trend) and Or2000P (retrogradational trend) in Goldwyer Formation Unit 3 and Unit 4 are a complete Stratpac (regression trend then followed by transgression trend) and the intervals of Or3000 (progradational trend) and Or3000P (retrogradational trend) in Nita Formation are another set of Stratpac

#### **4.5.5.4 Well correlation for Willara 1, Woods Hills 1 and Munro 1 (Figure 4.41)**

The regional correlations of the INPEFA curves of well Willara 1, well Woods Hills 1 and well Munro 1 are shown in Figure 4.41 from north-western to south-eastern in the Willara Sub-basin. These three wells consist of the complete

subdivision of the Nita and Goldwyer Formations (Or1000P: Goldwyer lower shale (Transgression); Or2000: Goldwyer middle carbonate (Regression); Or2000P: Goldwyer upper shale (Transgression); Or3000: Leo Member (Regression); Or3000P: Cudalgarra Member part 1 (Transgression); Or4000: Cudalgarra Member part 2 (Regression)). Figure 4.41 shows that these three wells correlate very well for each sub-unit for Nita and Goldwyer Formations and their thicknesses are thinning from well Willara 1 to well Munro 1. This indicates that the Nita and Goldwyer Formations are thinning from north-western to south-eastern in the Willara Sub-Basin.

These three wells matches with the intervals interpreted in well Looma 1 which also consists of the complete Nita and Goldwyer Formations on the Broome Platform (see Figure 4.9). Besides, they also match with wells Solanum 1 (Figure 4.22) and Acacia 2 (Figure 4.23) on Barbwire Terrace except the Goldwyer lower shale (Or1000P) from wells Acacia 2 and Solanum 1 which can be sub-divided into Goldwyer Unit 1 (Or1000P1) and Goldwyer Unit 2 (Or1000P2).

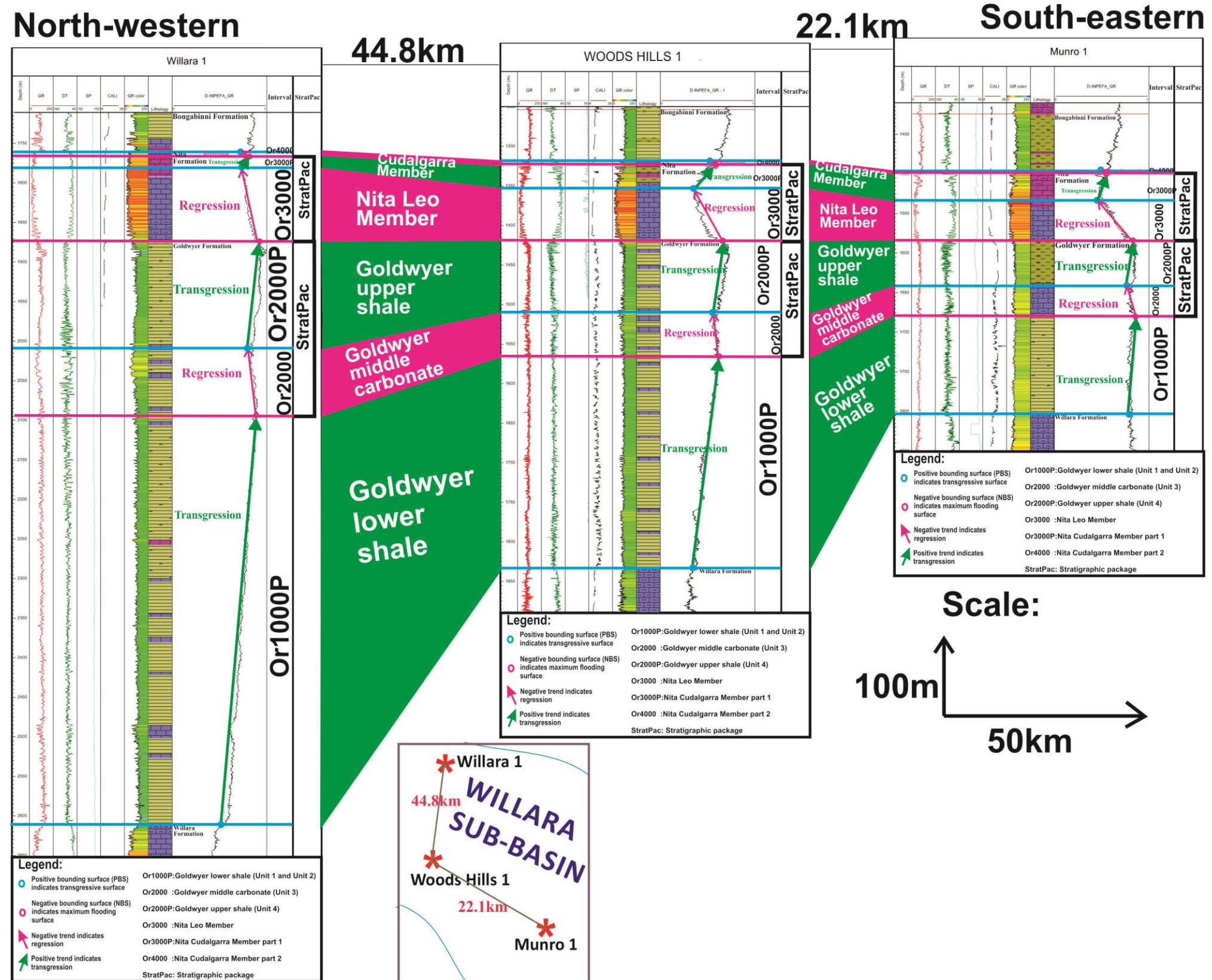


Figure 4.41: Well-to-well correlation of the INPEFA curves of wells Willara 1, Woods Hills 1 and Munro 1 on the Willara Sub-basin, all these three wells show the complete subdivision of the Nita and Goldwyer Formations (Or1000P: Goldwyer lower shale (Transgression); Or2000: Goldwyer middle carbonate (Regression); Or2000P: Goldwyer upper shale (Transgression); Or3000: Leo Member (Regression); Or3000P: Cudalgarra Member part 1 (Transgression); Or4000: Cudalgarra Member part 2 (Regression)).

## **4.6 Discussion**

### **4.6.3 Comparison between the previous known lithofacies and INPEFA curve in the Goldwyer Formation**

The Goldwyer Formation was deposited during the early Llanvirnian and four units are recognised on the Barbwire Terrace by Foster et al. (1986). These four units can be identified throughout most of the South Canning Basin. According to King (1998), the oldest units 1 and 2 comprise interbedded shales and limestones and were deposited in mid to outer ramp settings. The accommodation space increases from mid to outer ramp settings. Transgressive deposition happened for these units 1 and 2 or Goldwyer lower shale in the Goldwyer Formation. From the INPEFA analysis results from Figures 4.7 – 4.41, Goldwyer Unit 1 and Unit 2 or Goldwyer lower shale are at interval Or1000P which indicates transgression. This result of INPEFA curves matches with what King (1998) had mentioned. Goldwyer Unit 3 (Goldwyer middle carbonate) consists of shoaling-upwards limestones and minor shales that deposited in an inner to mid ramp setting (King, 1998). The accommodation space decreases from the outer ramp in Goldwyer Unit 1 and Goldwyer Unit 2 to inner ramp in Goldwyer Unit 3. The ramps prograded during regression and the sea level fell during unit 3 deposition. The Goldwyer Unit 3 deposition in the interval of Or2000 which indicates regression and this also matches with the previous lithofacies and depositional environments that had been discussed and studied in this project as part of core logging (see Chapter 3).

Foster et al. (1986) and Winchester-Seeto et al. (2000) reported that Goldwyer Unit 4 (Goldwyer upper shale) in the Goldwyer Formation has excellent liquid hydrocarbon source potential and King (1998) pointed out that the unit 4 consists predominantly of shales deposited in a subtidal-lagoonal environment. Sea level will increase from a carbonate ramp to the shaly facies and the accommodation space increases as well. This matches the result of INPEFA curves in this study in that the transgression occurred in unit 4 for interval Or2000P.

### **4.6.3 Comparison between the previous known lithofacies and INPEFA curve in the Nita Formation**

According to McCracken (1994), Nita Formation can be subdivided into 2 members along the Admiral Bay Fault Zone and across the Broome Platform where the Leo Member is below and the Cudalgarra Member on top of the Leo Member.

The lower part of Nita Formation displays classical shallowing upward carbonate cycles (Haines, 2004), as shown in this study. These cycles show characteristics of the shallowing upward carbonate sequences reported from peritidal carbonate successions (James, 1984). Karajas and Kernick (1984) reported that Nita Formation consists of 43 progradational cycles and it is a regressive sequence which deposited from subtidal to supratidal environments. The results of INPEFA curves in this study show that the interval Or3000 for Nita Formation has a negative trend which indicates regression. Lithofacies and depositional environments that had been discussed and studied in this project as part of core logging showing shallowing upwards cycles in Nita Leo Member furthermore supported the regression systems tract (sand prone units) of a negative trend in INPEFA analysis (see Chapter 3).

The upper part of Nita Formation is dominated by dolomite but also contains interbeds of argillaceous dolomite or limestone as well as interlamination of shale (Karajas and Kernick, 1984). Haines (2004) reported interbedded grey, green and reddish mudstone increases in abundance towards the top of Nita Formation and is commonly finely laminated or flaser bedded. During transgression, the lithology will change from sandy to shaly and this indicates that transgression happened at the upper Nita. From the result of INPEFA curves, the interval Or3000P at the upper Nita Formation which is a positive trend confirmed that transgression happened for upper Nita Formation. For the interval Or4000 which shows a regressive sequence, this is likely due to the intercrystalline diagenesis at ~30m beneath top of Nita Formation (King, 1998). Such intense diagenesis is likely to modify the log response leading to an error source.

### **4.6.3 Application of Embry's transgressive-regressive model (2002) to components of INPEFA stratigraphy**

Systems tracts are stratigraphic subdivisions of sequences. A schematic cross section illustrating the boundaries of the various types of systems tracts that have been

defined by various authors is shown in Figure 4.42 (Van Wagoner et al. 1988; Embry, 1993; Helland-Hansen and Gjelberg, 1994; Posamentier and Allen, 1999). Previously, the systems tracts are defined based on theoretical considerations rather than clear definitions that emphasize objective criteria for recognizing the boundaries of a given designated unit (Embry, 2002). This caused confusion in how systems tract boundaries are drawn and in what constitutes a given systems tract, such as lowstand, highstand, shelf margin, falling sea level, and forced regressive systems tract. These types of systems tracts which have one or more unrecognizable boundaries (hypothetical time lines) have no practical use. Embry (2002) argued that only the transgressive systems tracts (TST) and the regressive systems tract (RST) have boundaries that can be determined by objective scientific analysis. This study applies the results of INPEFA curves analysis to match with the transgressive-regressive model of Embry (2002).

Integrated prediction error filter analysis (INPEFA) curves which consist of complete Nita and Goldwyer Formations show that the Goldwyer Formation forms by transgressive systems tract (interval Or1000P), regressive systems tract (interval Or2000) and another transgressive systems tract (interval Or2000P) as top Goldwyer. Interval Or1000P matches the Goldwyer lower shale (Goldwyer Unit 1 and Unit 2) with transgressive systems tract; interval Or2000 matches the Goldwyer middle carbonate (Goldwyer Unit 3) with regressive systems tract; interval Or2000P matches the Goldwyer upper shale (Goldwyer Unit 4) with transgressive systems tract. Integrated prediction error filter analysis (INPEFA) curves show that the Nita Formation forms by regressive systems tract (interval Or3000), transgressive systems tract (interval Or3000p) and regressive systems tract (Or4000). Interval Or3000 is the Nita Formation Leo Member while intervals Or3000P and Or4000 are the Nita Formation Cudalgarra Member.

The result of the INPEFA curves in this study is applicable to Embry's model (1993) as shown in Figure 4.42.

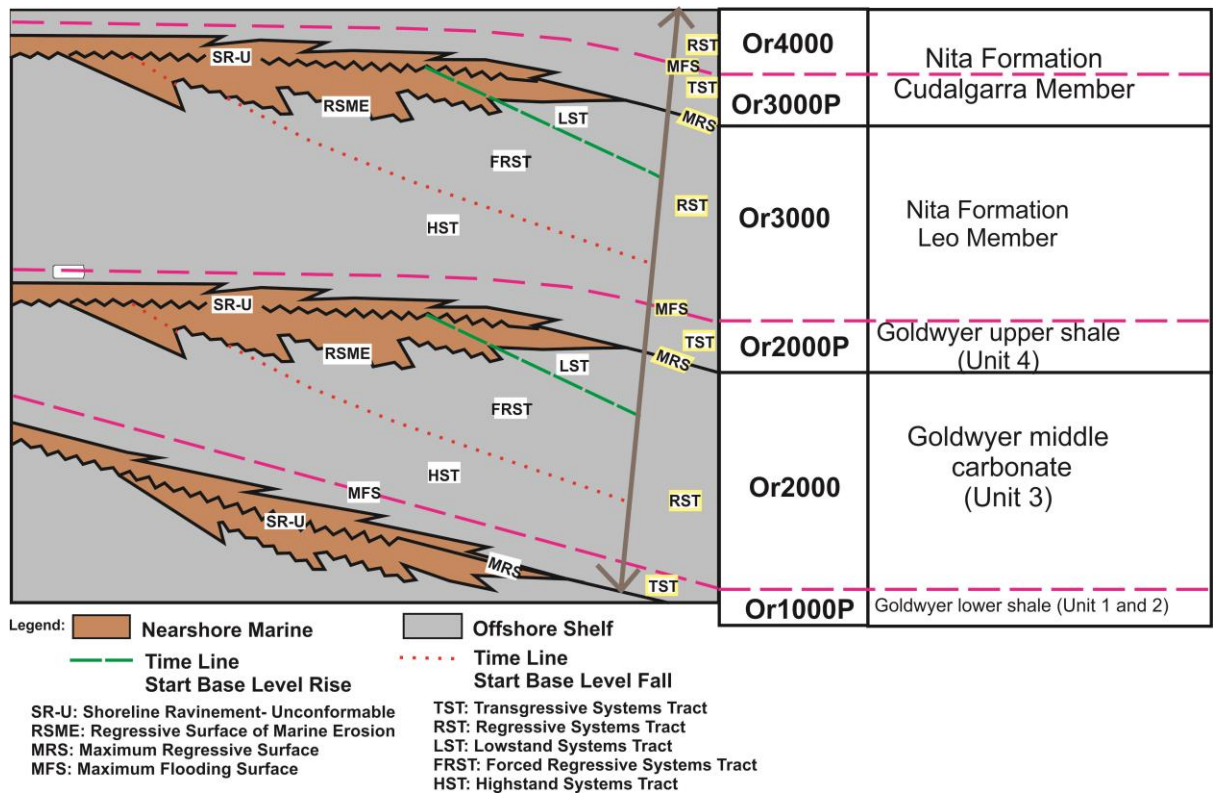


Figure 4.42: A schematic cross section illustrating the boundaries of the various types of systems tracts that have been defined by various authors (Van Wagoner et al. 1988; Embry, 1993; Helland-Hansen and Gjelberg, 1994; Posamentier and Allen, 1999). Embry (2002) argued that only the transgressive systems tracts (TST) and the regressive systems tract (RST) have boundaries that can be determined by objective scientific analysis. The other types have one or more unrecognizable boundaries (hypothetical time lines) which have no practical use. This study applies the results of INPEFA curves analysis to match with the transgressive-regressive model of Embry (2002). Note that this diagram is not to scale.

#### 4.7 Summary

As a conclusion, the comparison between litho-stratigraphy and the depositional environment using CycloLog software provides a methodology for recognising and regionally mapping the subsurface cycles at basin scale for the Nita and Goldwyer Formations (see Figure 4.43). INPEFA curves show that the Goldwyer Formation formed as a transgressive systems tract (interval Or1000P), regressive systems tract (interval Or2000) and a further transgressive systems tract (interval Or2000P) for the top Goldwyer. Interval Or1000P matches the Goldwyer lower shale (Goldwyer Unit 1 and Unit 2) with transgressive systems tract. Interval Or2000

matches the Goldwyer middle carbonate (Goldwyer Unit 3) with regressive systems tract. Interval Or2000P matches the Goldwyer upper shale (Goldwyer Unit 4) with transgressive systems tract and increasing relative sea-level. The Goldwyer Formation can be concluded as a largely transgressive unit due to the fact that it forms by mostly transgressive systems tracts for the shale packages, but it is regressive for the shallowing upwards subtidal cycles within the generally shallow carbonate package (Goldwyer Unit 3).

Integrated prediction error filter analysis (INPEFA) curves show that the Nita Formation formed by regressive systems tract (interval Or3000), transgressive systems tract (interval Or3000p) and regressive systems tract (Or4000). Interval Or3000 matches with the regressive Nita Formation Leo Member. Intervals Or3000P and Or4000 are matching with the Nita Cudalgarra member. The INPEFA methodology has potential for use in basin analysis and ongoing petroleum exploration.

Interpreted Events	Embry's model, 1993	Results of INPEFA stratigraphy in this study	Interval
Start Regression	RST MFS	NEGATIVE TREND Negative bounding surface (NBS)	Or4000
	TST MRS	POSITIVE TREND Positive bounding surface (PBS)	Or3000P
Start Regression	RST MFS	NEGATIVE TREND Negative bounding surface (NBS)	Or3000
	TST MRS	POSITIVE TREND Positive bounding surface (PBS)	Or2000P
Start Regression	RST MFS	NEGATIVE TREND Negative bounding surface (NBS)	Or2000
	TST MRS	POSITIVE TREND Positive bounding surface (PBS)	Or1000P

Figure 4.43.: Application of Embry's models (1993) to components of INPEFA stratigraphy including the stratigraphic packages and compare with the results of this study.

## CHAPTER 5

# SHALE GAS PROSPECTIVITY OF GOLDWYER FORMATION IN CANNING BASIN

### 5.1 Introduction

Chapter 4 uses the CycloLog software to analyse long term integrated prediction error filter analysis curves (INPEFA\_curves) of subsurface wells in part of the Canning Basin, WA to determine the depositional environment of Nita and Goldwyer Formations and have a detail understanding of sequence stratigraphy for the Middle Ordovician. In Chapter 4, it can be concluded that the positive INPEFA trend (transgression) at bottom part of Goldwyer Formation represents the Goldwyer lower shale, a negative trend (regression) represents the Goldwyer middle carbonate and the upper part positive trend (transgression) is the Goldwyer upper shale (see Figure 4.6 for an example). In this chapter, the short term INPEFA\_curves are used to correlate the Goldwyer Formation distribution for the Goldwyer lower shale and the Goldwyer upper shale across the Canning Basin because the Goldwyer Shale is not only source and seal rock for hydrocarbons, but also is a target of shale gas exploration. The Goldwyer upper shale or Goldwyer Unit 4 contains rich oil-prone source-beds with up to 5% TOC and hydrogen indices are up to 850 mg/g TOC on the Barbwire Terrace (Foster et al., 1986; EIA, 2011).

The objectives of this study were to access the thickness and lateral extent of Goldwyer Formation as a first stage to identify the potential for shale gas. Shale gas resources have expanded from near zero to about 20 per cent of the total gas market in the past ten years in the US; nearly all of this occurred in the past five years, as shale gas has become more economic (EIA, 2011). Table 5.1 shows the projections by the US Energy Information Administration estimates that shale gas will constitute 45 per cent of the US market by the year 2030 (EIA, 2011). The average thickness of Goldwyer Formation is about 400m and the thickest intersection is 736m (Ghori, 2013); the estimated shale gas resource is up to 288 trillion cubic feet (Tcf) (EIA, 2011). Importantly, the objective of this study is to estimate shale gas in place for the Goldwyer Formation and try to correlate this formation across the Canning Basin and determine the thickness of the Goldwyer lower shale and Goldwyer upper shale. This

is of initial importance for refining exploration potential and for locating exploration targets.

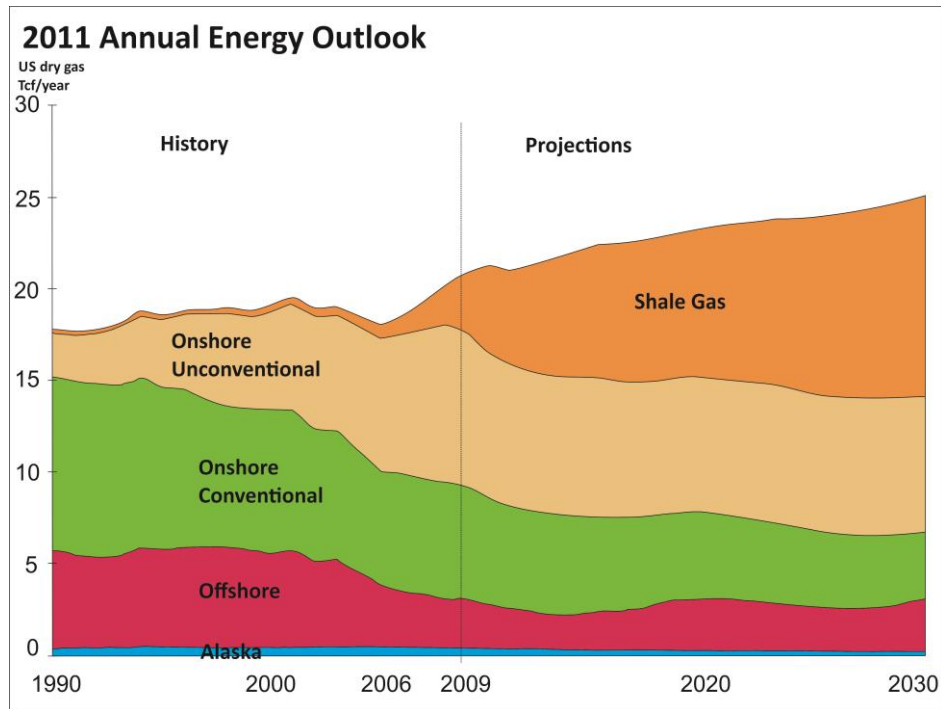


Table 5.1: Historical and projected US gas Production, year 1990-2030 (EIA, 2011).

## 5.2 Middle Ordovician Goldwyer Formation as shale gas resource

The Canning Basin has the largest estimated shale gas resource in Australia of up to 288 trillion cubic feet (Tcf) from Ordovician Goldwyer Formation shales (USGS, 2012). United States Energy Information Administration examined the shale gas potential in 14 countries outside of United States including the Canning Basin (EIA, 2011). They estimated that the Middle Ordovician Goldwyer Formation covered 124580km<sup>2</sup> of prospective area with 3660m depth average and 229 Tcf risked recoverable shale gas, which is 59 Tcf lower than 288 Tcf shale gas estimated by USGS (2012). According to EIA (2011) and Foster et al. (1986), the Ordovician Goldwyer Formation contains rich oil-prone source-beds with up to 5% total organic carbon (TOC) and hydrogen indices are up to 850 mg/g TOC on the Barbwire Terrace. New Standard Energy Ltd. drilled the well Nicolay 1 in October 2012 to evaluate shale gas potential within the Goldwyer Formation (NSE, 2012). Nicolay 1 is the first well drilled in the Canning Basin to target shale gas.

Figure 5.1 shows the very large area of shale gas prospectivity in the Canning Basin based on the Goldwyer Formation (EIA, 2011). Buru Energy and its joint venture partner Mitsubishi discovered 6.5 Tcf risked recoverable gas volume from the Carboniferous Laurel Formation in the Valhalla Field at northern Canning Basin while New Standard Energy and its joint venture partner ConocoPhillips have considerable acreage to the southwest of Buru/Mitsubishi in the Canning Basin and are largely focusing on the shale gas potential of the Goldwyer Formation (GSWA, 2013).

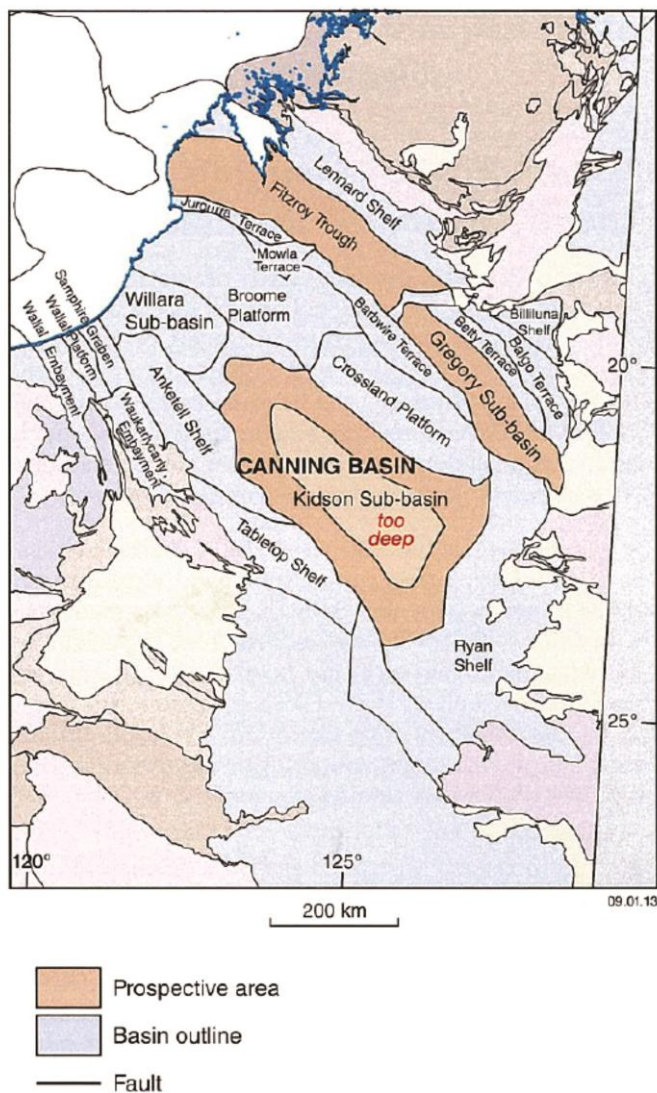


Figure 5.1: Prospective areas for shale gas resources in the Canning Basin (EIA, 2011).

### 5.3 Results

The short term integrated prediction error filter analysis (INPEFA) curves from thirty eight wells that penetrate the Goldwyer Formation were interpreted based on their positive trends, negative trends, positive turning points and negative turning points that were generated by CycloLog software. These components of INPEFA curves have been discussed in Chapter 1 and Chapter 4. The Goldwyer Formation can be sub-divided into lower shale, middle carbonate and upper shale in most of the areas in the Canning Basin but Foster et al. (1986) had sub-divided the Goldwyer Formation into 4 units. These units were characterized and correlated in this study based on the positive and negative trends based on the short term INPEFA curves. Eight section lines across the Canning Basin are chosen to correlate the Goldwyer Formation, which are A-A' (yellow line), B-B' (green line), C-C' (red line) and D-D' (orange line) from southwest to northeast while E-E' (dark blue line), F-F' (purple line), G-G' (brown line) and H-H' (grey line) are from northwest to southeast (Figure 5.2).

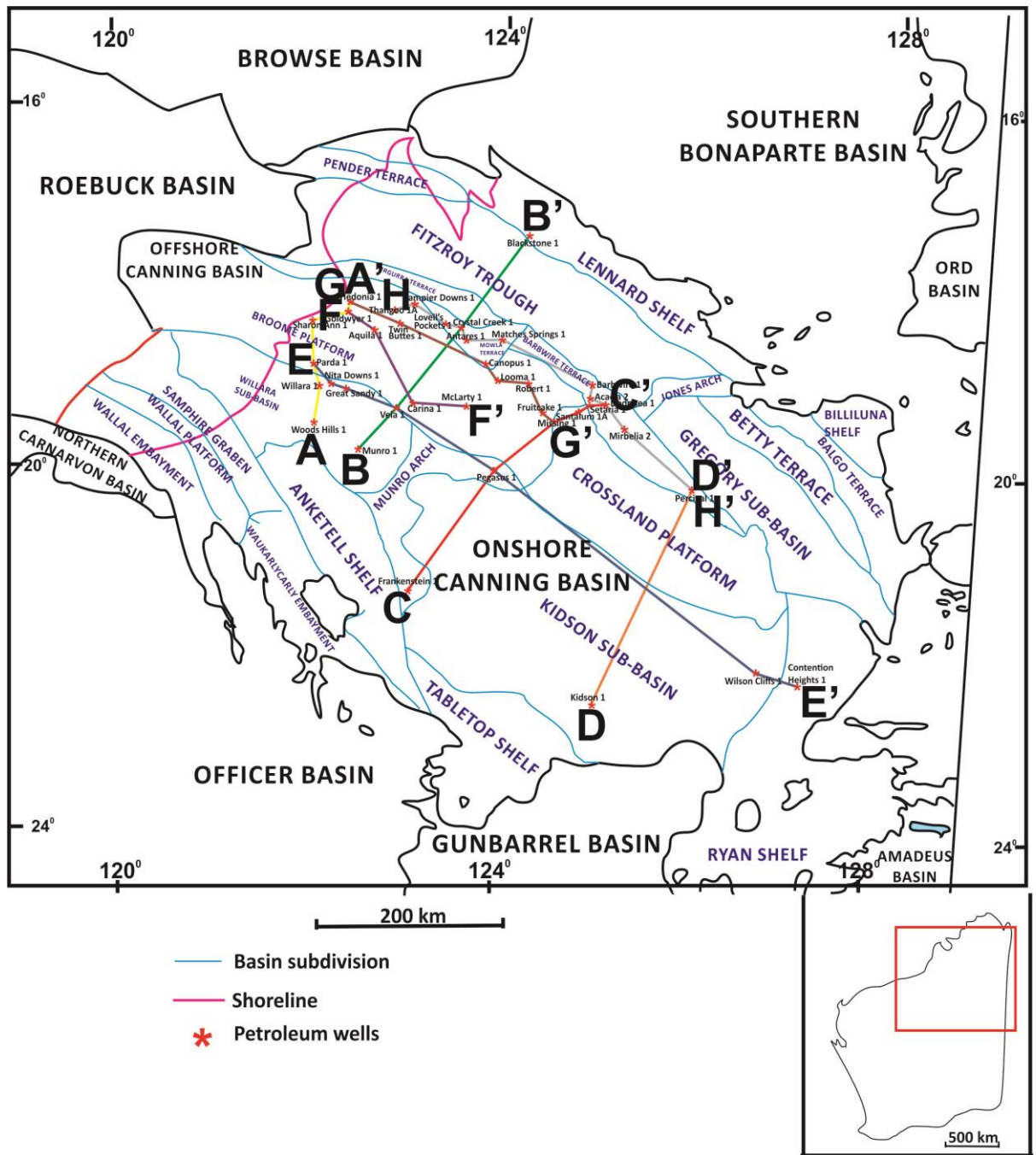


Figure 5.2: Well correlation lines, Canning Basin for Goldwyer Formation shale assessment. Each of the sections studied has three figures, first location map, then correlation diagrams and tables of shale distribution thickness. All of these figures are found after section 5.38 and following page 171.

### **5.3.1 Section A-A' (yellow line) (Figures 5.3, 5.4 and Table 5.2)**

The section A-A' (yellow line) in Figure 5.3 is a correlation between wells Woods Hills 1, Willara 1, Parda 1, Sharon Ann 1, Goldwyer 1 and Hedonia 1. It forms a SW-NE trending correlation line across the Willara Sub-basin and Broome Platform in the Canning Basin. This correlation line is based on the sub-units of the Goldwyer Formation, which are Goldwyer upper shale, Goldwyer middle carbonate and Goldwyer lower shale (Figure 5.4).

Table 5.2 shows the thickness for each sub-unit of the Goldwyer Formation for six different wells, which are wells Woods Hills 1, Willara 1, Parda 1, Sharon Ann 1, Goldwyer 1 and Hedonia 1. In this cross-section (Figure 5.4), the formation is the thickest in the Willara Sub-basin (well Willara 1), which is 736m. Although well Willara 1 contain the thickest Goldwyer Formation but it is deeper than other wells with the depth 1874-2610m. The next thickest section is in the Broome Platform (Sharon Ann 1). The area of least thickness is the north part of the Broome Platform (Hedonia 1); the upper part of the Goldwyer Formation in well Hedonia 1 was eroded by the unconformably overlying Permian Grant Group which left 135m thickness of lower shale. Besides Hedonia 1, parts of the upper shale of the Goldwyer 1 were also eroded by the Permian Grant Group glacial deposits characterize the base of this unit.

The total thickness of the Goldwyer upper shale (Goldwyer Unit 4) and Goldwyer lower shale (Goldwyer Unit 1 and Goldwyer Unit 2) is calculated for each well to determine the maximum shale contain in the Goldwyer Formation. Well Willara 1 on the Willara Sub-basin consists of 634m of shale units and well Woods Hills 1 which is also in the Willara Sub-Basin consists of 350m of shale units. On the Broome Platform, well Parda 1 consists of 187m shale units, well Sharon Ann consists of 335m of shale units, well Goldwyer 1 consists of 190m of shale units and well Hedonia 1 consists of 135m of shale units.

It can be concluded that the Goldwyer Formation pinches out from A to A' in this section. The Goldwyer Formation on the onshore Canning Basin which is situated near to the offshore Canning Basin is thinning from Willara Sub-basin to Broome Platform. This is probably due to the Permian erosion processes at wells Goldwyer 1 and Hedonia 1. The Nita Formation which lies conformably on top of the Goldwyer

Formation is missing together with upper part of the Goldwyer Formation due to post Ordovician erosion. The analysis of the data indicates the erosion events.

### **5.3.2 Section B-B' (Green line) (Figures 5.5, 5.6 and Table 5.3)**

The section B-B' (green line) in the Figure 5.5 is a correlation between wells Munro 1, Vela 1, Musca 1, Crystal Creek 1 and Blackstone 1. It forms a SW-NE trending correlation line across the Willara Sub-basin, Broome Platform, Mowla Terrace, Jurgurra Terrace, Fitzroy Trough to Lennard Shelf in the Canning Basin.

Goldwyer upper shale, Goldwyer middle carbonate and Goldwyer lower shale are sub-divided with INPEFA curves (Figure 5.6). A negative turning point which indicates the maximum flooding surface separated the Goldwyer lower shale (Unit 1 and 2) and Goldwyer middle carbonate (Unit 3) while a positive turning point which indicates maximum regressive surface or transgressive surface separated the Goldwyer middle carbonate and Goldwyer upper shale (Unit 4).

The thickness for each sub-unit of the Goldwyer Formation can be found in Table 5.3. The thickness of the Goldwyer shale is the total thicknesses of Goldwyer lower shale and upper shale. This can be calculated by subtracting the thickness of the Goldwyer middle carbonate from the thickness of the complete Goldwyer Formation. Figure 5.6 shows that the formation is the thickest in the Lennard Shelf (well Blackstone 1), which is more than 665m. This is because well Blackstone 1 reaches the well total depth and it might contain more Goldwyer lower shale in the unpenetrated stratigraphy. Although well Blackstone 1 contains the thickest Goldwyer Formation in this section, it is deeper than other wells with the depth 2310-2975m. The next thickest section is on the Mowla Terrace (well Crystal Creek 1) with 461m thickness. Well Munro 1 located on the Willara Sub-basin with the thickness of 219m for the Goldwyer Formation. Well Vela 1 on the boundary of Willara Sub-Basin and Broome Platform reaches well total depth at depth 1900m. It only covers 41m of the Goldwyer upper shale and it is predicted that the thickness of Goldwyer Formation should be between the thickness of Goldwyer Formation in wells Munro 1 and Crystal Creek 1 which fall in the ranges of 219m to 461m in this study. This is because the thickness of the Goldwyer Formation is thicker from south-western to north-western along the section B-B' (see Figure 5.6).

Unsurprisingly, well Blackstone 1 which consists of the thickest Goldwyer Formation contains the most shale units in this section. Then it is followed by well Crystal Creek 1 with 375m thickness shale units and well Munro 1 with 180m thickness shale units. Well Vela 1 reaches the total depth and the thickness of shale unit is not available but the thickness of the Goldwyer shale in this well will be estimated in following sections.

### **5.3.3 Section C-C' (Red line) (Figures 5.7, 5.8 and Table 5.4)**

The section C-C' (red line) in the Figure 5.7 is a correlation between wells Frankenstein 1, Pegasus 1, Sally May 1, Missing 1, Santalum 1A, Setaria 1 and Dodonea 1. It forms a SW-NE trending correlation line across the Munro Arch, Kidson Sub-basin, Broome Platform, Crossland Platform and Barbwire Terrace in the Canning Basin. The correlation of these wells can be found in Figure 5.8. In this cross-section (Figure 5.8), the formation is the thickest at the boundary of Crossland Platform and Broome Platform (well Missing 1), which is 380m. The next thickest section is on the Munro Arch (well Pegasus 1) with 288m but this well is deeper than other wells with the depth 2344-2632m. The area of least thickness is the western part of the Munro Arch (well Frankenstein 1) with only 111m thickness of the Goldwyer Formation. This shows that the Goldwyer Formation thins towards the western part of the Munro Arch.

The total thickness of the Goldwyer upper shale (Goldwyer Unit 4) and Goldwyer lower shale (Goldwyer Unit 1 and Goldwyer Unit 2) are shown in Table 5.4. Well Missing 1 on the Crossland Platform contains the most shale in this section C-C', which is 330m thickness of shale units and well Pegasus 1 which is on the eastern part of the Munro Arch consists of 254m of shale units as the well contains the next thickest shale section. Well Santalum 1A on the Crossland Platform consists of more than 101m thickness of shale because it reaches the well total depth at the Goldwyer lower shale. Wells Setaria 1 and Dodonea 1 on the Barbwire terrace consists of 164m and 159m of shale units respectively.

From the interpretation above, the Goldwyer Formation is thickening on the Broome Platform of the Canning Basin along this section C-C'. It pinches out towards Munro Arch from the Crossland Platform also thinning towards Barbwire Terrace. The Goldwyer Formation in well Setaria 1 (in Barbwire Terrace) was eroded by the

Permian Grant Group due to the Permian glaciation. This may be a reason for the Goldwyer Formation thinning towards the Barbwire Terrace.

#### **5.3.4 Section D-D' (Orange line) (Figures 5.9, 5.10 and Table 5.5)**

The section D-D' (orange line) in the Figure 5.9 is a correlation between wells Kidson 1 and Percival 1. It forms a SW-NE trending correlation line across the Kidson Sub-basin, Crossland Platform and Barbwire Terrace in the Canning Basin. The correlation for section D-D' (orange line) is based on the sub-units of the Goldwyer Formation (Figure 5.10).

The thickness for the whole Goldwyer Formation and the thickness for each sub-unit for the Goldwyer of wells Kidson 1 and Percival 1 are to be found at Table 5.5. In this cross-section (Figure 5.10), the formation correlates well and the thickness of Goldwyer Formation is 134m in well Kidson 1 and 153m in well Percival 1. However, the total thickness of shale units is higher in well Kidson 1 with 120m compared with 116m in well Percival 1. The Goldwyer middle carbonate in well Kidson 1 is quite thin with the thickness of 14m only. Although well Kidson 1 contains the thicker shale, it is the deepest Goldwyer Formation compared with other wells in the Canning Basin with depth 4270-4413m. This is far too deep for shale gas exploration because deeper drilling depths means more steel drilling pipe and this will give a higher cost to shale gas exploration and production.

#### **5.3.5 Section E-E' (Dark blue line) (Figures 5.11, 5.12 and Table 5.6)**

The section E-E' (dark blue line) in the Figure 5.11 is a correlation between wells Parda 1, Nita Downs 1, Cudalgarra North 1, Great Sandy 1, Vela 1, Pegasus 1, Wilson Cliffs 1 and Contention Heights 1. It forms a NW-SE trending correlation line across the Broome Platform, Willara Sub-basin, Munro Arch, Kidson Sub-basin and Ryan Shelf in the Canning Basin. The well-to-well correlation for this section is in Figure 5.12.

The formation is the thickest at the boundary Munro Arch (well Pegasus 1), which is 288m but the depth of Goldwyer Formation in this well is at 2344-2632m. The next thickest section is in the Willara Sub-basin (well Nita Downs 1) with 274m. The area of least thickness is the Ryan Shelf (well Contension Heights 1) with only

85m thickness of the Goldwyer Formation. This shows that the Goldwyer Formation thins towards the southeast on the Ryan Shelf (Table 5.6).

The total thickness of the Goldwyer shale units is calculated for each well to calculate the maximum shale contained in the Goldwyer Formation. Well Pegasus 1 on the Munro Arch consists the maximum thickness of 254m shale in this section E-E' and well Nita Downs 1 which is on the Willara Sub-Basin consists of 209m of shale as the well contains the next thickest of shale units. Well Great Sandy 1 which is at the bottom of well Nita Downs 1 (Figure 5.12) on the Willara Sub-Basin consists of only 111m thickness of shale although it is near to well Nita Downs 1 with distance 17.2km.

The Goldwyer Formation is thickening on the central part of the Canning Basin at Munro Arch along this section E-E; although it seems thins towards the north-western and south-eastern part of this section, the north-western part of this section consists of thicker Goldwyer shale units compared with the thickness of Goldwyer shale units in the south-eastern part.

### **5.3.6 Section F-F' (Purple line) (Figures 5.13, 5.14 and Table 5.7)**

The section F-F' (purple line) in the Figure 5.13 consists of wells Goldwyer 1, Aquila 1, Musca 1, Carina 1 and McLarty 1. It forms a NW-SE trending correlation line in the Broome Platform in the Canning Basin. The correlation for this section from northwest to southeast on the Broome Platform in the Canning Basin can be found in Figure 5.14.

Table 5.7 shows the thickness for each sub-unit of the Goldwyer Formation for each well. In this cross-section (Figure 5.14), the formation is the thickest at the wells McLarty 1 and Aquila 1 with the thickness 374m and 368m; this is because they consist of the complete Goldwyer Formation while well Carina 1 reaches well total depth with only 36m of Goldwyer upper shale penetrated. For well Goldwyer 1, the major part of the Goldwyer upper shale was eroded by the Permian Grant Group and left only 40m for this unit. The total thickness of Goldwyer shale units is 190m for well Goldwyer 1, 309m for well Aquila 1 and 302m for well McLarty 1.

### **5.3.7 Section G-G' (Brown line) (Figures 5.15, 5.16 and Table 5.8)**

The section G-G' (brown line) in the Figure 5.15 is a correlation between wells Hedonia 1, Twin Buttes 1, Canopus 1, Looma 1, Robert 1, Fruitcake 1 and Missing 1. The correlation for section G-G' (brown line) from northwest to southeast across the Broome Platform, Mowla Terrace, Broome Platform again and Crossland Platform in the Canning Basin is shown in Figure 5.16. In this cross-section, the formation is the thickest at the Broome Platform (well Looma 1), which is 560m. The next thickest section is on the Mowla Terrace (well Canopus 1) with 527m. The area of least thickness is well Hedonia 1 with only 135m of the Goldwyer lower shale; this is caused by the erosion by the Permian Grant Group.

The Goldwyer Formation is sub-divided into different units so as to calculate the maximum shale which is contained in this formation (Table 5.8). Well Looma 1 consists of the most shale in this section with 409m thickness of shale units and well Canopus 1 consists of 402m of shale units as the well contains next thickest of shale. Well Twin Buttes 1 on the Broome Platform consists of 288m thickness of shale units. Well Robert 1 on the Broome Platform consists of more than 155m thickness of shale units because it reaches the well total depth at the Goldwyer middle carbonate. Well Fruitcake 1 on the Broome Platform and well Missing 1 on the Crossland Platform consist of 352m and 330m of shale units respectively.

Compared with other sections in this study, the Goldwyer shale units are quite thick along the section G-G' with the thickness ranges from 135-527m.

### **5.3.8 Section H-H' (Grey line) (Figures 5.17, 5.18 and Table 5.9)**

The section H-H' (grey line) in the Figure 5.17 is a correlation between wells Thangoo 1A, Dampier Downs 1, Lovell's Pockets 1, Crystal Creek 1, Antares 1, Matches Springs 1, Barbwire 1, Acacia 2, Dodonea 1, Mirbelia 2 and Percival 1. The correlation for this section is from northwest to southeast across the Broome Platform, Mowla Terrace and Barbwire Terrace in the Canning Basin. Table 5.9 summarizes the thicknesses of each sub-unit of the Goldwyer Formation. In this cross-section (Figure 5.18), the formation is the thickest at the Mowla Terrace (well Matches Springs 1), which is more than 621m and reaches well total depth at the Goldwyer lower shale. The next thickest section is also on the Mowla Terrace (well

Crystal Creek 1) with 461m. Well Antares 1 on the Mowla Terrace reaches well total depth and only covers 47m of Goldwyer upper shale in the well composite chart. The Goldwyer Formation in well Antares 1 is expected to contain the complete sub-units because other wells in the Mowla Terrace (same tectonic sub-division) consist of the complete Goldwyer Formation from analysis in this study.

On the Mowla Terrace, Well Crystal Creek 1 comprises the bulk of the shale in this section HH ', a 375m thick shale unit and Matches Springs 1 consists of 360m of shale and also contains further thick shale unit. Thangoo Wells 1A and Dodonea 1 consists of 175 m and 159m respectively shale thickness; The Goldwyer upper shale is eroded by Permian Grant Group in both wells. A few wells do not cover complete Goldwyer Formation, Goldwyer shale units is therefore difficult to calculate. The other consists of Goldwyer shale units from 116m to 202m thickness.

The information collated confirms from this well analysis has allowed the construction of contour maps for shale thickness within sub-basins leading to an assessment of shale gas potential.

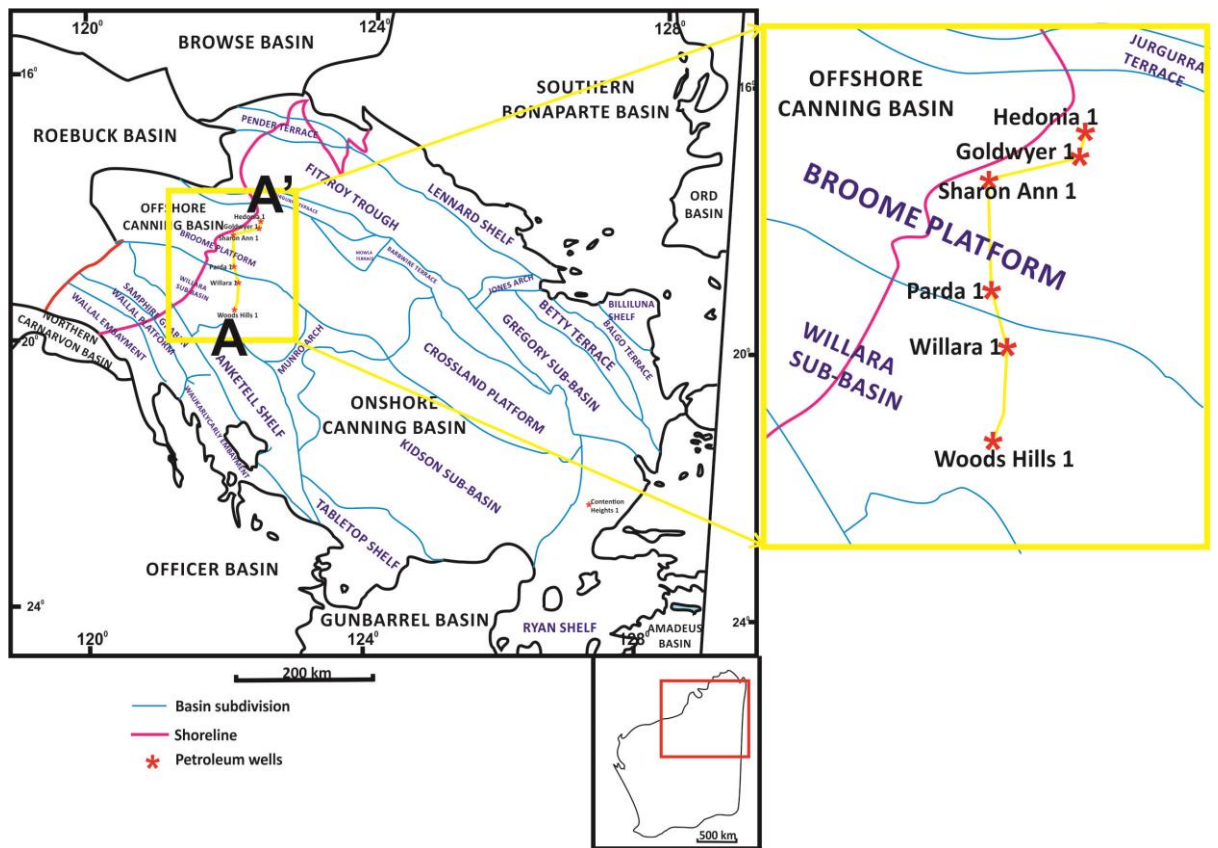


Figure 5.3: Map location of section A-A' (yellow line) for the Goldwyer Formation correlation from southwest to northeast in the Canning Basin.

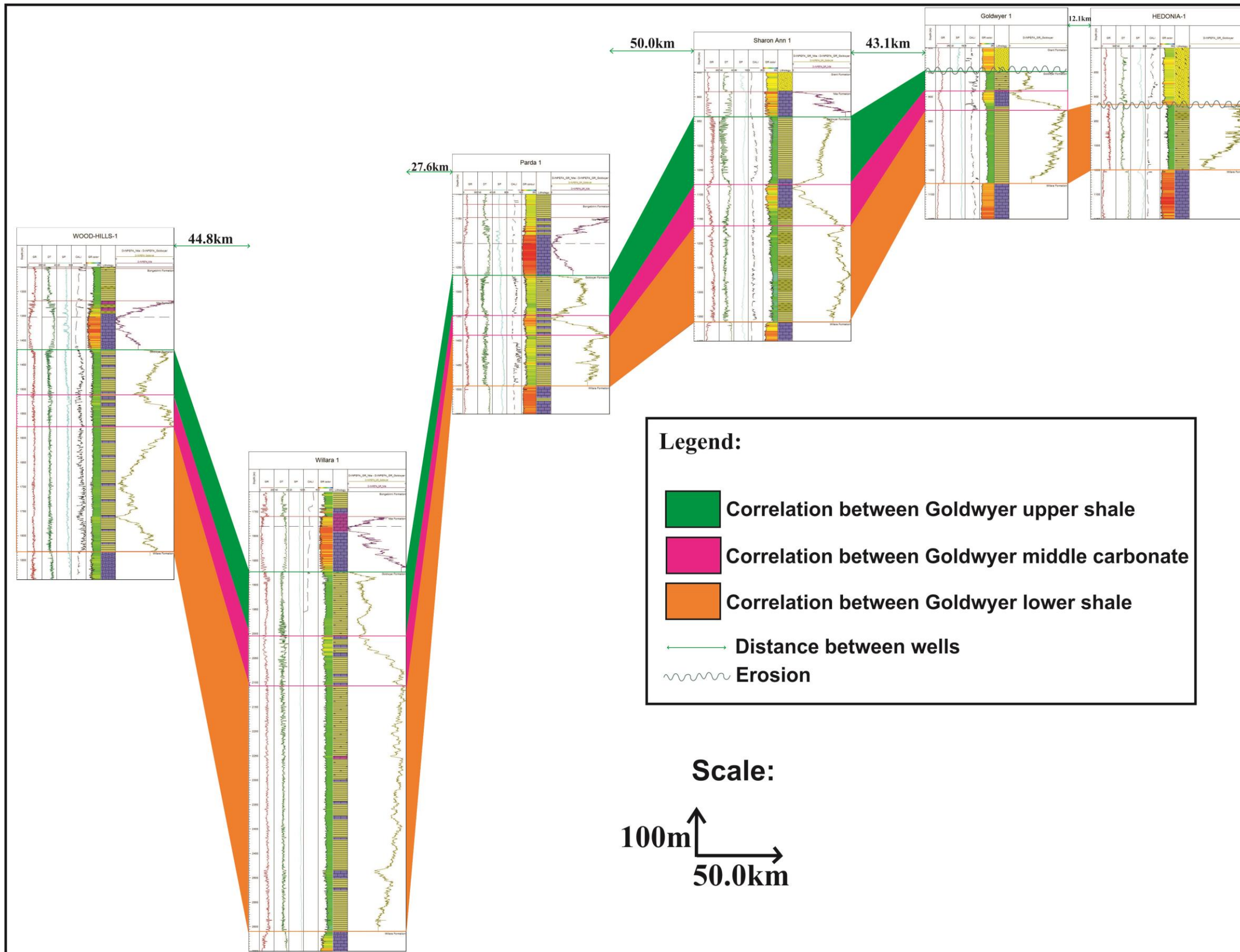


Figure 5.4: Well-to-well correlation for the section A-A' (yellow line) from southwest to northeast across Willara Sub-basin to Broome Platform in the Canning Basin for the Goldwyer Formation.

SW → NE

Distance between wells		44.8km		27.6km		50.0km		43.1km		12.1km			
WELLS		WOOD HILLS 1		WILLARA 1		PARDA 1		SHARON ANN 1		GOLDWYER 1		HEDONIA 1	
Formation	Sub-unit	Depth (m)	Thickness (m)	Depth (m)	Thickness (m)	Depth (m)	Thickness (m)	Depth (m)	Thickness (m)	Depth (m)	Thickness (m)	Depth (m)	Thickness (m)
GOLDWYER FORMATION	Upper Shale	1418-1511	93	1874-2005	131	1266-1349	83	941-1079	138	848-889	41		
	Middle Carbonate	1511-1576	65	2005-2107	102	1349-1389	40	1079-1164	85	889-928	39		
	Lower Shale	1576-1833	257	2107-2610	503	1389-1493	104	1164-1361	197	928-1077	149		
Thickness of the Goldwyer Formation (m)		415		736		227		420		229		135	
Total thickness of upper shale and lower shale (m)		350		634		187		335		190		135	

Table 5.2: Thickness correlation for the Goldwyer Formation based on the sub-units along the section A-A' (yellow line).

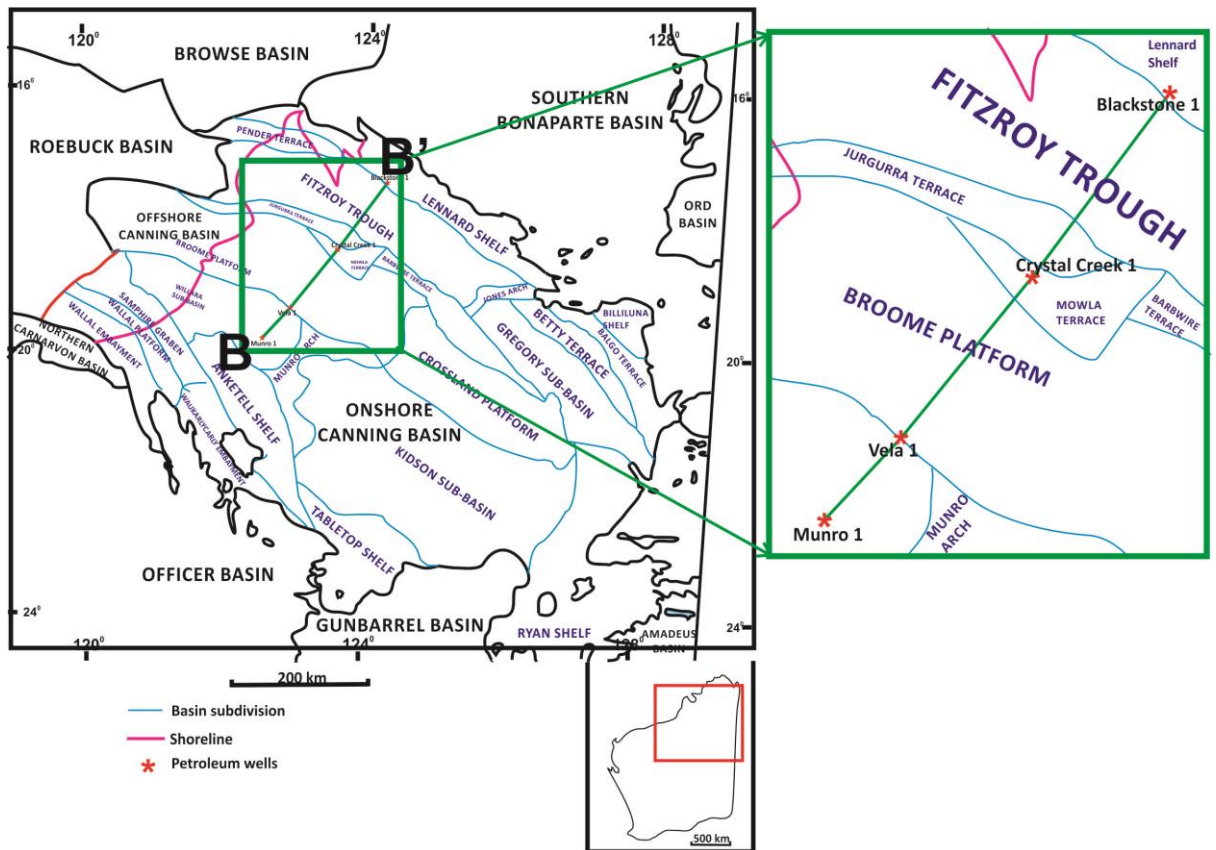


Figure 5.5: Map location of section B-B' (green line) for the Goldwyer Formation correlation from southwest to northeast in the Canning Basin.

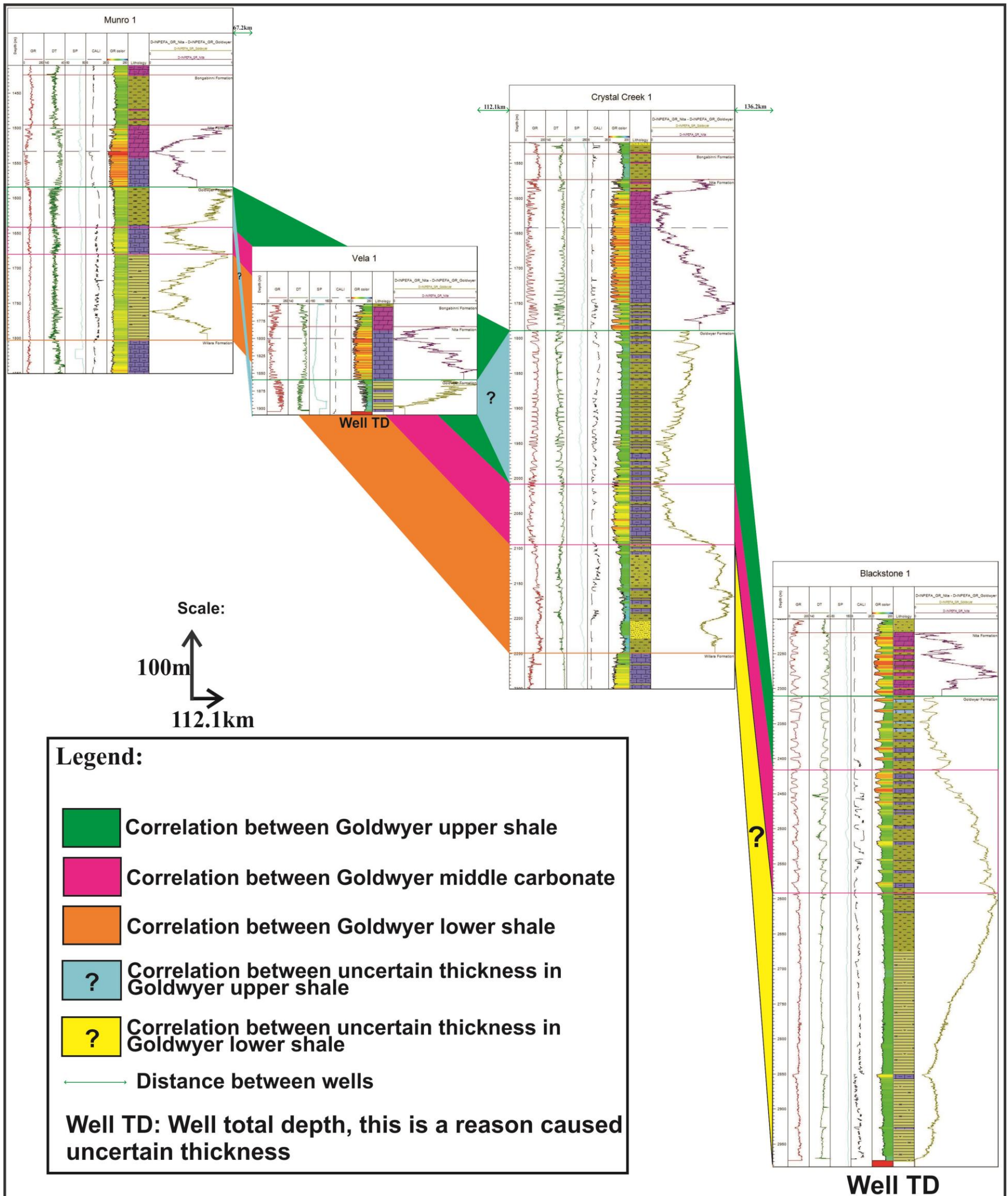


Figure 5.6: Well-to-well correlation for the section B-B' (green line) from southwest to northeast across Willara Sub-basin, Broome Platform, Mowla Terrace, Jurgurra Terrace, Fitzroy Trough to Lennard Shelf in the Canning Basin.

SW → NE

Distance between wells		67.2km		112.1km		136.2km			
WELLS		MUNRO 1		VELA 1		CRYSTAL CREEK 1		BLACKSTONE 1	
Formation	Sub-unit	Depth (m)	Thickness (m)	Depth (m)	Thickness (m)	Depth (m)	Thickness (m)	Depth (m)	Thickness (m)
GOLDWYER FORMATION	Upper Shale	1584-1641	57	1859-1900	>41	1789-2009	220	2310-2416	106
	Middle Carbonate	1641-1680	39	Depth 1900m is the well total depth (TD)		2009-2095	86	2416-2591	175
	Lower Shale	1680-1803	123			2095-2250	155	2591-2975 (well TD)	>384
Thickness of the Goldwyer Formation (m)		219		>41		461		>665	
Total thickness of upper shale and lower shale (m)		180		>41		375		>490	

Table 5.3: Thickness correlation for the Goldwyer Formation based on the sub-units along the section B-B' (green line).

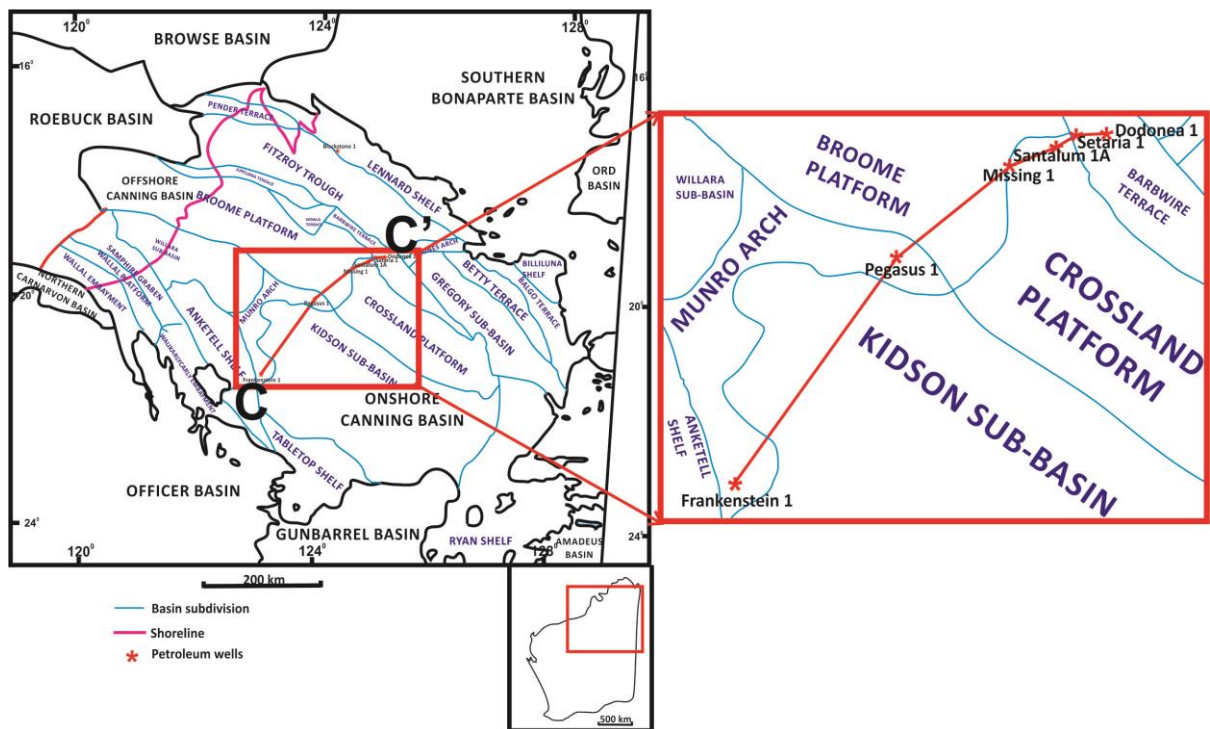


Figure 5.7: Map location of section C-C' (red line) for the Goldwyer Formation correlation from southwest to northeast in the Canning Basin.

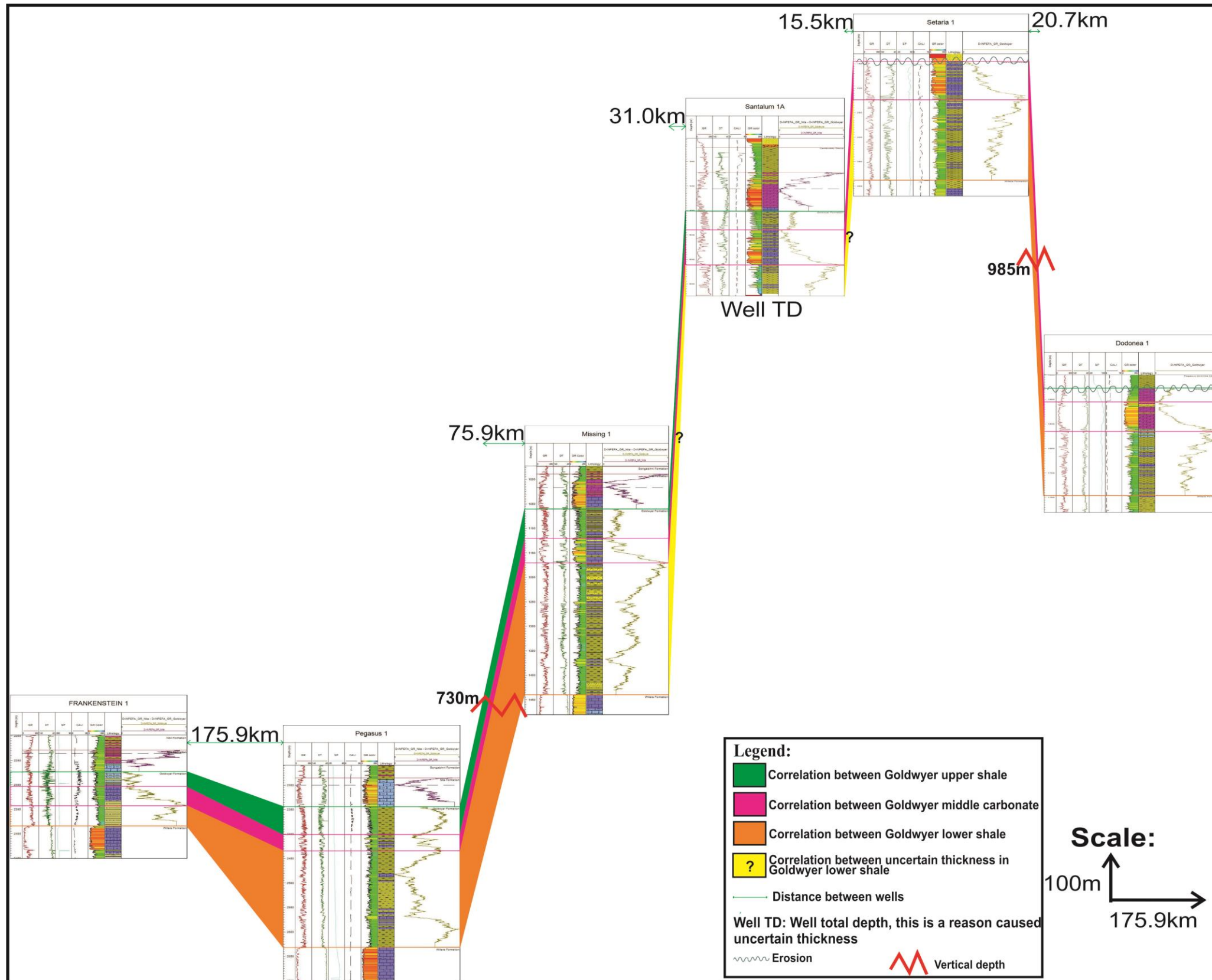


Figure 5.8: Well-to-well correlation for the section C-C' (red line) from southwest to northeast across Munro Arch, Kidson Sub-basin, Broome Platform, Crossland Platform and Barbwire Terrace in the Canning Basin.

SW

NE

Distance between wells		175.9km		75.9km		31.0km		15.5km		20.7km			
WELLS		FRANKENSTEIN 1		PEGASUS 1		MISSING 1		SANTALUM 1A		SETARIA 1		DODONEA 1	
Formation	Sub-unit	Depth (m)	Thickness (m)	Depth (m)	Thickness (m)	Depth (m)	Thickness (m)	Depth (m)	Thickness (m)	Depth (m)	Thickness (m)	Depth (m)	Thickness (m)
GOLDWYER FORMATION	Upper Shale	2274-2303	29	2344-2401	57	1060-1120	60	451-490	39			1527-1555	28
	Middle Carbonate	2303-2344	41	2401-2435	34	1120-1170	50	490-561	71	145-224	79	1555-1615	60
	Lower Shale	2344-2385	41	2435-2632	197	1170-1440	270	561-623 (TD)	>62	224-388	164	1615-1746	131
Thickness of the Goldwyer Formation (m)		111		288		380		>172		243		219	
Total thickness of upper shale and lower shale (m)		70		254		330		>101		164		159	

Table 5.4: Thickness correlation for the Goldwyer Formation based on the sub-units along the section C-C' (red line).

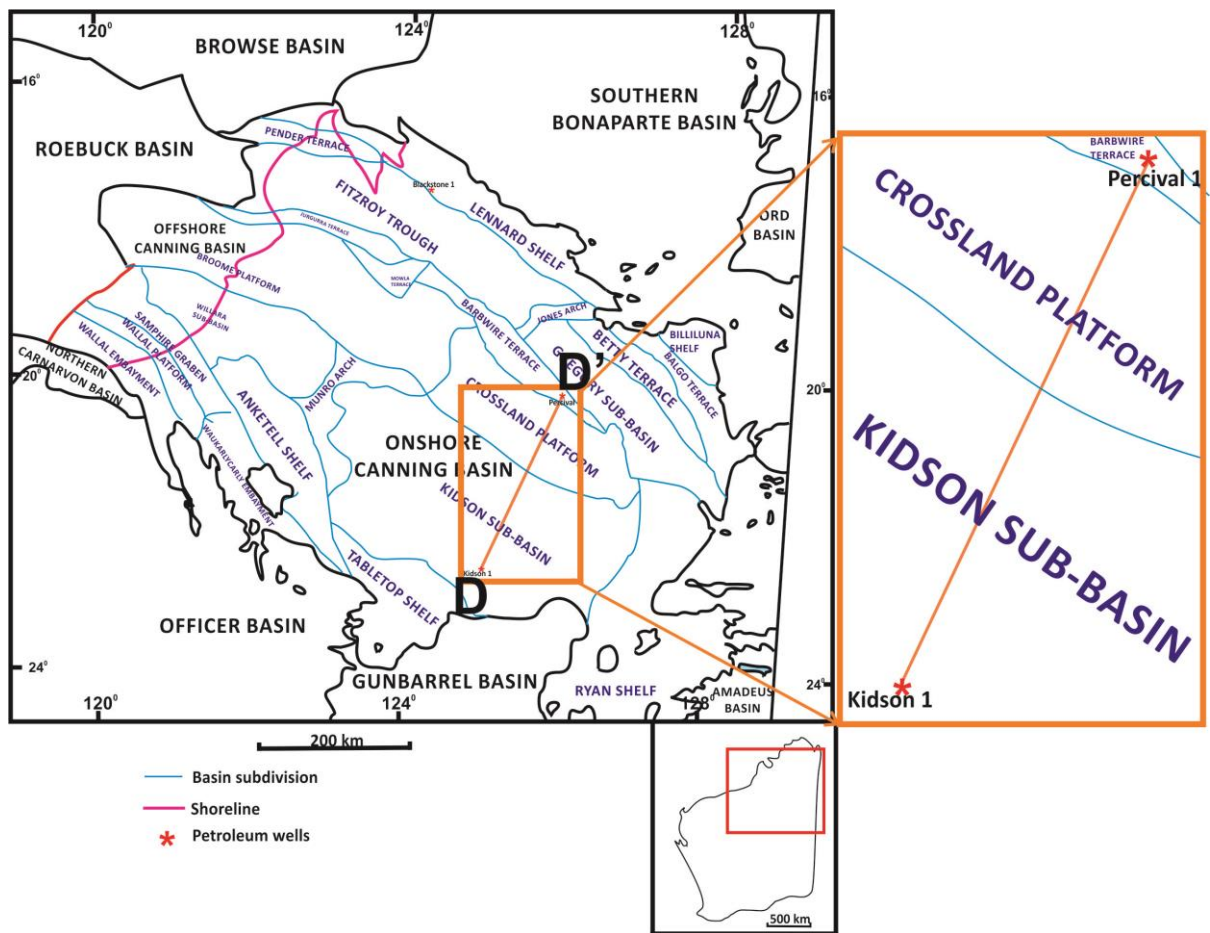


Figure 5.9: Map location of section D-D' (orange line) for the Goldwyer Formation correlation from southwest to northeast in the Canning Basin.

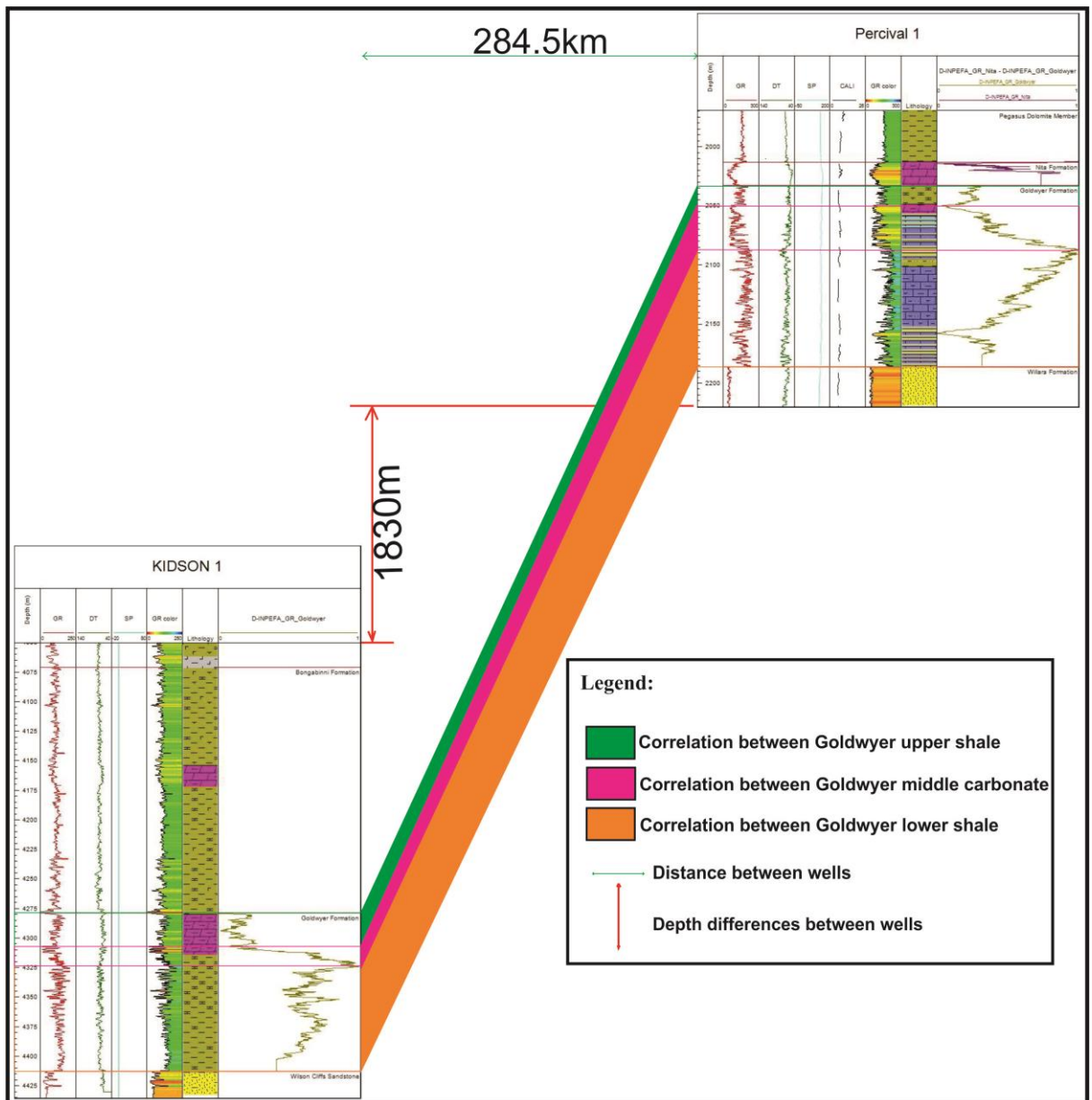


Figure 5.10: Well-to-well correlation for the section D-D' (orange line) from southwest to northeast across Kidson Sub-basin, Crossland Platform and Barbwire Terrace in the Canning Basin.

SW → NE

<b>Distance between wells</b>		284.5km			
<b>WELLS</b>		<b>KIDSON 1</b>		<b>PERCIVAL 1</b>	
<b>Formation</b>	<b>Sub-unit</b>	Depth (m)	Thickness (m)	Depth (m)	Thickness (m)
<b>GOLDWYER FORMATION</b>	<b>Upper Shale</b>	4279-4310	31	2033-2050	17
	Middle Carbonate	4310-4324	14	2050-2087	37
	<b>Lower Shale</b>	4324-4413	89	2087-2186	99
<b>Thickness of the Goldwyer Formation (m)</b>		134		153	
<b>Total thickness of upper shale and lower shale (m)</b>		120		116	

Table 5.5: Thickness correlation for the Goldwyer Formation based on the sub-units along the section D-D' (orange line).

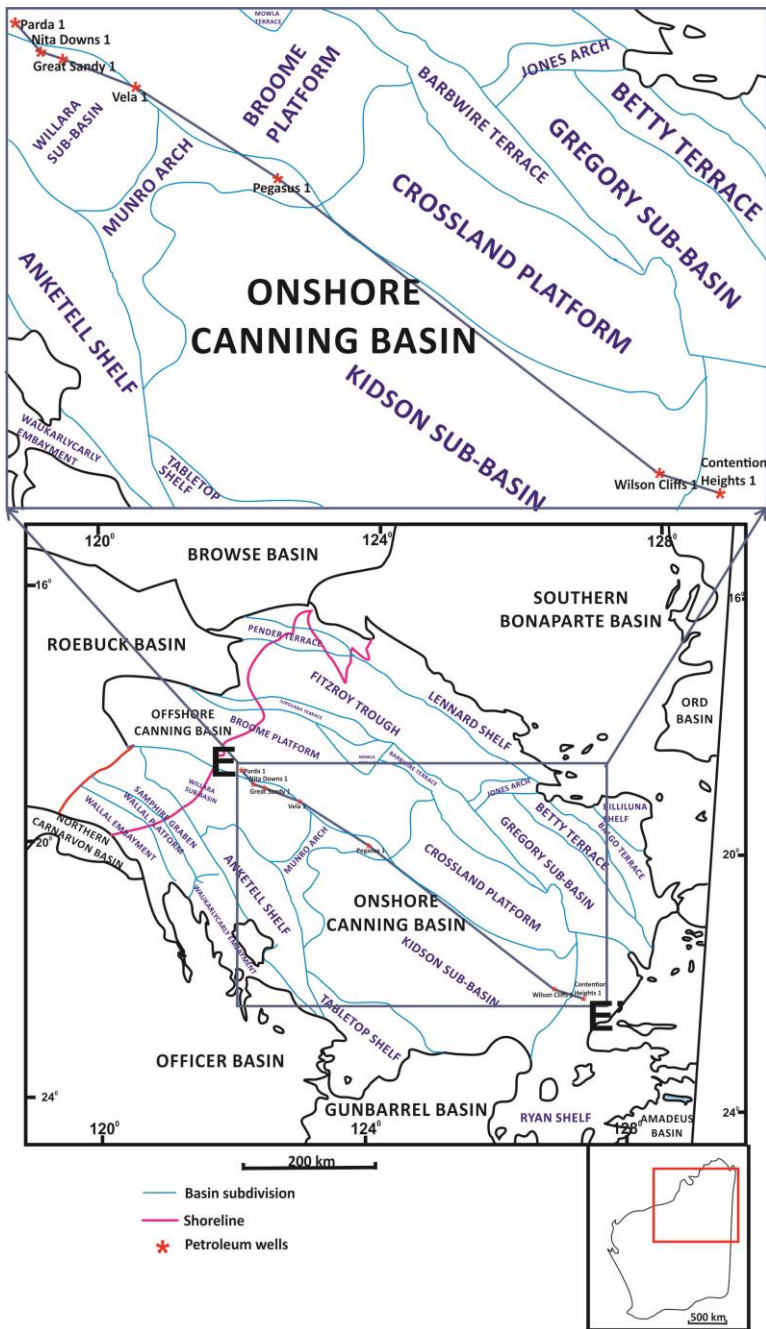


Figure 5.11: Map location of section E-E' (dark blue line) for the Goldwyer Formation correlation from northwest to southeast in the Canning Basin.

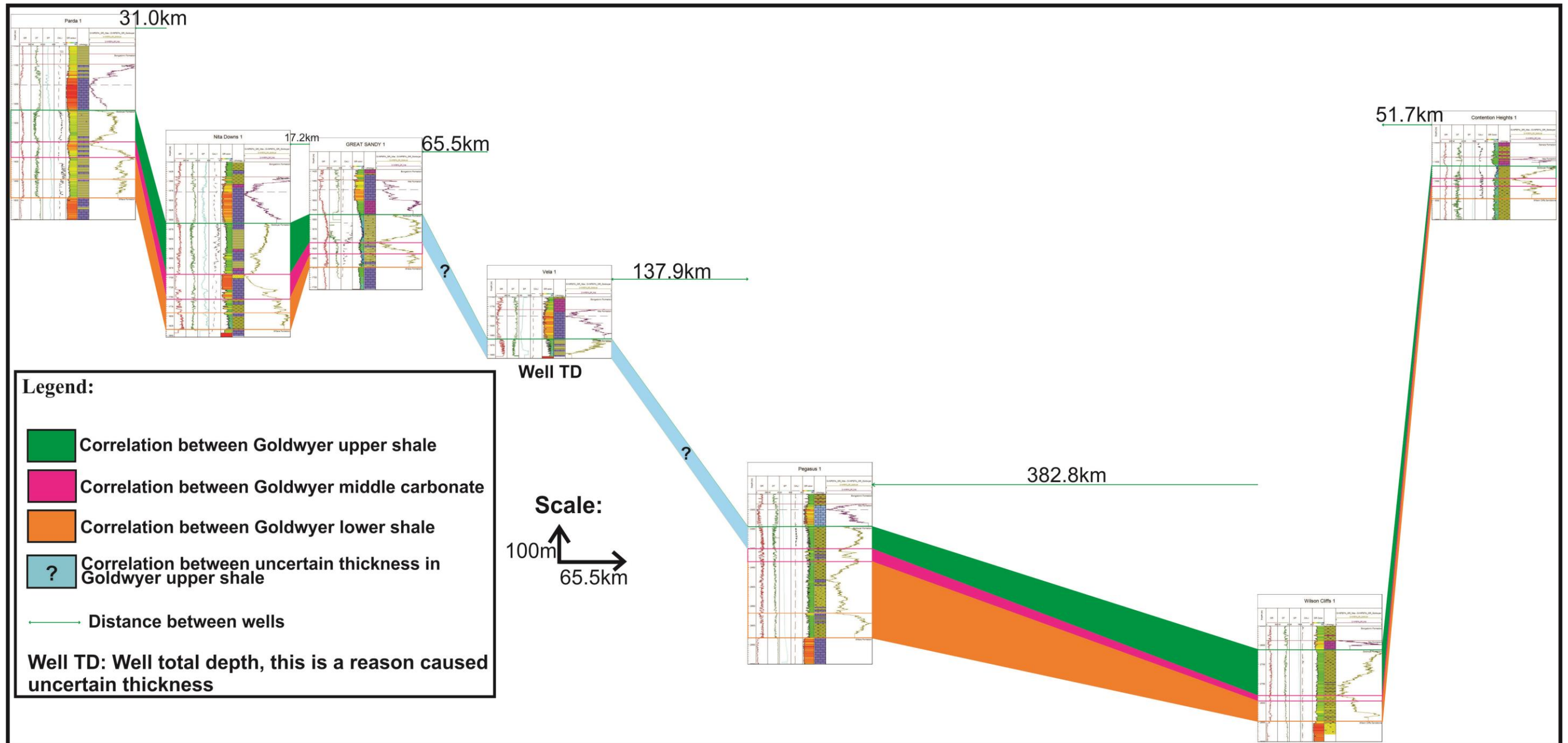


Figure 5.12: Well-to-well correlation for the section E-E' (dark blue line) from northwest to southeast across Broome Platform, Willara Sub-basin, Munro Arch, Kidson Sub-basin and Ryan Shelf in the Canning Basin.



Distance between wells		31.0km		17.2km		65.5km		137.9km		382.8km		51.7km				
WELLS		Parda 1		Nita Downs 1		Great Sandy 1		Vela 1		Pegasus 1		Wilson Cliffs 1		Contension Heights 1		
Formation	Sub-unit	Depth (m)	Thickness (m)	Depth (m)	Thickness (m)	Depth (m)	Thickness (m)	Depth (m)	Thickness (m)	Depth (m)	Thickness (m)	Depth (m)	Thickness (m)	Depth (m)	Thickness (m)	
GOLDWYER FORMATION	Upper Shale (Unit 4)	1266-1349	83	1560-1691	131	1536-1610	74	1860-1900 (TD)	>40	2344-2401	57	2662-2780	118	1410-1443	33	
	Middle Carbonate (Unit 3)	1349-1389	40	1691-1756	65	1610-1637	27			2401-2435	34	2780-2795	15	1443-1464	21	
	Lower Shale	Unit 2	1389-1445	56	1756-1791	35	1637-1674			37	2435-2568	133	2795-2842	47	1464-1495	31
		Unit 1	1445-1494	49	1791-1834	43					2568-2632	64				
Thickness of the Goldwyer Formation (m)		228		274		138		>40		288		180		85		
Total thickness of upper shale and lower shale (m)		188		209		111		>40		254		165		64		

Table 5.6: Thickness correlation for the Goldwyer Formation based on the sub-units along the E-E' (dark blue line).

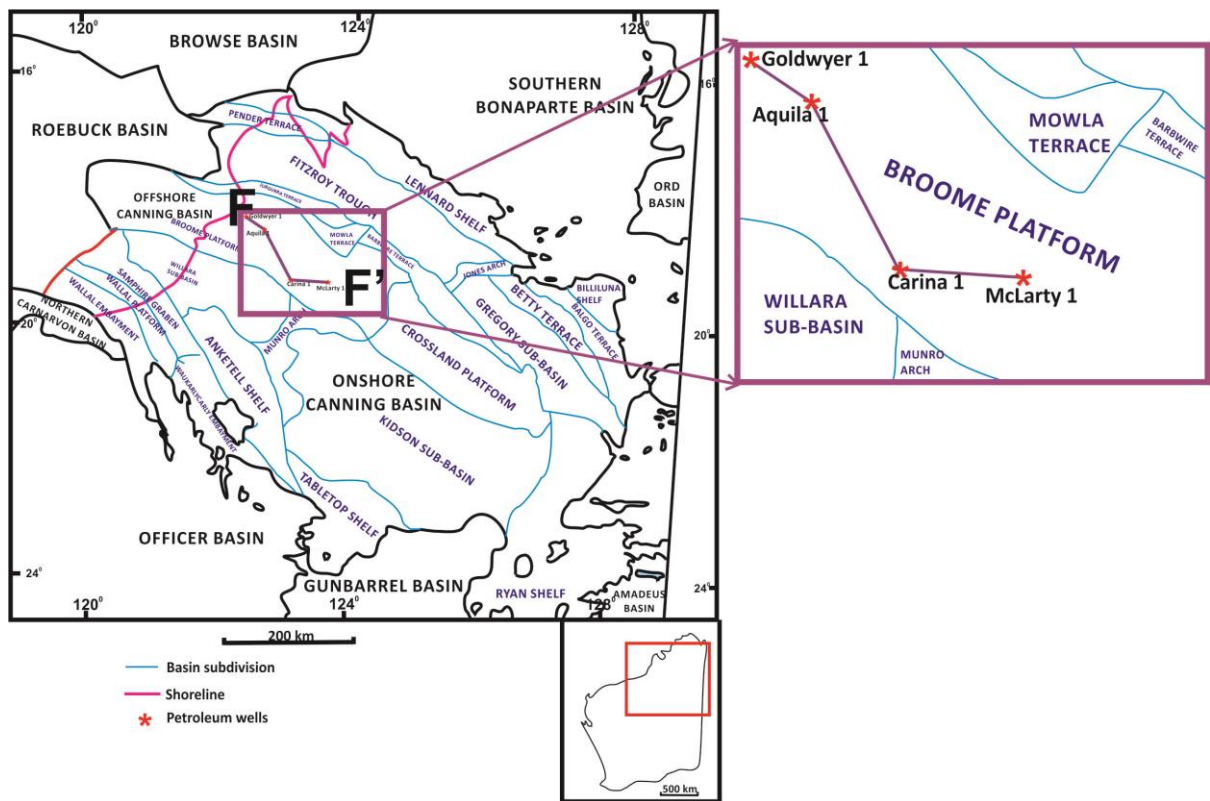


Figure 5.13: Map location of section F-F' (purple line) for the Goldwyer Formation correlation from northwest to southeast in the Canning Basin.

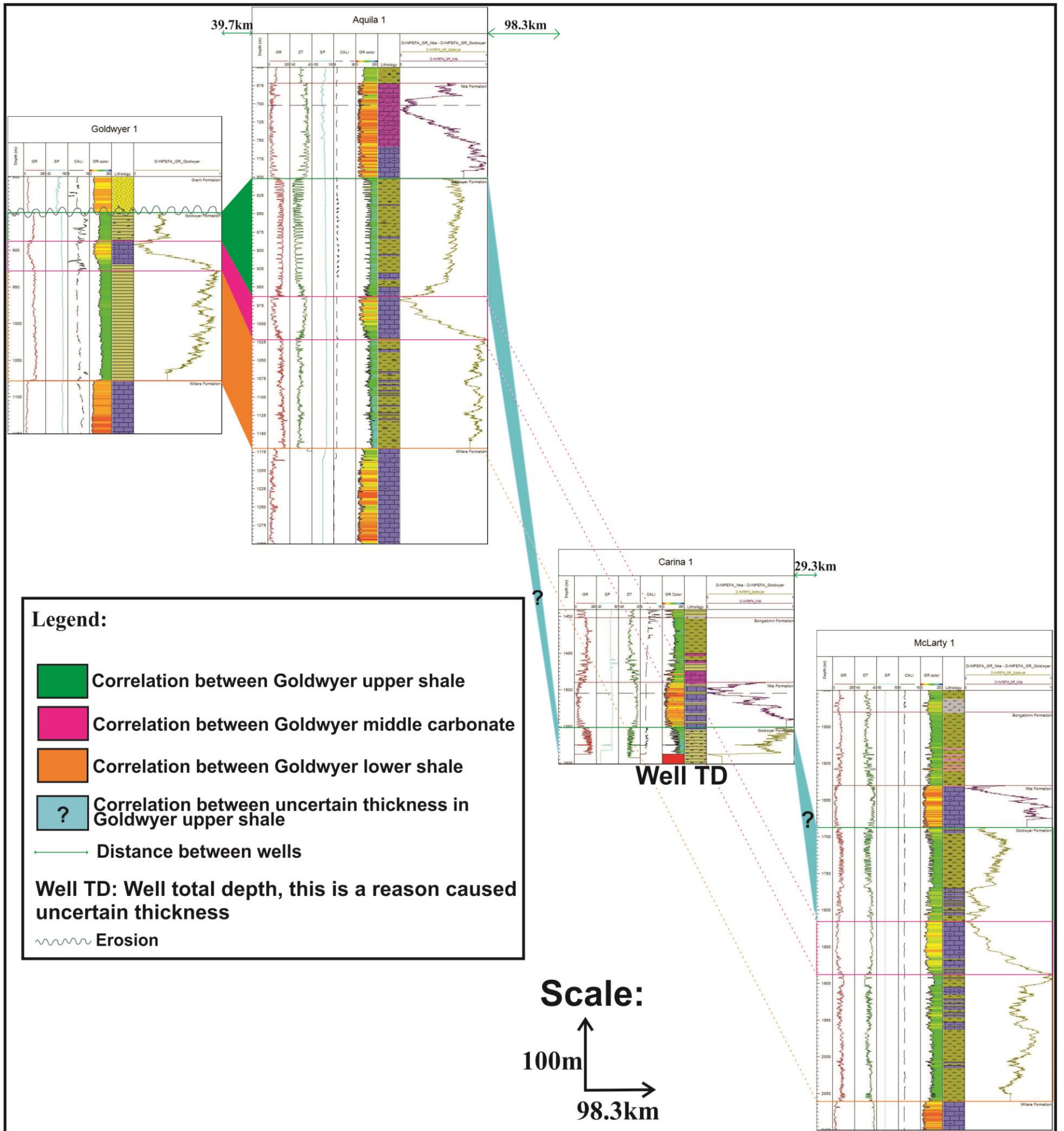


Figure 5.14: Well-to-well correlation for section F-F' (purple line) from northwest to southeast across Broome Platform in the Canning Basin.

NW → SE

Distance between wells		39.7km		98.3km		29.3km			
WELLS		GOLDWYER 1		AQUILA 1		CARINA 1		MCLARTY 1	
Formation	Sub-unit	Depth (m)	Thickness (m)	Depth (m)	Thickness (m)	Depth (m)	Thickness (m)	Depth (m)	Thickness (m)
GOLDWYER FORMATION	Upper Shale	848-888	40	802-963	161	1551-1587 (TD)	>36	1687-1816	129
	Middle Carbonate	888-928	40	963-1022	59			1816-1888	72
	Lower Shale	928-1078	150	1022-1170	148			1888-2061	173
Thickness of the Goldwyer Formation (m)		230		368		>36		374	
Total thickness of upper shale and lower shale (m)		190		309		>36		302	

Table 5.7: Thickness correlation for the Goldwyer Formation based on the sub-units along the section F-F' (purple line).

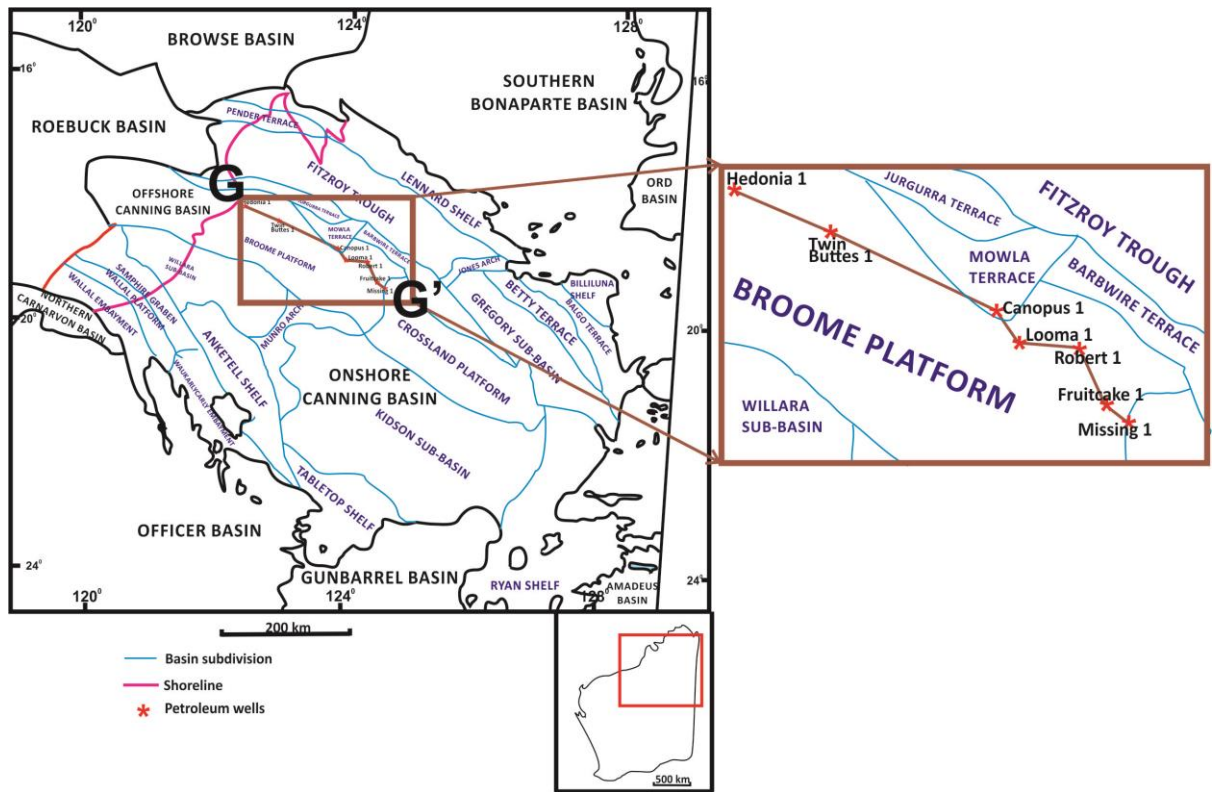


Figure 5.15: Map location of section G-G' (brown line) for the Goldwyer Formation correlation from northwest to southeast in the Canning Basin.

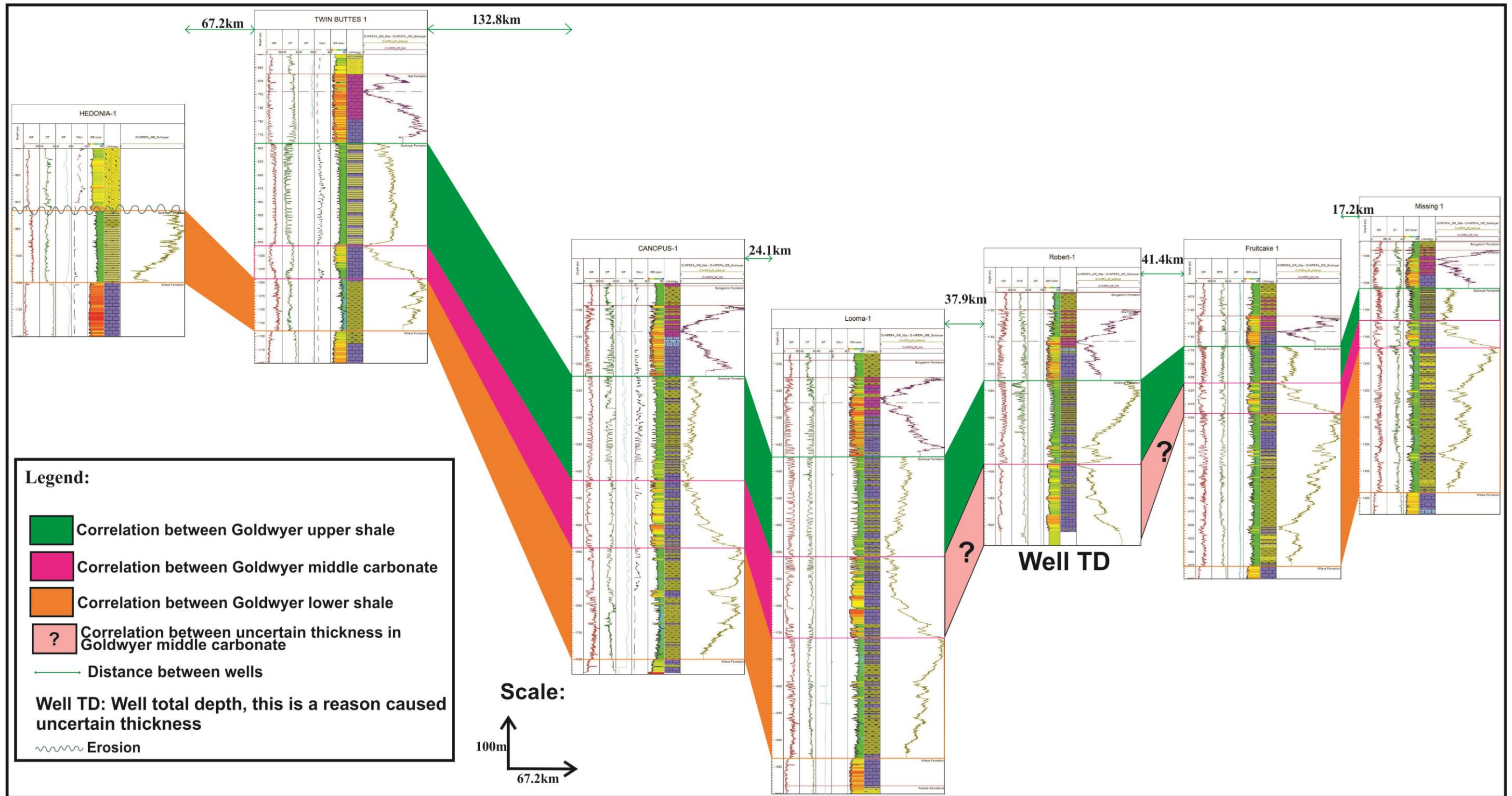


Figure 5.16: Well-to-well correlation for the section G-G' (brown line) from northwest to southeast across Broome Platform in the Canning Basin.

NW SE

Distance between wells		67.2km		132.8km		24.1km		37.9km		41.4km		17.2km			
WELLS		HEDONIA 1		TWIN BUTTES 1		CANOPUS 1		LOOMA 1		ROBERT 1		FRUITCAKE 1		MISSING 1	
Formation	Sub-unit	Depth (m)	Thickness (m)	Depth (m)	Thickness (m)	Depth (m)	Thickness (m)	Depth (m)	Thickness (m)	Depth (m)	Thickness (m)	Depth (m)	Thickness (m)	Depth (m)	Thickness (m)
GOLDWYER FORMATION	Upper Shale			791-982	191	1223-1417	194	1374-1559	185	1231-1386	155	1168-1236	68	1060-1120	60
	Middle Carbonate			982-1043	61	1417-1542	125	1559-1710	151	1386-1535 (TD)	149	1236-1293	57	1120-1170	50
	Lower Shale	915-1050	135	1043-1140	97	1542-1750	208	1710-1934	224			1293-1577	284	1170-1440	270
Thickness of the Goldwyer Formation (m)		135		349		527		560		>304		409		380	
Total thickness of upper shale and lower shale (m)		135		288		402		409		>155		352		330	

Table 5.8: Thickness correlation for the Goldwyer Formation based on the sub-units along the section G-G' (brown line).

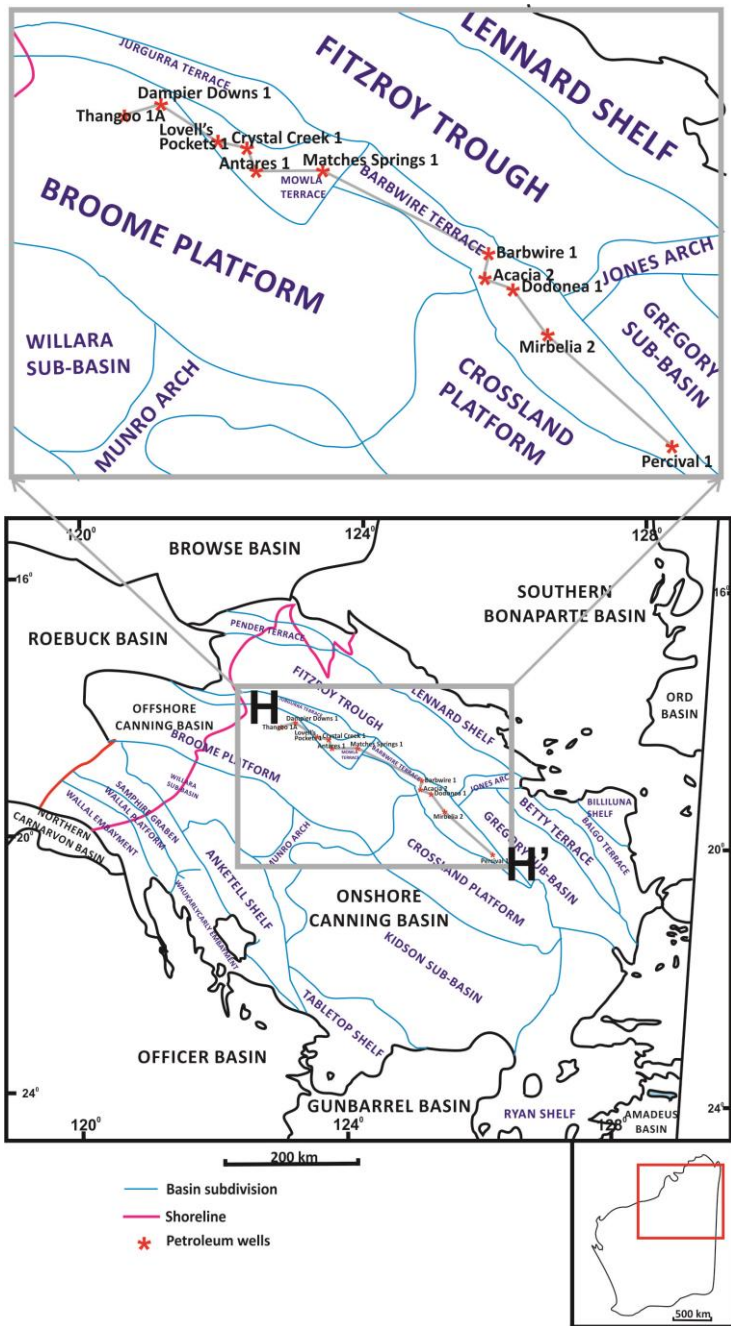


Figure 5.17: Map location of section H-H' (grey line) for the Goldwyer Formation correlation from northwest to southeast in the Canning Basin.

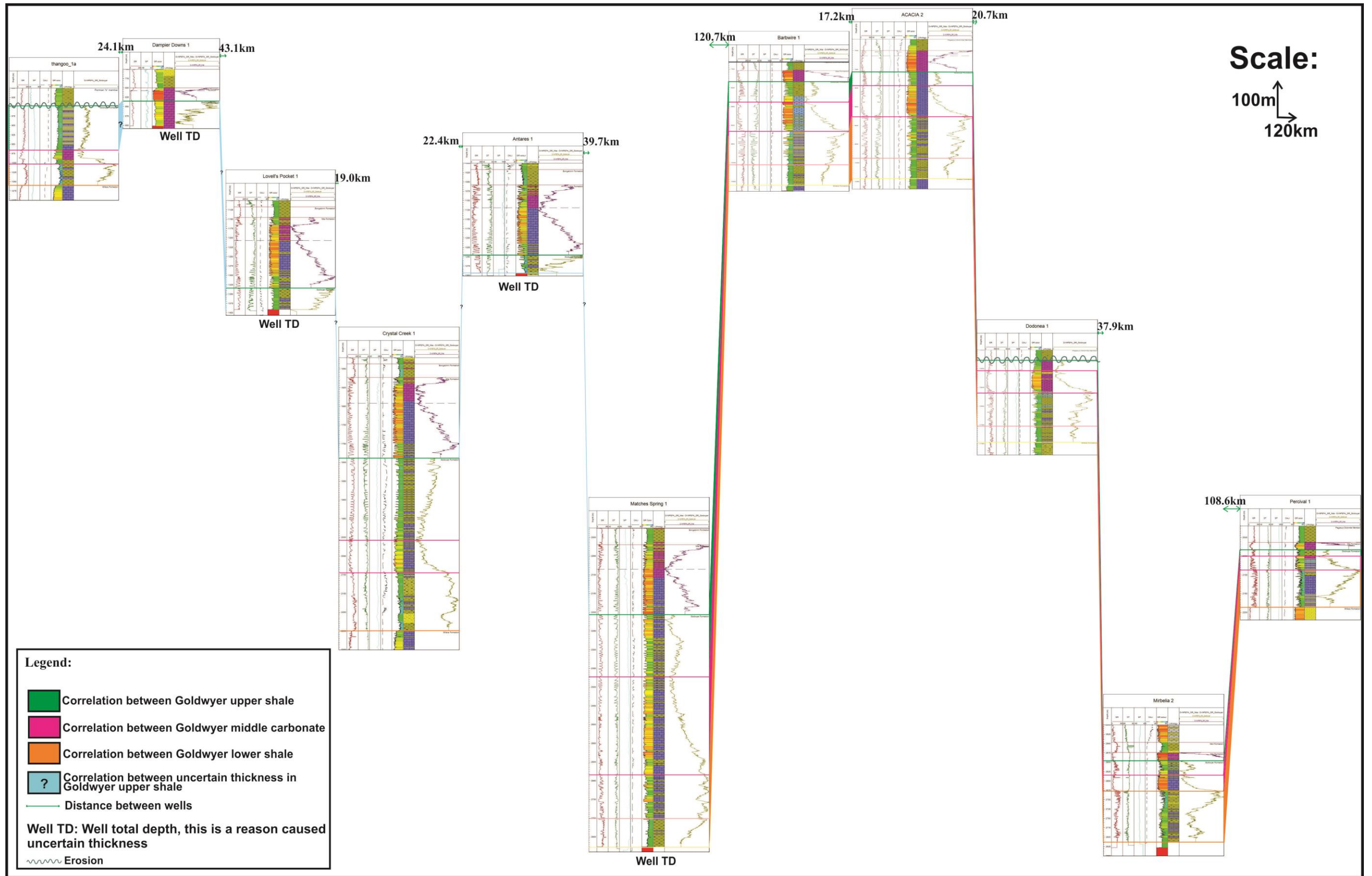


Figure 5.18: Well-to-well correlation for the section H-H' (grey line) from northwest to southeast across Broome Platform, Mowla Terrace and Barbwire Terrace in the Canning Basin.

NW SE

Distance between wells		24.1km	43.1km	19.0km	22.4km	39.7m	120.7km	17.2km	20.7km	37.9km	108.6km													
WELLS		THANGOO 1A		DAMPIER DOWNS 1		LOVELL'S POCKET 1		CRYSTAL CREEK 1		ANTARES 1		MATCHES SPRINGS 1		BARBWIRE 1		ACACIA 2		DODONEA 1		MIRBELIA 2		PERCIVAL 1		
Formation	Sub-unit	Depth (m)	Thickness (m)	Depth (m)	Thickness (m)	Depth (m)	Thickness (m)	Depth (m)	Thickness (m)	Depth (m)	Thickness (m)	Depth (m)	Thickness (m)	Depth (m)	Thickness (m)	Depth (m)	Thickness (m)	Depth (m)	Thickness (m)	Depth (m)	Thickness (m)	Depth (m)	Thickness (m)	
GOLDWYER FORMATION	Upper Shale (Unit 4)	848-966	118	835-900 (TD)	>65	1334-1392 (TD)	>58	1789-2009	220	1246-1293 (TD)	>47	2207-2374	167	783-838	55	757-794	37	1527-1555	28	2596-2635	39	2033-2050	17	
	Middle Carbonate (Unit 3)	966-1003	37					2009-2095	86			2374-2635	261	838-915	77	794-877	83	1555-1615	60	2635-2677	42	2050-2087	37	
	Lower Shale	Unit 2	1003-1060	57					2095-2250	155			2635-2751	116	915-1005	90	877-988	111	1615-1746	131	2677-2813	136	2087-2186	99
		Unit 1			2751-2828 (TD)	>77	1005-1060	55			988-1042	54												
Thickness of the Goldwyer Formation (m)		212		>65		>58		461		>47		>621		277		285		219		217		153		
Total thickness of upper shale and lower shale (m)		175		>65		>58		375		>47		>360		200		202		159		175		116		

Table 5.9: Thickness correlation for the Goldwyer Formation based on the sub-units along the section H-H' (grey line).

## 5.4 Discussion

The Goldwyer Formation spreads to a great extent in the Canning Basin. It has a varying thickness depending on the different tectonic sub-divisions of the basin. The Goldwyer Formation is found to be thickest in the Willara Sub-Basin from the well Willara 1. The next thickest part of the Goldwyer Formation is at Lennard Shelf as seen by the well Blackstone 1. The Goldwyer Formation is thins from section A towards A' (see Figure 5.4).

The Goldwyer Formation in this study can be divided into lower Goldwyer shale, middle Goldwyer carbonates and upper Goldwyer shale. However, in Barbwire Terrace, Foster et al. (1986) subdivided Goldwyer Formation into 4 units. This subdivision is shown in this study to apply only to the Barbwire Terrace.

Where the Nita Formation lies on top of the Goldwyer Formation and the Willara Formation below the Goldwyer Formation, that section represents the complete depth for the Goldwyer Formation, such as in wells Woods Hills 1, Willara 1, Parda 1, Sharon Ann 1, Munro 1, Crystal Creek 1, Aquila 1, McLarty 1, Twin Buttes 1, Canopus 1, Looma 1, Fruitcake 1, Missing 1, Matches Springs 1, Barbwire 1, Acacia 2, Percival 1, Frankenstein 1, Pegasus 1, Nita Downs 1, Great Sandy 1, Wilson Cliffs 1 and Contention Heights 1. In wells where the Permian Grant Formation overlies the Goldwyer Formation (such as wells Hedonia 1, Goldwyer 1), there was erosional loss of section during early Permian time. For some wells the total depth (TD) did not penetrate the whole Goldwyer Formation (such as wells Vela 1, Blackstone1), and this is certainly localised data on total thickness is limited. However, the results are still informative in terms of overall Goldwyer distribution and shale gas potential.

## 5.5 Isopach maps

Two maps were constructed based on the results of borehole analysis described in this chapter (Tables 5.2 to 5.9). The first map (Fig. 5.19) is the contour map showing the topography and indicating depth of Goldwyer Formation in various tectonic sub divisions of the Canning Basin. An isopach map (Figure 5.20) represents the thickness of the Goldwyer shale (Goldwyer upper shale, (Unit 4) and Goldwyer lower shale (Unit 1 and Unit 2)).

### **5.5.1 Contour map of the top Goldwyer Formation**

Topographic maps or contour maps show terrain in the area and help in planning the exploration of oil and gas industry. Figure 5.19 contain the contour map of the surface structure on Goldwyer Formation (Middle Ordovician) in the North West of Western Australia. Of these, the top of Goldwyer Formation from 38 wells were obtained from well completion reports on file at the Geology of Western Australia (GSWA) and via INPEFA analysis in this Chapter is to map the Goldwyer formation. In Figure 5.19, the depth shown is the depth below the surface. Close contour lines indicate a steep slope and flattens the surface where the contour lines even further.

In the extreme southeastern part of the Canning Basin, only a few wells have been drilled (wells Kidson 1, Wilson Cliffs 1 and Contention Heights 1) in the Kidson Sub-Basin and Ryan Shelf. Contour, therefore, is strongly influenced by the shape of tectonic sub-division. As in the Kidson Sub-basin, more data are needed to understand the distribution of Goldwyer Formation in more detail. The top Goldwyer in the Willara Sub-basin is deepening from southeast to northwest towards Broome Platform. It was shallower from the border Willara Sub-basin and Broome Platform (Admiral Bay Fault Zone) to the northern part of the Broome Platform. The bottom of the Broome Platform is deepening from east to west. For Mowla Terrace, top Goldwyer is shallowing from northeast to southwest. In Barbwire terrace, the top Goldwyer is particularly acute in the central part from northwest and southeast.

Areas other than the areas that were discussed are lack of data for the Goldwyer Formation. This is because not much wells penetrating into the Goldwyer Formation. More drilling is required to determine the full structure on Goldwyer Formation in the Canning Basin; however, the contoured area is approximately 180,000 square kilometers.

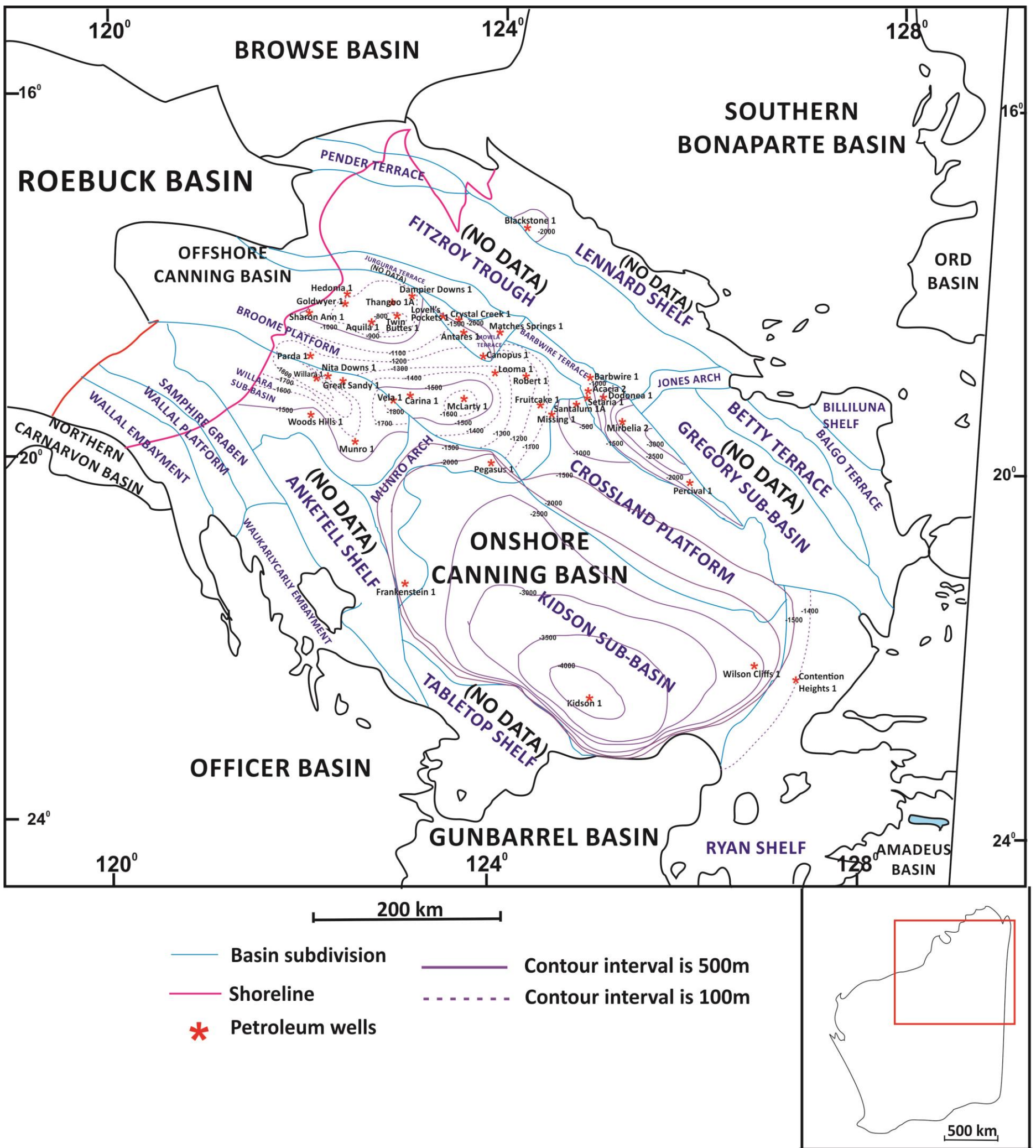


Figure 5.19: Contour map represents topography for the top Goldwyer Formation to show the depth and distribution of this formation in the subsurface of the Canning Basin. Note that negative sign of the depth means the depth is in the subsurface. The deepest depth of this formation is found in the Kidson Sub-basin while the shallowest of the top of this formation is in the Broome Platform.

### **5.5.2 Isopach map of the total Goldwyer shale thicknesses**

The isopach map of the thickness of the Goldwyer shale is shown in Figure 5.20. The thickness of the Goldwyer shale was calculated by subtracting the thickness of Goldwyer Unit 3 (carbonate successions) from the thickness of Goldwyer Formation. Goldwyer shale thickness ranges from 70m (Munro Arch) to 634m (Willara Sub-basin) in the Canning Basin region.

The isopach map (Figure 5.20) shows that it varies considerably in thickness throughout the Canning Basin based on the different tectonic sub-divisions. Shale thickness values (335m to 135m) across the northern Broome Platform which is near to the present shoreline because of erosion from Permian glaciation events. The Goldwyer shale is relatively thick in the centre part of the Broome Platform (409m) which is close to the Mowla Terrace. The Mowla Terrace consists of 375m to 402m thick shale.

Willara Sub-basin ranges in thickness between 111m and 634m. Most of the Ordovician rock units in the Canning Basin are thickening in the Willara Basin toward Broome Platform then they become thinner in the Broome Platform (Yeates et al., 1984; Ghorri, 2013). The Goldwyer shale follows this trend in Figure 5.20. The Goldwyer shale increases in thickness toward the Admiral Bay Fault Zone which separates the Willara Sub-basin and Broome Platform, reaching a maximum of 634m.

In the Barbwire Terrace, wells Barbwire 1 and Acacia 2 contain the greatest amount of shale (200m and 202m) compared with other wells in this tectonic sub-division. It can be concluded that the northwest part of the Barbwire Terrace is a potential area for shale gas exploration within the Barbwire Terrace.

There are only 5 control points (or 5 wells) for the Munro Arch, Kidson Sub-basin and Ryan Shelf due to lack of drilling (see Figure 5.20). Therefore, the contour lines might not be an accurate representation the actual situation. Other areas without contour lines reflect a lack of subsurface data.

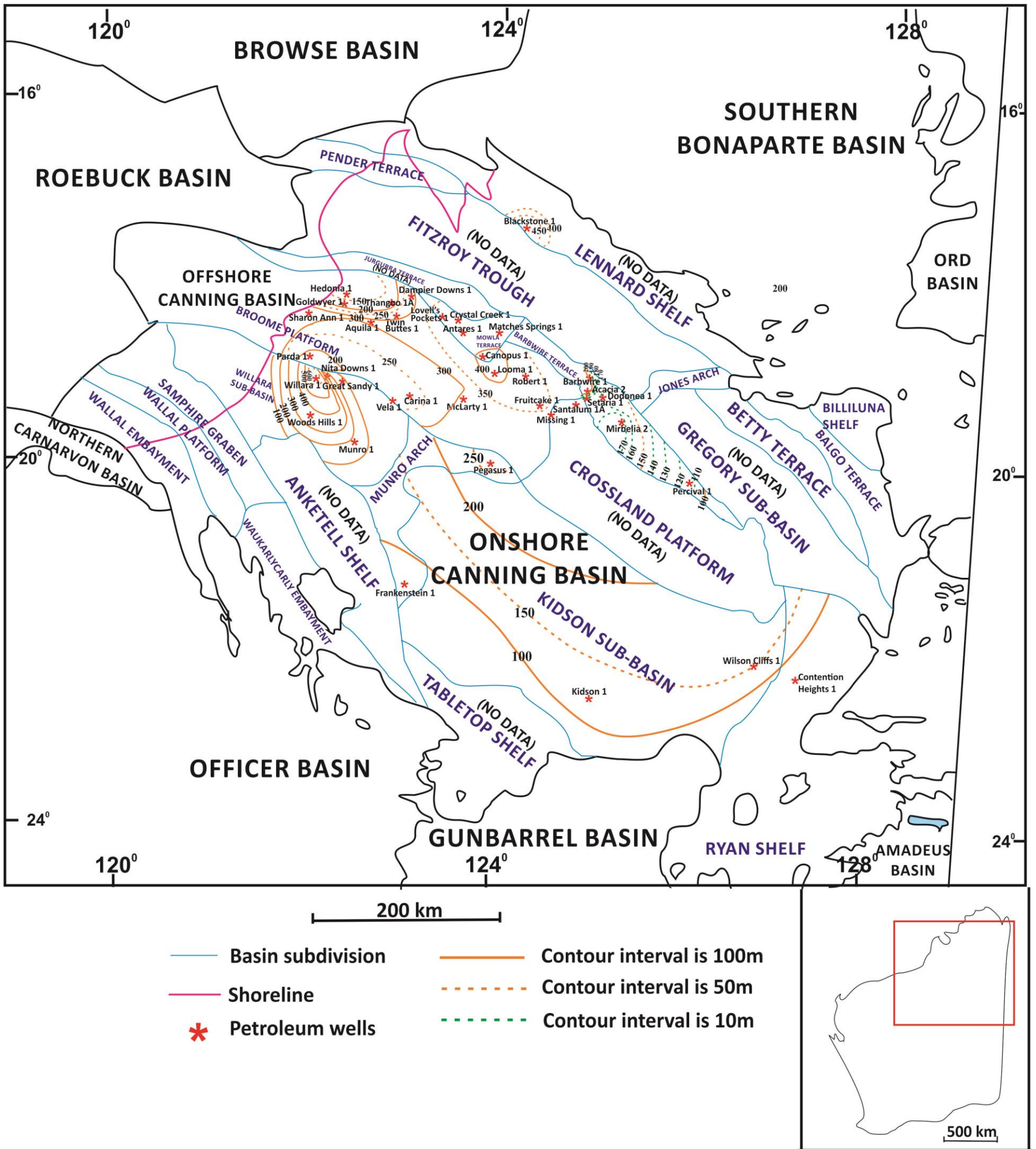


Figure 5.20: An isopach map of Canning Basin showing the thickness of the Goldwyer shale which is the total thickness of Goldwyer Unit 1, Unit 2 and Unit 4. This figure shows the thickness distribution of the Goldwyer shale in part of the Canning Basin where data is available. Note that the thickest Goldwyer shale is found in the Willara Sub-basin. The area contoured is approximately 180,000 sq km.

## 5.6 Resource estimation

The shale gas in shale rock is stored in two principle ways which are as gas adsorbed within the organic matrix and as free gas in pore spaces (Boyer et al., 2006; Jarvie et al., 2007). Adsorbed gas in place of the Goldwyer Formation shale was calculated for Willara Sub-basin, Broome Platform, Mowla Terrace, Barbwire Terrace and Kidson Sub-basin in the Canning Basin. A formula based approach will allow approximation of this shale resource present and the adsorbed shale gas content. The equation is shown below. According to Crain (2000), gas in place for the adsorbed gas is derived from:

$$\text{GIPadsorb} = \text{KG6} * \text{Gc} * \text{DENS} * \text{THICK} * \text{AREA}$$

Where:

GIPadsorb = gas in place for gas adsorbed (Bcf)

Gc = gas content (scf/ton) = KG11 \* TOC%

DENS = shale density (range of 2.20 to 2.60 g/cc so the average of this range which is 2.40 g/cc is used)

THICK = layer thickness (feet) (determined from INPEFA data in wells studied here)

AREA = spacing unit area (acres)

KG6 = 0.00000136 (a constant)

KG11 = gas parameter, varies between 5 and 15 (depending on petrophysical parameters)

TOC% = total organic carbon (%)

The minimum gas parameter which is 5 was used to estimate the minimum shale gas content with the formula in section 5.6. The maximum gas parameter (15) was used to calculate the maximum shale gas content while the median of the gas parameter (10) was used to estimate median shale gas content. Porosity of the Goldwyer shale is >8% and reaches a maximum of 22% in well McLarty 1 in Broome Platform (Finder, 2013). For the calculation in this study, the shale porosity of 10% is

being used from the range 8%-22% which was determined by Finder (2013). A TOC value of 5% is used based on data provided by EIA (2011).

Table 5.10 shows the calculation to estimate the gas in place (adsorbed gas) of the shale gas in the Middle Ordovician Goldwyer Formation. The tectonic sub-units with the vast significant maximum adsorbed gas potential are the Willara Sub-basin (58.8Tcf), Mowla Terrace (46.2Tcf), Broome Platform (143.6Tcf) and Kidson Sub-basin (151.9Tcf). Compared with 288 trillion cubic feet (Tcf) estimated total gas in place for shale gas resource in the Canning Basin by EIA (2011), this study predicted 139.4 Tcf to 418.2 Tcf shale gas (adsorbed gas) could be contained in the Goldwyer Formation. Triche (2012) compared US and WA shale gas play parameters. The result shows that the Barnett shale and Goldwyer shale have similar richness (5-6 TOC% values) and maturity (1.4-1.6 Ro% values). Thus, the ratio of adsorbed gas to free gas for Barnett shale which is 55:45 (Jarvie, 2012) can be applied to the Goldwyer shale in this study. With this ratio, the estimation of total gas in place for Goldwyer shale in Willara Sub-basin, Mowla Terrace, Barbwire Terrace, Broome Platform and Kidson Sub-Basin ranges from 253.5-760.4Tcf (minimum 253.5Tcf, median 506.9Tcf, and maximum 760.4Tcf).

## **5.7 Summary**

In conclusion, estimates of adsorbed gas based on INPEFA analysis is calculated in this study represent a significant potential gas reserves in the Canning Basin. Total gas includes both adsorbed and free gas and therefore it exceeds the values of the adsorbed gas. For this study only the adsorbed gas can be calculated from the available data. Therefore, the amount of gas estimated by the EIA (2011) for the Canning Basin (288 Tcf of gas in place) is a modest figure compared with estimates in Table 5.10, which covers only 5 of tectonic sub-division units in the basin (139.4- 418.2 TCF of adsorbed gas in place). Total gas in place is estimated in the areas of research ranges between 253.5-760.4 TCF (minimum 253.5Tcf, median 506.9 Tcf, and maximum 760.4Tcf). The minimum value is comparable with the EIA (2011) estimates, the median value is almost twice the previous estimate, and the maximum value is three times EIA estimates (760.4Tcf).

Willara Sub-basin (106.8Tcf), Mowla Terrace (83.9Tcf), Broome Platform (261.1Tcf) and Kidson Sub-basin (276.1Tcf) contain high value of total gas in place while the Barbwire terrace contains only the maximum amount of gas in place of 32.5Tcf. Therefore, these tectonic sub-divisions can be an important potential area for shale gas exploration. The Lennard Shelf showed good thickness of Goldwyer shale units in well Blackstone 1 but there is only one well drilled on the Lennard Shelf penetrate the Ordovician successions. Maps of depth and thickness depict the range of depth of the potential area from which most of the gas produced. This new resource estimates further value to new shale gas potential of the basin. It is suggested that more wells to be drilled in the Lennard Shelf to penetrate to the Goldwyer Formation to study the Goldwyer shale unit.

It is only in the last 5 years that Canning Basin shale gas potential has been recognized. Both the information about the distribution of shale and gas in place determined by this study provide further support for expanded exploration program. Combined with oil and gas production of the nearby northwest shelf, Browse Basin and Timor Sea, the realization of the onshore Canning Basin production will do much to enhance this already significant oil and gas province.



## CHAPTER 6

# MIDDLE ORDOVICIAN (LLANVIRNIAN) RELATIVE SEA-LEVEL FLUCTUATIONS

### 6.1 Introduction

The chapter discusses on the relative sea level fluctuation during part of Middle Ordovician. Fischer plot introduced by Fischer (1964) is used to identify long term change in rates of accommodation space creation. Goldhammer (1987) used Fischer plots of Middle Triassic carbonates in Italy to define third-order sea-level fluctuations. Read and Goldhammer (1988) also used Fischer plots to define third-order sea-level curves in Ordovician peritidal cyclic carbonates in the Appalachians. The sea-level curves therefore remain valid working models for the long-term trends of the base level, representing marine transgressions and regressions along the world's continental margins and flooding or desiccation of inland seas and wide interior epi-platform basins (Haq and Al-Qahtani, 2005).

The major control on carbonate deposition is relative sea-level fluctuation, determined by rates of eustatic sea-level variation and tectonic subsidence (Yoo and Lee, 1995). Particular depositional systems tracts are developed during specific phases of the sea-level cycle: transgressive-regressive systems tracts. Systems tracts are defined by their position within a sequence, boundary surfaces and internal strata geometries (Sarg, 1988; Van Wagoner et al., 1988; Yoo and Lee, 1995). The Llanvirnian age Nita and Goldwyer Formations consists of numerous shallowing-upwards cycles, which were formed on a shallow marine carbonate platform (see Chapter 3).

The objectives of this Chapter is to construct relative sea-level fluctuation based on Nita and Goldwyer Formations by using Fischer plots and compare with the eustatic sea-level change of comparable age. The correlation between third-order sea-level curves for the Middle Ordovician Nita Formation by using this technique provides a methodology for regional correlation for part of the Middle Ordovician sea-level fluctuations in the Broome Platform of Canning Basin, WA. The sea level curve for the Llanvirnian of Nita and Goldwyer Formations is plotted to correlate with the sea level curve for the Ordovician of Baltoscandia defined by Nielsen (2004).

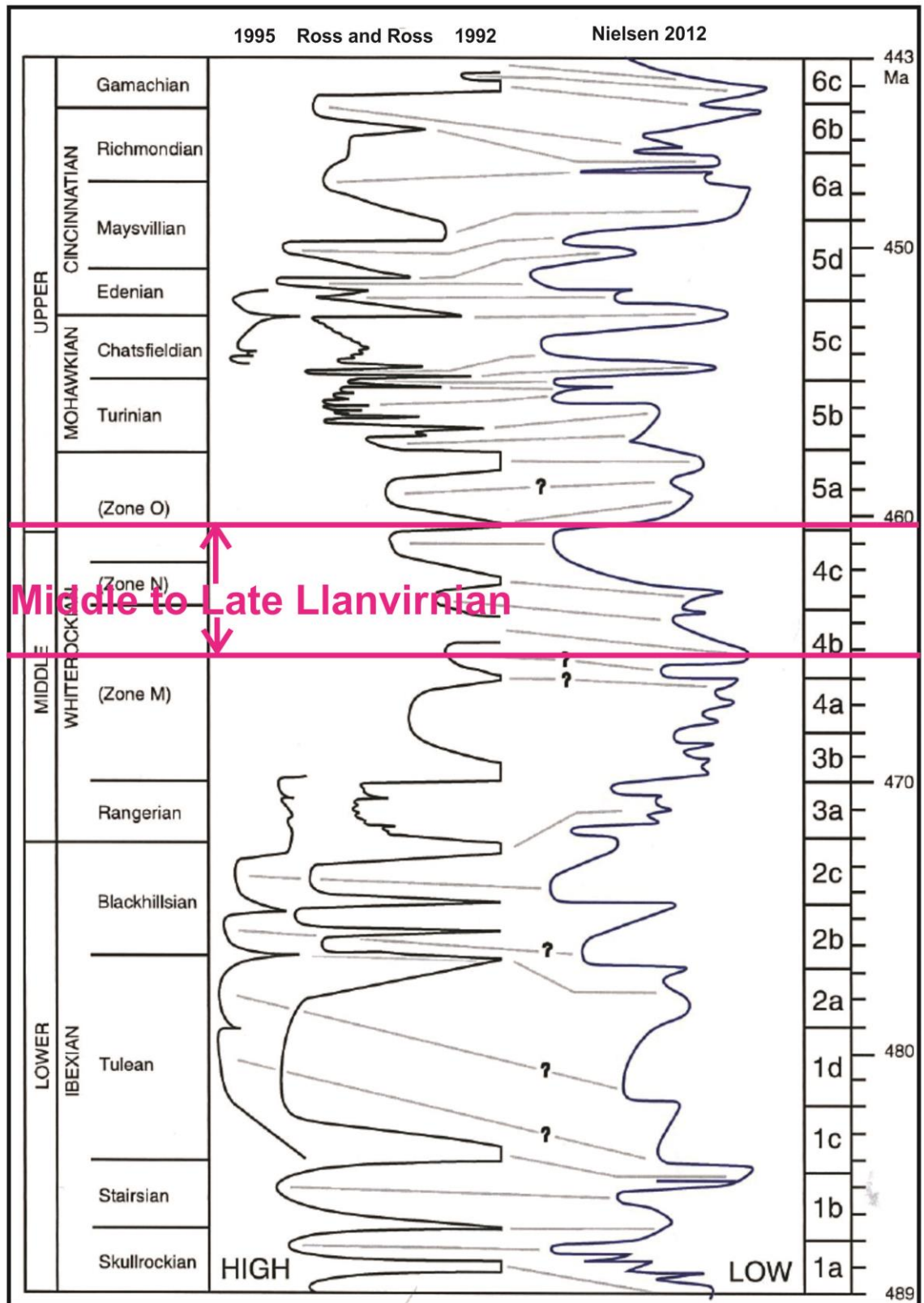


Figure 6.1: Comparison of North American and Baltoscandian third-order sea level curves. Ross and Ross (1992, 1995) defined the North American sea level curve while Nielsen (2004) illustrated the Baltoscandian sea level curve (after Nielsen, 2004). The middle to late Llanvirnian is approximately from 460.5 Ma to 465 million years, during where the Nita and Goldwyer Formations were deposited.

## **6.2 Middle Ordovician sea-level**

Nielsen (2004) correlated the Ordovician sea-level curves of Baltoscandia with North American sea-level curves defined by Ross and Ross (1992, 1995). Figure 6.1 shows the comparison of sea level curves for North America and Baltoscandia. Haq and Schutter (2008) determined most of the Paleozoic Era (542-251 million years ago) sea levels although an integrated history of sea levels has still remained unrealized. Figure 6.2 shows the Ordovician sea-level changes determined by Haq and Schutter (2008). There are three Ordovician sea-level change cycles of duration 1-2 million years (third order cycles) (Figure 6.2). The time scale and standard and regional stages in Figure 6.2 are modelled after Gradstein et al. (2004) and Ogg et al. (2008).

## **6.3 Parasequence stacking patterns and Fischer plots**

The vertical stacking patterns of parasequences (regressive and transgressive trend) are most likely controlled by long-term changes in accommodation space and therefore provide a critical link between individual cycles and the large scale depositional sequences (Goldhammer et al., 1990; Garland, 1997). The use of stacking patterns for correlation is particularly important where this is poor exposure of the successions, such as Nita and Goldwyer Formations in the present study. The Fischer plots were used to study the Llanvirnian relative sea level for Nita and Goldwyer Formations in the Canning Basin, WA in this study.

Fischer plots are a popular tool to graphically illustrating deviations from average cycle thickness in cycle stratigraphy; this graphical method can used to define accommodation changes and depositional sequences on “cyclic” carbonate platforms (Fischer, 1964; Sadler et al., 1993; Husinec et al., 2008). Figure 6.3 shows an example of the changes in accommodation space as a function of cycle number. Fischer (1964), Goldhammer et al. (1987) and Read and Goldhammer (1988) plotted the Fischer plots by graphing cumulative departure from mean cycle thickness as a function of time. However, Sadler et al. (1993) suggested that instead of a time scale, the horizontal axis of the plots should be labelled by cycle number to avoid problem of the poor absolute time control on the stratigraphic record. They also cautioned that Fischer

plots of less than 50 cycles may not ensure a robust estimate of average cycle-thickness, and therefore produce an insubstantial plot, especially when it is intended to apply a statistical analysis. Husinec et al. (2008) presents an easy to use Microsoft Excel spreadsheet program for Fischer plots which is used in this study.

Fischer plots were originally used to search for evidence of Milankovitch-scale (20-400kyr) eustatic sea-level oscillations in peritidal successions (Fischer, 1964; Goldhammer et al., 1987), but it was recognized that the plots were capable of qualitatively extracting long-term (1-5myr) relative sea-level changes from carbonate platform records (Goldhammer, et al. 1987; Read et al., 1991; Read and Goldhammer, 1988). The plots of peritidal successions more correctly plot changes in accommodation (sea level plus subsidence) rather than extracting relative sea-level change (Husinec et al., 2008).

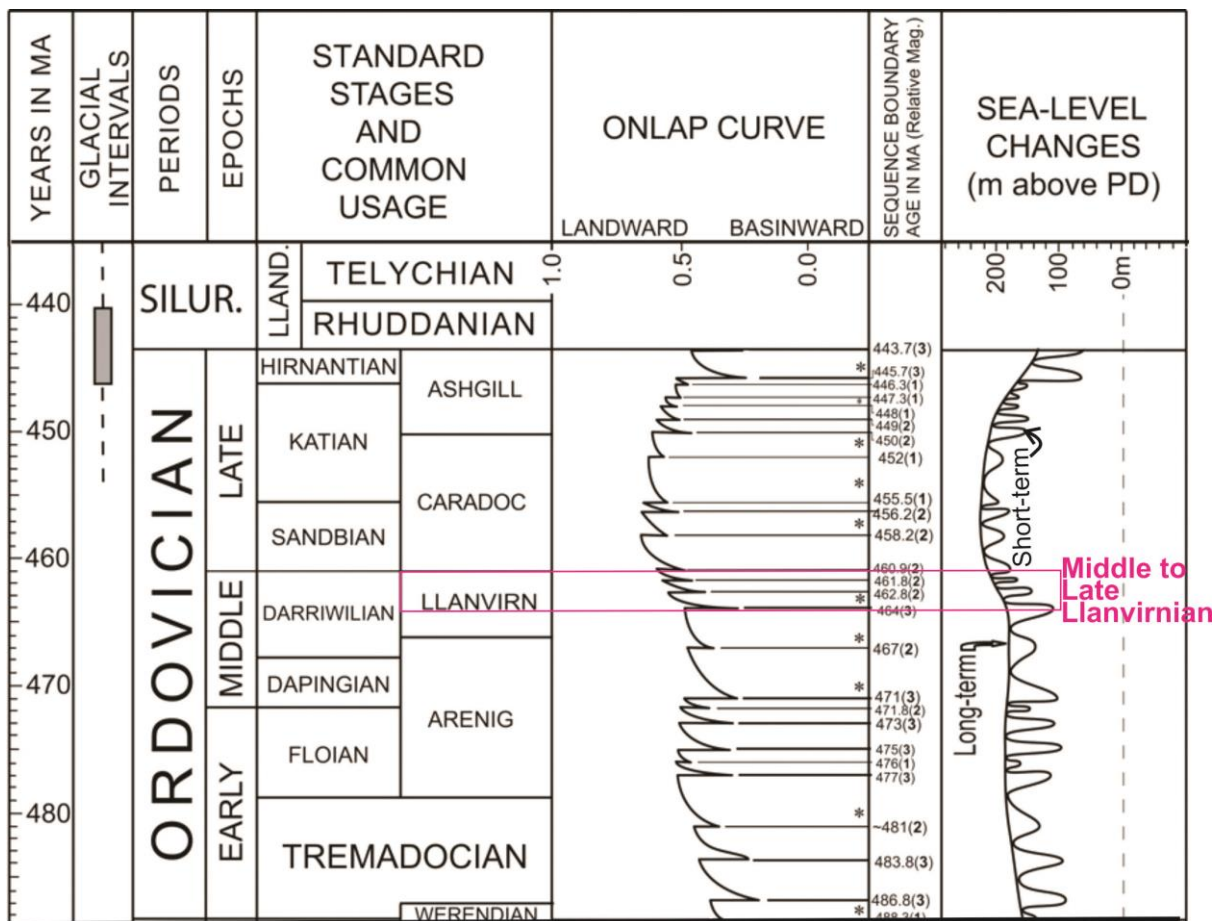


Figure 6.2: Ordovician sea level changes (Haq and Schutter, 2008).

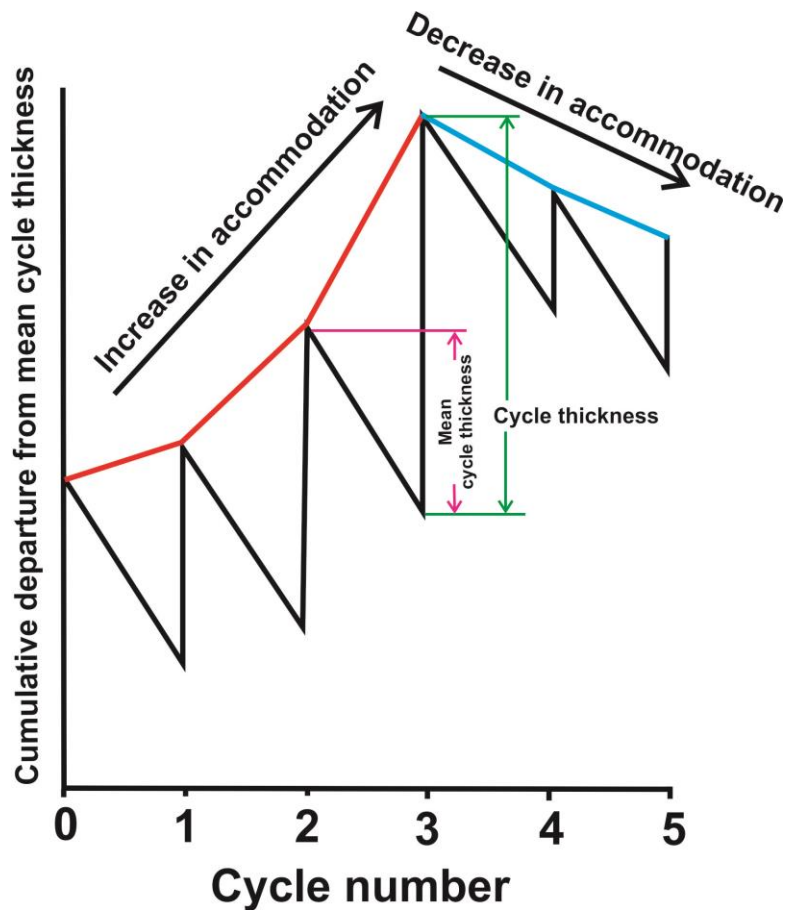


Figure 6.3: An example of Fischer plot showing changes in accommodation space as a function of cycle number. Thin green vertical line is individual cycle thickness. Increase in accommodation is shown by red line sloping up to the right while decrease in accommodation is shown by blue line (after Husinec et al., 2008).

#### 6.4 Sea-level fluctuations

Three wells (wells McLarty 1, Looma 1 and Robert 1) in Broome Platform, Canning Basin, Western Australia (Figure 6.5) were analysed by determining the cycle thickness based on the wireline logs, especially gamma ray logs, sonic logs and integrated prediction error filter analysis (INPEFA) curves, then keying the cycle thickness data to an Excel spreadsheet program (Figure 6.4) developed by Husinec et al. (2008) to generate Fischer plots. Appendix 3 shows the calculation using the Excel spreadsheet. The Fischer plots generated by using this excel spreadsheet are shown in Figures 6.6, 6.7 and 6.8. For the Llanvirnian sequences (Nita and Goldwyer Formations in the Canning Basin, Western Australia), the relative sea level curve is

illustrated based on well Looma 1 in Broome Platform subsurface wireline logs (Figure 6.6). Well McLarty 1 and well Robert 1 are located near to the well Looma 1 so the Fischer plots from these two wells can be compared with well Looma 1 regionally. These three wells on Broome Platform were chosen to study the relative sea-level fluctuations in Middle to Late Llanvirnian time.

The Fischer plots are used to recognize changes in accommodation space from cyclic carbonate successions (Husinec et al., 2008) and therefore extracting long-term relative sea-level changes from Nita and Goldwyer Formations in this study.

**Data Entry Sheet**

Number of covered Intervals:

Initial thickness:

Average cycle thickness:

Total number of cycles:

Covered interval thickness(m):

Assigned Cycles:

	Interval 1	Interval 2	Interval 3
Cycles:	0	0	0
	Thickness	Thickness	Thickness

Figure 6.4: Excel spreadsheet for data entry. Required input is number of covered intervals, thickness of each cycle in stratigraphic section between each covered interval and thickness of each covered interval (Husinec et al., 2008).

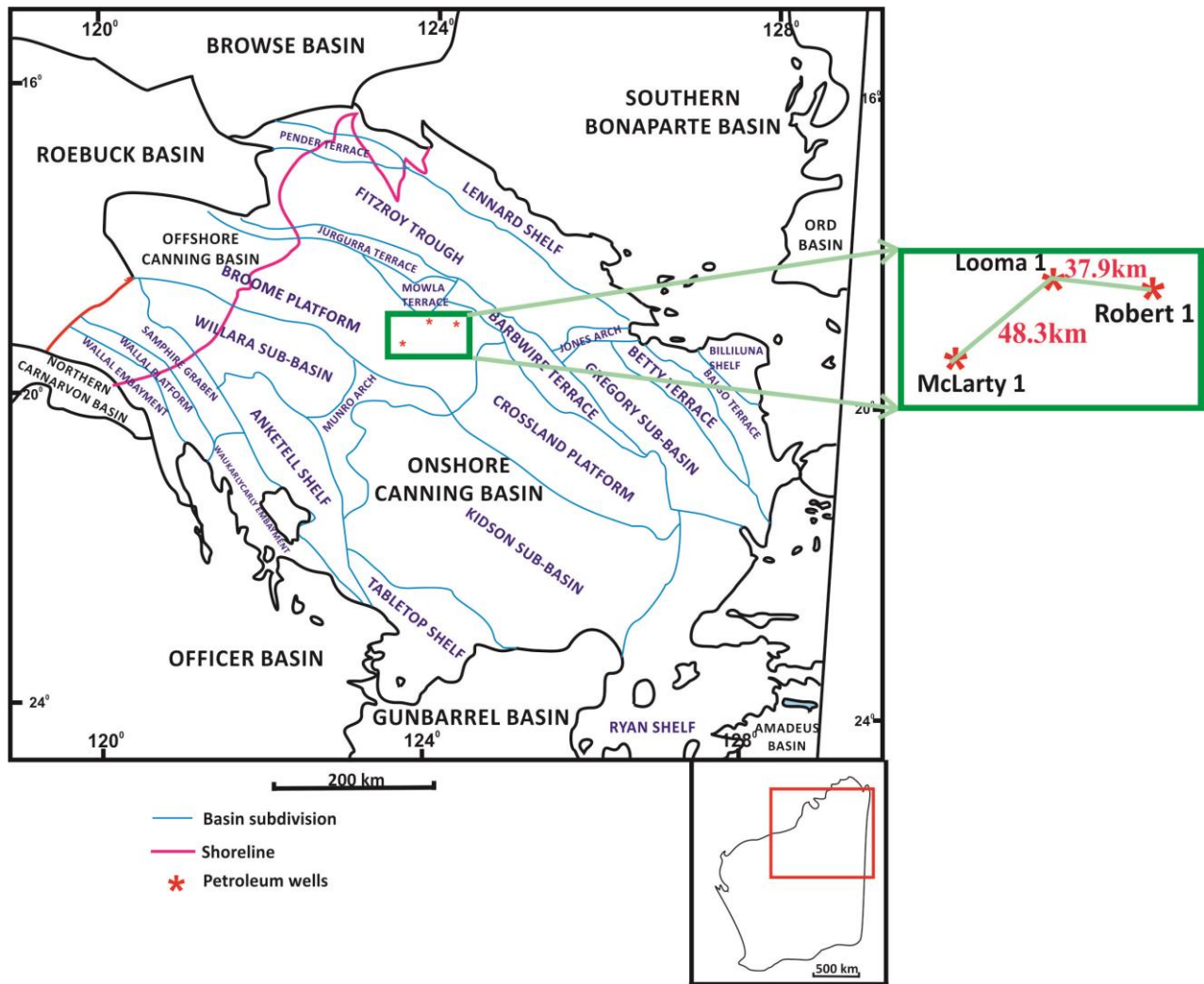


Figure 6.5: Well location maps of the studied wells in Broome Platform, Canning Basin, WA.

### 6.4.1 Fischer plots for well Looma 1

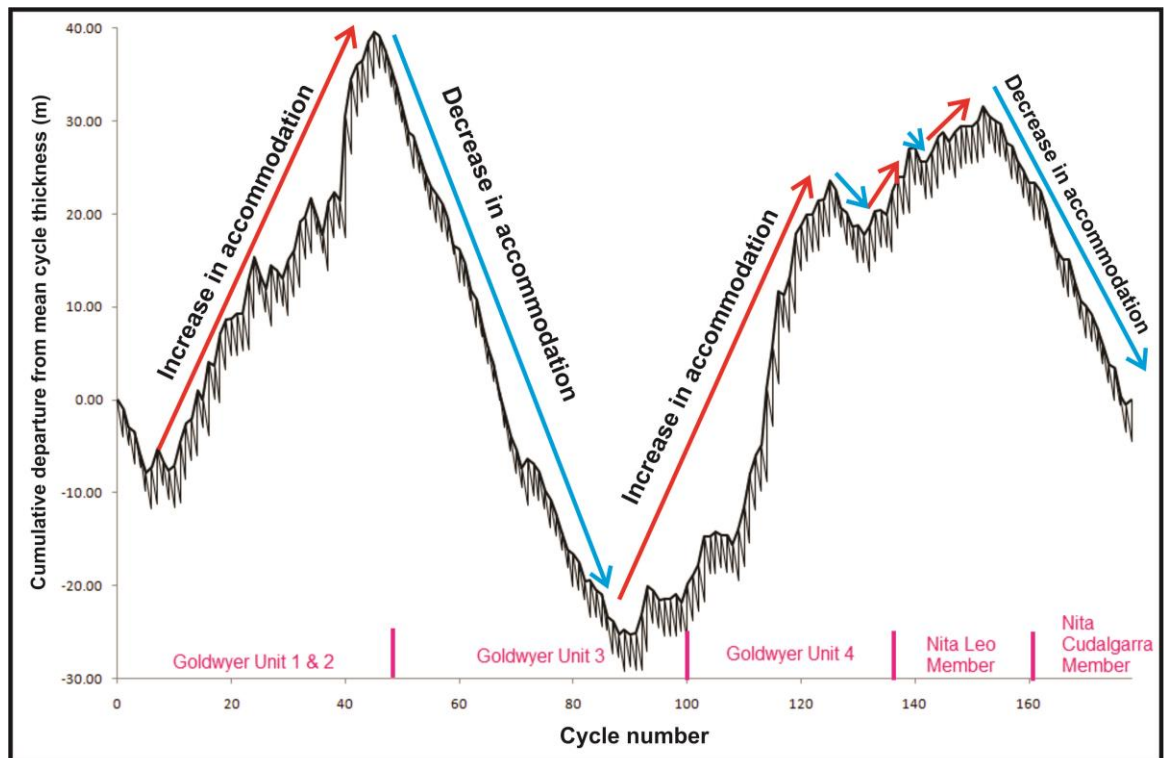


Figure 6.6 Fischer plots illustrated relative sea-level curve of well Looma 1 by showing changes in accommodation space as a function of cycle number. Increase in accommodation is shown by red arrow line sloping up to the right while decrease in accommodation is shown by blue arrow line.

#### 6.4.1.1 Interpretation for Looma 1

The Nita and Goldwyer Formation are complete in well Looma 1 (see Chapter 4). Fischer plots of well Looma 1 (Figure 6.6) were generated by keying in the cycle thickness to the excel spread sheet build by Husinec et al. (2008). The cycle thickness was determined based on the maximum regressive surface or positive bounding surface in INPEFA analysis. The thickness between two maximum regressive surfaces equals a cycle thickness.

Figure 6.6 shows that the accommodation space increases in Goldwyer lower shale (Goldwyer Unit 1 and Unit 2), decreases in Goldwyer middle carbonate (Goldwyer Unit 3), and increases in Goldwyer Unit 4. It does not have any clear trend with both increases and decreases in Nita Leo Member; therefore the accommodation space in

this sub-unit could not be defined. The accommodation decreases in Nita Cudalgarra Member.

#### 6.4.2 Fischer plots for well McLarty 1

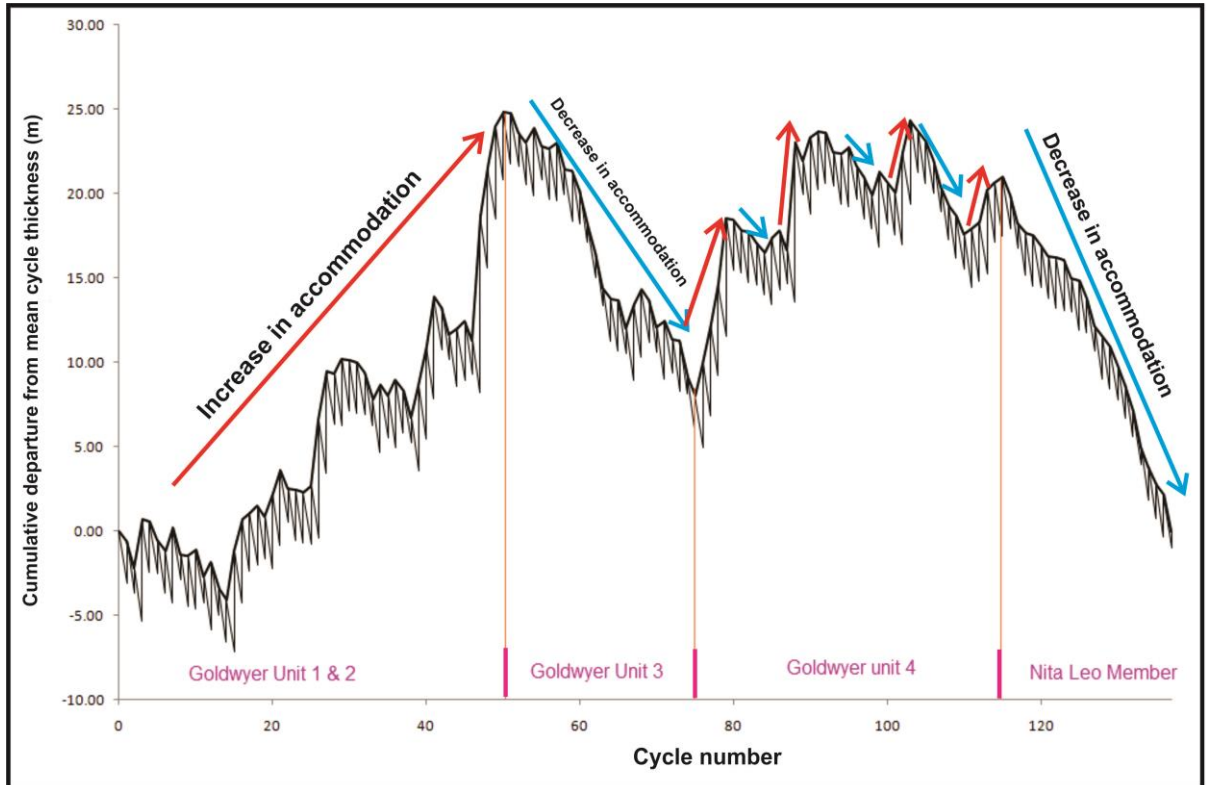


Figure 6.7: Fischer plots illustrated sea level curve of well McLarty 1 by showing changes in accommodation space as a function of cycle number. Increase in accommodation is shown by red arrow line sloping up to the right while decrease in accommodation is shown by blue arrow line.

##### 6.4.2.1 Interpretation for McLarty 1

The Nita Formation died out in well McLarty 1 (see Chapter 4) and this is the reason for the absence of Nita Cudalgarra Member. Fischer plots of Well McLarty 1 (Figure 6.7) were generated by keying in the cycle thickness to the excel spread sheet built by Husinec et al. (2008). The cycle thickness was determined based on the maximum regressive surface or positive bounding surface in INPEFA analysis. The thickness between two maximum regressive surfaces equals to a cycle thickness.

Figure 6.7 shows that the accommodation space increases in Goldwyer lower shale (Goldwyer Unit 1 and Unit 2), decreases in Goldwyer middle carbonate (Goldwyer

Unit 3), and decreases in Nita Leo Member. It does not have any clear trend (fluctuating trend in small scale) in Goldwyer upper shale (Goldwyer Unit 4), therefore the accommodation space in this sub-unit could not be clearly defined.

### 6.4.3 Fischer plots for well Robert 1

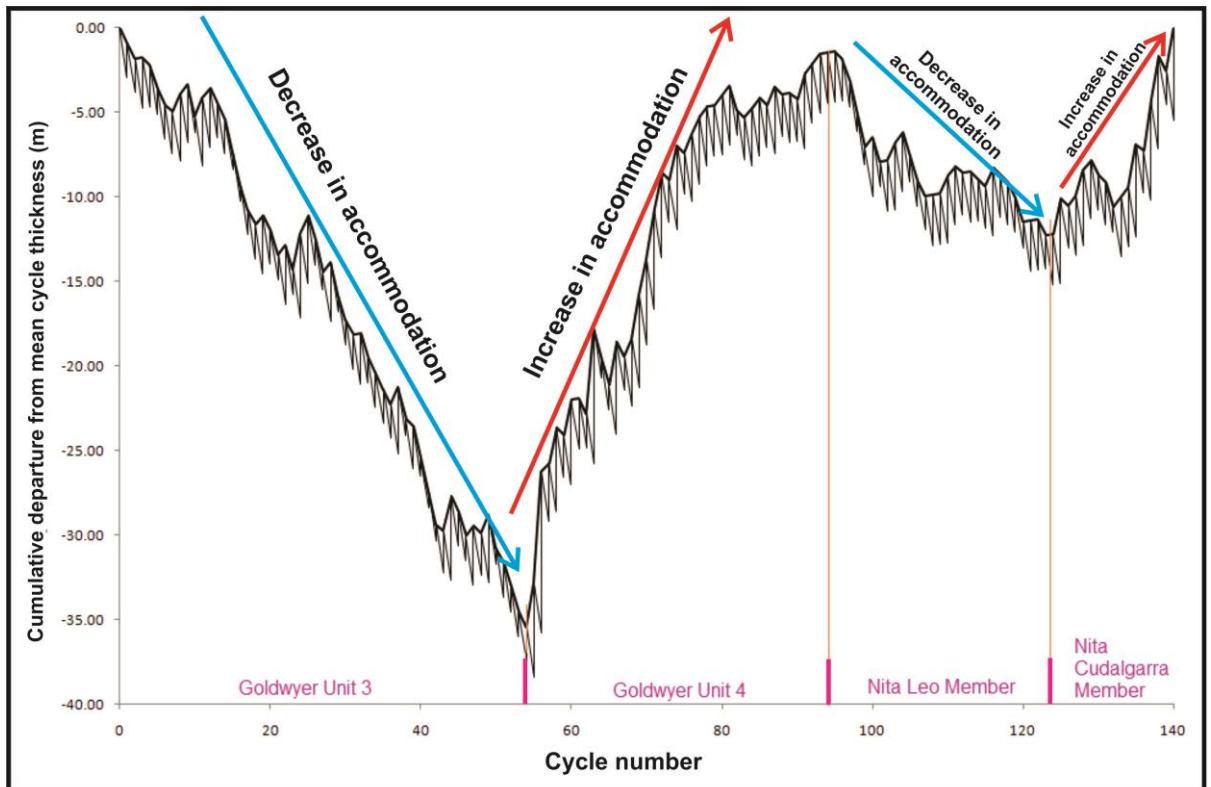


Figure 6.8: Fischer plots illustrated sea level curve of well Robert 1 by showing changes in accommodation space as a function of cycle number. Increase in accommodation is shown by red arrow line sloping up to the right while decrease in accommodation is shown by blue arrow line.

#### 6.4.3.1 Interpretation for Robert 1

Well Robert 1 reaches well total depth (see Chapter 4) at Goldwyer middle carbonate (Goldwyer Unit 3). Fischer plots of Well Robert 1 (Figure 6.8) were generated excel spread sheet built by Husinec et al. (2008). The cycle thickness was determined based on the maximum regressive surface or positive bounding surface in INPEFA analysis. The thickness between two maximum regressive surfaces equals a cycle thickness.

Figure 6.8 shows that the accommodation space decreases in Goldwyer middle carbonate (Goldwyer Unit 3), increases in Goldwyer Unit 4, decreases in Nita Leo Member, and increase again in Nita Cudalgarra Member.

### **6.5 Relationship of systems tracts with relative sea-level curves**

The column beside the relative sea-level curves contains the interpretation of the systems tracts which are represented by a negative trend and a positive trend of the integrated prediction error filter analysis (INPEFA) curves and discussed in Chapter 4, associated with each identifiable sub-unit for Nita and Goldwyer Formations (Figures 6.9, 6.10 and 6.11). In most cases, for transgressive systems tracts (TST) associated with the sea-level rise, the sea-level reaches a maximum represented by maximum flooding surface (MFS) and is overlain directly by regressive deposits.

For well Looma 1, there is a good match between the transgressive-regressive cycles for Goldwyer Formation as determined by the INPEFA curve and the sea-level curve (right hand column) as interpreted from the Fischer plots (Figure 6.9). The Goldwyer lower shale (interval Or1000P) which indicates transgression matches with the Fischer plots (sloping up trend) showing the increase of sea-level curve. The Goldwyer middle carbonate (interval Or2000) which indicates regression matches with the Fischer plots (dropping down trend) showing the decrease of sea-level curve. The Goldwyer upper shale (interval Or2000P) which indicates transgression consists of the same trend as the Goldwyer lower shale. But for the Nita Formation the correlation is weak. It may be because the Nita Formation comprises stacking of peritidal successions, such as shallow subtidal, intertidal and occasionally supratidal shallowing upward cycles. The plots of peritidal successions more correctly plot changes in accommodation (sea level plus subsidence) rather than extracting relative sea-level change (Husinec et al., 2008). Thus, Fischer plots of the Nita Formation in well Looma 1 more correctly show the changes in accommodation rather than sea-level fluctuations.

For well McLarty 1, there is a good match between the transgressive-regressive cycles for Goldwyer lower shale and Goldwyer middle carbonate as determined by the INPEFA curve and the sea-level curve (right hand column) as interpreted from the Fischer plots (Figure 6.10). But for the Goldwyer upper shale the correlation is weak. Nita Leo Member with regressive trend matches with the decreasing sea-level curve

(Figure 6.10). The Goldwyer lower shale (interval Or1000P) which indicates transgression matches with the Fischer plots (sloping up trend) showing the increase of sea-level curve. The Goldwyer middle carbonate (interval Or2000) which indicates regression matches with the Fischer plots (dropping down trend) showing the decrease of sea-level curve. The Goldwyer upper shale (interval Or2000P) which indicates transgression consists of the trend which fluctuates within small scale rather than sloping upwards trend as in well Looma 1 (see Figure 6.9). The Nita Formation pinched out in well McLarty 1 and the Nita Cudalgarra is absent here. The Nita Leo Member (interval Or3000) which indicates regression matches with the Fischer plots (dropping down trend) showing the decrease of sea-level.

For well Robert 1, there is a good match between the transgressive-regressive cycles for Nita and Goldwyer Formations as determined by the INPEFA curve and the sea-level curve (right hand column) as interpreted from the Fischer plots (Figure 6.11). However, it reaches well total depth at Goldwyer middle carbonate and Goldwyer lower shale (interval Or1000P) which indicates transgression is not found in this well. The Goldwyer middle carbonate (interval Or2000) which indicates regression matches with the Fischer plots (dropping down trend) showing the decrease of sea-level curve. The Goldwyer upper shale (interval Or2000P) which indicates transgression matches with the Fischer plots (sloping up trend) showing the increase of sea-level curve. The Nita Leo Member (interval Or3000) which indicates regression matches with the Fischer plots (dropping down trend) showing the decrease of sea-level. The Cudalgarra Member (intervals Or3000P and Or4000) with a majority transgressive trend which matches with the Fischer plots (sloping up trend) showing the increase of sea-level.

Goldwyer Formation units 1 and 2 (transgressive shale) show increasing accommodation. In Goldwyer Unit 3 (regressive thin carbonate parasequences) are shallow water packages which show decreasing accommodation. In general, small scale cyclicity (particularly in the upward shallowing carbonates) is controlled by Milankovitch cyclicity whereas the transgressive-regressive systems tracts are controlled by third order cyclicity.

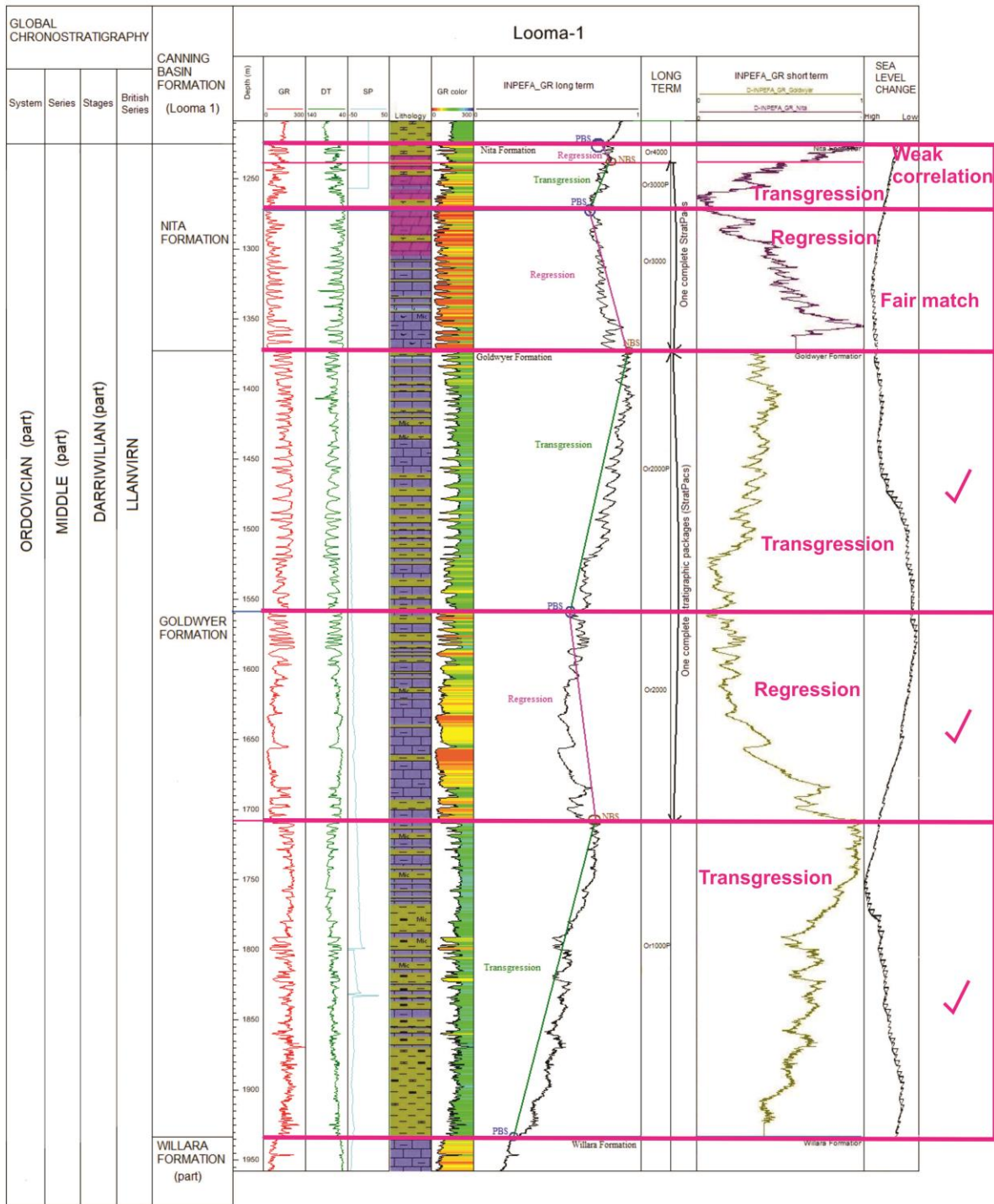


Figure 6.9: Comparison of Fischer plot and well composite chart for well Looma 1. There is a good match between the transgressive-regressive cycles for Goldwyer Formation as determined by the INPEFA curve and the sea-level curve (right hand column) as interpreted from the Fischer plots. But for the Nita Formation the correlation is weak.

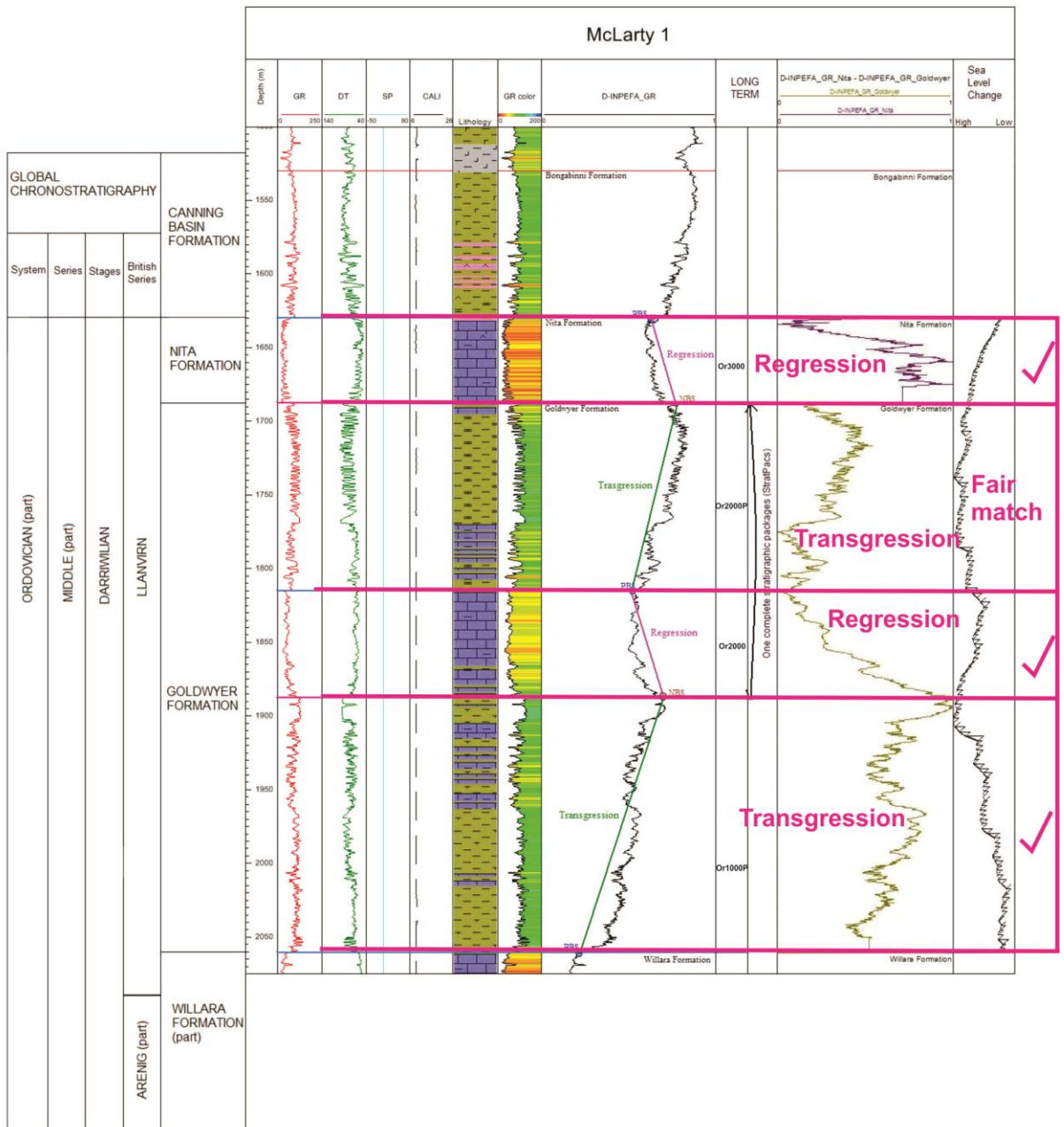


Figure 6.10: Comparison of Fischer plot and well composite chart for well McLarty 1. There is a good match between the transgressive-regressive cycles for Goldwyer lower shale and Goldwyer middle carbonate as determined by the INPEFA curve and the sea-level curve (right hand column) as interpreted from the Fischer plots. But for the Goldwyer upper shale the correlation is weak. Nita Leo Member with regressive trend matches with the decreasing sea-level curve.

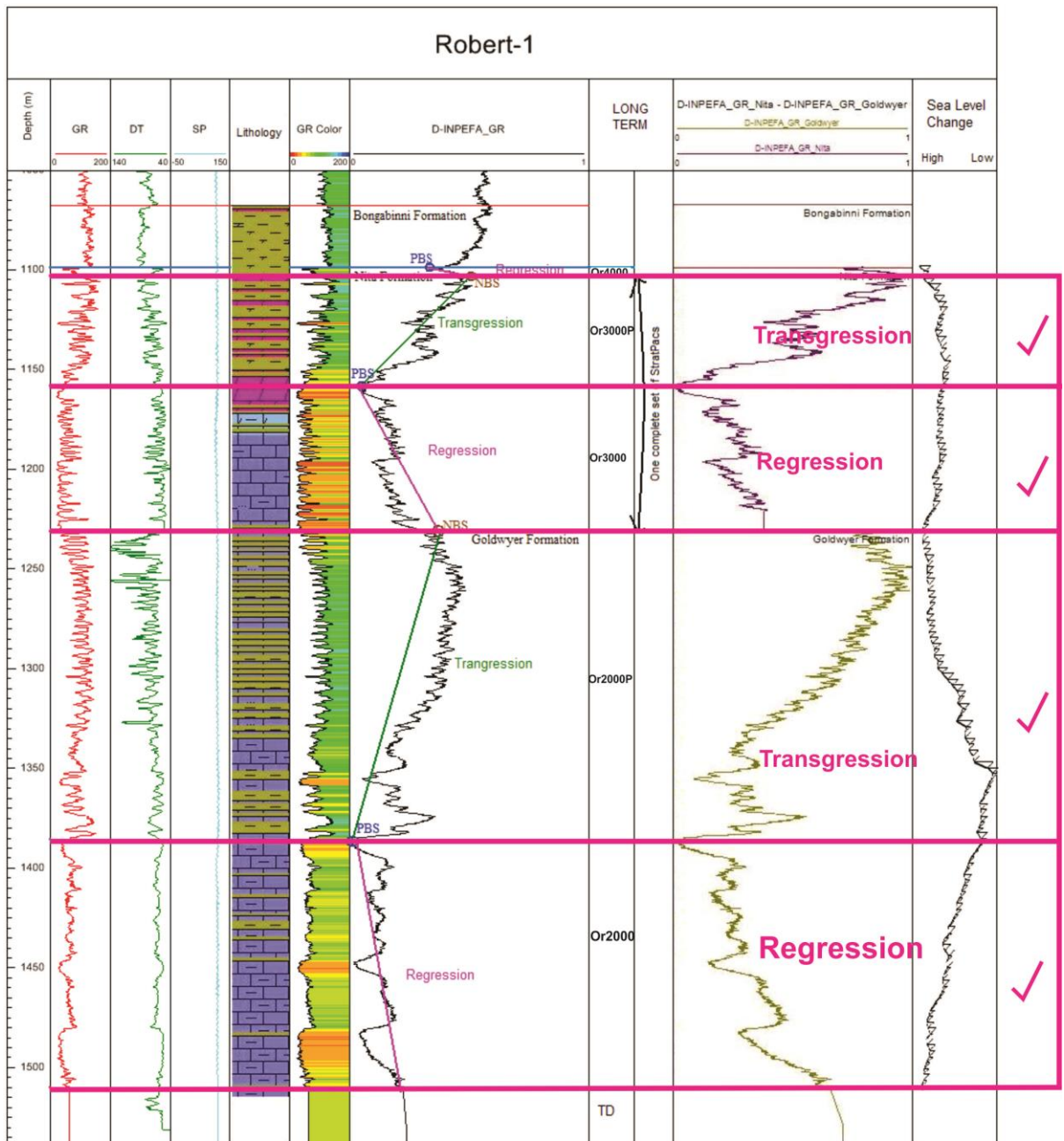


Figure 6.11: Comparison of Fischer plot and well composite chart for well Robert 1. In this well, there is a good match between the transgressive-regressive cycles for Nita and Goldwyer Formations as determined by the INPEFA curve and the sea-level curve (right hand column) as interpreted from the Fischer plots.

## 6.6 Comparison of Middle to Late Llanvirnian age relative sea-level curves

Besides comparing to regional sea level curves, the sea level curves of well Looma 1 which covers complete Nita and Goldwyer deposits illustrated in this study also compare with the North American sea level curve (Ross and Ross, 1992; Ross and Ross, 1995), Baltoscandian sea level curve (Nielsen, 2004) and Ordovician sea level changes determined by Haq and Schutter (2008). In this regard it needs to be underscored that sometimes the global events are applicable worldwide or their magnitude of change at various places may differ depending on local conditions (Haq and Qahtani, 2005), such as local tectonic changes. The third-order sea-level curve illustrated based on the Looma 1 well by using Fischer Plots correlates well with the third-order sea-level defined by others (Figure 6.12), and especially matches very well with the Ordovician sea level changes determined by Haq and Schutter (2008).

According to Havlicek and Fatka (1992), part of the Llanvirnian deposition in the Prague basin, Czechoslovakia took place in a deep water setting with black shale (probably shelf or shelf edge); this matches with the shaly transgressive systems tracts (intervals Or1000P and Or2000P) and increasing sea-level curves in the Goldwyer Formation.

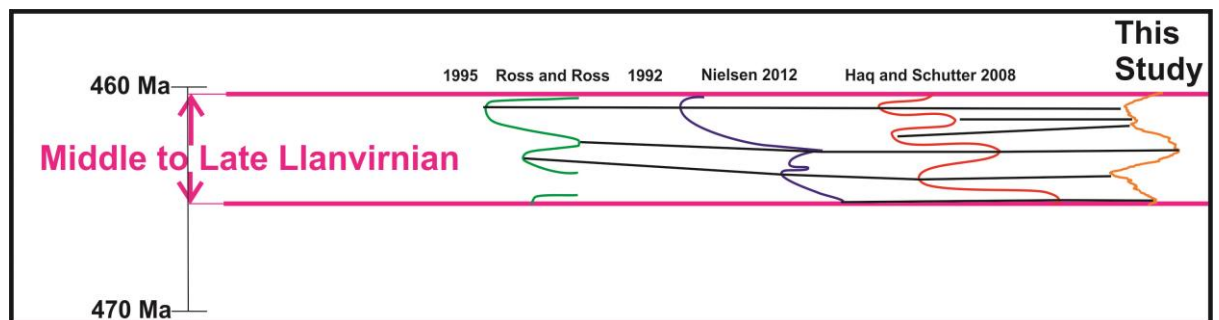


Figure 6.12: Comparison of third-order sea-level curves for Middle to Late Llanvirnian with various studies and this study. The middle to late Llanvirnian is approximately from 460.5 Ma to 465 million years, during which the Nita and Goldwyer Formations were deposited. The third-order sea-level illustrated with Fischer plots in this study correlates well with others shown.

## 6.7 Summary

Fischer plots in which cumulative cycle thickness against cycle number were constructed from three subsurface wells (wells Looma 1, McLarty 1 and Robert 1) in Broome Platform, Canning Basin, WA were constructed. The plots served as guides for correlating the Middle Ordovician (Middle to Late Llanvirnian) Nita and Goldwyer Formations. The formations comprise stacking of shelf or shelf edge, shallow subtidal, intertidal and occasionally supratidal shallowing upward cycles. The distribution of these cycles is related to the amount of accommodation space and controlled by subsidence and sea-level fluctuations because the comparison between the transgressive-regressive systems tracts and sea level illustrated by Fischer plots are matched. The INPEFA curves show clear patterns (see Chapter 4) and produce third-order depositional sequences of transgressive-regressive systems tracts. These systems tracts are recognised in the Nita and Goldwyer Formations of Llanvirnian age. Depositions of the transgressive deposits are attributed to the rise in relative sea level while the regressive deposits attributed to the decrease in relative sea level.

Signals of third-order sea-level fluctuation in the Goldwyer and Nita Formations (generated by using Fischer plots in this study) are compared with the systems tracts determined in Chapter 4. A relative change of sea-level also coincides with other sea-level curve for Llanvirn age. Therefore, the curve of eustatic sea-level during the Llanvirnian time relies on Nita and Goldwyer succession in this study.

# CHAPTER 7

## CONCLUSIONS

### 7.1 Conclusions of this study

This study has carried out an analysis of the sedimentology, stratigraphy and distribution of the Ordovician carbonate-shale packages of the Canning Basin, a vast intracratonic sag basin in northwest Australia. Whilst it remains relatively underexplored, the basin has proven hydrocarbons and significant potential for further discovery of oil, conventional gas, and shale gas. The major findings from this study are summarized below.

#### 1. Occurrence and lithofacies of the Ordovician Nita and Goldwyer Formations:

- Sedimentary well logging allowed characterisation of carbonate facies associations, cyclicity and environments. For the Nita Formation (major part of the Leo Member and part of the Cudalgarra Member) from well Looma 1 (Broome Platform), shallowing upwards cycles are from shallow subtidal (burrowed, fossiliferous mudstone/wackestone), to shoal (oolitic/peloidal/ intraclastic and bioclastic packstone/ grainstone), to intertidal (interlaminated shale and wackestone/packstone), to intertidal/supratidal (microbial laminites), and supratidal (evaporitic wackestone and terrestrial shale). This shows low energy tidal flat shallowing upward sequences dominated the formation.
- The Goldwyer middle carbonate (Unit 3) shallows upward and microfacies consist of gastropod bioclastic burrowed wackestone (subtidal below wave-base) to oncoidal-peloidal packstone/floatstone (shallow subtidal above wave-base) in well Acacia 2 (Barbwire Terrace). Wave energy was probably low in this shallow epeiric sea which is reflected in the overall muddy character of the facies present.
- The Nita Leo Member carbonate sediments in well Canopus 1 (Mowla Terrace) is shale-rich and is interbedded with dolomitised, stylonitic carbonates. Microfacies are weakly cemented burrowed mudstone with peloids and bioclasts with a depositional environment of subtidal below wave-base which coarsens upwards and is capped by peloidal/intraclastic

packstone floatstone which was deposited during storms or periods of lowered wave-base.

- The Nita and Goldwyer Formations for well Kunzea 1 (Crossland Platform) was further investigated in cores in this study.
    - Goldwyer Unit 3 was interpreted as upward coarsening thin cycles from below wave-base wackestone/packstone to oncoidal/peloidal packstone/floatstone. The interval at depth 404.6m was confirmed to contain thin stromatolite layers which likely represent shallow subtidal to lowermost intertidal environments near the top of this unit.
    - Goldwyer Unit 4 is strongly shaly at its base and this unit has upward coarsening cycles from shale to packstone. Near the top of this unit microfacies are oncoidal/peloidal packstone which may represent shoaling before onset of deposition of the Nita Leo Member (regressive carbonate package).
    - Nita Leo Member in this well consists of thin cyclicity from shallow subtidal (microfacies stylonodular burrowed wackestone) to storm lags (bioclastic floatstone horizons) intervals. The bioclastic floatstone horizons occur as thin intervals (a few centimetres to decimetre scale).
    - Bioclastic rudstone is present at the boundary of the Nita Leo Member and Nita Cudalgarra Member. This coarse grained unit matches with the positive bounding surface (the turning point between Leo Member and Cudalgarra Member from INPEFA analysis), which indicates a maximum regressive surface (see 2 below).
    - The Nita Cudalgarra Member consists of heavily dolomitised mudstone and diagenesis has prevented identification of microfacies and environmental analysis.
2. Application of INPEFA curves to well-to-well correlation and regional correlation in the Nita and Goldwyer Formations has been successful. The technique of generating INPEFA curve data, integrated with facies analysis of available cores, has been successfully applied to basin mapping, and to the identification of third order cycles and their transgressive-regressive systems tracts.

- INPEFA curves show that the Goldwyer Formation formed as a transgressive systems tract (interval Or1000P), regressive systems tract (interval Or2000) and a further transgressive systems tract (interval Or2000P) for the top Goldwyer.
  - Interval Or1000P matches the Goldwyer lower shale (Goldwyer Unit 1 and Unit 2) with transgressive systems tract.
  - Interval Or2000 matches the Goldwyer middle carbonate (Goldwyer Unit 3) with regressive systems tract.
  - Interval Or2000P matches the Goldwyer upper shale (Goldwyer Unit 4) with transgressive systems tract and increasing relative sea-level.
  - The Goldwyer Formation can be concluded as a largely transgressive unit due to the fact that it forms by mostly transgressive systems tracts for the shale packages, but it is regressive for the shallowing upwards subtidal cycles within the generally shallow carbonate package (Goldwyer Unit 3).
  - Integrated prediction error filter analysis (INPEFA) curves show that the Nita Formation formed by regressive systems tract (interval Or3000), transgressive systems tract (interval Or3000p) and regressive systems tract (Or4000).
  - Interval Or3000 matches with the regressive Nita Formation Leo Member.
  - Intervals Or3000P and Or4000 matches with the Nita Cudalgarra member.
  - Long-term (third order) evolution of the cyclicity packages through the Nita and Goldwyer Formations in the Canning Basin has been established as three cycles of shallowing upwards from transgression to regression from larger scale cycles in the Goldwyer Formation to smaller cycles in the Nita Formation.
  - Based on the sequence stratigraphic technology of Embry (which are regressive systems tracts (RST) and transgressive systems tracts (TST)), the INPEFA methodology has been shown in this study to be a useful technique in sequence stratigraphic analysis.
3. Shale gas potential of the Goldwyer Formation from INPEFA data:
- The Willara Sub-basin and Mowla Terrace are the areas with more than average thickness of Goldwyer shale units. These two tectonic sub-divisions could be potential areas for a major program of shale gas exploration.

- Lennard Shelf also shows good thickness of Goldwyer shale units in well Blackstone 1 but only one well was drilled in the Lennard Shelf that penetrate to Ordovician successions. More data are required here to access the shale gas potential.
  - Willara Sub-basin (106.8Tcf), Mowla Terrace (83.9Tcf), Broome Platform (261.1Tcf) and Kidson Sub-basin (276.1Tcf) contain high values of the estimated maximum total gas in place while the Barbwire Terrace only contains maximum total gas in place of 32.5Tcf. Therefore, these tectonic sub-divisions could be an important potential area for shale gas exploration.
  - The total gas in place that is estimated in these study areas ranges from 253.5-760.4Tcf (minimum 253.5Tcf, median 506.9Tcf, and maximum 760.4Tcf). The minimum value is comparable to the EIA (2011) estimate, the median value is almost twice the previous estimate, and the maximum value of 760.4Tcf is three times the EIA estimate. Shale gas in place (adsorbed gas) estimation derived from INPEFA data (139-418 Tcf) and total gas in place (253.5-760.4 Tcf) for Goldwyer shales with significant 5% TOC value and 10% shale porosity reinforce the resource potential of the Ordovician strata for future shale gas exploration and production.
4. Llanvirnian relative sea-level fluctuations from Fischer plots:
- Goldwyer lower shale (interval Or1000P) shows increasing relative sea-level and this matches with the transgressive systems tract.
  - Goldwyer middle carbonate (interval Or2000) shows relative sea-level drop and this matches with the regressive systems tract.
  - Goldwyer upper shale (interval Or2000P) shows relative sea-level drop and this matches with the transgressive systems tract.
  - Nita Formation Leo Member (interval Or3000) shows relative sea level drop and this matches with the regressive systems tract.
  - Nita Formation Cudalgarra Member (intervals Or3000P and Or4000) with transgressive systems tract then followed by the regressive systems tract does not correlate strongly with the relative sea-level curve in well Looma 1 but match with the relative sea-level curves in wells McLarty 1 and Robert 1. This is probably influenced by the fact that the thickness of this section is quite small.

- Fischer plots generally correlate well with trend and cyclicity determined by INPEFA curves and as a method of cross-checking INPEFA data and sea-level change.
- The Fischer plots for the Llanvirnian Goldwyer and Nita Formations show good agreement with the third order global sea level cycles of Haq and others.

## **7.2 Recommendations for future research**

Results in this study have helped to improved knowledge of the sequence stratigraphy and relative sea-level curves of the Middle Ordovician (Llanvirn) Nita and Goldwyer Formations in the Canning Basin, Western Australia. Microfacies and thin section analysis was also carried out for the available successions of these formations to understand the depositional environment. However, with respect to future exploration and research, the following recommendations are suggested:

1. The present study focuses only on Broome Platform, Mowla Terrace, Barbwire Terrace, Willara Sub-basin and Crossland Platform of the Canning Basin. It is recommended that more extensive areas in the basin, which are Kidson Sub-basin, Ryan Shelf and others be studied as new data becomes available. This will provide more valuable information to understand the depositional environment and cycles of Nita and Goldwyer Formations (Middle Ordovician). It is likely that further exploration success will be an outcome for this vast, still under explored basin.
2. The present study focuses on Goldwyer Formation correlation for shale gas assessment across the Canning Basin. No fluorescence studies and geochemical analysis were carried out. It is recommended that 1) the INPEFA technique should be further developed to generate shale isopach maps and 2) a more extensive and integrated work, which included fluorescence studies, geochemical analysis, more electric wireline logs together with the full cores to provide a more detailed evaluation of the prospectivity of the Goldwyer Formation and valuable information for future wells would follow. If this can be done, unconventional shale gas could eventually match or even exceed the potential of Western Australian conventional hydrocarbon deposits.

## REFERENCES

- Alexander, T., J. Baihly, C. Boyer, B. Clark, G. Waters, V. Jochen, J. Le Calvez, R. Lewis, C. K. Miller, and J. Thaeler. 2011. Shale gas revolution. *Oilfield Review* 23 (3): 40-55.
- Asquith, G., and D. Krygowski. 2004. Basic well log analysis. Edited by E. A. Mancini, AAPG methods in exploration series, no. 16.
- Asquith, G. B., and C. R. Gibson. 1982. Basic well log analysis for geologists. *AAPG Methods in Exploration* (3): 216.
- Baillie, P., C. M. Powell, Z. Li, and A. Ryall. 1994. The Sedimentary Basins of Western Australia, Proceedings of the Petroleum Exploration Society of Australia Symposium, Perth, The tectonic framework of Western Australia's Neoproterozoic to Recent sedimentary basins.
- Begg, J. 1987. Structuring and controls on Devonian reef development on the north-west Barbwire and adjacent terraces, Canning Basin. *APEA Journal* 27 (1): 137-151.
- Boyer, C., B. Clark, V. Jochen, R. Lewis, and C. K. Miller. 2011. Shale gas: A global resource. *Oilfield review* 23 (3): 28-39.
- Boyer, C., J. Kieschnick, R. Suarez-Rivera, R. E. Lewis, and G. Waters. 2006. Producing gas from its source. *Oilfield review* 18 (3): 36-49.
- Bradshaw, M., J. Bradshaw, A. Murray, D. Needham, L. Spencer, R. Summons, J. Wilmot, and S. Winn. 1994. The Sedimentary Basins of Western Australia, Proceedings of the Petroleum Exploration Society of Australia Symposium, Perth, Petroleum systems in West Australian basins.
- Broad, D. S. 1973. Geology and hydrocarbon potential of the South Canning Basin, Western Australia. West Australian Petroleum Pty. Ltd.
- Brown, S. A., I. M. Boserio, K. S. Jackson, and K. W. Spense, eds. 1984. The geological evolution of the Canning Basin – implications for petroleum exploration. Edited by P. Purcell, The Canning Basin, WA Perth, WA:

Proceedings Geological Society of Australia and Petroleum Exploration  
Society of Australia Canning Basin Symposium.

- Browne, W. 1947. A short history of the Tasman Geosyncline of eastern Australia. *Science Progress* 35 (140): 623-637.
- Cadman, S. J., L. Pain, V. Vuckovic, and S. R. Lepoidevin. 1993. Canning Basin, W.A. BRS, Canberra
- Carlsen, G., and K. Ghorri. 2005. Canning Basin and global Palaeozoic petroleum systems—a review: *APPEA Journal*, v. 45.
- Combaz, A., and G. Péniguel. 1972. Étude palynostratigraphique de l'Ordovicien dans quelques sondages du Bassin de Canning (Australie Occidentale). *Bulletin Centre de Recherches de Pau SNPA* 6: 121-167.
- Copp, I. 2008. Hydrothermal dolomite (HTD) reservoirs - A new Australian carbonate play. Pesa news resources.
- Crain, E. 2000. Crain's Petrophysical Handbook on CDROM,(3rd-Millennium Edition). Spectrum:
- David, T. W. E., and W. R. Browne. 1950. The geology of the Commonwealth of Australia. Vol. 1: E. Arnold London.
- De Jong, M., S. D. Nio, D. Smith, and A. R. Böhm. 2007. Subsurface correlation in the Upper Carboniferous (Westphalian) of the Anglo-Dutch Basin using the climate stratigraphic approach. *First break* 25 (12): 49-59.
- De Jong, M. G. G., D. G. Smith, S. D. Nio, and N. Hardy. 2006. Subsurface correlation of the Triassic of UK southern Central Garben: new look at an old problem. *First break* 24: 103-109.
- Demicco, R. V., and L. A. Hardie. 1994. Sedimentary structures and early diagenetic features of shallow marine carbonate deposits: *SEPM (Society of Sedimentary Geology)*.
- DMP. 2012. Shale gas in Western Australia. *Petroleum in Western Australia*, September 2012.

- Doll, H. 1948. *The SP log: theoretical analysis and principles of interpretation*: American Institute of Mining and Metallurgical Engineers.
- Doyle, P., and M. R. Bennett. 1998. *Interpreting paleoenvironments from fossils. Unlocking the Stratigraphical Record (Advance in Modern Stratigraphy)*. John Wiley & Sons, New York:
- Dunham, R. J., ed. 1962. *Classification of carbonate rocks according to depositional texture*. Edited by W. E. Ham. Vol. 1, *Classification of carbonate rocks*: American Association of Petroleum Geologists Memoir.
- Edwards, D., R. Summons, J. Kennard, R. Nicoll, J. Bradshaw, M. Bradshaw, C. Foster, G. O'Brien, and J. Zumberge. 1997. *Geochemical characterisation of Palaeozoic petroleum systems in north-western Australia*. *The APPEA Journal* 37 (1): 351-379.
- EIA. 2011. *World shale gas resources: An initial assessment of 14 regions outside the United States*. US Department of Energy, Arlington, VA, 365 p.
- Erick, M. 1995. *Cyclostratigraphy of Middle Devonian carbonates of the eastern Great Basin*. *Journal of Sedimentary Research* 65 (1):
- Embry, A. 1993. *Transgressive-regressive (TR) sequence analysis of the Jurassic succession of the Sverdrup Basin, Canadian Arctic Archipelago*. *Canadian Journal of Earth Sciences* 30 (2): 301-320.
- Embry, A. 2009. *Practical sequence stratigraphy*: Canadian Society of Petroleum Geologists, 81 p.
- Embry, A., and E. Johannessen. 1992. *TR sequence stratigraphy, facies analysis and reservoir distribution in the uppermost Triassic-Lower Jurassic succession, western Sverdrup Basin, Arctic Canada*. *Arctic geology and petroleum potential* 2: 121-146.
- Embry, A. F. 2002. *Sequence stratigraphic models for exploration and production: Evolving methodology, emerging models and application histories*: Proceedings of the 22nd Annual Gulf Coast Section SEPM Foundation, Bob

- F. Perkins Research Conference, Transgressive-regressive (TR) sequence stratigraphy. SEPM
- ENRES. 2011. ENRES stratigraphic methods and workflow approaches in subsurface well correlations, Report ID: ES484-2011, 23p
- Finder. 2013. Developing unconventional gas Australia, Release area L11-5. Royal International Convention Centre, Brisbane, Qld, Australia: Finder Shale Pty. Ltd.
- Fischer, A. G. 1964. The Lofer cyclothems of the Alpine Triassic. *Kansas Geol. Survey Bull.* 169: 107-149.
- Flügel, E. 2010. *Microfacies of carbonate rocks* 2nd ed. Sp. Verlag: 984 p.
- Folk, R. L. 1973. Evidence for peritidal deposition of Devonian Caballos Novaculite, Marathon Basin, Texas. *AAPG Bulletin* 57 (4): 702-725.
- Forman, D. J., and D. W. Wales. 1981. Geological evolution of the Canning Basin, Western Australia. *Australia BMR, Bulletin* 210: 91.
- Foster, C. B., G. W. O'Brien, and S. T. Watson. 1986. Hydrocarbon source potential of the Goldwyer Formation, Barbwire Terrace, Canning Basin, Western Australia. *APEA Journal* 26 (1): 142-155.
- France, R. E. 1986. Percival 1 well completion report. Western Mining Corporation Limited.
- Frazier, D. E. 1974. Depositional--episodes, Their Relationship to the Quaternary Stratigraphic Framework in the Northwestern Portion of the Gulf Basin: Bureau of Economic Geology, University of Texas at Austin.
- Frost III, E. L., and C. Kerans. 2010. Controls on syndepositional fracture patterns, Devonian reef complexes, Canning Basin, Western Australia. *Journal of Structural Geology* 32 (9): 1231-1249.
- Garland, J. 1997. Middle to upper Devonian (givetian and frasnian) shallow-water carbonates of Western Europe: facies analysis and cyclicity, Durham University

- Ghori, K., and P. Haines. 2007. American Association of Petroleum Geologists; AAPG International Conference and Exhibition, Perth, Western Australia, Paleozoic petroleum systems of the Canning Basin, Western Australia: a review.
- Ghori, K. A. R. 2013. Emerging unconventional shale plays in Western Australia. *APPEA Journal* 2013: 313-336.
- Goldhammer, R. K., P. Dunn, and L. Hardie. 1990. Depositional cycles, composite sea-level changes, cycle stacking patterns, and the hierarchy of stratigraphic forcing: examples from Alpine Triassic platform carbonates. *Geological Society of America Bulletin* 102 (5): 535-562.
- Goldhammer, R. K., P. A. Dunn, and L. A. Hardie. 1987. High-frequency glacio-eustatic sea-level oscillations with Milankovitch characteristics recorded in the Middle Triassic platform carbonate in northern Italy. *American Journal of Science* 287: 853-892.
- Gradstein, F. M., J. G. Ogg, and A. G. Smith. 2004. A geologic time scale 2004. Vol. 86: Cambridge University Press.
- Gregory, E. W. 2001. Famennian mud-mounds in the proximal fore-reef slope, Canning Basin, Western Australia. *Sedimentary Geology* 145: 295-315.
- GSWA. 2013. Geological Survey work program for 2012-13 and beyond: Geological Survey of Western Australia, Record 2012/1, 128p.
- Haines, P. 2004. Depositional facies and regional correlations of the Ordovician Goldwyer and Nita Formations. Canning Basin, Western Australia, with implications for petroleum exploration: Geological Survey of Western Australia, Record 7:
- Haines, P. 2009. The Carribuddy Group and Worrall Formation. Canning Basin, Western Australia: stratigraphy, sedimentology, and petroleum potential: Geological Survey of Western Australia, Report 105:
- Haines, P., and M. Wingate. 2005. Proceedings of the Central Australian Basins Symposium (CABS), Alice Springs, Northern Territory, Contrasting

depositional histories, detrital zircon provenance and hydrocarbon systems: Did the larapintine Seaway link the Canning and Amadeus basins during the Ordovician.

Haines, P. W., and K. A. R. Ghorri. 2006. AAPG 2006 International Conference and Exhibition, 5–8 November, 2006, Rich oil-prone Ordovician source beds, Bongabinni Formation, onshore Canning Basin, Western Australia. Perth, WA:

Hancock, E., and J. Huntington. 2010. The GSWA NVCL Hylogger: rapid mineralogical analysis for characterizing mineral and petroleum core. Geological Survey of Western Australia Record 2010/17: 21.

Haq, B. U., and A. M. Al-Qahtani. 2005. Phanerozoic cycles of sea-level change on the Arabian Platform. *GeoArabia* 10 (2): 127-160.

Haq, B. U., and S. R. Schutter. 2008. A chronology of Paleozoic sea-level changes. *Science* 322 (5898): 64-68.

Havlicek, V., and O. Fatka. 1992. Ordovician of the Prague Basin (Barrandian area, Czechoslovakia). *Global Perspectives on Ordovician Geology*. Balkema, Rotterdam: 461-172.

Helland-Hansen, W., and J. G. Gjelberg. 1994. Conceptual basis and variability in sequence stratigraphy: a different perspective. *Sedimentary Geology* 92 (1): 31-52.

Hillock, P. 1988. The Petrophysics of the Nita Formation central Canning Basin, Western Australia, Honours Thesis, University of Adelaide

Hocking, R., A. Mory, and I. Williams. 1994. The Sedimentary Basins of Western Australia: Proceedings of the Petroleum Exploration Society of Australia Symposium, Perth, An atlas of Neoproterozoic and Phanerozoic basins of Western Australia.

Hoffmann, C., C. Foster, T. Powell, and R. Summons. 1987. Hydrocarbon biomarkers from Ordovician sediments and the fossil alga *Gloeocapsomorpha*

*prisca* Zalessky 1917. *Geochimica et Cosmochimica Acta* 51 (10): 2681-2697.

Huntington, J. F., L. B. Whitbourn, M. A. Quigley, K. Yang, P. Mason, T. J. Cudahy, P. Connor, D. Coward, R. Hewson, and R. Phillips. 2007. Development and implementation of advanced automated core logging technology for enhanced mine feasibility and development in Western Australia: final report — Project M373. CSIRO, Exploration and Mining Report P2007/958: 62.

Husinec, A., D. Basch, B. Rose, and J. F. Read. 2008. FISCHERPLOTS: An Excel spreadsheet for computing Fischer plots of accommodation change in cyclic carbonate successions in both the time and depth domains. *Computers & Geosciences* 34 (3): 269-277.

James, N. P., ed. 1984. Shallowing-upward sequences in carbonates. Edited by R. G. Walker, *Facies models* (2nd edition).

James, N. P., and A. C. Kendall, eds. 1992. Introduction to carbonate and evaporite facies models. Edited by R. G. Walker and N. P. James, *Facies models, response to geological change*: Geological Association of Canada: 265-276.

Jarvie, D. M. 2012. Shale Resource Systems for Oil and Gas: Part 1—Shale-gas Resource Systems. *Shale reservoirs—Giant resources for the 21st century*: AAPG Memoir 97: 69-87.

Jarvie, D. M., R. J. Hill, T. E. Ruble, and R. M. Pollastro. 2007. Unconventional shale-gas systems: The Mississippian Barnett Shale of north-central Texas as one model for thermogenic shale-gas assessment. *AAPG Bulletin* 91 (4): 475-499.

Jones, P. J., R. S. Nicoll, D. S. Edwards, J. M. Kennard, and K. C. Glenn. 1998. Canning Basin biozonation and stratigraphy, 1998. Australian Geological Survey Organisation, chart 2.

Karajas, J., and C. N. Kernick, eds. 1984. A prospective Nita Formation reservoir trend on the Broome Platform, in the Canning Basin, W.A. . Edited by P. G. Purcell, *The Canning Basin, WA Perth, WA*: Proceedings Geological Society

of Australia and Petroleum Exploration Society of Australia Canning Basin Symposium.

Karajas, J., and D. Taylor. 1983. Aquila No. 1 well completion report Eagle Corporation Ltd. Western Australia Geological Survey.

Kennard, J. M., M. J. Jackson, K. K. Romine, R. D. Shaw, and P. N. Southgate, eds. 1994. Depositional sequences and associated petroleum systems of the Canning Basin WA. Edited by P. P. a. R. Purcell, The Sedimentary basins of Western Australia. Perth, WA: Petroleum exploration Society of Australia; West Australian Basins Symposium, 1994, Proceedings.

King, M. R. 1998. The Palaeozoic play in the south Canning Basin—results of Looma 1. The sedimentary basins of Western Australia 2: 695-714.

Kongkanoi, C. 2008. Subsurface Correlation of Formation 1, Platform B, Arthit Project, Gulf of Thailand Using the Climate. Master of Science (Petroleum Geosciences), Chiang Mai University

Krygowski, D. A. 2003. Guide to Petrophysical Interpretation. available through Classfronter) Wireline well logging:

Kui, Y., T. Servais, and L. Jun. 2010. Revision of the Ordovician acritarch genus *Ampullula* Righi 1991. Review of Palaeobotany and Palynology 163 (1): 11-25.

Legg, D. 1978. Ordovician biostratigraphy of the Canning Basin, Western Australia. Alcheringa 2 (4): 321-334.

McCracken, S. 1994. The Sedimentary Basins of Western Australia: Proceedings of the Western Australian Basins Symposium, Perth, Timing of hydrocarbon migration into the Admiral Bay Fault Zone, Canning Basin.

McCracken, S. R. 1997. Stratigraphic, diagenetic, and structural controls of the Admiral Bay carbonate-hosted Zn–Pb–Ag deposit, Canning Basin, Western Australia. PhD thesis University of Western Australia

Middleton, M. 1990. Canning Basin. Geology and mineral resources of Western Australia: Western Australia Geological Survey, Memoir 3: 425-457.

- Nicoll, R. S. 1984. Conodont distribution in the marginal-slope facies of the Upper Devonian reef complex, Canning Basin, Western Australia. Geological Society of America Special Papers 196: 127-142.
- Nielsen, A. T. 2004. Ordovician sea level changes: a Baltoscandian perspective. Edited by B. D. Webby, F. Paris, M. L. Droser and I. G. Percival, The great Ordovician biodiversification event: Columbia University Press, New York: 84-93.
- Nio, S. D., A. R. Böhm, J. H. Brouwer, M. G. G. De Jong, and D. G. Smith. 2006. Climate stratigraphy: Principles and applications in subsurface correlation. EAGE Short Course, Series 1: 1-130.
- Nio, S. D., J. H. Brouwer, D. G. Smith, M. G. G. De Jong, and A. R. Böhm. 2005. Spectral trend attribute analysis: applications in the stratigraphic analysis of wireline logs. First break 23: 71-75.
- Nio, S. D., M. G. G. De Jong, and A. R. Böhm. 2008. Climate stratigraphy - a new method of subsurface correlation: with examples from the Late Triassic of the northern Carnarvon Basin. PESA News February/March 2008: 50-55.
- NSE. 2012. New Standard Energy Limited : Nicolay No 1 Weekly Drilling Update12 August 2013).
- O'Brien, N. R., and R. M. Slatt. 1990. Argillaceous rock atlas.
- Ogg, J. G., G. Ogg, and F. M. Gradstein. 2008. The concise geologic time scale. Vol. 1.
- Oliver, T., and N. Cowper. 1963. Depositional environments of the Ireton Formation, central Alberta. Bulletin of Canadian Petroleum Geology 11 (2): 183-202.
- Perlmutter, M. A., and M. D. Matthews. 1992. Global cyclostratigraphy: Argonne National Laboratory, University of Chicago.
- Phipps, J., M. Trupp, and M. Nosiara. 1998. Looma 1 well completion report (EP 353). Shell Development (Australia) Pty. Ltd.

- Playford, G. 2009. Devonian reef complexes of the Canning Basin, Western Australia: review of Devonian palynology, Canning Basin. Geological Survey of Western Australia, Bulletin 145: 441-444.
- Playford, G., and F. Martin. 1984. Ordovician acritarchs from the Canning Basin, Western Australia. *Alcheringa* 8 (3): 187-223.
- Playford, P. E., N. F. Hurley, C. Kerans, and M. F. Middleton, eds. 1989. Reefal platform development, Devonian of the Canning Basin, Western Australia. . Edited by P. D. Crevello, J. L. Wilson, J. F. Sarg and J. F. Read. Vol. 44, Controls on carbonate platform and basin development: Soc. Econ. Paleontol. Mineral. Spec. Publ. .
- Posamentier, H. W., and G. P. Allen. 1999. Siliciclastic sequence stratigraphy: concepts and applications: SEPM (Society for Sedimentary Geology).
- Prospect. 2013. Balancing act: Canning Basin makes a 'comeback'. Western Australia's International Resources Development Magazine, 8p.
- Purcell, P. G. 1984. The Canning Basin, WA: Geological Society of Australia.
- Quintavalle, M., and G. Playford. 2008. Stratigraphic distribution of selected acritarchs in the Ordovician subsurface, Canning Basin, Western Australia. *Revue de micropaleontologie* 51 (1): 23-37.
- Read, J., and R. Goldhammer. 1988. Use of Fischer plots to define third-order sea-level curves in Ordovician peritidal cyclic carbonates, Appalachians. *Geology* 16 (10): 895-899.
- Read, J., W. Koerschner, D. Osleger, G. Bollinger, and C. Coruh. 1991. Field and modelling studies of Cambrian carbonate cycles, Virginia Appalachians; reply. *Journal of Sedimentary Research* 61 (4): 647-652.
- Reed, J., H. Illich, and B. Horsfield. 1986. Biochemical evolutionary significance of Ordovician oils and their sources. *Organic Geochemistry* 10 (1): 347-358.
- Romine, K. K., P. N. Southgate, J. M. Kennard, and M. J. Jackson, eds. 1994. The Ordovician to Silurian phase of the Canning Basin WA: structure and sequence evolution. Edited by P. G. Purcell and R. R. Purcell, The

sedimentary basins of Western Australia. Perth, Western Australia: Proceedings of the West Australian Basins Symposium.

- Ross, C. A., and J. R. Ross. 1995. North American Ordovician depositional sequences and correlations.
- Ross, J., and C. Ross. 1992. Ordovician sea-level fluctuations. *Global perspectives on Ordovician geology*: 327-335.
- Sadler, P. M., D. A. Osleger, and I. P. Montanez. 1993. On the labeling, length, and objective basis of Fischer plots. *Journal of Sedimentary Research* 63 (3): 360-368.
- Sarg, J. 1988. Carbonate sequence stratigraphy. *Sea-Level Changes: An Integrated Approach*: SEPM, Special Publication 42: 155-181.
- Scholle, P. A., and D. S. Ulmer-Scholle. 2003. A color guide to the petrography of carbonate rocks: grains, textures, porosity, diagenesis. Vol. 77: AAPG Online Bookstore.
- Shaw, R. D., M. J. Sexton, and I. Zeilinger. 1994. The tectonic framework of the Canning Basin, WA, including 1: 2 million structural elements map of the Canning Basin. Australian Geological Survey Organisation, Record 1994/48, 89 p.
- Smith, G. 1984. The tectonic development of the Gregory Sub-basin and adjacent areas, northeastern Canning Basin. *The Canning Basin, WA* edited by PG Purcell: Geological Society of Australia and Petroleum Exploration Society of Australia: 109-120.
- Triche, N. 2012. Shale gas in Western Australia - Wave of the future? *Petroleum in Western Australia*, 20-26.
- Tyler, I., and R. Hocking. 2000. A revision of the tectonic units of Western Australia. *Western Australia Geological Survey, Annual Review* 1: 33-44.
- USGS. 2012. Map of assessed shale gas in the United States, 2012. U.S. Geological Survey, Reston, Virginia: 16p.

- Vail, P., R. Mitchum Jr, and S. Thompson III. 1977. Seismic Stratigraphy and Global Changes of Sea Level: Part 3. Relative Changes of Sea Level from Coastal Onlap: Section 2. Application of Seismic Reflection Configuration to Stratigraphic Interpretation.
- Van Wagoner, J., H. Posamentier, R. Mitchum, P. Vail, J. Sarg, T. Loutit, and J. Hardenbol. 1988. An overview of the fundamentals of sequence stratigraphy and key definitions. *Sea-Level Changes: An Integrated Approach: SEPM, Special Publication 42*: 39-45.
- Van Wagoner, J. C. 1998. Sequence stratigraphy and marine to nonmarine facies architecture of foreland basin strata, Book Cliffs, Utah, USA; reply. *AAPG Bulletin* 82 (8): 1607-1618.
- Walker, R., and N. James. 1992. Facies models: response to sea level changes. Geological Association of Canada, St. John's, 409p:
- Wallace, M. W., C. Kerans, P. E. Playford, and A. McManus. 1991. Burial diagenesis in the Upper Devonian reef complexes of the Geikie Gorge Region, Canning Basin, Western Australia. *Bull. Am. Assoc. Pet. Geol.* 75: 1018-1038.
- Warris, B. J. 1993. The hydrocarbon potential of the Palaeozoic Basins of Western Australia. *APEA journal* 33: 123-137.
- Watson, S., and S. Derrington. 1982. Acacia 2 well completion report Canning Basin. Western Mining Corporation Limited, Exploration Division - Petroleum.
- Watson, S. T. 1988. Ordovician conodonts from the Canning Basin (W. Australia). *Palaeontographica Abteilung A* 203 (4-6): 91-147.
- Winchester-Seeto, T., C. Foster, and T. O Leary. 2000. Chitinozoans from the Middle Ordovician (Darriwilian) Goldwyer and Nita formations, Canning Basin (Western Australia). *Acta Palaeontologica Polonica* 45 (3): 271-300.
- Winchester-Seeto, T., C. Foster, and T. O'Leary. 2000. The environmental response of Middle Ordovician large organic walled microfossils from the Goldwyer and

Nita Formations, Canning Basin, Western Australia. Review of palaeobotany and palynology 113 (1): 197-212.

Wood, R. 1998. Novel reef fabrics from the Devonian Canning Basin, Western Australia. Sedimentary geology 121: 149-156.

Wright, V. 1986. Facies sequences on a carbonate ramp: the Carboniferous Limestone of South Wales. Sedimentology 33 (2): 221-241.

Yeates, A., D. Gibson, R. Towner, and R. Crowe. 1984. The Canning Basin, WA Proceedings of the Geological Society of Australia & Petroleum Exploration Society of Australia Symposium, Perth, Regional geology of the onshore Canning Basin, WA.

Yeates, A. N., D. L. Gibson, R. R. Towner, and R. W. A. Crowe, eds. 1984. Regional geology of the onshore Canning Basin, W.A. . Edited by P. Purcell, The Canning Basin, WA. Perth, WA: Proceedings Geological Society of Australia and Petroleum Exploration Society of Australia Canning Basin Symposium.

Yoo, C. M., and Y. I. Lee. 1995. Middle Ordovician (Llanvirnian) Sea Level Change Recorded in Shallow-Water Carbonates (Yeongheung Formation), Korea.

Zalesky, M. 1917. On marine sapropelite of Silurian age formed by a blue-green alga. Izv Imp Akad Nauk IV Ser 1: 3-18.

Zenger, D. H., J. B. Dunham, and R. L. Ethington, eds. 1980. Concepts and models of dolomitization. Vol. 28, Special Publication: Society of Economic Paleontologists and Mineralogists.

"Every reasonable effort has been made to acknowledge the owners of copyright material. I would be pleased to hear from any copyright owner who has been omitted or incorrectly acknowledged."

Ying Jia Teoh



Date: 27<sup>st</sup> September 2013

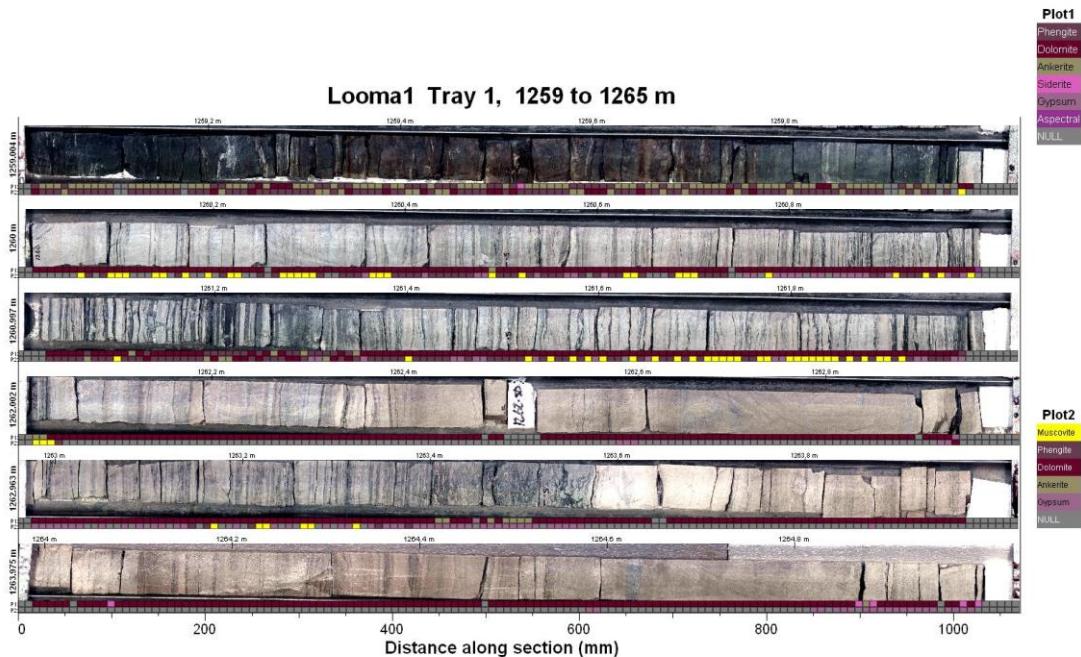
# APPENDIX 1

## CORE PHOTOS GENERATED BY TSG SOFTWARE

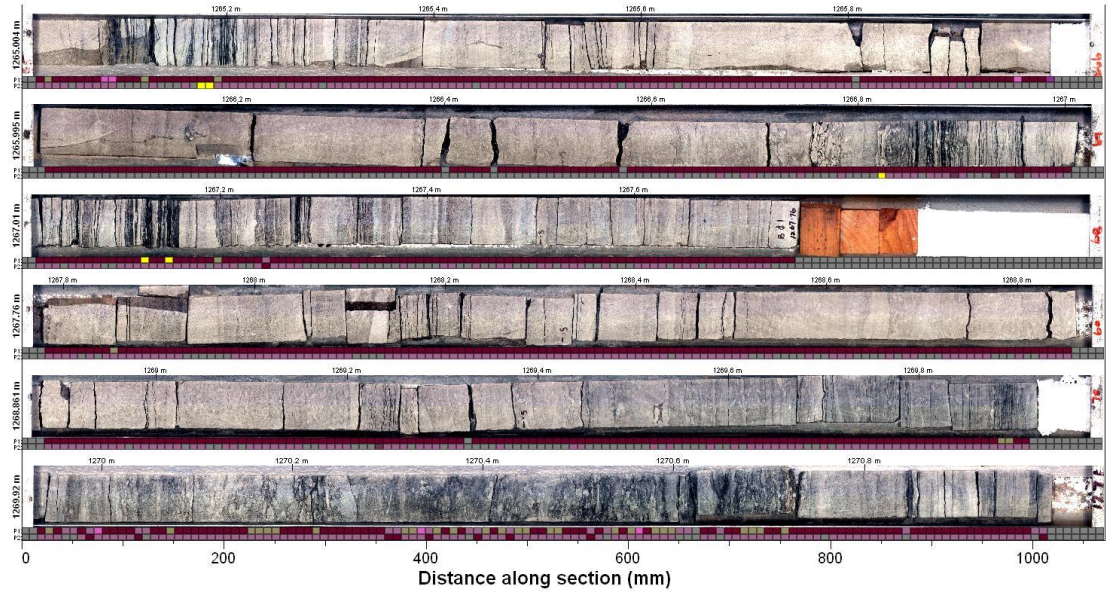
The sedimentary logs for Middle Ordovician carbonate successions of the Nita and Goldwyer Formations of the Canning basin were described and discussed in Chapter 3 (wells Looma 1, Acacia 2, Canopus 1 and Kunzea 1). Note that interpretation of mineralogy composition in the sedimentary logs was based on scan using hylogger method and TSG-software which are shown in this section. For the mineralogy legend, shale contains muscovite (yellow colour) and phengite (purple colour). Dolomite (dark purple colour) is a mineral for dolostone while limestone consists of calcite (light green). Occurrence of mineral gypsum (light purple colour) shows evaporitic rocks. Plot 1 is mineral which dominated the rocks and plot 2 shows the secondary mineral.

Acknowledgement: All wells are open file and held at the GSWA Core Library, Carisle, W.A.

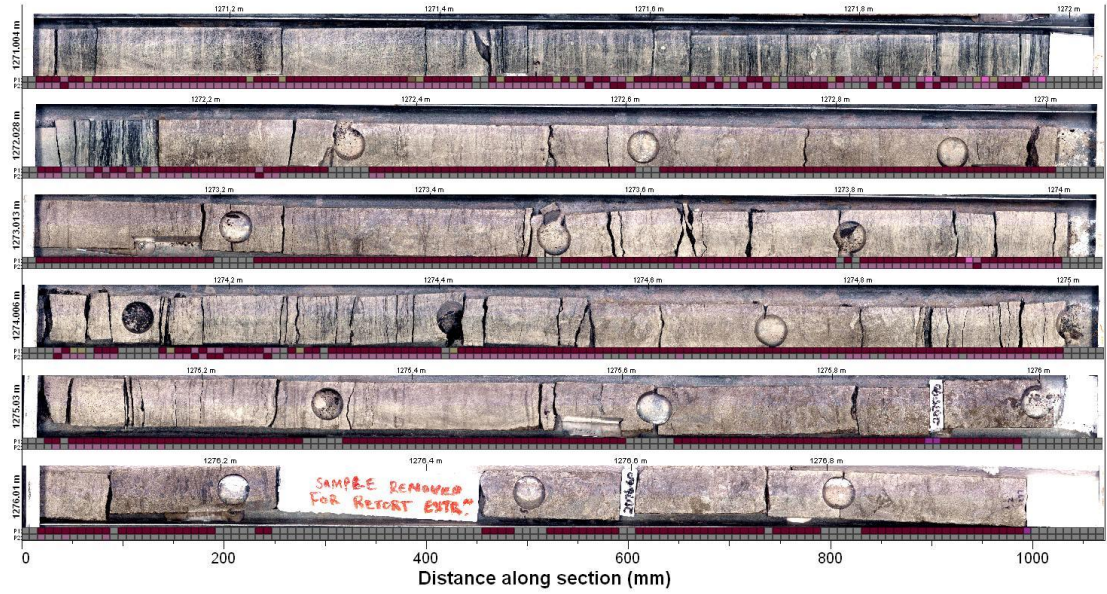
### Well Looma 1: Part of Nita Formation Cudalgarra Member (1259-1272.5m) and major part of Nita Formation Leo Member (1272.5-1350m)



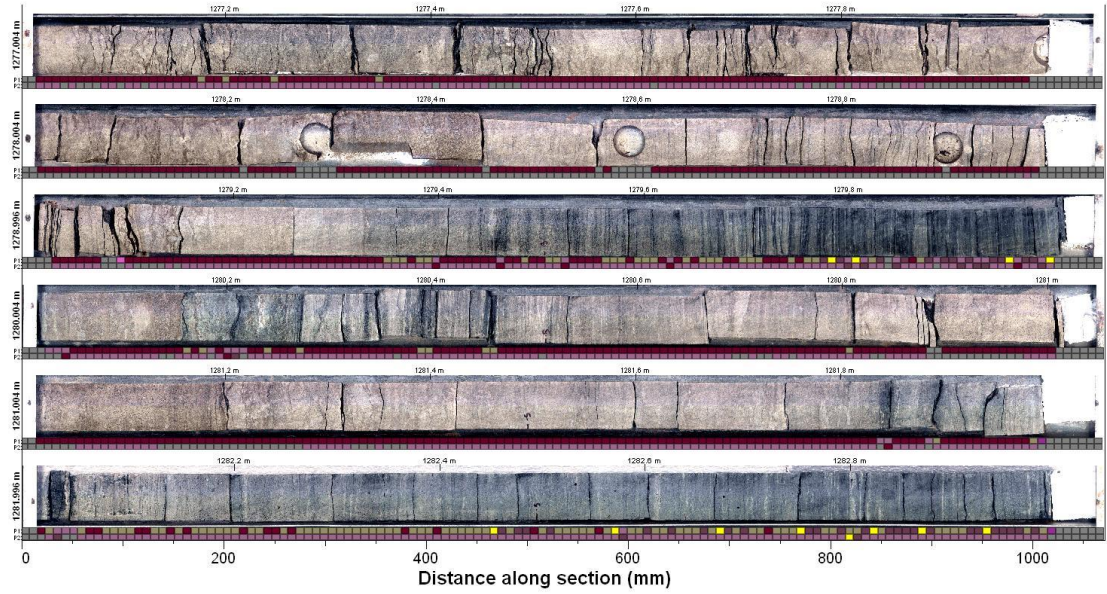
### Looma1 Tray 2, 1265 to 1271 m



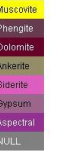
### Looma1 Tray 3, 1271 to 1277 m



### Looma1 Tray 4, 1277 to 1283 m



#### Plot1



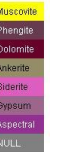
#### Plot2



### Looma1 Tray 5, 1283 to 1289 m



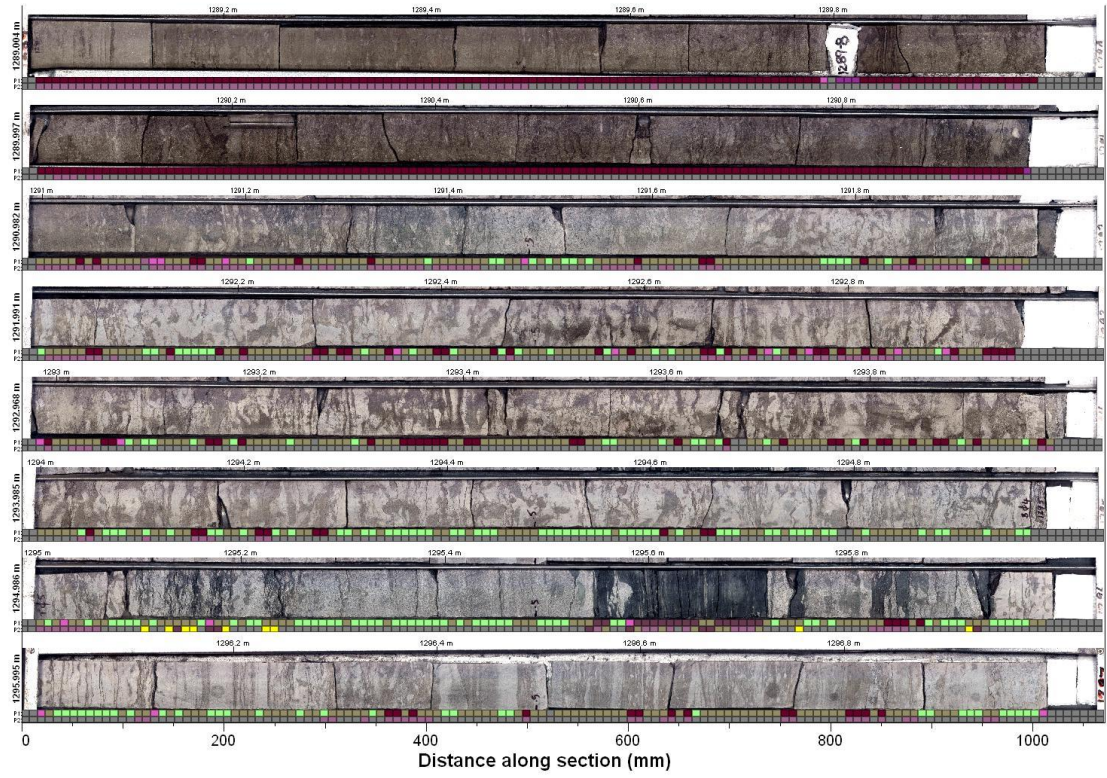
#### Plot1



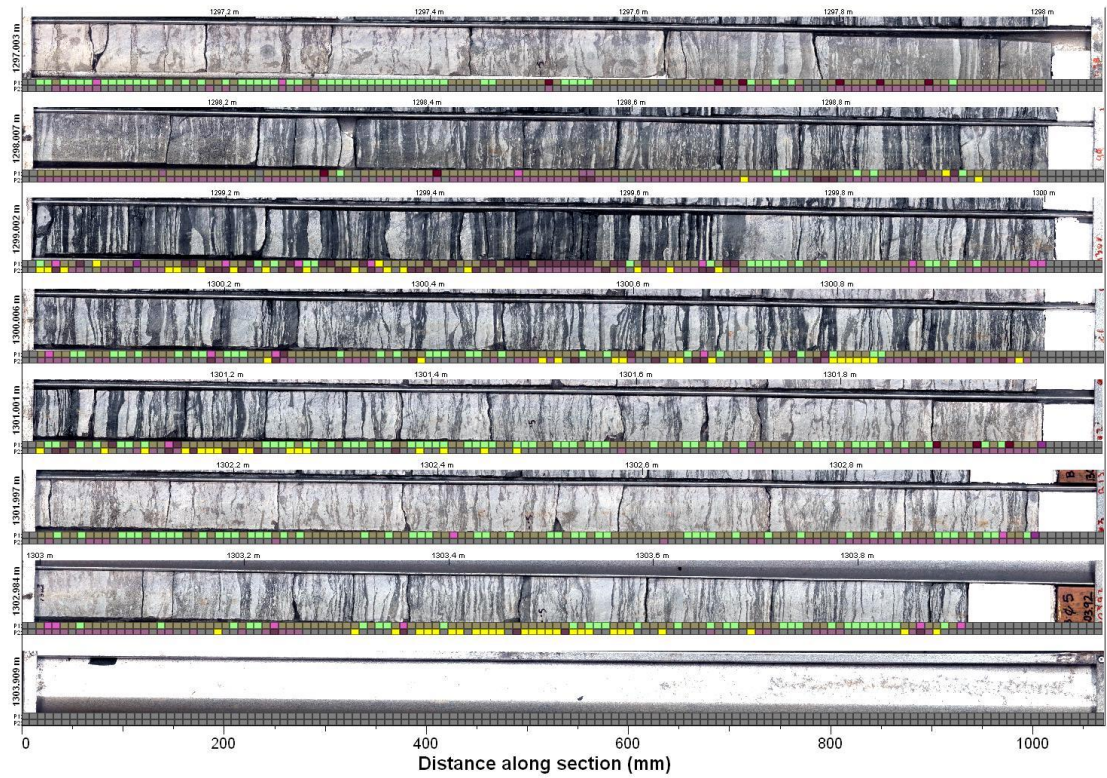
#### Plot2



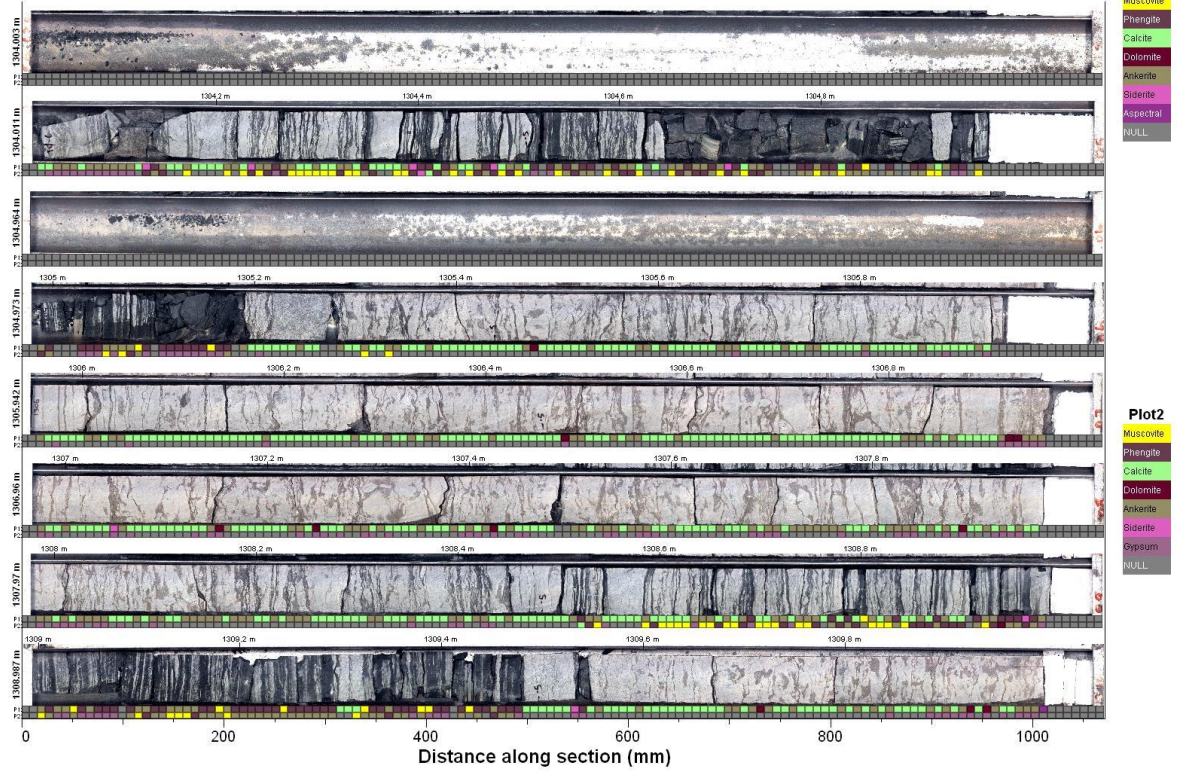
### Looma1 Tray 6, 1289 to 1297 m



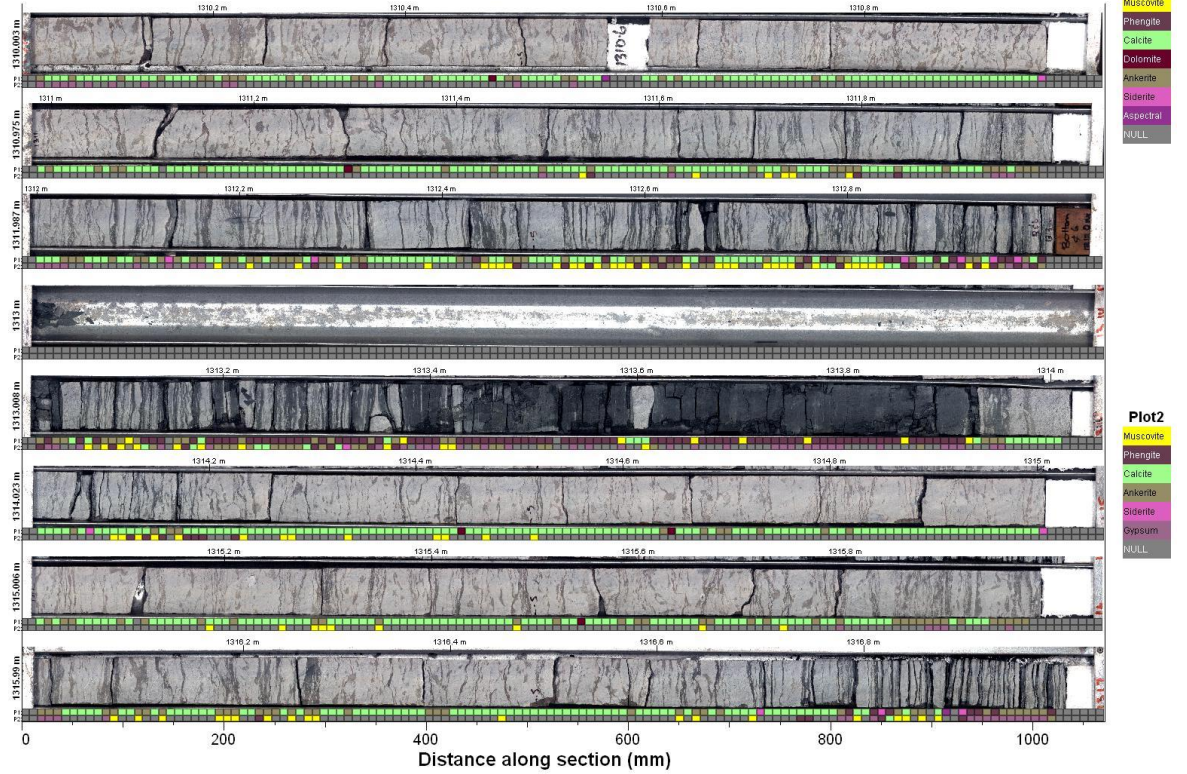
### Looma1 Tray 7, 1297 to 1303.9 m



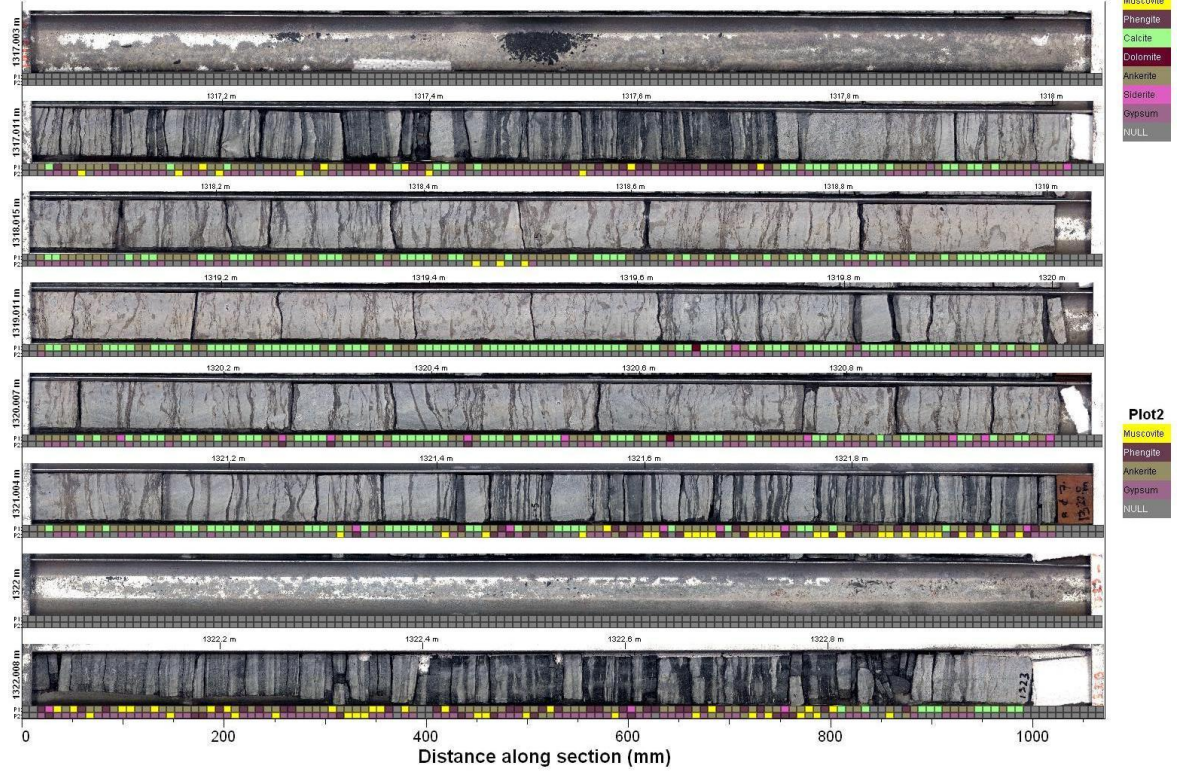
### Looma1 Tray 8, 1304 to 1310 m



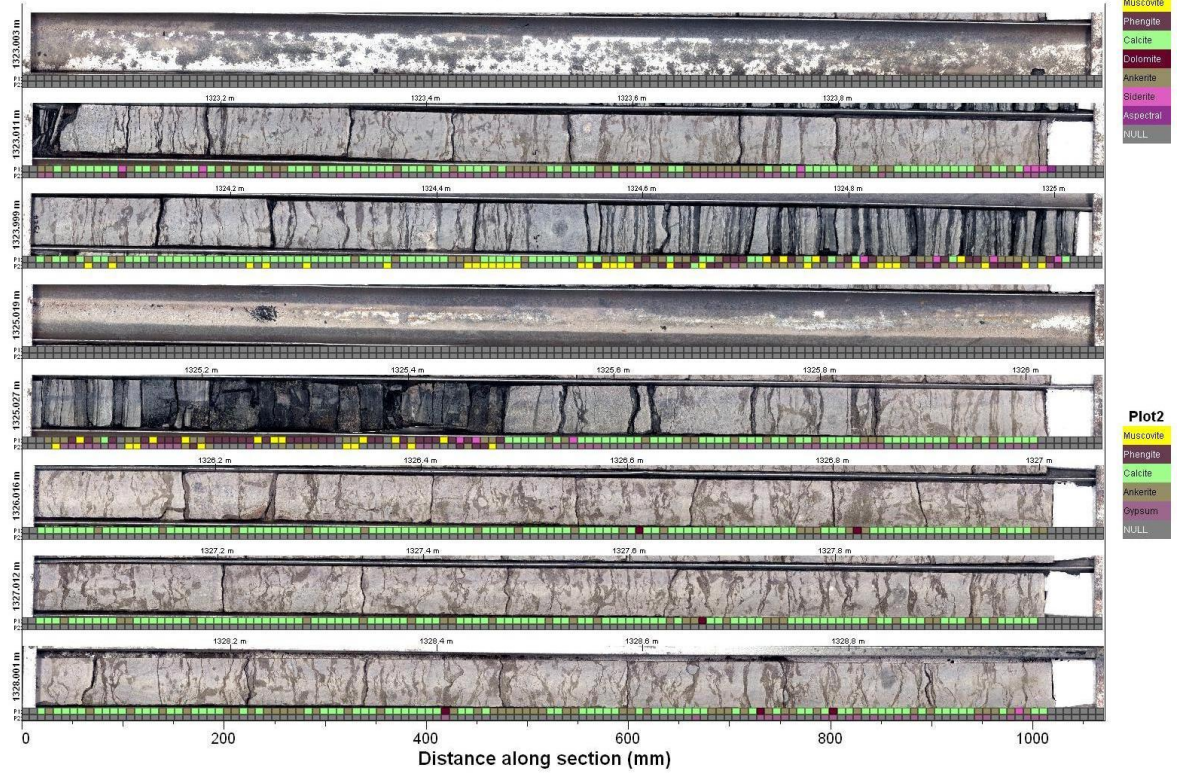
### Looma1 Tray 9, 1310 to 1317 m



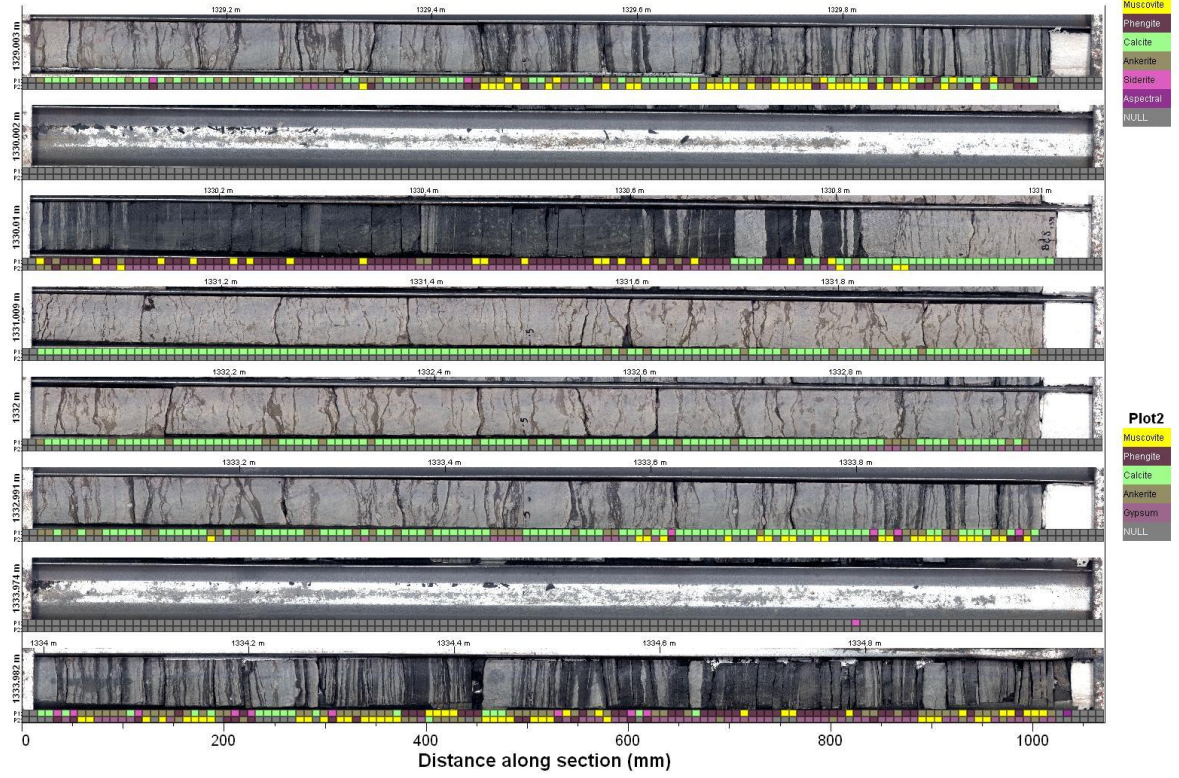
### Looma1 Tray 10, 1317 to 1323 m



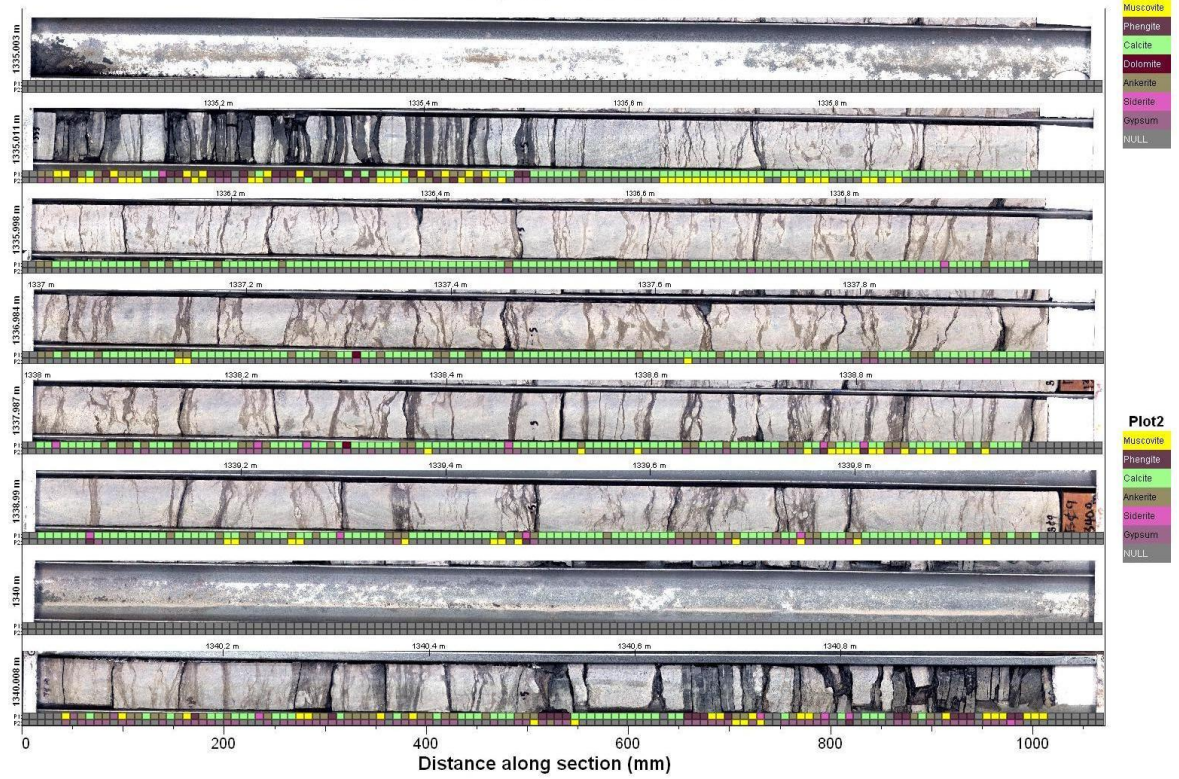
### Looma1 Tray 11, 1323 to 1329 m



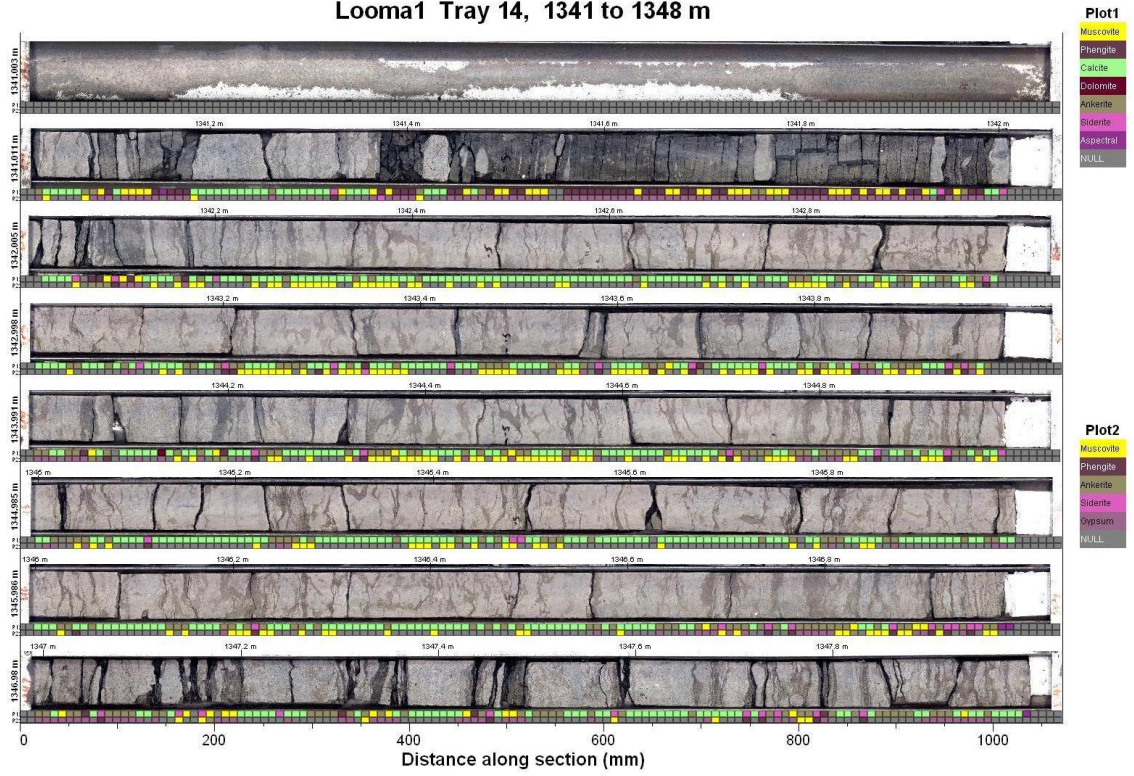
### Looma1 Tray 12, 1329 to 1335 m



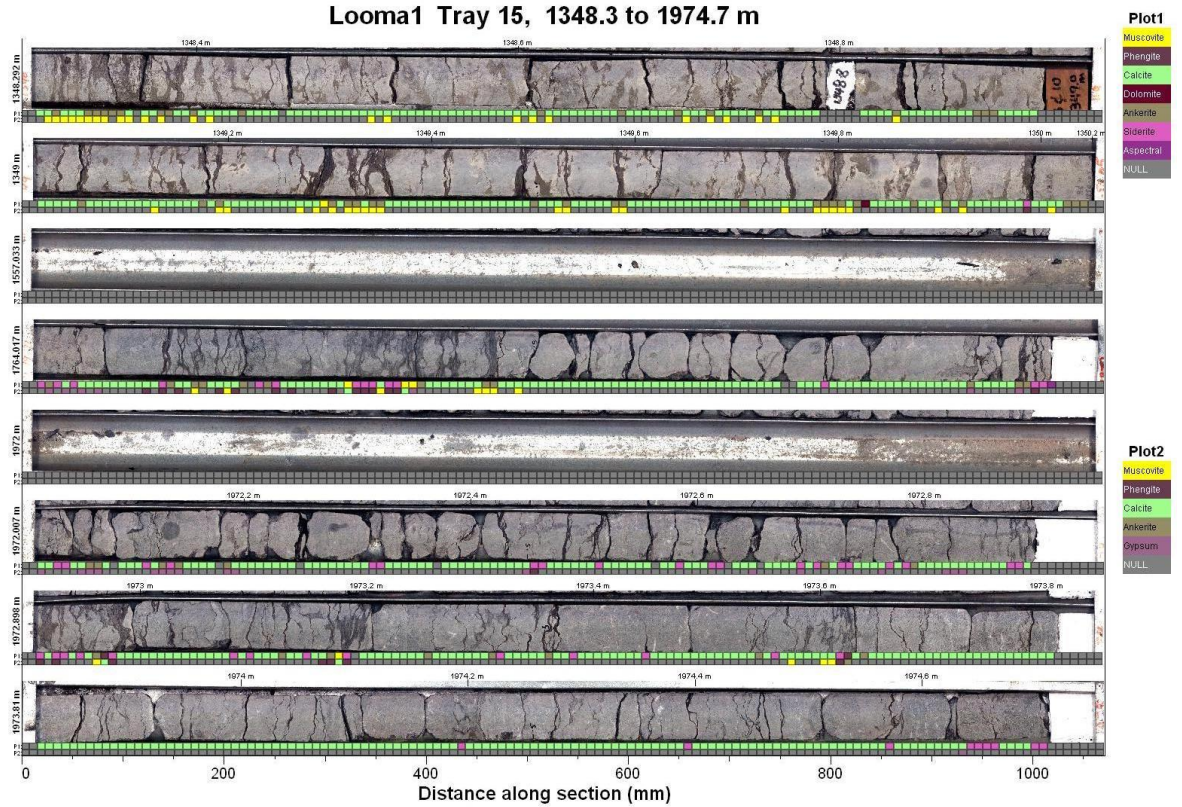
### Looma1 Tray 13, 1335 to 1341 m



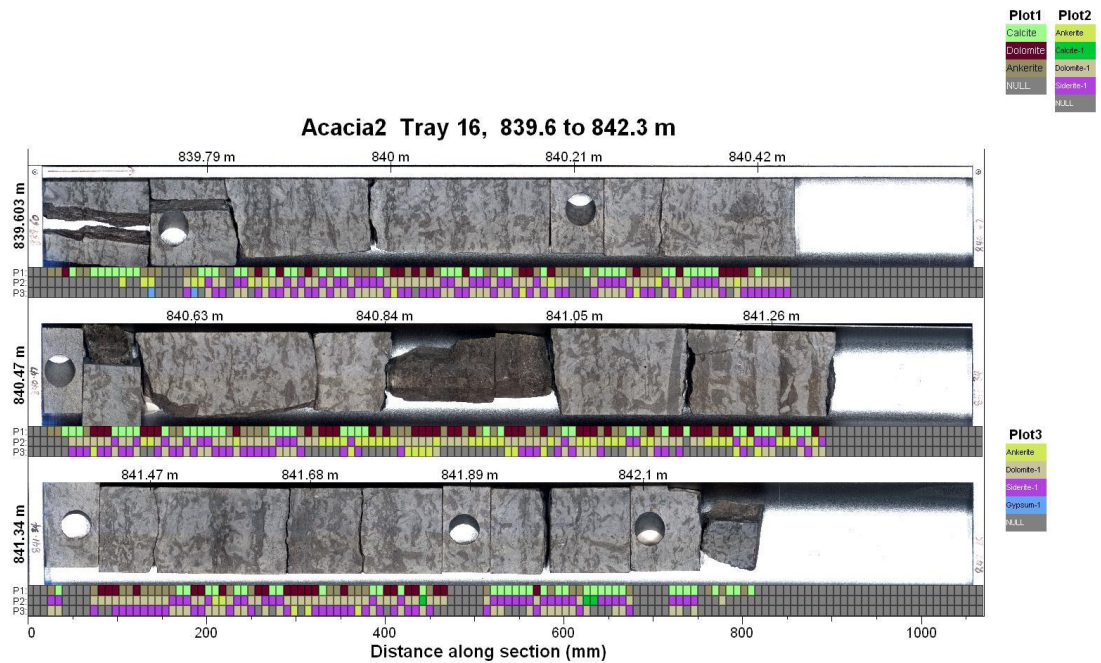
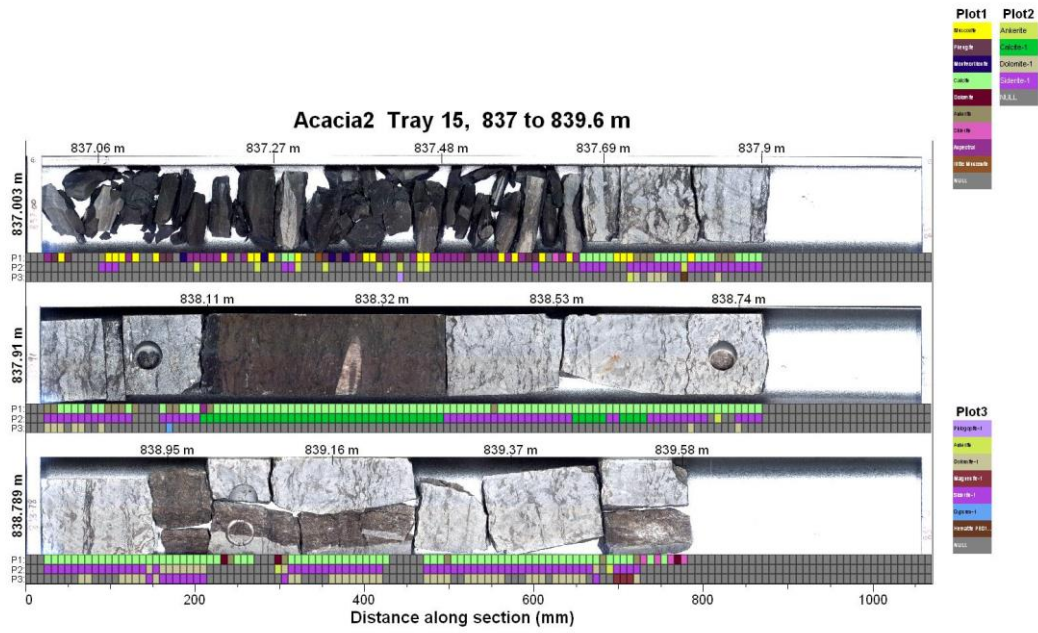
### Looma1 Tray 14, 1341 to 1348 m

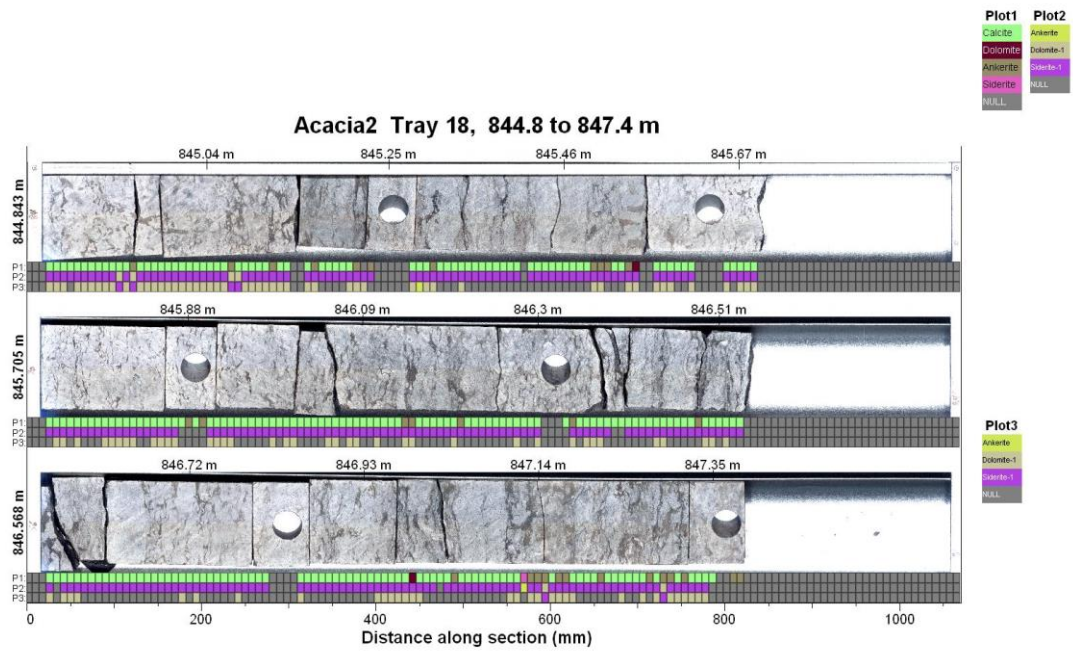
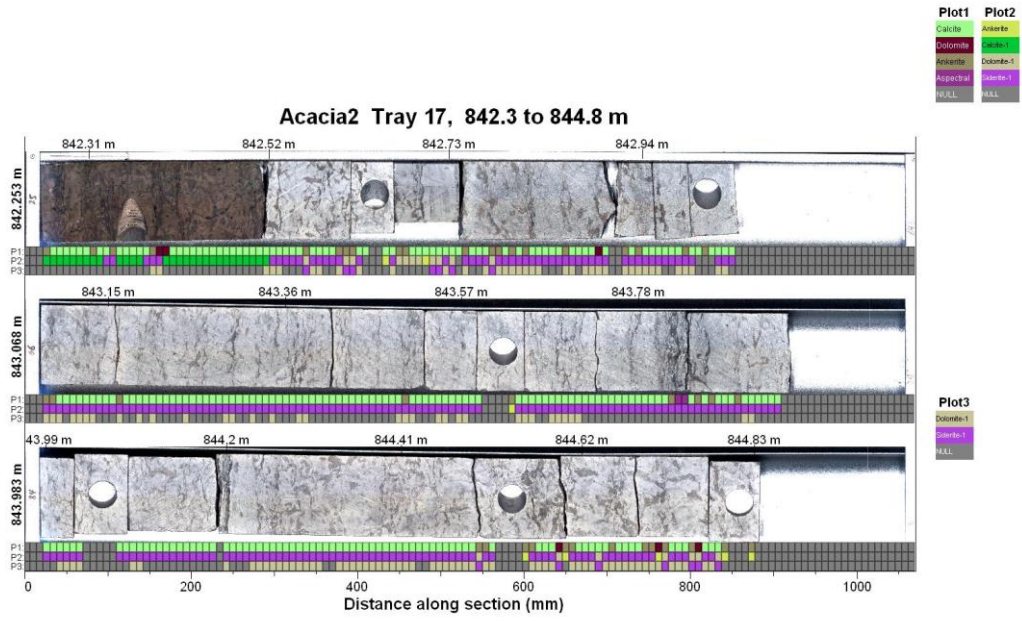


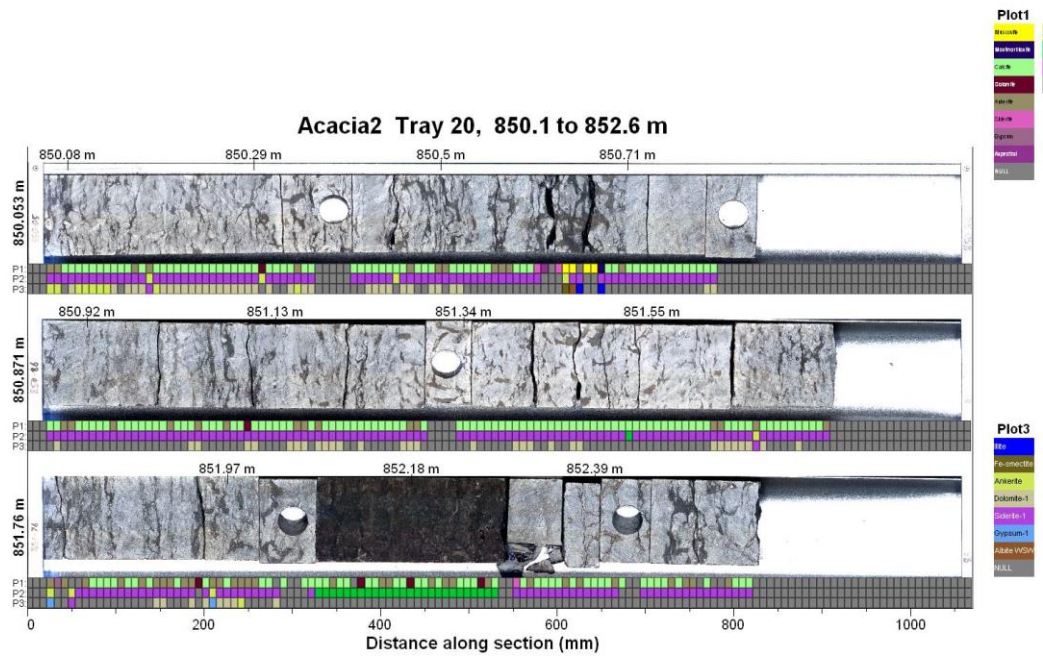
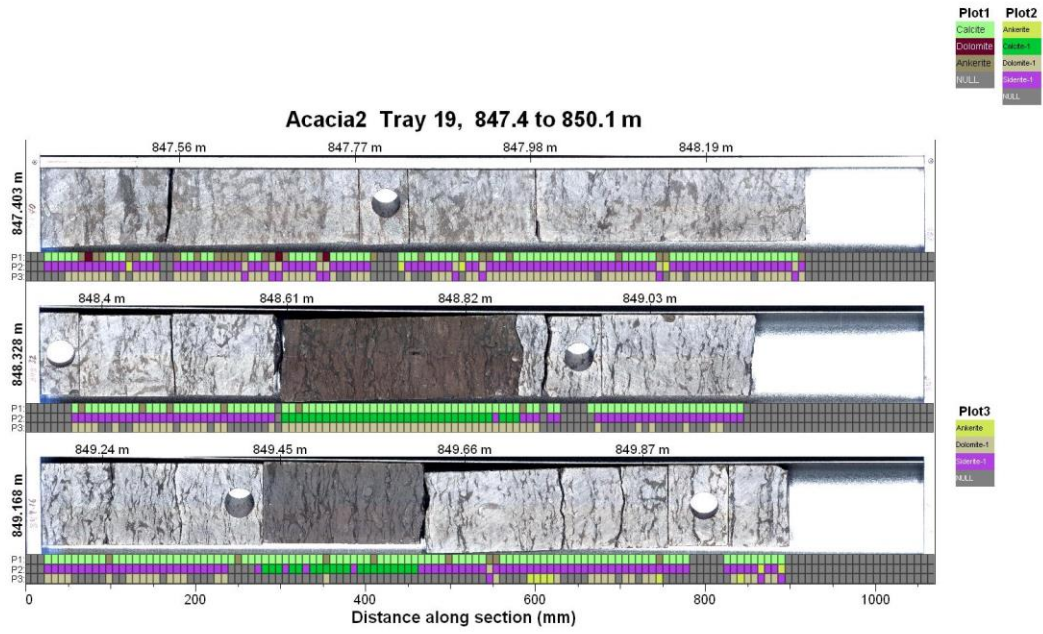
### Looma1 Tray 15, 1348.3 to 1974.7 m

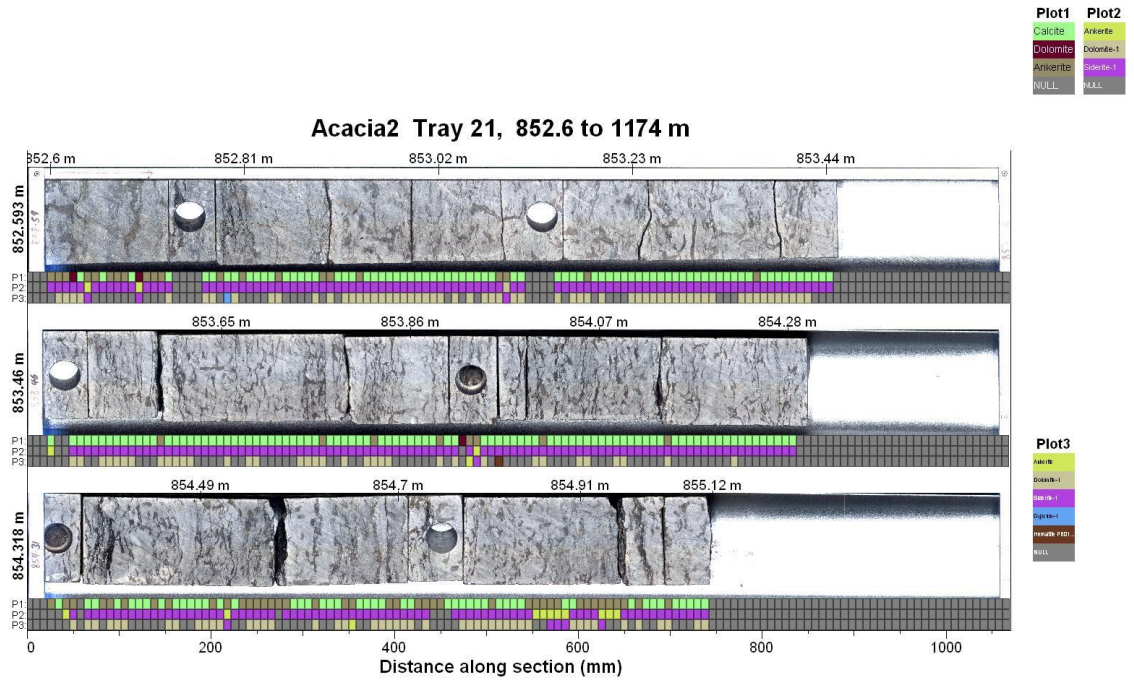


## Well Acacia 2: Goldwyer Formation, part of Unit 3 (837-855.12m)

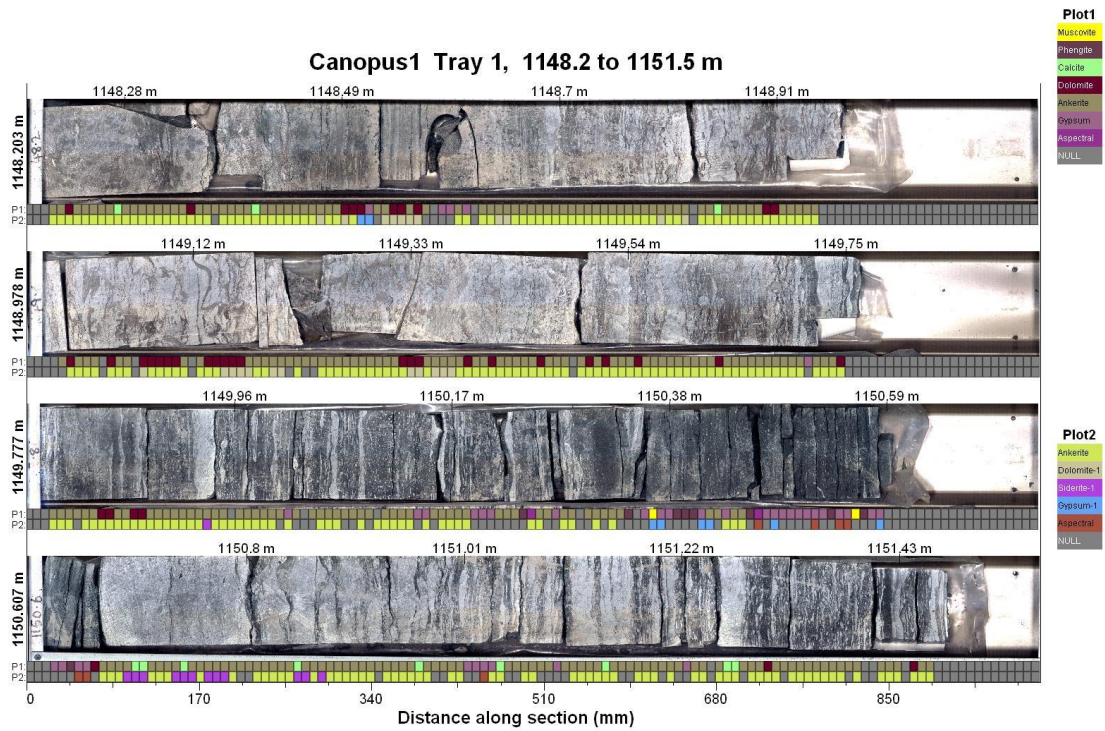


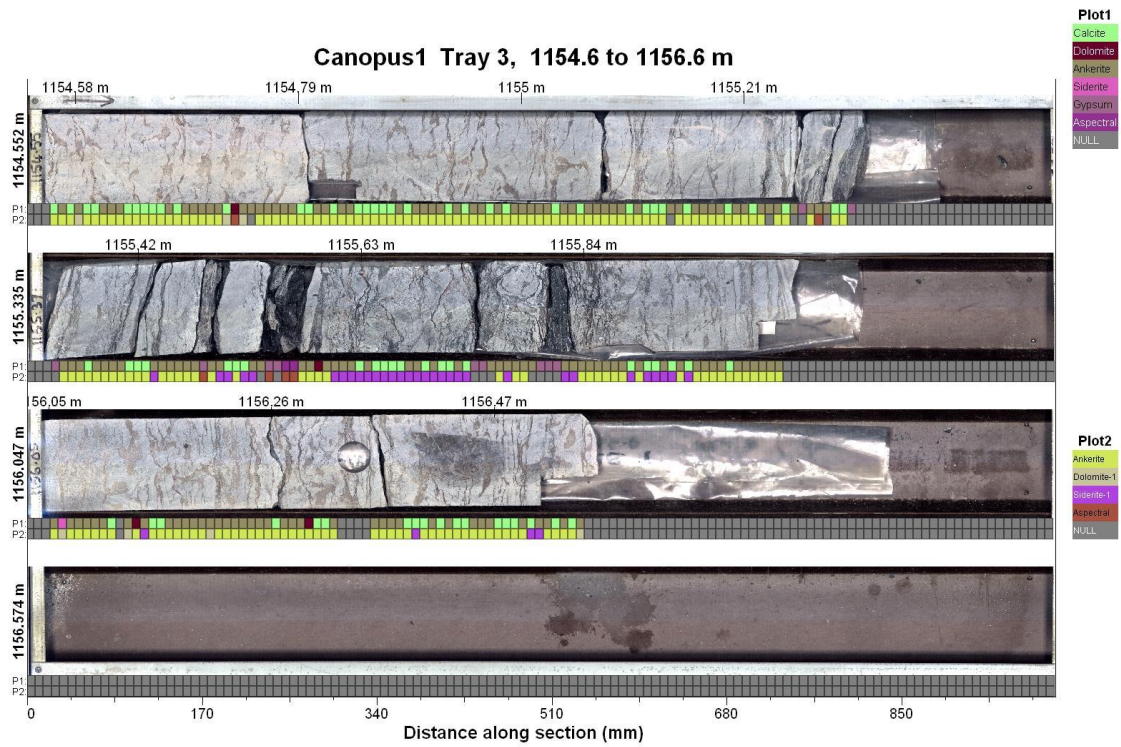
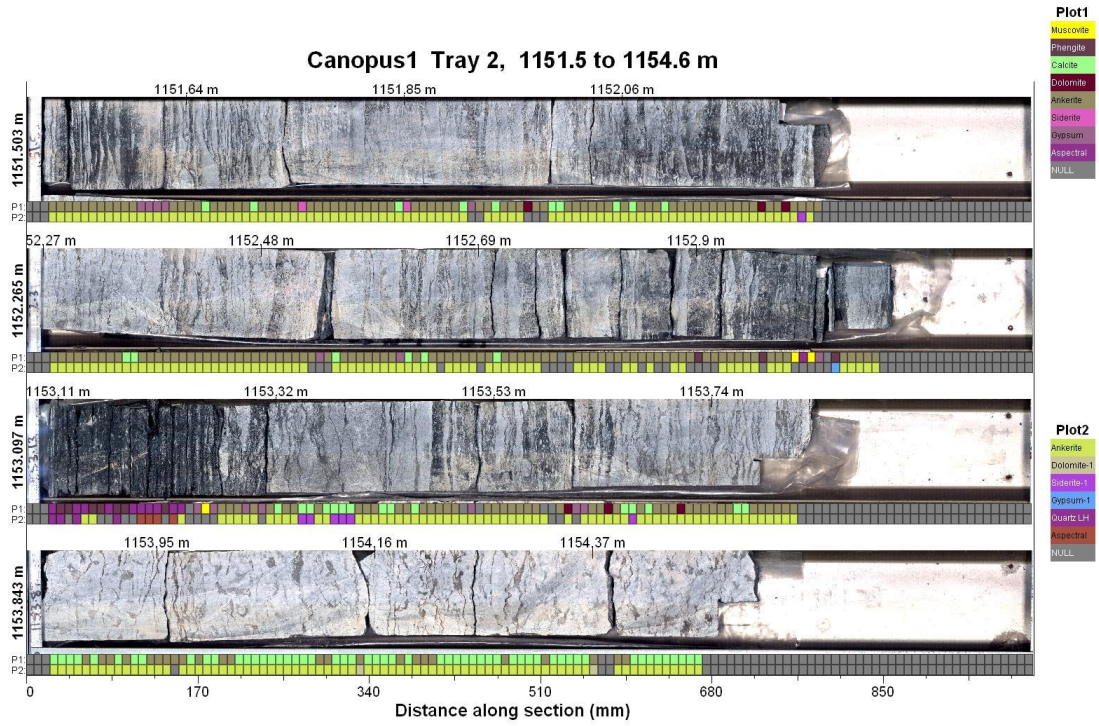




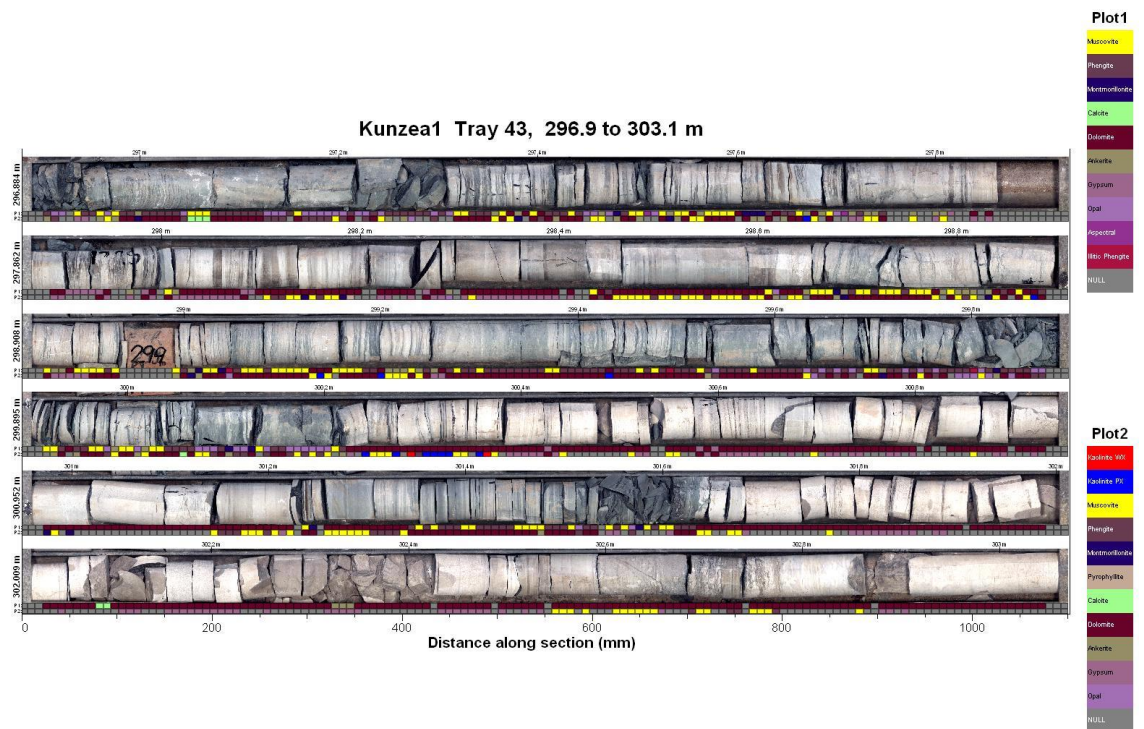
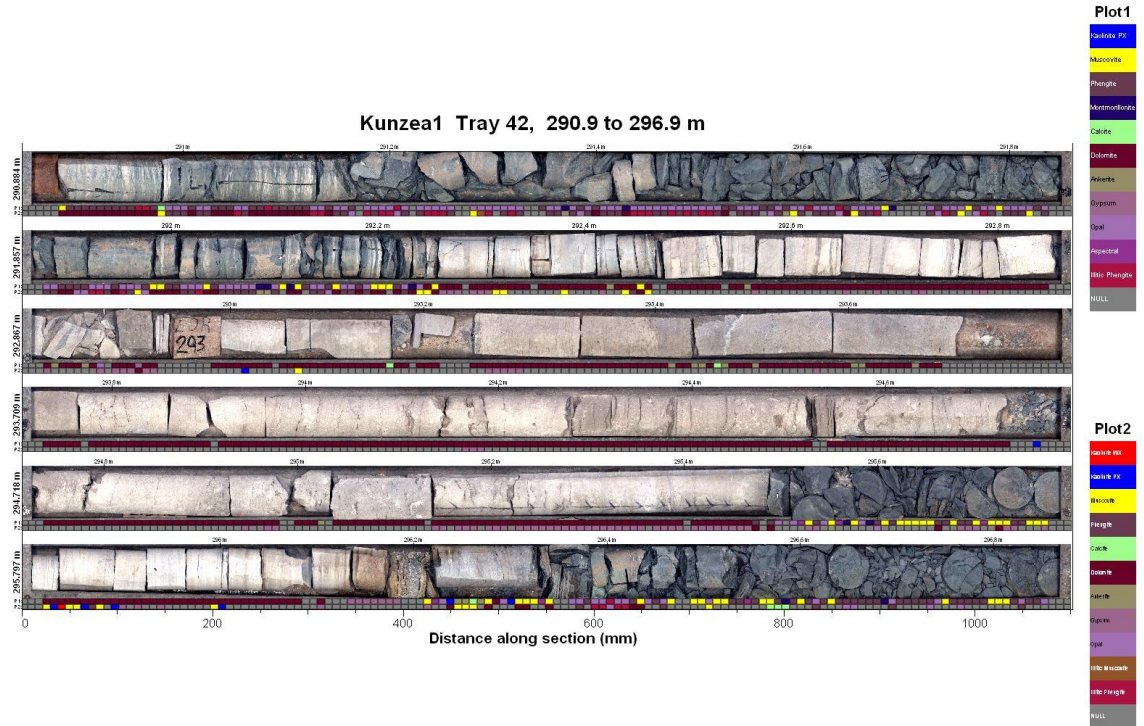


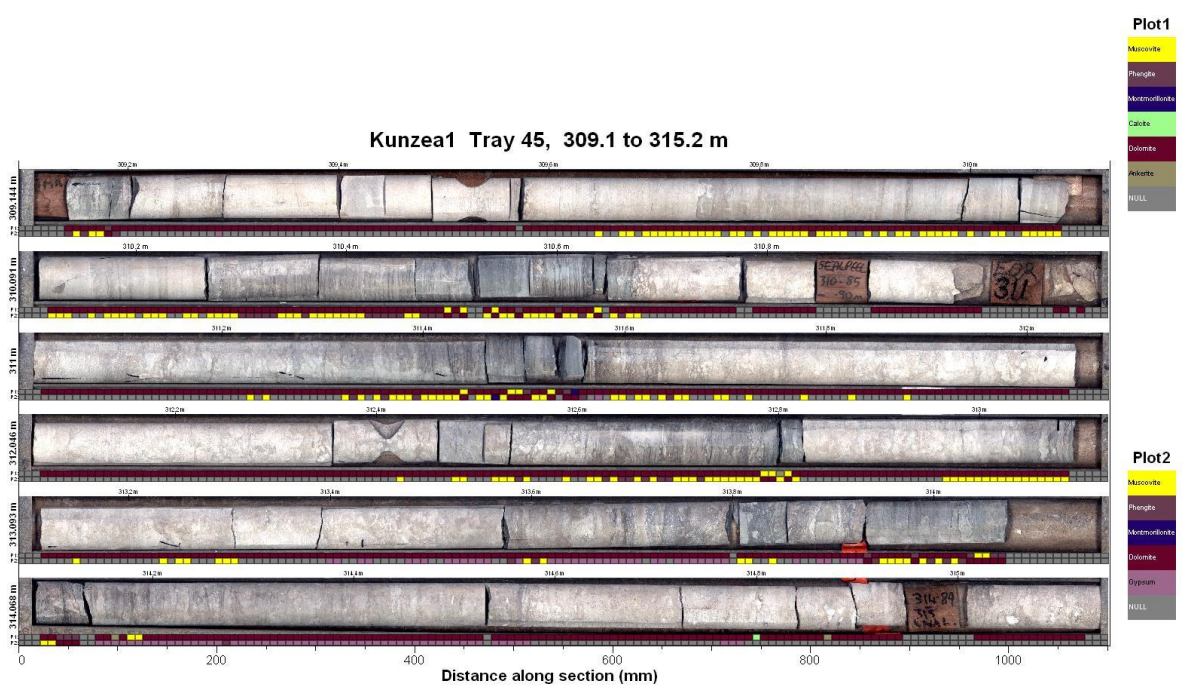
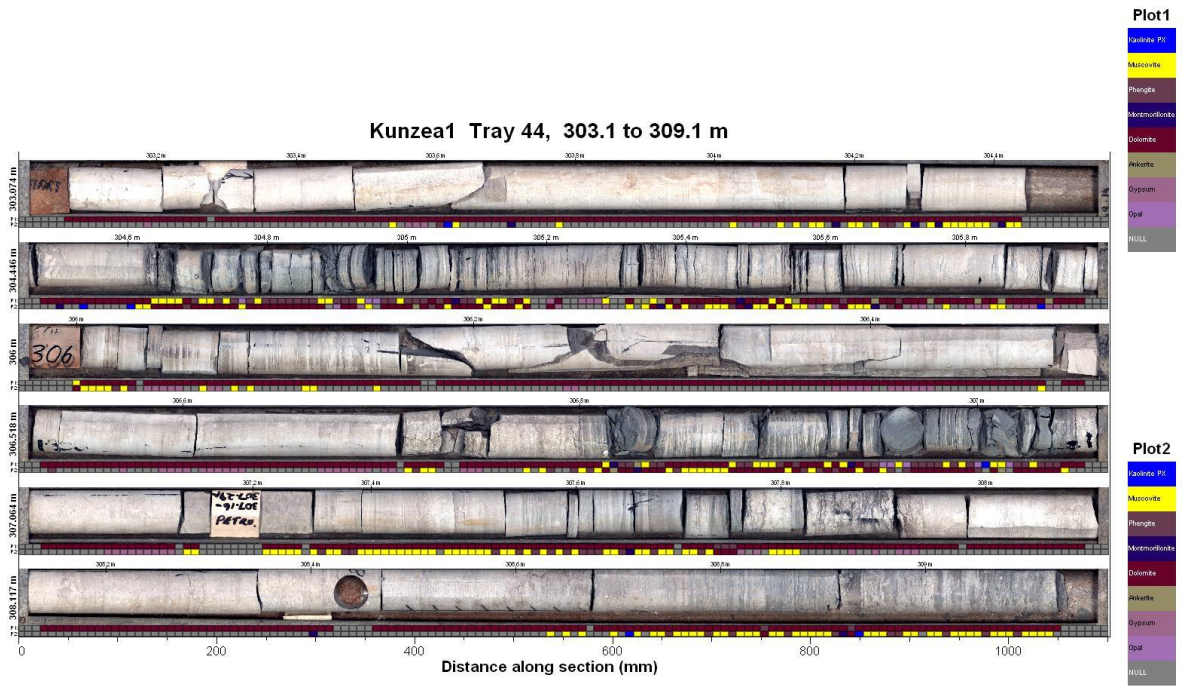
**Well Canopus 1: part of Nita Formation Leo Member (1148.2-1156.6m)**



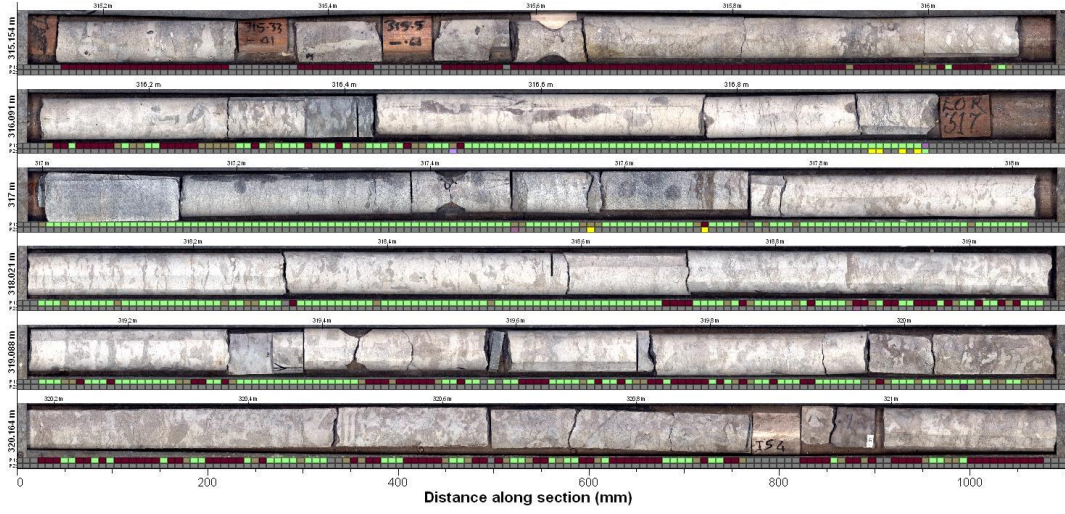


**Well Kunzea 1: Nita Formation Cudalgarra Member (292-315m), Nita Formation Leo Member (315-350m), Goldwyer Unit 4 (350-400m) and Goldwyer Unit 3 (400-450m)**

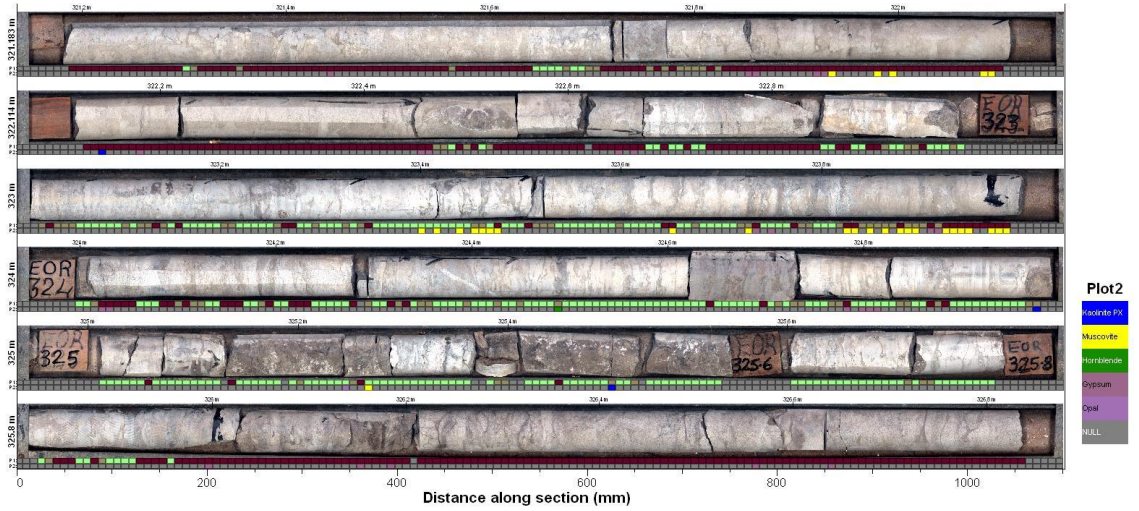




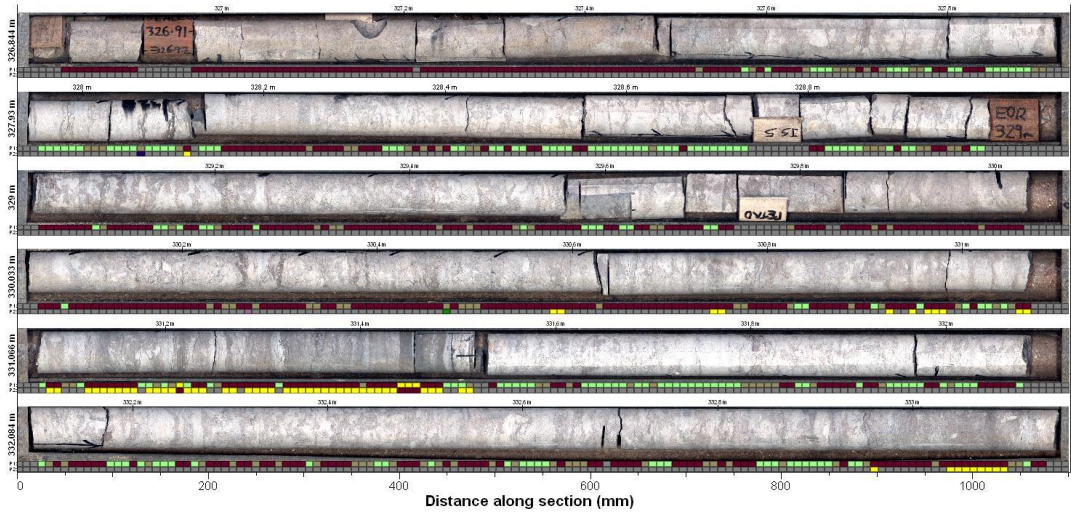
Kunzea1 Tray 46, 315.2 to 321.2 m



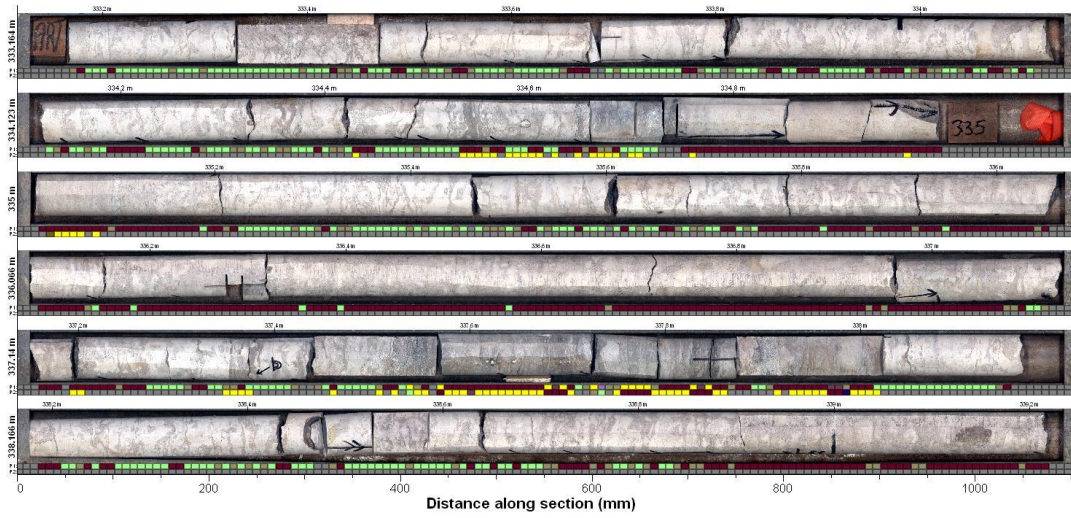
Kunzea1 Tray 47, 321.2 to 326.8 m



Kunzea1 Tray 48, 326.8 to 333.2 m



Kunzea1 Tray 49, 333.2 to 339.2 m



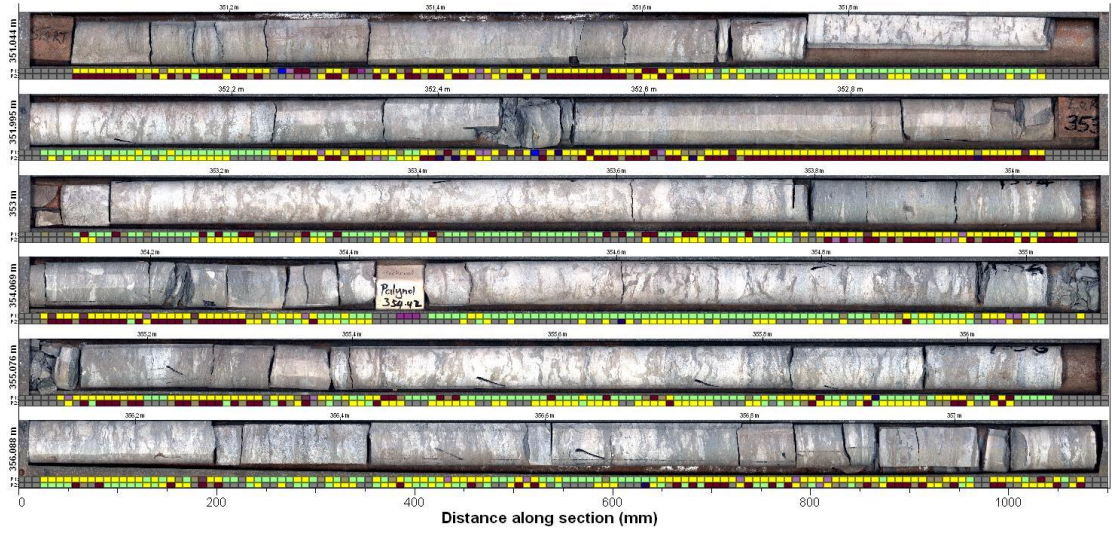
Kunzea1 Tray 50, 339.2 to 345.2 m



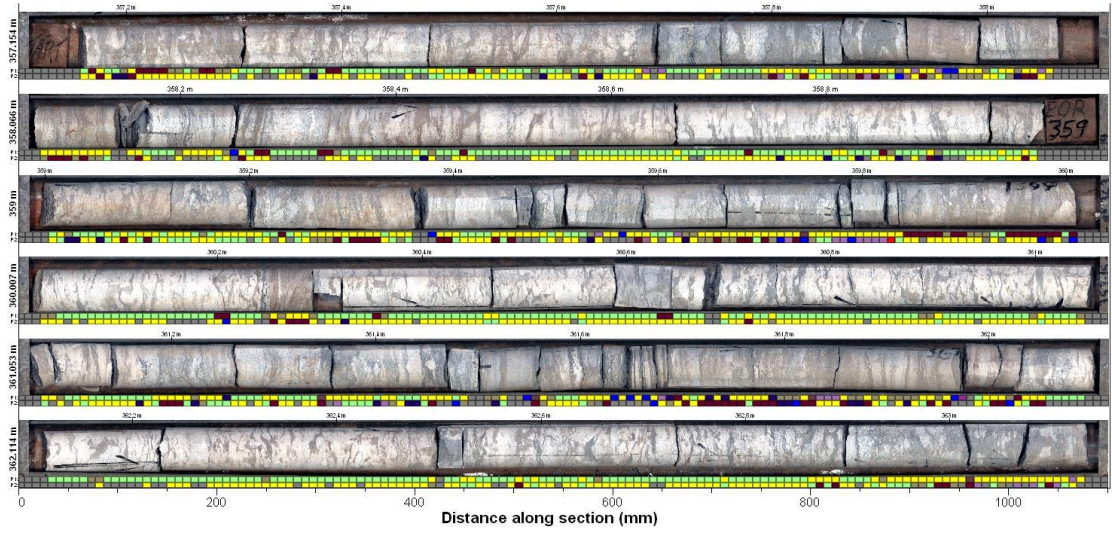
Kunzea1 Tray 51, 345.2 to 351 m



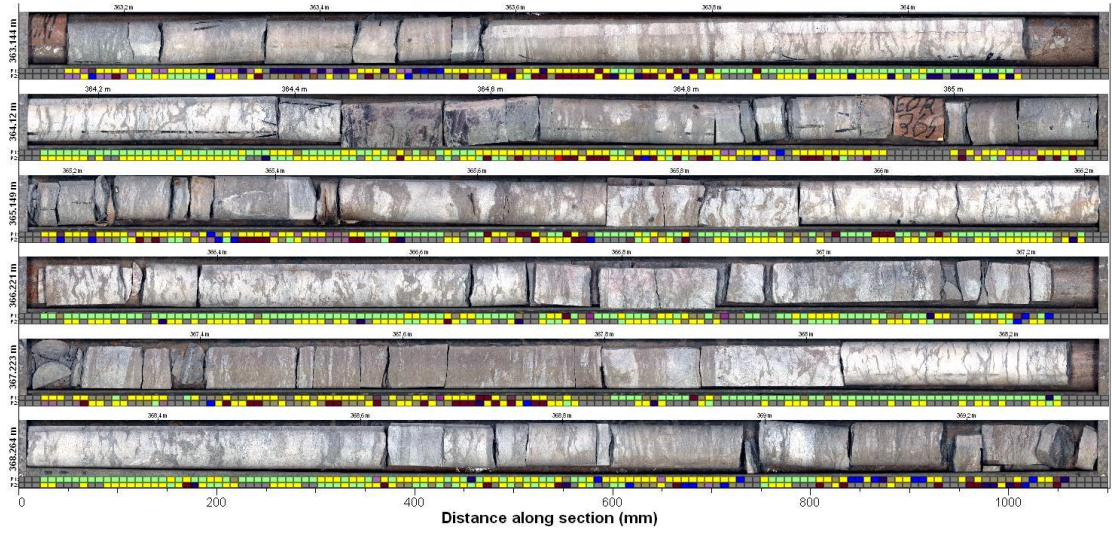
Kunzea1 Tray 52, 351 to 357.2 m



Kunzea1 Tray 53, 357.2 to 363.1 m



Kunzea1 Tray 54, 363.1 to 369.3 m



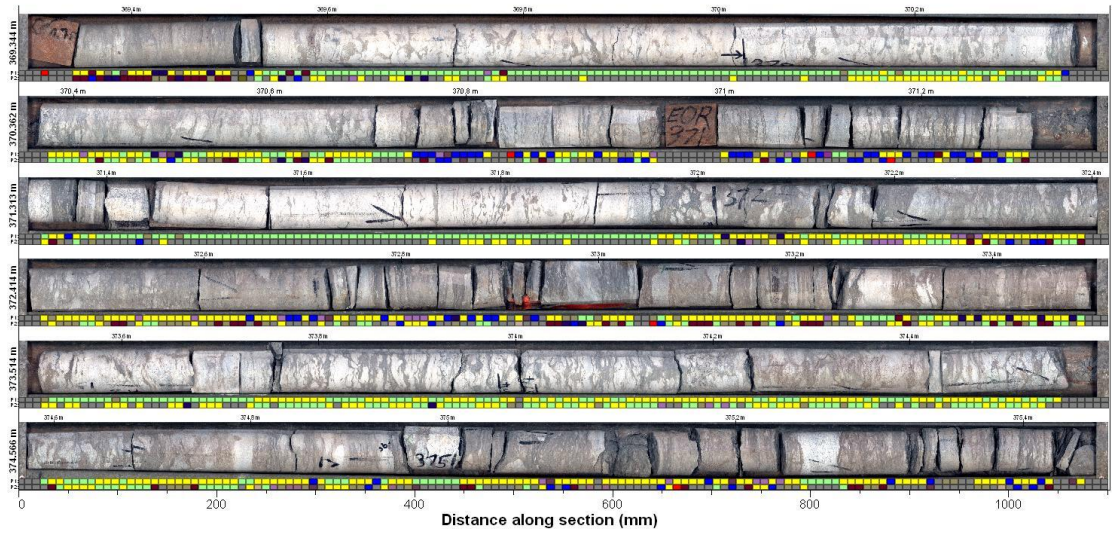
Plot1



Plot2



Kunzea1 Tray 55, 369.3 to 375.5 m



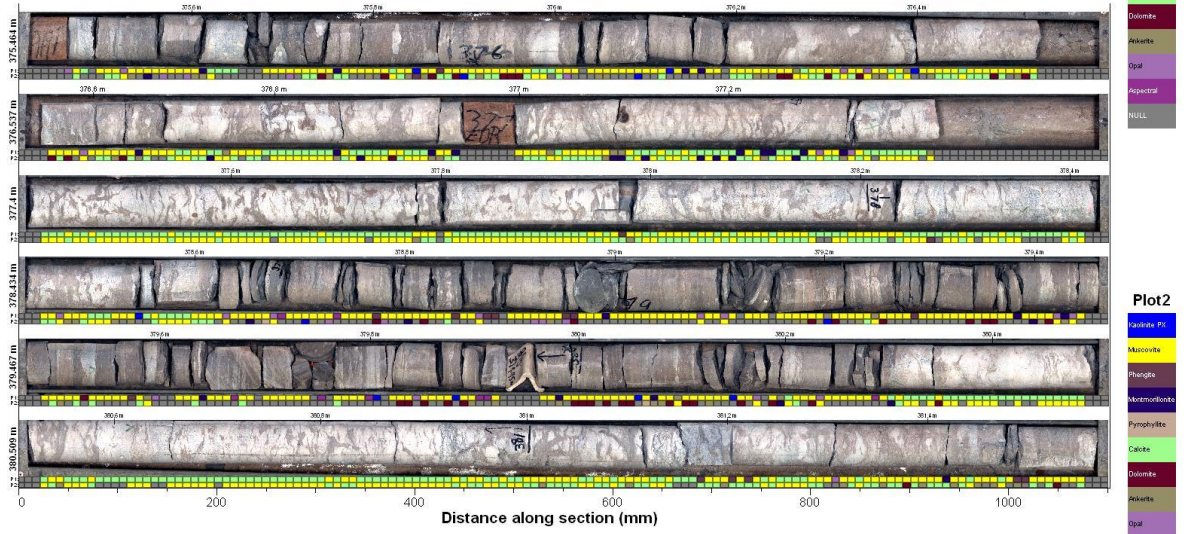
Plot1



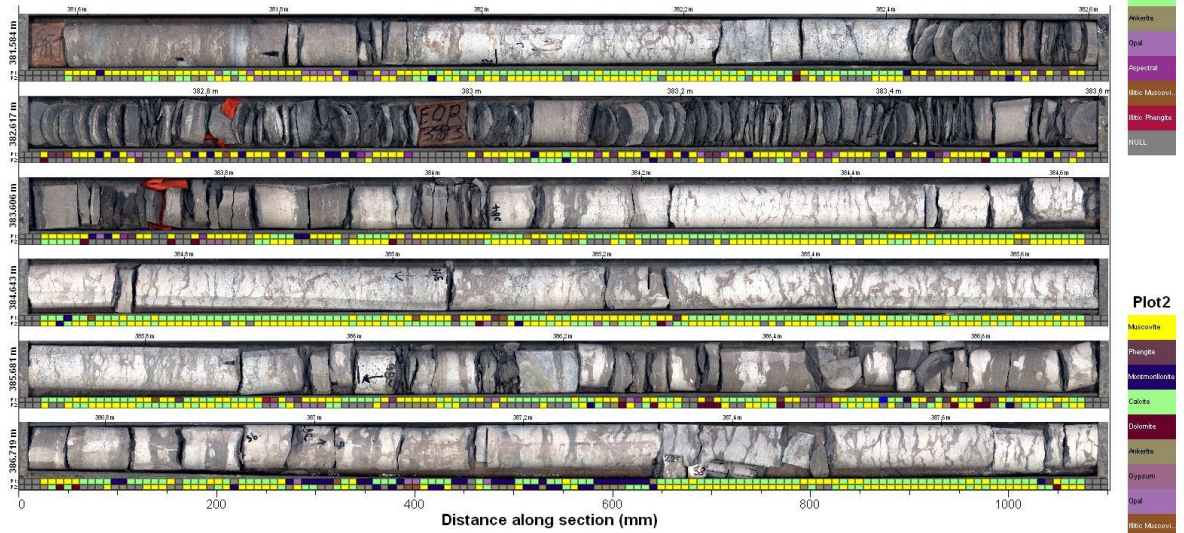
Plot2



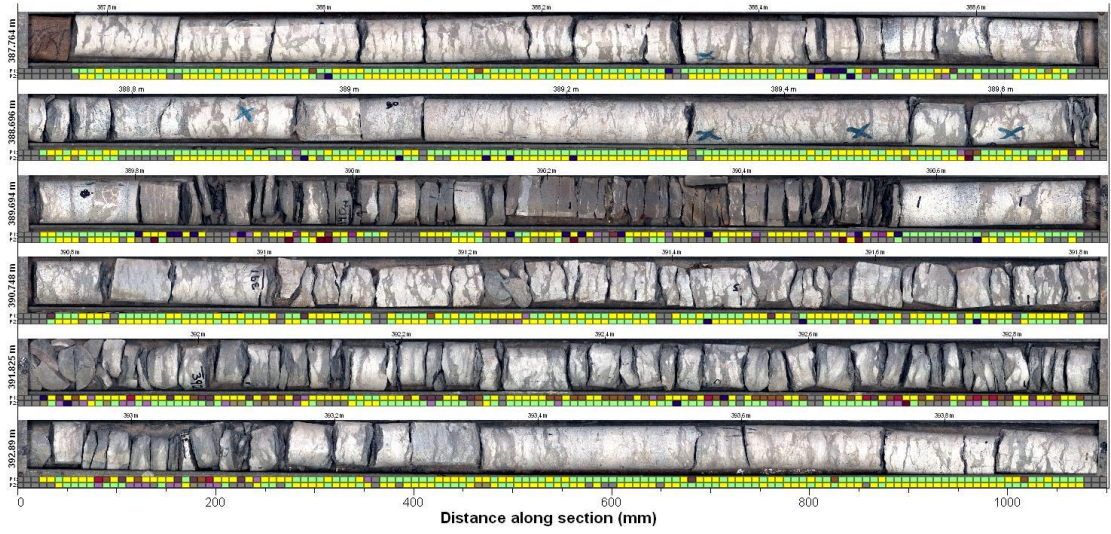
Kunzea1 Tray 56, 375.5 to 381.6 m



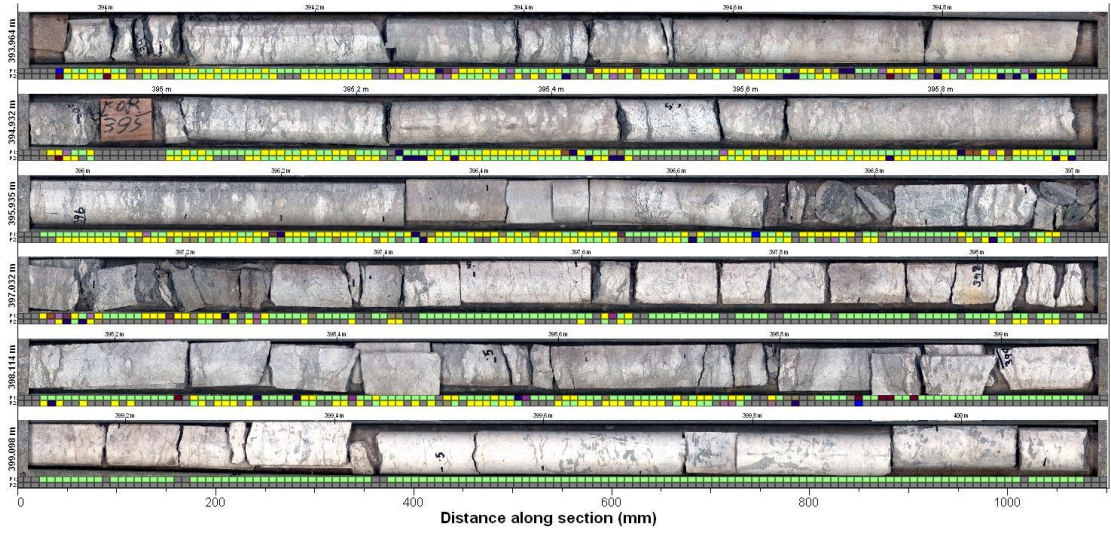
Kunzea1 Tray 57, 381.6 to 387.8 m



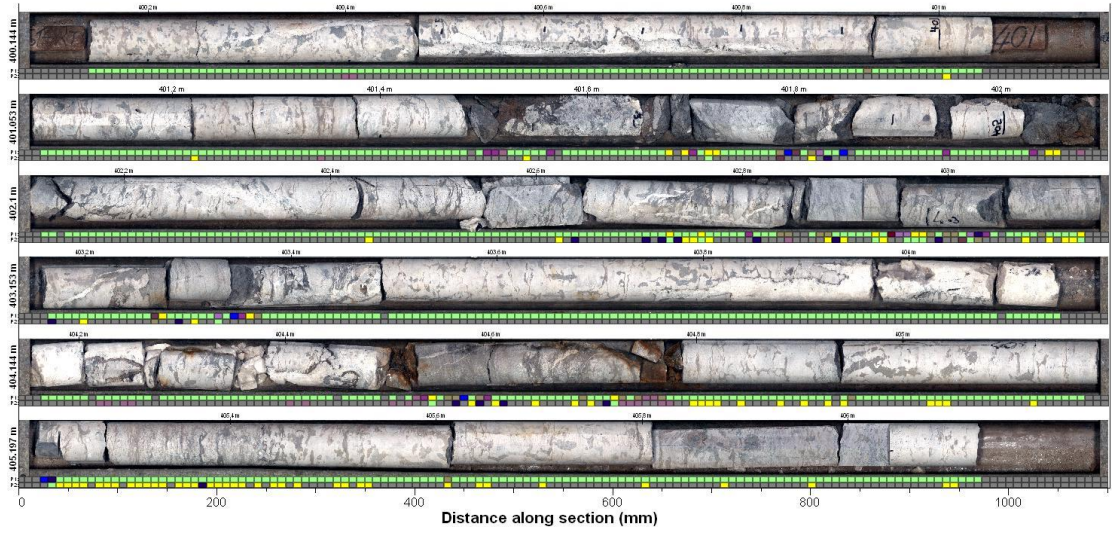
Kunzea1 Tray 58, 387.8 to 394 m



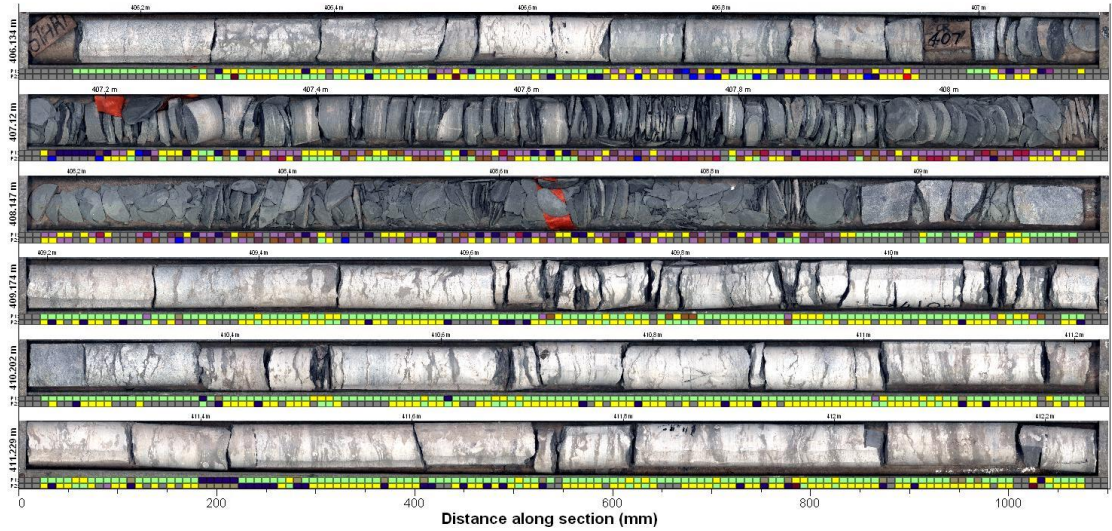
Kunzea1 Tray 59, 394 to 400.1 m



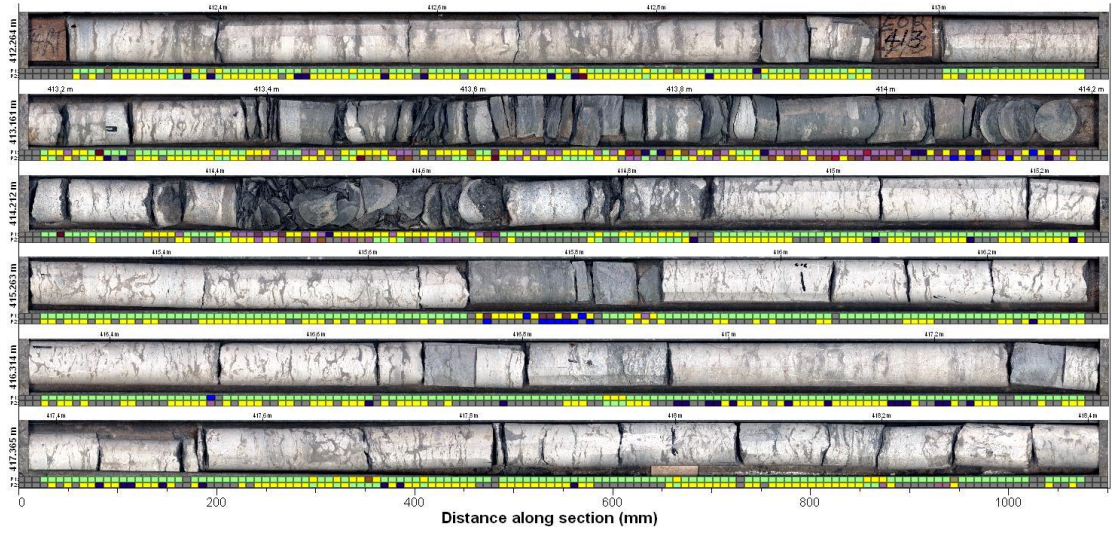
Kunzea1 Tray 60, 400.1 to 406.1 m



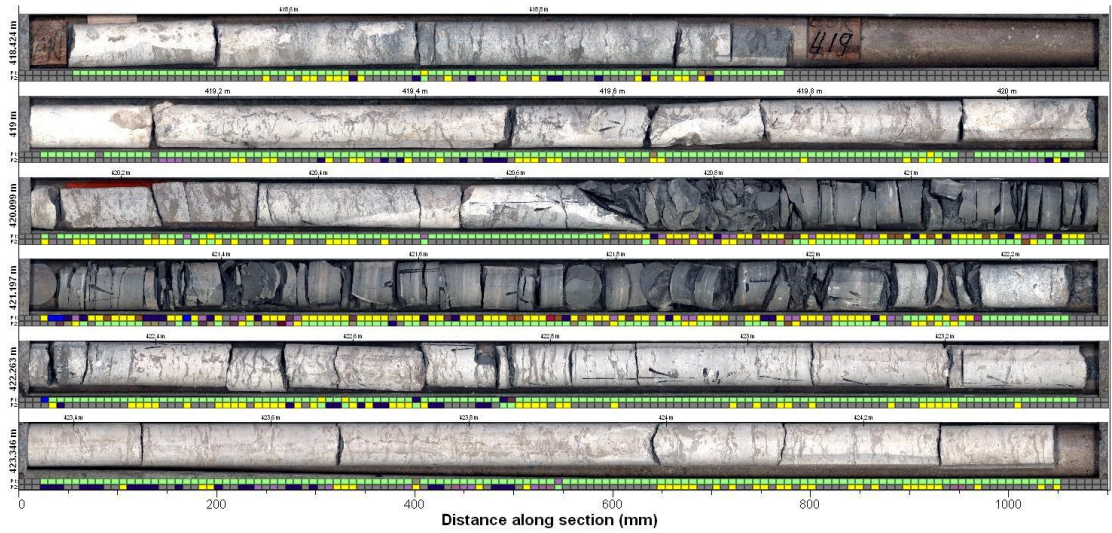
Kunzea1 Tray 61, 406.1 to 412.3 m



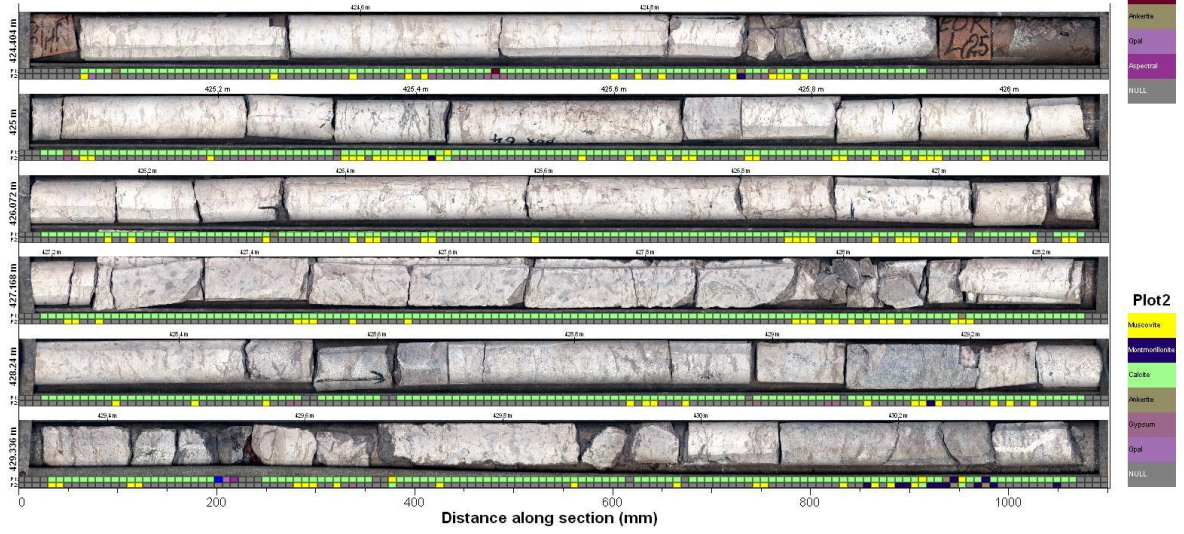
Kunzea1 Tray 62, 412.3 to 418.4 m



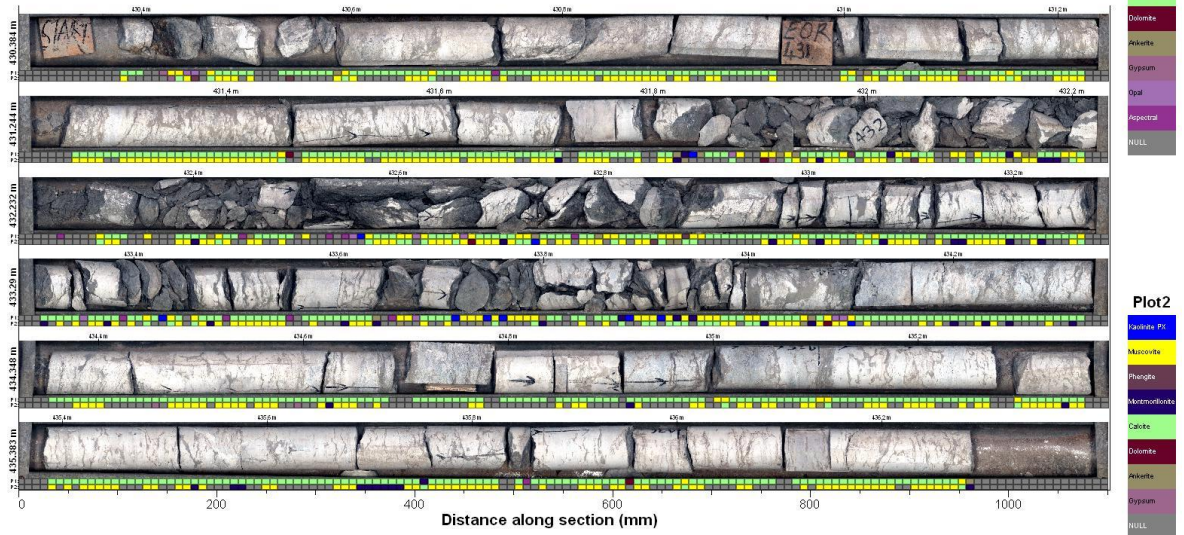
Kunzea1 Tray 63, 418.4 to 424.4 m



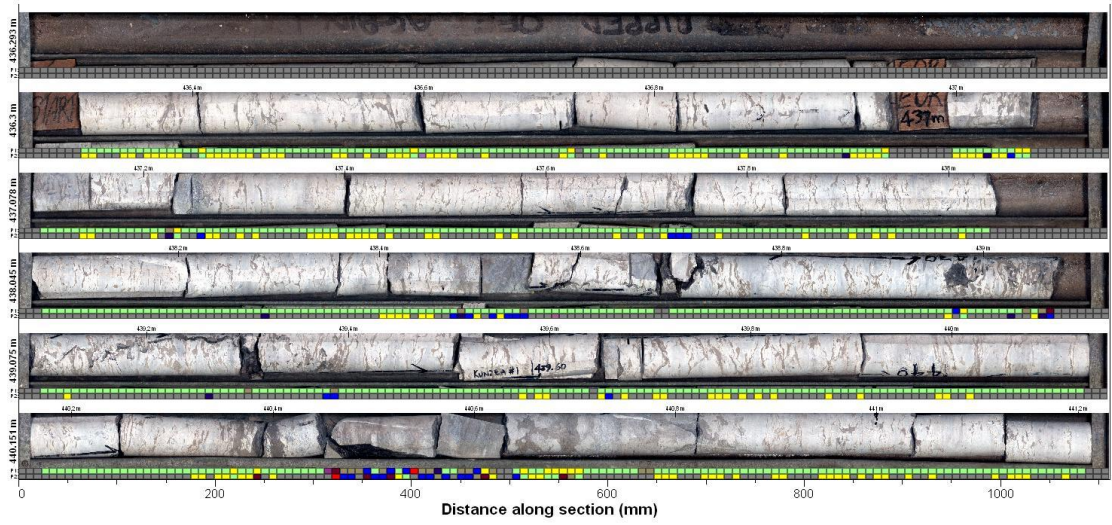
Kunzea1 Tray 64, 424.4 to 430.4 m



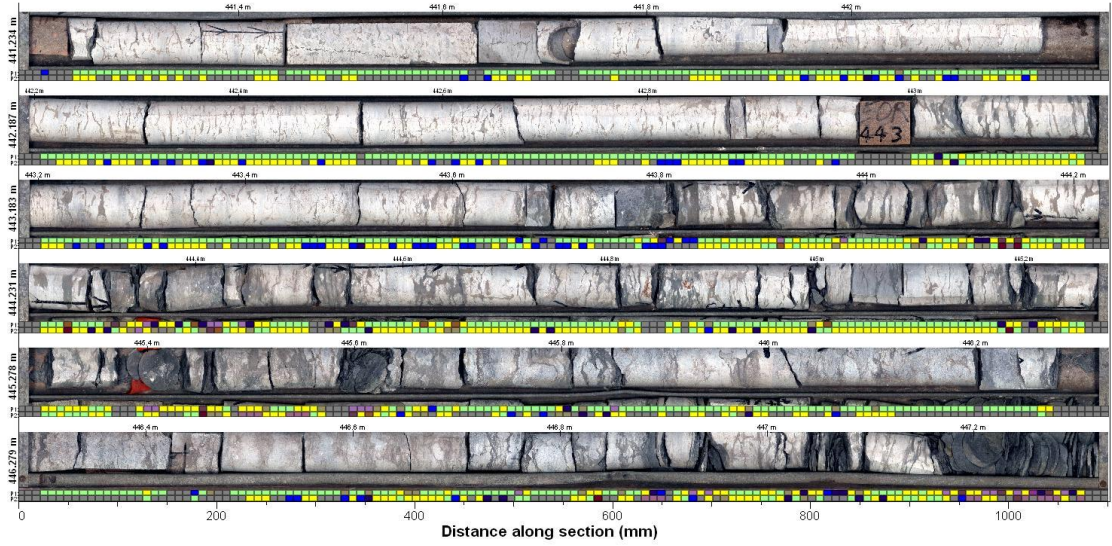
Kunzea1 Tray 65, 430.4 to 436.3 m



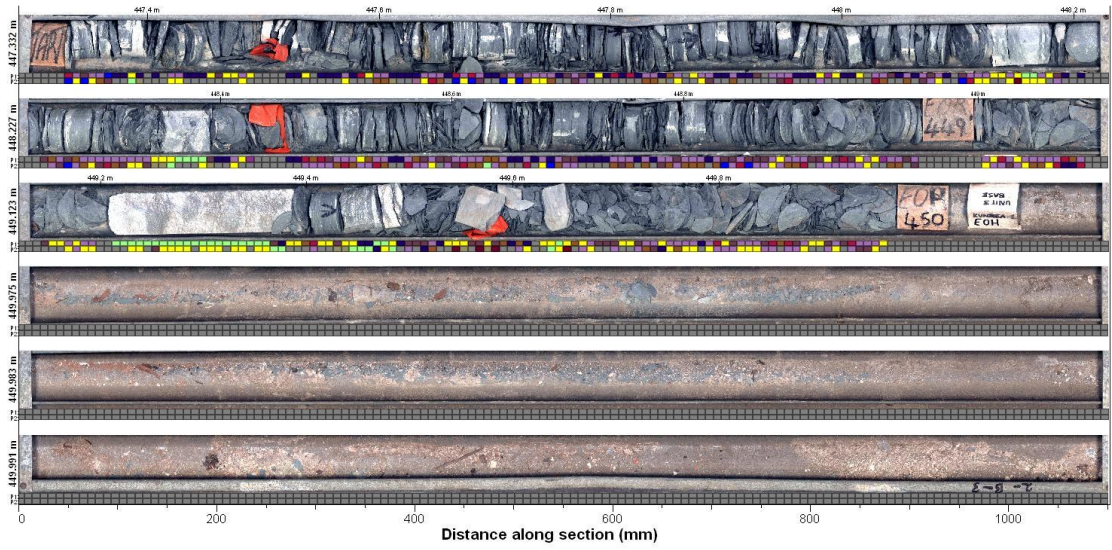
Kunzea1 Tray 66, 436.3 to 441.2 m



Kunzea1 Tray 67, 441.2 to 447.3 m



Kunzea1 Tray 68, 447.3 to 450 m



Plot1

- Caolinite PS
- Muscovite
- Phengite
- Mortmoreite
- Calcite
- Opal
- Pyroctral
- Basic Muscovite
- Basic Phengite
- NULL

Plot2

- Caolinite PS
- Muscovite
- Phengite
- Mortmoreite
- Calcite
- Dolomite
- Pyrite
- Gypsum
- Opal
- Basic Muscovite
- Basic Phengite
- NULL

## APPENDIX 2

### LIST OF WELL COMPLETION REPORTS

#### Well completion reports used in this study:

Johnson, N.E.A. 1968. Blackstone No. 1 well completion report. West Australian Petroleum Pty. Limited.

Phipps, J., Trupp, M. and Nosiara, M. 1998. Looma 1 well completion report (EP 353). Shell Development (Australia) Pty. Ltd.

Butcher, B. 1982. Canopus 1 well completion report (Permit EP 175). Getty oil Development Co. Ltd.

Command Petroleum N.L. 1989. Frankenstein 1 final well report (EP 232). Command Petroleum N.L.

Bentley, J. 1982. Carina 1 well completion report (Permit EP 175). Getty oil Development Co. Ltd.

Kufpec Australia Pty. Ltd. 1989. Crystal Creek 1 well completion report (EP 103). Kufpec Australia Pty. Ltd.

Bridge oil Limited. 1988. Antares 1 well completion report (EP 175). Bridge oil Limited.

Johnson, N.E.A. and Thornton, D.A. 2001. Fruitcake 1 combination well completion report (EP 353): composite well log. Hughes and Hughes Australia Pty. Ltd.

Watson, S. and S. Derrington, 1982. Acacia 2 well completion report Canning Basin. Western Mining Corporation Limited, Exploration Division – Petroleum.

Karajas, J. and D. Taylor. 1983. Aquila 1 well completion report. Eagle Corporation Ltd. and Geological Survey Western Australia.

Young, R.J.B. (1972). Barbwire 1 well completion report (EP 43). West Australian Petroleum Pty. Ltd.

McKeller, M.G. 1957. Dampier Downs 1 geological well summary. West Australian Petroleum Pty. Ltd.

Hough, J.K. and R.J. Weeden. 1986. Dodonea 1 well completion report. Western Mining Corporation Limited.

Elliott, R.M. 1959. Goldwyer 1 geological completion report. West Australian Petroleum Pty. Ltd.

Menzel, B. and K. Norlin. 1982. Great Sandy 1 well completion report. Meridian Oil N.L.

Bensimon, S., Klappa, C.F., Hamill, G.S. and H.M. McCaskey. 1985. Hedonia 1 well completion report (EP 114). Gulf Oil Australia Pty. Ltd.

Brown, R. Campbell, N. 1974. Contension Heights 1 well completion report. Australian Aquitaine Petroleum Pty. Ltd.

Johnson, N.E.A. 1966. Kidson 1 well completion report. West Australian Petroleum Pty. Ltd.

Kufpec Australia Pty. Ltd. 1990. Lovell's Pocket 1 well completion report (EP 103). Kufpec Australia Pty. Ltd.

Jacque, M., Strobel, P. and P.J. Sweeney, 1970. Matches Springs 1 well completion report. Total Exploration Australia Pty. Ltd.

Jacque, M., Sweeney, P.J. and P.H. Tricot. McLarty 1 well completion report. Total Exploration Australia Pty. Ltd.

Weeden, R. and G. Hodge. 1989. Mirbelia 2 well completion report. Western Mining Corporation Limited.

Hughes and Hughes Australia Pty. Ltd. 2001. Missing 1 well completion report: Revised geological and drilling program for Missing 1, Canning Basin, Western Australia.

Williams, C.T. 1972. Munro 1 well completion report (EP 3). West Australian Petroleum Pty. Ltd.

Sydney Oil Company Pty. Ltd. 1983. Nita Downs 1 well completion report (EP 142). Sydney Oil Company Pty. Ltd.

Johnson, N.E.A. and Thornton, D.A. 2001. Robert 1 end of well report: composite well log. Hughes and Hughes Australia Pty. Ltd.

Williams, C.T. 1965. Parda 1 well completion report. West Australian Petroleum Pty. Ltd.

Farrelly, J.J. 1988. Pegasus 1 geological well report. Amoco Australia Petroleum Company.

France, R.E. 1986. Percival 1 well completion report. Western Mining Corporation Limited.

Renison, M. 1987. Twin Buttes 1 well completion report (EP 142). Renison Petroleum Consultants Pty. Ltd.

- Pudovski, V. and S.P. Willmott. 1959. Thangoo 1A geological completion report. West Australian Petroleum Pty. Ltd.
- Creevey, K.J. 1969. Wilson Cliffs 1 well completion report (EP 152). Australian Aquitaine Petroleum Pty. Ltd.
- Watson, S.T. and R.E. France. 1983. Santalum 1A well completion report (EP 225). Western Mining Corporation Limited, exploration division - petroleum.
- Hillock, P. and M.Z. Al Abdin. 1989. Setaria 1 well completion report. Western Mining Corporation Limited.
- Jessop, R.G.C. and E.A. Webb. 1995. Sharon Ann 1 well completion report (EP 382). Maple Oil and Exploration N.L.
- Johnson, N.E.A. 1966. Willara 1 well completion report. West Australian Petroleum Pty. Limited.
- Royal Resources Exploration, INC. 1985. Woods Hills 1 final well report. Royal Resources Exploration, INC.
- Bentley, J. 1983. Vela 1 well completion report (EP 175). Getty oil development co. Ltd.

## APPENDIX 3

### FISCHER PLOTS CALCULATION

Fischer plots calculation for well Looma 1:

Cycle No.	Cycle thickness (m)	Cumulative thickness (m)	Cumulative departure (m)
0	0.00	0.00	0.00
1	3.00	3.00	-0.96
2	2.00	5.00	-2.93
3	3.50	8.50	-3.39
4	1.50	10.00	-5.85
5	2.00	12.00	-7.82
6	4.50	16.50	-7.28
7	6.00	22.50	-5.24
8	2.50	25.00	-6.71
9	3.00	28.00	-7.67
10	4.50	32.50	-7.13
11	6.50	39.00	-4.60
12	6.00	45.00	-2.56
13	4.50	49.50	-2.03
14	7.00	56.50	1.01
15	3.00	59.50	0.05
16	8.00	67.50	4.08
17	3.50	71.00	3.62
18	7.50	78.50	7.16
19	5.50	84.00	8.69
20	4.00	88.00	8.73
21	4.50	92.50	9.27
22	4.00	96.50	9.30
23	7.50	104.00	12.84
24	6.50	110.50	15.38
25	2.00	112.50	13.41
26	2.50	115.00	11.95
27	6.50	121.50	14.49
28	3.50	125.00	14.02
29	3.00	128.00	13.06
30	6.00	134.00	15.10
31	5.00	139.00	16.13
32	7.00	146.00	19.17
33	4.50	150.50	19.71
34	6.00	156.50	21.74

35	2.00	158.50	19.78
36	2.00	160.50	17.81
37	7.50	168.00	21.35
38	5.00	173.00	22.39
39	3.00	176.00	21.42
40	13.00	189.00	30.46
41	8.00	197.00	34.50
42	5.50	202.50	36.03
43	4.50	207.00	36.57
44	6.00	213.00	38.61
45	5.00	218.00	39.64
46	3.50	221.50	39.18
47	2.50	224.00	37.72
48	2.00	226.00	35.75
49	2.00	228.00	33.79
50	1.50	229.50	31.33
51	1.50	231.00	28.86
52	3.50	234.50	28.40
53	2.00	236.50	26.44
54	2.00	238.50	24.47
55	2.50	241.00	23.01
56	3.00	244.00	22.04
57	3.00	247.00	21.08
58	2.50	249.50	19.62
59	1.00	250.50	16.65
60	3.50	254.00	16.19
61	2.50	256.50	14.73
62	1.00	257.50	11.76
63	3.00	260.50	10.80
64	1.00	261.50	7.84
65	2.00	263.50	5.87
66	2.00	265.50	3.91
67	1.00	266.50	0.95
68	1.50	268.00	-1.52
69	1.50	269.50	-3.98
70	2.50	272.00	-5.44
71	2.00	274.00	-7.41
72	5.00	279.00	-6.37
73	3.50	282.50	-6.83
74	3.00	285.50	-7.80
75	2.00	287.50	-9.76
76	3.00	290.50	-10.72

77	2.50	293.00	-12.19
78	2.00	295.00	-14.15
79	2.00	297.00	-16.12
80	3.50	300.50	-16.58
81	3.00	303.50	-17.54
82	2.00	305.50	-19.51
83	4.00	309.50	-19.47
84	3.00	312.50	-20.43
85	3.50	316.00	-20.90
86	1.50	317.50	-23.36
87	3.50	321.00	-23.82
88	2.50	323.50	-25.29
89	4.50	328.00	-24.75
90	3.50	331.50	-25.21
91	4.00	335.50	-25.18
92	6.00	341.50	-23.14
93	7.00	348.50	-20.10
94	3.50	352.00	-20.57
95	3.00	355.00	-21.53
96	4.00	359.00	-21.49
97	4.00	363.00	-21.46
98	4.50	367.50	-20.92
99	3.00	370.50	-21.88
100	6.00	376.50	-19.85
101	5.00	381.50	-18.81
102	5.00	386.50	-17.78
103	7.00	393.50	-14.74
104	4.00	397.50	-14.70
105	4.50	402.00	-14.17
106	3.50	405.50	-14.63
107	4.00	409.50	-14.59
108	3.00	412.50	-15.56
109	5.50	418.00	-14.02
110	6.50	424.50	-11.48
111	7.50	432.00	-7.95
112	6.00	438.00	-5.91
113	5.00	443.00	-4.87
114	10.00	453.00	1.16
115	8.50	461.50	5.70
116	10.00	471.50	11.74
117	3.50	475.00	11.27
118	6.00	481.00	13.31

119	8.50	489.50	17.85
120	5.00	494.50	18.88
121	5.00	499.50	19.92
122	4.00	503.50	19.96
123	5.50	509.00	21.49
124	4.00	513.00	21.53
125	6.00	519.00	23.56
126	3.00	522.00	22.60
127	2.00	524.00	20.64
128	3.50	527.50	20.17
129	2.50	530.00	18.71
130	4.00	534.00	18.75
131	3.00	537.00	17.78
132	5.00	542.00	18.82
133	5.50	547.50	20.36
134	4.00	551.50	20.39
135	3.50	555.00	19.93
136	6.50	561.50	22.47
137	5.50	567.00	24.00
138	4.00	571.00	24.04
139	7.00	578.00	27.08
140	4.00	582.00	27.11
141	2.50	584.50	25.65
142	4.00	588.50	25.69
143	5.00	593.50	26.72
144	5.50	599.00	28.26
145	4.50	603.50	28.79
146	3.00	606.50	27.83
147	5.00	611.50	28.87
148	4.50	616.00	29.40
149	4.00	620.00	29.44
150	4.00	624.00	29.48
151	4.50	628.50	30.01
152	5.50	634.00	31.55
153	3.00	637.00	30.59
154	3.50	640.50	30.12
155	3.50	644.00	29.66
156	2.00	646.00	27.70
157	3.50	649.50	27.23
158	2.50	652.00	25.77

159	3.00	655.00	24.81
160	2.50	657.50	23.34
161	4.00	661.50	23.38
162	3.00	664.50	22.42
163	2.00	666.50	20.45
164	1.50	668.00	17.99
165	2.00	670.00	16.03
166	3.00	673.00	15.06
167	4.00	677.00	15.10
168	1.50	678.50	12.63
169	2.00	680.50	10.67
170	3.50	684.00	10.21
171	3.00	687.00	9.24
172	2.50	689.50	7.78
173	2.00	691.50	5.82
174	2.00	693.50	3.85
175	3.50	697.00	3.39
176	1.00	698.00	0.43
177	3.00	701.00	-0.54
178	4.50	705.50	0.00

**Fischer plots calculation for well McLarty 1:**

<b>Cycle No.</b>	<b>Cycle thickness (m)</b>	<b>Cumulative thickness (m)</b>	<b>Cumulative departure (m)</b>
0	0.00	0.00	0.00
1	2.50	2.50	-0.61
2	1.50	4.00	-2.23
3	6.00	10.00	0.66
4	3.00	13.00	0.55
5	2.00	15.00	-0.57
6	2.50	17.50	-1.18
7	4.50	22.00	0.21
8	1.50	23.50	-1.41
9	3.00	26.50	-1.52
10	3.50	30.00	-1.13
11	1.50	31.50	-2.74
12	4.00	35.50	-1.86
13	1.50	37.00	-3.47
14	2.50	39.50	-4.08
15	6.00	45.50	-1.20

16	5.00	50.50	0.69
17	3.50	54.00	1.08
18	3.50	57.50	1.46
19	2.50	60.00	0.85
20	4.50	64.50	2.24
21	4.50	69.00	3.62
22	2.00	71.00	2.51
23	3.00	74.00	2.40
24	3.00	77.00	2.28
25	3.50	80.50	2.67
26	7.00	87.50	6.56
27	6.00	93.50	9.45
28	3.00	96.50	9.33
29	4.00	100.50	10.22
30	3.00	103.50	10.11
31	3.00	106.50	9.99
32	2.50	109.00	9.38
33	1.50	110.50	7.77
34	4.00	114.50	8.65
35	2.50	117.00	8.04
36	4.00	121.00	8.93
37	2.50	123.50	8.31
38	1.50	125.00	6.70
39	5.00	130.00	8.59
40	5.50	135.50	10.97
41	6.00	141.50	13.86
42	2.50	144.00	13.25
43	1.50	145.50	11.64
44	3.50	149.00	12.02
45	3.50	152.50	12.41
46	2.00	154.50	11.30
47	10.50	165.00	18.68
48	6.00	171.00	21.57
49	5.50	176.50	23.96
50	4.00	180.50	24.84
51	3.00	183.50	24.73
52	2.00	185.50	23.62
53	2.50	188.00	23.00
54	4.00	192.00	23.89
55	2.00	194.00	22.78
56	3.00	197.00	22.66

57	3.50	200.50	23.05
58	1.50	202.00	21.44
59	3.00	205.00	21.32
60	2.00	207.00	20.21
61	1.00	208.00	18.10
62	1.50	209.50	16.49
63	1.00	210.50	14.37
64	2.50	213.00	13.76
65	3.00	216.00	13.65
66	1.50	217.50	12.03
67	4.50	222.00	13.42
68	4.00	226.00	14.31
69	2.50	228.50	13.69
70	1.50	230.00	12.08
71	3.50	233.50	12.47
72	2.00	235.50	11.35
73	3.00	238.50	11.24
74	1.00	239.50	9.13
75	2.00	241.50	8.01
76	5.00	246.50	9.90
77	5.50	252.00	12.29
78	5.50	257.50	14.68
79	7.00	264.50	18.56
80	3.00	267.50	18.45
81	2.50	270.00	17.84
82	3.00	273.00	17.72
83	2.50	275.50	17.11
84	2.50	278.00	16.50
85	4.00	282.00	17.38
86	3.50	285.50	17.77
87	2.00	287.50	16.66
88	9.50	297.00	23.04
89	2.00	299.00	21.93
90	4.50	303.50	23.32
91	3.50	307.00	23.70
92	3.00	310.00	23.59
93	2.00	312.00	22.48
94	3.00	315.00	22.36
95	3.50	318.50	22.75
96	2.00	320.50	21.64
97	2.50	323.00	21.03
98	2.00	325.00	19.91

99	4.50	329.50	21.30
100	2.50	332.00	20.69
101	2.50	334.50	20.07
102	5.50	340.00	22.46
103	5.00	345.00	24.35
104	2.50	347.50	23.73
105	2.50	350.00	23.12
106	2.00	352.00	22.01
107	1.50	353.50	20.39
108	2.00	355.50	19.28
109	2.50	358.00	18.67
110	2.00	360.00	17.55
111	3.50	363.50	17.94
112	3.50	367.00	18.33
113	5.00	372.00	20.22
114	3.50	375.50	20.60
115	3.50	379.00	20.99
116	2.00	381.00	19.88
117	1.50	382.50	18.26
118	2.50	385.00	17.65
119	3.00	388.00	17.54
120	2.50	390.50	16.92
121	2.50	393.00	16.31
122	3.00	396.00	16.20
123	3.00	399.00	16.08
124	2.00	401.00	14.97
125	3.00	404.00	14.86
126	2.00	406.00	13.74
127	1.50	407.50	12.13
128	2.50	410.00	11.52
129	2.50	412.50	10.91
130	2.00	414.50	9.79
131	2.00	416.50	8.68
132	1.50	418.00	7.07
133	1.00	419.00	4.95
134	2.00	421.00	3.84
135	2.00	423.00	2.73
136	2.50	425.50	2.11
137	1.00	426.50	0.00

**Fischer plots calculation for well Robert 1:**

<b>Cycle No.</b>	<b>Cycle thickness (m)</b>	<b>Cumulative thickness (m)</b>	<b>Cumulative departure (m)</b>
0	0.00	0.00	0.00
1	2.00	2.00	-0.93
2	2.00	4.00	-1.85
3	3.00	7.00	-1.78
4	2.50	9.50	-2.20
5	1.50	11.00	-3.63
6	2.00	13.00	-4.55
7	2.50	15.50	-4.98
8	4.00	19.50	-3.90
9	3.50	23.00	-3.33
10	1.00	24.00	-5.25
11	4.00	28.00	-4.18
12	3.50	31.50	-3.60
13	2.00	33.50	-4.53
14	2.00	35.50	-5.45
15	1.00	36.50	-7.38
16	1.00	37.50	-9.30
17	1.50	39.00	-10.73
18	2.00	41.00	-11.65
19	3.50	44.50	-11.08
20	2.00	46.50	-12.00
21	1.50	48.00	-13.43
22	3.50	51.50	-12.85
23	1.50	53.00	-14.28
24	5.00	58.00	-12.20
25	4.00	62.00	-11.13
26	1.50	63.50	-12.55
27	1.00	64.50	-14.48
28	3.50	68.00	-13.90
29	1.00	69.00	-15.83
30	1.50	70.50	-17.25
31	2.00	72.50	-18.18
32	3.00	75.50	-18.10
33	1.50	77.00	-19.53
34	2.00	79.00	-20.45
35	2.00	81.00	-21.38
36	2.00	83.00	-22.30
37	4.00	87.00	-21.23
38	1.00	88.00	-23.15

39	2.50	90.50	-23.58
40	1.00	91.50	-25.50
41	1.00	92.50	-27.43
42	1.00	93.50	-29.35
43	2.50	96.00	-29.78
44	5.00	101.00	-27.70
45	2.00	103.00	-28.63
46	1.50	104.50	-30.05
47	3.50	108.00	-29.48
48	2.50	110.50	-29.90
49	4.00	114.50	-28.83
50	1.00	115.50	-30.75
51	2.00	117.50	-31.68
52	1.50	119.00	-33.10
53	1.50	120.50	-34.53
54	2.00	122.50	-35.45
55	5.50	128.00	-32.88
56	9.50	137.50	-26.30
57	3.50	141.00	-25.73
58	5.00	146.00	-23.65
59	2.50	148.50	-24.08
60	5.00	153.50	-22.00
61	3.00	156.50	-21.93
62	2.00	158.50	-22.85
63	8.00	166.50	-17.78
64	1.00	167.50	-19.70
65	1.50	169.00	-21.13
66	5.50	174.50	-18.55
67	2.00	176.50	-19.48
68	4.00	180.50	-18.40
69	5.50	186.00	-15.83
70	5.00	191.00	-13.75
71	6.00	197.00	-10.68
72	5.00	202.00	-8.60
73	2.50	204.50	-9.03
74	5.00	209.50	-6.95
75	2.50	212.00	-7.38
76	4.00	216.00	-6.30
77	4.00	220.00	-5.23
78	3.50	223.50	-4.65
79	3.00	226.50	-4.58
80	3.50	230.00	-4.00

81	3.50	233.50	-3.43
82	1.50	235.00	-4.85
83	2.50	237.50	-5.28
84	3.50	241.00	-4.70
85	3.50	244.50	-4.13
86	2.50	247.00	-4.55
87	4.00	251.00	-3.45
88	2.50	253.50	-3.90
89	3.00	256.50	-3.83
90	2.50	259.00	-4.25
91	4.50	263.50	-2.68
92	3.50	267.00	-2.10
93	3.50	270.50	-1.53
94	3.00	273.50	-1.45
95	3.00	276.50	-1.38
96	2.50	279.00	-1.80
97	1.50	280.50	-3.23
98	1.00	281.50	-5.15
99	1.00	282.50	-7.08
100	3.50	286.00	-6.50
101	1.50	287.50	-7.93
102	3.00	290.50	-7.85
103	4.00	294.50	-6.78
104	3.50	298.00	-6.20
105	1.50	299.50	-7.63
106	1.50	301.00	-9.05
107	2.00	303.00	-9.98
108	3.00	306.00	-9.90
109	3.00	309.00	-9.83
110	4.00	313.00	-8.75
111	3.50	316.50	-8.18
112	2.50	319.00	-8.60
113	3.00	322.00	-8.53
114	2.50	324.50	-8.95
115	2.50	327.00	-9.38
116	4.00	331.00	-8.30
117	2.50	333.50	-8.73
118	2.50	336.00	-9.15
119	2.00	338.00	-10.08
120	1.50	339.50	-11.50

121	3.00	342.50	-11.43
122	3.00	345.50	-11.35
123	2.00	347.50	-12.28
124	3.00	350.50	-12.20
125	5.00	355.50	-10.13
126	2.50	358.00	-10.55
127	3.50	361.50	-9.98
128	4.50	366.00	-8.40
129	3.50	369.50	-7.83
130	2.00	371.50	-8.75
131	2.50	374.00	-9.18
132	1.50	375.50	-10.60
133	3.50	379.00	-10.03
134	3.50	382.50	-9.45
135	5.50	388.00	-6.88
136	2.50	390.50	-7.30
137	6.00	396.50	-4.23
138	5.50	402.00	-1.65
139	2.00	404.00	-2.58
140	5.50	409.50	0.00